Investigating Immune Reactivity to the Intestinal Microbiome in Myalgic Encephalomyelitis/Chronic Fatigue Syndrome

By Katharine Ann Seton

A thesis submitted to The University of East Anglia in accordance with the requirements for the degree of Doctor of Philosophy (PhD)

12th May 2022

ABSTRACT

Introduction: Myalgic encephalomyelitis/chronic fatigue syndrome (ME/CFS) pathogenesis is thought to be multisystemic, including the immune and gastrointestinal systems. A proportion of patients experience gastrointestinal disturbances with evidence suggesting a leaky gut. It was hypothesised that a leaky gut and microbial translocation causes a breach in immune tolerance, promoting inflammation and autoimmunity.

Aims: A) determine whether severe ME/CFS patients have increased systemic and mucosal immunoglobulin (Ig) reactivity to the intestinal microbiome, and B) determine which intestinal microbes serum IgG was directed against.

Methods: Serum and stool samples were collected from five pairs of severe ME/CFS patients and matched household controls. Enzyme linked immunosorbent assays were developed to quantify IgG in serum, bound and non-bound IgA in stool and serum IgG levels reactive with autologous and heterologous stool bacteria. Flow cytometry methods were developed to quantify both stool microbial load and the proportion of stool microbes reactive with mucosal IgA and serum IgG. A 'bug FACS' method was developed to identify and quantify serum IgG reactivity to stool bacteria and fungi.

Results: The main finding was that severe ME/CFS patients have significantly lower levels of serum IgG reactive to heterologous stool bacteria compared to their matched household controls. In addition, severe ME/CFS patients do not have higher levels of serum IgG reactive to heterologous stool bacteria than autologous stool bacteria. Severe ME/CFS patients also have a non-significant increase of IgG binding to *Campylobacter jejuni* and *Pseudomonas viridiflava* compared to their matched household controls. Analysis of mucosal IgA found ME/CFS patients with a long disease duration had higher microbe bound IgA concentrations compared to their matched household controls.

Conclusion: This thesis presents results from the first ME/CFS study to investigate serum IgG immune reactivity to stool microbes. Findings suggest ME/CFS patients have an impaired serum IgG immune response to the intestinal microbiome.

ACKNOWLEDGEMENTS

I would like to begin by acknowledging my primary supervisor Professor Simon Carding to whom I am extremely grateful for his knowledge and support throughout this project. I am also thankful to my secondary supervisory, Professor Tom Wileman, who provided excellent advice which guided my thesis. And to the rest of my supervisory team; Dr Alistair Noble, Dr Ana Carvalho and Dr Steve James for taking the time to provide demonstrations within the lab. Your assistance has been invaluable.

I would like to acknowledge everyone who provided help during my PhD in addition to my supervisory team; David Baker who assisted with sequencing, Dr Andrea Telatin, Dr Rebecca Ansorage and Dr Sumeet Tiwari who performed the bioinformatic analysis, Dr George Savva who helped with statistics and Dr Marianna Defernez who performed multivariate analysis. Thank you also to Professor Carding's lab group members who have provided the encouragement I have needed to complete this project.

This human study would not have been possible without the following people. Firstly, I would like to thank all of the incredible study participants, it was a pleasure to meet you all and I would like you all to know how inspirational you are. I would also like to thank Dr Amolak Bansal from Epsom and St Helier University Hospitals CFS Service who identified patients for the study. Thank you to the East Coast Community Healthcare Centre ME/CFS Service, particularly Joanne Wiggins and Louise Halliday who I liaised with and coordinated participant identification. Thank you to Antonietta Hayhoe for her help and guidance when making amendments to the human study. I would also like to thank Dr Fiona Newberry and Dr Shen Yuan Hsieh helping to process human samples. And thank you to Dr Daniel Vipond for setting up the first Norwich based ME/CFS human study, which made this human study so much easier.

Thank you to the Invest in ME Research charity who funded my research, and all who have donated to the charity, without whom this research would not have been possible. A special thanks to Richard and Pia Simpson for all the hard work they do for the ME/CFS community.

My time at Quadram has not been smooth sailing, as relapses in my own ME/CFS have set me back. Thank you to Dr Paul Kroon who has given me an incredible amount of support and guidance when applying for extensions. Thank you to my friends and housemates for keeping my spirits up when I was struggling. Thank you to my Mam, Dad and the rest of my family for providing emotional support and encouragement throughout my PhD despite living at the opposite end of the country.

I would like to dedicate this thesis to my late Grandpa, Anthony Seton, who was so excited to have the "first doctor in the family". I know he would be so proud.

TABLE OF CONTENTS

LIST OF FIGURES

LIST OF TABLES

LIST OF EQUATIONS

LIST OF SUPPLEMENTARY FIGURES

LIST OF APPENDICES

ABBREVIATIONS

AChR	Acetylcholine receptor
AdR	Adrenergic receptor
AHA	Anti-hypothalamic antibodies
ANA	Anti-nuclear antibodies
ANOVA	Analysis of variance
APA	Anti-pituitary antibodies
ATP	Adenosine triphosphate
BMI	Body mass index
BPRM	Bacteroides phage recovery medium
BSA	Bovine serum albumin
BSC	Back scatter
BSFS	Bristol stool form scale
CBT	Cognitive behavioural therapy
CCC	Canadian Consensus Criteria
CCL11	CC motif chemokine ligand 11
CD	Crohn's disease
CDC	Centers for Disease Control and Prevention
CFQ	Chalder fatigue questionnaire
CFS	Chronic fatigue syndrome
CFU	Colony forming unit
CLR	Centered log-ratio
CNS	Central nervous system
CRP	C-reactive protein
CSF	Cerebrospinal fluid

CSF1	Colony stimulating factor 1
DCs	Dendritic cells
DNA	Deoxyribonucleic acid
EBV	Epstein-Barr virus
EBVS	Chronic Epstein-Barr virus syndrome
ECCHC	East Coast Community Healthcare Centre
ECD	Epidemiological case definition
EDTA	Ethylenediaminetetraacetic acid
ELISA	Enzyme linked immunosorbent assay
ESTH	Epsom and St Helier University Hospitals
EU	European Union
FACS	Fluorescence activated cell sorting
FAO	Food and Agriculture Organization of the United Nations
FDR	False discovery rate
FMO	Fluorescence minus one
FMT	Faecal microbe transplantation
FSC	Forward scatter
GCP	Good Clinical Practice
GDPR	General Data Protection Regulation
GET	Graded exercise therapy
GI	Gastrointestinal
GM-CSF	Granulocyte-macrophage colony-stimulating factor
GU	Genitourinary
HADS	Hospital anxiety and depression scale
HIF-1	Hypoxia-inducible factor-1

HPA	Hypothalamic-pituitary-adrenal
HPT	Hypothalamic-pituitary-thyroid
HRA	Health Research Authority
hsCRP	High sensitivity C-reactive protein
HT	High throughput
IBD	Inflammatory bowel disease
IBS	Irritable bowel syndrome
IBS-C	Constipation predominant IBS
IBS-D	Diarrhoea predominant IBS
IBS-M	IBS with alternating diarrhoea and constipation
ICC	International Consensus Criteria
ICH	International council for harmonisation of technical requirements for pharmaceuticals for human use
IFN	Interferon
Ig	Immunoglobulin
IL	Interleukin
IOM	Institute of Medicine
IP-10	Interferon gamma-induced protein 10
IRAS	Integrated Research Application System
ITS	Internal transcribed spacer
LBP	Lipopolysaccharide binding protein
LPS	Lipopolysaccharide
M	Mean
MBL	Mannose-binding lectin
MDD	Major depressive disorder

MDS	Multi-dimensional scaling
ME	Myalgic encephalomyelitis
ME/CFS	Myalgic encephalomyelitis/chronic fatigue syndrome
MRS	de Man, Rogosa and Sharpe
MS	Multiple sclerosis
multiKAP	Multi-kingdom antibody profiling
NA	Not applicable
NHS	National Health Service
NICE	National Institute for Health and Care Excellence
NIH	National Institutes of Health
NIOF	Neuro-inflammatory and oxidative fatigue
NK	Natural killer
NMDS	Non-metric multi-dimensional scaling
NO	Nitroso
NRP	Norwich Research Park
NSAIDs	Non-steroidal anti-inflammatory drugs
OD	Optical density
OTU	Operational taxonomic unit
p	Probability value
PAMPs	Pathogen associated molecular patterns
PBMCs	Peripheral blood mononuclear cells
PBS	Phosphate buffered saline
PC	Principal component
PCA	Principal component analysis
PCR	Polymerase chain reaction

PEM	Post exertional malaise
PERMANOVA	Permutational multivariate analysis of variance
PET	Positron emission tomography
PFA	Paraformaldehyde
PhIP-Seq	Phage immunoprecipitation sequencing
PMN	Polymorphonuclear
PPIs	Proton pump inhibitors
POTS	Postural orthostatic tachycardia syndrome
PVFS	Post viral fatigue syndrome
QIB	Quadram Institute Bioscience
QMP	Quantitative microbiome profiling
q-PCR	Quantitative polymerase chain reaction
r	Pearson's correlation coefficient
RA	Rheumatoid arthritis
RAAS	Renin-angiotensin-aldosterone system
RANTES	Regulated upon activation, normal cell expressed and presumably secreted
REC	Regional ethics committee
RMP	Relative microbiome profiling
RPK	Reads per kilobase
rRNA	Ribosomal ribonucleic acid
RRV	Ross River virus
sCD14	Soluble CD14
SCFA	Short-chain fatty acid
SD	Standard deviation
SEID	Systemic exertion intolerance disease

SEM	Standard error of the mean
SF-36	Medical outcomes study 36-item short form health survey
sFasL	Soluble Fas ligand
SIBO	Small intestinal bacterial overgrowth
SLE	Systemic lupus erythematosus
SSC	Side scatter
SST	Serum separator tube
t	T-value
Tc	Effector CD8+ T cells
TCR	T cell receptor
Tfh	Follicular T-helper cell
TG	Thyreoglobulin
TGF	Transforming growth factor
Th	T helper cells
TJ	Tight junction
TLR	Toll-like receptor
TNF	Tumour necrosis factor
TPO	Thyreoperoxidase
Tregs	Regulatory T cells
TRPM	Transient receptor potential melastatin
UEA	University of East Anglia
UK	United Kingdon
US	United States
UV	Ultraviolet
WGA	Whole genome amplification

WGS	Whole genome shotgun
WHO	World Health Organization
β-NGF	Beta-nerve growth factor

1 CHAPTER ONE: INTRODUCTION

1.1 WHAT IS MYALGIC ENCEPHALOMYELITIS/CHRONIC FATIGUE SYNDROME?

1.1.1 Overview

Myalgic encephalomyelitis (ME) is also known as chronic fatigue syndrome (CFS) and is often referred to as ME/CFS. It is a chronic, heterogenous disease which leaves patients unable to undertake their pre-morbid work, sport and social activities. The disease is characterised by disabling fatigue and symptoms related to neurologic, neurocognitive, neuroendocrine, autonomic and immune dysfunction which worsen following physical, mental or emotional exertion. ME and CFS are currently listed under post viral fatigue syndrome (PVFS) and classified as a neurological disease by the World Health Organization (WHO) (ICD-11, 2022).

1.1.2 A historical perspective

In the 1930s outbreaks of neuromyasthenia with a striking resemblance to poliomyelitis began to emerge (Acheson, 1959). However, unlike poliomyelitis a cause by an infectious agent was not confirmed. These outbreaks of atypical poliomyelitis were characterised by the acute onset of headaches, muscular pain (myalgia) and muscle weakness (paresis), symptoms which indicated damage to the central or peripheral nervous system, as well as psychological symptoms and a low or absent fever. A proportion of patients did not recover after the acute phase of the illness and later went on to have long term health problems, suffering from myalgia, paresis, cognitive dysfunction with the worsening of symptoms during cold weather, menstruation and following exertion.

In 1955 there was a similar outbreak seen amongst staff in the Royal Free Hospital in London with nearly 300 recorded cases (The Medical Staff Of The Royal Free Hospital, 1957). The clinical presentation of these cases was heterogenous, with the predominant symptoms being headaches, sore throat, malaise, fatigue and dizziness. Despite the resemblance to an infectious disease, an aetiological agent could not be confirmed. This outbreak was named benign ME because of the signs of brain inflammation seen in the absence of death (Lindan, 1956). A follow up study found one subset did not recover and another subset did recover but experienced relapses in symptoms (Ramsay, 1978). Other outbreaks were recorded in the 1980's and referred to as 'chronic Epstein-Barr virus syndrome' and 'post viral fatigue syndrome (PVFS)' (Lim and Son, 2020).

In 1986 the first case definition of ME was made to encompass chronic long-term symptoms following infectious outbreaks (Ramsay, 1986). In 1988 the Centers for Disease Control and Prevention (CDC) renamed the disease as chronic fatigue syndrome (CFS) due to insufficient evidence surrounding a viral component to the disease (Holmes et al., 1988). In 2003 the Canadian

Consensus Criteria (CCC) was published and encompassed both ME and CFS which were consequently named ME/CFS (Carruthers et al., 2003). In 2015 the Institute of Medicine (IOM) proposed the term systemic exertion intolerance disease (SEID) (IOM, 2015). In addition, the term neuro-inflammatory and oxidative fatigue (NIOF) was also proposed in 2015 as a replacement for ME/CFS (Maes, 2015). Each name was altered in an attempt to better reflect the disease aetiology.

It is important to note that these outbreaks and case definitions have also been met with scepticism. The lack of evidence for an aetiological agent in these outbreaks led to the proposal that the outbreaks were instead mass hysteria with a psychosocial phenomenon and were referred to as myalgia nervosa (McEvedy and Beard, 1970). In the 1980s ME was referred to as 'yuppie flu' within the media (Blease and Geraghty, 2018). 20 % of US news articles published between 1987 and 2013 about ME/CFS trivialised the illness by instead referring to it as fatigue or a psychosomatic related disease (Siegel et al., 2018). The psycho-behavioural interventions put forward for ME/CFS treatment such as cognitive behavioural therapy (CBT) and graded exercise therapy (GET) has meant that the psychological stigma surrounding ME/CFS remains to this day (Sharpe, 1991, Wessely, 1996).

1.1.3 Epidemiology

To date there are 45 articles published that investigate the prevalence (disease frequency in a population at one time point) of ME/CFS from which there are 56 sets of prevalence data (Lim et al., 2020). The average prevalence from all of these studies was 1.40 %, with large variations across studies. Inconsistencies arose due to studies using different recruitment methods, case definitions, diagnostic methods and patient demographics (**Table 1.1**). Interestingly, the average prevalence of ME/CFS was greater in females than males and adults than in children and adolescents. However, incidence rates (frequency of newly diagnosed cases within a specified time period) were greater in children and adolescents than adults (Nacul et al., 2011, Rimes et al., 2007). Discrepancies between prevalence and incidence can be explained by the peak ages of onset; 10- to 19-years and 30- to 39-years (Bakken et al., 2014, Rowe et al., 2017). It is important to note the variation in prevalence rates seen by different case definitions. Nacul et al. (2011) applied the CDC-1994 case definition, the CCC-2003 and the epidemiological case definition (ECD) to the same study population and found different prevalence's in ME/CFS. This demonstrates that ME/CFS case definitions define different groups of participants which could impact research findings (discussed further in **section 1.1.4.4**).

Table 1.1: The study design aspects leading to differential prevalence rates of ME/CFS. *Adapted from (Lim et al., 2020).*

Study design aspect	Average prevalence of all studies (%)
Recruitment method	
Community	1.56 ± 1.80
Primary care	1.16 ± 1.13
Diagnostic method	
Interview (with medical test)	2.03 ± 2.13
Interview (without medical test)	1.17 ± 0.77
Physician diagnosis	0.10 ± 0.05
Medical records	1.25 ± 1.00
Case definition	
CDC-1994	1.46 ± 1.34
Holmes	0.34 ± 0.04
Australian	2.52 ± 2.99
Oxford	1.73 ± 1.35
CCC, ECD, PVFS, NICE	0.53 ± 0.77
Country	
Western	1.32 ± 1.45
Asian	1.51 ± 1.74
Other[a]	2.65 ± 2.37
Age	
≥ 18 years	1.45 ± 1.68
< 18 years	0.89 ± 0.82
Gender	
Female	2.24 ± 2.59
Male	1.11 ± 1.05

[a]Other countries included India and Nigeria

1.1.4 Case definitions

To date, 26 case definitions for ME, CFS, ME/CFS and SEID exist globally (**Table 1.2**) (Lim and Son, 2020, NICE, 2021). More than one case definition for ME, CFS and ME/CFS exist. In research the most widely used case definitions for ME, CFS and ME/CFS are the International Consensus Criteria (ICC)-2011, CDC-1994 criteria and the CCC-2003 respectively (Brurberg et al., 2014).

1.1.4.1 CDC-1994 criteria for CFS

The CDC-1994 criteria for CFS requires patients to have sudden onset of fatigue that has lasted for a minimum of 6 months and that is of a persistent or relapsing nature (Fukuda et al., 1994). In addition, a minimum of 4 additional symptoms are required for CFS diagnosis. These symptoms are as follows: 1) impaired memory or concentration, 2) sore throat, 3) tender cervical or axillary lymph nodes, 4) muscle pain, 5) joint pain, 6) headache, 7) unrefreshing sleep and 8) post-exertional malaise (PEM). Conditions that exclude a patient from CFS diagnosis include active medical conditions that cause chronic fatigue, chronic viral infections, major depressive disorder, substance abuse and severe obesity.

1.1.4.2 CCC-2003 for ME/CFS

The CCC-2003 criteria for ME/CFS requires patients to have sudden or gradual onset of persistent or relapsing physical and mental fatigue that results in a substantial reduction in activity level and has been present for a minimum of 6 months (Carruthers et al., 2003). PEM, sleep dysfunction and musculoskeletal pain also have to be present in patients for diagnosis. In addition, two or more neurological or cognitive symptoms have to be present; confusion, impaired concentration, impaired short-term memory, disorientation, impaired information processing, spatial instability, inability to focus vision, ataxia, paresis and sensory overload. Patients must also have at least one symptom from two of the following three categories: autonomic, neuroendocrine and immune manifestations. Autonomic symptoms listed were orthostatic intolerance, light-headedness, extreme pallor, gastrointestinal (GI) symptoms, genitourinary (GU) symptoms, heart palpitations and shortness of breath. Neuroendocrine symptoms listed were loss of thermostatic stability, feverishness and cold extremities, intolerance to extreme temperatures, anorexia and worsening of symptoms with stress. Immune symptoms listed were tender lymph nodes, recurrent sore throat, flu-like symptoms, general malaise, food, medication or chemical sensitivity. Illnesses that can cause fatigue, sleep disturbance, pain and cognitive dysfunction were listed as exclusionary conditions. Interestingly depression was listed as a comorbidity of ME/CFS.

1.1.4.3 ICC-2011 criteria for ME

The ICC-2011 criteria for ME were based upon the CCC-2003 ME/CFS definition (Carruthers et al., 2011). Instead of patients having to have fatigue present for a minimum of 6 months, patients can be diagnosed immediately if the fatigue experienced results in at least a 50 % reduction in premorbid activity. In addition, postexertional neuroimmune exhaustion is required for diagnosis. This is described as physical and/or cognitive fatigue in response to minimal exertion, which can be immediate or delayed, takes longer than 24 hours to recover from and causes ME symptom exacerbation. Patients must also present with at least one of the following neurological impairment symptoms; difficulty processing information, short-term memory loss, headaches, significant musculoskeletal pain, disturbed sleep patterns, unrefreshing sleep, sensory sensitivity or paresis. Patients must also present with at least one immune (e.g. flu-like symptoms), GI (e.g. irritable bowel syndrome (IBS)) or GU (e.g. altered urinary urgency) symptom. Finally, patients must have at least one of the following energy production impairments; orthostatic intolerance, hypotension, postural orthostatic tachycardia syndrome (POTS), palpitations, light-headedness, laboured breathing, fatigue of chest wall muscles, feeling feverish, cold extremities and intolerance of extreme temperatures. Exclusionary conditions include primary psychiatric disorders, somatoform disorder and substance abuse.

Table 1.2: Timeline of the development of case definitions for ME/CFS. *Adapted from (Lim and Son, 2020). ME = myalgic encephalomyelitis, CFS = chronic fatigue syndrome, CDC = Centers for Disease Control and Prevention, PVFS = post viral fatigue syndrome, NIH = National Institutes of Health, CCC = Canadian Consensus Criteria, ME/CFS = myalgic encephalomyelitis/chronic fatigue syndrome, NICE = National Institute for Health and Care Excellence, ICC = International Consensus Criteria, CF = chronic fatigue, IOM = Institute of Medicine, SEID = systemic exertion intolerance disease, NIOF = neuro-inflammatory and oxidative fatigue*

Year	Case definition	Country	Reference
1986	Ramsay's definition for ME	UK	(Ramsay, 1986)
1988	CDC-1988 definition for CFS	US	(Holmes et al., 1988)
1990	London-1990 definition for ME	UK	(Dowsett et al., 1990)
	Ho-yen Do definition for PVFS	UK	(Ho-Yen, 1990)
	Australian definition for CFS	Australia	(Lloyd et al., 1990)
1991	Oxford definition for CFS	UK	(Sharpe et al., 1991)
1992	NIH definition for CFS	US	(Schluederberg et al., 1992)
1994	London-1994 definition for ME	UK	(Dowsett et al., 1994)
	CDC-1994 definition for CFS	US	(Fukuda et al., 1994)
1996	Working case definition for CFS	US	(Komaroff et al., 1996)
1998	CFS-1998 definition for CFS	US	(Hartz et al., 1998)
2003	CCC-2003 for ME/CFS	Canada	(Carruthers et al., 2003)
2005	CDC-2005 empirical definition for CFS	US	(Reeves et al., 2005)
2007	NICE-2007 guidelines for ME/CFS	UK	(Baker and Shaw, 2007)
	Empirical-2007 definition for CFS	US	(Jason et al., 2007)
	The Nightingale definition for ME	Canada	(Hyde, 2007)
	Brighton Collaboration definition for CFS	US	(Jones et al., 2007)
	Epidemiological case definition for ME/CFS	UK	(Osoba et al., 2007)
2010	Revised CCC-2010 definition for ME	Canada	(Jason et al., 2010)
2011	ICC definition for ME	Canada	(Carruthers et al., 2011)
2012	ME-2011 for ME, ME/CFS	US	(Jason et al., 2012)
	Maes criteria for ME, CFS, CF	Thailand	(Maes et al., 2012b)
2015	IOM diagnostic criteria for SEID	US	(IOM, 2015)
	Maes criteria for NIOF	Australia	(Maes, 2015)
	Empirical case definition for CFS	US	(Jason et al., 2015)
2021	NICE-2021 guidelines for ME/CFS	UK	(NICE, 2021)

1.1.4.4 Similarities and differences between ME, CFS and ME/CFS case definitions

Whether ME and CFS are the same illness and can be classified as ME/CFS or are two distinct illnesses is still widely disputed. The CCC-2003 was the first case definition to merge ME and CFS together as ME/CFS. They explained that this was done because ME and CFS case definitions emphasise different aspects of what is "probably the same illness" and that in Canada ME and CFS definitions were used interchangeably (Carruthers et al., 2003). Indeed, the ICC-2011 ME criteria, CDC-1994 CFS criteria and CCC-2003 ME/CFS criteria share similarities. Fatigue, flu-like symptoms, sore throat, joint pain, tender lymph nodes, headache, myalgia, sleep disturbances, cognitive impairment and PEM are all listed as symptoms for ME, CFS and ME/CFS (**Figure 1.1**). But the CCC-2003 ME/CFS criteria and the ICC-2011 ME criteria also require additional symptoms for diagnosis which suggests the CDC-1994 CFS criteria is less stringent.

However, Maes et al. (2012b) argued that CFS is an umbrella term that also encompassed ME patients as PEM is a requirement for ME criteria to be met whereas PEM is a symptom but not a requirement for CFS diagnosis. Indeed only 65 % of patients who met the CDC-1994 criteria for CFS also met the ICC-2011 ME criteria (Brown et al., 2013). In addition, ME patients (those meeting the CDC-1994 CFS criteria and the ICC-2011 ME criteria) were more functionally impaired and experienced more severe neurocognitive symptoms, pain, sleep disturbances, neurosensory, perceptual and motor disturbances, immune impairment, GI and GU symptoms, cardiovascular symptoms and thermostatic stability than CFS patients (those meeting the CDC-1994 CFS criteria but not the ICC-2011 ME criteria). In light of these findings, an alternative view is that ME is a subgroup of severe CFS patients.

The name ME/CFS suggests a broader case definition including aspects of ME and CFS diagnostic criteria. However, only 50 % of the patients meeting the CDC-1994 CFS criteria also met the CCC-2003 ME/CFS criteria, despite the name suggesting a broader case definition (Jason et al., 2012). Interestingly, the UK diagnostic criteria are based on the National Institute for Health and Care Excellence (NICE) guidelines which refer to the illness as ME/CFS (see **section 1.1.4.5**).

This thesis subsequently refers to the illness as ME/CFS because of the following reasons: 1) the overlap observed between ME and CFS case definitions and 2) diagnosis of ME/CFS in the UK.

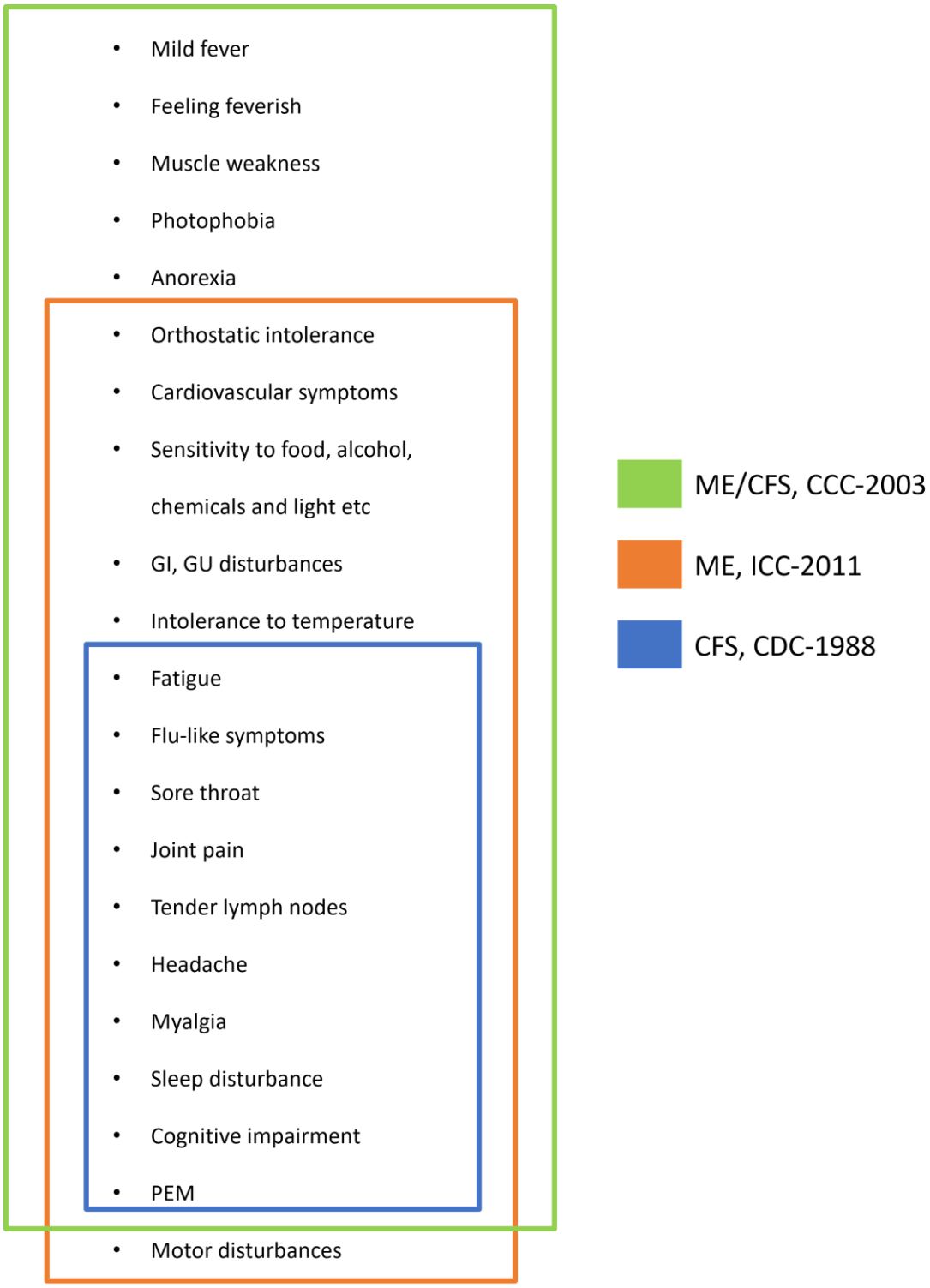

Figure 1.1: Overlap in symptom criteria for the most commonly used ME, CFS and ME/CFS case definitions. *Adapted from (Lim and Son, 2020). ME/CFS = myalgic encephalomyelitis/ chronic fatigue syndrome, ME = myalgic encephalomyelitis, CFS = chronic fatigue syndrome, CCC = Canadian Consensus Criteria, ICC = International Consensus Criteria, CDC = Centers for Disease Control and Prevention, GI = gastrointestinal, GU = genitourinary, PEM = post exertional malaise.*

1.1.4.5 UK diagnostic criteria

The NICE guidelines are used for diagnosing ME/CFS in the NHS. On the 29th of October 2021 NICE updated their guidelines (NG206) for the diagnosis and management of ME/CFS (NICE, 2021). These guidelines state that a diagnosis of ME/CFS can be made if all of the following symptoms persist for a minimum of three months: fatigue that is debilitating, made worse by activity and not alleviated by rest, PEM after activity which can last days or weeks, unrefreshing sleep and/or disturbed sleep where the patient still feels exhausted on waking, and cognitive difficulties which patients describe as 'brain fog' and lead to problems with communication, short-term memory and concentration. Symptoms have to impact the patient's life to such an extent that a reduction in their ability to participate in activities, both occupational and social, when compared to pre-illness levels, would be observed. Unlike many other illnesses, ME/CFS does not have diagnostic tests and instead diagnosis is based upon medical assessment to exclude generalised anxiety disorder or depression, physical examination and laboratory tests to exclude any other causes of symptoms (**Table 1.3**) (Bansal, 2016, Rowe et al., 2017).

Table 1.3: Laboratory measures used in the NHS prior to ME/CFS diagnosis to exclude other conditions that could cause symptoms. *Information collected from (Baker and Shaw, 2007, Bansal, 2016, Rowe et al., 2017).*

Laboratory measure	Exclusionary condition
Full blood count	Anaemia, polycythaemia, haematological malignancy
Erythrocyte sedimentation rate	Elevated levels indicative of immune activation
C-reactive protein concentration	Elevated levels in inflammation
Bilirubin, alkaline phosphatase, gamma glutamyl transaminase, aspartate transaminase, urea, creatinine, electrolytes	Liver function
Thyroid stimulating hormone and free thyroxine (free T4)	Hypo or hyperthyroidism
Autoimmune profile on a tissue block	Autoimmune diseases e.g. Sjogren's syndrome, early primary biliary cirrhosis, autoimmune hepatitis and atopic gastritis
Antinuclear antibodies	Autoimmune disease
Anti-tissue transglutaminase or endomysia antibodies	Coeliac disease
Urine dipstick analysis (level of red blood cells, white blood cells, protein, glucose, urea)	Renal inflammation/infection and renal tumours
Immunoglobulins and serum proteins electrophoresis	Elevated levels in chronic inflammation/infection, reduced levels in antibody deficiency
Calcium, serum iron, serum transferrin, serum ferritin, vitamin B12, folate, vitamin D3, 25-hydroxycholecalciferol	Vitamin and minerals deficiency
Fasting blood glucose	Diabetes

1.1.5 Symptoms

Symptoms experienced by ME/CFS patients include those required for diagnosis as well as those not specific to ME/CFS. They fall into five categories; autonomic, muscular, cognitive, neurological and immune symptoms (Castro-Marrero et al., 2017). Cognitive symptoms such as impaired concentration, information processing and memory were commonly reported in ME/CFS patients, at a prevalence of 81.7 %. 79.5 % of patients had neurological disturbances including sensory sensitivities, poor coordination and blurred vision. Muscular symptoms were seen in 75 % of patients and included muscle weakness, generalised chronic pain and myoclonic jerks. Autonomic symptoms were seen in 62.8 % of patients and included dizziness, orthostatic hypotension, palpitations, vertigo and IBS. Finally, immune symptoms were seen in 42.9 % of patients and included recurrent fever, recurrent sore throat, painful lymph nodes and intolerance to foods. It is important to also note the clinical heterogeneity seen amongst patients as they did not experience the same combinations or severity of symptoms. Interestingly, as the illness progressed the

symptoms experienced by patients changed with immune and muscular symptoms becoming less common in patients whereas cognitive symptoms and sensitivity to noise became more common (Chu et al., 2019). This adds another complexity when researching ME/CFS as patients have different clinical presentations at different time points.

1.1.6 Severity

ME/CFS patients can be categorised into four groups of severity based on the impact symptoms have on their ability to undertake activities of daily living (NICE, 2021). Patients who are able to care for themselves, undertake light domestic tasks and maintain work or education by stopping all leisure and social activities are classed as mild ME/CFS. Moderate ME/CFS patients have reduced mobility, are restricted in activities of daily living, unable to work or attend school, have poor quality sleep and require rest periods throughout the day. Severe ME/CFS patients are housebound, may be wheelchair dependent, unable to perform activities of daily living, suffer from severe cognitive difficulties and are extremely sensitive to light and sound. Very severe ME/CFS patients are bedbound and require full time care, sometimes needing to be tube fed. 25 % of ME/CFS patients are house- or bed-bound and fall into the severe and very severe ME/CFS categories (Pendergrast et al., 2016).

1.1.6.1 Measuring symptom severity

Symptom severity is an outcome often measured to determine whether patients have had a response to a clinical intervention (Kim et al., 2020). In addition, measuring symptom severity is also important for other research not involving clinical trials as correlations between symptom severity and biological alterations have been noted (Montoya et al., 2017). To date the most commonly used tools for measuring symptom outcome are the 36-item short form health survey (SF-36) which assesses functional impairment, and the checklist individual strength and Chalder fatigue questionnaire (CFQ) which both assess fatigue severity (Kim et al., 2020). However, these questionnaires are subjective as they are based on patient reported outcome measures, which are subject to inter-individual variability and ceiling effects (where more than 40 % of patients report the maximum score) (Haywood et al., 2012, Murdock et al., 2017). Another limitation is the use of patient reported outcome measures that were not specifically designed for use in ME/CFS patients. For example, the CFQ was not developed specifically for ME/CFS and consequently scores were unable to differentiate patients with ME/CFS from other illnesses with fatigue as a symptom such as multiple sclerosis, lupus and depression (Jason et al., 2011). However, the CFQ has been validated in ME/CFS and is a reliable measurement used to discriminate patients from controls (Jason et al., 2011). To overcome the aforementioned limitations, objective measures of symptom severity have now been developed and tested for ME/CFS, such as tracking physical activity and measuring oxygen consumption and saturation during exercise (van Campen et al., 2020b).

1.1.7 Comorbid illnesses

ME/CFS rarely occurs in isolation as more than 80 % of patients have at least one other illness (Castro-Marrero et al., 2017). There have been more than 30 recorded comorbid illnesses in ME/CFS patients which include autoimmune, cardiovascular, endocrine, GI, gynaecological, hematological, neurological, respiratory, rheumatological and psychological illnesses (Rowe et al., 2017). Interestingly, the aforementioned comorbid illnesses had a greater prevalence in ME/CFS patients than the general population (Chu et al., 2019).

Castro-Marrero et al. (2017) reported that the most common comorbid illness in ME/CFS patients was sicca syndrome, also known as Sjögren's syndrome, which is an autoimmune disease that affects fluid secretions in the body and presents as dry eyes and dry mouth. In contrast, Chu et al. (2019) grouped the prevalence of Sjögren's syndrome together with other autoimmune diseases (including Hashimoto's thyroiditis, coeliac disease, ulcerative colitis and multiple sclerosis) and found only 27 % of ME/CFS patients had a comorbid autoimmune disease. Discrepancies in the prevalence of comorbid illnesses across these two studies could have arisen due to the different use of ME/CFS case definitions in participant recruitment and also study design: Castro-Marrero et al. (2017) recorded the presence of comorbid illnesses following clinical assessment of all patients for all illnesses, whereas Chu et al. (2017) relied on previous diagnoses of the comorbid illnesses. Interestingly, the presence of comorbid illnesses was found to contribute to the subgrouping of ME/CFS patients (Castro-Marrero et al., 2017). To date studies analysing the prevalence of comorbid illnesses in ME/CFS patients have been retrospective. It would be interesting to perform prospective studies to determine whether these comorbid illnesses usually occur before, in parallel to, or following ME/CFS onset as it could provide valuable information for the aetiology of ME/CFS.

1.1.8 Treatment

There is currently no cure for ME/CFS. Instead, there are pharmacological and non-pharmacological treatments advised by the NHS for symptom management (NICE, 2021). These include management of sleep, physical functioning and mobility, orthostatic intolerance and pain. Chu et al. (2019) reported that over half of ME/CFS patients take medication for sleep, pain management and endocrine issues and 35 % take medication for GI disturbances such as pro- and pre- biotics, digestive enzymes and sodium bicarbonate. In addition, 36 % of patients take medication for anxiety, depression and general mental health.

The recent update of NICE guidelines in the diagnosis and management of ME/CFS has recognised that GET is of no benefit and is often harmful to patients, with a high proportion of patients experiencing relapses and symptom worsening following GET treatment which lasted months or years (McPhee et al., 2021, NICE, 2021). GET was an outdated approach based on theories that ME/CFS patients have reversible physiological changes due to deconditioning and exercise

avoidance (Bavinton et al., 2004). NICE have also updated their view on CBT and say that instead of being offered to patients as a treatment to instead offer it as a supportive therapy (NICE, 2021).

1.1.9 Course of illness

1.1.9.1 Onset

Many researchers propose that ME/CFS onset is initiated by an infectious disease (Blomberg et al., 2018, Underhill, 2015). The occurrence of ME/CFS outbreaks and sporadic cases across the world is suggestive of an infectious trigger (Acheson, 1959). However, a pathogen has not been identified that was associated with these outbreaks. Prospective studies following patients who had the acute viral infections Epstein-Barr virus (EBV) and Ross River virus (RRV) and the acute *Coxiella burnetii* bacterial infection found a subset of patients went on to develop ME/CFS (Hickie et al., 2006, Katz et al., 2009). In addition, a retrospective study found patients reported the following infections preceded ME/CFS onset, in order of decreasing prevalence: respiratory infection, non-specific infection presenting as fever, chills, sweats and muscle aches, GI infection and GU infection (Chu et al., 2019). This suggests the clinical end result of ME/CFS is triggered by more than one infectious disease. Interestingly, the SARS-CoV-2 pandemic has seen the emergence of a sister illness termed long COVID, with 16.8 % of long COVID patients fulfilling ME/CFS diagnostic criteria (Tokumasu et al., 2022).

Furthermore, only 64 % of patients reported an infectious trigger for the onset of ME/CFS (Chu et al., 2019). Other triggers of ME/CFS onset reported by patients include stress or a major life event, exposure to a chemical or environmental toxin, recent international or domestic travel, vaccination and surgery. This demonstrates the wide variety of events that preceded the onset of ME/CFS.

1.1.9.2 Prognosis

The prognosis for ME/CFS is poor, with less than 5 % of patients recovering their premorbid levels of activity and functioning (Chu et al., 2019). However, more than half of patients report fluctuations in the severity of illness, and a subset of patients experienced complete remission for more than one month. Events triggering relapses in ME/CFS were infectious illnesses and periods of stress. In addition, in females the menstrual cycle, pregnancy and menopause also exacerbated symptoms and could lead to relapses. More than half of females reported their monthly menstrual cycle negatively impacted their ME/CFS, and pregnancy and the menopause also impacted a significant proportion of females' ME/CFS. Interestingly, a follow up study 25 years after adolescents received an ME/CFS diagnosis found that 95 % of participants were no longer diagnosed with ME/CFS (Brown et al., 2012). However, they did not return to premorbid level of health as they were still significantly more impaired than healthy controls. This suggests that

ME/CFS has long term consequences on both patients who maintain a diagnosis and patients who improve to a point they no longer fit the ME/CFS diagnostic criteria.

1.1.10 A multisystemic disease

The pathophysiological changes that occur in ME/CFS patients affect multiple systems leading to immunological abnormalities, mitochondrial dysfunction and disturbances of GI, neurological, endocrine and metabolic systems (Missailidis et al., 2019). It is not known when these changes occur in the course of the illness, whether it is prior to or following the onset of ME/CFS (Nacul et al., 2020). Pathophysiology contributes to the heterogeneity of the disease as patients do not have dysfunction in all reported systems. This thesis focusses on pathophysiological changes in the immune system and GI system and how abnormalities in these two systems could be connected. The evidence for dysfunction in metabolism, mitochondria, the nervous system and the endocrine system are summarised in **Table 1.4**.

Table 1.4: A brief overview of the metabolic, mitochondrial, neurological and endocrine disturbances found in ME/CFS patients. *HPA = hypothalamic-pituitary-adrenal, RAAS = renin-angiotensin-aldosterone system, HPT = hypothalamic-pituitary-thyroid.*

Disturbance	Brief summary of key findings in ME/CFS patients	References
Metabolic	Blood metabolic disturbances in the following major biochemical pathways were found in more than one study: energy metabolism (e.g. amino acid metabolism, glycolysis), lipid metabolism, nucleotide metabolism and the urea pathway	(Germain et al., 2020, Germain et al., 2018, Nagy-Szakal et al., 2018, Germain et al., 2017, Yamano et al., 2016, Fluge et al., 2016, Armstrong et al., 2015, Armstrong et al., 2012, Jones et al., 2005)
	Urinary metabolite abnormalities, not consistent across studies	(Armstrong et al., 2015, Jones et al., 2005)
Mitochondrial	Lower mitochondrial membrane potential	(Mandarano et al., 2020, Missailidis et al., 2020)
	Lower proton leak	(Mandarano et al., 2020, Tomas et al., 2017)
	Greater proton leak	(Missailidis et al., 2020)
	Lower ATP production	(Mandarano et al., 2020, Tomas et al., 2017)
	Lowered complex V activation of ATP synthesis	(Missailidis et al., 2020)
	Lower respiratory reserve capacity	(Tomas et al., 2017)
	Greater respiratory reserve capacity	(Missailidis et al., 2020)
	Greater oxygen consumption rate	(Missailidis et al., 2020)
	Lower basal and maximal respiration	(Tomas et al., 2017)
	Lower levels of coenzyme Q10	(Castro-Marrero et al., 2013, Maes et al., 2009)

Table 1.4 continued

Disturbance	Brief summary of key findings in ME/CFS patients	References
Neurological	Reduced cerebral blood flow	(van Campen et al., 2020, van Campen et al., 2020a, van Campen et al., 2020c, van Campen et al., 2021, Yoshiuchi et al., 2006)
	Intracranial hypotension	(Bragée et al., 2020)
	Neuroinflammation	(Nakatomi et al., 2014)
	Reduced heart rate variability	(Escorihuela et al., 2020)
	Reduced serotonin receptors in different regions of the brain	(Cleare et al., 2005)
	Structural differences in the brain (reduction in grey matter volume, reduction in white matter volume and white matter atrophy)	(Okada et al., 2004, Shan et al., 2016, de Lange et al., 2004, Puri et al., 2012, Barnden et al., 2011, Barnden et al., 2015, Finkelmeyer et al., 2018, Shan et al., 2017)
	Altered electrical activity in the brain during sleep and wakefulness	(Decker et al., 2009, Le Bon et al., 2012, Sherlin et al., 2007, Zinn et al., 2016, Wu et al., 2016, Zinn et al., 2018, Flor-Henry et al., 2010)
	Altered functional connectivity between brain regions	(Boissoneault et al., 2018, Zinn et al., 2016, Kim et al., 2015, Boissoneault et al., 2016)
Endocrine	HPA axis disturbances (Hypocortisolism, hypo responsiveness to stimuli, elevated glucocorticoid negative feedback)	(Tak et al., 2011, Roberts et al., 2004, Jerjes et al., 2005, Gur et al., 2004, Demitrack et al., 1991, Scott et al., 1999, Scott et al., 1998, Dinan et al., 1997, Jerjes et al., 2007, Visser et al., 2001, Visser et al., 2000, Powell et al., 2013, Nijhof et al., 2014)
	RAAS system disturbances (lower renin activity, aldosterone and antidiuretic hormone)	(Miwa, 2017, Thomas et al., 2022)
	HPT axis disturbances (hypothyroidism)	(Ruiz-Núñez et al., 2018)

1.2 THE IMMUNE SYSTEM INVOLVEMENT IN ME/CFS

1.2.1 Impaired pathogen clearance

1.2.1.1 Impaired cell cytotoxicity

The most consistent finding of immune abnormalities in ME/CFS patients is reduced natural killer (NK) cell cytotoxicity (Eaton-Fitch et al., 2019). NK cells are part of the innate immune system and involved in removal of virus-infected cells and tumour cells (Vivier et al., 2008). $CD56^{dim}CD16^{+}$ NK cells are the main cytolytic NK cells making up 90 % of the NK cells in the peripheral blood. Reduced NK cell cytotoxicity in ME/CFS patients was not due to a reduced number of cytotoxic NK cells because the numbers of circulating $CD56^{dim}CD16^{+}$ NK cells does not vary between ME/CFS patients and controls (Brenu et al., 2010, Brenu et al., 2011, Huth et al., 2016a). Therefore, the $CD56^{dim}CD16^{+}$

NK cells must instead have functional impairment. NK cell cytotoxicity involves NK cell activation, granule polarisation, immune synapse formation and the release of cytotoxic granules (Krzewski and Coligan, 2012).

NK cell receptor and cell marker expression was assessed by multiple groups to determine the activation status of NK cells in ME/CFS patients. NK cells express activator receptors NKG2B, NKp46, NKp30 and NKp44 and signalling lymphocytic activation molecules which induce cytotoxic activity following target cell recognition (Chen et al., 2020). NK cells also express inhibitory killer-cell immunoglobulin-like receptors. NK cell phenotyping studies to determine the expression levels of the aforementioned receptors and cellular markers yielded conflicting results. Studies reported increased (Hardcastle et al., 2015c, Hardcastle et al., 2015a, Curriu et al., 2013), decreased (Hardcastle et al., 2015a, Hardcastle et al., 2015c, Rivas et al., 2018) and no significant differences (Huth et al., 2014, Brenu et al., 2014) in both activator and inhibitory receptor expression in ME/CFS patients. In addition, in ME/CFS patients increased expression of the activation marker CD69 (Curriu et al., 2013, Rivas et al., 2018) and increased expression of the maturation marker CD57 (Huth et al., 2016a) were reported. This suggests NK cells in ME/CFS patients are chronically activated. Indeed, chronic viral infections such as human herpesvirus have been reported in ME/CFS patients (Lee et al., 2021) which could contribute to the chronic activation of NK cells. In light of these findings the impaired NK cell cytotoxicity in ME/CFS patients appears not to be due to impaired NK cell activation.

There is evidence of impaired NK cell granule polarisation in ME/CFS patients. This process is dependent upon calcium (Ca^{2+}) ion mobilisation (Schwarz et al., 2013). The influx of Ca^{2+} through transient receptor potential melastatin (TRPM) ion channels and the expression of these ion channels have been investigated in ME/CFS patients. Reduced Ca^{2+} mobilisation was found in NK cells from ME/CFS patients (Nguyen et al., 2016a). In addition, impaired TRPM3 function (Cabanas et al., 2019, Cabanas et al., 2018), reduced surface expression of TRPM3 (Nguyen et al., 2016b) and TRPM2 overexpression (Balinas et al., 2019) was seen. Balinas et al. (2019) suggested TRPM2 overexpression on NK cells may be a compensatory mechanism for reduced Ca^{2+} mobilisation.

Cytotoxic granules contain perforin and granzymes (Prager and Watzl, 2019). Perforin forms pores in the membrane of target cells which facilitate the influx of granzymes which activate apoptosis of target cells. Therefore, a reduction in these cytolytic proteins could reduce NK cell cytotoxic activity. Indeed, decreased levels of granzyme B (Brenu et al., 2014, Huth et al., 2014), granzyme A (Brenu et al., 2011), granzyme K (Brenu et al., 2011) and perforin (Maher et al., 2005) have been observed in ME/CFS patients. However, this was not consistently found across studies, with the majority of studies reporting no significant differences (Brenu et al., 2014, Brenu et al., 2010, Brenu et al., 2011, Hardcastle et al., 2015a, Huth et al., 2016a, Huth et al., 2016b).

In addition, $CD8^+$ T cell cytotoxicity was also impaired in ME/CFS patients, as seen by a reduced percentage of lysed tumour cells incubated with $CD8^+$ T cells (Brenu et al., 2011). $CD8^+$ T cells, also known as cytotoxic T lymphocytes, are a part of the adaptive immune system and are involved in the clearance of intracellular pathogen infected cells and tumour cells (Zhang and Bevan, 2011). A reduction in granzyme A expression in the $CD8^+$ T cells from ME/CFS patients was seen which could be a possible mechanism for the reduced cytotoxic activity of $CD8^+$ T cells (Brenu et al., 2011).

In conclusion, impaired NK cells cytotoxicity and impaired $CD8^+$ T cells cytotoxicity by the aforementioned mechanisms could mean ME/CFS patients have impaired mechanisms to clear virally infected cells, enabling viral persistence.

1.2.1.2 Complement impairment

Another aspect of impaired pathogen clearance in ME/CFS patients involves complement activation. Complement can be activated by three pathways (classical, lectin and alternative pathways) and results in the opsonisation and lysis of pathogens (Dunkelberger and Song, 2010). Activation of the complement cascade via the classical pathway involves antigen-antibody immune complexes binding to C1q, C1r and C1s. Impairment in the classical pathway in ME/CFS patients is suggested as immunoglobulin (Ig)G1 and IgG3 deficiency occurs in a subset of ME/CFS patients (Guenther et al., 2015, Peterson et al., 1990). Indeed, when ME/CFS patients with IgG deficiency were treated with subcutaneous IgG therapy, the frequency and severity of infections reduced in 90 % of patients (Scheibenbogen et al., 2021).

In addition, deficiencies in the lectin pathway have been found in ME/CFS patients. Activation of the complement cascade via the lectin pathway involves the recognition of and binding to pathogen associated molecular patterns (PAMPS) by mannose-binding lectin (MBL) (Dunkelberger and Song, 2010). Studies analysing the MBL levels in ME/CFS patients found reduced levels (Guenther et al., 2015, Lutz et al., 2021). One study found 32 % of ME/CFS patients had reduced MBL levels and 7 % of patients fulfilled the criteria for MBL deficiency (Lutz et al., 2021). A second study found 12-15 % of ME/CFS patients had MBL deficiency (Guenther et al., 2015). MBL deficiency is known to cause susceptibility to infectious diseases (Hoeflich et al., 2009). Indeed 47-55 % of ME/CFS patients with MBL deficiency had increased susceptibility to upper and lower respiratory tract infections (Guenther et al., 2015). However, approximately 30 % of ME/CFS patients without MBL deficiency also had increased susceptibility to upper and lower respiratory tract infections.

1.2.2 Chronic inflammation

1.2.2.1 Circulating cytokines

Cytokines are cell signalling molecules which have immunomodulatory effects. Circulating cytokine levels in ME/CFS patients have been extensively analysed and provides evidence of low-level

chronic inflammation in patients, despite most studies yielding conflicting results. Elevated levels of interleukin (IL)-1, IL-6 and tumour necrosis factor (TNF)-α were reported in a number of studies and as these cytokines have pro-inflammatory effects authors concluded ME/CFS patients have chronic inflammation (Maes et al., 2012c, Maes et al., 2013, Maes et al., 2012d, Fletcher et al., 2009). However, Blundell et al. (2015) reported that IL-1, IL-6 and TNF-α were the most researched cytokines in ME/CFS patients and that 71-80 % of studies reported no significant differences in the levels of these cytokines. This systematic review reported the most consistent finding was elevated levels of transforming growth factor (TGF)-β in ME/CFS patients, found in 63 % of studies. In addition, Strawbridge et al. (2019) performed a meta-analysis of 42 studies which found elevated levels of TGF-β, TNF-α, IL-4 and IL-2 in ME/CFS patients compared to healthy controls. However, Blundell et al. (2015) rated 50 % of cytokine studies as poor quality because they failed to account for the following confounding variables of cytokine studies: age, activity level, gender, body mass index (BMI), menstrual cycle, psychiatric disorders and anti-depressants.

Inconsistent findings of cytokine abnormalities across studies could also reflect disease heterogeneity. Hardcastle et al. (2015b) grouped ME/CFS patients based on disease severity and identified cytokine differences between moderate and severe ME/CFS patients. Moderate ME/CFS patients had higher levels of IL-1B and regulated upon activation, normal cell expressed and presumably secreted (RANTES) and lower levels of IL-6 compared to severe ME/CFS patients. Severe ME/CFS patients had higher levels of interferon (IFN)-γ, IL-8 and IL-7 compared to moderate ME/CFS patients. In addition, another study found the levels of 13 proinflammatory cytokines, including IFN-γ, IL-7 and IL-8, had a positive correlation with disease severity (Montoya et al., 2017). These findings suggests that the level of chronic inflammation could determine disease severity.

The correlation of cytokine levels with symptom severity has also been investigated. Jonsjö et al. (2020) found a positive correlation between the severity of PEM and beta-nerve growth factor (β-NGF) levels. β-NGF also positively correlated with the severity of impaired cognitive processing, as well as CC motif chemokine ligand 11 (CCL11). In addition, β-NGF, IL-7 and TGF-β positively correlated with severity of musculoskeletal pain. The severity of flu-like symptoms correlated with the level of TNF-α, which was also confirmed in other studies (Maes et al., 2012c, Maes et al., 2012d). In contrast, conflicting cytokines were correlated with fatigue severity in different studies. Jonsjö et al. (2020) found levels of β-NGF correlated with levels of fatigue whereas Maes et al. (2012c, 2012d) found the levels of IL-1 and TNF-α correlated with levels of fatigue. Finally, poorer sleep quality correlated with higher levels of proinflammatory cytokines IL-1β, IL-6 and TNF-α (Milrad et al., 2017). However, elevated levels of circulating TNF-α and IL-6 occur as a consequence of sleep deprivation (Irwin et al., 2006).

Horning et al. (2015) demonstrated that stratifying ME/CFS patients based on illness duration identifies further cytokine abnormalities. When comparing unstratified ME/CFS patients to controls, decreased levels of anti-inflammatory cytokines (IL-10 and colony-stimulating factor 1 (CSF1)) as well as decreased levels of pro-inflammatory cytokines (IL-17A, IL-8, IL-6, TNF-β, interferon gamma-induced protein 10 (IP-10) and soluble Fas ligand (sFasL)) were found. When ME/CFS patients were stratified into short illness duration (up to three years) and long illness duration (over three years) additional cytokine abnormalities were identified. ME/CFS patients with short illness duration had elevated levels of IFN-γ and IL-12p40 and depleted levels of TNF-α, granulocyte-macrophage colony-stimulating factor (GM-CSF) and IL-12p70. In addition, more than half of the measured cytokines were elevated in short illness duration but depleted in long illness duration.

1.2.2.2 T cells

The differentiation of naïve $CD4^+$ T cells into T helper (Th) cell subsets following T cell receptor (TCR) stimulation is influenced by cytokines (**Figure 1.2**) (Jiang and Dong, 2013). In addition, different Th cell subsets produce different cytokines. As mentioned in **section 1.2.2.1** the most consistent finding is elevated TGF-β in ME/CFS patients. Elevated TGF-β levels could lead to the polarisation of naïve $CD4^+$ T cells into either regulatory T cells (Tregs) or Th17 cells, suggesting ME/CFS patients may have elevated levels of circulating Tregs and Th17 cells. The percentage of $FOXP3^+$ Tregs in the $CD4^+$ T cells population was found to be both increased (Brenu et al., 2011) and decreased (Rivas et al., 2018) in ME/CFS patients compared to healthy controls. Another study found no significant difference in the percentage of $CD4^+$ T cells producing IL-10 between ME/CFS patients and healthy controls (Skowera et al., 2004). Instead, they found an increased proportion of IL-4 and IFN-γ producing $CD4^+$ T cells in ME/CFS patients. Following polyclonal activation of $CD4^+$ T cells the proportion of IL-4, but not IFN-γ producing $CD4^+$ T cells, was higher in ME/CFS patients compared to controls. In contrast, another study measured the concentration of cytokines produced by $CD4^+$ T cells following activation of the TCR and found elevated levels of both anti-inflammatory (IL-10) and proinflammatory (IFN-γ and TNF-α) cytokines produced by ME/CFS patients' $CD4^+$ T cells (Brenu et al., 2011). Therefore, the contribution of $CD4^+$ T cells to chronic inflammation in ME/CFS patients is not clear.

Like naïve $CD4^+$ T cells, the differentiation of naïve $CD8^+$ T cells into effector cell (Tc) subsets is influenced by the cytokine environment (St. Paul and Ohashi, 2020) (**Figure 1.3**). The percentage of $CD8^+$ T cells producing IL-4, IL-10 and IFN-γ were higher in ME/CFS patients than healthy controls which reflects higher levels of Tc1, Tc2 and $CD8^+$ regulatory T cells (Skowera et al., 2004). Whereas only the percentage of activated $CD8^+$ T cells producing IL-4 was higher in ME/CFS patients than healthy controls.

Therefore, the contribution of T cells to the maintenance of chronic inflammation in ME/CFS patients is controversial as T cells producing both pro- and anti-inflammatory cytokines are elevated.

1.2.2.3 Inflammatory markers

In addition to cytokines there are other inflammatory markers in the blood, including C-reactive protein (CRP), polymorphonuclear (PMN) elastase and lysozyme. CRP is an acute phase protein secreted by the liver following detection of inflammatory cytokines (Du Clos, 2000). Levels of circulating CRP in ME/CFS patients has been investigated and found to be higher in ME/CFS patients compared to healthy controls (Groeger et al., 2013, Spence et al., 2008, Sulheim et al., 2014). High sensitivity CRP (hsCRP) has also been measured, with elevated levels seen in ME/CFS patients (Groven et al., 2019) and no differences between ME/CFS patients and healthy controls also found (Giloteaux et al., 2016a, Ruiz-Núñez et al., 2018). Another study found ME/CFS patients had significantly higher plasma hsCRP before, but not after, adjustment for confounding variables such as age, gender, race, geographical location and BMI (Raison et al., 2009).

PMN elastase is a protease secreted by neutrophils during inflammation and lysozyme is a marker for monocyte/macrophage activity in inflammation and both proteins have been found to be elevated in ME/CFS patients (Maes et al., 2012c). In addition, levels of PMN elastase positively correlated with disease severity and flu-like malaise.

1.2.2.4 Inflammation in the central nervous system

Evidence for neuroinflammation in ME/CFS has been found using positron emission tomography (PET) scans of the brain (Nakatomi et al., 2014). Cytokines in cerebrospinal fluid (CSF) have also been assessed to confirm inflammation in the central nervous system (CNS). Peterson et al. (2015) investigated the levels of 27 cytokines in the CSF of 18 ME/CFS patients and 5 healthy controls and found patients had significantly lower levels of IL-10. Hornig et al. (2016) investigated 51 cytokines in the CSF in a larger cohort comprising 32 ME/CFS patients and 19 healthy controls. They found that as well as IL-10, 19 other cytokines were also significantly lower in ME/CFS patients compared to controls. These included both pro- and anti-inflammatory cytokines. In addition, two pro-inflammatory chemokines were elevated in ME/CFS patients.

In addition, Hornig et al. (2017) compared cytokine abnormalities in the CSF of classical ME/CFS patients to atypical ME/CFS patients. They classified classical ME/CFS as patients with acute onset of illness following an infection. Atypical ME/CFS was classified as patients with less common modes of onset and who also experienced subsequent onset of co-morbidities such as seizures, atypical multiple sclerosis, cancer, autoimmune disorders and inflammatory disorders. They found classical ME/CFS patients had higher levels of CSF IL-17A and CXCL9 compared to atypical ME/CFS patients.

This demonstrates that ME/CFS patients with different illness onset have different pathophysiology.

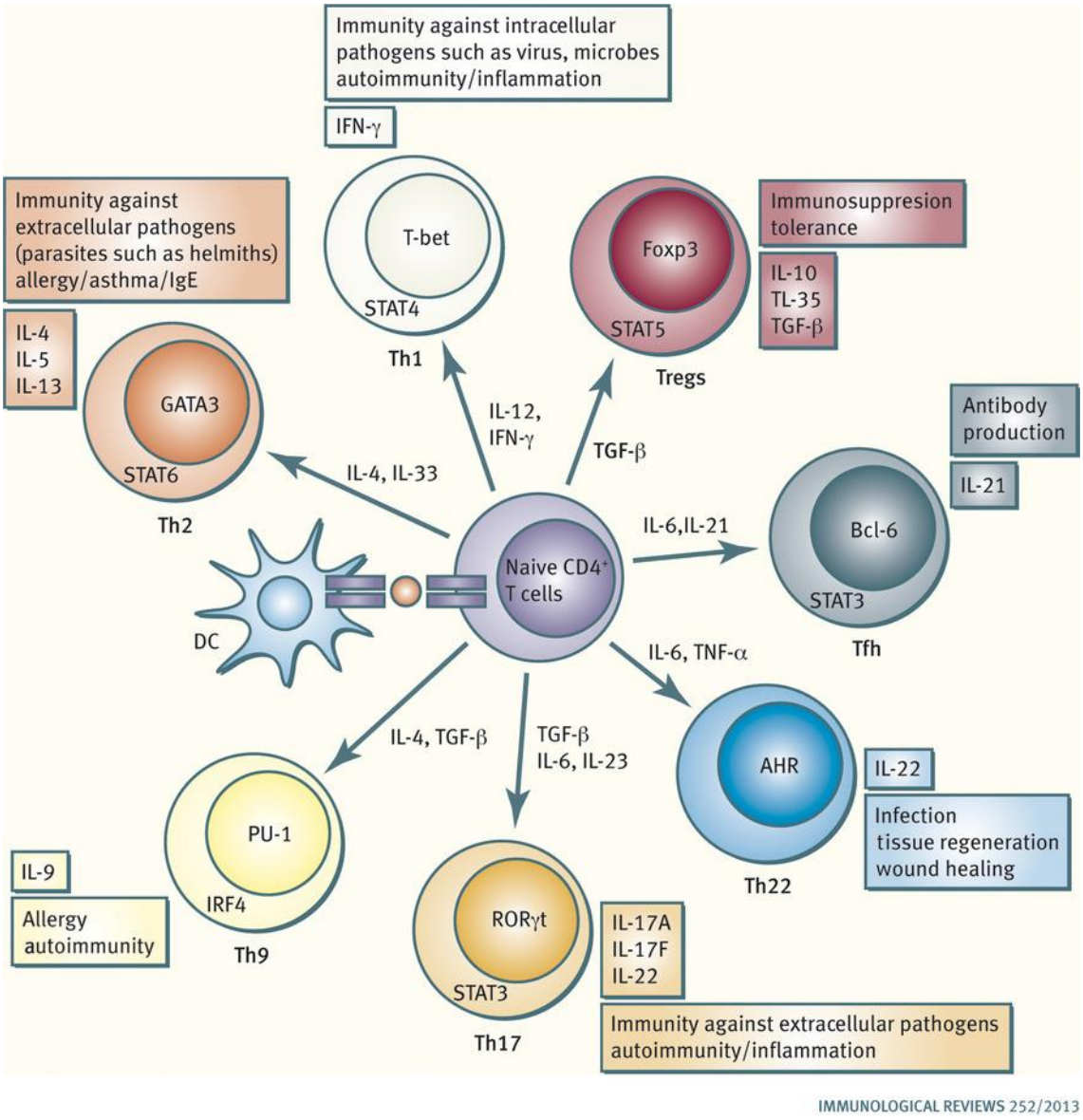

Figure 1.2: The polarisation of naïve CD4⁺ T cells into T helper subsets and their subsequent functions. *Upon activation of their T cell receptor, naïve CD4⁺ T cells differentiate into Th1, Th2, Th9, Th17, Th22, Tfh or Tregs. Cytokines within the environment at the time of activation determine the subset CD4⁺ T cells are polarised into. The Th1, Th2, Th9, Th17, Th22, Tfh and Tregs cell subsets are characterised by their transcription factor and the combination of cytokines they produce. Each CD4⁺ T cell subset has a distinct function in adaptive immunity. Tfh = follicular T-helper cells, Tregs = CD4⁺ regulatory T cells. This figure was sourced from Jiang and Dong (2013).*

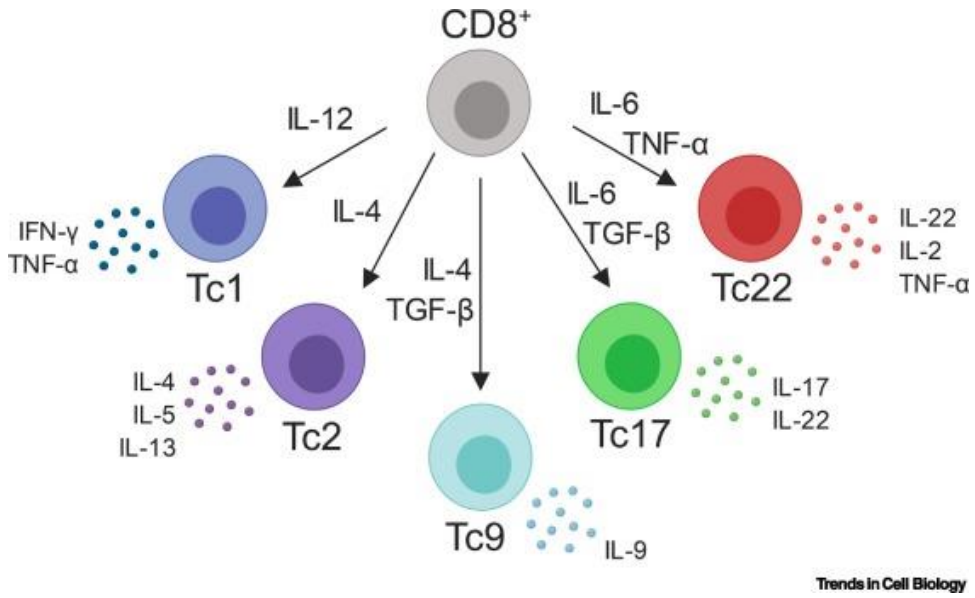

Figure 1.3: The polarisation of naïve CD8⁺ T cells into effector CD8⁺ T cell subsets. *Upon activation naïve CD8⁺ T cells differentiate into Tc1, Tc2, Tc9, Tc17, Tc22 and regulatory CD8⁺ T cells (not shown). Environmental cytokines determine the subset CD8⁺ T cells differentiate into. Each effector CD8⁺ T cell subset produces a distinct combination of cytokines which aid identification of each cell subset. This figure was sourced from St. Paul and Ohashi (2020).*

1.2.3 Autoimmunity

1.2.3.1 Autoantibodies in ME/CFS

In an autoimmune disease there is a loss of self-tolerance and the generation of autoreactive T and B cells and autoantibodies. Multiple research groups have investigated the presence of autoantibodies in ME/CFS patients to provide evidence of an autoimmune component to the disease. Loebel et al. (2016) measured the levels of serum IgG antibodies to human α and β adrenergic receptors (AdR), muscarinic 1-5 acetylcholine receptors (aChR), endothelin receptors, dopamine receptors, serotonin receptors, angiotensin receptors, thyreoperoxidase (TPO)/ thyreoglobulin (TG) and anti-nuclear antibodies (ANA). They found ME/CFS patients had significantly higher levels of autoantibodies to β2-AdR, M3/4-aChR, TPO/TG and ANA. Similarly, Bynke et al. (2020) measured the levels of IgG antibodies to α1/2 AdR, β1-3 AdR and M1-5 aChR in two cohorts of ME/CFS patients. One ME/CFS cohort had elevated IgG antibodies to β1/2 AdR and M3/4 AChR whereas the second ME/CFS cohort just had elevated IgG antibodies to M3/4 AChR only. Abnormal levels of autoantibodies to AdR and aChR occurred more frequently in ME/CFS patients (79-91 %) compared to controls (29.5 %) (Bynke et al., 2020). In addition, anti-pituitary antibodies (APA) and anti-hypothalamic antibodies (AHA) were present in 56 % and 33 % of ME/CFS patients, respectively, and absent in controls (De Bellis et al., 2021). This suggests that autoimmunity is present only in a subset of ME/CFS patients. Blomberg et al. (2018) proposed that autoimmunity in ME/CFS patients developed following an infectious trigger seen at the time of onset. As only a proportion of ME/CFS patients have an infectious disease prior to the onset of ME/CFS it suggests that in patients without an infectious onset the pathophysiology does not involve autoimmunity. However, a recent study found no significant difference between the level of autoantibodies in ME/CFS patients with infectious onset compared to ME/CFS patients without infectious onset (Freitag et al., 2021). Alternatively, the chronic inflammation seen in a subset of ME/CFS patients (detailed in **section 1.2.2**) could promote the development of autoimmunity. Indeed, in ME/CFS patients with serotonin autoantibodies there were significantly higher levels of IL-1, TNF-α and neopterin, compared to ME/CFS patients without serotonin autoantibodies (Maes et al., 2013).

Maes et al. (2012a) investigated whether autoantibodies contribute to the pathophysiology of ME/CFS. They compared the levels of IgM antibodies to anchorage molecules (palmitic acid, myristic acid, 5-farnesyl-L-cysteine), acetylcholine, NO adducts (NO-tyrosine, NO-phenylalanine, NO-aspartate, NO-histidine and NO-creatine) and oxidatively modified anchorage molecules (palmitic acid and myristic acid) between ME/CFS patients, chronic fatigue patients, major depressive disorder (MDD) patients and healthy controls. Although all IgM antibodies were higher in ME/CFS patients than healthy controls, only IgM antibodies to anchorage molecules, NO-

phenylalanine and oxidatively modified neoepitopes were significantly higher in ME/CFS patients than MDD patients. The severity of physio-somatic symptoms (aches and pains, muscular tension, fatigue, neurocognitive difficulties, IBS and flu-like malaise), but not depressive symptoms (sadness, irritability, sleep disturbances and autonomic symptoms), correlated with elevated IgM to self and neo-epitopes. Another study found the severity of fatigue and other somatic symptoms in ME/CFS patients with infectious onset also correlated with levels of IgG antibodies to neuropeptide and hormone receptors (Freitag et al., 2021).

For an autoantibody to contribute to symptom severity it needs to have functional consequences. Autoantibodies can induce pathology through the following mechanisms: agnostic or antagonistic effects on receptors or enzymes, cause direct cell lysis or induce inflammation (Ludwig et al., 2017). The functional consequence of AHA and APA in ME/CFS patients was investigated by measuring the levels of circulating hormones produced by the hypothalamic-pituitary-adrenal (HPA) axis (De Bellis et al., 2021). ME/CFS patients with high levels of AHA and/or APA had lower levels of adrenocorticotropin/cortisol and growth hormone peak/insulin-like growth factor-1 than patients without AHA or APA. Therefore, AHA and APA could contribute to the dysfunctional HPA-axis reported in ME/CFS patients. In addition, antibodies to β1/2-AdR also correlated with structural alterations in the brain of ME/CFS patients (Fujii et al., 2020). This suggests that these autoantibodies could bind to β1/2-AdR in the brain and cause damage.

1.2.3.2 Effectiveness of autoimmune therapies in ME/CFS

Evidence for a link between autoantibodies and ME/CFS symptom manifestation suggests therapeutic interventions aimed to reduce the level of autoantibodies could be of benefit. Rituximab is a monoclonal anti-CD20 antibody which depletes B cell numbers. Clinical trials of Rituximab therapy in ME/CFS began following evidence of clinical improvement in three patients (Fluge and Mella, 2009). The first clinical trial undertaken was a randomised placebo-controlled phase II study (Fluge et al., 2011). In 67 % of patients an overall clinical response to Rituximab treatment emerged 2 months following infusions. A second open-label phase II clinical trial reported 62 % of patients had an overall clinical response (Fluge et al., 2015). Again, this trial reported a lag phase following treatment during which no clinical improvement was seen. The lag phase in patients with a major response was shorter than the lag phase in patients with a moderate response, being an average of 23 and 53 weeks respectively. In both trials the level of circulating B cells depleted one month following treatment, regardless of a clinical response. The authors hypothesised that the delay in response could be due to the presence of long-lived autoantibodies. Indeed, clinical response was linked to the depletion of autoantibodies to β2-AdR and M3/4 AChR following treatment (Loebel et al., 2016). However, when Rituximab was trialled in a larger cohort of ME/CFS patients during a randomised, double-blind, placebo-controlled phase III study there

were negative findings (Fluge et al., 2019). A clinical response was seen in 35.1 % of the placebo group but only 26 % of the rituximab group. This halted all further clinical trials of Rituximab therapy in ME/CFS patients. The authors noted that rituximab therapy is not suitable for the treatment of all autoimmune diseases. Therefore, the negative findings of Rituximab as a treatment for ME/CFS does not disprove an autoimmune component in the disease.

An alternative therapy for reducing autoantibody levels is immunoadsorption. This therapy selectively removes IgG from the blood. A pilot study in ME/CFS showed that immunoadsorption significantly reduced the levels of β1/2 AdR autoantibodies 6 months after treatment, but M3/4 AChR autoantibodies were not significantly different from pre-treatment levels (Scheibenbogen et al., 2018). Despite only reducing the levels of some, but not all, IgG autoantibodies 7/10 patients had a rapid improvement of symptoms during immunoadsorption, with 3 patients sustaining symptom improvement for more than 12 months. Placebo-controlled trials of immunoadsorption need to be undertaken before clinical response in ME/CFS patients due to the treatment can be confirmed.

1.3 INTESTINAL ORIGIN OF ME/CFS

1.3.1 Microbiome

1.3.1.1 Overview

The GI tract harbours approximately 100 trillion microbes which together with their genetic material form the intestinal microbiome (Rinninella et al., 2019). The intestinal microbiome contributes to human health by aiding digestion of food (Oliphant and Allen-Vercoe, 2019), inducing tolerance to food (Tordesillas and Berin, 2018), contributing to the development of the immune system (Gensollen et al., 2016) and providing protection against pathogen colonisation of the GI tract (Pickard et al., 2017). However, an altered intestinal microbiome and a reduction in microbial diversity, referred to as dysbiosis, can initiate or propagate disease (DeGruttola et al., 2016). Microbial dysbiosis is seen in both intestinal diseases such as Crohn's disease (CD) (Pascal et al., 2017) and IBS (Wang et al., 2020) and extraintestinal diseases such as multiple sclerosis (MS) (Noto and Miyake, 2022) and depression (Sanada et al., 2020).

1.3.1.2 Alterations in the ME/CFS intestinal microbiome

Microbial dysbiosis is also seen in ME/CFS with patients having reduced microbial diversity in their stool samples (Giloteaux et al., 2016a). In addition, several studies used sequencing technologies to investigate the bacterial composition of the intestinal microbiome in ME/CFS patients and provided evidence for bacterial dysbiosis (König et al., 2021). However, only a small number of significant findings were replicated in more than one study (**Table 1.5**). Only two studies analysed microbiome changes at the family-level and the relative abundance of Lachnospiraceae was

depleted in ME/CFS patients compared to healthy controls in both studies (Lupo et al., 2021, Nagy-Szakal et al., 2017). In contrast, microbiome changes at the genus-level were analysed in all seven studies. The most remarkable finding was a depletion in the relative abundance of *Faecalibacterium* replicated in five studies (Giloteaux et al., 2016a, Guo et al., 2021, Kitami et al., 2020, Lupo et al., 2021, Nagy-Szakal et al., 2017). In addition, *Faecalibacterium prausnitzii* was depleted in two studies (Guo et al., 2021, Nagy-Szakal et al., 2017). *F. prausnitzii* is important in GI health as it produces anti-inflammatory metabolites (Ferreira-Halder et al., 2017). A reduction in *F. prausnitzii* is also seen in other diseases, such as CD (Björkqvist et al., 2019). Therefore, a reduction in *F. prausnitzii* could contribute to the initiation or propagation of intestinal inflammation. In addition, the enrichment of *Coprobacillus* was found in four studies (Giloteaux et al., 2016a, Kitami et al., 2020, Lupo et al., 2021, Nagy-Szakal et al., 2017). This could also contribute to the initiation or propagation of intestinal inflammation as elevated *Coprobacillus* is associated with a high fat diet in mice and intestinal inflammation (Terzo et al., 2020, Wang et al., 2018).

Despite four studies analysing microbiome changes at the species-level, significant differences were not replicated in more than two studies. An enrichment of *Ruminococcus torques* (Nagy-Szakal et al., 2017, Raijmakers et al., 2020) and *Ruminococcus bromii* (Lupo et al., 2021, Raijmakers et al., 2020) and a depletion of *Alistipes putredinis* (Nagy-Szakal et al., 2017, Raijmakers et al., 2020) *Eubacterium rectale* (Guo et al., 2021, Nagy-Szakal et al., 2017) and *Faecalibacterium prausnitzii* (Guo et al., 2021, Nagy-Szakal et al., 2017) in ME/CFS patients were found. However, Raijmakers et al. (2020) found an enrichment of *E. rectale* and *F. prausnitzii* in ME/CFS patients reducing certainty of these findings. Newberry et al. (2018) explained that these discrepancies could be caused by both methodological restrictions (differing sequencing depth, the use of different sequencing platforms and bioinformatics pipelines) and study design (small sample sizes, different diagnostic criteria, patient selection criteria, and choice of control).

Furthermore, relative microbiome profiling (RMP) using shotgun metagenomic and 16S ribosomal ribonucleic acid (rRNA) sequencing is limited in its interpretation of microbial composition because the relative abundance of one taxon is affected by the relative abundance of other taxa present within the microbial community and is therefore not strictly quantitative (Vandeputte et al., 2017, Galazzo et al., 2020). In addition, relative abundances do not account for microbial load. Whereas quantitative microbiome profiling (QMP) is not constrained by the aforementioned factors and is subsequently gaining interest. QMP involves the conversion of relative abundances to counts using microbial loads (quantified using quantitative polymerase chain reaction (q-PCR) or flow cytometry enumeration). To date, QMP on ME/CFS patients has only been performed in one study which used q-PCR and found increased total bacteria in stool from ME/CFS patients and lower quantities of

Roseburia, *Eubacterium* and *F. prausnitzii* (Guo et al., 2021). These findings need to be confirmed in future studies.

Table 1.5: Compilation of previously reported significant alterations in the intestinal microbiome of ME/CFS patients. *Upward arrows indicate taxa whose relative abundance was significantly higher in ME/CFS patients compared to controls and downward arrows indicate taxa whose relative abundance was significantly lower in ME/CFS patients compared to controls. Taxa with the same alterations reported in two or more papers were highlighted in grey.*

Taxa	Fremont et al. (2013)	Giloteaux et al. (2016a)	Nagy-Szakal et al. (2017)	Raijmakers et al. (2020)	Kitami et al. (2020)	Lupo et al. (2021)	Guo et al. (2021)
Phylum							
Bacteroidetes						↑	
Class							
Bacteroidia						↑	
Clostridia						↓	
Order							
Bacteroidales						↑	
Clostridiales						↓	
Pasteruellales			↓				
Pseudomonadales			↑				
Family							
Bacteroidaceae						↑	
Barnesiellaceae						↑	
Clostridiaceae			↑				
Lachnospiraceae			↓			↓	
Pasteruellaceae			↓				
Pseudomonadaceae			↑				
unclassified Bacillales			↓				
Genus							
Aggregatibacter		↓					
Alistipes							
Anaerostipes			↑			↓	
Anaerotruncus		↑					
Asaccharobacter							
Atopobium		↓					
Bacteroides						↑	
Bifidobacterium		↓					
Blauti					↑	↑	
Clostridium		↓	↑				
Collinsella		↓			↓	↓	
Coprobacillus		↑	↑		↑	↑	
Coprococcus			↓				

Table 1.5 continued

Taxa	Fremont et al. (2013)	Giloteaux et al. (2016a)	Nagy-Szakal et al. (2017)	Raijmakers et al. (2020)	Kitami et al. (2020)	Lupo et al. (2021)	Guo et al. (2021)
Genus							
Dialister							
Dorea			↓				↓
Eggerthella		↑			↑	↑	
Eubacterium							↓
Faecalibacterium		↓	↓		↓	↓	↓
Fusicatenibacter							↓
Gemella			↓				
Gemmiger							↓
Haemophilus		↓	↓				
Holdemania							
Lachnoclostridium							↑
Lachnospira					↓	↓	
Lactococcus		↑					
Lactonifactor	↑						
Marvynbryantia			↑				
Odoribacter			↓				
Oscillospira		↑					
Peptococcus		↓					
Phascolarctobacterium						↑	
Pseudoflavonifractor			↑				
Pseudomonas			↑				
Roseburia			↓				↓
Ruminococcus		↓					
Suturella		↓					
Syntrophococcus							
Unclassified Bacteria		↓					
Unclassified Clostridiaceae		↓					
Unclassified Clostridiales		↓					
Unclassified Coriobacteriaceae		↓					
Unclassified Dehalobacteriaceae		↑					
Unclassified ML615J-28		↓					
Unclassified Mogibacteriaceae		↓					
Unclassified Ruminococcaceae		↓					
Species							
Alistipes finegoldii				↓			
Alistipes indistinctus				↓			

Table 1.5 continued

Taxa	Fremont et al. (2013)	Giloteaux et al. (2016a)	Nagy-Szakal et al. (2017)	Raijmakers et al. (2020)	Kitami et al. (2020)	Lupo et al. (2021)	Guo et al. (2021)
Species							
Alistipes onderdonkii				↓			
Alistipes putredinis			↓	↓			
Alistipes shahii				↓			
Alistipes sp AP11				↓			
Alistipes unclassified				↓			
Anaerostipes caccae			↑				
Bacterioidales bacterium ph8				↓			
Bacteroides cellulosilyticus				↓			
Bacteroides massiliensis				↓			
Bacteroides ovatus				↓		↑	
Bacteroides stercoris				↓			
Bacteroides uniformis				↓		↑	
Bifidobacterium adolescentis				↑			
Bifidobacterium bifidum				↑			
Bifidobacterium longum				↑			
Bilophila unclassified				↓			
Clostridium asparagiforme			↑				
Clostridium bolteae			↑				
Clostridium scindens			↑				
Clostridium symbiosum			↑				
Collinsella aerofaciens				↑			
Coprobacillus bacterium			↑				
Coprococcus catus			↓				
Coprococcus comes				↑			
Coprococcus sp ART55 1				↑			
Dorea formicigenerans			↓	↑			
Dorea longicatena			↓	↑			
Eubacterium biforme				↑			
Eubacterium hallii			↓	↑			
Eubacterium rectale			↓	↑			↓
Eubacterium ventriosum			↓				
Faecalibacterium cf			↓				
Faecalibacterium prausnitzii			↓	↑			↓

Table 1.5 continued

Taxa	Fremont et al. (2013)	Giloteaux et al. (2016a)	Nagy-Szakal et al. (2017)	Raijmakers et al. (2020)	Kitami et al. (2020)	Lupo et al. (2021)	Guo et al. (2021)
Species							
Fusicatenibacter saccharivorans							↓
Gemminger formicilis							↓
Haemophilus parainfluenzae			↓				
Lachnospiraceae bacterium 1 1 57FAA				↑			
Marvynbryantia formatexigens			↑				
Methanobrevibacter smithii				↓			
Odoribacter splanchnicus			↓				
Oscillibacter unclassified				↓			
Parabacteroides distasonis			↓				
Parabacteroides merdea			↓				
Paraprevotella unclassified				↓			
Pseudoflavonifractor capillosus			↑				
Roseburia inulivorans			↓	↑			
Ruminococcus bromii				↑		↑	
Ruminococcus gnavus			↑				
Ruminococcus lactaris				↑			
Ruminococcus obeum			↓	↑			
Ruminococcus sp 5 1 30BFAA				↑			
Ruminococcus torques			↑	↑			
Streptococcus thermophilus				↑			
Sutterella wadsworthensis				↓			
unclassified Alistipes			↑				
unclassified Bacteroides			↑				
unclassified Dorea			↑				
unclassified Faecalibacterium			↓				

1.3.1.3 Geographical location affects microbiome biomarkers for ME/CFS

The composition of the microbiome is affected by environmental factors such as diet (Redondo-Useros et al., 2020), geography (Conlon and Bird, 2014) and genetics (Goodrich et al., 2014). Lupo et al. (2021) demonstrated the importance of accounting for environment induced microbiome changes in ME/CFS microbiome studies through the use of internal (relatives of the patient) and external controls. Comparing ME/CFS patients to internal controls reduced the number of taxa found to be differentially abundant between patients and external controls. For example, at the genus-level the abundance of *Bacteroides, Anaerostipes* and *Phascolarctobacterium* were significantly different between ME/CFS patients and external controls, but only *Bacteroides* and *Anaerostipes* were significantly different between ME/CFS patients and internal controls. In addition, the utilisation of internal controls also enabled the identification of ME/CFS associated microbiome changes that were masked by environmental differences.

Another study recruited ME/CFS patients and healthy controls from Norway and Belgium and demonstrated the composition of stool microbiome differed both regionally and in disease (Frémont et al., 2013). In the Belgian population stool samples from ME/CFS patients had an enrichment of *Lactonifactor* and a depletion of *Asaccharobacter*. Whereas in the Norwegian population ME/CFS patients had enriched *Alistipes* and *Lactonifactor* and a depletion of *Holdemania, Roseburia* and *Syntrophococcus*. Only an enrichment of *Lactonifactor* was found in both geographical locations which could suggest a pivotal role of this microbe in ME/CFS. However, enrichment of *Lactonifactor* was not found in any other microbiome study in ME/CFS patients (**Table 1.5**).

1.3.1.4 Comorbid IBS affects microbiome biomarkers for ME/CFS

Gastrointestinal disturbances, such as IBS, affect 38 % of ME/CFS patients (Chu et al., 2019). IBS patients have alterations in their intestinal microbiome, with small intestinal bacterial overgrowth (SIBO) occurring in patients with diarrhoea predominant IBS (IBS-D) and increased abundance of the archaea *Methanobrevibacter smithii* in patients with constipation predominant IBS (IBS-C) (Pimentel and Lembo, 2020). This suggests ME/CFS patients with co-morbid IBS may have different microbiome alterations to those ME/CFS patients without co-morbid IBS.

Indeed, Nagy-Szakal et al. (2017) demonstrated the importance of stratifying the ME/CFS patient population into those with and those without IBS as this enabled microbial differences found within the unstratified ME/CFS patient population to be assigned to IBS comorbidity or ME/CFS. When comparing the unstratified ME/CFS patient population to healthy controls 23 bacterial species were differentially abundant. 7 of these were associated with IBS comorbidity as they were only seen when comparing ME/CFS patients with comorbid IBS to controls but not when comparing ME/CFS

patients without co-morbid IBS to controls. 12 bacterial species were associated with the disease itself as they were seen in both the ME/CFS cohort with and without comorbid IBS.

In contrast, Guo et al. (2021) did not find the stratification of ME/CFS patients into those with and those without comorbid IBS aided the discovery of additional bacterial species differentially abundant in ME/CFS. Instead, *Faecalibacterium prausnitzii* and *Eubacterium rectale* were the only two bacterial species differentially abundant in the unstratified ME/CFS cohort and they were also the only two bacterial species differentially abundant when comparing ME/CFS patients without comorbid IBS to controls. These bacterial species were also depleted in the ME/CFS with IBS cohort, along with 13 other microbial changes. Whereas Nagy-Szakal et al. (2017) only found a depletion of *E. rectale* in the unstratified ME/CFS cohort and found a depletion of *F. prausnitzii* in the unstratified ME/CFS cohort and the ME/CFS with IBS cohort, but not the ME/CFS without IBS cohort.

1.3.1.5 The neglected components of the intestinal microbiome

Thus far the bacterial composition of the intestinal microbiome in ME/CFS patients has been discussed. However, the intestinal microbiome is also inhabited by both viruses and eukaryotes (Rinninella et al., 2019). Viruses outnumber bacterial cells in the intestine by 10:1 (Mukhopadhya et al., 2019). Despite the abundance of viruses in the intestine, virome research is still in its infancy due to laboratory and computational limitations hindering its characterisation. In addition, microbiome studies have overlooked eukaryotes because of their low genetic content within stool samples (Qin et al., 2010). Recent technological advances and evidence of eukaryome involvement in health and disease has meant these components of the microbiome are gaining traction (Khan Mirzaei et al., 2021, Tiew et al., 2020). Given reports of the onset of ME/CFS following enteroviral and eukaryotic infections in some patients, investigation of the virome and eukaryome in ME/CFS patients is of interest (Mørch et al., 2013, O'Neal and Hanson, 2021).

To date, a limited number of studies have investigated the intestinal virome of ME/CFS patients. One study investigated alterations of eukaryotic viruses in intestinal biopsies and found an increased abundance and frequency of *Parvovirus B19* (Frémont et al., 2009). Another study investigated the relative abundance of bacteriophages in a pair of monozygotic twins, one with and one without ME/CFS, and found an increased relative abundance of Siphoviridae and Myoviridae in stool samples (Giloteaux et al., 2016b). However, the former study did not report statistical measures and the latter study's sample size was not large enough to perform statistical tests and therefore conclusions from these studies are limited.

The mycobiome in ME/CFS patients is also poorly characterised. One study using a culture-based technique identified an increased abundance of *Candida albicans* in the faecal samples of ME/CFS patients during the acute phase of the disease compared to when that patient was in remission

(Evengård et al., 2007). Interestingly, *C. albicans* was also elevated in the active phase in CD patients, but not in those who were in remission (Qiu et al., 2020). Another study used 18S rRNA marker gene sequencing to investigate the composition of eukaryotes in stool samples from ME/CFS patients (Mandarano et al., 2018). They found a non-significant increase in the ratio of Basidiomycota to Ascomycota in ME/CFS patients, which was also found in the CD patients (Li et al., 2014).

1.3.1.6 Microbiome targeted therapeutic interventions

Therapeutic interventions aiming to reverse intestinal microbial dysbiosis, referred to as bacteriotherapy, have been trialled in ME/CFS patients. Bacteriotherapy's include probiotics, prebiotics and faecal microbe transplantation (FMT). Probiotics are defined by the Food and Agriculture Organization of the United Nations (FAO) and the WHO as "live microorganisms which when administered in adequate amounts confer a health benefit on the host" (Hill et al., 2014). Oral administration of *Bifidobacterium infantis* 35624 was able to reduce the significantly elevated levels of systemic inflammation as evidenced by the reduction of CRP, TNF-α and IL-6 levels in the blood of ME/CFS patients (Groeger et al., 2013).

70 % of ME/CFS patients were reported to have a clinical response to probiotic intake (a mixture of 13 non-pathogenic enteric bacteria from the Bacteroidetes phylum, Clostridia phylum and *Escherichia coli*) defined as the resolution of sleep disturbances and fatigue, which was sustained in 58 % of participants at 15-20 years follow up (Borody et al., 2012). In contrast, Sullivan et al. (2009) found an improvement in neurocognitive functions but no significant improvements in fatigue severity or physical activity levels following administration of *Lactobacillus paracasei* ssp. *Paracasei* F19, *Lactobacillus acidophilus* NCFB 1748 and *Bifidobacterium lactis* Bb12. The discrepancies in improvement of fatigue following probiotic intervention seen in these two papers could reflect the administration of different probiotic bacteria, which could have different functions in the human body. In contrast, the administration of different probiotic bacteria could result in the same clinical outcome due to functional redundancy of probiotic bacteria. For example, an improvement in anxiety and depressive symptoms were seen in ME/CFS patients following probiotic intervention with *Lactobacillus casei Shirota* (Rao et al., 2009) and a combination of *Enterococcus faecium, Saccharomyces boulardii, Bifidobacterium longum, Bifidobacterium breve, Bifidobacterium bifidum, Bifidobacterium infantis, B. longum AR81, L. casei, B. lactis, Lactobacillus rhamnosus* GG and *L. acidophilus* (Venturini et al., 2019). Interestingly, one study compared FMT to a mixture of probiotic and prebiotic intake and found greater clinical improvement in ME/CFS patients treated with FMT (Kenyon et al., 2019). The difference in clinical improvement between the two interventions could be because FMT is not restricted to bacteriotherapy as faecal samples also contain viruses and eukaryotes. It is worth noting that a systematic review of bacteriotherapy

interventions in ME/CFS patients regarded the majority of these studies as poor quality and concluded more research was required before bacteriotherapy can be used as a treatment for ME/CFS (Corbitt et al., 2018).

1.3.2 Leaky gut

1.3.2.1 Overview

A consequence of microbial dysbiosis is the initiation of intestinal inflammation which results in a leaky gut (Kinashi and Hase, 2021). A leaky gut is the term used to describe the increased permeability of the gut barrier. When the integrity of the intestinal barrier is compromised systemic translocation of enteric microbes and their products can occur which can initiate or propagate systemic inflammation. This is witnessed in intestinal diseases such as IBS (Singh et al., 2019), autoimmune diseases (Kinashi and Hase, 2021) and major depressive disorders (Ohlsson et al., 2019). In addition, a leaky gut alters the bidirectional communications along the gut-brain axis as the systemic inflammation can disrupt the blood-brain barrier enabling the translocated microbes and microbial products to reach the brain and activate neuroinflammation (Houser and Tansey, 2017). It is also worth noting that a transient breach in the intestinal barrier can also occur in health during periods of stress (Kiecolt-Glaser et al., 2018), intensive exercise (Karhu et al., 2017), acute binge drinking (Bala et al., 2014) and a high-fat diet (Rohr et al., 2019).

1.3.2.2 Evidence for a leaky gut in ME/CFS

There is evidence for microbial dysbiosis and autoimmunity in ME/CFS patients, as described earlier (see **section 1.3.1.2** and **section 1.2.3**). In addition, there is evidence for a leaky gut. ME/CFS patients had elevated levels of leaky gut biomarkers such as lipopolysaccharide (LPS) binding protein (LBP) and soluble CD14 (sCD14) (Giloteaux et al., 2016a). Maes et al. (2007) investigated the levels of serum IgA and IgM to the LPS of the following seven Gram-negative enterobacteria: *Hafnia alvei, Pseudomonas aeruginosa, Morganella morganii, Proteus mirabilis, Pseudomonas putida, Citrobacter koseri* and *Klebsiella pneumoniae*. They found over 70 % of ME/CFS patients had abnormally high IgA levels to the LPS of at least one Gram-negative enterobacteria and 40 % of ME/CFS patients had abnormally high IgM levels to the LPS of at least one Gram-negative enterobacteria. Elevated levels of serum antibodies to the LPS of Gram-negative enterobacteria could reflect higher circulating endotoxin levels as a consequence of a leaky gut. Indeed, higher concentrations of LPS in the blood of ME/CFS patients were found (Giloteaux et al., 2016a). In addition, following exercise the abundance of Bacilli in the blood significantly increased in ME/CFS patients but not healthy controls (Shukla et al., 2015). This suggests that exercise induced intestinal permeability is greater in ME/CFS patients than in healthy controls.

Bacterial translocation has also been linked to the severity of other common ME/CFS symptoms. There was a significant positive correlation between the level of serum IgA to the LPS of Gram-

negative enterobacteria and the severity of the following symptoms: irritable bowel, muscle tension, fatigue, impaired concentration and failing memory (Maes et al., 2007). Another study found higher serum IgA and IgM antibodies to the LPS of Gram-negative enterobacteria in patients with GI disturbances compared to those without (Maes et al., 2014). In addition, clinical improvement of ME/CFS symptom severity, measured using the fibromyalgia and chronic fatigue syndrome rating scale, was seen in ME/CFS patients after having a leaky gut diet (dairy free, gluten free and low carbohydrate intake) and taking natural anti-inflammatory and anti-oxidative substances (e.g. glutamine, N-acetyl cysteine and zinc) (Maes and Leunis, 2008). 63.5 % of patients were clinical responders to this treatment and they had significantly lower IgM levels against *P. aeruginosa, P. putida* and *H. alvei* and significantly lower IgA levels against *C. koseri* compared to non-responders. In addition, clinical responders to the leaky gut diet had a shorter duration of ME/CFS suggesting a leaky gut and bacterial translocation could be involved in the early stages of the illness, such as disease initiation. Furthermore, events which predispose the onset of ME/CFS such as infection, stress and surgery can disrupt the intestinal epithelial barrier.

However, measuring serum IgM and IgA reactivity to enterobacteria gives limited information about the systemic immune response that occurs as a consequence of a leaky gut and bacterial translocation. IgM functions during primary immune responses where there is a small window of IgM production which has low specificity for antigens (Keyt et al., 2020). Therefore, measuring serum IgM to enterobacteria only provides information about the presence of non-specific antibody reactivity. The majority of IgA is produced at mucosal sites, such as the gastrointestinal tract, and therefore is not suitable for studying systemic immune responses (de Sousa-Pereira et al., 2019). In contrast, IgG is the predominant immunoglobulin subclass in serum and is the main antibody in secondary immune responses (immunological memory) (Schroeder et al., 2010). This was the rationale for developing a method to determine IgG reactivity to intestinal microbes in **chapter 3**.

1.3.2.3 Potential mechanisms for the induction of a leaky gut in ME/CFS

Many factors affect the integrity of the intestinal barrier including genetic susceptibility, drugs (e.g. antibiotics), inflammation (e.g. cytokines and pattern recognition receptor (PRR) engagement), pathogenic microorganisms and microbiome alterations (Chelakkot, et al. 2018). This section discusses the microbiome alterations in ME/CFS patients which have independently been shown to affect intestinal permeability.

A leaky gut in ME/CFS patients could be caused by reduced levels of butyrate producing bacteria and reduced levels of butyrate in the stool (König et al., 2021). Butyrate is a short-chain fatty acid (SCFA) which is utilised by intestinal epithelial cells as a source of energy, generating a hypoxic environment which stabilises the transcription factor hypoxia-inducible factor-1 (HIF-1) (Kelly et al.,

2015). HIF-1 transcribes tight junction (TJ) proteins claudin-1 and occludin which maintain the epithelial barrier. Decreased butyrate levels result in a reduction of stabilised HIF-1, which in turn would reduce the production of TJ proteins, increasing the permeability of the intestinal epithelial barrier.

The mucus layer in the intestine protects the epithelial barrier integrity (Paone and Cani, 2020). Butyrate increases mucus production and secretion by inducing the transcription of MUC2 (Burger-van Paassen et al., 2009). Therefore, decreased butyrate levels can lead to mucus layer impairment which enables commensal and pathogenic microorganisms to reach the intestinal epithelium, triggering inflammation (Paone and Cani, 2020). Therefore, the reduced butyrate producing bacteria and butyrate levels in stool of ME/CFS patients could contribute to the breakdown of the mucosal and epithelial barrier in the intestine. However, one study found increased butyrate levels in the stool of ME/CFS patients, suggesting other mechanisms also contribute to a leaky gut in these patients (Armstrong et al., 2016).

Proinflammatory cytokines regulate TJs and, therefore, epithelial barrier integrity (Capaldo and Nusrat, 2010). Elevated levels of TGF-β, TNF-α, IL-4 and IL-2 are frequently found in ME/CFS patients (Strawbridge et al., 2019). TNF-α and IL-4 have been shown to increase intestinal permeability whereas TGF-β decreases intestinal permeability (Capaldo and Nusrat, 2010). In addition, cytokines also regulate mucus production and therefore the mucus barrier (Paone and Cani, 2020). TNF-α can signal through the JNK pathway to reduce MUC2 expression and secretion, leading to mucus layer impairment. However, TNF-α along with IL-4 can increase MUC2 expression and secretion, which enhances the mucus barrier. Therefore, it is difficult to conclude whether altered cytokine levels contribute to the induction of a leaky gut in ME/CFS patients.

LPS stimulation of Toll-like receptor (TLR)-4 on the basolateral (in interstitial fluid) but not apical (luminal) side of intestinal epithelial cells increases intestinal epithelial TJ permeability (Guo et al., 2013). LPS is therefore not thought to initiate intestinal permeability but instead perpetuate it as a defective TJ barrier is required for the paracellular flux of LPS from the apical to basolateral side of the intestinal epithelial barrier. Hence elevated LPS in the blood of ME/CFS patients (Giloteaux et al., 2016a) could contribute to the chronicity of ME/CFS by perpetuating a leaky gut.

1.3.2.4 Leaky gut and autoimmunity in ME/CFS

Evidence for a leaky gut and autoimmunity in ME/CFS patients has been provided. A leaky gut is also witnessed in other autoimmune diseases such as MS (Buscarinu et al., 2018), ankylosing spondylitis (Ciccia et al., 2017), rheumatoid arthritis (RA) (Tajik et al., 2020) and type 1 diabetes (Harbison et al., 2019). Whether a leaky gut is a cause or consequence of these autoimmune diseases is still being debated. However, ME/CFS patients with a leaky gut have a higher incidence

of serotonin autoimmunity than those without, suggesting a leaky gut could contribute to the initiation or propagation of autoimmunity in ME/CFS patients (Maes et al., 2013).

Systemic inflammation following a leaky gut and microbial translocation leads to elevated levels of oxidative and nitrosative stress and the formation of neoepitopes (Morris and Maes, 2014). Oxidation can alter the structure and function of self-epitopes, converting them to neoepitopes which are recognised as 'foreign' by the immune system (James et al, 2018). The generation of neoepitopes is an example of epitope spreading, which is one mechanism of autoimmune development (James et al., 2018). As discussed in **section 1.2.3.1** ME/CFS patients have elevated levels of antibodies to neoepitopes, suggesting patients have elevated neoepitope levels. Therefore, the leaky gut seen in ME/CFS patients could cause epitope spreading and an autoimmune response.

Systemic inflammation caused by a leaky gut and microbial translocation into the systemic circulation could cause or augment autoimmune responses through bystander activation of T or B cells in a pro-inflammatory environment through antigen non-specific mechanisms (Pacheco et al., 2019). These mechanisms involve innate immune responses, for example recognition of PAMPs and the secretion of cytokines. ME/CFS patients had a positive correlation between the levels of IgA to the LPS of Gram-negative enterobacteria and the levels of IL-1, TNF-α, and elastase (markers of inflammation) and neopterin (a marker of cell-mediated immune activation) (Maes et al., 2012d). This indicates that the leaky gut in ME/CFS patients causes the systemic inflammation which is a suitable environment in which bystander activation could occur.

Another mechanism through which a leaky gut could cause autoimmunity is molecular mimicry. Molecular mimicry can generate cross reactive T cells, B cells and autoantibodies. For example, T cells reactive to Ro60 and Sjögren's syndrome antigen A, two autoantigens in Sjögren's syndrome, share structural similarity with four peptides from gut-derived commensal bacteria (Szymula et al., 2014). In addition, RA patients have autoantibodies to anti-citrullinated α-enolase which can cross react with the homologous *P. gingivalis* derived α-enolase (Lundberg et al., 2008). *P. gingivalis* is an oral pathogen that can cause intestinal dysbiosis and inflammation if ingested (Arimatsu et al., 2014). Evidence for molecular mimicry as a mechanism for leaky gut induced autoimmunity in ME/CFS patients is limited as cross-reactive autoantibodies, B cells and T cells have yet to be explored.

1.3.3 The gut-brain axis

1.3.3.1 Overview

The gut is able to bidirectionally communicate with other organs such as the liver (Konturek et al., 2018) and brain (Cryan et al., 2019). Microbial dysbiosis and a leaky gut disturbs these bidirectional

communications and can contribute to extra-intestinal diseases (Di Tommaso et al., 2021). The gut-brain axis, also referred to as the microbiome-gut-brain axis, involves the bidirectional communication between the central nervous system and the GI tract and is mediated by four main routes: I) neural, II) endocrine, III) immune and VI) metabolic pathways (Cryan et al., 2019). The microbiome is able to produce neuropeptides, hormones and metabolites which can directly or indirectly impact the CNS along these four routes influencing sleep, mood, memory and cognition. The gut-brain axis is implicated in the pathogenesis of many diseases including, but not limited to, neuropsychiatric diseases (depression (Liang et al., 2018) and autism spectrum disorder (ASD) (Yu and Zhao, 2021)), neurodegenerative diseases (Parkinson's disease (Klann et al., 2022), Alzheimer's disease (Megur et al., 2020) and multiple sclerosis (Parodi and Kerlero de Rosbo, 2021)) and GI diseases (IBS (Tait and Sayuk, 2021)).

1.3.3.2 Evidence for altered gut-brain axis in ME/CFS

As fatigue, disturbed sleep, impaired memory, poor concentration and low mood are experienced in patients with ME/CFS it is speculated that the dysregulation of the gut-brain axis is involved in pathogenesis. To date, evidence of a dysregulated gut-brain axis in ME/CFS is limited and the role of the gut-brain axis in ME/CFS pathogenesis has not been directly investigated. This is primarily due to the progression of gut-brain axis research being driven by the use of animal models (Cryan et al., 2019) and there is not yet an animal model that reflects the clinical aspects of ME/CFS to be able to research disease pathogenesis (Lee et al., 2020). Instead, human trials using bacteriotherapy indirectly provide evidence of the involvement of the gut-brain axis because upon altering the intestinal microbiome there is an improvement in neurocognitive symptoms (detailed in **section 1.3.1.6**).

1.4 HYPOTHESIS

The working hypothesis for the research presented within this thesis is that the microbial dysbiosis witnessed in ME/CFS patients causes intestinal inflammation, resulting in a leaky gut which enables the systemic translocation of small quantities of microbes and microbial products into the circulation. This results in an increased immune response to enteric microbes, promoting inflammation and ultimately autoimmunity by either bystander activation, epitope spreading or molecular mimicry.

1.5 AIMS AND OBJECTIVES

The primary aim of this thesis was to demonstrate that ME/CFS patients have an elevated systemic immune response to the microbiome. The secondary aim was to determine which enteric microbes the immune response was directed against. The thesis had the following objectives:

1. To set up a human study recruiting severe ME/CFS patients and matched household controls for the collection of blood and stool samples (chapter 2),
2. To use blood and stool samples to develop methods to identify enteric microbes reacting to circulating antibodies (chapter 3),
3. Determine the level and specificity of stool IgA and serum IgG for the microbiome in severe ME/CFS patients compared to their matched household controls (chapter 4),
4. To identify differences in the reactivity of stool microbes to serum IgG in severe ME/CFS patients compared to their matched household controls (chapter 5).

2 CHAPTER TWO: HUMAN STUDY PROTOCOL

2.1 SUMMARY

The results presented within this thesis were obtained using samples collected from the human study "Defining autoimmune aspects of myalgic encephalomyelitis/chronic fatigue syndrome (ME/CFS) (AI-ME/CFS)". This was a case control pilot study recruiting severe ME/CFS patients from the Epsom and St Helier (ESTH) CFS Service and the East Coast Community Healthcare Centre (ECCHC) ME/CFS Service. Matched household controls were recruited through severe ME/CFS patients interested in participating in this study.

2.2 ETHICAL CONSIDERATIONS

An application for the ethical approval of the study "Defining autoimmune aspects of myalgic encephalomyelitis/chronic fatigue syndrome (ME/CFS) (AI-ME/CFS)" was submitted through the Integrated Research Application System (IRAS) to the Health Research Authority (HRA). The application was reviewed by and received HRA approval from London Hampstead regional ethics committee (REC) on the 19th of July 2017, reference number 17/LO/1102 (**Appendix I**).

All research undertaken for this human study complied with the Declaration of Helsinki seventh version (2013) and ICH-Good Clinical Practice (GCP). All data was handled in accordance with the EU General Data Protection Regulation (GDPR) and the UK Data Protection Act 2018.

2.3 STUDY PERSONNEL

Tracey Moulton, Contracts Manager at the University of East Anglia (UEA), was appointed study sponsor until 2019. In 2019, sponsorship of the study was transferred to the Quadram Institute Bioscience (QIB), where Dr Antonietta Melchini, Human Studies Lead, assumed the post.

As the chief investigator of this human study, it was my responsibility to design the study, acquire ethical approval and set up the study. I also corresponded with eligible participants who had expressed interest in study participation, coordinated and attended study visits and obtained written informed consent from participants.

Blood sample collection was undertaken at participants' homes by Shelina Rajan, QIB, or by research nurses from St Helier Hospital.

The processing of samples for long term storage was aided by the PhD students Shen-Yuan Hsieh and Fiona Newberry.

2.4 STUDY OBJECTIVES

This human study was set up to investigate the hypothesis that *ME/CFS is an autoimmune disease initiated or sustained by microbial dysbiosis which drives intestinal inflammation, leading to a breakdown in the epithelial barrier and subsequent exposure of the intestinal microbiome to the immune system.*

2.5 SAMPLE SIZE

Four assumptions were made in the power calculation: 1) The McNemar's exact test with a two-sided significance level of 5 % was used in the main analysis, 2) the presence of immune reactivity to intestinal microbiome is in less than 10 % of the general population, 3) the presence of immune reactivity to intestinal microbiome is in more than 70 % of the severe ME/CFS population (based on Maes et al. (2007) findings that more than 70 % of ME/CFS patients had elevated IgM levels to the LPS of Gram-negative enterobacteria), 4) there is a weak correlation of outcome between cases and controls (phi < 0.1). Based upon these assumptions, ten pairs of patients and household controls would give an 80 % chance of proving the hypothesis and concluding a difference between patients and household controls, with 95 % statistical power.

2.6 STUDY PROCEDURES

2.6.1 Participant identification

2.6.1.1 Patient cohort

The patient cohort for this study were severe ME/CFS patients between the ages of 18 and 70 years. Jason et al (2005) reviewed the importance of subgrouping patients when undertaking ME/CFS research. For this study patients were sub grouped by severity of the illness, recruiting severe ME/CFS patients as they have a more homogeneous clinical presentation than mild and moderate subgroups of patients (Collin et al., 2016).

Participant identification was undertaken at the ESTH CFS Service by Dr Amolak Bansal, and at the ECCHC ME/CFS Service by occupational therapists. These services identified ME/CFS patients meeting the eligibility criteria (**Table 2.1**).

Participants had to fulfil the 2007 NICE guidelines' clinical diagnostic criteria for ME/CFS (CG53): sudden onset of disabling fatigue present for a minimum of four months, experiencing symptoms such as disturbed sleep, musculoskeletal pain, severe headaches, sore throat and glands in the absence of swelling, memory and concentration deficit, flu-like symptoms, dizziness, nausea, heart palpitations or post exertional malaise (Baker and Shaw, 2007). In addition, participants had to be classified as severe. Categorisation of severity was based on a patient's ability to undertake

activities of daily living, such as bathing, dressing, mobility, eating and toileting. Patients in the severe category were unable to perform the activities of daily living, were wheelchair dependent or bed-bound, and experienced severe cognitive impairment and sensitivity to light and sound.

Table 2.1: Patient cohort eligibility criteria.

Inclusion	**Exclusion**
18-70 years old	Antibiotic consumption
Confirmed ME/CFS diagnosis	Probiotic capsule consumption
Severe ME/CFS symptoms	Anxiety diagnosis
Able to provide informed consent	Depression diagnosis

2.6.1.2 Control cohort

Matched household controls were used for this study. This cohort was chosen because of the increased power of detecting disease associated alterations relating to the intestinal microbiome, which is strongly influenced by environmental factors (Norman et al., 2015). For the purpose of this study, a matched household control was defined as a relative or non-relative, living with or caring for the patient. Household controls had to fulfil the inclusion/exclusion criteria (**Table 2.2**), which was confirmed with an eligibility questionnaire completed prior to recruitment (**Appendix VI**). This cohort was identified through interested patient cohort participants.

Table 2.2: Control cohort eligibility criteria.

Inclusion	Exclusion
18-70 years old	Antibiotic consumption
Able to provide informed consent	Probiotic capsule consumption
Living with or caring for the patient	Long term medical condition affecting the stomach or bowel
Healthy	Autoimmune disease diagnosis
	Anxiety diagnosis
	Depression diagnosis
	Recipient of immunomodulatory drugs, statins, beta blockers or steroids

2.6.2 Participant recruitment

Once clinicians and occupational therapists at the ESTH CFS Service and the ECCHC ME/CFS Service identified patients fulfilling the severe ME/CFS eligibility criteria, they mailed them a cover letter explaining the study (**Appendix II**), a summary patient information sheet (**Appendix III**), a full patient information sheet (**Appendix IV**) and a household control information sheet (**Appendix V**). Patients interested in participating in the study were asked to identify and inform eligible household controls about the study using the relevant participant information sheets.

Pairs of participants interested in being a part of the study contacted me to express their interest. To ensure participants were fully informed and made their own independent decision, telephone interviews were carried out to explain the study further and ensure all their questions were answered. Following this they had a 72-hour consideration period prior to booking a consenting appointment.

2.6.3 Study visits

Study visits were undertaken at participants' homes, due to the severity and the nature of the patient cohort's illness.

2.6.4 Informed consent

Prior to 16th March 2020 consent appointments were undertaken during study visits. Following the national COVID lockdown on the 26th of March 2020, all consent appointments were undertaken remotely. Participants chose whether they gave their remote consent through a telephone appointment or a video conference call, using a paper or an electronic copy of the consent form (**Appendix VII and VIII**).

Prior to the appointment for informed consent participants were given a copy of the consent form, to ensure they fully understood what they were being asked to do. During their consent appointment, participants were given the opportunity to ask any further questions. When participants received satisfactory answers, a GCP trained member of the research team guided participants through the consenting process. Consent forms consisted of required and optional sections. Optional sections enabled participants to decide whether they wanted their samples to be transferred to the Norwich Research Park (NRP) Biorepository at the end of the study for long term storage and use in other research projects and whether they were happy for samples to be used in ethically approved animal research. Participants were asked to complete two copies of the consent form, one for the research team and one for the individual to keep.

2.6.5 Sample collection

During a 24-hour window of the scheduled sample collection appointment, participants collected a stool sample. Following printed instructions (**Appendix IX**) participants defecated into a Fecotainer® (AT Medical BV, catalogue number: 39233000), added an Oxoid™ AnaeroGen™ compact sachet (Thermo Scientific™, catalogue number: AN0020D) and sealed the Fecotainer®. Samples were stored at 4 °C by the participant until their appointment.

During the home visit a trained phlebotomist collected a total of 50 ml of blood by venepuncture using BD Vacutainer® push button blood collection set with pre-attached holder (Becton Dickinson UK LTD, catalogue number: 367355 and 367354). 30 ml of blood was collected into BD Vacutainer® plastic whole blood tube with spray-coated K2EDTA (Thomas Scientific, catalogue number: 366643) and 20 ml of blood was collected into BD Vacutainer® plus plastic SST tube with double polymer gel (Thomas Scientific, catalogue number: 367985).

2.6.6 Sample processing

2.6.6.1 Stool

The consistency of stool samples was scored according to the Bristol stool form scale (BSFS) by a member of the research team (**Table 2.3**). Stool samples were homogenised by mixing. 100 mg ±10 mg aliquots were stored at -80 °C. Stool microbial glycerol stocks were made by diluting 1.5 g of stool sample 10 % w/v with sterile phosphate buffered saline (PBS) (Sigma Aldrich), homogenised by vortexing, centrifugated for 5 minutes at 300 x g and the supernatant was diluted 1:1 with 80 % v/v glycerol. Stool microbial glycerol stocks were aliquoted and stored at -80 °C.

Table 2.3: The seven types of stool consistency defined by the Bristol stool form scale (Lewis and Heaton, 1997).

Type	Description
1	Separate hard lumps, like nuts
2	Sausage shaped, formed by hard lumps
3	Sausage shaped, with a cracked surface
4	Smooth and soft sausage shape
5	Soft, clear-cut blobs
6	Fluffy pieces with ragged edges and no clear form
7	Watery

2.6.6.2 Peripheral blood mononuclear cells

Peripheral blood mononuclear cells (PBMCs) were isolated from whole blood collected in BD Vacutainer® plastic whole blood tubes with spray coated K2EDTA. EDTA anticoagulated blood was diluted three-fold with sterile Dulbecco's phosphate buffered saline solution (Merck Life Sciences UK Limited, catalogue number: D8537). Ficoll-Paque™ PLUS (GE Healthcare Life Sciences, catalogue number: 17-1440-03) was used for density gradient centrifugation. 15 ml was added to a Leucosep™ tube (Greiner Bio-one International) and subsequently centrifuged for 1 minute at 1000 x g at 20 °C. Diluted blood was poured into the Leucosep™ tubes to form an overlay. Leucosep™ tubes were centrifuged at 800 x g for 20 minutes at 20 °C with the break switched off. PBMCs were recovered from the buffy coat and washed three times with sterile PBS, centrifuging once at 600 x g and twice at 300 x g for 5 minutes each. PBMCs were resuspended in 1 ml of 10 % dimethyl sulfoxide (Sigma-Aldrich) in heat inactivated foetal bovine serum (Biosera). They were then cryopreserved using Nalgene® Mr. Frosty® cryo 1 °C freezing containers (Nalgene Nunc International, Rochester, New York) which when placed at -80 °C lowers the temperature of the PBMCs at a rate of 1 °C/min. PBMCs were stored long term at -80 °C.

2.6.6.3 Plasma

Plasma was isolated from whole blood during the density gradient centrifugation process described in **section 2.6.6.2**. It was recovered from the upper phase, aliquoted and stored long term at -80 °C.

2.6.6.4 Serum

BD Vacutainer® plus plastic SST tubes with double polymer gel were centrifuged at 1000 x g for 10 min. The upper phase was aliquoted and stored long term at -80 °C.

2.6.7 Obtaining clinical metadata

ME/CFS is a complex illness with numerous events reported to occur prior to onset and different combinations of symptoms and disability, it was important therefore to collect clinical information relating to the patient cohort's ME/CFS diagnoses to enable associations to be made between clinical aspects and research findings. Clinical metadata was obtained using the following tools used in clinic for ME/CFS diagnosis: shortened SF-36 (**Appendix X**), CFQ (**Appendix XI**), hospital anxiety and depression scale (HADS) (**Appendix XII**), self-efficacy questionnaire, (**Appendix XIII**), visual analogue pain rating scale (**Appendix XIV**) and the Epworth sleepiness scale (**Appendix XV**). ME/CFS symptoms experienced, duration of illness and mode of onset were also provided using the studies CFS/ME symptom questionnaire (**Appendix XVI**). Either clinicians at ESTH CFS Service or occupational therapists at the ECCHC ME/CFS Service provided participant scores for each questionnaire, or participants completed the questionnaires and returned them to the research team where the chief investigator scored the questionnaires.

2.7 STUDY OUTCOMES

2.7.1 Enrolment

At the time of participant identification, there were 3812 ME/CFS patients registered with the ESTH CFS Service and the ECCHC ME/CFS Service, 36 of which were invited to the study with a response rate of 58.3 %. Of the 21 pairs responding to study invitation, only 12 pairs were eligible to participate due to one or more of the following reasons: 1) patients not having a matched household control, 2) household control or patients were recipients of medication excluding them from the study, 3) patient unable to provide written informed consent. Of the 12 eligible pairs 6 were consented and the other 6 withdrew their interest or could not be contacted again. Samples from one pair of consented participants were unable to be collected because they were enrolled onto the study just before the COVID-19 national lockdown was announced. This meant a total of 5 pairs of severe ME/CFS patients and matched household controls donated samples to this study (**Figure 2.1**).

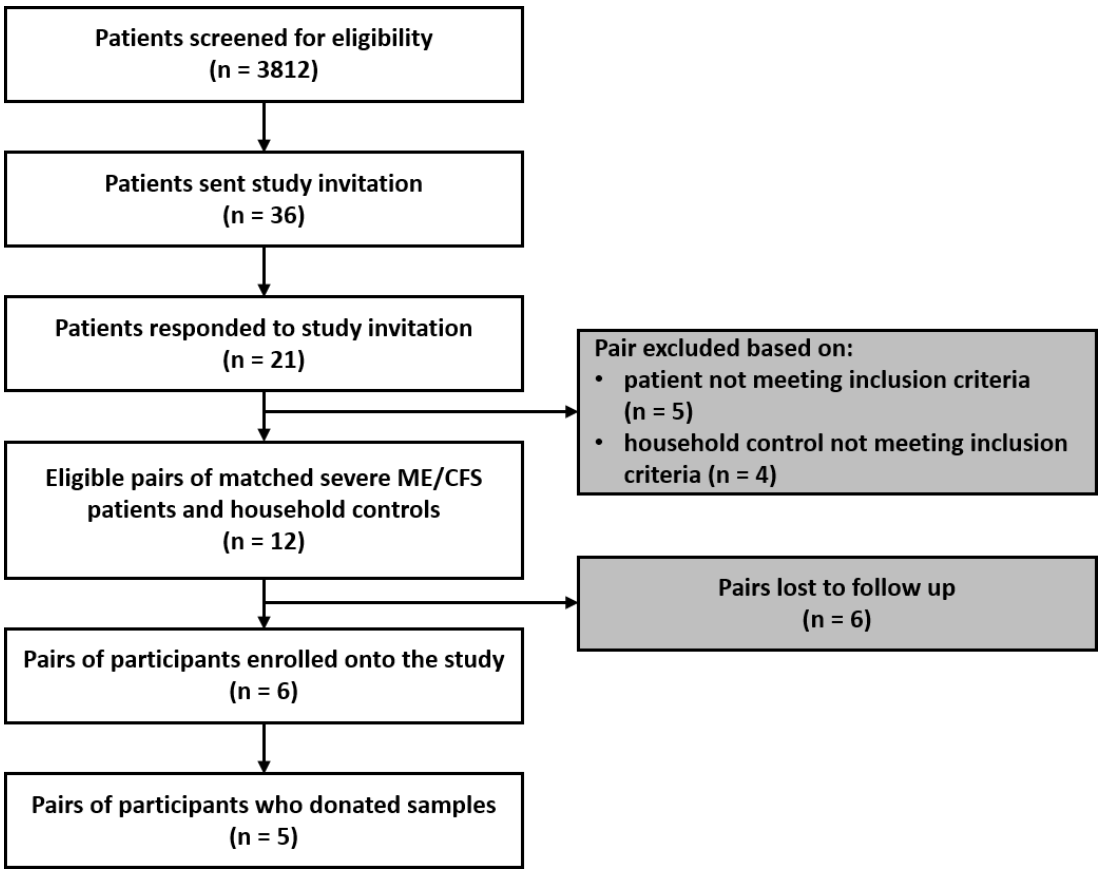

Figure 2.1: Flowchart of the AI-ME/CFS study population recruited through the Epsom and St Helier CFS Service and the East Coast Community Healthcare Centre ME/CFS Service.

2.7.2 Demographics

Table 2.4 describes the demographic information collected from each pair of participants.

Table 2.4: Demographics of participant pairs recruited onto AI-ME/CFS human study.

Pair	Gender		Age		Recruitment Site	Relation
	Patient	**Control**	**Patient**	**Control**		
1	Female	male	59	62	ECCHC	spouse
2	Female	male	38	38	ECCHC	spouse
3	Female	female	22	57	ESTH	parent
4	Female	male	26	23	ESTH	spouse
5	Male	male	24	22	ESTH	sibling
Mean (±SD)			33.8 (13.76)	40.4 (16.67)		

The patient cohort varied in length of illness and age of onset (**Table 2.5**). All patients experienced a sudden onset of fatigue, three reported onset after viral infection, one following vaccination and another following surgery. All patients experienced post exertional malaise, disturbed sleep, cognitive difficulties and sensitivity to light or sound (**Table 2.6**). Scores from ME/CFS questionnaires confirmed the severity of ME/CFS experienced by the patient cohort (**Table 2.7**).

Table 2.5: Age of onset and length of illness in the severe ME/CFS patient cohort.

	Mean (SD)	**Range**
Age of onset (years)	25.0 (9.34)	12-38
Length of ME/CFS (years)	8.4 (6.83)	2-21

Table 2.6: ME/CFS symptoms experienced by the AI-ME/CFS human study patient cohort.

Symptom	Affected
Post exertional malaise	100 %
Non-restorative sleep	100 %
Headaches of a new onset, pattern and severity	80 %
Recurrent sore throat	40 %
Impaired concentration	100 %
Impaired memory	80 %
Joint pain	60 %
Muscle pain	80 %
Visual and/or auditory hypersensitivity	100 %

Table 2.7: AI-ME/CFS human study patient cohort scores in questionnaires relating to patients' diagnosis.

Questionnaire (maximum score)	Mean (SD)	Range
Shortened SF-36 (30) *	11.0 (1.73)	10-14
Chalder fatigue – physical (28) *	24.0 (3.67)	18-27
Chalder fatigue – mental (16) *	13.5 (1.12)	12-15
HADS – anxiety (21) *	7.8 (4.55)	3-15
HADS – depression (21) *	6.5 (5.50)	3-16
Self-efficacy (60) **	12.0 (7.35)	3-21
Visual analogue (100) *	62.5 (36.31)	0-90
Epworth sleepiness (24) ***	7.5 (14)	1-14

* questionnaire completed by 4 patients
** questionnaire completed by 3 patients
*** questionnaire completed by 2 patients

2.7.3 Gastrointestinal health

All ME/CFS patients and no matched household controls reported symptoms of GI complaints, such as IBS. Interestingly, the BSFS score of 60 % of severe ME/CFS patients was normal, compared with 40 % of matched household controls (**Table 2.8**).

Table 2.8: Consistency of stool samples from severe ME/CFS patients and matched household controls recruited onto the AI-ME/CFS human study. *BSFS = Bristol stool form scale.*

Stool form (BSFS type)	patients	controls
hard (1-2)	2	1
normal (3-5)	3	2
loose (6-7)	0	2

2.7.4 Limitations

During the implementation of the AI-ME/CFS study unanticipated difficulties were encountered which required changes to the study design. The original study design submitted through IRAS for ethical review was longitudinal with six sample collection time points. However, as sample collection was undertaken at participants' homes, there were a limited number of appointments where trained phlebotomists were available for home visits and so 30 study visits were unable to be scheduled. To overcome this, a substantial amendment was submitted to the HRA (approved 22/01/20) to change the study to a single time point study, prioritising resources for collecting samples from the target population size. Unfortunately, the target number was not met. This was because only a small pool of patients were eligible for the study, as severe ME/CFS patients make up 25 % of the ME/CFS population (Pendergrast et al., 2016). Furthermore, because of the difficulties arranging study visits, time had lapsed between participants expressing interest in the study and the sample collection appointments, during which 6 pairs of participants were lost to follow up. Future research should focus on recruitment of moderately affected patients, who make up 50 % of the ME/CFS population, as this would increase the pool of eligible patients, and study visits would be more accessible as they would be undertaken at NHS or research centres, negating the issue of phlebotomist availability.

3 CHAPTER THREE: OPTIMISING A FLUORESCENT ACTIVATED CELL SORTING PROTOCOL TO IDENTIFY CELLS IN THE INTESTINAL MICROBIOME REACTIVE WITH SYSTEMIC IMMUNOGLOBULIN G

3.1 INTRODUCTION

3.1.1 ME/CFS and the leaky gut

ME/CFS is a complex, multi-factorial disease. Up to 92 % of ME/CFS patients experience comorbid GI disturbances, such as IBS, which contribute to the morbidity these patients experience (Sperber and Dekel, 2010). Maes et al. (2007) proposed that patients with ME/CFS have a leaky gut. Leaky gut syndrome is a phenomenon which is thought to occur in many autoimmune diseases (Kinashi and Hase, 2021). It is characterised by dysbiosis of the intestinal microbiome leading to an increase in pathobionts (opportunistic microbes) and a decrease in symbionts (health promoting microbes). This causes inflammation in the GI tract, which reduces the integrity of TJs, leading to a breach of the intestinal epithelial barrier. Consequently, metabolites, microbial cell wall components and viable microbes can translocate into the circulation and trigger systemic inflammation (McPherson et al., 2021). This hypothesis is supported by findings that ME/CFS patients have increased pro-inflammatory and decreased anti-inflammatory microbes within the intestinal microbiota (Giloteaux et al., 2016a), elevated inflammatory proteins CRP, TNF-α and IL-6 in blood plasma (Groeger et al., 2013) and elevated serum IgA and IgM to the LPS of Gram-negative enterobacteria (Maes et al., 2007, Maes et al., 2012d).

Another hallmark of a leaky gut and microbial translocation is the presence of serum IgGs specific for gut microbes (Balmer et al., 2014). However, serum IgG recognition of gut bacteria is not just seen in inflammatory disorders such as inflammatory bowel disease (IBD) (Adams et al., 2008, Haas et al., 2011, Harmsen et al., 2012, Landers et al., 2002, Macpherson et al., 1996, Targan et al., 2005) and systemic lupus erythematosus (SLE) (Azzouz et al., 2019), but it is also seen in healthy individuals (Christmann et al., 2015, Fadlallah et al., 2019, Haas et al., 2011, Harmsen et al., 2012, Sterlin et al., 2020). One theory as to how anti-microbiota IgGs arises in health is that antigen recognition occurs within the intestine leading to the generation of memory B cells which can enter and circulate in the blood. This theory was formulated from the finding that memory B cells to gut bacteria arising from a single progenitor cell were found in both lamina propria and in the blood (Rollenske et al., 2018). However, the presence of LPS and bacterial DNA in the serum of healthy individuals following a high-fat meal, which can induce a temporary breach of the epithelial barrier, raises the possibility of antibody priming in the periphery (Mannon, 2019). Furthermore, transient

increases in intestinal permeability can also be induced by other environmental factors such as excessive alcohol consumption and use of drugs such as proton pump inhibitors (PPIs) and non-steroidal anti-inflammatory drugs (NSAIDs). Zeng et al. (2016) speculated that this temporary increase was insufficient to cause disease but could generate humoral immune memory. Indeed, healthy individuals have anti-microbiota IgG antibodies that persist for years within the serum (Haas et al., 2011).

The contribution of anti-microbiota IgG to health and disease is not yet fully understood, but previous studies have suggested both a protective and pathogenic role for these antibodies. Anti-microbiota IgG is transferred passively from mother to baby through breast milk and contributes to immunomodulation in early life (Sterlin et al., 2020). Furthermore, serum IgG reacting to commensal bacteria can recognise conserved antigens and protect against systemic infections through opsonisation (Zeng et al., 2016). Interestingly, Fadlallah et al. (2019) showed that serum anti-microbiota IgG was able to bind both pathobionts and symbionts, with a stronger response to the latter. More evidence that anti-microbiota IgG has a protective role in health was that there was a negative correlation between levels of systemic anti-microbiota IgG and inflammation (Fadlallah et al., 2019). Disputing this was the finding that serum IgG antibodies to *Sacchromyces cerevisiae* were a clinical biomarker of disease activity in CD (Vasiliauskas et al., 2000) with IBD patients having an elevated (Harmsen et al., 2012) and biased (Haas et al., 2011) anti-microbiota IgG response. Furthermore, translocated bacteria could initiate or worsen autoimmune diseases, such as RA (Lundberg et al., 2008) and antiphospholipid syndrome (Ruff et al., 2019), as patients have systemic anti-microbiota IgG that is cross-reactive with autoantigens. Given the pathogenic role systemic anti-microbiota IgGs may play in autoimmune diseases and the potential of using them as a clinical biomarker, investigating the serum anti-microbiota IgG response in ME/CFS could provide insight into the pathogenesis of this disease and has yet to be fully explored.

3.1.2 Investigating systemic anti-microbiota IgG response

A range of *in vitro* assays have been used to investigate systemic anti-microbiota IgG responses. These include enzyme linked immunosorbent assays (ELISA), immunoblotting, leverage phage immunoprecipitation sequencing (PhIP-Seq) (Vogl et al., 2021) and fluorescence activated cell sorting (FACS). Methods are split into two categories based on whether they investigate low affinity, cross-reactive antibodies for conserved intracellular antigens or high affinity and specificity antibodies for microbe specific outer membrane antigens (Zimmermann et al., 2012). ELISA and immunoblotting can measure serum IgG levels to cell lysates which contain intracellular antigens obtained through the sonication of cells. Alternatively, PhIP-Seq can identity the specific antigen with which serum IgG is reacting by using phage to present libraries of synthetic oligonucleotides encoding microbiota derived peptide antigens (Vogl et al., 2021). ELISA can also measure levels of

serum IgG levels to cell surface antigens by coating plates with intact, whole cells (Haas et al., 2011). Similarly, FACS is a liquid phase assay that can be used to analyse serum IgG response to live cells. The source of antigens or whole cells used for investigating anti-microbiota IgG responses can either be from cells grown in a pure culture or mixed microbial populations from stool samples (Fadlallah et al., 2019). An advantage of using pure cultures is the ability to identify the species/strains serum IgG reacts against and quantify the specific IgGs. However, Harmsen et al. (2012) highlighted the importance of using autologous intestinal microbes, as it was found that where CD patients had higher levels of anti-microbiota IgG, it was due to the composition of microbes present in the stool rather than the composition of anti-microbiota IgG antibodies in sera.

Palm et al. (2014) developed a method called IgA-SEQ, also referred to as 'bug FACS', which identified bacterial taxa from stool that were reactive with secretory IgA. Fadlallah et al. (2019) adapted this method to enable identification of bacterial taxa from stool reactive with serum IgG. Briefly, stool microbes incubated with serum were separated into 'IgG positive' and 'IgG negative' fractions using FACS and 16s rRNA sequencing was performed on each fraction for taxonomic classification. However, 16S rRNA gene sequencing only enables the identification of bacterial taxa reactive with serum IgG, which was insufficient given the aforementioned clinical relevance of anti-fungi serum IgG in CD. Doron et al. (2021) developed this method further, creating multi-kingdom antibody profiling (multiKAP), a method that also detects serum antibody reactivity to fungi within stool samples using fungal specific fluorescent probes and internal transcribed spacer (ITS) rRNA sequencing.

3.1.3 Identifying bacterial and fungal cells during 'bug FACS'

To date analysis of antibody reactivity to intestinal microbes using 'bug FACS' has primarily focussed on the bacterial counterpart. Previous studies prepared stool samples by homogenisation, separation of microbes from debris using centrifugation or filtration and thereafter referred to the cells as 'bacteria' (Fadlallah et al., 2019, Harmsen et al., 2012, Huus et al., 2021, Jackson et al., 2021, Janzon et al., 2019, Liu et al., 2020, Palm et al., 2014, Shapiro et al., 2021, Sugahara et al., 2017, Zeng et al., 2016). This could be because authors preferentially isolated bacteria from stool by using either: 1) low centrifugal speeds that only pelleted larger cells meaning only bacteria were recovered in the supernatant, or 2) by using a filter size that only allowed the passage and therefore recovery of cells as small as bacteria. Interestingly, Doron et al. (2021) used a 35 µm cell strainer to isolate microbes from stool in a study analysing bacteria and fungi, whereas a 70 µm cell strainer was used in studies analysing bacteria only (Huus et al., 2021, Jackson et al., 2021). Following filtration to remove stool debris, Doron et al. (2021) performed centrifugation at a speed of 900 x g for the separation of bacterial cells from fungal cells (recovered from the supernatant and pellet respectively). Studies focussing on bacterial cells used lower centrifugal speeds, ranging from 50 to

700 x g, to separate bacterial cells in the supernatant from stool debris in the pellet (Harmsen et al., 2012, Liu et al., 2020, Palm et al., 2014, Shapiro et al., 2021, Sugahara et al., 2017).

Another way in which previous studies utilising 'bug FACS' focussed on bacterial cells could be through the use of bacterial specific parameters on FACS. The identification of bacterial cells isolated from stool sample using FACS has been performed in previous studies using four different approaches: 1) use of light scatter properties to discriminate cellular events from background noise (Janson et al., 2019, Liu et al., 2020, Palm et al., 2014, Shapiro et al., 2021, Sugahara et al., 2017), 2) use of a permeable nucleic acid stain to identify live and dead cells (Doron et al., 2021, Huus et al., 2021, Jackson et al., 2021), 3) use of an impermeable nucleic acid stain which stains dead cells allowing identification of live cells (Harmsen et al., 2012, Zeng et al., 2016) and 4) use of primary amine stain to monitor cell proliferation (Fadlallah et al., 2019). In contrast, the identification of fungal cells isolated from stool has been less commonly performed (Doron et al., 2021, Moreno-Sabater et al., 2020). Doron et al. (2021) used SYBR™ green I nucleic acid gel stain and calcofluor white stain, a fungal specific extracellular stain that binds chitin and cellulose, for the identification of fungi. Whereas Moreno-Sabater et al. (2020) used calcofluor white stain and light scatter properties.

The structure of the cell wall is different in Gram-positive bacteria, Gram-negative bacteria, and fungi (Huang et al., 2008, Garcia-Rubio et al., 2020). A crucial step in DNA extraction is the disruption of the cell wall using mechanical, enzymatic or chemical lysis. The efficiency of cell lysis of each technique varies depending on the structure of the cell wall. DNA extraction kits fall into a further two categories: 1) extraction of DNA from a small concentration of cells from the same taxonomic domain, 2) extraction of DNA from biological material which is high in cell number and contains more than one taxonomic domain. Previous 'bug FACS' studies focussing on bacteria have used QIAGEN's DNeasy® PowerSoil® HTP 96 kit (Khan et al., 2019), MO BIO's PowerSoil®-htp 96-well soil DNA isolation kit (Bunker et al., 2017, Bunker et al., 2015, Janzon et al., 2019) or used phenol-chloroform extraction (Jackson et al., 2021, Palm et al., 2014, Shapiro et al., 2021). Whereas QIAGEN's QIAamp® DNA mini kit (Doron et al., 2021) was used when studying bacteria and fungi. With the exception of phenol-chloroform extraction, all of the methods utilised were kits designed to isolate DNA from a large number of cells within a biological sample, despite the number of cells per fraction collected ranging from 5×10^4 to 2×10^6 cells only (Fadlallah et al., 2019, Huus et al., 2021, Janzon et al., 2019, Palm et al., 2014, Shapiro et al., 2021). Based on the average bacterial genome size (Nayfach and Pollard, 2015), 5×10^4 to 2×10^6 cells would extract 0.27 ng and 10.8 ng of DNA respectively with 100 % DNA extraction efficiency. However, DNA yield recovered using different DNA extraction procedures varies (Fiedorová et al., 2019, Huseyin et al., 2017). Following DNA extraction, taxonomic classification of bacteria and fungi when performing 'bug FACS' was

carried out by sequencing the 16S and ITS rRNA marker genes respectively (Doron et al., 2021). However, 16S rRNA and ITS rRNA sequencing are limited due to their ability to only resolve sequence identification to the genus-level, whereas whole genome shotgun sequencing (WGS) enables species level taxonomic identification and profiling of the functional potential of microbial communities (Ma et al., 2014).

Therefore, the following elements of 'bug FACS' could be optimised for the analysis of both bacterial and fungal cells: 1) isolation of cells from stool debris, 2) FACS identification and 3) DNA extraction.

3.1.4 Confounding variables of 'bug FACS'

The microbial load in stool samples varies between individuals (Vandeputte et al., 2017). If two individuals have the same levels of serum antibody reactive to the microbiome but a different microbial load, the individual with the lower microbial load would have a higher proportion of microbes coated with antibody when incubated with serum. This means that microbial load is a confounding variable and therefore it was imperative to ensure serum was incubated with consistent microbial concentrations. This requires quantifying microbial load in stool samples. Methods to quantify bacterial or fungal cells in pure cultures include counting colony forming unit (CFU), measuring optical density, q-PCR, counting cells using a microscope with a hemacytometer and FACS enumeration (Hazan et al., 2012). CFUs and optical density cannot be used to quantify the total number of cells in mixed microbial populations, such as those extracted from stool samples, because different species require different culture conditions and the optical densities change with different species. FACS and q-PCR have previously been used for the quantification of bacteria in stool (Galazzo et al., 2020), however, q-PCR cannot be used to simultaneously quantify bacteria and fungi as it requires the use of a marker gene.

3.1.5 Aims and objectives

The primary aim of the work discussed in this chapter was to develop a protocol, based on 'bug FACS', able to identify fungal and bacterial microbes, at the species level, reactive with serum IgG (**Figure 3.1**) with the following objectives:

1. Optimise the isolation of bacteria and fungi from stool samples
2. Optimise the detection of bacterial and fungal cells by flow cytometry
3. Optimise the incubation procedure for serum IgG binding to stool microbes
4. Determine the optimal number of 'IgG positive' and 'IgG negative' cells to be collected during cell sorting
5. Optimise DNA extraction from bacterial and fungal cells

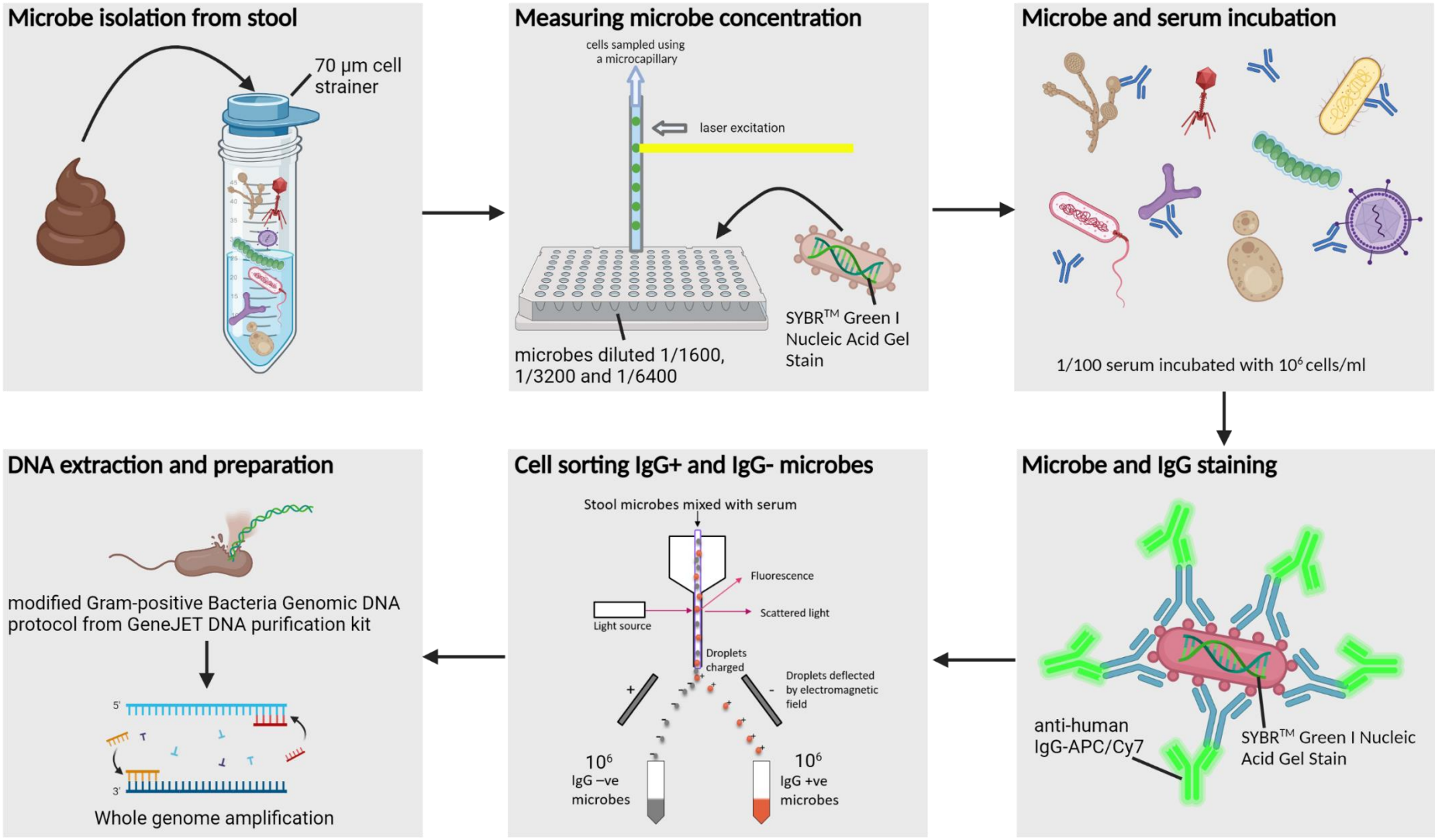
Microbe isolation from stool
70 µm cell strainer
Measuring microbe concentration
cells sampled using a microcapillary
laser excitation
SYBR™ Green I Nucleic Acid Gel Stain
microbes diluted 1/1600, 1/3200 and 1/6400
Microbe and serum incubation
1/100 serum incubated with 10⁶ cells/ml
Microbe and IgG staining
anti-human IgG-APC/Cy7
SYBR™ Green I Nucleic Acid Gel Stain
Cell sorting IgG+ and IgG- microbes
Stool microbes mixed with serum
Fluorescence
Scattered light
Light source
Droplets charged
Droplets deflected by electromagnetic field
10⁶ IgG –ve microbes
10⁶ IgG +ve microbes
DNA extraction and preparation
modified Gram-positive Bacteria Genomic DNA protocol from GeneJET DNA purification kit
Whole genome amplification

← *Figure 3.1: Optimised protocol for cell sorting 'IgG positive' stool microbes from IgG negative stool microbes.* *Stool microbes were diluted 1 % w/v, homogenised, and filtered through a 70 µm cell strainer. Microbes were stained with SYBR™ green I nucleic acid gel stain, diluted 1 in 1600, 1 in 3200 and 1 in 6400 and concentration of microbes was measured using the Guava® easyCyte™ HT system. Microbes were resuspended to 10^6 cells/ml and incubated with 1 in 100 complement inactivated serum. Microbes were stained for identification using 10^{-3} SYBR™ green I nucleic acid gel stain and anti-human IgG-APC/Cy7. 10^6 'sybr green high' cells bound by IgG ('IgG positive') and not bound by IgG ('IgG negative') were collected using the Sony SH800S cell sorter. DNA was extracted using the modified Gram-positive bacteria genomic DNA protocol from the GeneJET genomic DNA purification kit and DNA was amplified using QIAGEN's REPLI-g advanced DNA single cell kit to ensure sufficient DNA quantity for shotgun sequencing. Figure created with BioRender.com.*

3.2 METHODS

3.2.1 Study population

Stool and serum samples used for method development were acquired from the study population and were collected and processed as described in **chapter 2 section 2.6**.

3.2.2 Microbe isolation from stool

3.2.2.1 Centrifugation

100 mg ±10 mg frozen stool aliquots were thawed on ice and diluted 1 % w/v with FACS buffer (0.22µm-filter sterilised PBS + 0.1 % w/v bovine serum albumin (BSA) fraction V (Sigma-Aldrich)). Samples were homogenised using a Kimble™ Kontes™ Pellet Pestle™ Cordless Motor and then centrifuged at 300 x g for 5 minutes and the supernatant was recovered.

3.2.2.2 Filtration

100 mg ±10 mg frozen stool aliquots were thawed on ice and diluted 1 % w/v with FACS buffer. Samples were homogenised using a Kimble™ Kontes™ Pellet Pestle™ Cordless Motor and then filtered through a 70 µm cell strainer (Falcon™).

3.2.3 Complement inactivation of serum

Aliquots of serum were thawed and heated to 56 °C for 30 minutes and then centrifuged at 16,100 x g for 5 minutes. The supernatant was recovered.

3.2.4 Cell culture

3.2.4.1 Bacteria

Bifidobacterium bifidum and *Bifidobacterium longum* were cultured in BD Difco™ Lactobacilli MRS broth (Fisherscientific) + 50 mg/l mupirocin (USP) pure, pharma grade (PanReac AppliChem) + 0.5 g/l cysteine (L- Cysteine Hydrochloride, Sigma Life Science) at 37 °C for 3 days under anaerobic conditions. Cell concentrations were calculated using the growth of colony forming units on solid agar BD Difco™ Lactobacilli MRS broth (Fisherscientific) + FORMEDIUM agar + 50 mg/l mupirocin (USP) pure, pharma grade (PanReac AppliChem) + 0.5g/l cysteine (L- Cysteine Hydrochloride, Sigma Life Science), at 37 °C for 2 days under anaerobic conditions.

E. coli was cultured aerobically in a shaking incubator in lysogeny broth + 100 mg/ml ampicillin (Sigma Aldrich) at 37 °C, 889.4 x g, overnight. To calculate cell concentration, the optical density of the culture was measured. An $OD_{600\ nm}$ of 1.0 was equivalent to 8 x 10^8 cells/ml.

Bacteroides fragilis was cultured anaerobically in *Bacteroides* phage recovery medium (BPRM) broth (**Table 3.1**) at 37 °C overnight. To calculate cell concentration, the optical density of the culture was measured. An $OD_{600\,nm}$ of 1.0 was equivalent to 1.4 x 10^9 cells/ml.

Bacteroides thetaiotaomicron was cultured anaerobically in brain heart infusion salt broth + 5 µg/ml erythromycin + 50 ug/ml gentamycin at 37 °C overnight. To calculate cell concentration, the optical density of the culture was measured. An $OD_{600\,nm}$ of 1 was equivalent to 1 = 1.4 x 10^9 cells/ml.

Bacillus subtilis was cultured aerobically in a shaking incubator in lysogeny broth at 37 °C, 567.94 x g, overnight. Cell concentration was measured using a hemacytometer.

Prior to use in downstream experiments, culture medias were washed from bacterial cells with PBS by centrifugation at 6000 x g for 10 minutes.

Table 3.1: Constituents of the Bacteroides phage recovery medium (BPRM) broth. *All reagents except for those highlighted grey were added before autoclaving. Reagents highlighted in grey were filter sterilised and added to the medium after autoclaving.*

Reagent	**Concentration**
Peptone	10 g/l
Tryptone	10 g/l
Yeast Extract	2 g/l
NaCl	5 g/l
L-cysteine	0.5 mg/l
Glucose	1.8 g/l
$CaCl_2$	0.45 mM
Na_2CO_3	25 mM/l
Hemin (dissolved with 1 M/L NaOH)	0.001 % w/v

3.2.4.2 Yeast

Candida albicans, Candida glabrata and *S. cerevisiae* were cultured at 37 °C in Sabouraud dextrose broth (40 g/l dextrose, 10 g/l peptone) under aerobic conditions for 3 days. Cell concentrations were measured using a hemacytometer.

Prior to use in downstream experiments, the culture media was washed from 1 ml aliquots of yeast cells with PBS by centrifugation at 800 x g for 5 minutes.

3.2.5 Guava® easyCyte™ HT system

The Guava® easyCyte™ HT system is a benchtop FACS designed to be used for accurate absolute cell counting. It was equipped with a 488 nm (blue) laser and had the following bandpass filters and their respective detectors: 488/16 (Side Scatter), 525/30 (Green-B), 583/26 (Yellow-B), 695/50 (Red-B). Prior to each experiment, the Guava® easyCyte™ HT system was cleaned following manufacturer's instructions and calibrated using the Guava® easyCheck™ kit. Then the threshold parameter was set on side scatter (SSC) using FACS buffer. Forward scatter (FSC) and SSC gain were adjusted using unstained stool microbes and the gain for the Green-B parameter was adjusted using stool microbes stained with SYBR™ green I nucleic acid gel stain (Thermofischer Scientific). Prior to sample acquisition, cell suspensions were diluted using FACS buffer to ensure the concentration did not exceed 250 cells/µl. A minimum of 10^4 events were acquired for downstream analysis using Guava® Suite Software version 3.3.

3.2.5.1 Comparing light scatter properties of yeast, bacteria, and stool samples

Pure cultures of *B. bifidum* and *E. coli* were grown, counted, and washed using methods described in **section 3.2.4.1**. Pure cultures of *C. albicans* and *C. glabrata* were grown, counted, and washed using methods described in **section 3.2.4.2**. Bacteria and yeast isolates were resuspended to a concentration of 2.5 x 10^6 cells/ml. Microbes were isolated from stool samples using filtration (see **section 3.2.2.2**) and then diluted 5000-fold. Following set up of the Guava® easyCyte™ HT system and sample acquisition (explained in **section 3.2.5**), FSC and SSC were used to compare the size and internal complexity, respectively, of pure bacteria populations, yeast populations and mixed microbial populations isolated from stool.

3.2.5.2 Stool microbe concentration optimisation

An optimal stool dilution was defined by the concentration of measured 'sybr green' events halved when the dilution of stool microbes doubled. At high concentrations of stool microbes this pattern would not be seen as multiple cells could pass through the laser simultaneously and register as a single event, meaning the number of events the machine can register reaches saturation. At low concentrations replicates could have high variation. Microbes were extracted from a single homogenised stool sample using filtration (see **section 3.2.2.2**). The microbial suspension was diluted 1 in 200 with FACS buffer, followed by two-fold serial dilutions. 200 µl of each of the following dilutions were plated in triplicate and incubated with 10 µl of 1:100 SYBR™ green I nucleic acid gel stain for 30 minutes: 1 in 400, 1 in 800, 1 in 1600, 1 in 3200, 1 in 6400, 1 in 12800, 1 in 25600, 1 in 51200, 1 in 102400 and 1 in 204800. The concentration of microbes at each stool dilution was measured using the Guava® easyCyte™ HT system. The optimal stool dilutions were determined through performing linear regression analysis on every combination of three dilutions.

3.2.5.3 Measuring microbe concentration in stool suspension

Microbes were isolated from stool samples using filtration (see **section 3.2.2.2**). Filtered microbial suspensions were diluted 1 in 1600, 1 in 3200 and 1 in 6400. 200 µl of each dilution was plated in triplicate and incubated with 10 µl of 1 in 100 SYBR™ green I nucleic acid gel stain (Thermofischer Scientific) for 30 minutes, prior to sample acquisition. To determine the concentration of microbes acquired by the Guava® easyCyte™ HT system, data was analysed according to the gating strategy (**Figure 3.2**). The original concentration of microbes in the homogenised stool suspension was calculated using **Equation 3.1**.

3.2.6 BD LSRFortessa™

The BD LSRFortessa™ equipped with BD FACS diva software version 7.0 was used for microbial FACS experiments. The laser and filters on the BD LSRFortessa™ are described in **Table 3.2**. Prior to each experiment, the threshold and voltages on the BD LSRFortessa™ were optimised. The threshold was set on SSC using FACS buffer. The FSC and SSC voltages were set using microbial samples. When required, the voltage on the blue (488 nm) laser was set using microbes stained with SYBR™ green I nucleic acid gel stain and the voltage on the red (633 nm) laser was set using either anti-human IgG-APC/Cy7 antibody stained UltraComp ebeads™ Compensation beads (Invitrogen) or anti-human IgA-APC antibody stained UltraComp ebeads™ Compensation beads and compensation for spectral overlap between channels was calculated. Prior to sample acquisition, cell suspensions were diluted using FACS buffer to ensure the event rate did not exceed 1 x 10^3 events per second. A minimum of 1 x 10^4 events were acquired for downstream analysis using the software FlowJo™ v10.7.1.

3.2.6.1 Centrifuged vs filtered

The BD LSRFortessa™ was used to profile the FSC and SSC of microbes isolated from stool by centrifugation (**3.2.2.1**) and microbes isolated from stool by filtration (**3.2.2.2**). 1 % w/v microbial suspensions were diluted 100-fold in FACS buffer and then fixed with 1 % paraformaldehyde (PFA) (Santa Cruz Biotechnology). Following set up of the BD LSRFortessa™ and sample acquisition (explained in **section 3.2.6**), FSC was used to compare the cells isolated from centrifuged and filtered stool microbes, as FSC enables the discrimination of cells by size.

3.2.6.2 Optimising SYBR™ green I nucleic acid gel stain concentration

B. fragilis was grown, counted and washed using methods described in **section 3.2.4.1**. Cells were resuspended to 1 x 10^6 cells/ml and incubated with SYBR™ green I nucleic acid gel stain diluted 1 in 50, 1 in 100 and 1 in 1000 for 30 minutes in the dark at 20 °C, then fixed with 1 % PFA for acquisition and analysis on the BD LSRFortessa™.

3.2.6.3 Comparing cellular stains for fungal identification

Pure cultures of two strains of *S. cerevisiae* were grown, counted and washed using methods described in **section 3.2.4.2**. Microbes from two stool samples were isolated (see **section 3.2.2.2**) and the cell concentration was measured (see **section 3.2.5.3**). Yeast isolates and stool microbes were resuspended to 1 x 10^6 cells/ml then stained with 10^{-3} SYBR™ green I nucleic acid gel stain or 25 µM calcofluor white (Biotium) for 30 minutes in the dark. Cells were then fixed with 1 % PFA for acquisition and analysis on the BD LSRFortessa™.

3.2.6.4 Serum concentration optimisation

Serum samples were complement inactivated (see **section 3.2.3**) and diluted 1 in 50, 1 in 100, 1 in 200, 1 in 400 and 1 in 800 with FACS buffer. Microbes were isolated from stool samples using filtration (see **section 3.2.2.2**) and quantified (see **section 3.2.5.3**). 200 µl of 1 x 10^6 cells/ml stool microbes were incubated with 500 µl of each serum dilution for 30 minutes at 20 °C. Samples were centrifuged for 5 minutes at 13,400 x g and resuspended in 100 µl of FACS buffer. 50 µl of each reaction was incubated with anti-human IgG-APC/Cy7 (Biolegend UK Ltd) and 10^{-3} SYBR™ green I nucleic acid gel stain. The remainder of each reaction was incubated with APC/Cy7 mouse IgG2a, κ isotype control antibody (Biolegend UK Ltd) and 10^{-3} SYBR™ green I nucleic acid gel stain. Samples were incubated with stains for 30 minutes in the dark at 20 °C, then fixed with 1 % PFA. Set up and sample acquisition on the BD LSRFortessa™ was undertaken as described in **section 3.2.6**. Results were normalised by subtracting the isotype control value from the values of corresponding samples.

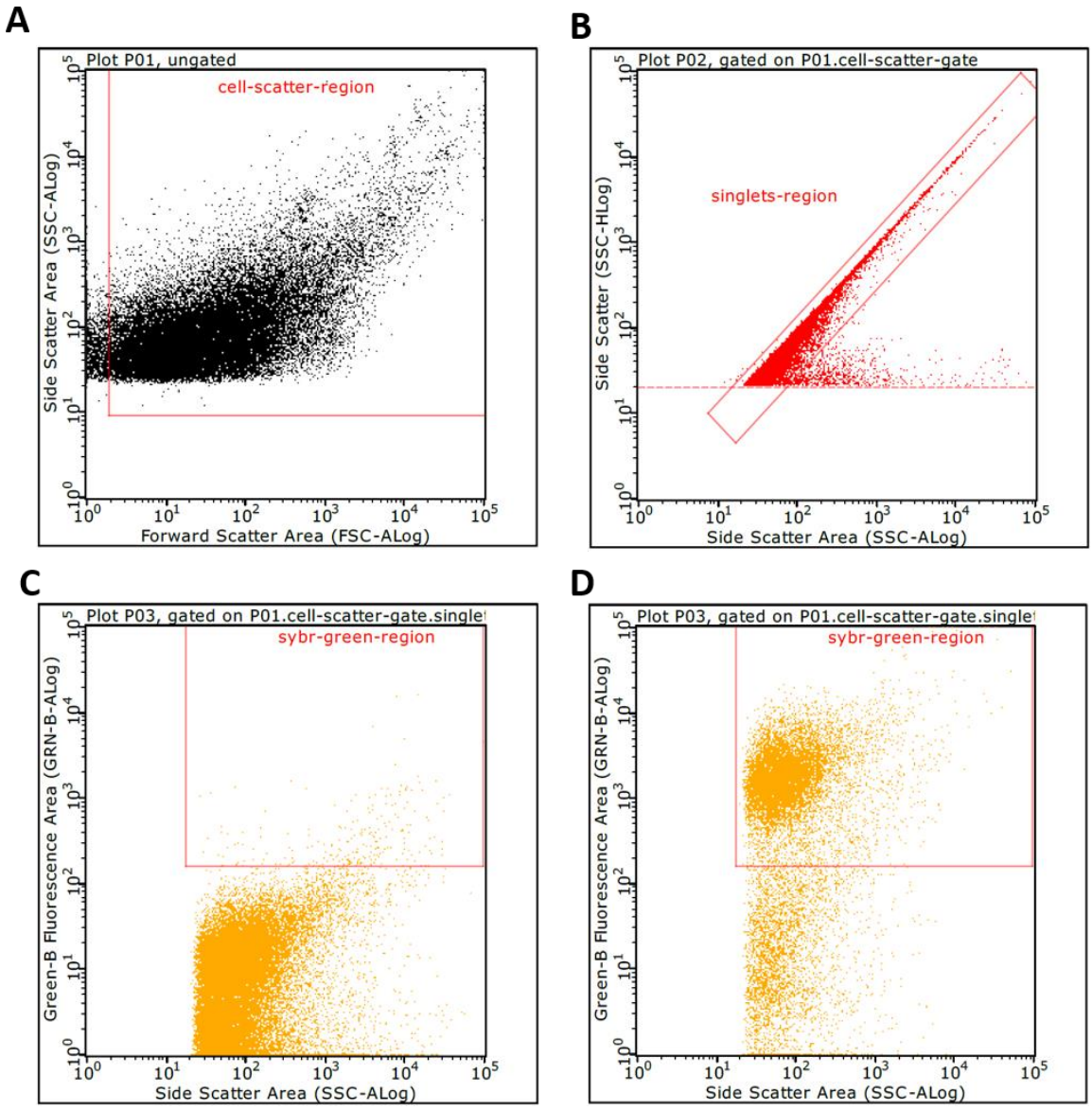

Figure 3.2: Stool microbe quantification gating strategy. *Representative data of microbes isolated from stool samples. Microbes isolated from stool samples were stained with SYBR™ green I nucleic acid gel stain and 'sybr green' events were counted on the Guava® easCyte HT system in triplicate. At least 1 x 10^4 'sybr green' events were acquired. Gates were drawn using InCyte 3.3 software. A) FSC versus SSC plot allowed cells to be gated and debris and noise to be excluded based on light scatter properties of cells. B) Events from the cell scatter region were plotted as SSC-A versus SSC-H to gate singlets. C) A non-stained sample was used to set the 'sybr green region' on singlets. D) An example of a stained sample with events falling into the 'sybr green region' which was used to calculate the concentration of microbes per stool sample.*

Equation 3.1: Formula for calculating cell concentration in a liquid suspension

$$concentration\ (cells\ ml^{-1}) = measured\ concentration\ \times \left(\frac{210}{200}\right) \times dilution\ factor$$

Table 3.2: Laser and filter configurations of the BD LSRFortessa™.

Laser (nm)	Long Pass Filter	Band Pass Filter
UV (355)	505	530/30
	NA	379/28
Violet (405)	750	780/60
	685	705/70
	630	660/20
	595	610/20
	505	552/50
	NA	450/45
Blue (488)	670	695/40
	NA	552/50
	NA	530/30
Yellow/Green (561)	750	780/60
	635	670/30
	600	610/20
	NA	582/12
Red (633)	750	780/60
	685	730/45
	NA	670/14

3.2.7 Sony SH800S cell sorter

The Sony SH800S cell sorter was operated within a category II biosafety cabinet for aerosol management. The Sony SH00S cell sorter has four excitation lasers: 488 nm (blue), 405 nm (violet), 638 nm (red) and 651 nm (yellow/green). The detectors and filters are described in **Table 3.3**. Sterile deionised water was used for sheath fluid. The Sony SH800S cell sorter set up was done according to the manufacturer's instructions. In brief, 'automated alignment and sort setup' was done to align the 100 µm sorting chip and to check the fluidics for sheath fluid droplet formation, followed by 'autocalibration' using the sort calibration beads (Sony). Prior to sample acquisition, the system was cleaned using 1 % sodium hypochlorite. The threshold parameter was then set on back scatter (BSC)

using FACS buffer, FSC and BSC gain were adjusted using unstained stool microbes, and the gain for FL2 detector was adjusted using stool microbes stained with SYBR™ green I nucleic acid gel stain.

Sample tubes were maintained at 4 °C and the agitation setting was selected to ensure a homogenous cellular suspension. Collection tubes were maintained at 4 °C.

3.2.7.1 Collecting known quantities of microbes from centrifuged and filtered stool

Microbes were isolated from stool by centrifugation (see **3.2.2.1**) and filtration (see **3.2.2.2**) and cell concentrations were measured (see **3.2.5.3**). Cells were resuspended to 1 x 10^7 cells/ml prior to acquisition. Set up of the Sony SH800S cell sorter was performed as described in **section 3.2.7**. The gating parameters (**Figure 3.3**) were used to collect 10^3, 10^4, 10^5, 10^6, 2.5 x 10^6 and 5 x 10^6 microbes isolated from stool by centrifugation and filtration. After collection cells were snap frozen at -20 °C.

3.2.7.2 Cell sorting 'sybr green high', 'sybr green low' and 'all' microbes from stool

Microbes were isolated from stool using filtration (see **3.2.2.2**) and the concentration of cells was measured (see **3.2.5.3**). Cells were resuspended to 1 x 10^6 cells/ml before incubation with 10^{-3} SYBR™ green I nucleic acid gel stain for 30 minutes in the dark at 20 °C. Cells were resuspended to 1 x 10^7 cells/ml prior to acquisition. Set up of the Sony SH800S cell sorter was performed as described in **section 3.2.7**. The gating parameters (**Figure 3.4**) were used to collect approximately 10^6 cells in the 'sybr green high' gate, 'sybr green low' gate and 'all' gate. After collection cells were snap frozen at -20 °C.

Table 3.3: Sony SH800S cell sorter filter configurations and their respective detectors.

Detector	Long Pass Filter	Band Pass Filter
FL1	487.5	450/50
FL2	487.5	525/50
FL3	561.0	600/60
FL4	685.0	665/30
FL5	685.0	720/60
FL6	752.0	785/60

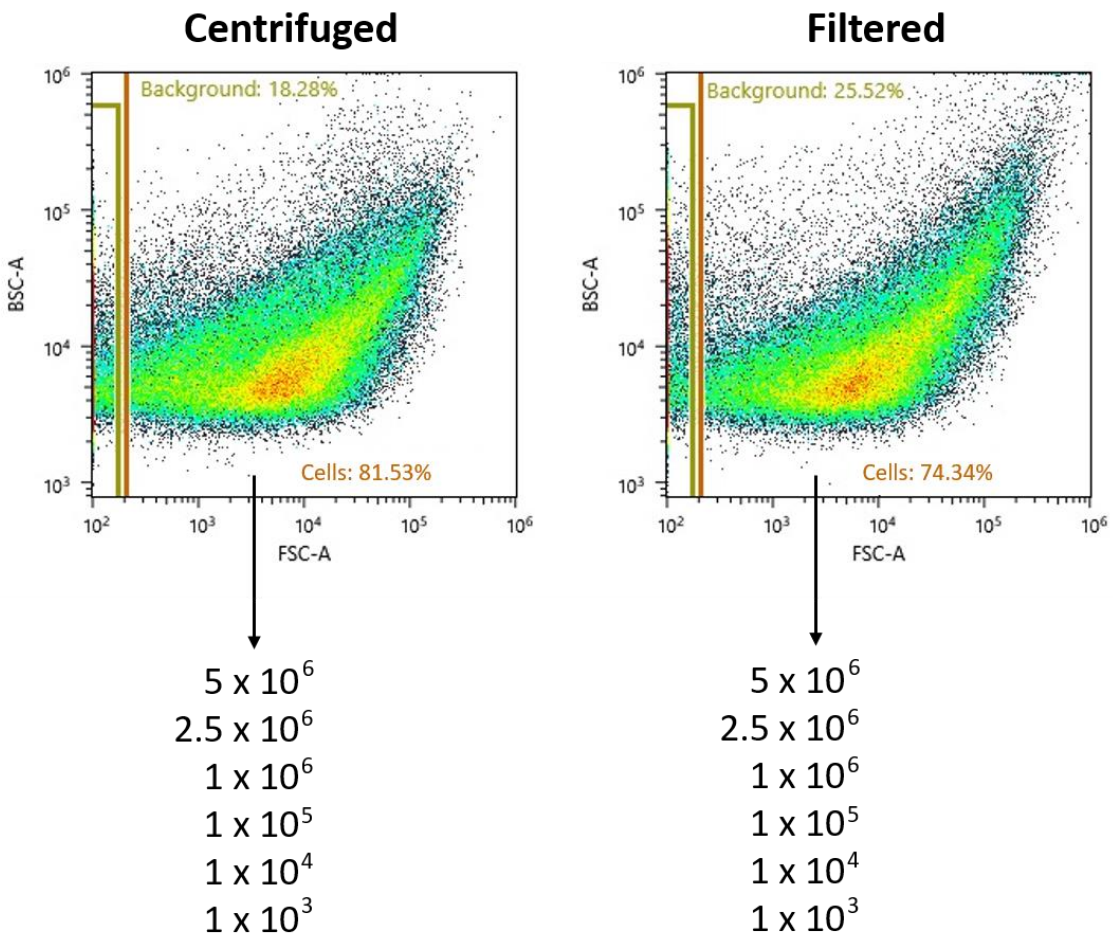

Figure 3.3: Gating strategy for optimising stool microbe isolation protocol. *Prior to microbe acquisition a buffer only control was acquired on the Sony SH800S cell sorter to set a background noise gate on forward scatter (FSC) versus back scatter (BSC) plot. Microbes were acquired on the Sony SH800S cell sorter and a 'cells' gate was drawn around events with a larger FSC than background noise. 1 x 10^3, 1 x 10^4, 1 x 10^5, 1 x 10^6, 2.5 x 10^6 and 5 x 10^6 events acquired from centrifuged and filtered stool samples falling in the 'cells' gate were collected for downstream analysis.*

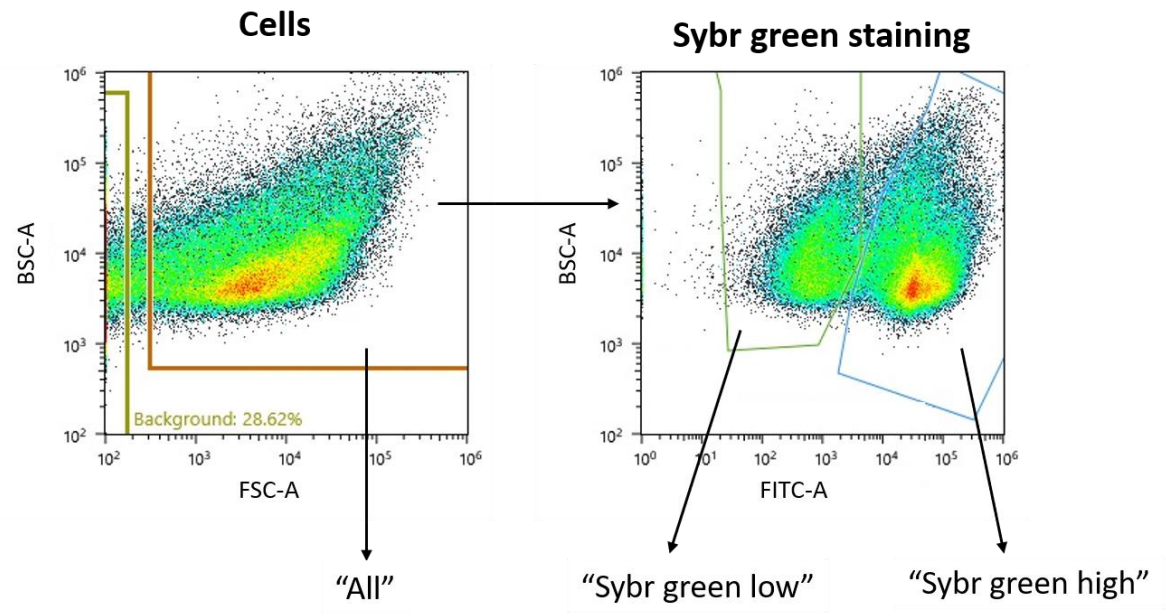

Figure 3.4: Gating strategy for the separation and collection of 'sybr green high', 'sybr green low' and 'all' microbes. *A buffer only control was first acquired on the Sony SH800S cell sorter to set a background noise gate on the forward scatter (FSC) versus back scatter (BSC) plot. Microbes were acquired and a 'cells' gate was drawn. Events falling in the 'cells' gate were plotted on BSC versus FITC and microbes stained with SYBR™ green I nucleic acid gel stain were used to draw a gate on 'sybr green high' and 'sybr green low' populations. 'All' microbes were acquired from the 'cells gate', 'sybr green high' microbes were acquired from the 'sybr green high' gate and 'sybr green low' microbes were acquired from the 'sybr green low' gate.*

3.2.8 DNA extraction

DNA extraction kits fall into two categories: 1) DNA extraction from a small concentration of cells from the same taxonomic domain, 2) DNA extraction from biological material which is high in cell number and contains more than one taxonomic domain.

3.2.8.1 Gram-positive bacteria genomic DNA purification protocol

The Gram-positive bacteria genomic DNA purification protocol from the GeneJET DNA genomic DNA purification kit (Thermoscientific) was designed to extract DNA from up to 2 x 10^9 Gram-positive bacterial cells. The protocol was followed according to manufacturer's guidelines: cells were pelleted by centrifuging for 10 minutes at 5000 x g. The pellet was resuspended in 180 µl of Gram-positive bacteria lysis buffer (20 mM Tris-HCl, pH 8.0, 2 mM EDTA, 1.2 % Triton X-100, 20 mg/ml lysozyme) and incubated for 30 minutes at 37 °C. 200 µl of lysis solution and 20 µl of proteinase K were then added and incubated at 56 °C for 30 minutes and vortexed at 10-minute intervals. 20 µl of RNase A solution was added and incubated for 10 minutes at 20 °C. 400 µl of 50 % ethanol was added, the mixture was vortexed and then transferred to a GeneJET genomic DNA purification column inserted into a collection tube. The column was centrifuged for 1 minute at 6000 x g and then placed into a new collection tube. The column was washed once with 500 µl of wash buffer I by centrifugation for 1 minute at 8000 x g and then once with 500 µl of wash buffer II by centrifugation for 3 minutes at 12000 x g. The column was then transferred to a sterile 1.5 ml microcentrifuge tube. DNA was eluted into the microcentrifuge tube by the addition of 200 µl of elution buffer to the membrane of the column which was then incubated for 2 minutes at 20 °C and centrifuged for 1 minute at 8000 x g.

3.2.8.2 Gram-negative bacteria genomic DNA purification protocol

The Gram-negative bacteria genomic DNA purification protocol from the GeneJET genomic DNA purification kit was designed to extract DNA from up to 2 x 10^9 Gram-negative bacterial cells. Briefly, cells were pelleted by centrifugation for 10 minutes at 5000 x g. The pellet was resuspended in 180 µl of digestion solution and 20 µl of proteinase K solution, vortexed and then incubated at 56 °C for 30 min, vortexing at 10-minute intervals. This was then incubated at 20 °C for 10 minutes with 20 µl of RNase A solution. 200 µl of lysis solution was added and the sample was vortexed for 15 seconds. 400 µl of 50 % ethanol was added, the mixture was vortexed and then transferred to a GeneJET genomic DNA purification column inserted into a collection tube. The column was centrifuged for 1 minute at 6000 x g and placed into a new collection tube, then washed once with 500 µl of wash buffer I by centrifugation for 1 minute at 8000 x g. The second wash step was with 500 µl of wash buffer II by centrifugation for 3 minutes at 12000 x g. The column was then transferred to a sterile 1.5 ml microcentrifuge tube. DNA was eluted into the microcentrifuge tube

by the addition of 200 µl of elution buffer to the membrane of the column which was then incubated for 2 minutes at 20 °C and centrifuged for 1 minute at 8000 x g.

3.2.8.3 Modified Gram-positive bacteria genomic DNA purification protocol

The Gram-positive bacteria genomic DNA purification protocol (as described in **3.2.8.1**) was performed with the modifications described in **Table 3.4**.

Table 3.4: Modification of the Gram-positive bacteria genomic DNA purification protocol from the GeneJET genomic DNA purification kit. *The Gram-positive bacteria genomic DNA purification protocol was optimised by altering the Gram-positive bacterial lysis buffer and extending the length of time for chemical and enzymatic lysis.*

Step	Manufacturer's instructions	Modification
Composition of Gram-positive bacteria lysis buffer	20 mM Tris-HCl, pH 8.0, 2 mM EDTA, 1.2 % Triton X-100, lysozyme 20 mg/ml.	20 mM Tris-HCl, pH 8.0, 2 mM EDTA, 1.2 % Triton X-100, lysozyme 20 mg/ml, achromopeptidase 0.52 kU/ml.
Incubation period with Gram-positive bacteria lysis buffer	30 minutes	60 minutes
Incubation period with lysis solution and proteinase K	30 minutes	50 minutes

3.2.8.4 QIAamp® PowerFecal® Pro DNA Kit

The QIAamp® PowerFecal® pro DNA kit (QIAGEN) was designed to extract DNA from up to 250 mg of stool. The kit was followed according to manufacturer's guidelines. Cells for DNA extraction were mixed with 800 µl of solution CD1 in the PowerBead pro tube by vortexing. The tube was vortexed at maximum speed for 10 minutes and then centrifuged at 15,000 x g for 1 minute. The supernatant was transferred to a clean 2 ml microcentrifuge tube. 200 µl of solution CD2 was added, vortexed for 5 seconds and then centrifuged at 15,000 x g for 1 minute. The supernatant was transferred to a clean 2 ml microcentrifuge tube and mixed with 600 µl of solution CD3 by vortexing for 5 seconds and then 650 µl was transferred onto an MB spin column. This was centrifuged at 15,000 x g for 1 minute, the flow-through was discarded and then centrifugation was repeated. The MB spin column was then transferred to a clean 2 ml collection tube. 500 µl of solution EA was added to the MB spin column and centrifuged at 15,000 x g for 1 minute and the flow-through was discarded. 500 µl of solution C5 was added and the MB spin column was centrifuged at 15,000 x g for 1 minute, before

being placed in a new 2 ml collection tube. After centrifugation at 16,000 x g for 2 minutes, the MB spin column was transferred to a 1.5 ml elution tube. DNA was eluted into the elution tube by the addition of 50 µL of solution C6 which was centrifuged for 1 minute at 15,000 x g.

3.2.8.5 FastDNA™ Spin Kit for Soil

The FastDNA™ spin kit for soil (MP Bio) was designed to extract DNA from up to 500 mg of soil. The kit was used according to manufacturer's guidelines. Cells, 978 µl sodium phosphate buffer and 122 µl MT buffer were added to a lysing matrix E tube, then vortexed on the FastPrep instrument for 40 seconds at speed setting 6.0. Then the lysing matrix E tube was centrifuged at 14,000 x g for 15 minutes. The supernatant was mixed with 250 µl protein precipitation solution in a clean 2 ml microcentrifuge tube by inverting 10 times. This was then centrifuged at 14,000 x g for 10 minutes and the supernatant was transferred to a 15 ml tube and mixed with 1 ml binding matrix solution by inverting for 2 minutes. Then the 15 ml tube was left for 3 minutes to allow the silica matrix to settle. 500 µl of the supernatant was removed and the binding matrix was resuspended in the remaining supernatant. 600 µl of the mixture was transferred to a SPIN™ filter and centrifuged at 14,000 x g for 1 minute. The catch tube was emptied, and the remaining mixture was transferred to the SPIN™ filter and centrifuged at 14,000 x g for 1 minute. The pellet formed on the membrane of the SPIN™ filter was resuspended in 500 µl of SEWS-M. This was then centrifuged twice at 14,000 x g for 5 minutes, emptying the catch tube between spins. The SPIN™ filter was transferred to a clean 1.5 ml Eppendorf DNA LoBind® tube and air dried for 5 minutes at 20 °C. The binding matrix was then resuspended with 50 µl of DNase/pyrogen-free water, incubated at 20 °C for 5 minutes and then the DNA was eluted by centrifugation at 14,000 x g for 1 minute.

3.2.9 DNA quantification

Microbial DNA quantities were measured on a Qubit™ 4 Fluorometer (Thermofischer Scientific) either using the Qubit™ dsDNA broad range assay kit or the Qubit™ dsDNA high sensitivity assay kit, depending on whether the quantity of DNA present was expected to be above or below 100 ng/µl respectively.

3.2.9.1 DNA extraction efficiency

The amount of DNA expected from a given number of cells was calculated using **Equation 3.2**.

Equation 3.2: Formula for calculating DNA mass within a known cell quantity. *Where x = cell number, n = genome length, 650 g/mol = average mass of 1 base pair of double stranded DNA.*

$$DNA\ mass\ (ng) = \frac{x\ \times (n\ \times 650\ gram\ mol^{-1}) \times (1\ \times\ 10^{9}\ ng\ g^{-1})}{6.022\ \times 10^{23}\ gram\ mol^{-1}}$$

The efficiency of DNA extraction was calculated using **Equation 3.3**.

Equation 3.3: Formula for calculating DNA extraction efficiency.

$$DNA\ extraction\ efficiency\ (\%) = \left(\frac{amount\ of\ DNA\ extracted\ (ng)}{expected\ amount\ of\ DNA\ extracted\ (ng)}\right) \times 100$$

3.2.10 DNA precipitation

Glycogen (Thermoscientific) was used to precipitate DNA from diluted solutions, following the manufacturer's protocol. First, 1 in 10 volume of 3 M sodium acetate, pH 5.2, was added to the nucleic acid solution, then glycogen was added to a final concentration of 1 µg/µl and then 1 volume of isopropanol was added. The solution was mixed and incubated for 1 hour at -20 °C before centrifuging at 12,000 x g at 4 °C for 15 minutes. Supernatant was discarded and the pellet was air dried for 10 minutes, then dissolved in 4 µl of TE buffer, pH 8.

3.2.11 Whole genome amplification

The REPLI-g advanced DNA single cell kit (QIAGEN) was used to perform whole genome amplification (WGA) on precipitated DNA. 2.5 µl of precipitated DNA was mixed with 2.5 µl of buffer D1 in a 0.2 ml reaction tube by vortexing before incubation at 20 °C for 3 minutes. 5 µl of buffer N1 was added, mixed by vortexing, and then stored on ice. Then 40 µl of master mix (9 µl H_2O sc + 29 µl REPLI-g advanced sc reaction buffer + 9 µl REPLI-g sc DNA polymerase) was added and incubated at 30 °C for 2 hours, then immediately incubated at 65 °C for 3 minutes. Amplified DNA was stored at -20 °C.

3.2.12 16S rRNA and ITS rRNA DNA sequencing

David Baker from the QIB Core Sequencing team performed the amplification of 16S rRNA and ITS rRNA genes (see **3.2.12.1**), prepared the DNA libraries for sequencing (see **3.2.12.2**) and performed paired-end sequencing on the DNA libraries (see **3.2.12.3**). Dr Andrea Telatin and Dr Rebecca Ansorge, bioinformaticians at the QIB, performed the processing and taxonomic classification of sequencing reads (see **3.2.12.4**).

3.2.12.1 Polymerase chain reaction

The following procedure was used for both the amplification of the V3+V4 16S rRNA gene and the amplification of the ITS1 sub-region of the ITS rRNA gene, using the primers from Sigma Aldrich detailed in **Table 3.5**. Extracted microbial DNA was normalised to 5 ng/µl using 10 mM Tris-HCl. A polymerase chain reaction (PCR) master mix was made of 4 µl KAPA2G buffer, 0.4 µl of 10 mM KAPA dNTP mix, 0.08 µl of 5U/µl KAPA2G robust DNA polymerase, 13.72 µl of PCR-grade water from the KAPA2G robust PCR kit (Sigma Aldrich), 0.4 µl 10µM forward primer and 0.4 µl 10 µM reverse primer. 19 µl of PCR master mix was used per reaction, with 1 µl of 5 ng/µl DNA. The following PCR protocol was then used to amplify the 16S rRNA gene and the ITS rRNA gene: 95°C for 1 minute, 30

cycles of 95°C for 30 seconds, 55°C for 30 seconds and 72°C for 30 seconds, followed by a final extension at 72°C for 5 minutes.

Table 3.5: Primers sourced from Sigma Aldrich used for 16S rRNA and ITS rRNA sequencing.

Primer name	Gene	Primer direction	Sequence
16S_V3-4_F	16S rRNA	Forward	5' TCGTCGGCAGCGTCAGATGTGTATAAGAGACAG
16S_V3-4_R	16S rRNA	Reverse	5' GTCTCGTGGGCTCGGAGATGTGTATAAGAGACAG
ITS1F	ITS rRNA	Forward	CTTGGTCATTTAGAGGAAGTAA
ITS2	ITS rRNA	Reverse	GCTGCGTTCTTCATCGATGC

3.2.12.2 Library preparation and quality control

A 0.7X solid phase reversible immobilisation bead clean-up was performed on amplified DNA using KAPA pure beads (Roche), eluting DNA into 20 µl 10 mM Tris-HCl.

A PCR master mix was made of 4 µl KAPA2G buffer, 0.4 µl of 10 mM KAPA dNTP mix, 0.08 µl of 5U/µl KAPA2G robust DNA polymerase, and 6.52 µl of PCR-grade water from the KAPA2G robust PCR kit. 11 µl was used per reaction. 2 µl of P5 index primer and 2 µl of P7 index primer from Nextera XT index kit (Illumina) were added to each reaction. 5 µl of cleaned DNA from **section 3.2.12.1** was added. A PCR was run using the following cycling protocol: 95°C for 5 minutes, 10 cycles of 95°C for 30 seconds, 55°C for 30 seconds and 72°C for 30 seconds, followed by a final extension at 72°C for 5 minutes.

The Quanti-iT™ dsDNA high sensitivity assay kit (Fisher Scientific) was used to quantify libraries on the FLUOstar Optima plate reader. Libraries were pooled in equal quantities and a 0.7X solid phase reversible immobilisation bead clean-up was performed using KAPA pure beads. The final pool was quantified using the Qubit™ dsDNA high sensitivity assay kit (see **3.2.9**). Molarity of the final pool was measured on a high sensitivity D1000 screen tape (Agilent) using the Agilent TapeStation 4200.

3.2.12.3 Amplicon sequencing

The final pool was run at a concentration of 8pM on an Illumina MiSeq instrument using MiSeq® reagent kit v3 (600-cycle) (Illumina) for sequencing 2 x 300 bp paired end readings. A 20 % PhiX control v3 (Illumina) spike was run in a separate lane for validation. The raw reads generated were in FASTQ format.

3.2.12.4 Processing sequenced data

Quality control was undertaken using *Fastp* (version 0.20.0) (Chen et al., 2018), where low-quality reads containing ambiguous bases were removed. Adapters were removed using *SeqFu* (version 0.96) (Telatin et al., 2021).

Operational taxonomic units (OTUs) were identified and classified using the LotuS tool (version 1.64) (Hildebrand et al., 2014). The reads remaining after low-quality filtering were clustered using UPARSE (Edgar, 2013). Taxonomic annotation of OTUs was performed using the Ribosomal Database Project by aligning OTUs against a reference database (Cole et al., 2005). The SILVA database (Quast et al., 2013) was used for 16S ribosomal sequences and the UNITE database for ITS1 sequences (Nilsson et al., 2019).

Following analysis using LotuS, ITS1 unclassified OTUs were analysed using blastn, and taxonomy was assigned to OTUs that had 100 % query cover and 100 % percentage identity.

3.2.13 Taxonomic analysis

The Rhea pipeline developed by Lagkouvardos et al. (2017) was implemented in R for the analysis of OTU tables. The pipeline was composed of 6 R scripts: 1) normalisation, 2) alpha-diversity, 3) beta-diversity, 4) taxonomic-binning, 5) serial group comparisons and 6) correlations. This section describes how the Rhea pipeline was used to transform sequence counts, compare relative abundances of taxa, measure alpha and beta diversity and compare abundance of individual taxa between sample groups.

3.2.13.1 Normalisation

A common artifact of sequencing is that individual samples from the same sequencing run have different sequencing depths, meaning the feature table generated has different numbers of sequences per sample (Knight et al., 2018). Normalisation is a form of data transformation which was used to remove the confounding effects of different numbers of read counts per sample.

The read counts were normalised by dividing by their sample size and then multiplying by the size of the smallest sample using the 'normalization' script from the Rhea pipeline. This script produced a second table which also contained relative abundances.

3.2.13.2 Taxonomic binning

Taxonomic binning is the process of amalgamating OTUs sharing the same root at each taxonomic level. This enables the comparison of relative abundances at each taxonomic level across samples.

The 'taxonomic-binning' script from the Rhea pipeline was used to split the OTUs into 5 tables for each taxonomic level: kingdom, phylum, class, order, family and genus. Bubble plots were then

created to compare the relative abundance of the top 10 taxa per sample at the families and genus-level, which was done in R independently of the Rhea pipeline.

3.2.13.3 Alpha diversity

Alpha diversity is a measure of diversity within a sample. There are alpha diversity measures that enumerate the number of taxa within a sample (richness) or the variation of taxa abundance within a sample (evenness). There are also alpha diversity measures that capture community structure with an emphasis on rare taxa (Shannon) or an emphasis on the most abundant taxa (Simpson). Shannon and Simpson diversity indices are not linear and can be converted into intuitive scores by calculating the effective diversities (Jost, 2006).

Richness, evenness and Shannon effective scores were calculated for normalised counts with a value of 0.5 or higher using the 'alpha-diversity' script from the Rhea pipeline.

3.2.13.4 Beta diversity

Beta diversity is a measure of variance across samples, expressed as distances based on feature similarity. There are many distance metrics that can be used to generate a distance matrix, for example Jaccard index, Bray-Curtis index and UniFrac distances (Knight et al., 2018). The Jaccard index is limited in its ability to measure variance across samples as it is based on presence and absence data only (Lozupone et al., 2007). UniFrac is superior to Bray-Curtis analysis as it accounts for the phylogenetic distance between OTUs. There are two versions of UniFrac distances: unweighted and weighted. Weighted UniFrac considers OTU relative abundances whereas unweighted UniFrac does not and they are therefore sensitive to dominant and rare lineages respectively. Chen et al. (2012) developed a generalised UniFrac distance metric which has more power to detect changes in taxa present at low, moderate and high abundances.

The 'beta-diversity' script from the Rhea pipeline was used to generate a matrix of generalised UniFrac distances which were visualised in two dimensions on a multi-dimensional scaling (MDS) plot and a permutational multivariate analysis of variance (PERMANOVA) test was performed to determine the significance of group separation. The hierarchical clustering of samples was assessed using Ward's clustering method (Murtagh and Legendre, 2014) and presented as a dendrogram.

3.2.13.5 Differential abundance analysis

Differential abundance analysis is the process of comparing the abundance of individual taxa in each group. There are two types of differential abundance analysis, univariate and multivariate, which compare the abundance of taxa between groups based on one and many variables, respectively. Due to small sample sizes, univariate differential analysis was performed using non-classical analysis of variance (ANOVA) which does not assume normality of distribution.

ANOVA was performed using the 'serial group comparisons' script from the Rhea pipeline. For the experiment comparing 'filtered' and 'centrifuged' microbes, the non-parametric Kruskal-Wallis rank sum test was used to calculate the likelihood of the abundance of an OTU in the two groups being from different distributions. For the experiment comparing 'sybr green high', 'sybr green low' and 'all' microbes, the non-parametric Mann-Whitney test was used to analyse pairwise differences in abundances of OTUs. *P*-values were corrected for multiple testing using the Benjamini-Hochberg method (Benjamini and Hochberg, 1995).

The following parameters were used for analysis: 1) at least 50 % of a sample group must have the OTU present at a relative abundance of 0.1 % to be considered for analysis, 2) OTUs with a relative abundance less than 0.1 % were treated as missing values and removed from statistical calculations, 3) OTUs had to have a median relative abundance of 0.1 % across all groups to be considered for analysis.

3.3 RESULTS

3.3.1 Optimising bacteria and fungi isolation from stool

A method was first sought which isolated all microbes from stool, including fungi. The two methods compared were centrifugation and filtration. When comparing light scatter properties of microbes isolated from aliquots of one stool sample using centrifugation or filtration, the percentage of larger cells isolated by centrifugation was 12.2 % compared to 16.6 % from the filtered stool samples. In addition, there were events with higher FSC from filtered stool samples (**Figure 3.5**).

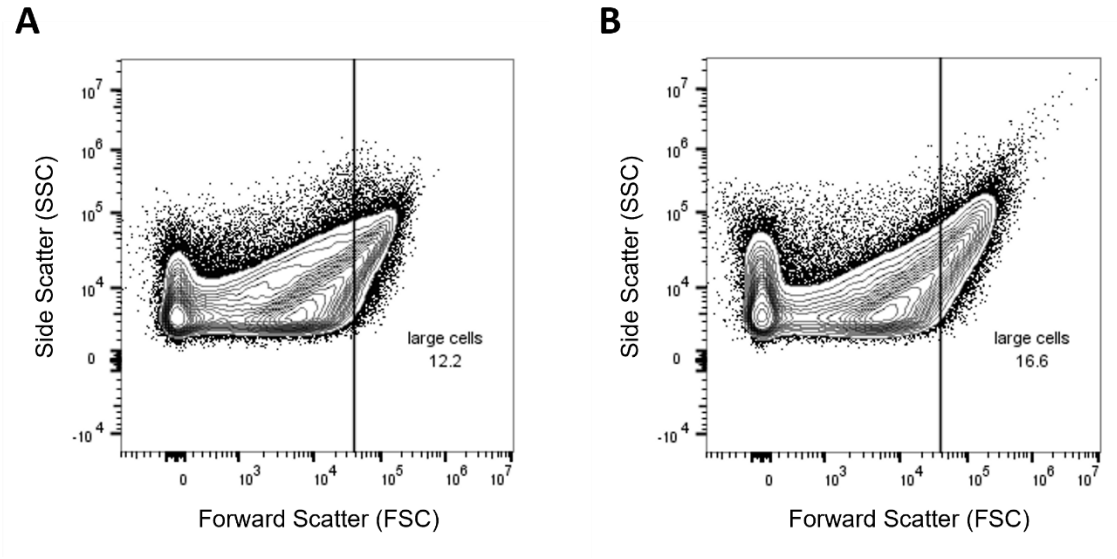

Figure 3.5: Comparison of the size of microbes isolated from aliquots of the same stool sample using A) centrifugation and B) filtration. *Two aliquots of the same frozen stool sample underwent centrifugation or filtration to isolate microbes from stool debris and forward scatter and side scatter were analysed using the BD LSRFortessa™. The 'large cells' gate was set to the same position on forward scatter as this measurement is proportional to the diameter of a cell. The percentage of cells falling in this gate was measured.*

A comparison of the bacterial taxonomic composition of cells isolated from a single stool sample by centrifugation or by filtration was carried out. At the family-level it was found that 9 of the 10 most abundant taxa per sample were shared between 5 x 10^6 cells sampled from the centrifuged and the filtered stool microbes: Lachnospiraceae (43.4 % vs 39.1 %), Ruminococcaceae (26.8 % vs 22.7 %), Bacteroidaceae (6.5 % vs 2.9 %), Bifidobacteriaceae (6.4 % vs 12.0 %), Xanthomonadaceae (5.0 % vs 4.9 %), Rhizobiaceae (4.3 % vs 13.5 %), Veillonellaceae (2.2 % vs 1.6 %), Rikenellaceae (0.7 % vs 0.4 %) and Clostridiaceae 1 (0.7 % vs 0.3 %) (**Figure 3.6**). In both the centrifugation and filtration method the abundance of Xanthomonadaceae and Rhizobiaceae decreased as the number of cells sampled increased and the abundance of Ruminococcaceae, Lachnospiraceae, Bifidobacteriaceae and Bacteroidaceae increased.

At the genus-level, 9 of the 10 most abundant taxa per sample were shared between 5 x 10^6 cells sampled from centrifuged and filtered stool microbes: unclassified *Lachnospiraceae* (16.1 % vs 11.7 %), *Faecalibacterium* (14.8 % vs 9.1 %), *Lanchnospira* (11.4 % vs 7.8 %), *Blautia* (9.6 % vs 14.9 %), *Bacteroides* (6.5 % vs 2.9 %), *Bifidobacterium* (6.4 % vs 12.0 %), *Lysobacter* (5.0 % vs 4.9 %), *Subdoligranulum* (4.2 % vs 5.8 %), *Allorhizobium-Neorhizobium-Pararhizobium-Rhizobium* (3.4 % vs 11.5 %) and *Dialister* (2.2 % vs 1.6 %) (**Figure 3.7**). In both the centrifugation method and filtration method the abundance of *Lysobacter* decreased as the number of cells sampled increased and the abundance of unclassified *Lachnospiraceae*, *Lachnospira*, *Faecalibacterium* and *Blauti* increased.

The taxonomic composition of fungi isolated from a single stool sample using centrifugation and filtration had greater variation than bacteria. The top 10 taxa per sample at the family and genera taxonomic level varied in composition and relative abundance at different cell concentrations and with different microbe isolation methods. At the family-level 10^3 cells were dominated by one taxon, which was different for centrifuged and filtered cells: Mrakiaceae (83.6 %) and Fomitopsidaceae (98.1 %) respectively (**Figure 3.8**). At the genus-level: *Mrakia,* which is part of the Mrakiaceae family, dominated 10^3 cells sampled from centrifuged microbes (83.6 %) and *Piptoporus,* which is part of the Fomitopsidaceae family, dominated 10^3 cells sampled from filtered microbes (98.1 %) (**Figure 3.9**). At the family-level only 4 of the 10 most abundant fungal taxa were shared between 5 x 10^6 cells sampled from the centrifuged and filtered stool *microbes:* Saccharomycodaceae (99.0 % vs 30.5 %), Malasseziaceae (0.7 % vs 35.1 %), Fomitopsidaceae (0.01 % vs 0.02 %) and Cordycipitaceae (0.3 % vs 0.007 %). At the genus-level 4 out of 10 most abundant taxa were shared between 5 million cells sampled from centrifuged and filtered stool microbes: *Piptoporus* (0.01 % vs 0.02 %), *Malassezia* (0.7 % vs 35.1 %), *Hanseniaspora* (99.0 % vs 30.5 %) and *Engyodontium* (0.3 % vs 0.007 %).

The alpha diversity within bacterial and fungal communities of microbes isolated from a single stool sample using centrifugation or filtration was then analysed (**Figure 3.10)**. The following measures

were used to analyse the diversity of taxa within a sample: Shannon effective, richness and evenness. All three measures followed the same trend for bacterial communities from both centrifuged and filtered stool samples: scores increased from 1 x 10^3 cells to 1 x 10^6 cells where they reached saturation. Shannon effective indices, evenness scores and richness scores were higher from the filtered stool sample compared to the centrifuged stool sample at the following cell numbers: 1 x 10^3 to 2.5 x 10^6 cells, 1 x 10^3 to 1 x 10^6 cells and 1 x 10^3 to 1 x 10^6 cells respectively.

Alpha diversity scores of fungal taxa did not follow the same trend as their bacterial counterparts. Scores varied across cell concentration measured and neither microbe isolation method had consistently higher scores compared to the other. It is worth noting that the range of Shannon effective scores measured from fungal taxa was 0.07-1.6 whereas Shannon effective scores measured from bacterial taxa ranged from 0.4-3.4. In addition, richness scores from fungal communities ranged from 5-20 whereas richness scores from bacterial communities ranged from 82-253.

Finally, the similarity between fungal and bacteria communities from centrifuged and filtered stool microbes was analysed. Beta diversity was measured using the generalised UniFrac distance metric and distances between samples were visualised using a MDS plot (**Figure 3.11**). PERMANOVA analysis showed there were no significant differences between centrifuged and filtered microbes in the bacterial or fungal communities ($p=0.634$ and $p=0.729$). In addition, differential abundance analysis of bacteria and fungi did not find the abundance of any taxa significantly different between the two methods of microbe isolation.

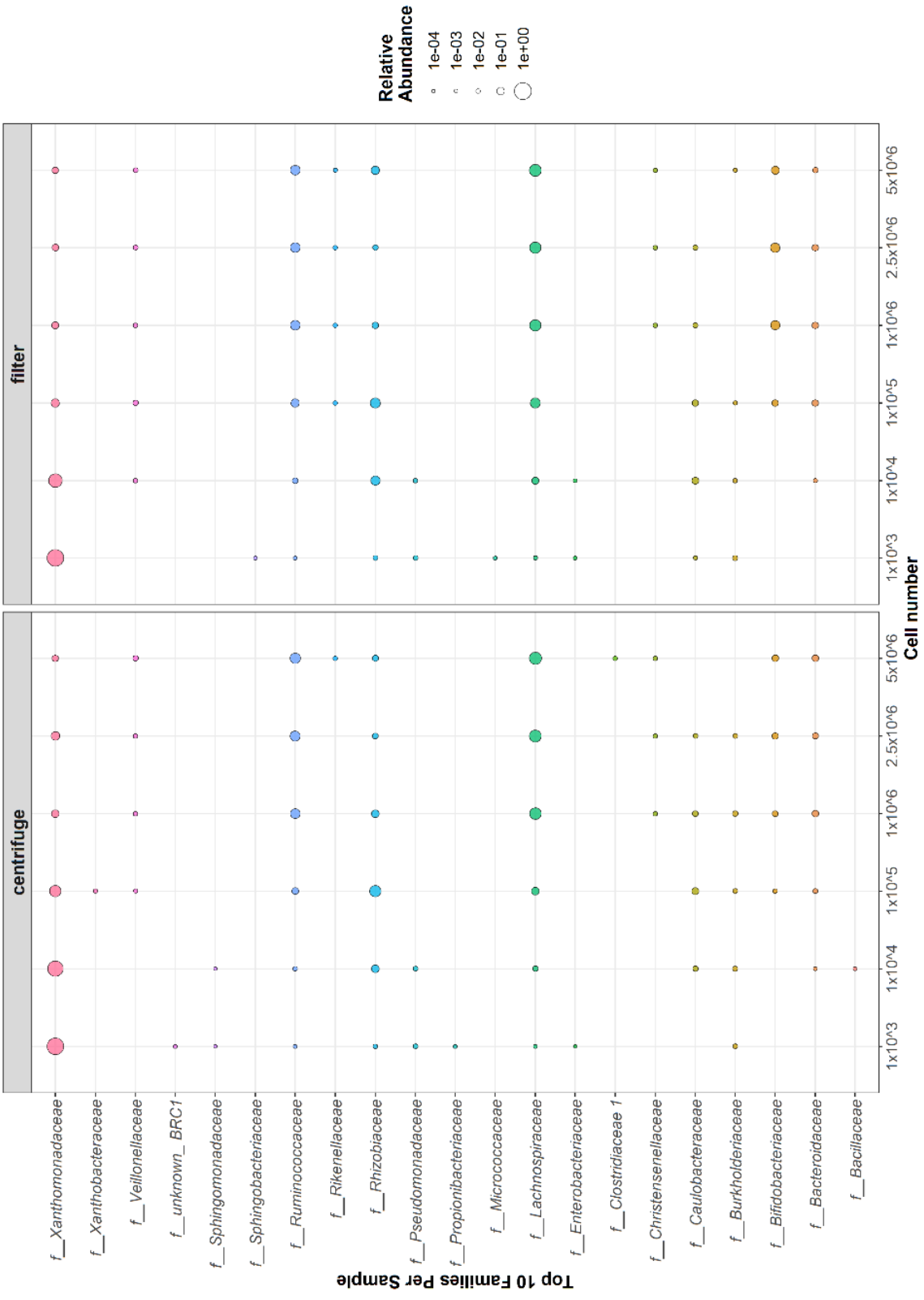
centrifuge
filter
Relative Abundance
1e-04
1e-03
1e-02
1e-01
1e+00
Top 10 Families Per Sample
f__Xanthomonadaceae
f__Xanthobacteraceae
f__Veillonellaceae
f__unknown_ BRC1
f__Sphingomonadaceae
f__Sphingobacteriaceae
f__Ruminococcaceae
f__Rikenellaceae
f__Rhizobiaceae
f__Pseudomonadaceae
f__Propionibacteriaceae
f__Micrococcaceae
f__Lachnospiraceae
f__Enterobacteriaceae
f__Clostridiaceae 1
f__Christensenellaceae
f__Caulobacteraceae
f__Burkholderiaceae
f__Bifidobacteriaceae
f__Bacteroidaceae
f__Bacillaceae
1x10^3
1x10^4
1x10^5
1x10^6
2.5x10^6
5x10^6
Cell number

←Figure 3.6: Relative abundances of the top 10 bacterial families of microbes isolated from a stool sample using centrifugation (left) or filtration (right). *Two aliquots of the same stool sample underwent centrifugation or filtration to isolate microbes from stool debris. 1 x 10^3, 1 x 10^4, 1 x 10^5, 1 x 10^6, 2.5 x 10^6 and 5 x 10^6 cells from each method were collected on the Sony SH800S cell sorter for comparison. 16S rRNA gene sequencing was used for identification of bacterial microbes and relative abundances were calculated from classified reads that were rarefied to the minimum sequencing depth.*

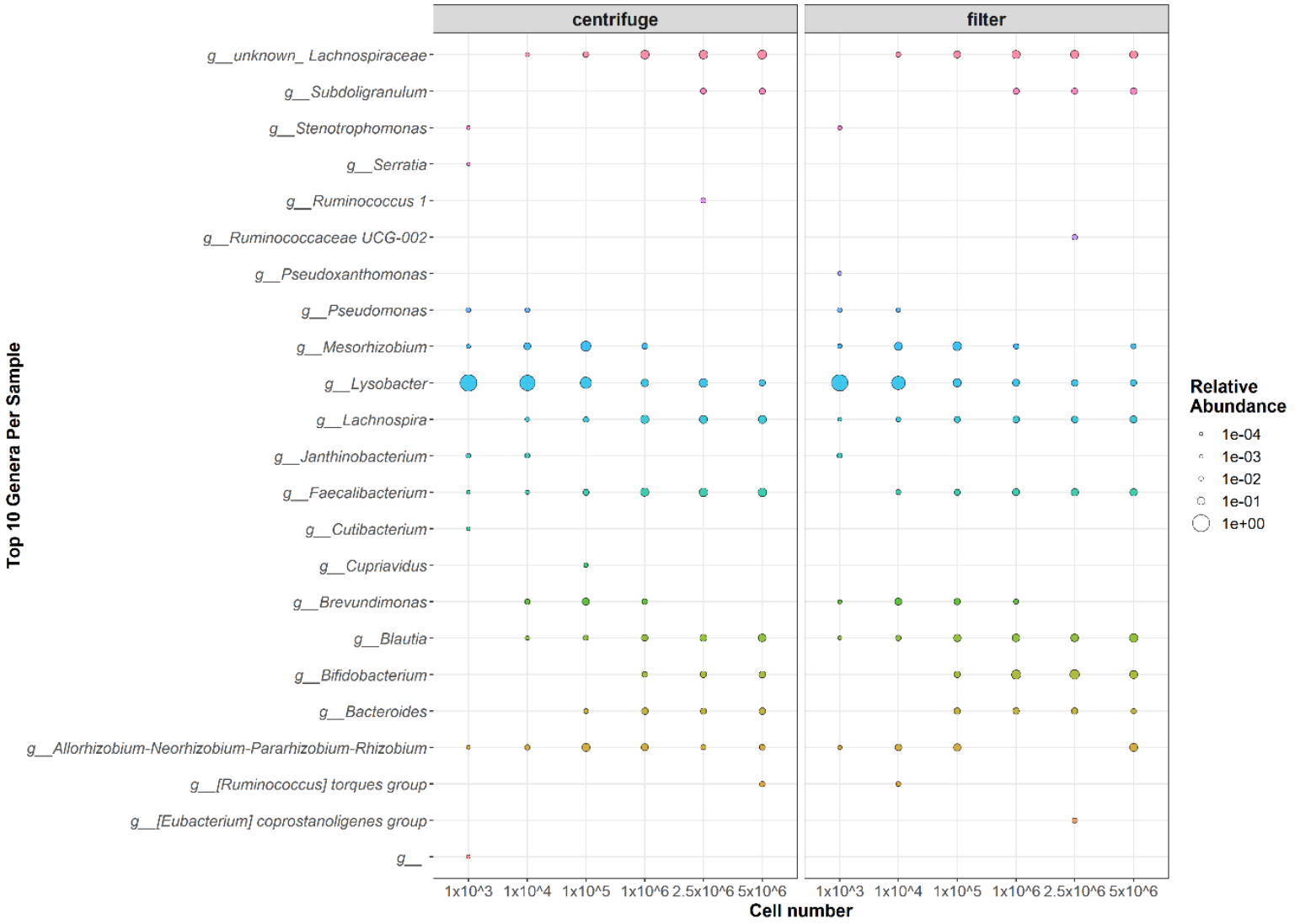
centrifuge
filter
g__unknown_ Lachnospiraceae
g__Subdoligranulum
g__Stenotrophomonas
g__Serratia
g__Ruminococcus 1
g__Ruminococcaceae UCG-002
g__Pseudoxanthomonas
g__Pseudomonas
g__Mesorhizobium
g__Lysobacter
g__Lachnospira
g__Janthinobacterium
g__Faecalibacterium
g__Cutibacterium
g__Cupriavidus
g__Brevundimonas
g__Blautia
g__Bifidobacterium
g__Bacteroides
g__Allorhizobium-Neorhizobium-Pararhizobium-Rhizobium
g__[Ruminococcus] torques group
g__[Eubacterium] coprostanoligenes group
g__
Top 10 Genera Per Sample
1x10^3 1x10^4 1x10^5 1x10^6 2.5x10^6 5x10^6
Cell number
Relative Abundance
1e-04
1e-03
1e-02
1e-01
1e+00

← ***Figure 3.7: Relative abundances of the top 10 bacterial genera of microbes isolated from a stool sample using centrifugation (left) or filtration (right).*** *Two aliquots of the same stool sample underwent centrifugation or filtration to isolate microbes from stool debris. 1 x 10^3, 1 x 10^4, 1 x 10^5, 1 x 10^6, 2.5 x 10^6 and 5 x 10^6 cells from each method were collected on the Sony SH800S cell sorter for comparison. 16S rRNA gene sequencing was used for identification of bacterial microbes and relative abundances were calculated from classified reads that were rarefied to the minimum sequencing depth.*

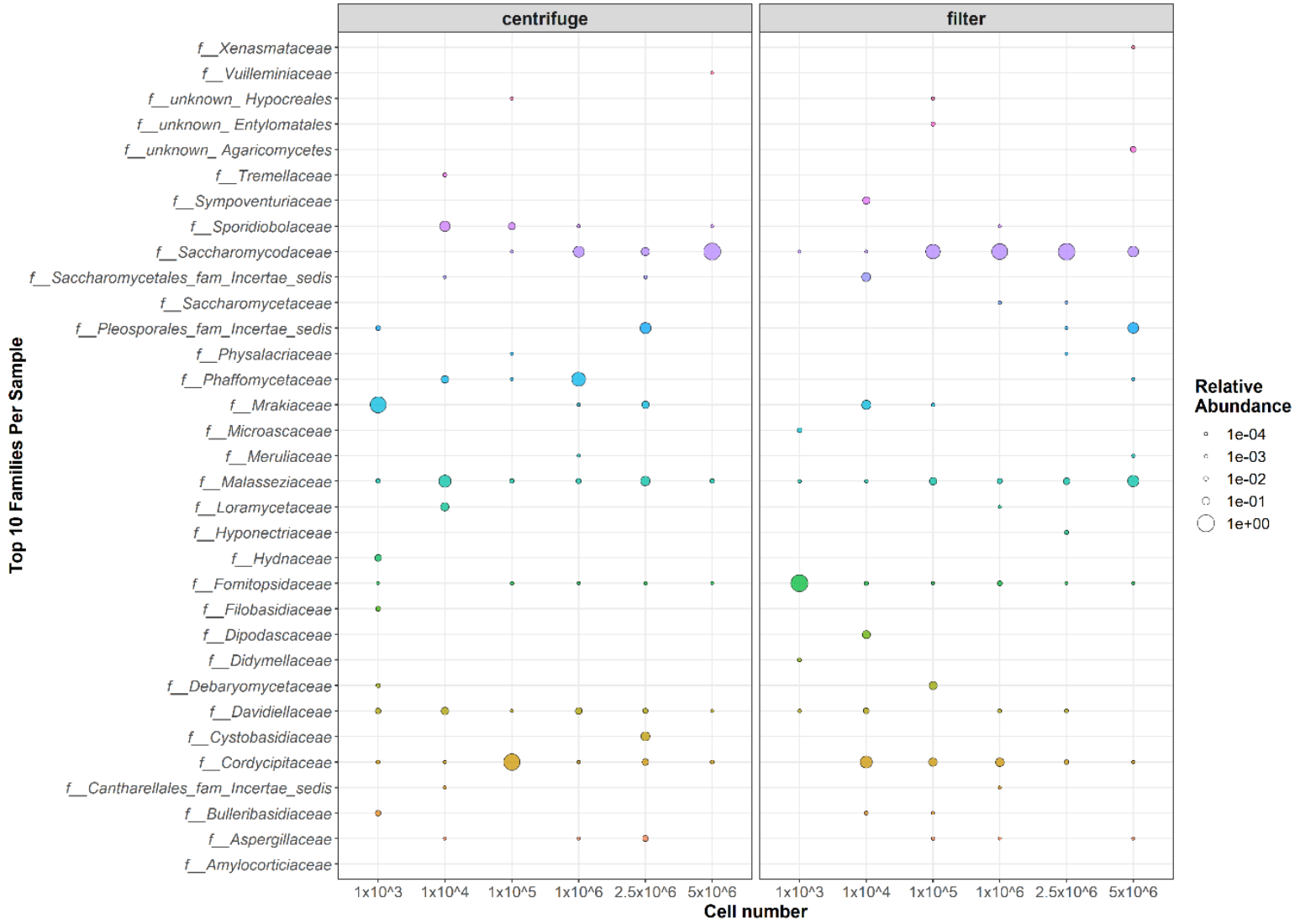
centrifuge
filter
Top 10 Families Per Sample
f__Xenasmataceae
f__Vuilleminiaceae
f__unknown_ Hypocreales
f__unknown_ Entylomatales
f__unknown_ Agaricomycetes
f__Tremellaceae
f__Sympoventuriaceae
f__Sporidiobolaceae
f__Saccharomycodaceae
f__Saccharomycetales_fam_Incertae_sedis
f__Saccharomycetaceae
f__Pleosporales_fam_Incertae_sedis
f__Physalacriaceae
f__Phaffomycetaceae
f__Mrakiaceae
f__Microascaceae
f__Meruliaceae
f__Malasseziaceae
f__Loramycetaceae
f__Hyponectriaceae
f__Hydnaceae
f__Fomitopsidaceae
f__Filobasidiaceae
f__Dipodascaceae
f__Didymellaceae
f__Debaryomycetaceae
f__Davidiellaceae
f__Cystobasidiaceae
f__Cordycipitaceae
f__Cantharellales_fam_Incertae_sedis
f__Bulleribasidiaceae
f__Aspergillaceae
f__Amylocorticiaceae
1x10^3
1x10^4
1x10^5
1x10^6
2.5x10^6
5x10^6
Cell number
Relative Abundance
1e-04
1e-03
1e-02
1e-01
1e+00

← *Figure 3.8: Relative abundances of the top 10 fungal families of microbes isolated from a stool sample using centrifugation (left) or filtration (right).* *Two aliquots of the same frozen stool sample underwent centrifugation or filtration to isolate microbes from stool debris. 1 x 10^3, 1 x 10^4, 1 x 10^5, 1 x 10^6, 2.5 x 10^6 and 5 x 10^6 cells from each method were collected on the Sony SH800S cell sorter for comparison. ITS rRNA gene sequencing was used for identification of fungal microbes and relative abundances were calculated from classified reads that were rarefied to the minimum sequencing depth.*

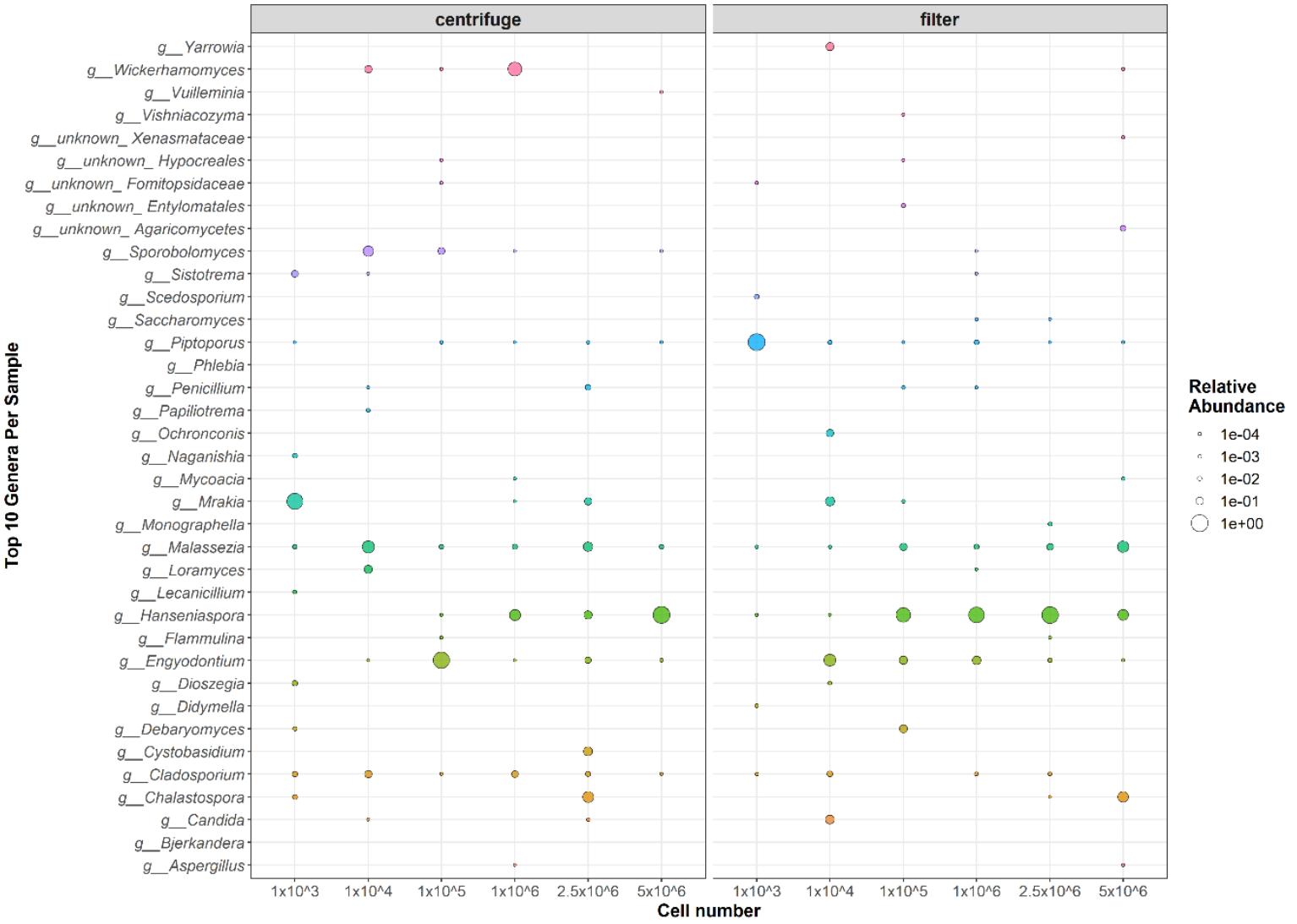
centrifuge
filter
Top 10 Genera Per Sample
g__Yarrowia
g__Wickerhamomyces
g__Vuilleminia
g__Vishniacozyma
g__unknown_ Xenasmataceae
g__unknown_ Hypocreales
g__unknown_ Fomitopsidaceae
g__unknown_ Entylomatales
g__unknown_ Agaricomycetes
g__Sporobolomyces
g__Sistotrema
g__Scedosporium
g__Saccharomyces
g__Piptoporus
g__Phlebia
g__Penicillium
g__Papiliotrema
g__Ochronconis
g__Naganishia
g__Mycoacia
g__Mrakia
g__Monographella
g__Malassezia
g__Loramyces
g__Lecanicillium
g__Hanseniaspora
g__Flammulina
g__Engyodontium
g__Dioszegia
g__Didymella
g__Debaryomyces
g__Cystobasidium
g__Cladosporium
g__Chalastospora
g__Candida
g__Bjerkandera
g__Aspergillus
1x10^3
1x10^4
1x10^5
1x10^6
2.5x10^6
5x10^6
Cell number
Relative Abundance
1e-04
1e-03
1e-02
1e-01
1e+00

← *Figure 3.9: Relative abundances of the top 10 fungal genera of microbes isolated from a stool sample using centrifugation (left) or filtration (right).* *Two aliquots of the same frozen stool sample underwent centrifugation or filtration to isolate microbes from stool debris. 1 x 10^3, 1 x 10^4, 1 x 10^5, 1 x 10^6, 2.5 x 10^6 and 5 x 10^6 cells from each method were collected on the Sony SH800S cell sorter for comparison. ITS rRNA gene sequencing was used for identification of fungal microbes and relative abundances were calculated from classified reads that were rarefied to the minimum sequencing depth.*

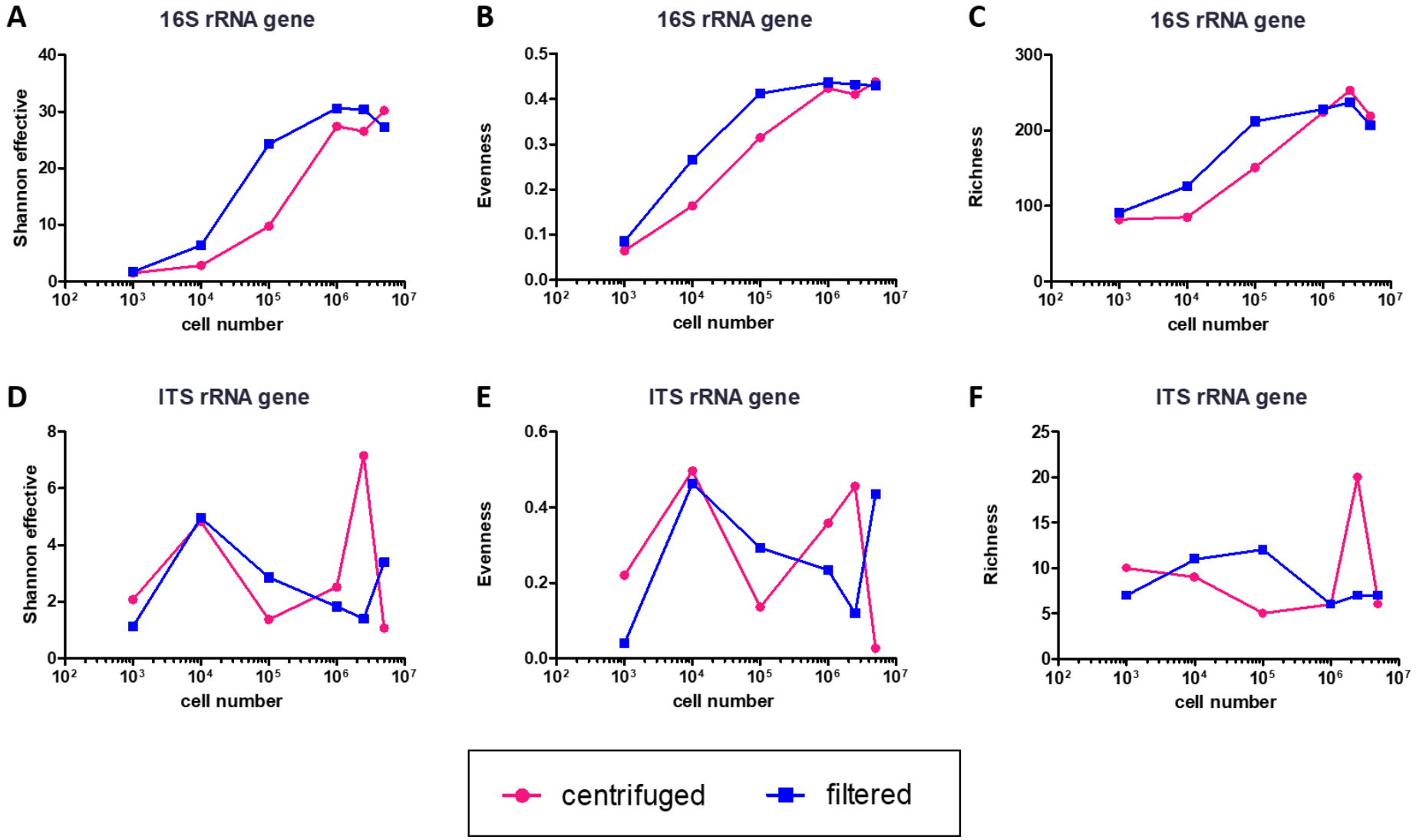
A
16S rRNA gene
Shannon effective
cell number
B
16S rRNA gene
Evenness
cell number
C
16S rRNA gene
Richness
cell number
D
ITS rRNA gene
Shannon effective
cell number
E
ITS rRNA gene
Evenness
cell number
F
ITS rRNA gene
Richness
cell number
centrifuged
filtered

←Figure 3.10: Alpha diversity of bacterial and fungal communities of microbes isolated from a stool sample using centrifugation (pink) or filtration (blue). *Aliquots of the same stool sample underwent centrifugation or filtration. 16S rRNA and ITS rRNA gene sequencing of extracted DNA from 1 x 10^3, 1 x 10^4, 1 x 10^5, 1 x 10^6, 2.5 x 10^6 and 5 x 10^6 cells from each method were performed and then Shannon effective (A+D), evenness (B+E) and richness (C+F) were analysed. Each point represents a single measurement.*

A

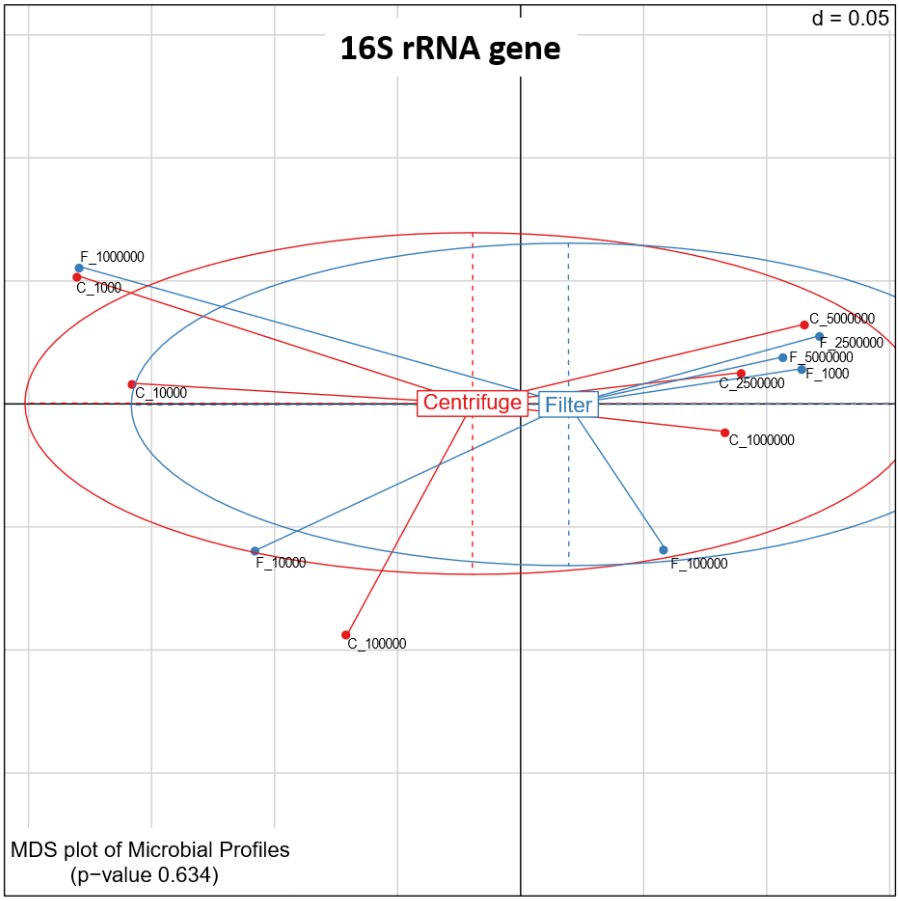
16S rRNA gene
d = 0.05
F_1000000
C_1000
C_10000
C_5000000
F_2500000
F_5000000
F_1000
C_2500000
Centrifuge
Filter
C_1000000
F_10000
F_100000
C_100000
MDS plot of Microbial Profiles
(p−value 0.634)

B

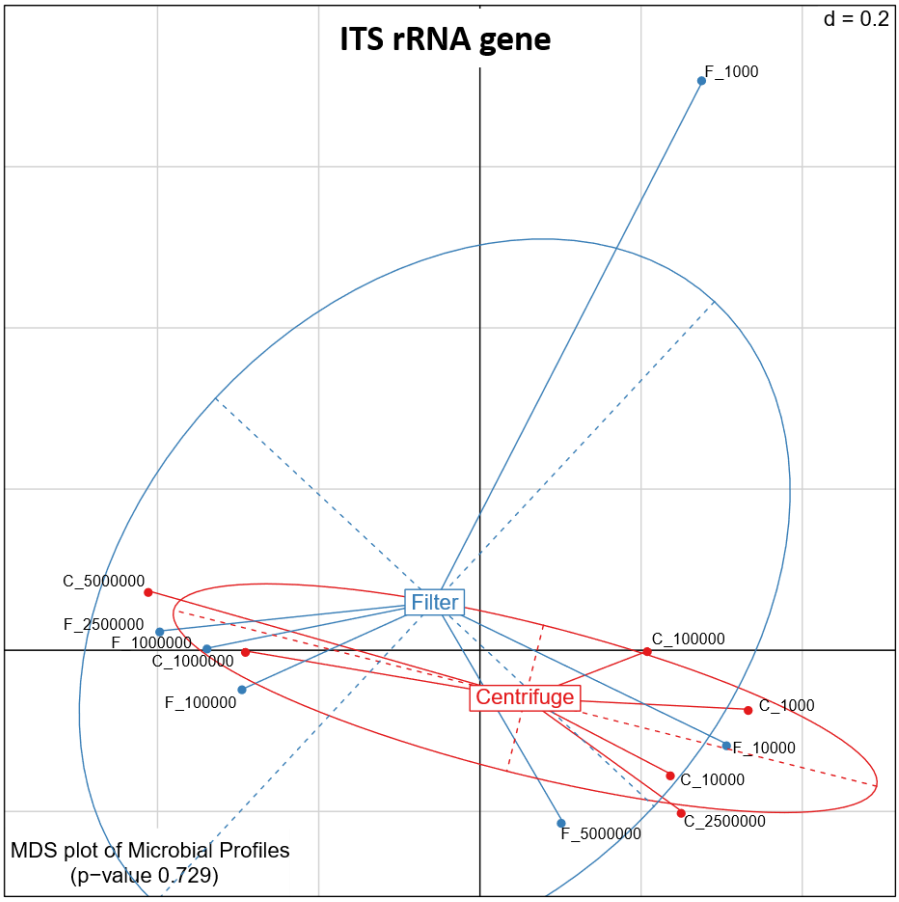
ITS rRNA gene
d = 0.2
F_1000
C_5000000
F_2500000
F_1000000
C_1000000
F_100000
Filter
Centrifuge
C_100000
C_1000
F_10000
C_10000
C_2500000
F_5000000
MDS plot of Microbial Profiles
(p−value 0.729)

← ***Figure 3.11: Beta diversity of bacterial (A) and fungal (B) communities within microbes extracted from a stool sample using centrifugation (red) or filtration (blue).*** *Aliquots of the same stool sample underwent centrifugation or filtration, followed by 16s rRNA and ITS rRNA gene sequencing on DNA extracted from 1 x 10^3, 1 x 10^4, 1 x 10^5, 1 x 10^6, 2.5 x 10^6 and 5 x 10^6 cells collected using the Sony SH800S cell sorter. Generalised UniFrac distances were used to generate a MDS plot for visualising dissimilarity between centrifuged and filtered microbes. 'D' is a measure of dissimilarity. Significance was measured using PERMANOVA.*

3.3.2 Optimising the detection of bacterial and fungal cells by flow cytometry

To perform FACS on intestinal microbes a reliable parameter was needed in order to segregate intestinal microbes from background noise caused by debris. Initially, the use of light refraction properties for identification of bacteria and fungi within stool samples were investigated (**Figure 3.12**). The yeast isolates *Candida albicans* and *Candida glabrata* had higher forward and side scatter levels than bacterial isolates *Bifidobacterium bifidum* and *Escherichia coli*. When comparing the light scatter profile of stool microbes, both samples had events with low forward and side scatter levels similar to those seen in bacteria, and fewer events with high forward and side scatter levels similar to those seen in yeast. Both stool samples had a high proportion of background noise seen in the 'noise' gate. Forward scatter levels of bacteria overlapped with background noise, therefore light refraction properties were not able to accurately segregate microbes from background noise.

Fluorescent dyes were analysed for their ability to segregate intestinal microbes from background noise and identify bacterial and fungal cells. The concentration of SYBR™ green I nucleic acid gel stain was optimised for staining bacterial cells by comparing the percentage of 'sybr green positive' events at three dilutions (**Table 3.6**). The highest dilution tested, 1×10^{-3}, had the highest staining capacity, staining 92.8 % of *B. fragilis* cells. Next, SYBR™ green I nucleic acid gel stain and calcofluor white stain were tested for their staining capacity of stool microbes and yeast (**Figure 3.13**). SYBR™ green I nucleic acid gel stain stained a higher proportion of yeast than calcofluor white stain, 74.7 % and 49.0 % respectively. Calcofluor white stained 34.9 % of stool microbes. As only 66.0 % of stool microbes were stained with the optimised concentration of SYBR™ green I nucleic acid gel stain, it was hypothesised that some microbes were resistant to staining with SYBR™ green I nucleic acid gel stain.

To test this hypothesis, microbes were separated into 'sybr green high' and 'sybr green low' populations and also 'all' microbes were collected based on their light scatter properties. Stool samples from two pairs of severe ME/CFS patients and their matched household controls were analysed. Cell populations were sequenced using the 16S rRNA gene and the ITS rRNA gene to profile bacterial and fungal populations respectively.

Initially, the bacterial taxonomic composition of 'sybr green high', 'sybr green low' and 'all' microbes were analysed. When comparing the families present in every sample, 5 of the 10 most abundant taxa were shared: Xanthomonadaceae, Ruminococcaceae, Lachnospiraceae, Bifidobacteriaceae and Bacteroidaceae (**Figure 3.14**). In addition to the 5 aforementioned taxa, all cell populations from participant pair one also shared a further 2 taxa (Veillonellaceae and Christensellaceae) and all cell populations from participant pair two shared one further taxon (Acidaminococcaceae). Each participant had a high proportion of the top 10 bacterial families shared by their 'sybr green high', 'sybr green low' and 'all' cell populations: 8 taxa were shared between cell populations in patient

one, 8 taxa were shared between cell populations in control one, 9 taxa were shared between cell populations in patient two and 9 taxa were shared between cell populations in control two. At the genus-level, 5 of the 10 most abundant taxa were shared across all samples: unclassified *Lachnospiraceae, Subdoligranulum, Lysobacter, Faecalibacterium* and *Blautia* (**Figure 3.15**). In addition, all cell populations from pair one also shared a further 2 taxa: *Lachnospira* and *Bacteroides*. As seen with the top 10 families, each participant had a high proportion of the top 10 genus shared across their 'sybr green high', 'sybr green low' and 'all' populations. 9 taxa were shared between cell populations in patient one, 9 taxa were shared between cell populations in control one, 7 taxa were shared between cell populations in patient two and 8 taxa were shared between cell populations in control two.

Unlike the bacterial taxonomic composition, the fungal taxonomic composition of the top 10 families and genera was more heterogenous between samples. Only one of the top 10 most abundant families per sample was shared across all samples: Davidiellaceae (**Figure 3.16**). *Cladosporium,* a genus in the Davidiellaceae family, was the only genus from the top 10 abundant taxa shared across all samples (**Figure 3.17**). The number of top 10 fungal taxa shared across a participant's 'sybr green high', 'sybr green low' and 'all' cell populations was also lower. At the family-level, patient one had 2, control one had 4, patient two had 3 and control two had 3 out of the 10 most abundant taxa shared between their 'sybr green high', 'sybr green low' and 'all' cell populations. At the genus-level, patient one had 2, control one had 4, patient two had 3 and control two had 3 out of the 10 most abundant taxa shared between their 'sybr green high', 'sybr green low' and 'all' cell populations.

The number and diversity of taxa within bacterial and fungal communities in 'sybr green high', 'sybr green low' and 'all' populations were then analysed using three alpha diversity measures: Shannon effective, richness and evenness (**Figure 3.18**). The 'all' population had the highest alpha diversity scores, which was the case with fungal taxa as the average diversity scores were higher in the 'all' fraction compared to 'sybr green high' and 'sybr green low' populations. But for bacterial taxa, the 'sybr green high' population had the highest average richness score and the 'sybr green low' population had the highest average evenness and Shannon effective scores.

Next, the richness scores were compared between 'sybr green high' cells and 'sybr green low' cells isolated from the same participant to determine whether SYBR™ green I nucleic acid gel stain identified more or less taxa than cells remaining unstained. In pair one, the richness scores for bacterial taxa were higher in the 'sybr green high' cell population than the 'sybr green low' cell population (**Figure 3.18**). Patients had higher richness scores for fungal taxa in their 'sybr green high' cell population compared to their 'sybr green low' cell population. Whereas controls had

higher richness scores for fungal taxa in their 'sybr green low' cell population compared to their 'sybr green high' cell population.

Next, the hierarchical clustering of samples based on their bacterial and fungal communities using phylograms based on Ward's minimum variance were analysed (**Figure 3.19**). Bacterial communities clustered based on sample origin: the 'sybr green high', 'sybr green low' and 'all' cell populations originating from the same participant shared the highest similarity. For all participants, the 'sybr green high' and 'all' cell populations shared the most similarity. The distance between samples based on fungal communities was greater with no clear grouping based on cell population, participant, disease status or participant pairing.

The beta diversity of the bacterial and fungal communities isolated from 'sybr green high', 'sybr green low' and 'all' cell populations was then analysed (**Figure 3.20**). To analyse the effect of cell population on the composition of microbial profiles similarities were calculated using the generalised UniFrac distance metric. Distance matrices were plotted on a MDS plot and significance was calculated using PERMANOVA. There were no significant differences between 'sybr green high', 'sybr green low' and 'all' cells in the bacterial or fungal communities ($p=0.958$ and $p=0.852$), with there being smaller dissimilarities between the cell populations in the bacterial communities (5 % dissimilarity) compared to the fungal communities (20 % dissimilarity).

To perform taxonomic classification of 'IgG positive' and 'IgG negative' stool microbes as much DNA as possible was required. The DNA extraction efficiencies from 'sybr green high', 'sybr green low' and 'all' stool microbes (**Table 3.7**) were measured using the DNA extraction method optimised in **section 0**. As 90 % of the microbiome is made up of bacteria, the average bacterial genome size of 5 Mb (Nayfach and Pollard, 2015) was used to calculate DNA extraction efficiency. For all participants the DNA extraction efficiency was highest from 'sybr green high' microbes and therefore the optimised protocol would isolate 'IgG positive' and 'IgG negative' microbes from the 'sybr green high' cell population.

To summarise, SYBR™ green I nucleic acid gel stain stained a greater proportion of fungal cells than the eukaryotic cell specific dye calcofluor white stain. By comparing the bacterial composition of 'sybr green high' and 'sybr green low' cells it was determined that there were no significant differences or bacteria resistant to staining with SYBR™ green I nucleic acid gel stain but it could instead reflect the genetic content of live and dead bacterial cells respectively. Conclusions on 'sybr green high' and 'sybr green low' fungal cells were unable to be drawn and this was assumed to be due to low fungal content in stool samples. As SYBR™ green I nucleic acid gel stain was the best stain for the detection of fungal cells and 'sybr green high' cell populations yielded higher DNA concentrations, 'sybr green high' cell populations were chosen to be used in the optimised protocol.

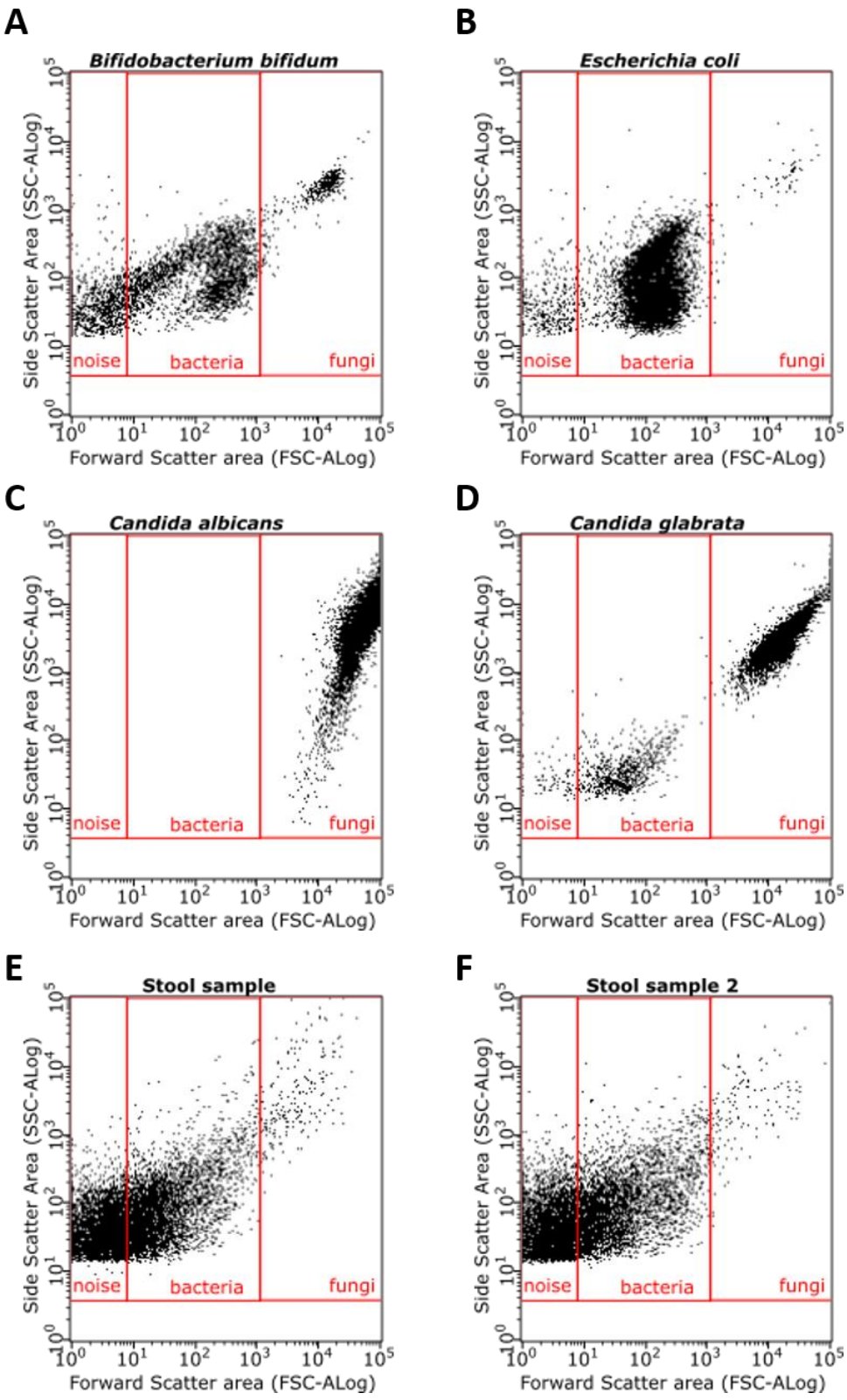

Figure 3.12: Flow cytometry detection of yeast and bacteria using forward and side scatter profiles. *Aliquots of two bacterial species (A+B), two yeast species (C+D) and two stool samples (E+F) were analysed on the Guava® easCyte HT system and forward and side scatter properties of each sample were collected. A buffer only control was used to set the noise gate, Escherichia coli was used to set the bacteria gate and Candida albicans was used to set the fungi gate.*

Table 3.6: Optimising the SYBR™ green I nucleic acid gel stain concentration for bacterial staining. *Bacteroides fragilis cells were stained with different concentrations of SYBR™ green I nucleic acid gel stain and then analysed on the BD LSRFortessa™ to measure the percentage of sybr green positive cells.*

SYBR™ green I nucleic acid gel stain dilution (concentration)	**'SYBR green positive' (%)**
2 x 10^{-2} (200 X)	84.2
1 x 10^{-2} (100 X)	85.8
1 x 10^{-3} (10 X)	92.8

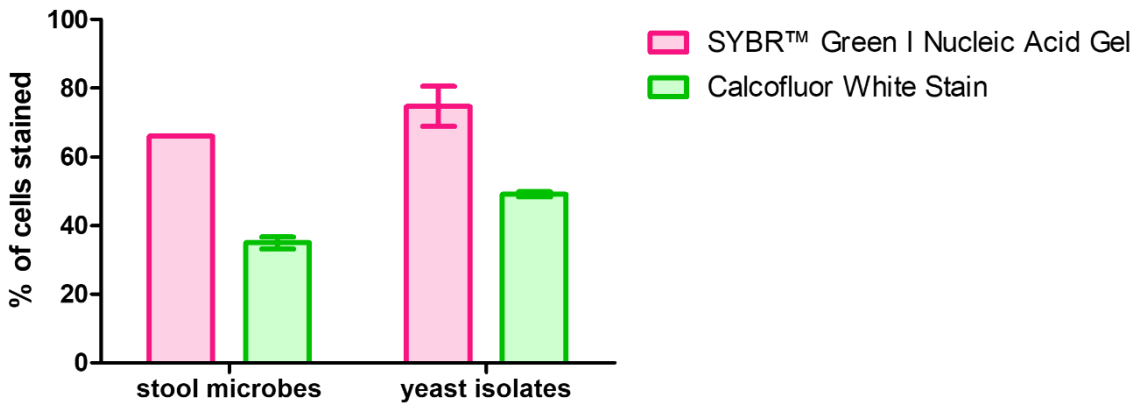

Figure 3.13: Comparing SYBR™ green I nucleic acid gel stain's and calcofluor white's staining of faecal microbes and yeast isolates. *Two stool samples and two strains of S. cerevisiae were stained with SYBR™ green I nucleic acid gel stain and calcofluor white stain, a stain which binds cellulose and chitin in the cell wall of fungi. The percentage of cells positive for each stain was analysed using the BD LSRFortessa™. Error bars on the graph show the range.*

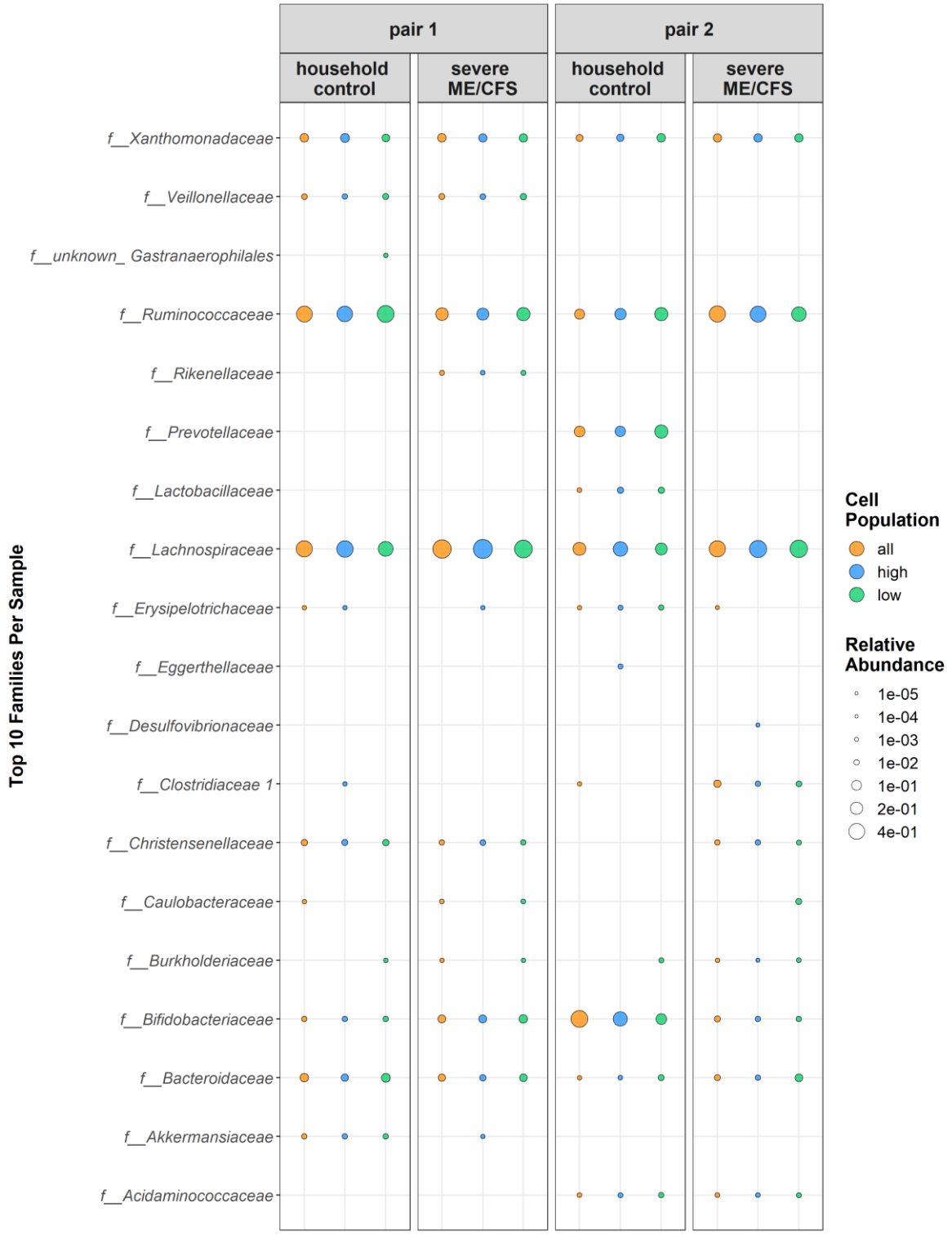

Figure 3.14: Relative abundances of the top 10 bacterial families that stain high and low with SYBR™ green I nucleic acid gel stain. *Stool microbes from two pairs of severe ME/CFS patients and their matched household controls (n=4) were stained with SYBR™ green I nucleic acid gel stain and analysed on the Sony SH800S cell sorter. Cells were sorted into 'sybr green high' populations, 'sybr green low' populations and 'all' events in the scatter gate were also collected. DNA from each cell population was sequenced by 16S rRNA gene sequencing and relative abundances at the family taxonomic rank were visualised using a bubble plot.*

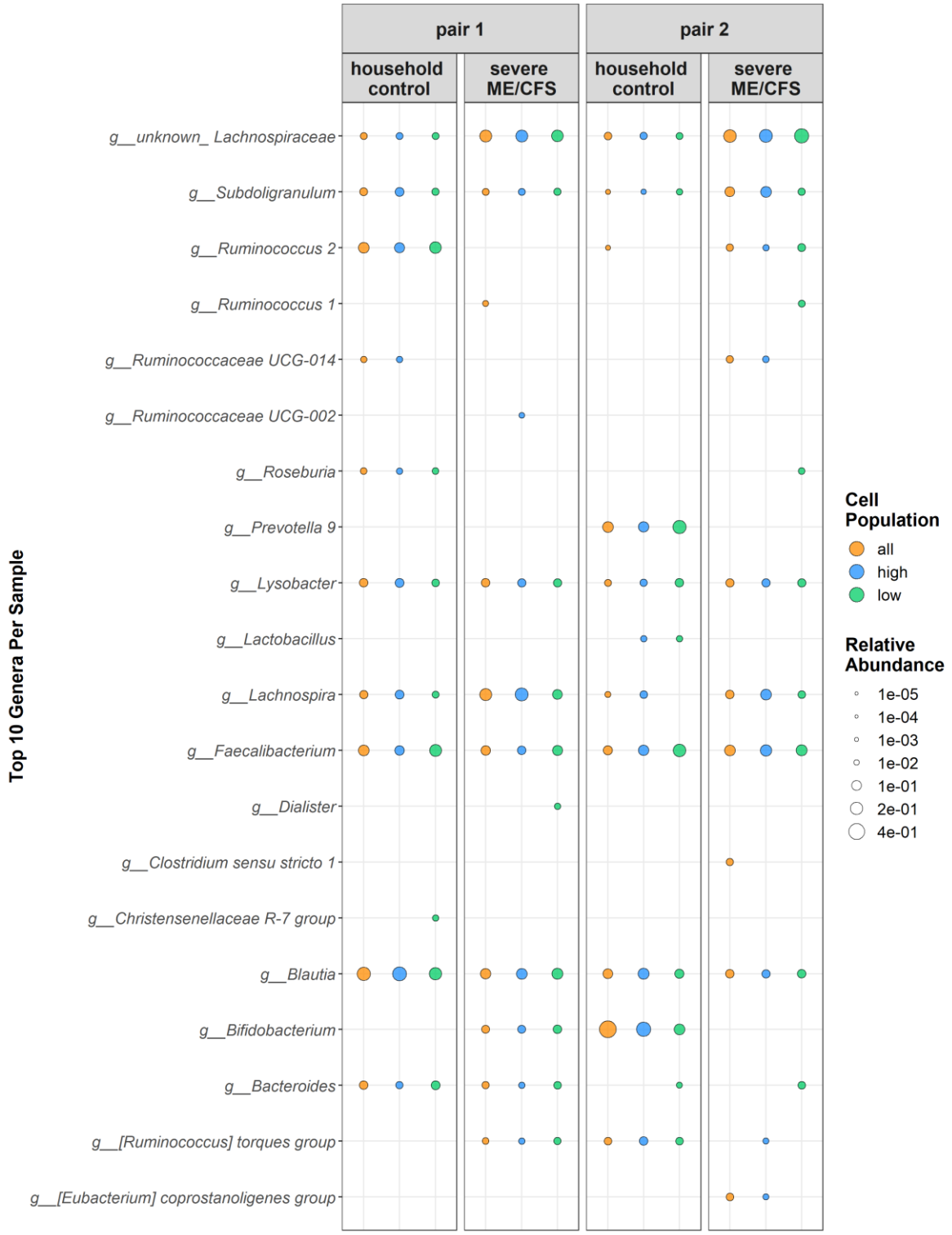

Figure 3.15: Relative abundances of the top 10 bacterial genera that stain high and low with SYBR™ green I nucleic acid gel stain. *Stool microbes from two pairs of severe ME/CFS patients and their matched household controls (n=4) were stained with SYBR™ green I nucleic acid gel stain and analysed on the Sony SH800S cell sorter. Cells were sorted into 'sybr green high' populations, 'sybr green low' populations and 'all' events in the scatter gate were also collected. DNA from each cell population was sequenced by 16S rRNA gene sequencing and relative abundances at the genera taxonomic rank were visualised using a bubble plot.*

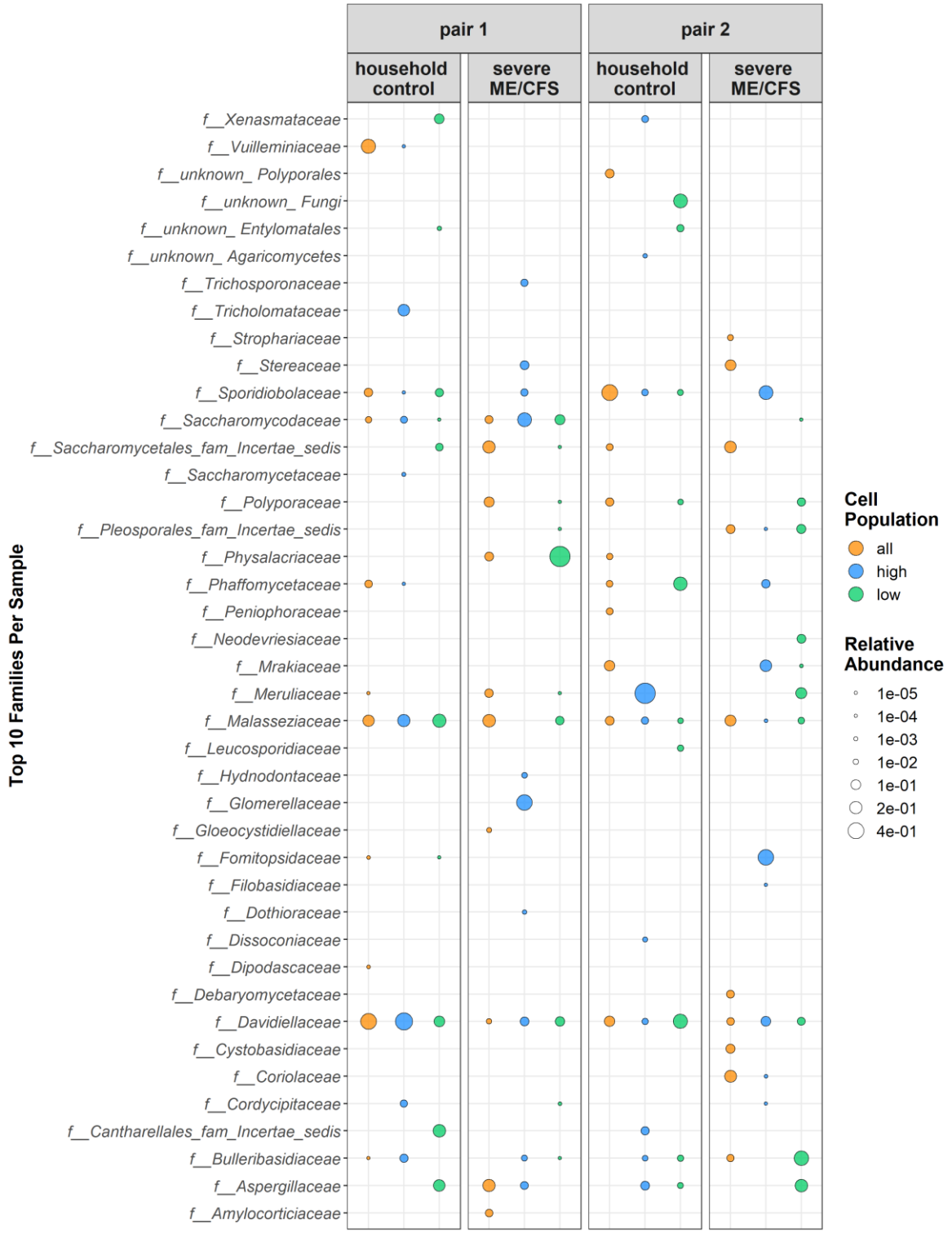

Figure 3.16: Relative abundances of the top 10 fungal families that stain high and low with SYBR™ green I nucleic acid gel stain. *Stool microbes from two pairs of severe ME/CFS patients and their matched household controls (n=4) were stained with SYBR™ green I nucleic acid gel stain and analysed on the Sony SH800S cell sorter. Cells were sorted into 'sybr green high' populations, 'sybr green low' populations and 'all' events in the scatter gate were also collected. DNA from each cell population was sequenced by ITS rRNA gene sequencing and relative abundances at the family taxonomic rank were visualised using a bubble plot.*

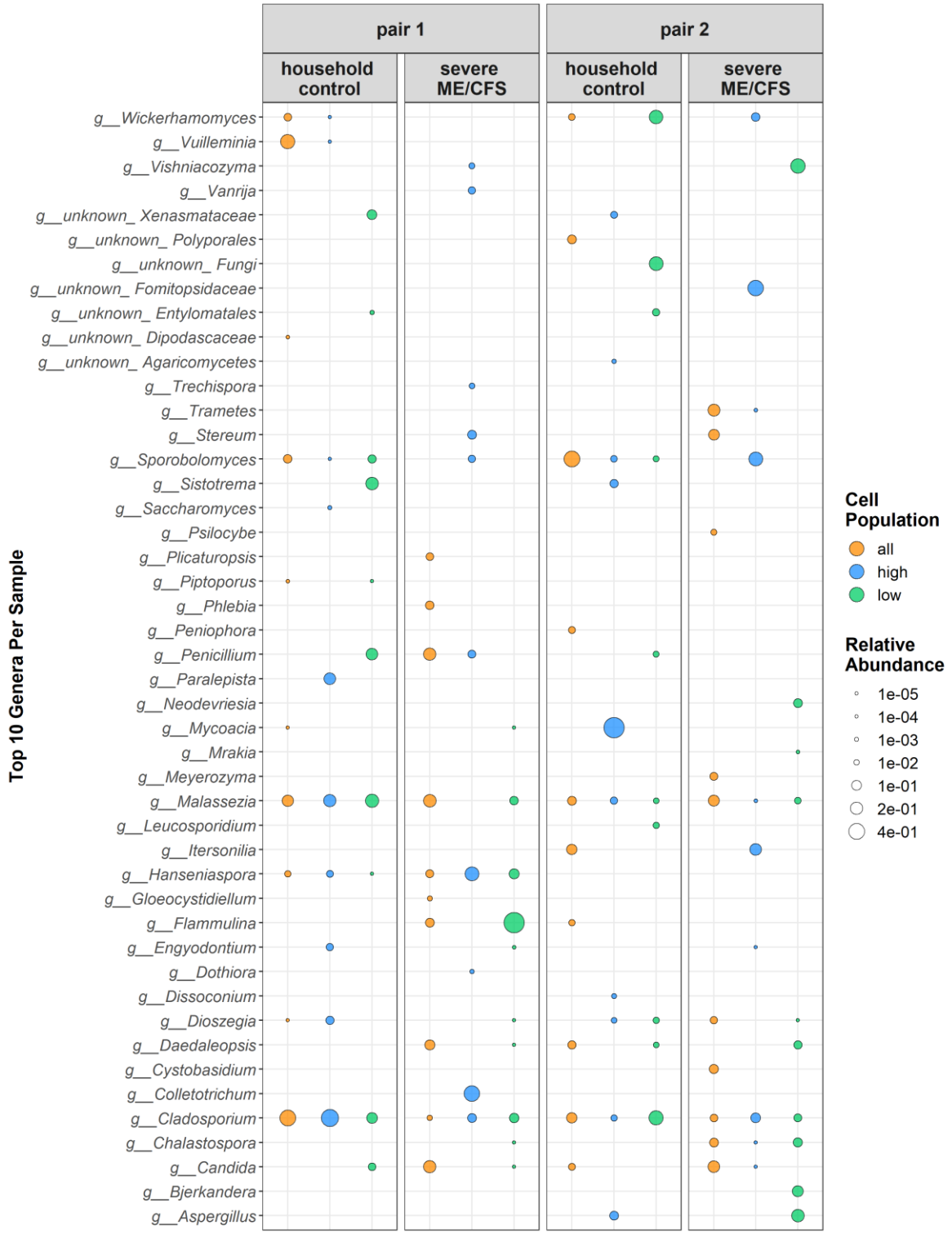

Figure 3.17: Relative abundances of the top 10 fungal genera that stain high and low with SYBR™ green I nucleic acid gel stain. *Stool microbes from two pairs of severe ME/CFS patients and their matched household controls (n=4) were stained with SYBR™ green I nucleic acid gel stain and analysed on the Sony SH800S cell sorter. Cells were sorted into 'sybr green high' populations, 'sybr green low' populations and 'all' events in the scatter gate were also collected. DNA from each cell population was sequenced by ITS rRNA gene sequencing and relative abundances at the genera taxonomic rank were visualised using a bubble plot.*

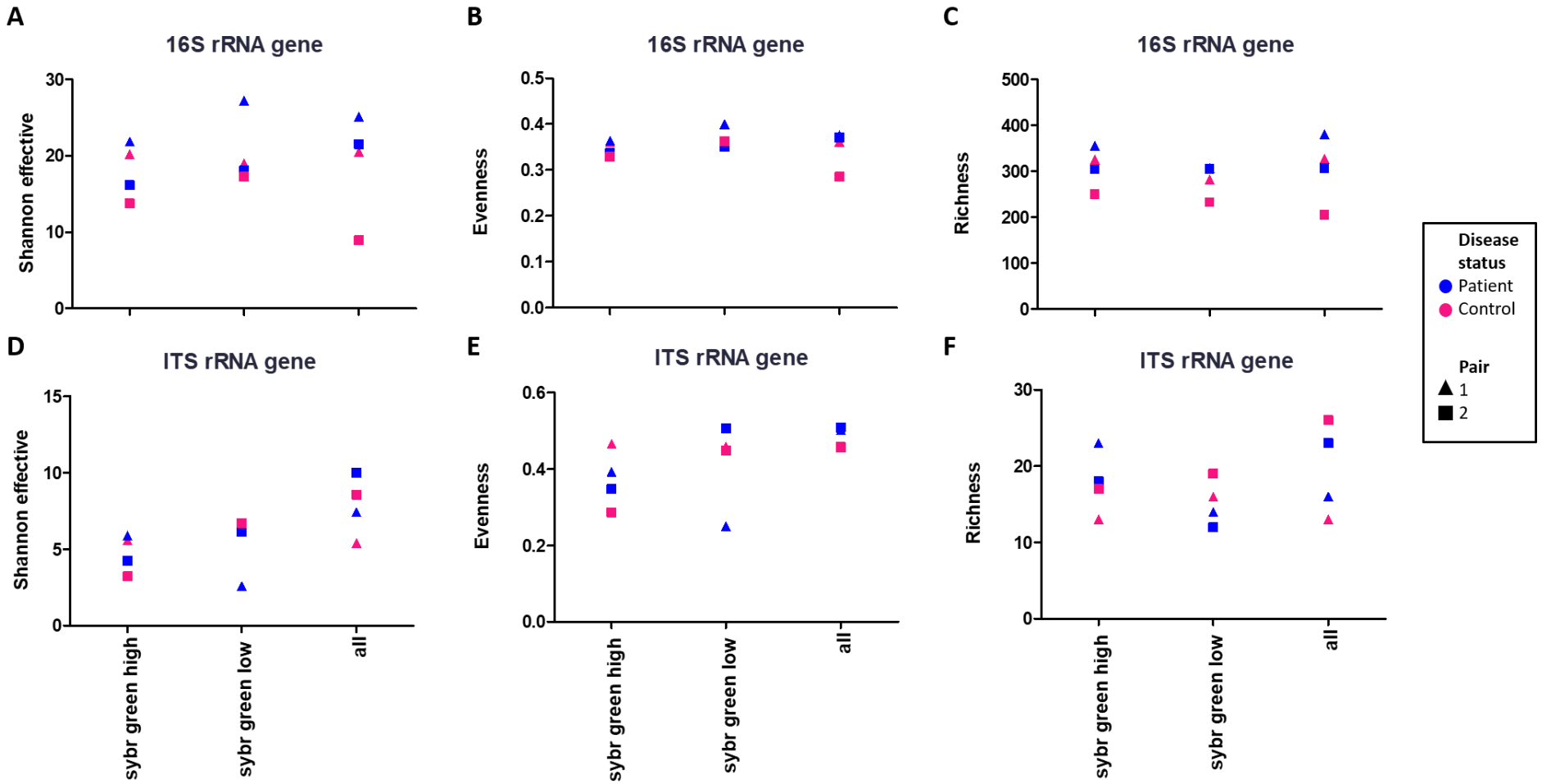
A
16S rRNA gene
Shannon effective
30
20
10
0
B
16S rRNA gene
Evenness
0.5
0.4
0.3
0.2
0.1
0.0
C
16S rRNA gene
Richness
500
400
300
200
100
0
D
ITS rRNA gene
Shannon effective
15
10
5
0
E
ITS rRNA gene
Evenness
0.6
0.4
0.2
0.0
F
ITS rRNA gene
Richness
30
20
10
0
sybr green high
sybr green low
all
Disease status
Patient
Control
Pair
1
2

Figure 3.18: Alpha diversity of bacterial and fungal communities staining high and low with SYBR™ green I nucleic acid gel stain. *Stool microbes from two pairs of severe ME/CFS patients and their matched household controls (n=4) were stained with SYBR™ green I nucleic acid gel stain and analysed on the Sony SH800S cell sorter. Cells were sorted into 'sybr green high' populations, 'sybr green low' populations and 'all' events in the scatter gate were also collected. 16S rRNA and ITS rRNA gene sequencing of each sample were analysed using Shannon effective (A+D), evenness (B+E) and richness (C+F). Each point represents a single measurement.*

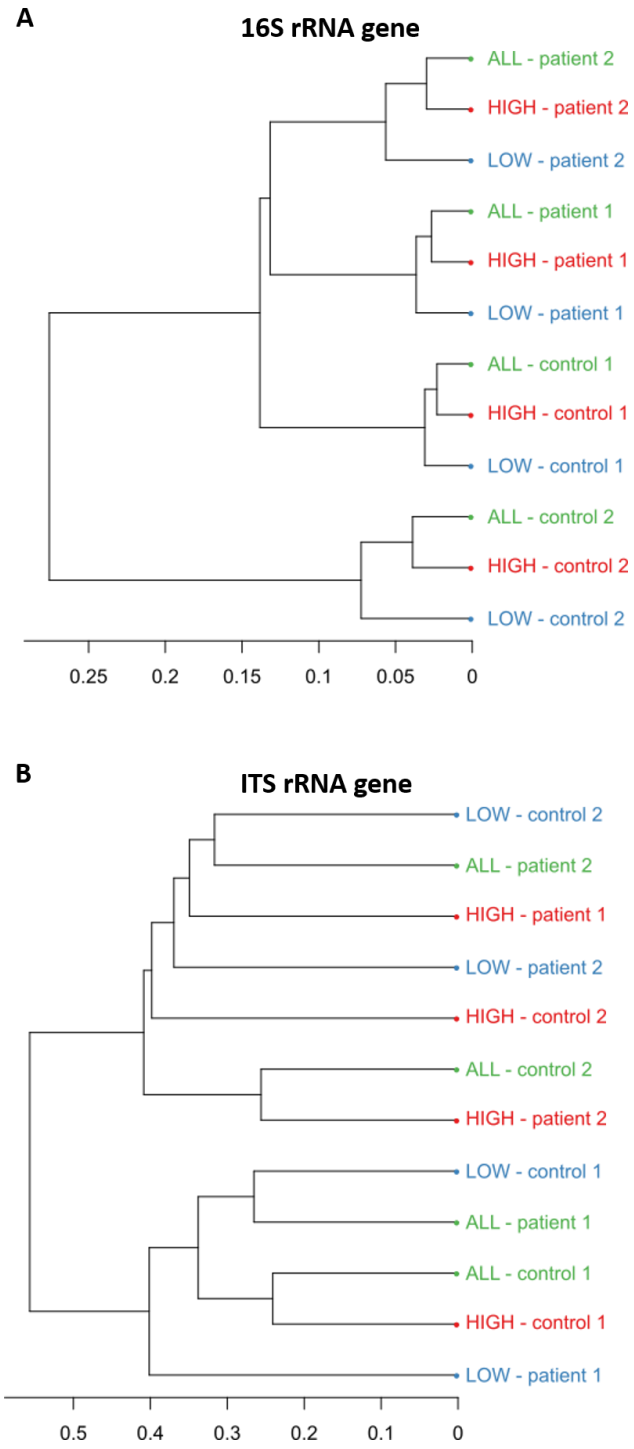

Figure 3.19: Hierarchical clustering of 'sybr green high' (red), 'sybr green low' (blue) and 'all' (green) stool microbes. *Stool microbes from two pairs of severe ME/CFS patients and their matched household controls (n=4) were stained with SYBR™ green I nucleic acid gel stain and separated into 'sybr green high', 'sybr green low' and 'all' cell populations using the SH800S cell sorter. 16S rRNA and ITS rRNA gene sequencing were performed. Ward's minimum variance was used to generate phylograms of A) bacterial communities identified using 16S rRNA gene sequencing and B) fungal communities identified using ITS rRNA gene sequencing.*

A

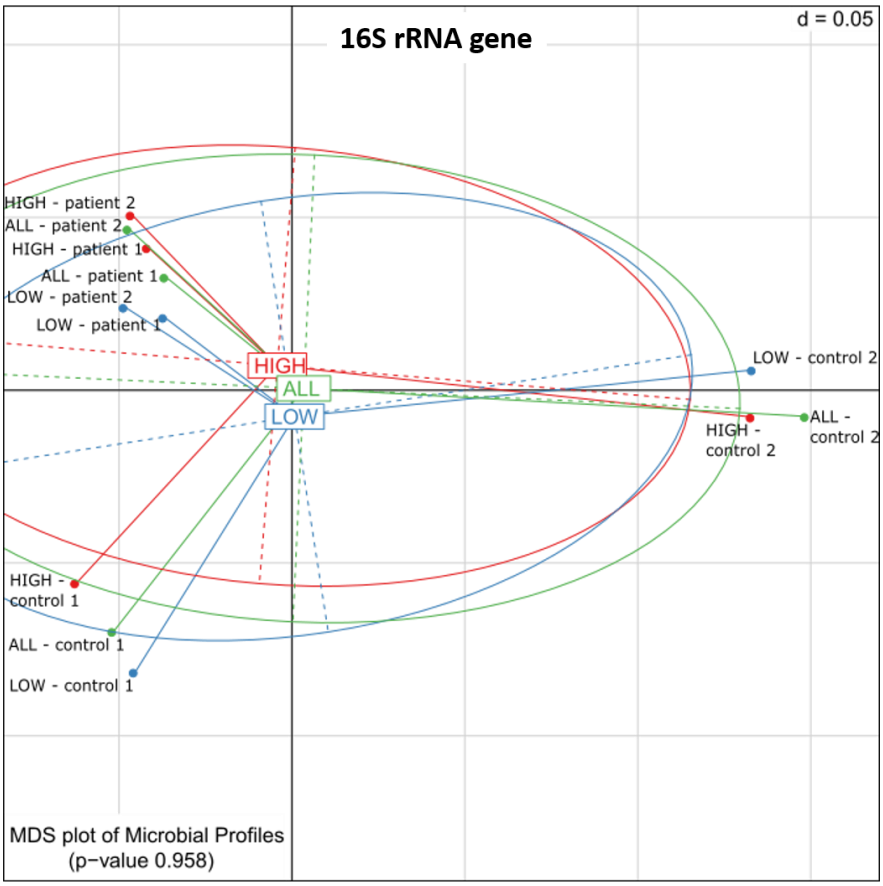
16S rRNA gene
d = 0.05
HIGH - patient 2
ALL - patient 2
HIGH - patient 1
ALL - patient 1
LOW - patient 2
LOW - patient 1
HIGH
ALL
LOW
LOW - control 2
ALL - control 2
HIGH - control 2
HIGH - control 1
ALL - control 1
LOW - control 1
MDS plot of Microbial Profiles
(p−value 0.958)

B

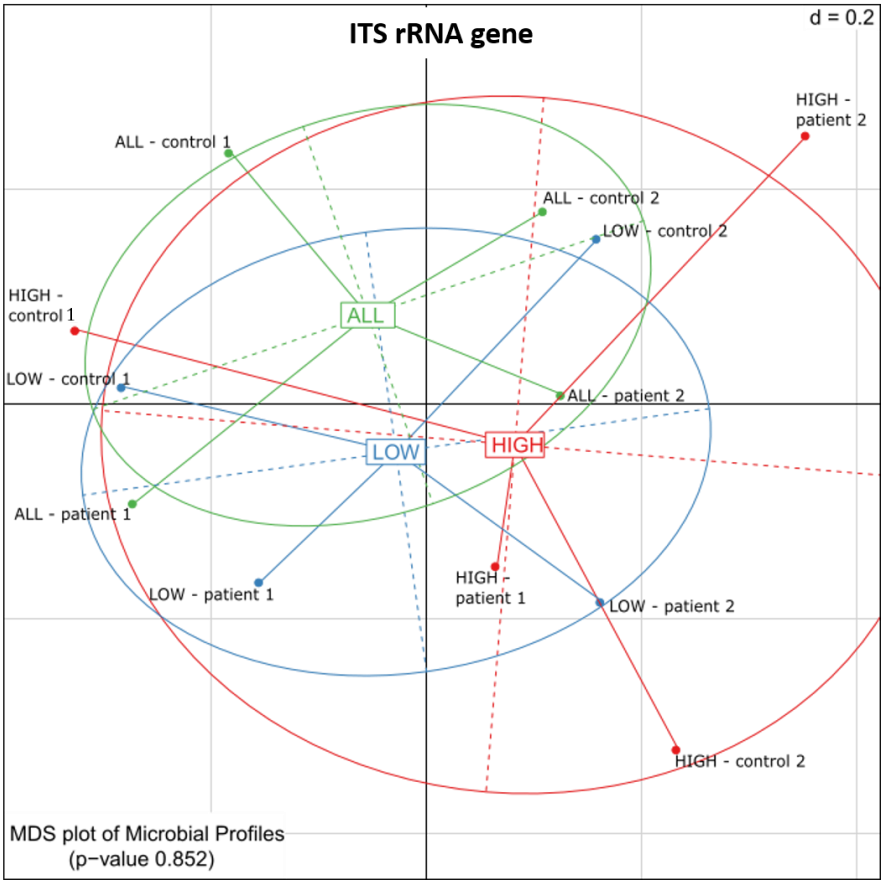
ITS rRNA gene
d = 0.2
HIGH - patient 2
ALL - control 1
ALL - control 2
LOW - control 2
HIGH - control 1
ALL
LOW - control 1
ALL - patient 2
HIGH
LOW
ALL - patient 1
HIGH - patient 1
LOW - patient 1
LOW - patient 2
HIGH - control 2
MDS plot of Microbial Profiles
(p−value 0.852)

← Figure 3.20: Beta diversity of bacterial (A) and fungal (B) communities of 'sybr green high' (red), 'sybr green low' (blue) and 'all' (green) stool microbes. *Stool microbes from two pairs of severe ME/CFS patients and their matched household controls (n=4) were stained with SYBR™ green I nucleic acid gel stain and separated into 'sybr green high', 'sybr green low' and 'all' cell populations using the Sony SH800S cell sorter. 16S rRNA and ITS rRNA gene sequencing were performed. Generalised UniFrac distances were used to generate a MDS plot for visualising dissimilarity between centrifuged and filtered microbes. 'D' is a measure of dissimilarity. Significance was measured using PERMANOVA.*

Table 3.7: DNA extraction efficiency from 'sybr green high', 'sybr green low' and 'all' stool microbes. *Stool microbes from two pairs of severe ME/CFS patients and their matched household controls (n=4) were stained with SYBR™ green I nucleic acid gel stain and separated into 'sybr green high', 'sybr green low' and 'all' cell populations using the Sony SH800S cell sorter. DNA was stained with the Qubit™ dsDNA high sensitivity assay kit and total DNA was measured on the Qubit™ fluorometer. The DNA extraction efficiency was calculated based on the assumption that the average genome size of a stool microbe is 5 MB.*

Pair number	Disease status	Cell population	Cell number	Total DNA (ng)	DNA extraction efficiency (%)
1	Patient	High	7,388,751	15	37.62
		Low	10,000,000	7.5	13.90
		All	6,000,000	5.8	17.91
1	Control	High	7,243,987	14.4	36.83
		Low	8,000,000	8.1	18.76
		All	8,000,000	7.9	18.30
2	Patient	High	7,500,000	12.2	30.14
		Low	6,317,228	-	-
		All	8,000,927	11.1	25.70
2	Control	High	8,561,127	9.2	19.91
		Low	6,658,823	-	-
		All	8,000,000	7.5	17.37

3.3.3 Optimising the detection of IgG reactive stool microbes

3.3.3.1 Optimising the quantification of microbes in stool

Part of the cell sorting procedure for identifying intestinal microbes reactive with systemic IgG is the incubation of serum samples with stool microbes. For this step, stool microbes needed to be suspended at a concentration of 1 x 10^6 cells/ml. To determine the optimal stool dilutions for microbial quantification the concentration of 'sybr green high' events in 2-fold dilutions of microbes isolated from a single stool sample were measured using the Guava® easyCyte™ HT system, in triplicate (**Figure 3.21A**). The three stool dilutions with the highest correlation coefficient value (R^2 = 0.9812) were 1 in 160000, 1 in 320000 and 1 in 640000 and were therefore the dilutions chosen for quantifying stool microbe concentration (**Figure 3.21B**).

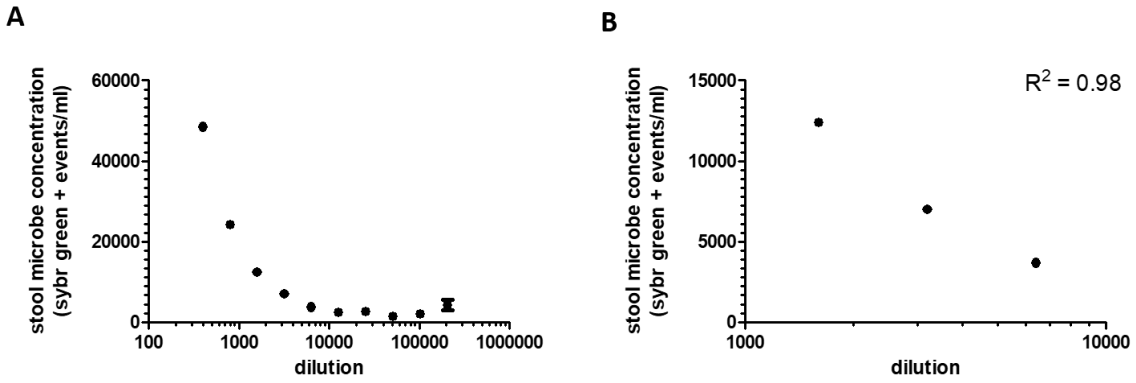

Figure 3.21: Stool microbe titration curve. *2-fold serial dilutions of stool microbes were stained with SYBR™ green I nucleic acid gel stain. Concentrations of sybr green stained microbes were measured for each dilution using the Guava® easCyte HT system. Readings were measured in triplicate and results presented as mean ±SEM. A) Concentrations of sybr green positive stool microbes at 2-fold dilutions. B) The stool microbe dilutions that have a correlation coefficient value (R^2) closest to 1.*

3.3.3.2 Optimising serum incubation with stool microbes

In order to detect all of the stool microbes reactive with serum IgG the optimal serum concentration to be used in the assay needed to be determined. Two-fold dilutions of serum from two pairs of severe ME/CFS patients and their matched household controls were incubated with autologous stool microbes and analysed using the BD LSRFortessa™. The percentage of 'IgG positive' events reached saturation in three of the four participants measured at the serum dilution 1 in 100 (**Figure 3.22**). Therefore, the dilution used for the assay was 1 in 100.

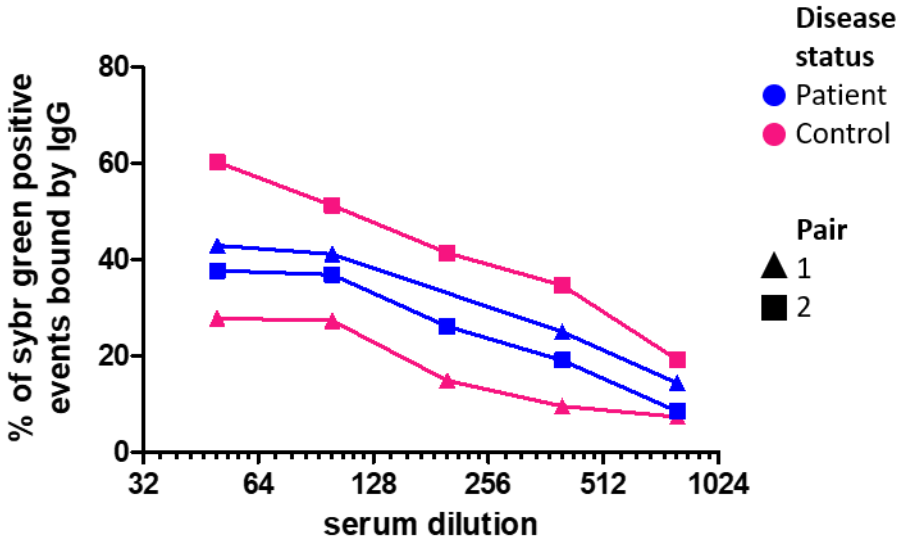

Figure 3.22: Serum titration curve. *2-fold serial dilutions of serum were incubated with stool microbes from two pairs of severe ME/CFS patients and their matched household controls (n=4). Following incubation, samples were stained with SYBR™ green I nucleic acid gel stain and anti-human IgG-APC/Cy7 antibody. The percentage of 'IgG positive' events from the 'sybr green high' cell population was measured on the BD LSRFortessa™. 1 x 10^4 events were acquired for analysis.*

3.3.4 Determining the optimal number of 'IgG positive' and 'IgG negative' stool microbes to be collected during cell sorting

The next step of optimisation was to determine the number of 'IgG positive', 'IgG negative' and 'all' stool microbes to be collected using the Sony SH800S cell sorter aiming to find the lowest number of cells that could be collected without compromising the diversity of samples. This was done by analysing the bacterial taxa composition, alpha and beta diversity of 10^3, 10^4, 10^5, 10^6, 2.5 x 10^6 and 5 x 10^6 microbes isolated from stool using filtration. As the number of cells analysed increased from 10^3 to 10^5, the number of top 10 bacterial families shared with 5 x 10^6 cells increased (**Figure 3.6**). There was little change in composition and abundance of top 10 fungal families from 10^5 cells to 5 x 10^6 cells (**Figure 3.8**). Whereas at the genus-level, the cell counts with the most similarity to the highest cell count tested were 10^5 and 10^6 as they shared 9 of the top 10 bacterial taxa with 5 x 10^6 cells (**Figure 3.7**). The relationship between cell counts and alpha diversity measures based on bacterial taxa were then examined. Shannon effective, richness and evenness scores increased as cell counts increased from 10^3 to 10^6 and alpha diversity scores reached saturation at 10^6 cells (**Figure 3.10**). When analysing the phylogenetic distances between samples 10^6 and 2.5 x 10^6 cells were most similar to 5 x 10^6 cells (**Figure 3.23**). The lowest number of cells with a similar bacteria composition and diversity to 5 x 10^6 cells was 10^6 cells. Therefore, the optimised protocol aimed to collect 10^6 cells from each condition on the Sony SH800S cell sorter.

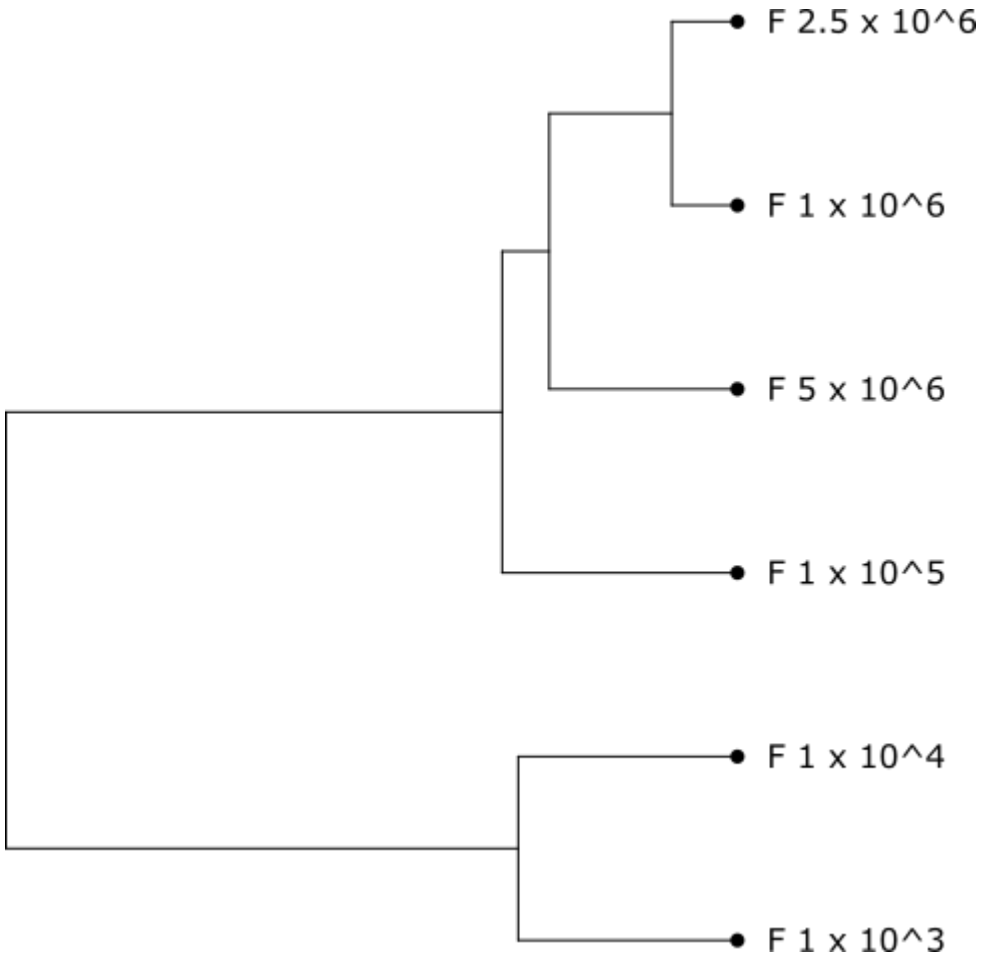

Figure 3.23: Hierarchical clustering of different concentrations of filtered stool microbes. *A single stool sample underwent filtration, followed by 16s rRNA gene sequencing on DNA extracted from 1 x 10^3, 1 x 10^4, 1 x 10^5, 1 x 10^6, 2.5 x 10^6 and 5 x 10^6 cells collected using the Sony SH800S cell sorter. Ward's minimum variance was used to generate phylograms of bacterial communities identified using 16S rRNA gene sequencing.*

3.3.5 Optimising DNA extraction from bacterial and fungal cells

Following isolation of 10^6 'IgG positive', 'IgG negative' and 'all' microbes, DNA was to be extracted from cells for whole genome shotgun sequencing. First the DNA extraction efficiency of the 'Gram-positive bacteria genomic DNA purification protocol' was tested using Gram-negative bacteria *B. fragilis* and Gram-positive bacteria *B. longum* for two reasons: 1) bacteria outnumber yeast in stool (Qin et al., 2010), 2) Gram-negative bacteria are harder to lyse than Gram-positive bacteria (Wright et al., 2017). Surprisingly, the DNA extraction efficiency was higher from the Gram-negative bacteria than the Gram-positive bacteria (**Figure 3.24A**). However, the 'Gram-positive bacteria genomic DNA purification protocol' needed optimising because the DNA extraction efficiency was low from both Gram-positive bacteria, 13.7 %, and Gram-negative bacteria, 27.2 %.

The 'Gram-positive bacteria genomic DNA protocol' from the GeneJET genomic DNA purification kit was modified by adding achromopeptidase to the lysis buffer, increasing the first lysis step from 30 to 60 minutes and the second lysis step from 30 to 50 minutes (**Table 3.4**). The Gram-positive bacteria *B. longum* was used to compare the DNA extraction efficiency of the original and modified 'Gram-positive bacteria genomic DNA purification protocol'. The DNA extraction efficiency from 5 x 10^6 cells using the modified protocol was higher than the original protocol (**Figure 3.24B**). In addition, the DNA extraction efficiency of the modified protocol on lower cell numbers was tested: at 1.4 x 10^6 cells, DNA extraction efficiency was 96 %.

Next the efficiency of the modified 'Gram-positive bacteria genomic DNA purification protocol' for DNA extraction from Gram-negative bacteria was determined. The quantity of DNA extracted from *B. fragilis* using the modified 'Gram-positive bacteria genomic DNA purification protocol' was compared to the quantity of DNA extracted from *B. fragilis* using the 'Gram-negative bacteria genomic DNA purification protocol'. The quantity of DNA extracted from 5 x 10^7 cells was two-fold higher using the 'Gram-negative bacteria genomic DNA purification protocol' than the modified 'Gram-positive bacteria genomic DNA purification protocol' (**Figure 3.24C**). At the lower cell concentration 9.2 x 10^6 cells the extracted DNA quantity from the 'Gram-negative bacteria genomic DNA purification protocol' and the modified 'Gram-positive bacteria genomic DNA purification protocol' was 34.8 ng and 29.2 ng respectively. Therefore, the modified 'Gram-positive bacteria genomic DNA purification protocol' from the GeneJET genomic DNA purification kit was suitable for DNA extraction from both Gram-positive and Gram-negative bacteria.

The quantity of DNA extracted from Gram-positive bacteria, Gram-negative bacteria and yeast using the modified 'Gram-positive bacteria genomic DNA purification protocol', QIAamp® PowerFecal® pro DNA kit and MP Bio FastDNA spin kit for soil was then compared. No quantifiable DNA was isolated from 10^5, 10^6 or 10^7 Gram-negative bacteria, 10^5 or 10^6 Gram-positive bacteria and 10^5 or 10^6 yeast using the MP Bio FastDNA spin kit for soil. Whereas the modified 'Gram-positive

bacteria genomic DNA purification protocol' and QIAamp® PowerFecal® pro DNA kit isolated DNA from 10^5, 10^6 and 10^7 Gram-positive and Gram-negative bacteria and yeast (**Figure 3.25**). The modified 'Gram-positive bacteria genomic DNA purification protocol' isolated higher quantities of DNA from 10^5, 10^6 and 10^7 Gram-positive and Gram-negative bacterial cells than the QIAamp® PowerFecal® pro DNA kit, but lower quantities of DNA from 10^6 and 10^7 yeast cells. The modified 'Gram-positive bacteria genomic DNA purification protocol' isolated 35.2 ng and 3.6 ng of DNA from 10^6 Gram-positive and Gram-negative bacteria respectively. Whereas the QIAamp® PowerFecal® pro DNA kit only isolated 5.8 ng and 0.7 ng of DNA from 10^6 Gram-positive and Gram-negative bacteria respectively. The QIAamp® PowerFecal® pro DNA kit isolated 5.6 ng of DNA from 10^6 yeast cells, which was higher than the 2.96 ng of DNA isolated using the modified 'Gram-positive bacteria genomic DNA purification protocol'. However, the modified 'Gram-positive bacteria genomic DNA purification protocol' isolated 2.1 ng of DNA from 10^5 yeast cells, which was higher than the 1.0 ng of DNA isolated using the QIAamp® PowerFecal® pro DNA kit (**Figure 3.25C**). Therefore, the modified 'Gram-positive bacteria genomic DNA purification protocol' from the GeneJET genomic DNA purification kit was the most efficient method for extracting DNA from 10^5 yeast, 10^6 Gram-positive and 10^6 Gram-negative bacteria.

To analyse the microbial composition of 'IgG positive', 'IgG negative' and 'all' cell populations isolated from stool a minimum quantity of 5 ng of DNA was required to perform whole genome shotgun sequencing. Based on 90 % of the microbiome being bacteria and the average bacterial genome size being 5 Mb (Nayfach and Pollard, 2015), it was calculated that 1 x 10^6 cells were needed to extract 5 ng of DNA. The DNA quantities extracted from 10^3, 10^4, 10^5 and 10^6 stool microbes using the modified 'Gram-positive bacteria genomic DNA protocol' were less than 5 ng. Whereas DNA extracted from 2.5 x 10^6 and 5 x 10^6 stool microbes was 10.72 ng and 29.36 ng respectively (**Table 3.8**). WGA of DNA extracted from 10^3, 10^4, 10^5, 10^6, 2.5 x 10^6 and 5 x 10^6 stool microbes increased DNA quantities more than 70-fold (**Table 3.8**).

A

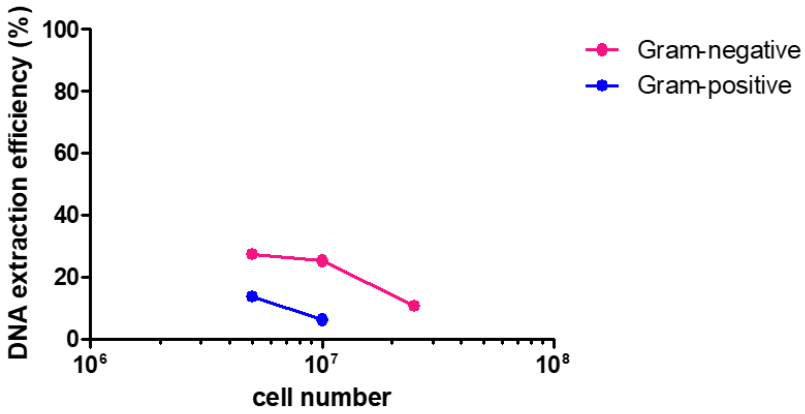
DNA extraction efficiency (%)
100
80
60
40
20
0
10^6
10^7
10^8
cell number
Gram-negative
Gram-positive

B

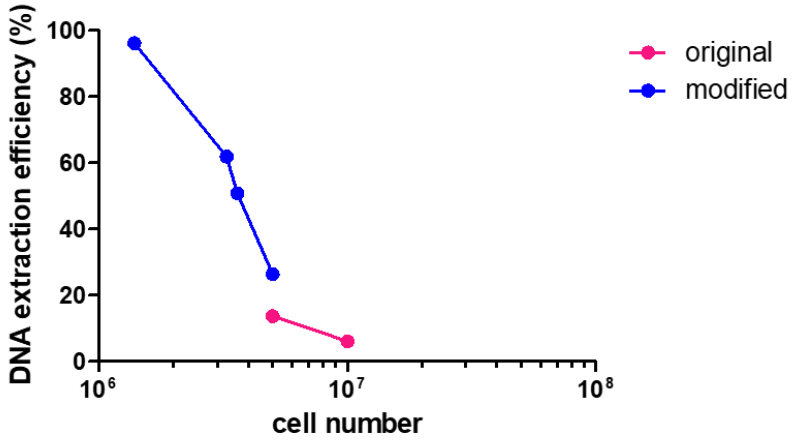
DNA extraction efficiency (%)
100
80
60
40
20
0
10^6
10^7
10^8
cell number
original
modified

C

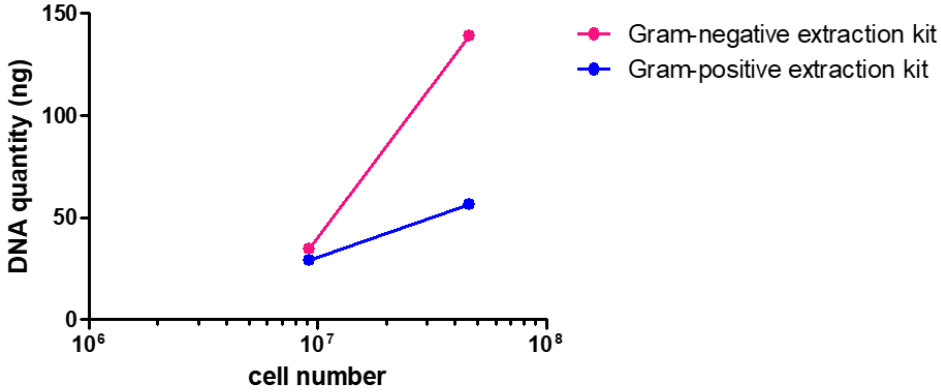
DNA quantity (ng)
150
100
50
0
10^6
10^7
10^8
cell number
Gram-negative extraction kit
Gram-positive extraction kit

←Figure 3.24: Optimising the GeneJET genomic DNA purification kit. *A) Comparing DNA extraction efficiency of the 'Gram-positive bacteria genomic DNA purification protocol' from the GeneJET genomic DNA purification kit on the Gram-positive bacteria Bifidobacterium longum and the Gram-negative bacteria Bacteroides fragilis. B) Comparing DNA extraction of original versus modified 'Gram-positive bacteria genomic DNA purification protocol' from Gram-positive bacteria. C) Comparing the amount of DNA extracted from Gram-negative bacteria using the modified 'Gram-positive bacteria genomic DNA purification protocol' and the 'Gram-negative bacteria genomic DNA purification protocol'. The 'Gram-positive bacteria genomic DNA purification protocol' had three modifications: 1) addition of achromopeptidase in the lysis buffer, 2) incubation step with Gram-positive bacteria lysis buffer was increased from 30 to 60 minutes, 3) incubation step with lysis solution and proteinase K was increased from 30 to 50 minutes. Extracted DNA was stained with the Qubit™ dsDNA high sensitivity assay kit and quantity was measured on the Qubit™ fluorometer.*

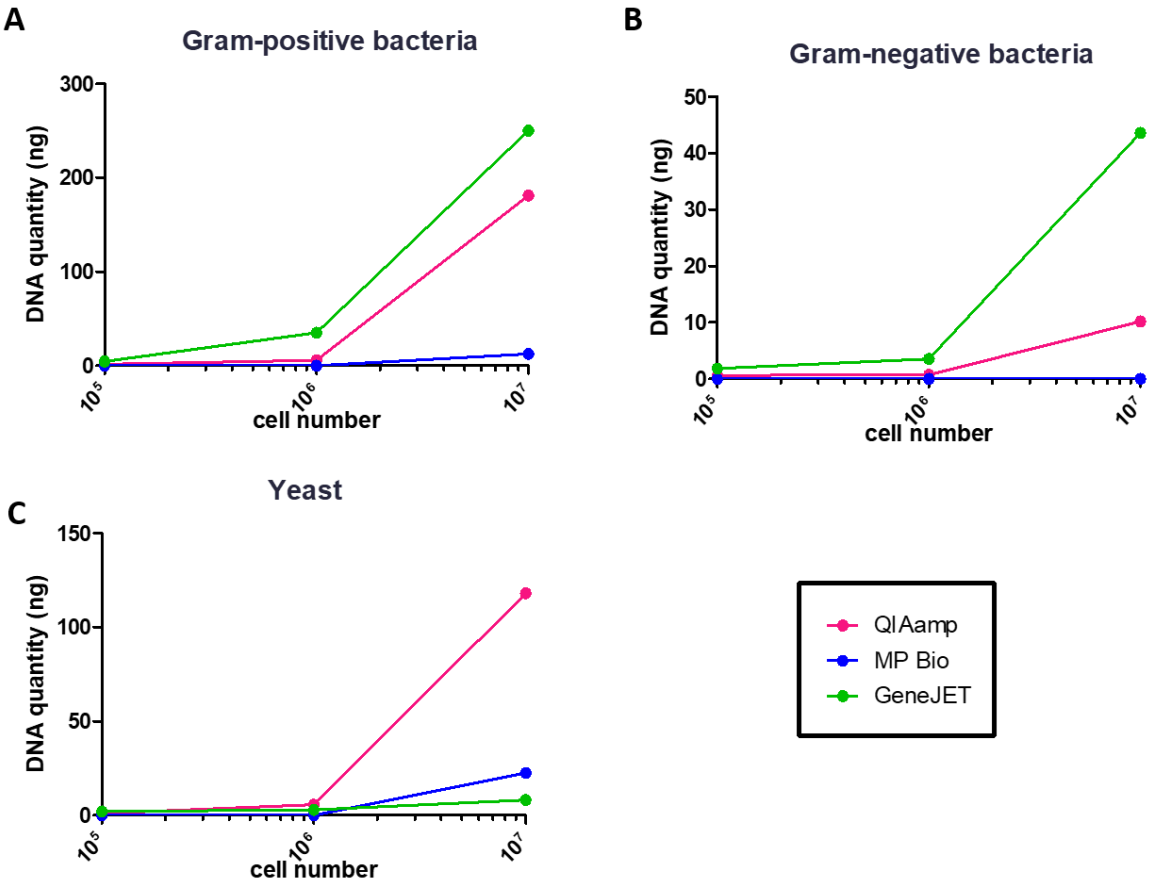

Figure 3.25: Comparing DNA extraction methods. *Three methods were used to extract DNA from A) Gram-positive bacteria, B) Gram-negative bacteria and C) yeast: QIAamp® PowerFecal® pro DNA kit, MP Bio FastDNA spin kit for soil and the modified Gram-positive GeneJET genomic DNA purification kit. DNA was measured on the Qubit™ fluorometer using the Qubit™ dsDNA high sensitivity assay kit.*

Table 3.8: Amount of DNA extracted from stool microbes before and after whole genome amplification (WGA). *Stool microbes from a single sample were run on the Sony SH800S cell sorter and different numbers of cells were collected for DNA extraction. DNA was stained with the Qubit™ dsDNA high sensitivity assay kit and quantities were measured on the Qubit™ fluorometer before and after samples underwent WGA using REPLI-g advanced DNA single cell kit.*

Cell number	Total DNA pre-WGA (ng)	Total DNA post WGA (ng)
5×10^6	29.36	2,048.00
2.5×10^6	10.72	6,944.00
1×10^6	3.35	6,048.00
1×10^5	3.38	10,480.00
1×10^4	1.92	6,784.00
1×10^3	2.98	7,392.00
0	0	401.60

3.4 DISCUSSION

This chapter explains the development of an experimental workflow based on 'bug FACS' to identify bacteria and fungi from stool that are reactive with serum IgG. The key findings from optimisation are: 1) filtration of stool microbes recovers larger cells than centrifugation, 2) SYBR™ green I nucleic acid gel stain identifies bacteria and fungi in FACS, 3) accurate quantification of stool microbes requires stool to be diluted to 1 in 160000, 1 in 320000 and 1 in 640000, 4) 1 in 100 diluted serum identifies all microbes reactive with serum IgG, 5) 1×10^6 cells captures diversity within a stool sample, 6) a modified version of the 'Gram-positive bacterial genomic DNA purification protocol' from the GeneJET genomic DNA purification kit extracts DNA from Gram-positive bacteria, Gram-negative bacteria and yeast, 7) WGA is required to obtain sufficient DNA for whole genome shotgun sequencing.

First, the effect of centrifugation and filtration on the diversity of bacteria and fungi in stool was compared. By using a single sample the inter-individual variability of the faecal microbiome was avoided enabling focus to be on investigating methodological variation (Huseyin et al., 2017). It was found that bacterial diversity was not altered by the microbial isolation method used. It was difficult

to draw conclusions on the effect of the microbial isolation method on fungal diversity because the diversity was low in both methods. This was to be expected, as the abundance of fungi in the microbiome is reported to be around 0.1 % (Qin et al., 2010). Therefore, when isolating 1 x 10^3 to 5 x 10^6 cells only 1 to 5 x 10^3 fungal cells were being analysed. However, using FSC in FACS as an arbitrary measure of cell size showed that there are more cells of a larger size in microbes isolated from stool samples by filtration compared to centrifugation. As fungi are larger than bacteria it was hypothesised that the cells isolated from stool with high FSC were fungi. This was confirmed by analysing the FSC of yeast isolates. This suggests that the centrifugation method for isolating microbes from stool debris may also pellet some fungal cells.

'Bug FACS' involves the detection of microbes on a flow cytometer. Unlike with fungi, FSC and SSC gating is not effective for identifying bacteria in FACS whereas the fluorescent dye SYBR™ green I nucleic acid gel stain is able to identify bacteria in FACS. The eukaryotic specific dye calcofluor white stain is not required for fungal identification on FACS as SYBR™ green I Nucleic Acid Stain is able to stain a larger portion of fungal cells. When staining stool microbes with SYBR™ green I nucleic acid gel stain, stool microbes had different fluorescent intensities and formed two populations based on their level of staining, referred to as 'sybr green high' and 'sybr green low' cell populations. The fluorescence intensity of SYBR™ green I nucleic acid gel stain directly reflects the nucleic acid content of cells (Zipper et al., 2004), which in turn differs based on the type of bacteria, cell viability and cell cycle stage (Günther et al., 2008, Lebaron et al., 2002, Müller et al., 2000). To determine why stool microbes segregate into 'sybr green high' and 'sybr green low' cell populations, 'sybr green high', 'sybr green low' and 'all' microbes were FACS sorted, DNA was extracted and analysed for the bacterial and fungal profiles of these cell populations. It was found that 'sybr green high' and 'sybr green low' bacterial populations originating from the same stool sample had a smaller phylogenetic distance than 'sybr green low' bacterial populations isolated from different stool samples. Therefore, there is no evidence for a specific group of microbes resistant to staining with SYBR™ green I nucleic acid gel stain. One limitation of using the DNA intercalation dye SYBR™ green I nucleic acid gel stain is that it has been shown to have inhibitory effects on PCR and could therefore affect DNA sequencing (Gudnason et al., 2007). However, larger DNA quantities were extracted from 'sybr green high' cells than from 'sybr green low' cells, which suggests SYBR™ green I nucleic acid gel stain does not inhibit DNA extraction and sequencing. Alternatively, 'sybr green low' cells could have a lower DNA content because they are dead and consequently undergoing DNA degradation (Lebaron et al., 2002). Future studies could be done to a) confirm SYBR™ green I nucleic acid gel stain does not inhibit DNA extraction and sequencing by comparing the DNA quantity and microbial diversity of equal amounts of stool microbes stained with SYBR™ green I nucleic acid gel stain, unstained stool microbes and stool microbes stained with other DNA intercalating dyes previously shown not to inhibit PCR (Gudnason et al., 2007), and b) confirm 'sybr green low' cells

are dead cells by performing dead cell discrimination using amine-reactive dyes (Perfetto et al., 2011).

The 'bug FACS' protocol was optimised to enable the identification and quantification of all stool microbes reactive with serum IgG by investigating the dilutions of stool required to accurately quantify microbial load, investigating serum dilution required to bind all stool microbes and investigating the number of cells required to capture diversity. 1 in 160000, 1 in 320000 and 1 in 640000 dilutions of stool were found to accurately quantify stool microbes. Accurate quantification of stool microbes enables the investigation of absolute abundances of 'IgG positive' microbes in stool, which can overcome the limitations associated with relative abundances (Barlow et al., 2020). As the microbial load in stool samples varies between individuals (Vandeputte et al., 2017), stool microbes were resuspended to a known concentration prior to incubation with serum, to avoid participants with the same levels of serum antibody reactivity to the microbiome having different proportions of microbes coated with antibody when incubated with serum. The optimal serum dilution for identifying all microbes reactive with serum IgG is 1 in 100. Doron et al. (2021) also incubated stool microbes with 1 in 100 diluted sera. Whereas Morento-Sabater et al. (2020) and Fadlallah et al. (2019) selected serum concentration based on total IgG content, which accounts for the inter-individual variation in serum IgG concentrations. Finally, comparing the diversity measures of stool microbes ranging from 1×10^3 to 5×10^6 cells found that a minimum of one million cells were required to capture diversity. This was double the number of cells previous authors found were required (Jackson et al., 2021).

Other experimental conditions such as incubation time, temperature and buffer composition affect specific (Fab-mediated) antibody binding (Reverberi and Reverberi, 2007). In the future, experiments could be done to compare the effect of altering these conditions on the level of antibody bound stool microbes. For example, the concentration and type of protein added to the FACS buffer could be compared to ensure the absence of false positives due to non-specific (Fc region) antibody binding. In addition, use of positive and negative controls would confirm specific (Fab-mediated) antibody binding. In **chapter 4** positive and negative controls were used to develop an ELISA based method for detecting levels of serum antibody binding to autologous and heterologous stool microbes (see **supplementary figure 4.5**). These controls were serum collected at day 0 (negative control) and day 57 (positive control) from rabbits inoculated with stool microbes.

Based on the average bacterial genome size (Nayfach and Pollard, 2015) it was calculated that 1×10^6 cells contain 5.4 ng of DNA. The efficiency of three DNA extraction kits were compared because shotgun metagenomic sequencing requires at least 5 ng of DNA for analysis and previous authors found the DNA yield recovered varied with different extraction procedures (Fiedorová et al., 2019,

Huseyin et al., 2017). The main step of DNA extraction is cell lysis. Gram-positive bacteria, Gram-negative bacteria and yeast have different cell wall structures. Therefore, DNA extraction kits were tested for DNA extraction efficiency from each cell type. It was found that for both Gram-positive and Gram-negative bacteria the modified 'Gram-positive bacteria genomic DNA purification protocol' from the GeneJET genomic DNA purification kit had the highest DNA extraction efficiency. As this was the only method without a mechanical lysis step it could suggest that bead-beating negatively impacted the DNA yield from bacteria. In contrast, methods involving mechanical lysis had greater DNA extraction efficiency from the highest number of yeast cells tested. At the lowest number of yeast cells analysed DNA yield was greater from cells when methods without mechanical lysis were used, suggesting mechanical lysis became redundant with decreasing numbers of yeast cells. As the concentration of fungi in stool is low (Huseyin et al., 2017), it was decided that the modified 'Gram-positive bacteria genomic DNA purification protocol' would be used to extract DNA from 1 x 10^6 'IgG positive' and 1 x 10^6 'IgG negative' stool microbes. Despite attempts to optimise a DNA extraction procedure, the DNA yield extracted from one million stool microbes was still too low to perform shotgun metagenomic sequencing. Therefore, WGA was utilised in the optimised protocol. WGA is a technique able to amplify DNA from a range of species. However, caution has to be taken when interpreting metagenomic results due to the introduction of sequencing bias during WGA (Quince et al., 2017).

3.4.1 Conclusion

This chapter shows the development of an optimised 'bug FACS' protocol for the identification of fungal and bacterial cells reactive with serum IgG. This method is important because of the growing evidence for systemic anti-microbiota IgG as a biomarker of disease. This optimised protocol was used for the work detailed in chapter 5 which compared intestinal microbes reactive with serum IgG in severe ME/CFS patients to their matched household controls.

4 CHAPTER FOUR: QUANTIFYING ANTIBODY LEVELS REACTIVE WITH THE INTESTINAL MICROBIOME IN MYALGIC ENCEPHALOMYELITIS/CHRONIC FATIGUE SYNDROME

4.1 INTRODUCTION

4.1.1 Immune tolerance in health and chronic inflammatory diseases

The GI tract is a source of dietary and microbial antigens, to which the intestinal immune system is tolerant (Zheng et al., 2020). There is a 'mucosal firewall' consisting of an intact epithelial barrier and mucosal layer which prevents the dissemination of microbes into the systemic circulation (Belkaid and Hand, 2014). Immune tolerance is maintained by tolerogenic dendritic cells (DCs) in gut associated lymphoid tissues which sample both innocuous and pathogenic antigens within the intestinal lumen and promote the differentiation of naïve $CD4^+$ T cells into regulatory T cells (Stagg, 2018) and the production of IgA-secreting plasma cells (Tezuka and Ohteki, 2019). IgA-secreting plasma cells can be produced via both T cell-dependent (Zeng et al., 2016) and T cell-independent (He et al., 2007) routes and function to maintain homeostasis through a process called immune exclusion: by coating pathogenic microbes, IgA prevents their adherence to and invasion of the intestinal epithelium (Xiong and Hu, 2015).

In microbial dysbiosis bacterial access and adherence to the epithelium results in a pro-inflammatory immune response (Atarashi et al., 2015, Zheng et al., 2020). Intestinal inflammation is associated with the breakdown of the epithelial barrier and enables translocation of microbes and microbial antigens, such as endotoxins, which can trigger systemic inflammation (Nagpal and Yadav, 2017, Kinashi and Hase, 2021). Intestinal inflammation also compromises the tolerogenic properties of intestinal DCs leading to the differentiation of naïve $CD4^+$ T cells into effector T cells such as Th1 and Th17 cells, resulting in a pro-inflammatory immune response targeting both pathobionts and commensals (Morris et al., 2016). In addition, the level of secretory IgA in the intestine increases which coats inflammatory microbes (Palm et al., 2014). There is an ongoing debate as to whether the generation of anti-microbiota IgG antibodies and microbiota reactive $CD4^+$ T cells present in the circulation occurs in health or when there is a breach in the intestinal epithelial barrier due to inflammation, physical insults or chemical insults (Mowat, 2018). Nevertheless, the levels of circulating anti-microbiota IgG antibodies increase during chronic inflammatory diseases, such as IBD (Harmsen et al., 2012).

4.1.2 Immune tolerance and autoimmunity

A breakdown in immune tolerance and systemic translocation of commensal microbes, pathogens or pathobionts can initiate or propagate autoimmune disease by the following mechanisms: molecular mimicry, bystander activation, epitope spreading, T helper cell skewing and post-translational modification of autoantigens (Ruff et al., 2020). Examples of autoimmune diseases initiated or propagated by the intestinal microbiota include RA (Pianta et al., 2017), SLE (Greiling et al., 2018), MS (Planas et al., 2018) and antiphospholipid syndrome (Ruff et al., 2019). ME/CFS is a complex multisystemic disease with an autoimmune component, as evidenced by autoantibodies to muscarinic and acetylcholine receptors (Fujii et al., 2020), which has the potential to be initiated by the intestinal microbiota (detailed in **section 1.3.2.4**). As in the other autoimmune diseases, patients with ME/CFS show evidence of microbial dysbiosis, characterised by decreased diversity of the microbiome, decreased prevalence of anti-inflammatory microbes such as *Faecalibacterium* and *Bifidobacterium* (Giloteaux et al., 2016a) and evidence of a leaky gut (Maes et al., 2007, Maes et al., 2012d). Whether microbial dysbiosis results in a breakdown in immune tolerance and therefore is a potential mechanism for the initiation or propagation of autoimmunity in ME/CFS has yet to be explored. Therefore, the research in this chapter investigated the levels of serum IgG and stool IgA antibodies to the intestinal microbiome of severe ME/CFS patients, as indicators of a breach in tolerance in the systemic and intestinal immune responses respectively.

4.1.3 Aims and objectives

The primary aim of this chapter was to determine whether severe ME/CFS patients had a heightened local and systemic humoral immune response to intestinal microbes compared to their matched household controls. To investigate this, the following objectives were undertaken:

1. Determine the concentration of IgA in stool which is bound to microbes
2. Determine the concentration of stool microbes coated by IgA
3. Quantify the level of serum IgG reactive to autologous and heterologous stool microbes
4. Determine the concentration of stool microbes reactive with serum IgG

4.2 METHODS

Stool and serum samples from the study population were collected and processed as described in **Section 2.6**.

4.2.1 Stool sample water content quantification

100 mg ± 10 mg aliquots of frozen stool samples were weighed before and after freeze drying in the ModulyoD freeze dryer (Thermo Electron Corporation) for 12 hours. Water content of the stool sample was calculated using **Equation 4.1**.

Equation 4.1: Calculating water content of stool samples.

$$\frac{(wet\ weight\ (mg) - dry\ weight\ (mg))}{wet\ weight\ (mg)} \times 100$$

4.2.2 Quantifying total microbes in stool

The concentration of stool microbes in a liquid suspension was measured as described in **section 3.2.5.3**. Using **Equation 4.2** the concentration of stool microbes per gram of stool was calculated.

Equation 4.2: Calculating the number of microbes per gram of stool.

$$concentration\ (cells\ gram^{-1}) = 1\%\ w/v\ stool\ suspension\ (cell\ ml^{-1}) \times 100$$

4.2.3 Quantification of microbe bound IgA and non-bound IgA in stool

100 mg ± 10 mg aliquots of frozen stool samples were processed as described in **section 3.2.2.2** with the following modification: samples were diluted to 10 % w/v with coating buffer (0.2 M $NaHCO_3$ pH 9.4). Stool microbes were then centrifuged at 16,000 x g for 5 minutes and the supernatant was aspirated and centrifuged a second time. The supernatant from the second round of centrifugation was used to analyse free non-bound IgA. The pellets from both rounds of centrifugation were combined, washed with coating buffer, resuspended to the original volume and then used to analyse levels of microbe bound IgA.

Levels of microbe bound IgA and non-bound IgA in the stool were quantified using an indirect ELISA, the optimisation of which is detailed in **Supplementary figure 4.1** and **Supplementary figure 4.2**. Briefly, the protocol published by Scholtens et al. (2008) which measured non-bound IgA1 (the predominant isotype in the blood) and IgA2 (the predominant isotype in mucosal secretions) in stool samples was optimised to reduce background noise by determining the highest signal detected when altering the following parameters: blocking step duration, format of the ELISA, concentration of detection antibody and concentration of HRP-conjugated streptavidin.

The standard (IgA from human colostrum reagent grade, buffered aqueous solution, Sigma Aldrich) was 2-fold serial diluted from 250 ng/ml to 3.9 ng/ml and samples were diluted 10-fold from 1 to 1 in 10^6 in coating buffer. 100 µl/well of each dilution of samples and standards were added in duplicate and incubated for 16 hours at 4 °C. Plates were washed three times with 200 µl/well wash buffer (PBS, 0.05 % Tween™ 20) and then incubated with 300 µl/well blocking buffer (PBS + 0.05 % Tween™ 20 + 2 % BSA fraction V + 1 % normal mouse serum (Thermo Fisher Scientific)) for 3 hours at 20 °C on a shaking plate. Plates were washed three times and then incubated with 100 µl/well of 1000 ng/ml detection antibody (biotin mouse anti-human IgA1/IgA2, clone G20-359 (RUO), BD Biosciences) diluted in blocking buffer at 20 °C on a shaking plate for 1 hour. Plates were washed three times and then incubated with 100 µl/well of 1 in 8 x 10^4 HRP-conjugated streptavidin

(Thermo Fisher Scientific) diluted in blocking buffer at 20 °C on a shaking plate for 30 minutes. Plates were washed six times and then incubated with 100 µl/well TMB high sensitivity substrate solution (BioLegend® UK Ltd) for 5 minutes. The reaction was quenched with 100 µl/well stop solution (2N H_2SO_4). Absorbance was determined by analysing OD 450 nm.

Background absorbance readings were subtracted from sample measurements. Sample concentrations were interpolated from the standard curve by performing quadratic polynomial regression analysis.

4.2.4 Relative quantification of IgA binding stool microbes

Concentration of microbes in stool samples were quantified following **section 3.2.5.3**. Stool microbes were resuspended to 2 x 10^6 cells/ml in FACS buffer (PBS + 0.1 % BSA) and 50 µl of this was incubated with either 50 µl of isotype control master mix (PBS + 0.1 % BSA + 1 in 500 SYBR™ green I nucleic acid stain + 1 in 50 isotype control antibody, mouse IgG1, APC (Miltenyi Biotec)) or sample master mix (PBS + 0.1 % BSA + 1 in 500 SYBR™ green I Nucleic Acid Stain + 1 in 50 anti-human IgA-APC (Miltenyi Biotec)) for 30 minutes at 20 °C in the dark. Samples were then fixed with 300 µl of 1 % PFA.

Cells were acquired using the BD LSRFortessa™ as described previously in **section 3.2.6**. Unstained samples and fluorescence minus one controls (FMO) were used to set the gating parameters used (

←**Figure 4.1**).

The percentage of IgA positive microbes was normalised by subtracting false positive events measured using the isotype control.

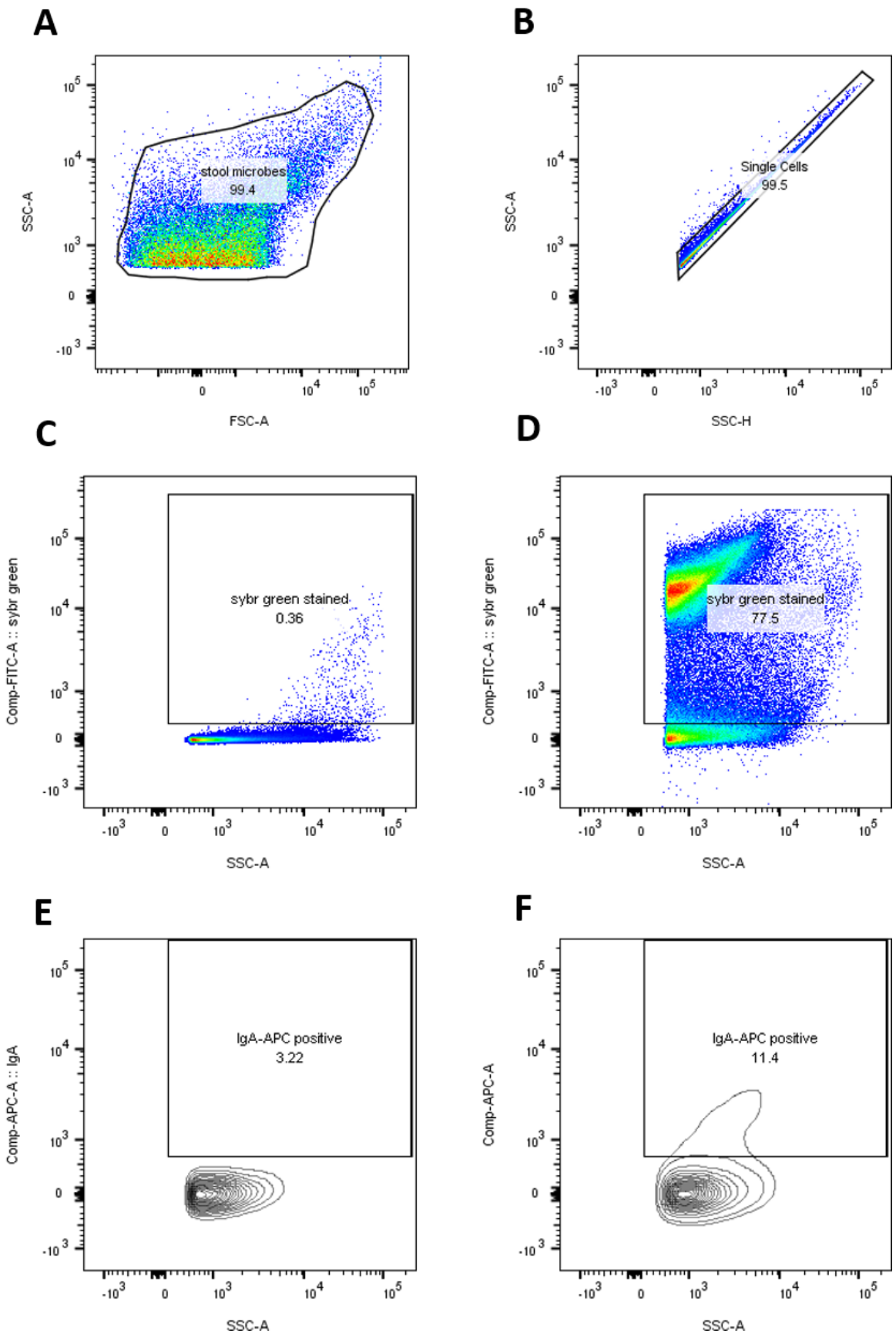
A
stool microbes
99.4
SSC-A
FSC-A
B
Single Cells
99.5
SSC-A
SSC-H
C
sybr green stained
0.36
Comp-FITC-A :: sybr green
SSC-A
D
sybr green stained
77.5
Comp-FITC-A :: sybr green
SSC-A
E
IgA-APC positive
3.22
Comp-APC-A :: IgA
SSC-A
F
IgA-APC positive
11.4
Comp-APC-A
SSC-A

←Figure 4.1: Gating strategy to identify IgA bound stool microbes. *Representative data of IgA positive microbes isolated from stool samples. Microbes were extracted from stool samples and stained with SYBR™ green I nucleic acid gel stain and anti-human IgA-APC antibody or a mouse IgG1-APC isotype control antibody. Stained samples were fixed with 1 % PFA before running on the BD LSRFortessa™. 10^4 events were acquired and analysed using FlowJo™ software version 10.7.1. A) Acquired events were gated to exclude debris based on light scatter properties. B) Events from the stool microbes gate were plotted on SSC-A versus SSC-H to exclude doublets. C) A fluorescence minus one control (stained with IgA-APC only) was used to set the 'sybr green stained' gate on singlets. D) An example of a stool sample stained with SYBR™ green I nucleic acid gel stain. E) A mouse IgG1-APC isotype control was used to set the 'IgA-APC positive' gate on 'sybr green stained' stool microbes. F) An example of the IgA profile of a stained stool sample.*

4.2.5 Serum IgG quantification

Total IgG serum was measured using a commercial Invitrogen ELISA kit (Thermo Fisher Scientific, catalogue number: 88-50550-22) according to the manufacturer's protocol. Capture antibody (pre-titrated, purified anti-human IgG monoclonal antibody) was diluted 1 in 250 in coating buffer (PBS), 100 µl/well was added to the Corning™ Costar™ 9018 ELISA plate and incubated for 16 hours at 4°C. Plates were washed twice with 400 µl/well wash buffer (PBS + 0.05 % Tween™ 20) following aspiration of diluted capture antibody. Plates were incubated with 250 µl/well blocking buffer (2x PBS + 1 % Tween™ 20 + 10 % BSA) for 2 hours at 20 °C. Plates were washed twice following aspiration of blocking buffer. Serum samples were thawed and diluted 2-fold from 1 in 1 x 10^5 to 1 in 8 x 10^5 and standards (recombinant human IgG) provided with the kit were diluted 2-fold from 100 ng/ml to 1.6 ng/ml with assay buffer A (1x PBS + 1 % Tween™ 20 + 10 % BSA). 100 µl/well of diluted samples and standards were added in duplicate and incubated for 2 hours at 20 °C. Plates were washed four times and then 100 µl/well of 1 in 250 detection antibody (pre-titrated, HRP-conjugated anti-human IgG monoclonal antibody) diluted in assay buffer A was incubated at 20 °C for 1 hour. Plates were washed four times with 400 µl/well wash buffer following aspiration of diluted detection antibody. The plate was incubated with 100 µl/well substrate solution (TMB) for 15 minutes at 20 °C. The reaction was quenched with 100 µl/well stop solution (2N H_2SO_4). Absorbance was determined by analysing OD 450 nm – 750 nm.

Background absorbance readings were subtracted from sample measurements. Quadratic polynomial regression analysis of the standard curve was performed to interpolate the concentration of IgG in samples.

4.2.6 Qualitative assay measuring serum IgG reactivity to autologous and heterologous stool samples

Levels of serum IgG reactive to autologous and heterologous stool microbes were measured using an optimised ELISA based protocol (optimisation detailed in **Supplementary figure 4.5**). Briefly, the duration of the coating step was optimised to ensure maximum signal detection and background noise was reduced by optimising the washing step. Finally, bacteria, serum and detection antibody were titrated.

1 ml microbial glycerol stocks from stool samples processed as described in **section 2.6.6.1** were thawed and washed three times with sterile PBS at 8000 x g for 5 minutes and then the pellet was resuspended to 1 ml. 2-fold serial dilutions of stool microbes in PBS were plated in duplicate in a 96-well flat bottom Corning™ Costar™ 9018 ELISA plate. Absorbance was measured at 570 nm. Stool microbes were resuspended to an optical density (OD) of 0.05 with coating buffer (0.1 M $NaHCO_3$ pH 9.4).

100 µl/well of stool microbes were added to Nunc™ Maxisorp™ flat-bottom 96 well plates and incubated for 16 hours at 4 °C. Plates were washed three times with 200 µl/well wash buffer (PBS + 0.1 % Tween™ 20) following aspiration of stool microbes. Plates were incubated with 200 µl/well blocking buffer (PBS + 2 % BSA + 1 % normal goat serum (Sigma-Aldrich)) for 3 hours at 20 °C on a shaking plate. Serum samples were thawed and complement inactivated following **section 3.2.3** and then three dilutions were made in blocking buffer: 1 in 80, 1 in 160 and 1 in 320. 50 µl/well of each serum dilution were added to wells with autologous stool microbes and wells with heterologous stool microbes and incubated for 1 hour at 20 °C on a shaking plate. Plates were washed three times and then incubated with 100 µl/well of 1 in 500 detection antibody (goat anti-human IgG H&L (HRP), Abcam) diluted in blocking buffer, at 20 °C on a shaking plate for 1 hour. Plates were washed six times and then incubated with 100 µl/well substrate solution (TMB high sensitivity substrate solution, BioLegend®) for 5 minutes at 20 °C. The reaction was quenched with 100 µl/well stop solution (0.16 M H_2SO_4). Absorbance was determined by analysing OD 450 nm.

Results were normalised by subtracting negative control (serum only) 450 nm absorbance readings from sample readings.

4.2.7 Relative quantification of serum IgG binding stool microbes

Serum aliquots were thawed and complement inactivated as described in **section 3.2.3**. 100 mg ± 10 mg aliquots of frozen stool samples were thawed and microbe concentration was measured as described in **section 3.2.5.3**. 500 µl of complement inactivated serum diluted 1 in 100 in FACS buffer was incubated with 200 µl of 1 x 10^6 cells/ml stool microbes for 30 minutes at 20 °C. Reactions were centrifuged at 1.2 x 10^4 rpm for 5 minutes and the pellet was resuspended to 100 µl with FACS buffer. 50 µl of this was incubated with 50 µl of sample master mix (PBS + 0.1 % BSA + 1 in 500 SYBR™ green I nucleic acid gel stain + 1 in 50 anti-human IgG-APC/Cy7 (BioLegend®)) and 50 µl of the sample was incubated with 50 µl of isotype control master mix (PBS + 0.1 % BSA + 1 in 500 SYBR™ green I nucleic acid stain + 1 in 50 APC/Cy7 mouse IgG2a, k isotype control antibody (BioLegend®)), for 30 minutes at 20 °C in the dark. Samples were then fixed with 300 µl of 1 % PFA.

Cell acquisition on the BD LSRFortessa™ was performed as described in **section 3.2.6**. Gating parameters for downstream analysis were set using unstained samples and FMO controls (

← **Figure 4.2**).

The percentage of microbes bound by IgG was normalised by subtracting false positive events measured using the isotype control.

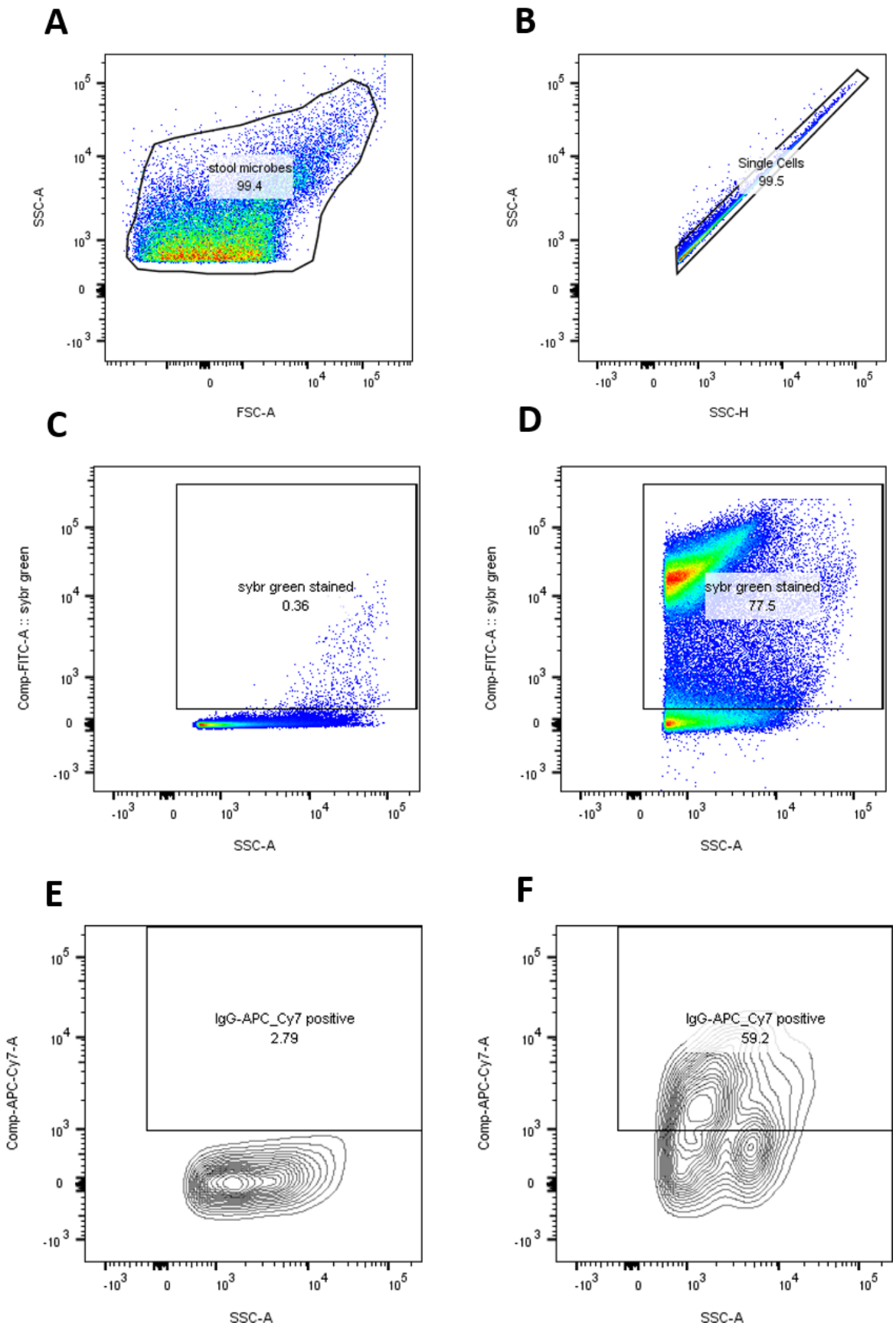
A
stool microbes
99.4
SSC-A
FSC-A
B
Single Cells
99.5
SSC-A
SSC-H
C
sybr green stained
0.36
Comp-FITC-A :: sybr green
SSC-A
D
sybr green stained
77.5
Comp-FITC-A :: sybr green
SSC-A
E
IgG-APC_Cy7 positive
2.79
Comp-APC-Cy7-A
SSC-A
F
IgG-APC_Cy7 positive
59.2
Comp-APC-Cy7-A
SSC-A

← ***Figure 4.2: Gating strategy to detect serum IgG bound stool microbes.*** *Representative data of 'IgG positive'microbes from stool samples incubated with serum. Stool microbes were isolated, quantified using the Guava® easyCyte™ HT system and resuspended to 1 x 10^6 cells/ml. Resuspended stool microbes were incubated with serum then stained with SYBR™ green I nucleic acid gel stain and anti-human IgG-APC/Cy7 antibody or APC/Cy7 mouse IgG2a k isotype control antibody. Stained samples were fixed with 1 % PFA before running on the BD LSRFortessa™. 10^4 events were acquired and analysed using FlowJo™ software version 10. A) Acquired events were gated to exclude debris based on light scatter properties. B) Events from the stool microbes gate were plotted on SSC-A versus SSC-H to exclude doublets. C) A fluorescence minus one control ('sybr green negative') was used to set the 'sybr green stained' gate on singlets. D) An example of a SYBR™ green I nucleic acid gel stained stool sample. E) An APC/Cy7 mouse IgG2a k isotype control antibody was used to set the 'IgG positive' gate on 'sybr green stained' stool microbes. F) An example of an IgG profile of a stained stool sample.*

4.2.8 Statistical analysis

Prior to making comparisons between severe ME/CFS patients and their matched household controls, the distribution of differences (control – patient) was analysed for Gaussian distribution using Shapiro-Wilk's test. When there was no evidence for non-normality ($p > .05$) a two-tailed paired *t*-test was performed. When there was evidence for non-normality ($p < .05$) data was log-transformed prior to performing a two-tailed paired *t*-test.

Prior to correlation analysis the distribution of a variable was tested for normality using Shapiro-Wilk's test. If one of the variables was not normally distributed then both of the variables underwent log-transformation, a variation of which was used on variables containing zero values (see **Equation 4.3**). Then correlations were analysed using the Pearson (*r*) correlation test.

Statistical analyses were undertaken using R v4.0.4. All statistical tests were performed at the 0.05 level of significance and were two-sided.

Equation 4.3: Log transformation of datasets containing zero values.

$$\log_{10}(x+1)$$

4.3 RESULTS

4.3.1 Analysis of stool consistency and microbial load

The consistency of severe ME/CFS patients and their matched household controls stool samples were measured indirectly by investigating stool water content. Severe ME/CFS patients from pairs 1 and 3 had lower stool water content than their matched household control while the other three patients had similar amounts of stool water content as their matched household control (**Figure 4.3A**). However, the lower water content in patients (M = 67.91 %, SD = 6.01) was not significantly different ($t(4) = 1.06$, $p = .351$) to that of matched household controls (M = 72.57 %, SD = 7.24). The two patients with lower stool water content than their matched household controls had abnormally hard stools according to the BSFS, while the matched household controls had abnormally loose stools (see **section 2.7.3**). The rest of the patients and 2 of 3 of the remaining controls had a 'normal' BSFS Score. In addition, a positive correlation between stool water contents with BSFS scores was noted when not accounting for disease status, $r(8) = .67$, $p = .033$ (**Figure 4.3B**).

The microbial loads of stool samples were measured by quantifying the concentration of cells per gram of stool stained with SYBR™ green I nucleic acid gel stain. Three severe ME/CFS patients had a higher stool microbial load than their matched household control and the two remaining patients had a lower stool microbial load than their matched household controls (**Figure 4.3C**). However, there was no significant difference in the stool microbial load from severe ME/CFS patients (M =

1.66 x 10^{11} cells/gram, *SD* = 7.12 x 10^{10}) compared to their matched household controls (*M* = 1.50 x 10^{11} cells/gram, *SD* = 3.14 x 10^{10}) (*t*(4) = -.45, *p* = .677). The participant with the lowest stool microbial load, 6.32 x 10^{10} cells/gram, was the severe ME/CFS patient from pair three. This patient also had the lowest BSFS Score and the second lowest stool water content. However, the patient from pair one and the control from pair 4 had the highest microbial load in stool, 2.64 x 10^{11} cells/gram and 2.01 x 10^{11} cells/gram respectively but had a low water content and a BSFS Score of 2. This suggests there was no correlation between stool microbial load and stool consistency, supported by the lack of correlation between stool microbial load and stool water content, *r*(8) = -.23, *p* = .515 (**Figure 4.3D**).

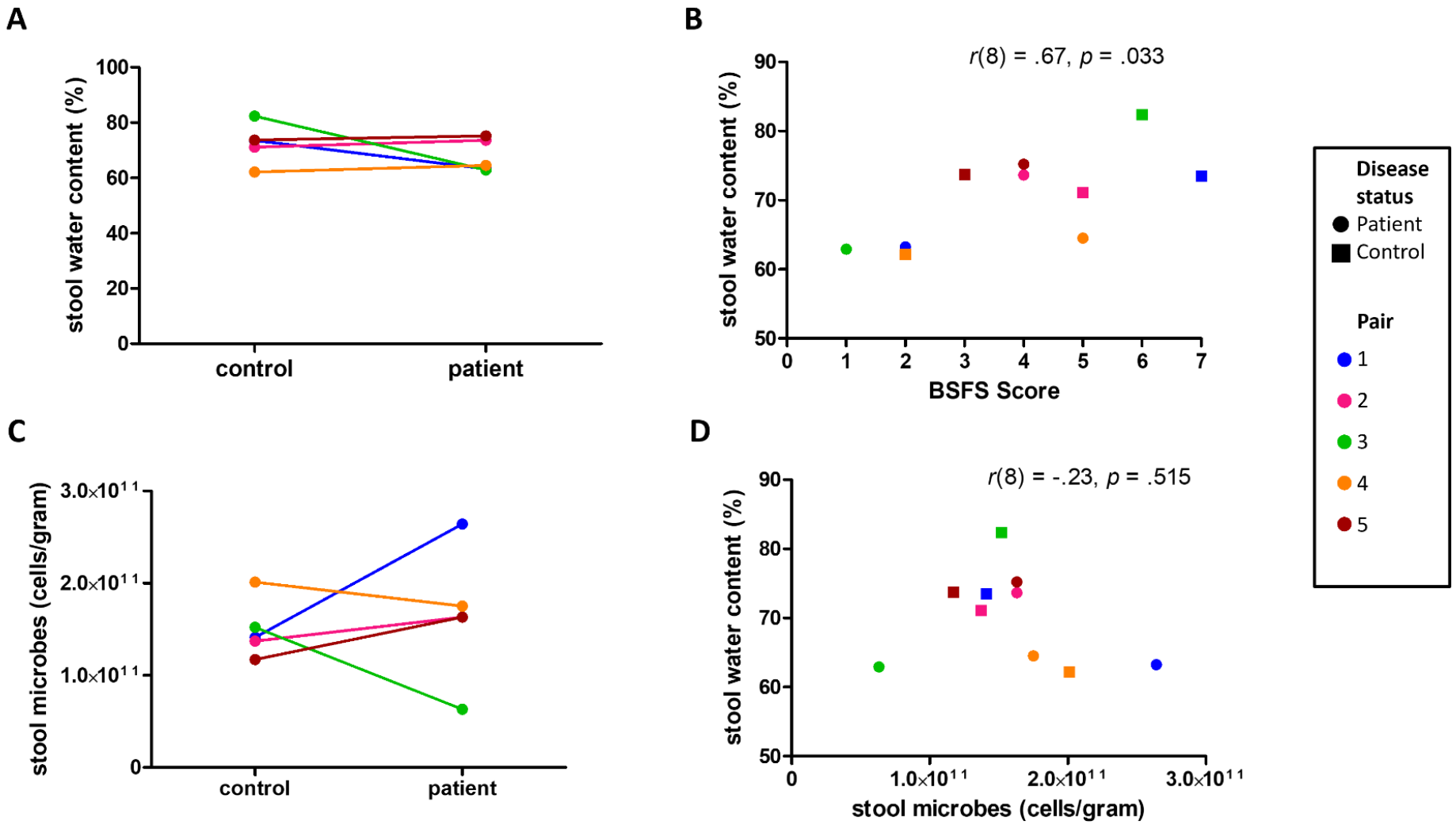
A
stool water content (%)
100
80
60
40
20
0
control
patient
B
r(8) = .67, p = .033
stool water content (%)
90
80
70
60
50
0
1
2
3
4
5
6
7
BSFS Score
Disease status
Patient
Control
Pair
1
2
3
4
5
C
stool microbes (cells/gram)
3.0×10^11
2.0×10^11
1.0×10^11
0
control
patient
D
r(8) = -.23, p = .515
stool water content (%)
90
80
70
60
50
0
1.0×10^11
2.0×10^11
3.0×10^11
stool microbes (cells/gram)

←Figure 4.3: Water and microbial content of stool samples. *Stool samples from severe ME/CFS patients (n=5) and matched household controls (n=5) were analysed for: A) Water content of stool samples, measured in duplicate with the average depicted on the graph. B) Correlation between the Bristol stool form scale (BSFS) score and the average water content of stool measured using Pearson's correlation coefficient. C) Stool microbial load, measured in triplicate, with the average depicted on the graph. D) Correlation between stool microbial load and stool water content measured using Pearson's correlation coefficient. Water and microbial content of severe ME/CFS patients' stool samples were compared to those of matched household controls' using a paired* t-*test.*

4.3.2 Analysis of stool IgA

The concentrations of microbe bound and non-bound IgA1/2 in severe ME/CFS patients and their matched household controls were interpolated from a standard curve (**Supplementary figure 4.3**). The sample dilutions used for this analysis were based on the following conditions: 1) being in the linear part of the curve, and 2) the lowest coefficient of variation. Total IgA1/2 in stool was calculated from the microbe bound and non-bound IgA1/2 levels. Severe ME/CFS patients (*M* = 687.39 µg/g, *SD* = 504.72) and matched household controls (*M* = 451.80 µg/g, *SD* = 214.62) exhibited a large range of total stool IgA1/2 concentrations. For severe ME/CFS patients, this variation was due to a large range of both microbe bound IgA1/2 concentrations (0 to 892.62 µg/mg) and of non-bound IgA1/2 concentrations (0 to 886.78 µg/mg). Whereas microbe bound IgA1/2 concentrations in matched household controls had less variation (4.24 to 130.15 µg/mg) and the range in total IgA1/2 concentrations seen in matched household controls was due to a wide variation in non-bound IgA1/2 (96.71 to 556.48 µg/mg). The concentration of stool microbe bound IgA1/2 was higher in two and lower in one patient compared to their matched household controls, non-bound IgA1/2 was higher in two and lower in three patients compared to their matched household controls, and total IgA1/2 was higher in three and lower in two patients compared to their matched household controls. However, pairwise comparisons of severe ME/CFS patients and their matched household controls did not reveal any significant differences between total IgA1/2, $t(4) = -.86$, $p = .436$, microbe bound IgA1/2, $t(4) = -1.36$, $p = .244$, or non-bound IgA1/2, $t(4) = -.02$, $p = .988$, IgA1/2 (**Figure 4.4**). When comparing a participant's microbe bound IgA1/2 concentrations to their non-bound IgA1/2 concentrations, every household control had higher levels of non-bound IgA1/2 than levels of microbe bound IgA1/2, whereas only three severe ME/CFS patients had higher levels of non-bound IgA1/2 than microbe bound IgA1/2. Interestingly, the patient from pair 5 did not have any detectable IgA1/2. Also, 100 % of IgA1/2 in stool from the patient in pair 3 was microbe bound.

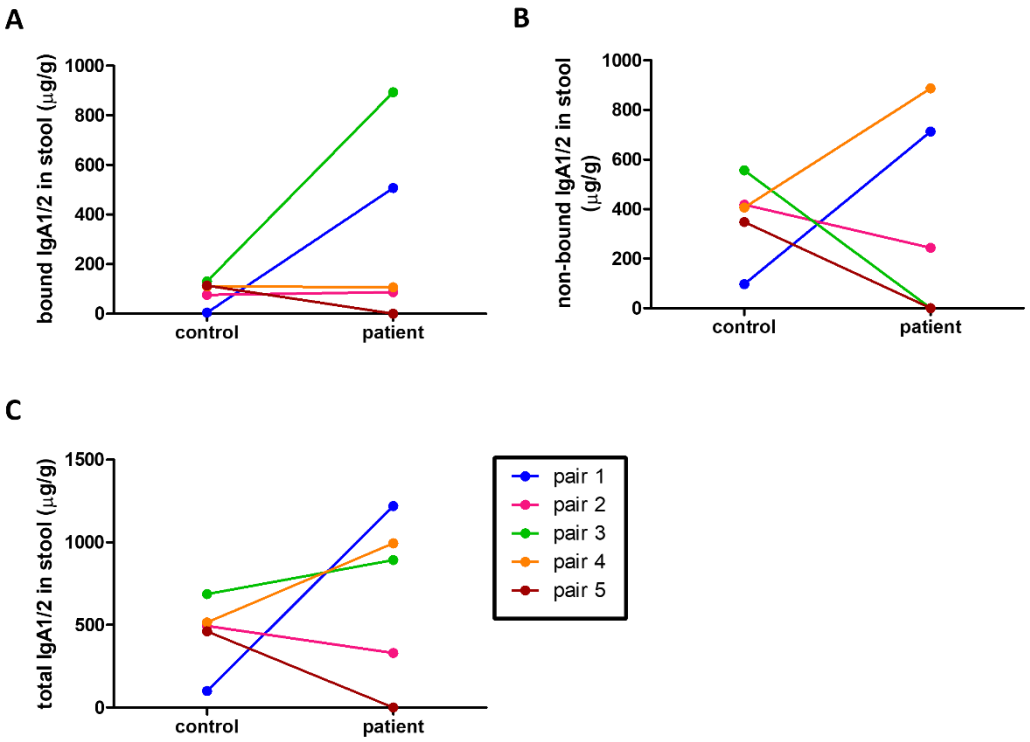

Figure 4.4: Quantifying stool IgA levels. *The concentrations of A) microbe bound IgA1/2, B) non-bound IgA1/2 and C) total IgA1/2 in stool samples were measured in severe ME/CFS patients (n=5) and their matched household controls (n=5). Samples were assayed in duplicate. The means are shown on the graphs. IgA concentrations of severe ME/CFS patients' stool samples were compared to those of matched household controls' using a paired* t*-test.*

Levels of stool microbes coated by IgA in severe ME/CFS patients and their matched household controls were measured using flow cytometry. All participants had less than 10 % of stool microbes coated by IgA, except for the patient from pair 3 who had 41.26 % of microbes coated by IgA (**Figure 4.5A**). This was the only patient with a higher proportion of IgA coated stool microbes than their matched household control and two patients had a lower proportion of IgA coated stool microbes than their matched household control. However, there was no significant difference ($t(4) = .04$, $p = .973$) between the proportion of IgA coated stool microbes in severe ME/CFS patients (M = 10.59 %, SD = 17.23) and their matched household controls (M = 5.01 %, SD = 2.49). Relative levels of microbes coated by IgA were then converted to absolute levels of microbes coated by IgA, which considers the microbial load in stool samples. This enhanced the differences between severe ME/CFS patients ($M = 9.76 \times 10^9$ cells/gram, $SD = 9.70 \times 10^9$) and their matched household controls ($M = 7.29 \times 10^9$ cells/gram, $SD = 3.32 \times 10^9$) as two patients had lower and three patients had higher quantities of IgA bound microbes in stool samples than their matched household controls (**Figure 4.5B**). However, the difference between severe ME/CFS patients and matched household controls remained non-significant ($t(4) = -.54$, $p = .617$). A positive correlation was found between the concentration of IgA bound to stool microbes and the quantity of microbes bound by IgA in stool in participants when disease status was not taken into account, $r(8) = .64$, $p = .045$ (**Figure 4.6**).

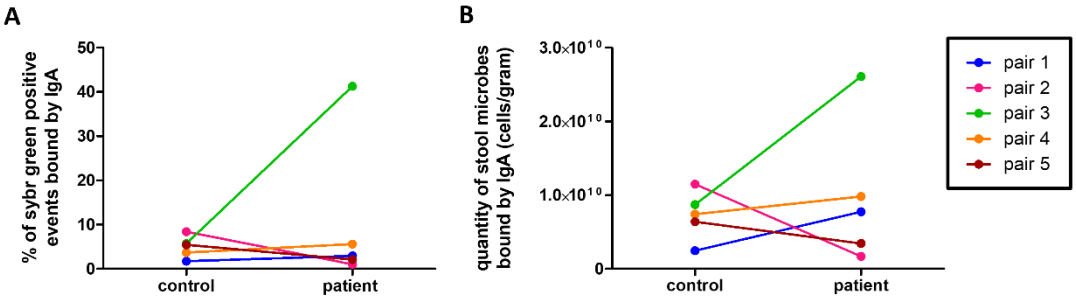

Figure 4.5: Quantifying levels of stool microbes bound by IgA. *Stool samples from severe ME/CFS patients (n=5) and their matched household controls (n=5) were stained with SYBR™ green I nucleic acid gel stain and anti-human IgA-APC and analysed on the BD LSRFortessa™. A) the percentage of sybr green events IgA positive. B) The quantities of stool microbes bound by IgA were calculated by multiplying the percentage of sybr green cells IgA positive by the concentration of microbes in the stool sample. Severe ME/CFS patients were compared to their matched household controls using a paired* t*-test.*

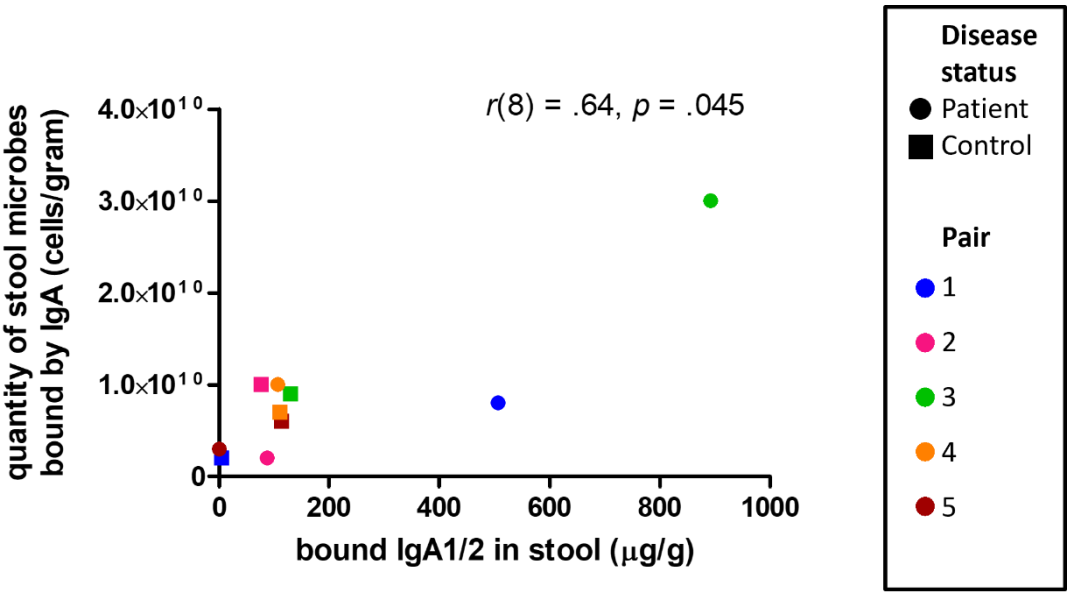

Figure 4.6: Correlation between levels of microbe bound IgA and quantity of IgA bound microbes in stool. *The relationship between the concentration of microbe bound IgA in stool and the concentration of IgA bound stool microbes from five pairs of severe ME/CFS patients and their matched household controls (n=10) was measured using Pearson's correlation coefficient.*

4.3.3 Analysis of serum IgG binding to stool microbes

Concentrations of total IgG in serum from severe ME/CFS patients and their matched household controls were interpolated from a standard curve (**Supplementary figure 4.4**). Of the four serum dilutions measured, 1 in 4 x 10^6 and 1 in 8 x 10^6 dilutions were excluded from further analysis because two and five participants respectively had readings out of the standard curve range. Therefore, the average interpolated concentrations from 1 in 10^6 and 1 in 2 x 10^6 diluted serum samples were used to compare total IgG concentrations in serum between severe ME/CFS patients (*M* = 20.59 mg/ml, *SD* = 11.11) and their matched household controls (*M* = 24.66 mg/ml, *SD* = 15.08). Pairwise comparisons revealed two patients had lower total IgG levels in serum than their matched household controls and two patients had higher total IgG levels than their matched household controls (**Figure 4.7**). However, the differences seen between the total serum IgG in severe ME/CFS patients and matched household controls was not significant ($t(4) = .46$, $p = .669$).

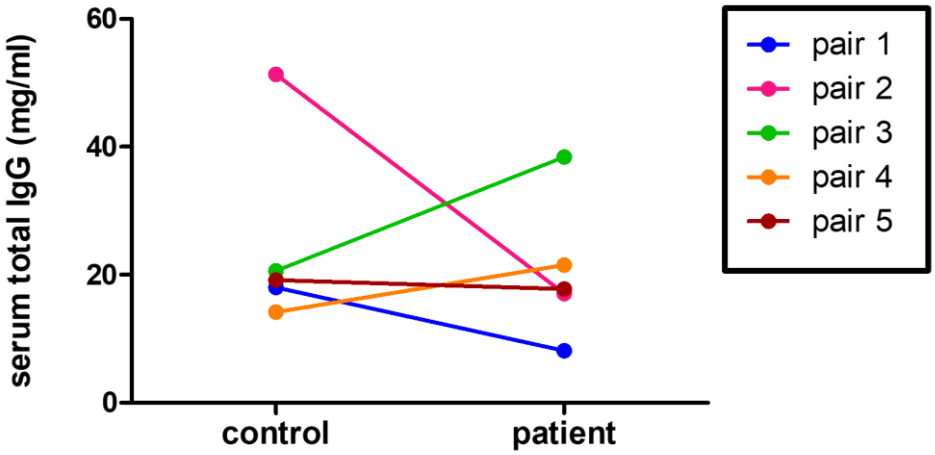

Figure 4.7: Quantifying serum IgG levels. *Serum samples from severe ME/CFS patients (n=5) and their matched household controls (n=5) were measured for the concentration of IgG. Samples were measured in duplicate and the average is depicated on the graph. Serum IgG concentrations from severe ME/CFS patients were compared to their matched household controls using a paired* t*-test.*

The proportion of stool microbes bound by serum IgG was determined using flow cytometry. Three patients had a higher proportion and two patients had a lower proportion of microbes bound by IgG compared to their matched household controls (**Figure 4.8A**). However, the differences between the percentage of serum 'IgG positive' stool microbes in severe ME/CFS patients (M = 44.01 %, SD = 10.28) and their matched household controls (M = 40.16 %, SD = 9.90) were not significant ($t(4) = -.52$, $p = .630$). Relative levels of microbes coated by serum IgG were then converted to absolute levels. Two severe ME/CFS patients had higher numbers of microbes bound by serum IgG than their matched household controls and three patients had lower numbers of microbes bound by serum IgG than their matched household controls (**Figure 4.8B**). However, the quantity of IgG bound microbes from severe ME/CFS patients ($M = 6.86 \times 10^{10}$ cells/gram, $SD = 2.53 \times 10^{10}$) compared to their matched household controls ($M = 6.12 \times 10^{10}$ cells/gram, $SD = 2.44 \times 10^{10}$) was not significantly different ($t(4) = -.39$, $p = .713$). By converting relative abundances to absolute abundances, which accounts for microbial load, the patient from pair three went from having the highest percentage of stool microbes reactive with serum IgG to having the lowest quantity of microbes in stool reactive with serum IgG. When comparing the relationship between total IgG concentration in serum and the proportion of microbes bound by IgG, no correlation was found $r(8) = .45$, $p = .191$ (**Figure 4.9**).

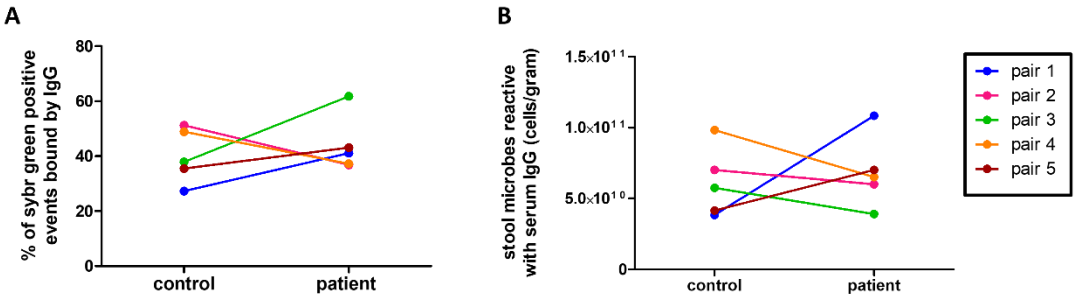

Figure 4.8: Quantifying levels of stool microbes reactive with serum IgG. *Stool samples from severe ME/CFS patients (n = 5) and their matched household controls (n = 5) incubated with serum samples from the same individual were stained with SYBR™ green I nucleic acid gel stain and anti-human IgG-APC/Cy7 and analysed on the BD LSRFortessa™. A) The percentage of sybr green cells bound by serum IgG. B) The quantities of stool microbes reactive with serum IgG were calculated by multiplying the percentage of sybr green cells 'IgG positive' by the concentration of microbes in the stool sample. Severe ME/CFS patients were compared to their matched household controls using a paired* t*-test.*

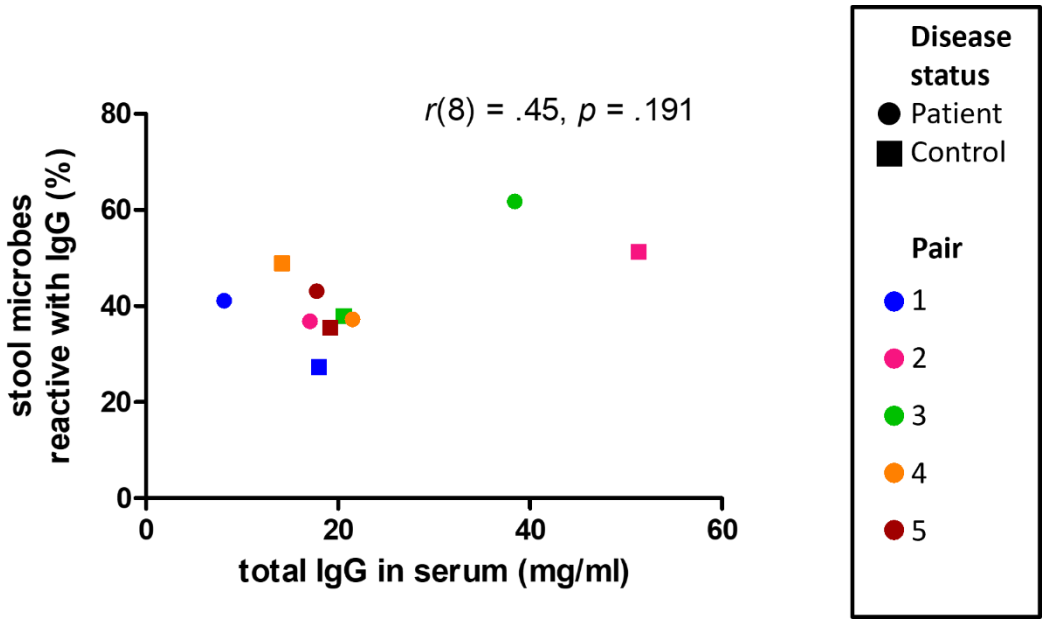

Figure 4.9: Correlation between levels of serum IgG and the proportion of stool microbes reactive to serum IgG. *The relationship between the concentration of IgG in serum and the proportion of microbes bound by serum IgG from five pairs of severe ME/CFS patients and their matched household controls (n = 10) was measured using Pearson's correlation coefficient.*

4.3.4 Analysis of serum IgG binding to autologous and heterologous stool microbes

An indirect ELISA approach was used to analyse the levels of serum IgG to autologous and heterologous stool microbes in severe ME/CFS patients and their matched household controls.

Serum IgG binding to autologous stool microbes was analysed by incubating serum samples from severe ME/CFS patients and matched household controls with their own stool microbes. Four of the five severe ME/CFS patients (M = 0.83 $OD_{450\ nm}$, SD = 0.43) had lower serum IgG binding to autologous stool microbes than their matched household controls (M = 1.25 $OD_{450\ nm}$, SD = 0.64), although these differences were not significant ($t(4) = 1.87$, $p = .135$ (**Figure 4.10A**)).

Severe ME/CFS patient serum IgG binding to heterologous stool microbes was analysed by incubating the patients' serum sample with the stool sample from their matched household control. In addition, household control serum was incubated with the stool sample from their matched severe ME/CFS patient to analyse household control serum IgG binding to heterologous stool microbes. Severe ME/CFS patients (M = 0.80 $OD_{450\ nm}$, SD = 0.45) had significantly lower serum IgG binding to heterologous stool microbes than their matched household controls (M = 1.92 $OD_{450\ nm}$, SD = 1.01), $t(4) = 3.34$, $p = .028$ (**Figure 4.10B**).

Finally, the levels of serum IgG binding autologous stool microbes were compared to the levels of serum IgG binding to heterologous stool microbes. Household controls had significantly higher serum IgG levels binding heterologous stool microbes (M = 1.92 $OD_{450\ nm}$, SD = 1.01) than autologous stool microbes (M = 1.25 $OD_{450\ nm}$, SD = 0.64). $t(4) = -2.85$, $p = .046$ (**Figure 4.10C**). By comparison, in severe ME/CFS patients, serum IgG levels binding heterologous stool microbes (M = 0.80 $OD_{450\ nm}$, SD = 0.43) and autologous stool microbes (M = 0.80 $OD_{450\ nm}$, SD = 0.45) were equivalent, $t(4) = 0.54$, $p = .619$ (**Figure 4.10D**).

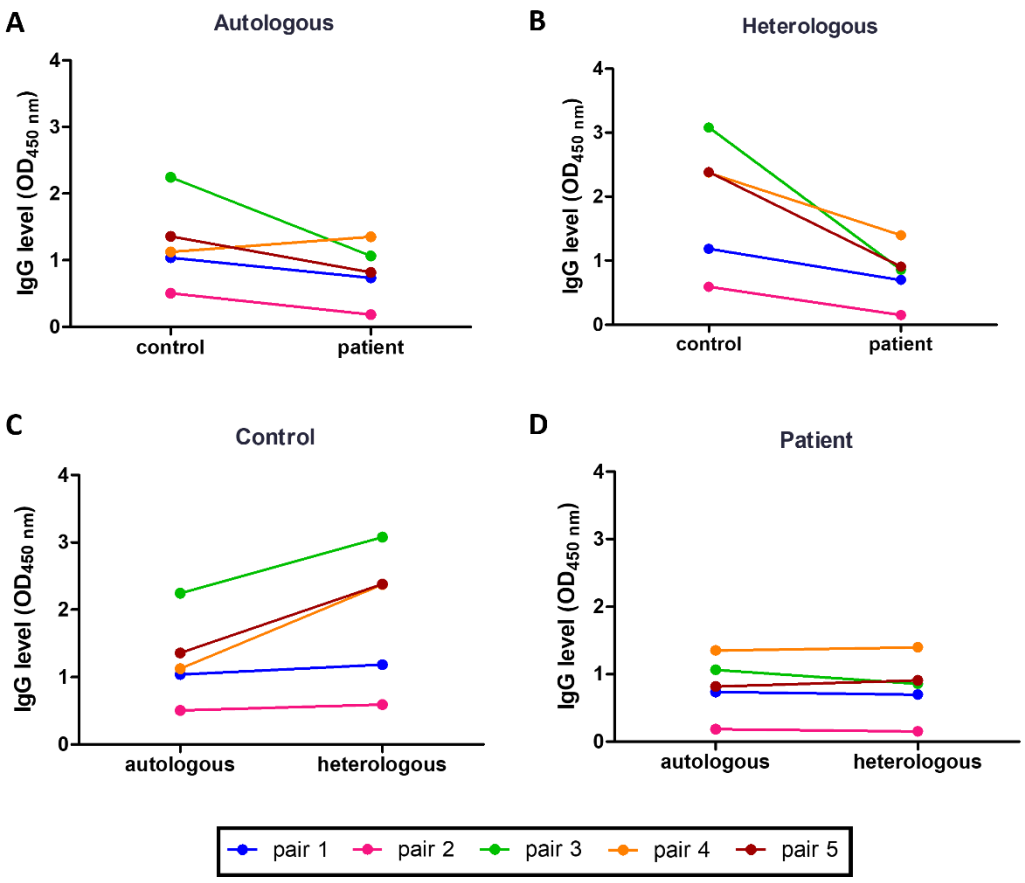

Figure 4.10: Serum IgG reactivity to autologous and heterologous stool microbes. *Serum samples from severe ME/CFS patients (n=5) and their matched household controls (n=5) were incubated with self (autologous) or matched (heterologous) stool samples and the amount of serum IgG binding stool microbes was measured using an enzyme linked immunosorbent assay. A) Comparing serum IgG levels bound to autologous stool microbes in severe ME/CFS patients and matched household controls, B) comparing serum IgG levels bound to heterologous stool microbes in severe ME/CFS patients and matched household controls, C) comparing household control serum IgG levels bound to autologous and heterologous stool microbes, D) comparing severe ME/CFS patient serum IgG levels bound to autologous and heterologous stool microbes. Single measurements were taken. Significance was measured using a paired* t*-test.*

4.4 DISCUSSION

This chapter investigates the binding of mucosal IgA and systemic IgG to the intestinal microbiome in severe ME/CFS patients and their matched household controls. The key findings are:

1. the water content and microbial load of stool samples did not significantly differ between severe ME/CFS patients and their matched household controls,
2. the levels of microbe bound and non-bound stool IgA did not significantly differ between severe ME/CFS patients and their matched household controls,
3. the proportion and quantity of microbes bound by secretory IgA in stool did not significantly differ between severe ME/CFS patients and their matched household controls,
4. the concentration of serum IgG did not significantly differ between severe ME/CFS patients and their matched household controls,
5. the proportion and quantity of microbes reactive with serum IgG did not significantly differ between severe ME/CFS patients and their matched household controls,
6. heterologous, but not autologous, stool bacteria elicited significantly lower levels of serum IgG reactivity in severe ME/CFS patients than their matched household controls,
7. matched household controls, but not severe ME/CFS patients, had significantly higher levels of serum IgG reactive with heterologous stool bacteria than autologous stool bacteria.

4.4.1 Severe ME/CFS patients report comorbid IBS, but their stool consistency is not significantly altered

Water content and the BSFS are two indirect indicators of stool consistency, which is a measure of bowel function. There is a significant positive correlation between the two measures, irrespective of disease status. Another study comparing the BSFS to stool water content in healthy controls also found a significant positive correlation (Blake et al., 2016). As the BSFS is a subjective scale with high variance and is positively correlated with stool water content, water content was used as an indicator of bowel function. Despite only severe ME/CFS participants having IBS-like complaints, the water content of stool samples is similar between severe ME/CFS patients and their matched household controls. As 28 % and 14 % of healthy controls have previously been shown to have abnormally hard and abnormally loose stool, respectively (Blake et al., 2016), it is not surprising that the matched household controls in this study also have varying stool consistencies. Despite all five severe ME/CFS patients having IBS, three of the stool samples are of normal consistency. As the diagnosis of IBS is characterised by the frequency and consistency of stool samples over a period of time (Lacy and Patel, 2017), this experiment could be improved by sampling stool longitudinally. Another limitation of this study is that IBS was not categorised into IBS-D, IBS-C and IBS with alternating diarrhoea and constipation (IBS-M) (Lacy and Patel, 2017), each of which is typically

associated with very different stool consistencies (Palsson et al., 2012). Finally, another confounding variable is the time of sample collection, as the consistency of stool samples passed in the morning is usually softer than stool samples passed in the afternoon or evening (Matsuda et al., 2021).

4.4.2 IgA in stool is not significantly altered in severe ME/CFS patients

The concentration of secretory IgA in stool increases in the context of intestinal inflammation. Despite previous evidence of intestinal inflammation in ME/CFS patients (Venturini et al., 2019), the results detailed in this chapter found the levels of microbe bound and non-bound secretory IgA in stool samples are not higher in severe ME/CFS patients compared to their matched household controls. Lin et al. (2018) examined the levels of soluble IgA (free IgA) in stool of patients with IBD and found a significant increase in IBD patients with intestinal inflammation (active IBD), but not IBD patients without intestinal inflammation (IBD in remission). Therefore, intestinal inflammation in any of the patients or controls that was unaccounted for may have confounded the measure of free IgA stool levels. Another variable that could affect the content of IgA in stool is stool consistency. In IBS-D patients the concentration of IgA in stool is significantly higher than healthy controls (Liu et al., 2020). Similarly, the severe ME/CFS patient with the loosest stool sample in this study also has the highest concentration of free IgA in stool. Studies in mice also give insight into other variables that could affect the concentration of IgA in stool; the concentration of IgA in the colon increased with age (Nagafusa and Sayama, 2020) and the secretion of IgA was diurnal and changed based on the time of sample collection (Penny et al., 2021).

In addition to measuring the concentration of IgA in stool, this study also measured the percentage of microbes coated by IgA in stool samples. The proportion of IgA positive microbes in stool are not significantly higher in severe ME/CFS patients compared to their matched household controls. Liu et al. (2020) reported patients with IBS have a higher proportion of IgA positive microbes in stool samples than healthy controls. Interestingly, despite all severe ME/CFS patients and no matched household controls in this study reporting co-morbid IBS, only one severe ME/CFS patient has a higher proportion of IgA coated stool microbes than their matched household control. To confirm whether the absence of the IBS associated elevation of IgA coated stool microbes in the current patient population is associated with ME/CFS pathogenesis future studies comparing the proportion of IgA coated stool microbes in severe ME/CFS patients with co-morbid IBS to severe ME/CFS patients without co-morbid IBS should be undertaken.

Finally, previous studies have reported that between 2 % and 35 % of microbes in stool are coated by IgA in health (Sterlin et al., 2020), whereas the highest proportion of stool microbes coated with IgA of healthy controls in this study is only 10 %. This may have been caused by IgA-degrading

proteases produced by microbial communities within the microbiome (Moon et al., 2015). To overcome this, future studies could use a protease inhibitor to preserve IgA in stool.

4.4.3 Total serum IgG concentration is not significantly different between severe ME/CFS patients and their matched household controls

Patients with autoimmune diseases tend to have a higher concentration of total IgG in serum compared to healthy controls (Zhang et al., 2015). Due to the presence of autoantibodies in patients (Wirth and Scheibenbogen, 2020), ME/CFS is thought to be an autoimmune disease and thus this study hypothesised that severe ME/CFS patients have elevated levels of serum IgG. However, in this study only two severe ME/CFS patients have higher serum IgG levels than their matched household control. In addition, two of five severe ME/CFS patients have lower serum IgG levels than their matched household control, which supports previous studies which found 6.5 % (Lutz et al., 2021) and 39.3 % (Peterson et al., 1990) of ME/CFS patients have a decrease in serum IgG levels. Studies analysing the levels of IgG in serum in ME/CFS patients also measured the concentration of IgG subclasses and results suggested a subset of patients have reduced levels of serum IgG1 (Guenther et al., 2015, Peterson et al., 1990), IgG2 (Peterson et al., 1990), IgG3 (Guenther et al., 2015, Lutz et al., 2021, Peterson et al., 1990) and IgG4 (Guenther et al., 2015, Lutz et al., 2021), with reduced serum IgG3 levels being the most prominent reduction, affecting as many as 64.3 % of ME/CFS patients (Peterson et al., 1990).

4.4.4 The proportion of 'IgG positive' microbes is high in both health and ME/CFS

Intestinal inflammation results in a leaky gut, bacterial translocation and an elevated serum IgG response to enteric microbes (Zheng et al., 2020). As there is evidence of bacterial translocation and elevated serum IgA and IgM reactivity to the LPS of Gram-negative enteric bacteria in ME/CFS patients (Maes et al., 2007), it was hypothesised that ME/CFS patients would also have elevated serum IgG reactivity to enteric microbes. However, only three of five severe ME/CFS patients had a higher proportion of serum IgG binding stool microbes compared to their matched household controls. In addition, the proportion of stool microbes bound by serum IgG ranges from 36.83 to 61.78 % in severe ME/CFS patients and 27.30 to 51.25 % in matched household controls, which is higher than a previous study which only found 1.10 % of stool bacteria binding to serum IgG from healthy controls (Fadlallah et al., 2019). This discrepancy could be due to the current study analysing both bacteria and fungi reactivity to serum IgG as another study analysing serum IgG binding to fungi from stool found that approximately 70 % of fungi were reactive to serum IgG in health (Doron et al., 2021).

Patients with secretory IgA deficiency have higher levels of anti-microbiota IgG (Fadlallah et al., 2019). This would suggest that secretory IgA either confines microbes to the intestine and in the absence of secretory IgA microbial translocation increases and triggers serum anti-microbiota IgG

production, or it competes with serum IgG for binding sites on microbes. However, in this study both the severe ME/CFS patient with the highest proportion of IgA coated microbes and the household control with the highest proportion of IgA coated microbes also had the highest proportion of serum IgG coated microbes. Furthermore, the proportion of microbes bound by serum IgG is higher than the proportion of microbes bound by secretory IgA in both severe ME/CFS patients and their matched household controls. In contrast, Fadlallah et al. (2019) found that in health the proportion of IgA positive microbes were greater than the proportion of serum 'IgG positive' microbes.

4.4.5 Serum IgG reactivity to heterologous stool microbes is significantly lower in severe ME/CFS patients

The level of serum IgG reactive to intestinal microbes was investigated by incubating serum from severe ME/CFS patients and matched household controls with autologous and heterologous stool bacteria. Household controls have significantly higher serum IgG levels to heterologous stool bacteria than autologous stool bacteria. This was expected because Duchmann et al. (1995) found in healthy participants PBMC reactivity to heterologous intestinal bacteria was higher than PBMC reactivity to autologous intestinal bacteria due to immune tolerance towards autologous intestinal microbes. In contrast, the current study found patients' serum IgG levels reacting to their own stool bacteria to be comparable to serum IgG levels reacting to stool bacteria from their matched household control. This suggests severe ME/CFS patients either have loss of self-tolerance towards autologous intestinal bacteria, or they have reduced serum IgG levels to heterologous stool bacteria. This study found evidence to support the latter: severe ME/CFS patients had significantly lower serum IgG levels to heterologous stool bacteria compared to their matched household controls.

One limitation of this research is that matched household controls were used to assess patients' serum IgG levels to heterologous stool bacteria and vice versa. It is well known that the environment influences microbiome composition and the microbiomes of individuals living within the same household share greater similarity than the microbiomes of individuals living in different households (Lax et al., 2014). Therefore, measuring serum IgG levels to stool from members of the same household is limited in its interpretation as the heterologous stool bacteria tested will be of a similar composition to the autologous stool bacteria. Further experiments using unmatched controls would be able to confirm severe ME/CFS patients have significantly lower serum IgG levels to heterologous stool bacteria.

4.4.6 Conclusion

The hypothesis that severe ME/CFS have a heightened local secretory IgA and systemic IgG immune response to autologous intestinal microbes is not supported by the data obtained in this study.

However, there is evidence that severe ME/CFS patients have reduced systemic IgG response to heterologous intestinal bacteria. These findings warrant further investigation as they may provide important insights into why patients with ME/CFS have a higher susceptibility to infections (Guenther et al., 2015) with a longer recovery time (Ghali et al., 2020).

5 CHAPTER FIVE: IDENTIFYING INTESTINAL MICROBES REACTIVE WITH SERUM ANTIBODIES IN MYALGIC ENCEPHALOMYELITIS/CHRONIC FATIGUE SYNDROME

5.1 INTRODUCTION

5.1.1 Functional profiling of the ME/CFS intestinal microbiome

Taxonomic classification of the microbiome is limited in its interpretation as it only provides information about which microbes are present and not what they are doing. In 2017 Rosen and Palm highlighted two main approaches for functionally classifying the microbiome: 'omics'-based approaches and 'targeted' approaches. 'Omics' based approaches include methods to look at the functional potential (shotgun metagenomics) and methods to look at the functional activity of the microbial community (metatranscriptomics, metaproteomics and metabolomics) (Franzosa et al., 2015). 'Targeted' approaches for functional classification of the microbiome include immunological profiling using 'bug FACS' (Rosen and Palm, 2017). To date, only 'omics' based functional profiling of the intestinal microbiome has been investigated in ME/CFS patients using metabolomics (Armstrong et al., 2016, Lupo et al., 2021, Guo et al., 2021) and metagenomics (Guo et al., 2021, Nagy-Szakal et al., 2017, Raijmakers et al., 2020). Findings were not comparable due to the use of different methods and reference databases.

Guo et al. (2021) demonstrated the importance of combining taxonomy and functional profiling of the microbiome to corroborate findings. Interestingly they analysed the RMP and QMP of ME/CFS patients and found both a relative and quantitative decrease in butyrate-producing bacteria. Using metabolomics and metagenomics they confirmed a reduction of butyrate in the stool and a deficiency in the butyrate metabolism pathway respectively. Given the role of butyrate in preventing inflammation (Schulthess et al., 2019) and maintaining the structure of the intestinal epithelial barrier (Kelly et al., 2015), a decrease in butyrate could contribute to intestinal inflammation and a leaky gut hypothesised in ME/CFS patients. Therefore, immunological profiling of the intestinal microbiome in ME/CFS patients would be beneficial to both confirm these findings and determine the immunological consequences of a leaky gut.

5.1.2 Aims and objectives

The aim of this chapter was to identify compositional and functional alterations in the stool microbiome of ME/CFS patients by:

1. Comparing the microbiome profiles of stool samples in severe ME/CFS patients and their matched household controls using shotgun metagenomics,
2. Quantifying serum IgG binding to each taxa using 'bug FACS' and the IgG probability ratio and
3. Identifying patterns in serum IgG binding to stool microbes using multivariate analyses on the abundance of gene families in 'IgG positive' microbes and 'IgG negative' microbes.

5.2 METHODS

Stool and serum samples from the study population were collected and processed as described in **Chapter 2 section 2.6**.

5.2.1 Cell sorting of 'IgG positive' and 'IgG negative' stool microbes

The concentration of microbes in stool samples was measured as described in **section 3.2.5.3** and microbes were resuspended to 1 x 10^6 cells/ml in FACS buffer. Serum was complement inactivated as described in **section 3.2.3**. Then 20 ml of 1 x 10^6 cells/ml faecal microbes were incubated with 50 ml of 1:100 dilution of serum for 30 minutes. Samples were then centrifuged at 8000 x g for 5 minutes and the pellet was resuspended in 20 ml of staining buffer and incubated with 100 µl of anti-human IgG-APC/Cy7 (BioLegend® UK Ltd) and 20 µl SYBR™ green I nucleic acid gel stain (Thermo Fisher Scientific) for 30 minutes in the dark at 20 °C. Samples were centrifuged again and resuspended to 1 x 10^7 cells/ml.

The Sony SH800S cell sorter was set up as described in **3.2.7**. In addition, the gain for FL6 was adjusted using samples double stained with SYBR™ green I nucleic acid gel stain and anti-human IgG-APC/Cy7. The gating parameters (**Figure 5.1**) were used to collect approximately 1 million cells in the following three fractions: 1) SYBR™ green I nucleic acid gel positive microbes, herein referred to as the 'all' fraction, 2) SYBR™ green I nucleic acid gel positive microbes positive for anti-human IgG-APC/Cy7, hereafter referred to as the 'IgG positive' fraction, 3) SYBR™ green I nucleic acid gel positive microbes negative for anti-human IgG-APC/Cy7, herein referred to as the 'IgG negative' fraction. After cell sorting, the cell fractions were centrifuged at 8000 x g for 5 minutes and the cell pellets were frozen at -20°C until DNA extraction.

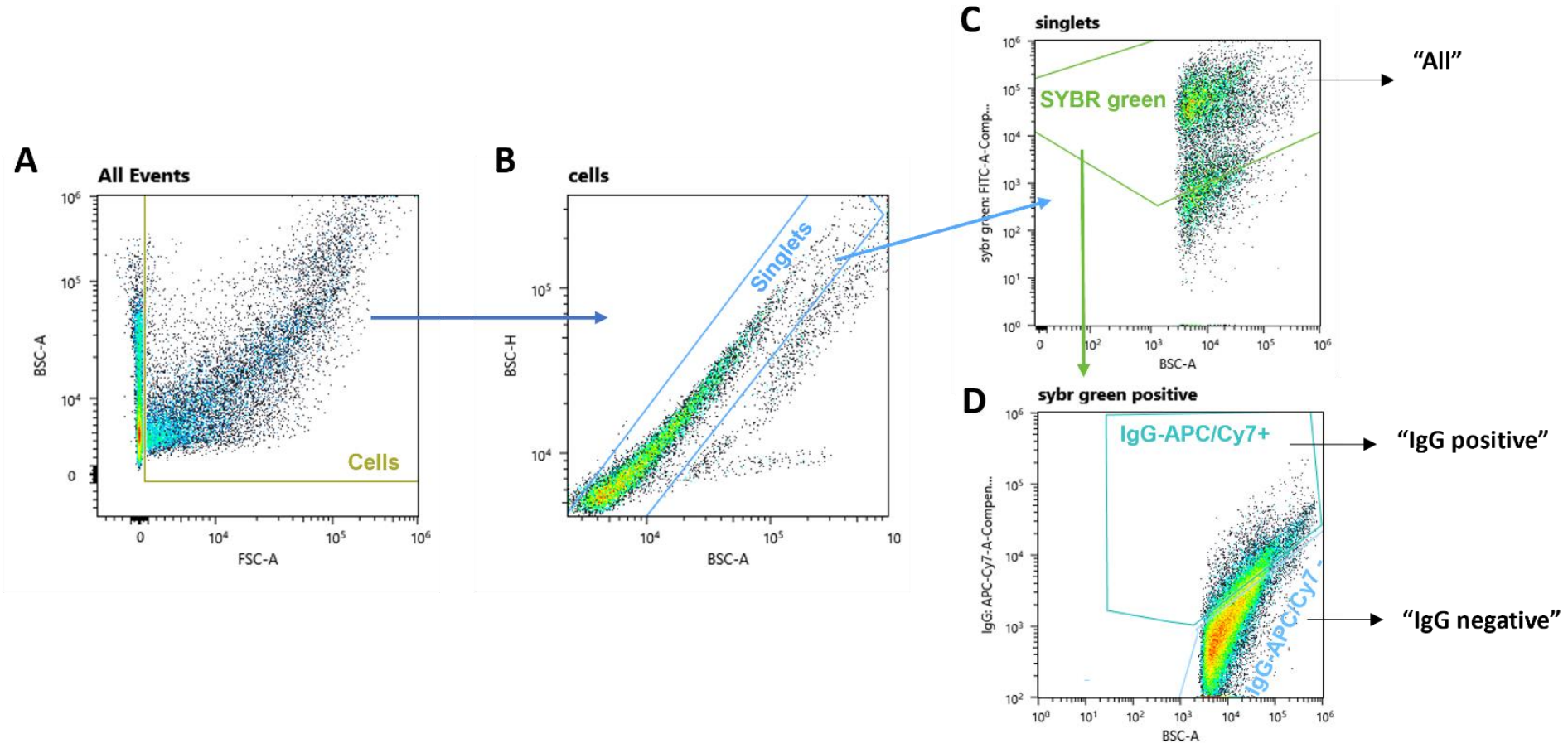
A
All Events
BSC-A
FSC-A
Cells
B
cells
BSC-H
BSC-A
Singlets
C
singlets
SYBR green
sybr green: FITC-A-Comp...
BSC-A
"All"
D
sybr green positive
IgG-APC/Cy7+
IgG: APC-Cy7-A-Compen...
BSC-A
"IgG positive"
"IgG negative"

←Figure 5.1: Gating strategy for the separation and collection of 'IgG positive', 'IgG negative' and 'all' microbes. *Representative data of 'IgG positive' microbes from stool samples incubated with serum from severe ME/CFS patients and their matched household controls. Samples were stained with SYBR™ green I nucleic acid gel stain and anti-human IgG-APC/Cy7 antibody. Prior to sample acquisition using the Sony SH800S cell sorter the following gates were set: A) 'cells' gate using a buffer only control (not shown) and an unstained stool sample, B) 'singlets' gate using an unstained stool sample, C) 'SYBR green' gate using an unstained stool sample (not shown) and a SYBR™ green I nucleic acid gel stained stool sample, D) 'IgG positive' and 'IgG negative' gate using a SYBR™ green I nucleic acid gel stained stool sample (not shown) and a stool sample incubated with both SYBR™ green I nucleic acid gel stain and anti-human IgG-APC/Cy7 antibody. 'all' microbes were acquired from the 'SYBR green' gate, 'IgG positive' microbes were acquired from the 'IgG positive' gate and 'IgG negative' microbes were acquired from the 'IgG negative' gate.*

5.2.2 DNA preparation for shotgun metagenomic sequencing

DNA from the 'all', 'IgG positive' and 'IgG negative' fractions was extracted using the modified Gram-positive bacterial genomic DNA purification protocol (as described in **3.2.8.3**). Members of the QIB Sequencing Facility then used vacuum DNA precipitation followed by 0.7X solid phase reversible immobilisation bead clean-up using KAPA pure beads (Roche) to precipitate DNA. WGA was performed on the precipitated DNA (as described in **3.2.11**). DNA was quantified (as described in **3.2.9**) and resuspended to 5 ng/µl in 10 mM Tris-HCl.

DNA tagmentation was performed by the QIB Sequencing Facility using the Illumina DNA prep kit (Illumina, catalogue number: 20018704). Briefly, a master mix was made using 0.5 µl tagmentation buffer 1, 0.5 µl of bead-linked transposomes and 4 µl of PCR grade water. 5 µl of the master mix was added to a chilled 96 well plate and mixed with 2 µl of 5 ng/µl DNA before being heated to 55 °C for 15 minutes.

Then the QIB Sequencing Facility amplified DNA using the KAPA2G Robust PCR kit (Sigma, catalogue number: KK5005). A PCR master mix was made up of 4 µl KAPA2G buffer, 0.4 µl KAPA dNTP mix, 0.08 µl KAPA2G robust DNA polymerase and 4.52 µl of PCR grade water. 9 µl was used per reaction. 2 µl of P7 Nextera XT index kit v2 index primers (Illumina, catalogue number: FC-131-2001) and 2 µl of P5 Nextera XT index kit v2 index primers (Illumina, catalogue number: FC-131-2004) were added to each reaction and then 7 µl of tagmented DNA was added. A PCR was run using the following profile: 72 °C for 3 minutes, 95 °C for 1 minute, 14 cycles of 95 °C for 10 seconds, 55 °C for 20 seconds and 72 °C for 3 minutes. The Quanti-iT™ dsDNA high sensitivity assay kit (Thermo Fisher Scientific, catalogue number: 10164582) was used to quantify DNA on the FLUOstar Optima plate reader. Libraries were pooled in equal quantities and double solid phase reversible immobilisation bead clean-up was performed with 0.5X and 0.7X bead volumes using KAPA pure beads (Roche, catalogue number: 07983298001). The final pool was quantified (as described in **3.2.9**) and the molarity of the final pool was measured on a D500 ScreenTape (Agilent, catalogue number: 5067-5588 & 5067 – 5589) using the Agilent Tapestation 4200.

q-PCR was then performed by the QIB Sequencing Facility on the Applied Biosystems StepOne Plus machine. A PCR master mix was made of 10 µl KAPA SYBR FAST q-PCR master mix (2X) (Sigma, catalogue number: KK4600), 0.4 µl ROX high, 0.4 µl 10 µM forward primer, 0.4 µl of 10 µM reverse primer, 4 µl of 1 in 10^4 diluted template DNA and 4.8 µl PCR grade water. A PCR was run using the following cycling protocol: 95 °C for 3 minutes, 40 cycles of 95 °C for 10 seconds and 60 °C for 30 seconds. A standard range of 10-fold dilutions of phix from 20 pmol to 0.0002 pmol was used.

The final pool was sent to Novogene and was sequenced using an Illumina NovaSeq 6000 system on a S4 flow cell in a single lane.

5.2.3 Processing shotgun metagenomics sequence data

Dr Andrea Telatin performed the following steps to make the raw sequences ready for taxonomic analysis. All of the following tools mentioned were retrieved from the BioConda repository (Grüning et al., 2018). The quality of raw sequences was assessed using SeqFu (version 1.8.5) (Telatin et al., 2021) and sequences with bases below Phred quality score of 15 were removed using Fastp (version 0.20.0) (Chen et al., 2018). Removal of human reads was done by mapping against the human genome (release hg19) using Kraken 2 (Wood et al., 2019). Taxonomic assignment of filtered metagenomics sequencing reads was done using Kraken 2 against the 'PlusPF' database containing archaea, bacteria, viral, plasmid, human1, UniVec_Core, Protozoa and Fungi (Wood et al., 2019). The following was then performed for a) taxonomic profiling and b) functional profiling:

a) Bracken was used to estimate the abundance of reads at the species-level (Lu J, 2017).
b) The HMP Unified Metabolic Analysis Network 3.0 (HUMAnN 3.0) package from the bioBakery 3 suite (McIver et al., 2018, Beghini et al., 2021)

5.2.4 Taxonomic analysis of stool microbes

5.2.4.1 Relative microbiome profiling

The bracken table was split into the following taxonomic ranks: domain, phylum, class, order, family, genus and species. For each taxonomic level read counts were converted to relative abundances by total sum scaling to 1 (**Equation 5.1**). The cut-off threshold was 1 x 10^{-6}; any values less than this were zeroed. RMP was performed on the relative abundances of taxa in each sample. RMP of each taxonomic level were displayed as stacked bar charts in R (v.4.1.2) using the following R packages: ggplot2 (v.3.3.5), reshape2 (v.1.3.3), ggsci (v.2.9) and ggh4x (v.0.2.1). As only relative abundances greater than 0.01 are visible on stacked bar charts, any taxa with a relative abundance less than 0.01 were not shown on the graphs and were instead grouped into '_Other'. For taxonomic levels with more than 15 taxa present at a relative abundance greater than 0.01 only the top 15 most abundant taxa were shown.

Equation 5.1: Calculating relative abundance of a taxa (i) in sample (j).

$$relative\ abundance_{ij} = \frac{number\ of\ reads_{ij}}{total\ number\ of\ reads_{j}}$$

5.2.4.2 Quantitative microbiome profiling

Absolute abundances were calculated from relative abundances (calculated in **section 5.2.4.1**) and total cell ('sybr green high') concentration in stool samples (calculated in **section 4.2.2**) (**Equation 5.2**). QMP was then performed on the absolute abundances of taxa in each sample. Stacked bar

charts were again used to visualise the absolute abundances of the taxa presented within the RMP plots.

Equation 5.2: Calculating the microbial load of taxa (i) in sample (j).

$$absolute\ abundance\ (cells/g)_{ij} = relative\ abundance_{ij} \times total\ cell\ concentration\ (cells/g)_j$$

5.2.4.3 Analysing IgG binding of taxa

For each participant, at each taxonomic level, counts were zeroed in the 'IgG positive' and 'IgG negative' fraction if they were not present in the 'all' fraction. Next relative abundances for each taxonomic rank in the 'IgG positive' and 'IgG negative' fractions were calculated (**Equation 5.1**). The cut-off threshold applied was 1 x 10^{-6} and any values less than this were zeroed. Relative abundances of taxa in each taxonomic level from the 'IgG positive' and 'IgG negative' fractions were displayed as bubble plots in R (v.4.1.2) using the following R packages: ggplot2 (v.3.3.5), reshape2 (v.1.3.3) and ggh4x (v.0.2.1). For taxonomic levels with more than 20 taxa present the top 20 most abundant taxa were shown.

5.2.4.4 IgG probability ratio

Next, IgG probability ratios (**Equation 5.3**) for each taxon in each taxonomic level were calculated using the igascores function within the IgAScores (v 0.1.2) R package with the method set to 'probratio'. The pseudocount was set to 1 x 10^{-6} as this was the minimum observed abundance due to the threshold being set to 1 x 10^{-6}. The scaleratio was set to TRUE meaning the probability ratio scores were scaled to the pseudocount with scores ranging from -1 to 1. Summary plots for probability ratios were made in R (v.4.1.2) using ggplot2 (v.3.3.5) and reshape2 (v.1.3.3) and displayed taxa that were present in four or more complete participant pairs. Paired *t* tests were performed on IgG probability ratios from taxa present in four or more complete participant pairs using R (v.4.1.2). P values were adjusted for multiple comparisons using the false discovery rate (FDR) method and applied using the p.adjust function in R.

Equation 5.3: Calculating the IgG probability ratio of taxa (i) in sample (j).

$$Probability\ ratio_{ij} = log2\left(\frac{\left(IgG_{ij}^{+} \times FracSize_j^{IgG^+}\right) + c}{\left(IgG_{ij}^{-} \times FracSize_j^{IgG^-}\right) + c}\right)$$

5.2.4.5 Statistical analysis

The following analyses were performed in R (v.4.1.2). To test whether there were any taxa differentially abundant in severe ME/CFS patients compared to their matched household controls paired *t*-tests were performed with FDR correction. For RMP, taxa with relative abundances less than 1 x 10^{-6} (including zeroes) were converted to 1 x 10^{-7} prior to analysis of significance. In

addition, these new relative abundances were used to calculate microbial loads to analyse differential abundance in QMP. Prior to performing paired *t*-tests the distribution of differences (control – patient) was analysed for Gaussian distribution using Shapiro-Wilk's test. When there was evidence for non-normality RMP data was centred log ratio (CLR) transformed and QMP data was log10-transformed prior to paired *t*-tests.

Alpha diversity was calculated at the species-level on read counts. The diversity function from vegan (v.2.5-7) was used to calculate Shannon indices and inverse Simpson indices. Then total reads per sample were calculated and the rarefy function from vegan (v.2.5-7) was used to rarefy reads to the lowest sequencing depth. Observed species' richness was the number of species remaining following rarefaction.

Beta diversity was assessed at the species-level for RMP and QMP. Bray-Curtis indices were calculated using the vegdist function from vegan (v.2.5-7). Non-metric multi-dimensional scaling (NMDS) on Bray-Curtis indices was performed using the metMDS function from vegan (v.2.5-7) and plotted using ggplot2 (v.3.3.5). PERMANOVA analysis could not be performed on only 5 pairs of participants and therefore the differences between severe ME/CFS patients and their matched household controls could not be assessed for significance.

5.2.5 Functional analysis of shotgun metagenomics

5.2.5.1 Analysing the 'all' fraction

Dr Sumeet Tiwari, a bioinformatician at QIB, converted gene families from reads per kilobase (RPK) to relative abundances using the humann_renorm_table utility script from HUMAnN (v 3.0) (Beghini et al., 2021). Subsequent analyses were performed in R (v.4.1.2) by Dr Marianne Defernez from the QIB Core Science Resources team. Community level classifications of gene families were used in downstream analysis. A threshold of 1×10^{-6} was applied and if the relative abundance of a gene family was below this threshold it was set to zero. Gene families that were below the threshold level in 7 or more samples were discarded from downstream analysis. CLR transformation of gene families' relative abundance was calculated using the clr function from the compositions package (v 2.0-4). Then principal component analysis (PCA) was performed using the pca function from the mixOmics package (v 6.18.1). Severe ME/CFS patients and their matched household controls were not treated as paired samples in this analysis.

5.2.5.2 Analysing the 'IgG positive' and 'IgG negative' fractions

All analyses were performed in R (v.4.1.2) by Dr Marianne Defernez on community level classifications of gene families. In every sample each gene family was filtered by the following: if the gene family was not present in the 'all' fraction the RPK was zeroed in the 'IgG positive' and 'IgG negative' fraction. Then gene families were normalised to relative abundances using total sum

scaling. A threshold of 1 x 10^{-6} was applied and if the relative abundance of a gene family was below this threshold it was set to zero. Then IgG probability ratios for each gene family were calculated as described in **section 5.2.6.1**. Only gene families with IgG probability ratios present in all samples were used in downstream analysis. PCA was then performed on IgG probability ratios of gene families using the pca function from the mixOmics package (v 6.18.1). Severe ME/CFS patients and household controls were treated as two unrelated groups in this analysis.

5.3 RESULTS

5.3.1 Taxonomic analysis of the gut microbiota

The average number of 'sybr green high' microbes collected on the Sony SH800S cell sorter was 1,473,548 cells (*SD* = 83,648.57). Therefore, all taxa present at a relative abundance greater than 1 x 10^{-6} were included in downstream analysis. This cell population was used to represent the gut microbiota in the severe ME/CFS patient group and matched household control group.

5.3.1.1 Taxonomic composition

5.3.1.1.1 Domain

At the domain-level, bacteria, viruses and archaea were detected. Only bacteria and viruses were detected in every sample. However, only bacteria (*M* = 0.981, *SD* = 0.056) and archaea (*M* = 0.018, *SD* = 0.056) had a relative abundance greater than 0.01 in at least one participant (**Figure 5.2A**). Interestingly, only the severe ME/CFS patient from pair 3 had a relative abundance of archaea greater than 0.01, at 0.18. When the total concentration of cells in stool samples (presented in **chapter 4**) was used to convert RMP to QMP the variance of abundance of bacteria across stool samples increased, ranging from 5.19 x 10^{10} cells/gram to 2.64 x 10^{11} cells/gram (**Figure 5.2B**). Three severe ME/CFS patients had a higher and two patients had a lower concentration of bacteria in their stool sample compared to their matched household controls. There were no taxa at the domain-level whose relative abundance or microbial load were significantly different between the patient and control groups.

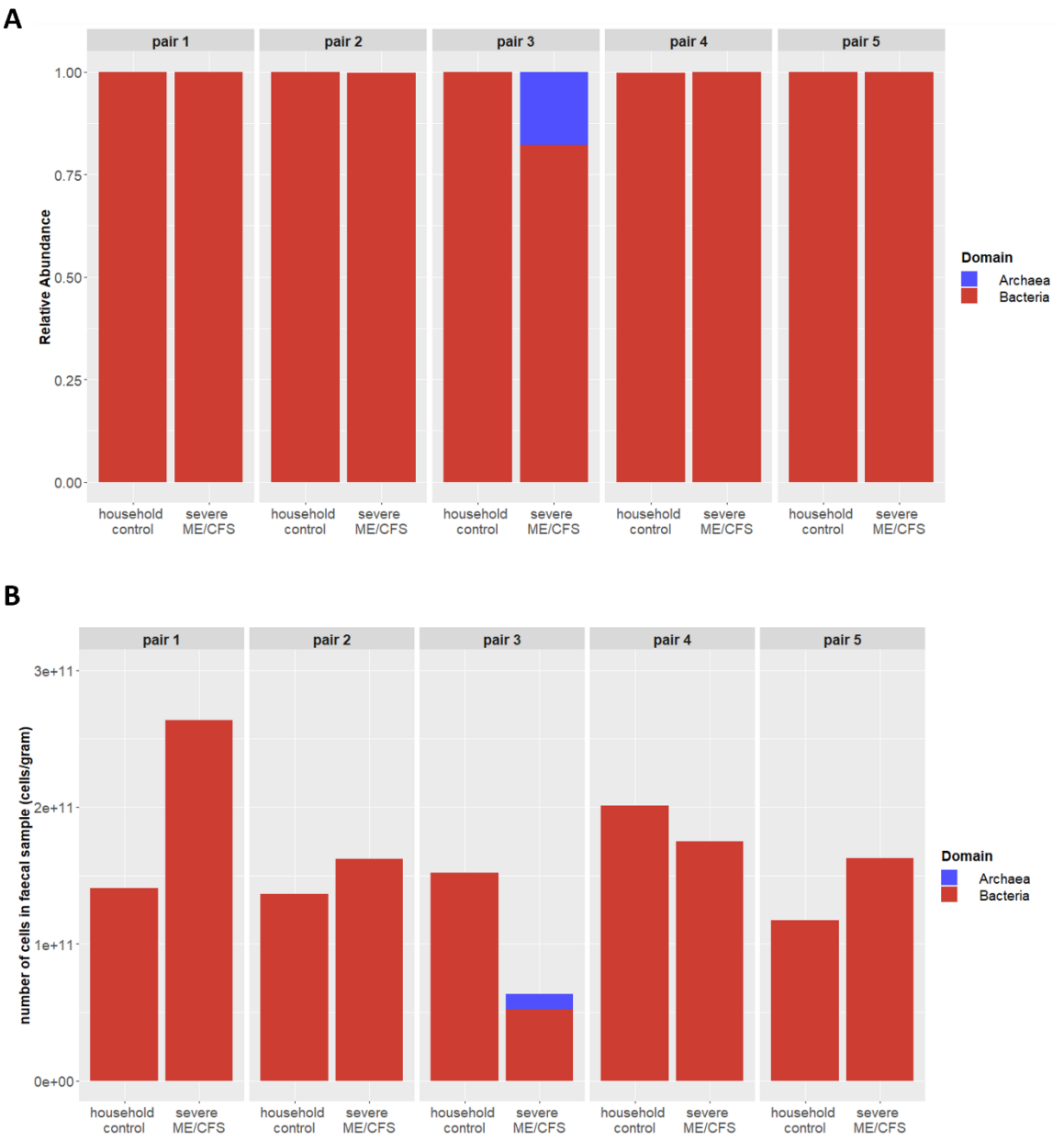

Figure 5.2: Composition of stool samples from severe ME/CFS patients and their matched household controls at the domain-level. *A) Relative microbiome profiling and B) quantitative microbiome profiling of taxa present at a relative abundance greater than 0.01. Stool microbes from severe ME/CFS patients (n=5) and their matched household controls (n=5) were stained with SYBR™ green I nucleic acid gel stain and 'all' cells were collected using the Sony SH800S cell sorter and shotgun metagenomic sequencing was performed to identify the taxa present in each sample.*

5.3.1.1.2 Phylum

A total of 20 taxa at the phylum-level were detected, 5 of which were detected in every sample. However, only 6 taxa had a relative abundance greater than 0.01 in at least one participant (**Figure 5.3A**). These were as follows in decreasing order: Firmicutes (*M* = 0.514, *SD* = 0.147), Bacteroidetes (*M* = 0.219, *SD* = 0.167), Proteobacteria (*M* = 0.181, *SD* = 0.122), Verrucomicrobia (*M* = 0.043, *SD* = 0.078), Actinobacteria (*M* = 0.024, *SD* = 0.019) and Euryarchaeota (*M* = 0.018, *SD* = 0.057). All of the aforementioned taxa were present in at least five samples at a relative abundance greater than 0.01, except for Euryarchaeota which was only present in the sample from patient in pair 3 at a relative abundance greater than 0.01.

Firmicutes was not the dominant phyla in all samples; the relative abundance of Proteobacteria was 0.348 which was slightly higher than the relative abundance of Firmicutes, at 0.338, in the sample from the severe ME/CFS patient from pair 3, and in the samples from household control from pair 3 and the severe ME/CFS patient from pair 5 the dominant phyla was Bacteroides.

Converting the RMP to QMP increased the heterogeneity of samples at the phylum-level (**Figure 5.3B**). For example, when considering RMP, the relative abundance of Firmicutes is comparable between severe ME/CFS patient and their matched household control in pair 1 and pair 3; the relative abundance of Firmicutes in pair 1 was 0.54 and 0.56 in the patient and household control respectively and the relative abundance of Firmicutes in pair 3 was 0.34 and 0.33 in the patient and household control respectively. But when RMP was converted to QMP, the abundance of Firmicutes was no longer comparable within these pairs; in pair 1 the microbial load was 1.43×10^{11} cells/gram in the severe ME/CFS patient compared to 7.92×10^{10} cells/gram in the matched household control and in pair 3 the microbial load was 2.14×10^{10} cells/gram in the severe ME/CFS patient compared to 5×10^{10} cells/gram in the matched household control.

To determine whether there were any taxa at the phylum-level with differentially abundant RMP or QMP paired *t*-tests with FDR correction were performed on CLR-transformed relative abundances and log10-transformed microbial loads (**Figure 5.4, Table 5.1**). All severe ME/CFS patients had lower CLR-transformed relative abundances of Apicomplexa and Ascomycota than their matched household controls, but these differences were not significant following FDR correction. In addition, four severe ME/CFS patients had higher CLR-transformed relative abundances of Basidiomycota than their matched household controls, but this difference was not significant following FDR correction. In contrast, microbial loads of Basidiomycota were higher in all severe ME/CFS patients compared to their matched household controls, but again this difference was not significant following FDR correction.

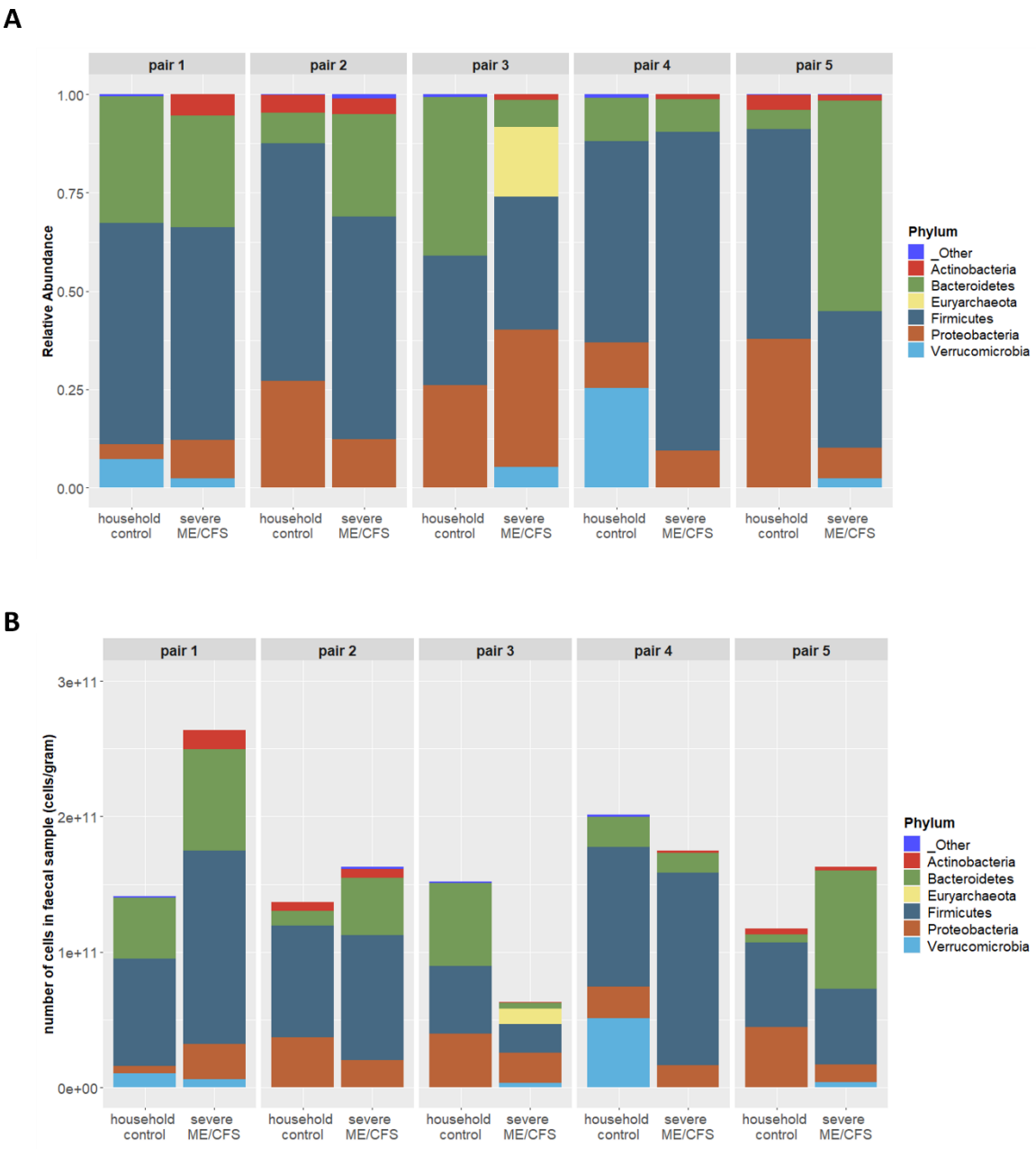

Figure 5.3: Composition of stool samples from severe ME/CFS patients and their matched household controls at the phylum-level. *A) Relative microbiome profiling and B) quantitative microbiome profiling of taxa present at a relative abundance greater than 0.01. Stool microbes from severe ME/CFS patients (n=5) and their matched household controls (n=5) were stained with SYBR™ green I nucleic acid gel stain and 'all' cells were collected using the Sony SH800S cell sorter and shotgun metagenomic sequencing was performed to identify the taxa present in each sample.*

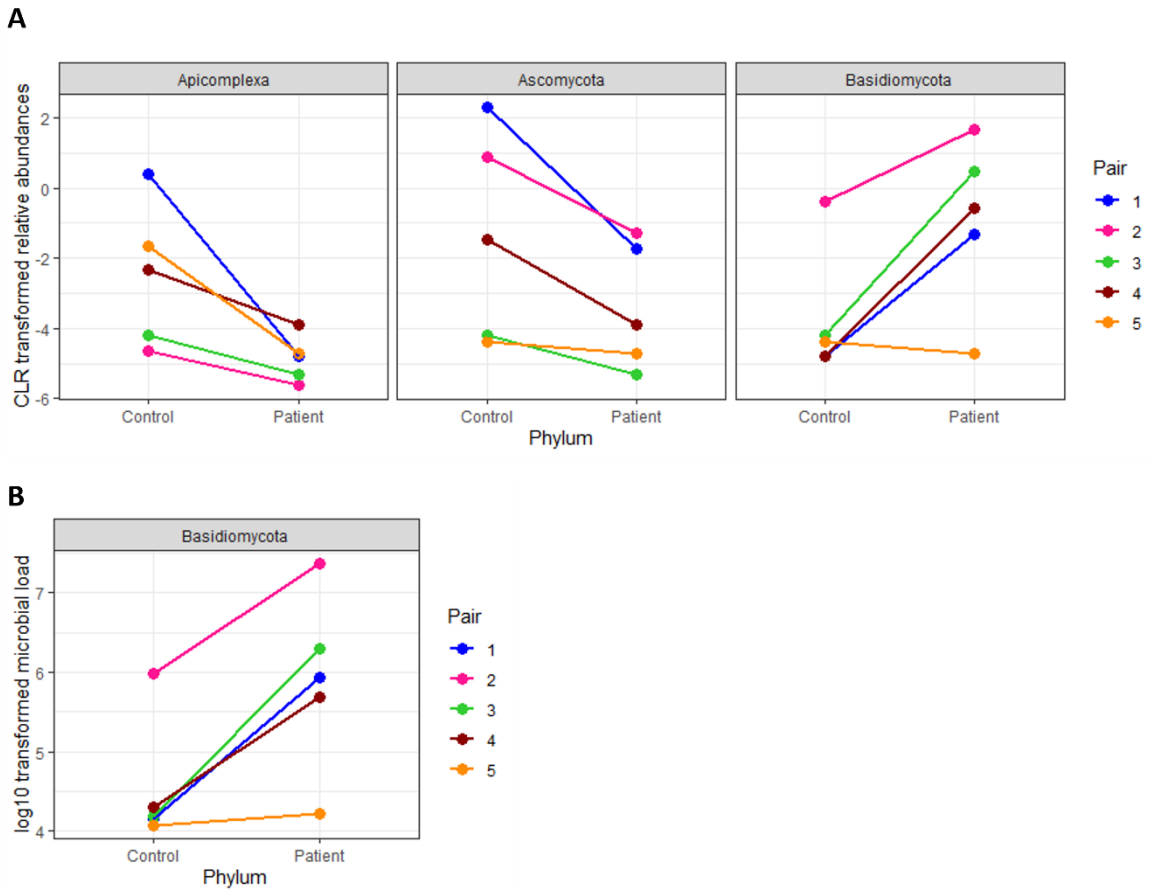

Figure 5.4: Pairwise comparisons of the abundance of taxa at the phylum-level in severe ME/CFS patients and their matched household controls. *Paired t-tests were performed on A) CLR transformed relative abundances and B) log10-transformed microbial loads. Stool microbes from severe ME/CFS patients (n = 5) and their matched household controls (n=5) were stained with SYBR™ green I nucleic acid gel stain and 'all' cells were collected using the Sony SH800S cell sorter and shotgun metagenomic sequencing was performed to identify the taxa present in each sample. Taxa with a p-value < 0.05 (prior to FDR correction) are shown on the graph.*

5.3.1.1.3 Class

A total of 30 taxa at the class-level were detected, 13 of which were detected in every sample. Of the 30 taxa only 13 had a relative abundance greater than 0.01 in at least one participant (**Figure 5.5A**). These were as follows in decreasing order: Clostridia (*M* = 0.464, *SD* = 0.162), Bacteroidia (*M* = 0.219, *SD* = 0.167), Gammaproteobacteria (*M* = 0.108, *SD* = 0.078), Verrucomicrobiae (*M* = 0.043, *SD* = 0.078), Alphaproteobacteria (*M* = 0.039, *SD* = 0.053), Epsilonproteobacteria (*M* = 0.029, *SD* = 0.054), Erysipelotrichia (*M* = 0.028, *SD* = 0.019), Actinobacteria (*M* = 0.019, *SD* = 0.018), Bacilli (*M* = 0.019, *SD* = 0.015), Methanobacteria (*M* = 0.018, *SD* = 0.057), Betaproteobacteria (*M* = 0.005, *SD* = 0.006), Coriobacteriia (*M* = 0.004, *SD* = 0.003) and Negativicutes (*M* = 0.004, *SD* = 0.006). Only 3 taxa had a relative abundance greater than 0.01 in all participants: Clostridia, Bacteroidia and Gammaproteobacteria. Clostridia dominated samples from 4 severe ME/CFS patients and 4 household controls, which was not surprising as Clostridia belongs to the Firmicutes phylum, which was the most abundant taxa. The dominant class in the sample from the control in pair 3 and the patient in pair 5 was Bacteroidia, belonging to the Bacteroidetes phylum. Other taxa dominating individual samples included Alphaproteobacteria and Methanobacteria in the patient from pair 3, Epsilonproteobacteria in the control from pair 3, and Verrucomicrobiae in the control from pair 5.

When converting RMP to QMP at the class-level the heterogeneity of samples increased (**Figure 5.5B**). For example, the relative abundance of Clostridia was comparable between the severe ME/CFS patient and matched household control in pair 1, but the microbial load of Clostridia was 1.8-fold higher in the severe ME/CFS patient than the matched household control. In addition, converting RMP to QMP also decreases the variation between samples of some taxa. For example, the patient from pair 3 had the highest relative abundance of Bacilli but when converted to microbial load the patient from pair 3 no longer had the highest abundance of Bacilli as the microbial load was higher in the patients from pair 1 and 5 and comparable to the concentration of Bacilli in the patient from pair 2 and the control from pair 4.

To determine whether there were any taxa at the class-level with differentially abundant RMP or QMP, paired *t*-tests with FDR correction were performed on CLR-transformed relative abundances and log10-transformed microbial loads (**Figure 5.6, Table 5.1**). All severe ME/CFS patients had higher CLR-transformed relative abundances and log10-transformed microbial loads of Malasseziomycetes than their matched household controls, but these differences were not significant following FDR correction.

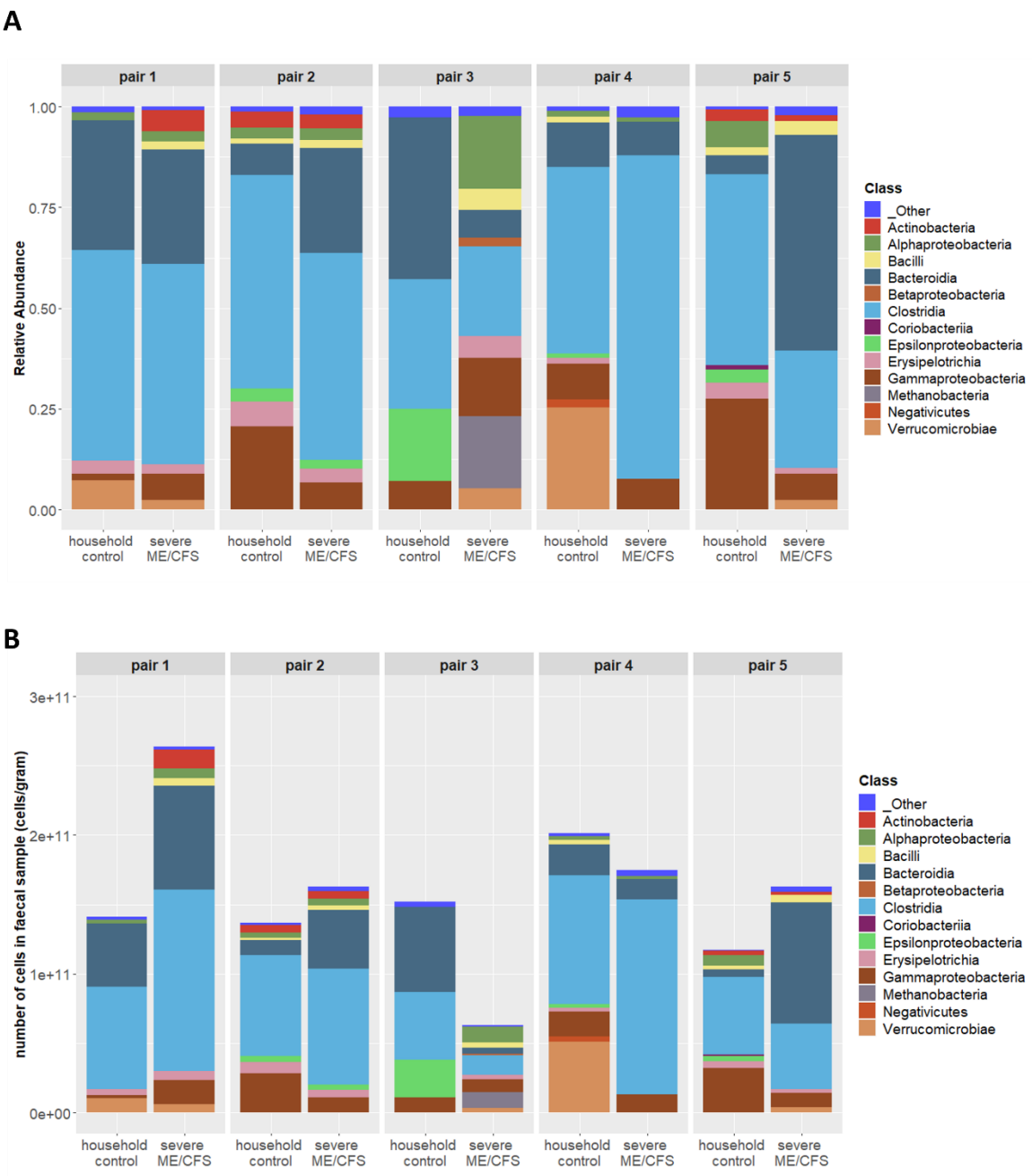

Figure 5.5: Composition of stool samples from severe ME/CFS patients and their matched household controls at the class-level. *A) Relative microbiome profiling and B) quantitative microbiome profiling of taxa present at a relative abundance greater than 0.01. Stool microbes from severe ME/CFS patients (n=5) and their matched household controls (n=5) were stained with SYBR™ green I nucleic acid gel stain and 'all' cells were collected using the Sony SH800S cell sorter and shotgun metagenomic sequencing was performed to identify the taxa present in each sample.*

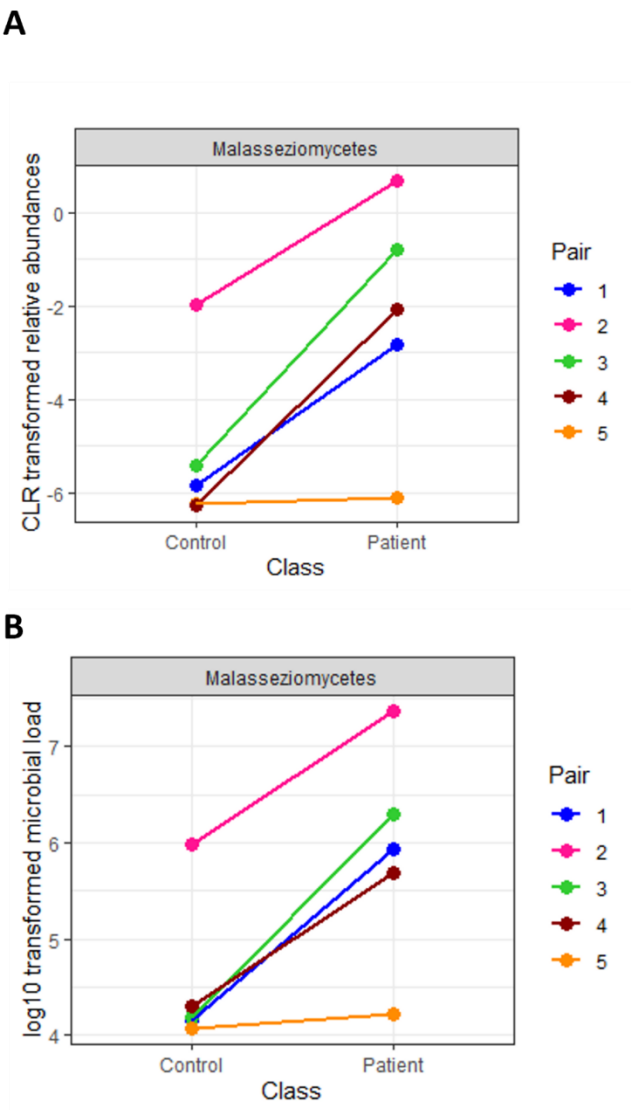

Figure 5.6: Pairwise comparisons of the abundance of taxa at the class-level in severe ME/CFS patients and their matched household controls. *Paired* t*-tests were performed on A) CLR transformed relative abundances and B) log10-transformed microbial loads. Stool microbes from severe ME/CFS patients (n = 5) and their matched household controls (n=5) were stained with SYBR™ green I nucleic acid gel stain and 'all' cells were collected using the Sony SH800S cell sorter and shotgun metagenomic sequencing was performed to identify the taxa present in each sample. Taxa with a p-value < 0.05 (prior to FDR correction) are shown on the graph.*

5.3.1.1.4 Order

At the order-level a total of 56 taxa were detected, 25 of which were detected in every sample. However, only 14 taxa had a relative abundance greater than 0.01 in at least one participant. These were as follows in decreasing order: Clostridiales (*M* = 0.464, *SD* = 0.162), Bacteroidales (*M* = 0.219, *SD* = 0.167), Xanthomonadales (*M* = 0.095, *SD* = 0.079), Verrucomicrobiales (*M* = 0.043, *SD* = 0.078), Rhizobiales (*M* = 0.036, *SD* = 0.049), Campylobacterales (*M* = 0.029, *SD* = 0.054), Erysipelotrichales (*M* = 0.028, *SD* = 0.019), Bifidobacteriales (*M* = 0.019, *SD* = 0.018), Lactobacillales (*M* = 0.018, *SD* = 0.015), Methanobacteriales (*M* = 0.018, *SD* = 0.057), Enterobacterales (*M* = 0.010, *SD* = 0.010), Burkholderiales (*M* = 0.005, *SD* = 0.006), Coriobacteriales (*M* = 0.003, *SD* = 0.003) and Acidaminococcales (*M* = 0.003, *SD* = 0.006) (**Figure 5.7A**). Only 3 taxa had a relative abundance greater than 0.01 in all participants; Clostridiales, Bacteroidales and Xanthomonadales, which belong to the classes Clostridia, Bacteroidia and Gammaproteobacteria respectively. The cumulative relative abundance of these three classes was greater than 0.79 in all but one participant; the cumulative relative abundance was only 0.41 in the patient from pair 3. Other taxa making up a large proportion of the stool sample of the patient from pair 3 were Methanobacteriales, at a relative abundance of 0.179, and Rhizobiales, at a relative abundance of 0.169. Interestingly, Methanobacteriales was not detected at a relative abundance greater than 0.01 in the stool samples from any other participant and the relative abundance of Rhizobiales was highest in the patient from pair 3. Despite having the lowest total microbial load, when the RMP of Rhizobiales was converted to QMP, the patient from pair 3 had the highest microbial load of Rhizobiales (**Figure 5.7B**).

To determine whether there were any taxa at the order-level with differentially abundant RMP or QMP, paired *t*-tests with FDR correction were performed on CLR-transformed relative abundances and log10-transformed microbial loads (**Figure 5.8, Table 5.1**). All severe ME/CFS patients had higher CLR-transformed relative abundances of Malasseziales and Nitrosomonadales than their matched household controls, but these differences were not significant following FDR correction. In addition, severe ME/CFS patients had lower CLR-transformed relative abundances of Neisseriales than their matched household controls, but this difference was not significant following FDR correction. In contrast, only the microbial load of Malasseziales was higher in all severe ME/CFS patients compared to their matched household controls, but again this difference was not significant following FDR correction.

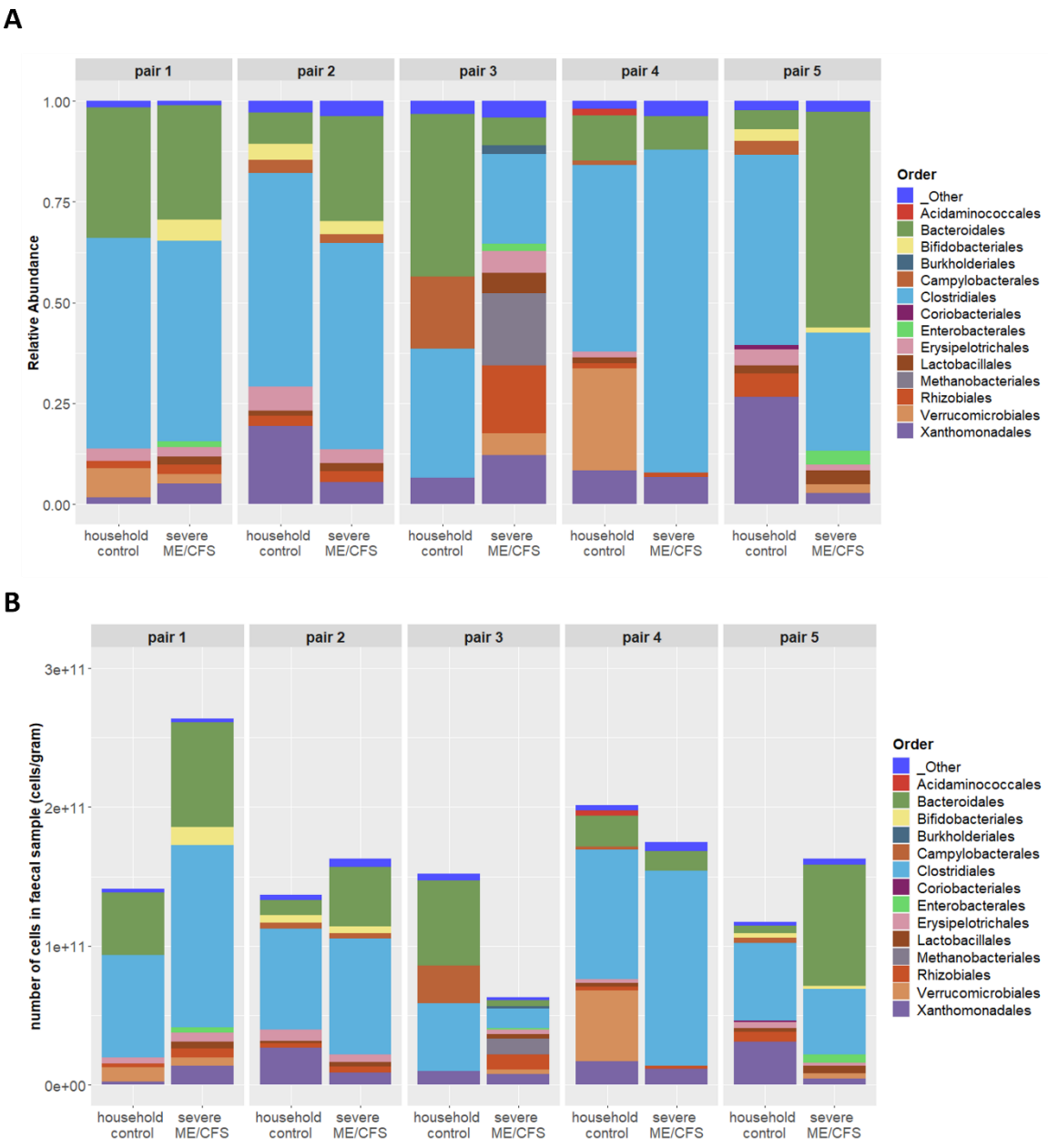

Figure 5.7: Composition of stool samples from severe ME/CFS patients and their matched household controls at the order-level. *A) Relative microbiome profiling and B) quantitative microbiome profiling of taxa present at a relative abundance greater than 0.01. Stool microbes from severe ME/CFS patients (n=5) and their matched household controls (n=5) were stained with SYBR™ green I nucleic acid gel stain and 'all' cells were collected using the Sony SH800S cell sorter and shotgun metagenomic sequencing was performed to identify the taxa present in each sample.*

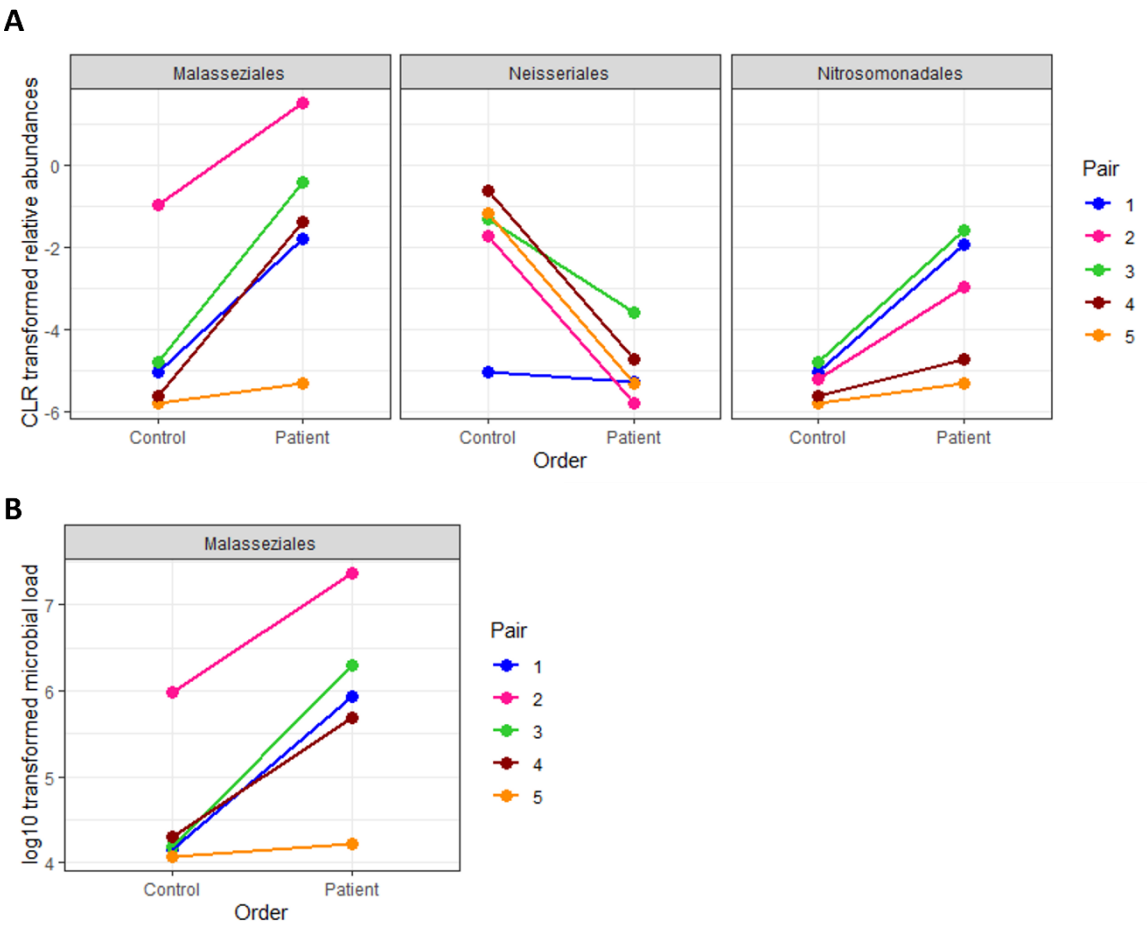

Figure 5.8: Pairwise comparisons of the abundance of taxa at the order-level in severe ME/CFS patients and their matched household controls. *Paired* t*-tests were performed on A) CLR transformed relative abundances and B) log10-transformed microbial loads. Stool microbes from severe ME/CFS patients (n = 5) and their matched household controls (n=5) were stained with SYBR™ green I nucleic acid gel stain and 'all' cells were collected using the Sony SH800S cell sorter and shotgun metagenomic sequencing was performed to identify the taxa present in each sample. Taxa with a p-value < 0.05 (prior to FDR correction) are shown on the graph.*

5.3.1.1.5 Family

A total of 110 taxa at the family-level were detected, 42 of which were detected in every sample. However, only 22 taxa had a relative abundance greater than 0.01 in at least one participant (**Supplementary figure 5.1A**). The 15 most abundant families were as follows in decreasing order: Lachnospiraceae (*M* = 0.274, *SD* = 0.122), Bacteroidaceae (*M* = 0.120, *SD* = 0.094), Ruminococcaceae (*M* = 0.109, *SD* = 0.077), Xanthomonadaceae (*M* = 0.102, *SD* = 0.077), Peptostreptococcaeceae (*M* = 0.100, *SD* = 0.229), Akkermansiaceae (*M* = 0.048, *SD* = 0.080), Camplylobacteraceae (*M* = 0.033, *SD* = 0.062), Erysipelotrichaceae (*M* = 0.031, *SD* = 0.019), Rhizobiaceae (*M* = 0.029, *SD* = 0.041), Bifidobacteriaceae (*M* = 0.022, *SD* = 0.021), Methanobacteriaceae (*M* = 0.020, *SD* = 0.061), Streptococcaceae (*M* = 0.017, *SD* = 0.017), Enterobacteriaceae (*M* = 0.14, *SD* = 0.019), Oscillospiraceae (*M* = 0.010, *SD* = 0.007), Tannerellaceae (*M* = 0.010, *SD* = 0.007) (**Figure 5.9A**). All of the aforementioned taxa were present in at least three samples at a relative abundance greater than 0.01, except for Methanobacteriaceae which was only present in the sample from the severe ME/CFS patient in pair 3 at a relative abundance greater than 0.01. Despite this, Methanobacteriaceae made the top 15 most abundant families because of its high relative abundance at 0.19 in this one patient. Peptostreptococcaceae had the highest variation across samples; in pair 4 the relative abundance of this taxa in the severe ME/CFS patient was 0.75 and 0.12 in the matched household control whereas the relative abundance in all other participants was less than 0.03. Another taxon with a high variation in relative abundance across samples was Lachnospiraceae, varying from 0.05 to 0.39, with all but two severe ME/CFS patients having a relative abundance greater than 0.1. There were no taxa at the family-level whose relative abundance was significantly different between the patient and control groups.

When RMP was converted to QMP the heterogeneity of samples increased at the family-level (**Figure 5.9B, Supplementary figure 5.1B**). This can be demonstrated by comparing the severe ME/CFS patient to the matched household control in pair one. The relative abundance of some taxa, such as Lachnospiraceae and Ruminococcaceae, were comparable between the severe ME/CFS patient and the matched household control, but became nearly 2-fold higher in the severe ME/CFS patient when relative abundances were converted to microbial loads. Conversely, when taxa such as Bacteroidaceae with a relative abundance nearly 2-fold higher in the matched household control compared to the severe ME/CFS patient was converted to microbial load, the abundance of Bacteroidaceae in the severe ME/CFS patient and matched household control was similar. This occurred because the total microbial load of the stool sample from the patient in pair one was double that of their matched household control.

To determine whether there were any taxa at the family-level with differentially abundant RMP or QMP, paired *t*-tests with FDR correction were performed on CLR-transformed relative abundances

and log10-transformed microbial loads (**Figure 5.10, Table 5.1**). All severe ME/CFS patients had higher CLR-transformed relative abundances of Malasseziaceae and Sulfuricellaceae than their matched household controls, but these differences were not significant following FDR correction. In addition, severe ME/CFS patients had lower CLR-transformed relative abundances of Chromobacteriaceae than their matched household controls, but this difference was not significant following FDR correction. When comparing log10-transformed microbial loads between severe ME/CFS patients and their matched household controls, 4 patients had a lower log10-transformed microbial load of Chromobacteriaceae than their matched household control, and all patients had higher microbial loads of Corynebacteriaceae, Erythrobacteraceae and Malasseziaceae than their matched household controls.

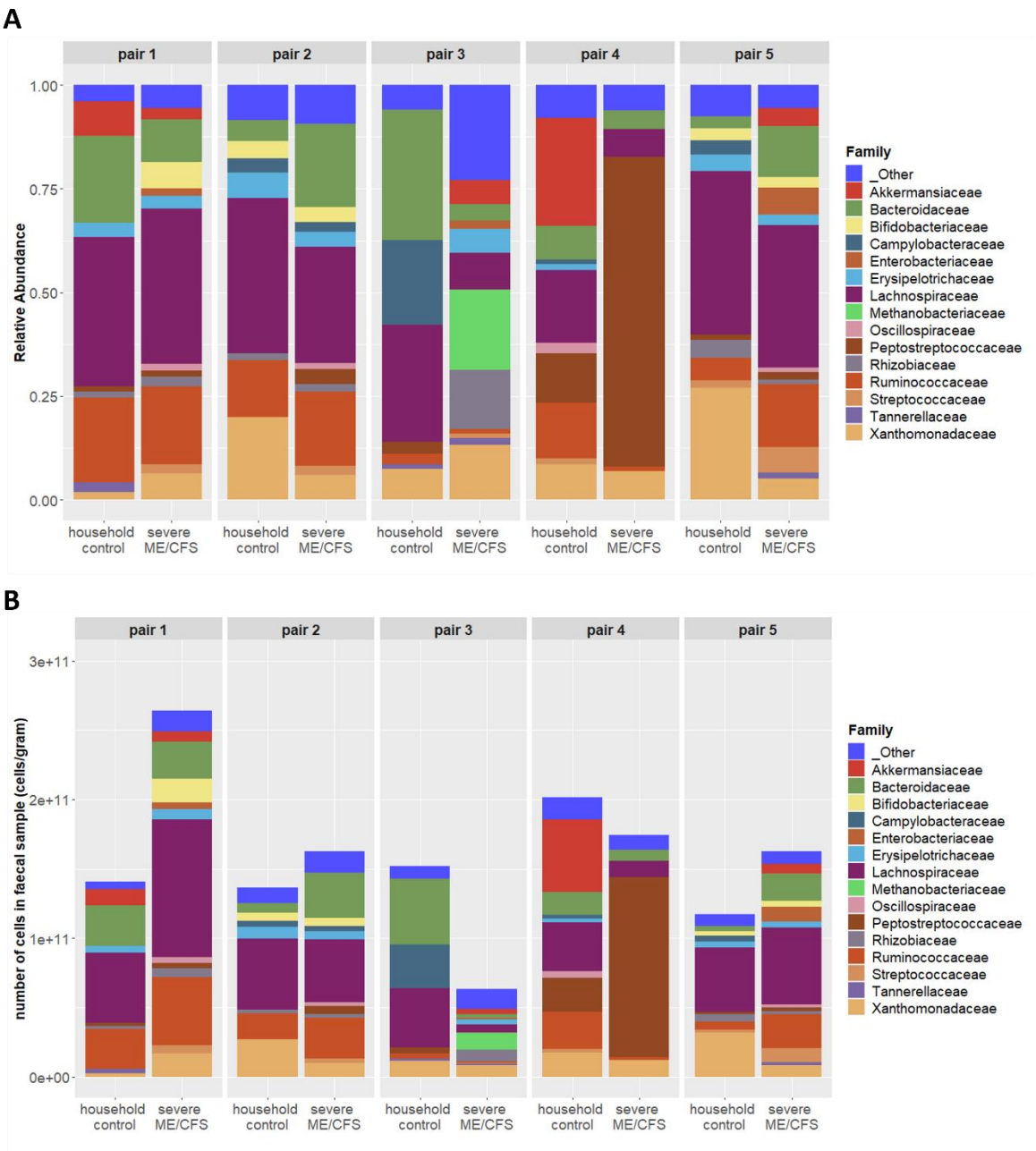

Figure 5.9: Top 15 families in stool samples from severe ME/CFS patients and their matched household controls at the family-level. *A) Relative microbiome profiling and B) quantitative microbiome profiling of taxa present at a relative abundance greater than 0.01. Stool microbes from severe ME/CFS patients (n=5) and their matched household controls (n=5) were stained with SYBR™ green I nucleic acid gel stain and 'all' cells were collected using the Sony SH800S cell sorter and shotgun metagenomic sequencing was performed to identify the taxa present in each sample.*

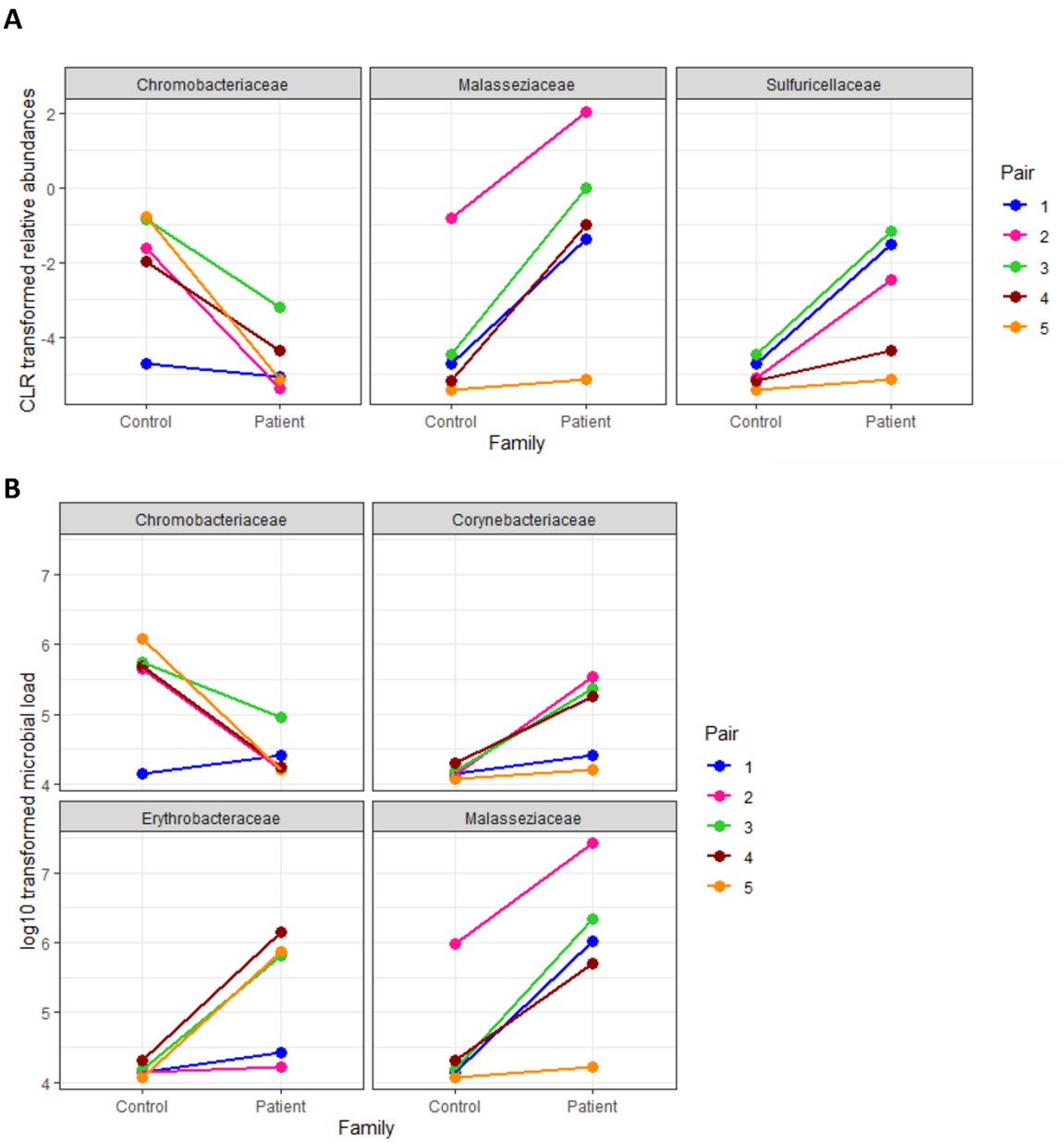

Figure 5.10: Pairwise comparisons of the abundance of taxa at the family-level in severe ME/CFS patients and their matched household controls. *Paired* t*-tests were performed on A) CLR transformed relative abundances and B) log10-transformed microbial loads. Stool microbes from severe ME/CFS patients (n = 5) and their matched household controls (n=5) were stained with SYBR™ green I nucleic acid gel stain and 'all' cells were collected using the Sony SH800S cell sorter and shotgun metagenomic sequencing was performed to identify the taxa present in each sample. Taxa with a p-value < 0.05 (prior to FDR correction) are shown on the graph.*

5.3.1.1.6 Genus

At the genus-level a total of 275 taxa were detected, 84 of which were detected in every sample. However, only 33 taxa had a relative abundance greater than 0.01 in at least one participant (**Supplementary figure 5.2A**). The 15 most abundant genera were as follows in decreasing order: *Bacteroides* (*M* = 0.104, *SD* = 0.083), *Phocaeicola* (*M* = 0.101, *SD* = 0.137), *Clostridioides* (*M* = 0.095, *SD* = 0.222), *Lysobacter* (*M* = 0.094, *SD* = 0.079), *Faecalibacterium* (*M* = 0.086, *SD* = 0.062), *Blautia* (*M* = 0.071, *SD* = 0.048), *Roseburia* (*M* = 0.058, *SD* = 0.044), *Anaerostipes* (*M* = 0.055, *SD* = 0.048), *Akkermansia* (*M* = 0.044, *SD* = 0.078), *Campylobacter* (*M* = 0.029, *SD* = 0.054), *Agrobacterium* (*M* = 0.026, *SD* = 0.039), *Methanobrevibacter* (*M* = 0.019, *SD* = 0.059), *Bifidobacterium* (*M* = 0.019, *SD* = 0.018), *Anaerobutyricum* (*M* = 0.015, *SD* = 0.011) and *Streptococcus* (*M* = 0.013, *SD* = 0.010) (**Figure 5.11A**). All of the aforementioned taxa were present in at least four samples at a relative abundance greater than 0.01, except for *Methanobrevibacter* which was only present in the sample from the severe ME/CFS patient in pair 3 at a relative abundance greater than 0.01. *Clostridioides* had the highest variation in relative abundances across samples; in pair 4 the relative abundance of this taxa in the severe ME/CFS patient was 0.720 and 0.116 in the matched household control whereas the relative abundance in all other pairs was 0.031 or less. To determine whether there were any taxa at the genus-level with differentially abundant RMP, paired *t*-tests with FDR correction were performed on CLR-transformed relative abundances (**Figure 5.12, Table 5.1**). All severe ME/CFS patients had higher CLR-transformed relative abundances of *Malassezia* and *Sulfuriferula*, and lower CLR-transformed relative abundances of *Citrobacter, Ligilactobacillus, Longibaculum, Microvirgula, Pluralibacter* and *Roseburia* than their matched household controls, but these differences were not significant following FDR correction.

When converting the RMP to QMP, differences between pairs of severe ME/CFS patients and their matched household controls became more visible (**Figure 5.11B, Supplementary figure 5.2B**). For example, relative abundances of *Faecalibacterium* in both the severe ME/CFS patient and the matched household control in pair 2 were the same, at 0.133. By converting RMP to QMP the abundance of *Faecalibacterium* became higher in the patient, at 2.16 x 10^{10} cells/gram compared to 1.82 x 10^{10} in the matched household control. In addition, conversion of RMP to QMP also enhanced differences already seen in the taxa's RMP. For example, the relative abundance of *Lysobacter* in the patient from pair 1 was 3-fold higher than their matched household control, and this difference increased to a 6-fold difference when relative abundance was converted to microbial load. In pair 3, the household control had 7-fold higher relative abundance of *Bacteroides* than the patient, which increased to a 17-fold difference when converted to microbial load.

To determine which taxa had differentially abundant QMP, paired *t*-tests with FDR correction were performed on log10-transformed microbial loads (**Figure 5.12, Table 5.1**). All severe ME/CFS

patients had lower log10-transformed microbial loads of *Ligilactobacillus, Longibaculum, Pluralibacter* and *Roseburia* than their matched household controls, but these differences were not significant following FDR correction. Four severe ME/CFS patients had lower log10-transformed microbial loads of *Citrobacter* and *Microvirgula* than their matched household controls, which were not significant following FDR correction. Finally, all severe ME/CFS patients had higher log10-transformed microbial loads of *Malassezia* than their matched household controls, which were not significant following FDR correction.

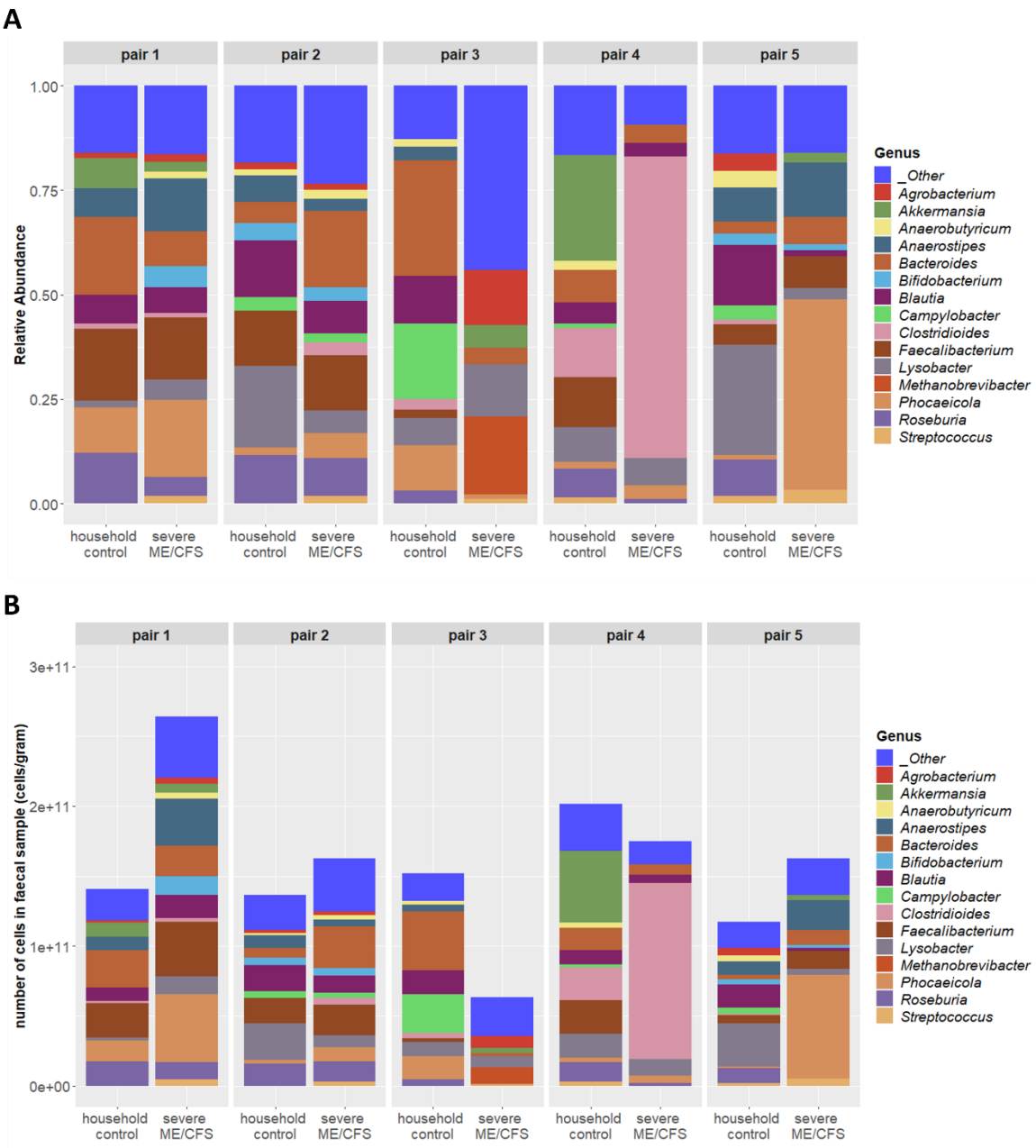

Figure 5.11: Top 15 genera in stool samples from severe ME/CFS patients and their matched household controls. *A) Relative microbiome profiling and B) quantitative microbiome profiling of taxa present at a relative abundance greater than 0.01. Stool microbes from severe ME/CFS patients (n=5) and their matched household controls (n=5) were stained with SYBR™ green I nucleic acid gel stain and 'all' cells were collected using the Sony SH800S cell sorter and shotgun metagenomic sequencing was performed to identify the taxa present in each sample.*

A

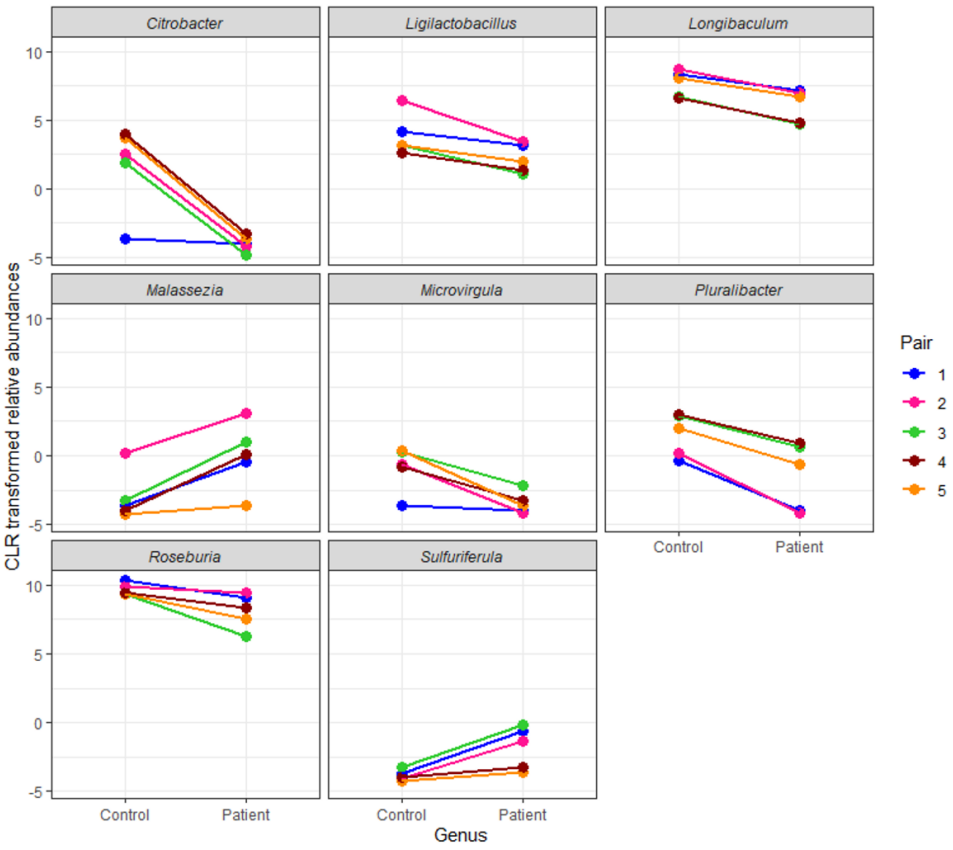
Citrobacter
Ligilactobacillus
Longibaculum
Malassezia
Microvirgula
Pluralibacter
Roseburia
Sulfuriferula
CLR transformed relative abundances
10
5
0
-5
Control
Patient
Genus
Pair
1
2
3
4
5

B

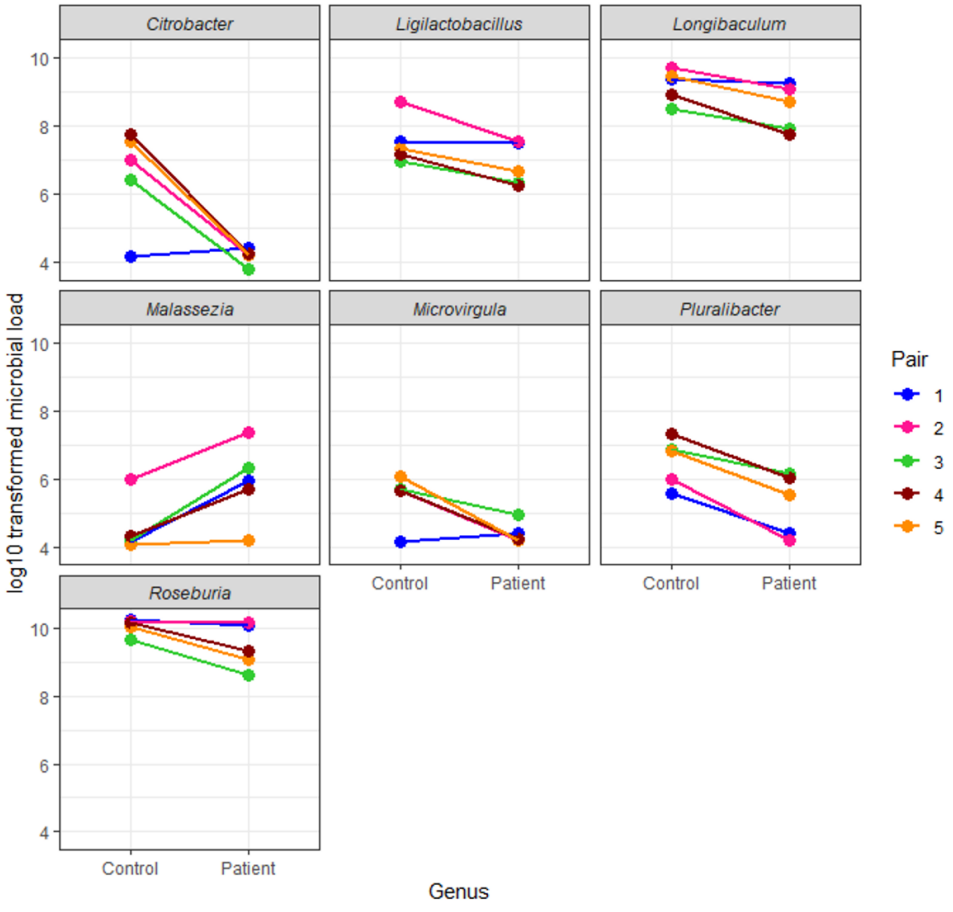
Citrobacter
Ligilactobacillus
Longibaculum
Malassezia
Microvirgula
Pluralibacter
Roseburia
log10 transformed microbial load
10
8
6
4
Control
Patient
Genus
Pair
1
2
3
4
5

← ***Figure 5.12: Pairwise comparisons of the abundance of taxa at the genus-level in severe ME/CFS patients and their matched household controls.*** *Paired* t*-tests were performed on A) CLR transformed relative abundances and B) log10-transformed microbial loads. Stool microbes from severe ME/CFS patients (n = 5) and their matched household controls (n=5) were stained with SYBR™ green I nucleic acid gel stain and 'all' cells were collected using the Sony SH800S cell sorter and shotgun metagenomic sequencing was performed to identify the taxa present in each sample. Taxa with a p-value < 0.05 (prior to FDR correction) are shown on the graph.*

5.3.1.1.7 Species

At the species-level a total of 705 taxa were detected, 159 of which were detected in every sample. Only 48 taxa had a relative abundance greater than 0.01 in at least one participant (**Supplementary figure 5.3A**). The 15 most abundant species were as follows in decreasing order: *Clostridioides difficile* (*M* = 0.095, *SD* = 0.222), *Lysobacter enzymogenes* (*M* = 0.094, *SD* = 0.078), *Faecalibacterium prausnitzii* (*M* = 0.086, *SD* = 0.062), *Phocaeicola dorei* (*M* = 0.064, *SD* = 0.139), *Blautia sp. SC05B48* (*M* = 0.063, *SD* = 0.046), *Anaerostipes hadrus* (*M* = 0.054, *SD* = 0.047), *Roseburia intestinalis* (*M* = 0.045, *SD* = 0.040), *Akkermansia muciniphila* (*M* = 0.043, *SD* = 0.078), *Bacteroides uniformis* (*M* = 0.037, *SD* = 0.034), *Phocaeicola vulgatus* (*M* = 0.036, *SD* = 0.058), *Agrobacterium tumefaciens* (*M* = 0.025, *SD* = 0.036), *Methanobrevibacter smithii* (*M* = 0.018, *SD* = 0.057), *Bacteroides cellulosilyticus* (*M* = 0.016, *SD* = 0.040), *Anaerobutyricum hallii* (*M* = 0.015, *SD* = 0.011) and *Campylobacter jejuni* (*M* = 0.015, *SD* = 0.016) (**Figure 5.13A**). All but one of the aforementioned taxa were present in at least two samples at a relative abundance greater than 0.01; *Methanobrevibacter smithii* was only present in the sample from the patient in pair 3 at a relative abundance greater than 0.01.

The conversion of RMP to QMP both heightened and reduced the fold-change seen within pairs of severe ME/CFS patients and matched household controls (**Figure 5.13B, Supplementary figure 5.3B**). An example of a species where the within pair differences are heightened by conversion to QMP is *B. uniformis*. The relative abundance of this species in the severe ME/CFS patient from pair 2 is 8-fold higher than their matched household control, whereas the microbial load of this species is 10-fold higher in the patient than their matched household control. Conversely, *C. difficile* was an example of a species where the within pair differences were reduced by the conversion of RMP to QMP. In pair 4 the relative abundance of *C. difficile* was 6-fold higher in the patient but the microbial load of *C. difficile* was only 5-fold higher in the patient compared to their matched household control. In addition, converting RMP to QMP highlights species which have a greater microbial load in some participants than the total microbial load in other participants. For example, the microbial load of *C. difficile* in the stool sample of the patient from pair 4 was greater than the total microbial load in the stool sample from the patient in pair 3 and the control in pair 5. In addition, the microbial load of *Phocaeicola dorei* in the stool sample of the patient from pair 5 was greater than the total microbial load in the stool sample from the patient in pair 3.

To determine whether there were any taxa at the species-level with differentially abundant RMP or QMP, paired *t*-tests with FDR correction were performed on CLR-transformed relative abundances and log10-transformed microbial loads (**Figure 5.14, Table 5.1**). All severe ME/CFS patients had higher CLR-transformed relative abundances and log10-transformed microbial loads of *Eubacterium callanderi* and *Malassezia restricta* than their matched household controls. In addition, severe ME/CFS patients had lower CLR-transformed relative abundances and log10-

transformed microbial loads of *Alistipes megaguti, Ligilactobacillus ruminis, Longibaculum sp. KGMB06250, Pluralibacter gergoviae* and *Roseburia intestinalis* than their matched household controls. All severe ME/CFS patients had lower CLR-transformed relative abundances of *Microvirgula aerodenitrificans* than their matched household controls whereas four severe ME/CFS patients had lower log10-transformed microbial loads of *Microvirgula aerodenitrificans* than their matched household controls. In addition, the CLR-transformed relative abundances of *Alistipes indistinctus, Streptococcus milleri* and *Sulfuriferula plumbiphila* were higher in patients compared to their matched household controls whereas *Citrobacter freundii, Enterococcus faecium, Pseudomonas alcaliphila, Pseudomonas azotoformans* and *Ruminococcus sp. JE7A12* were lower in patients compared to their matched household controls. Additional taxa observed to have different log10-transformed microbial abundances between patients and matched household controls were *Eggerthella sp. HF1101* and *Pseudomonas sp. BIOMIG1BAC* and *Streptococcus sp. HSISm1*. However, in all of the aforementioned differences observed between severe ME/CFS patients and controls RMP and QMP were not significantly different following FDR correction.

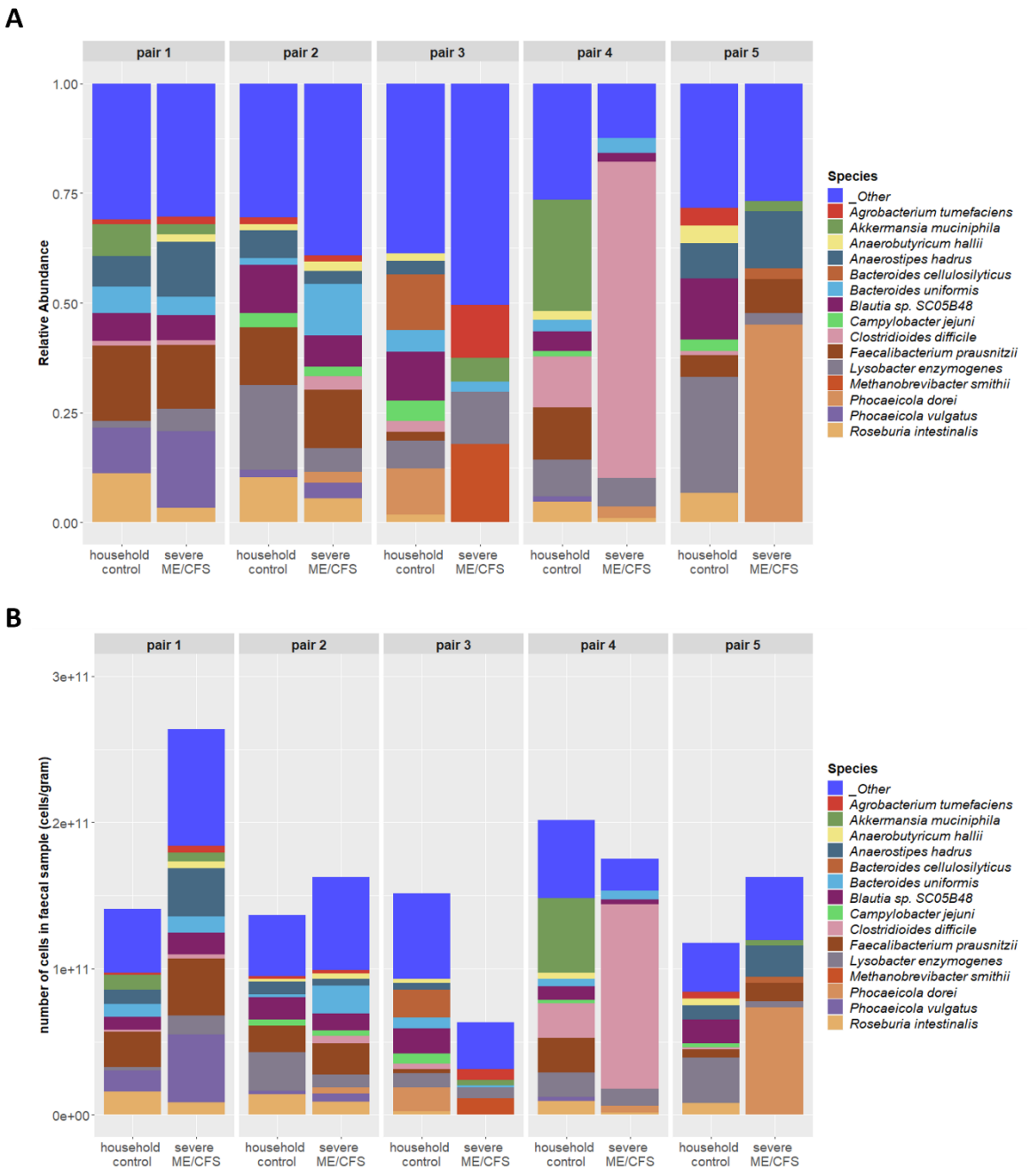

Figure 5.13: Top 15 species in stool samples from severe ME/CFS patients and their matched household controls. *A) Relative microbiome profiling and B) quantitative microbiome profiling of taxa present at a relative abundance greater than 0.01. Stool microbes from severe ME/CFS patients (n=5) and their matched household controls (n=5) were stained with SYBR™ green I nucleic acid gel stain and 'all' cells were collected using the Sony SH800S cell sorter and shotgun metagenomic sequencing was performed to identify the taxa present in each sample.*

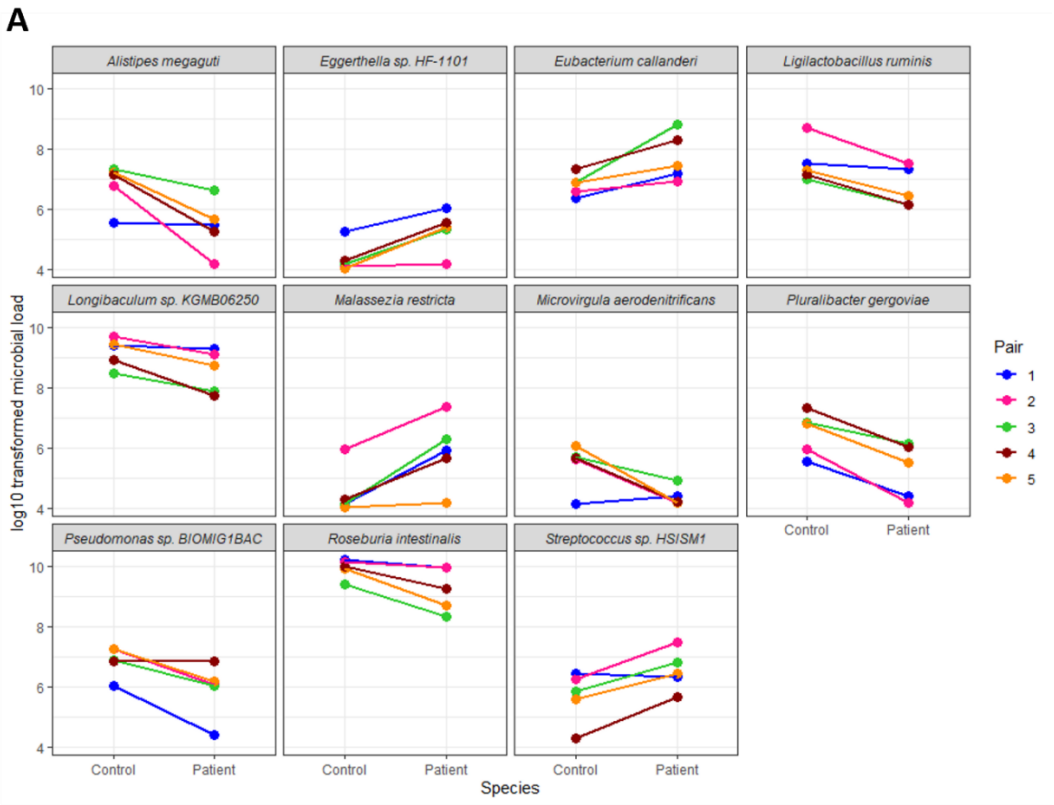
A
Alistipes megaguti
Eggerthella sp. HF-1101
Eubacterium callanderi
Ligilactobacillus ruminis
Longibaculum sp. KGMB06250
Malassezia restricta
Microvirgula aerodenitrificans
Pluralibacter gergoviae
Pseudomonas sp. BIOMIG1BAC
Roseburia intestinalis
Streptococcus sp. HSISM1
log10 transformed microbial load
Control
Patient
Species
Pair
1
2
3
4
5

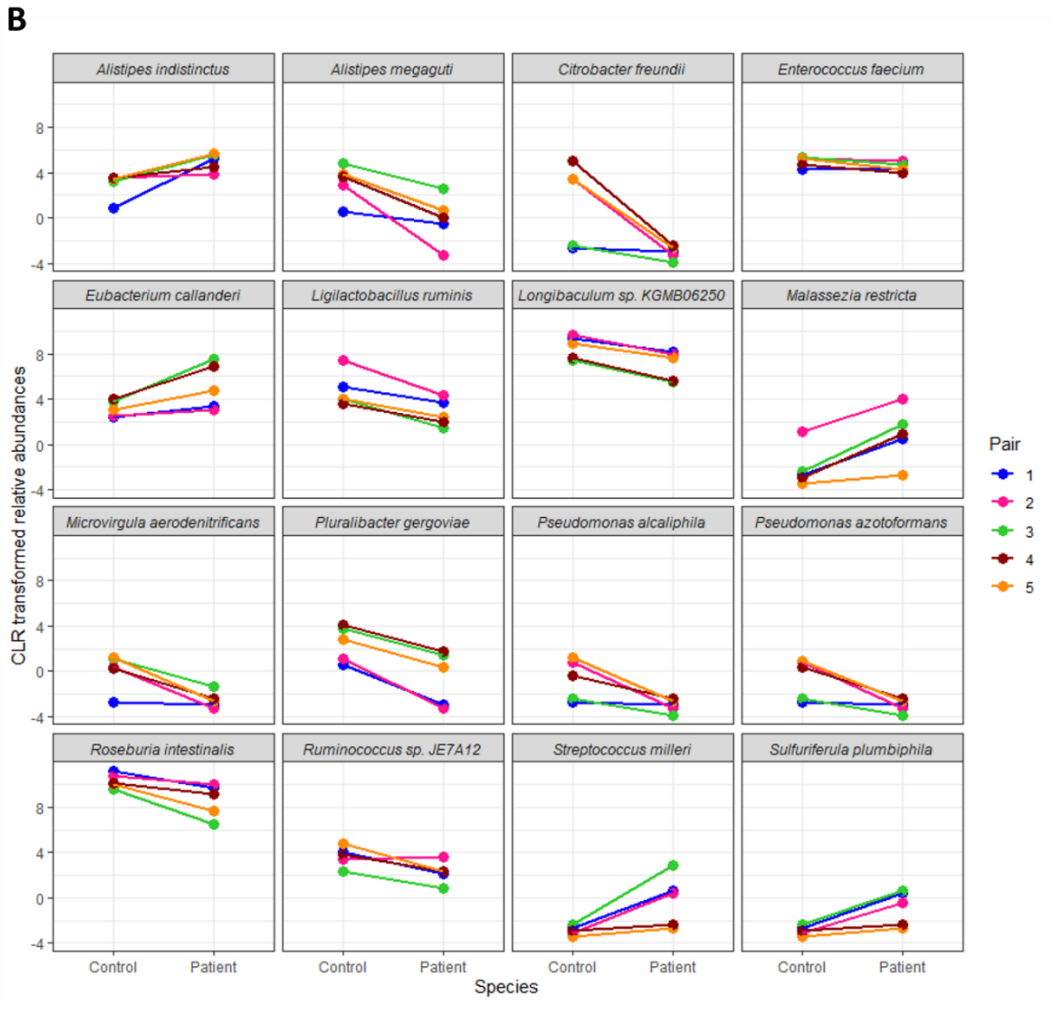
B
Alistipes indistinctus
Alistipes megaguti
Citrobacter freundii
Enterococcus faecium
Eubacterium callanderi
Ligilactobacillus ruminis
Longibaculum sp. KGMB06250
Malassezia restricta
Microvirgula aerodenitrificans
Pluralibacter gergoviae
Pseudomonas alcaliphila
Pseudomonas azotoformans
Roseburia intestinalis
Ruminococcus sp. JE7A12
Streptococcus milleri
Sulfuriferula plumbiphila
CLR transformed relative abundances
Control
Patient
Species
Pair
1
2
3
4
5

← ***Figure 5.14: Pairwise comparisons of the abundance of taxa at the species-level in severe ME/CFS patients and their matched household controls.*** *Paired* t*-tests were performed on A) CLR transformed relative abundances and B) log10-transformed microbial loads. Stool microbes from severe ME/CFS patients (n = 5) and their matched household controls (n=5) were stained with SYBR™ green I nucleic acid gel stain and 'all' cells were collected using the Sony SH800S cell sorter and shotgun metagenomic sequencing was performed to identify the taxa present in each sample. Taxa with a p-value < 0.05 (prior to FDR correction) are shown on the graph.*

Table 5.1:* P *values pre and post FDR correction from differential abundance analysis on taxa at the phylum-, class-, order-, family-, genus- and species-levels. *Paired* t*-tests were performed on the relative microbiome profile (RMP) and the quantitative microbiome profile (QMP) of stool microbes from severe ME/CFS patients (n = 5) and their matched household controls (n=5). Stool microbes were stained with SYBR™ green I nucleic acid gel stain and 'all' cells were collected using the Sony SH800S cell sorter and shotgun metagenomic sequencing was performed to identify the taxa present in each sample. Taxa with a p-value < 0.05 (prior to FDR correction) are shown.*

Taxa	**Profiling**	***p*-value prior to FDR correction**	***p*-value with FDR correction**
Phylum			
Apicomplexa	RMP	0.0390	0.2731
Ascomycota	RMP	0.0314	0.2731
Basidiomycota	RMP	0.0360	0.2731
Basidiomycota	QMP	0.0150	0.3160
Class			
Malasseziomycetes	RMP	0.0205	0.6339
Malasseziomycetes	QMP	0.0150	0.4665
Order			
Malasseziales	RMP	0.0136	0.4417
Malasseziales	QMP	0.0150	0.7171
Neisseriales	RMP	0.0182	0.4417
Nitrosomonadales	RMP	0.0232	0.4417
Family			
Chromobacteriaceae	RMP	0.0187	0.8816
Chromobacteriaceae	QMP	0.0477	0.8952
Corynebacteriaceae	QMP	0.0337	0.8952
Erythrobacteraceae	QMP	0.0452	0.8952
Malasseziaceae	RMP	0.0148	0.8816
Malasseziaceae	QMP	0.0152	0.8952
Sulfuricellaceae	RMP	0.0306	0.8816
Genus			
Citrobacter	RMP	0.0138	0.7691
Citrobacter	QMP	0.0252	0.8561
Ligilactobacillus	RMP	0.0100	0.6987
Ligilactobacillus	QMP	0.0207	0.8561

Table 5.1 continued

Taxa	Profiling	*p*-value prior to FDR correction	*p*-value with FDR correction
Genus			
Longibaculum	RMP	0.0004	0.1157
Longibaculum	QMP	0.0193	0.8561
Malassezia	RMP	0.0095	0.6987
Malassezia	QMP	0.0153	0.8561
Microvirgula	RMP	0.0171	0.7971
Microvirgula	QMP	0.0495	0.8561
Pluralibacter	RMP	0.0021	0.2952
Pluralibacter	QMP	0.0018	0.5064
Roseburia	RMP	0.0264	0.8615
Roseburia	QMP	0.0456	0.8561
Sulfuriferula	RMP	0.0217	0.8615
Species			
Alistipes indistinctus	RMP	0.0411	0.7364
Alistipes megaguti	RMP	0.0177	0.7364
Alistipes megaguti	QMP	0.0354	0.7831
Citrobacter freundii	RMP	0.0388	0.7364
Eggerthella sp. HF 1101	QMP	0.0168	0.7831
Enterococcus faecium	RMP	0.0396	0.7364
Eubacterium callanderi	RMP	0.0302	0.7364
Eubacterium callanderi	QMP	0.0278	0.7831
Ligilactobacillus ruminis	RMP	0.0035	0.7364
Ligilactobacillus ruminis	QMP	0.0088	0.7831
Longibaculum sp KGMB06250	RMP	0.0009	0.6004
Longibaculum sp KGMB06250	QMP	0.0188	0.7831
Malassezia restricta	RMP	0.0075	0.7364
Malassezia restricta	QMP	0.0150	0.7831
Microvirgula aerodenitrificans	RMP	0.0153	0.7364
Microvirgula aerodenitrificans	QMP	0.0489	0.7831
Pluralibacter gergoviae	RMP	0.0017	0.6004
Pluralibacter gergoviae	QMP	0.0017	0.7831
Pseudomonas alcaliphila	RMP	0.0303	0.7364

Table 5.1 continues

Taxa	Profiling	*p*-value prior to FDR correction	*p*-value with FDR correction
Species			
Pseudomonas azotoformans	RMP	0.0233	0.7364
Pseudomonas sp. BIOMIG1BAC	QMP	0.0243	0.7831
Roseburia intestinalis	RMP	0.0162	0.7364
Roseburia intestinalis	QMP	0.0275	0.7831
Ruminococcus sp JE7A12	RMP	0.0338	0.7364
Streptococcus milleri	RMP	0.0411	0.7364
Streptococcus sp. HSISM1	QMP	0.0284	0.7831
Sulfuriferula plumbiphila	RMP	0.0234	0.7364

5.3.1.1.8 Summary

The analysis of the RMP and QMP of 'sybr green high' stool microbes found non-significant alterations in the abundance of taxa at phylum-, class-, order-, family-, genus- and species-levels in severe ME/CFS patients compared to their matched household controls. In addition, the conversion of relative abundances to microbial load increased the heterogeneity of samples at each taxonomic level. Interestingly, the taxonomic composition of microbes from the severe ME/CFS patient in pair 3 was markedly different from all other patient and control stool samples. This was partly due to this stool sample having different taxa detected and also different taxa dominating the sample. In addition, the QMP of the stool sample from the patient in pair 3 did not compare to other stool samples, due to this sample having the smallest microbial load.

5.3.1.2 Alpha diversity

The inter-sample diversity of the gut microbiome from severe ME/CFS patients and their matched household controls was measured on 'sybr green high' microbes at the species-level using the following alpha diversity measures: Shannon index, inverse Simpson index and observed richness.

The average Shannon index score was lower in severe ME/CFS patients (M = 2.809, SD = 0.865) compared to household controls (M = 3.060, SD = 0.053) but the severe ME/CFS patients had a larger variation in scores. When comparing patients to their matched household controls Shannon index scores in the severe ME/CFS patients from pairs 1, 2 and 3 were higher than their matched household controls and the patients from pairs 4 and 5 were lower than their matched household controls (**Figure 5.15A**).

The average inverse Simpson index in severe ME/CFS patients (*M* = 10.259, *SD* = 7.086) was lower than household controls (*M* = 11.305, *SD* = 2.045), but patients had a large variation in scores. When making paired comparisons the inverse Simpson indices, like the Shannon indices, were higher in the patient from pair 2 and lower in patients from pairs 4 and 5 compared to their matched household controls (**Figure 5.15B**). Pairs 1 and 3 had slightly larger Shannon indices in patients compared to controls, but the inverse Simpson indices were slightly smaller in patients compared to their matched household controls.

Observed richness, measured following rarefaction to the lowest read count, was used to give an indication of the number of species present in each sample. The average observed richness score was higher in severe ME/CFS patients (*M* = 366.849, *SD* = 62.076) compared to household controls (*M* = 331.998, *SD* = 46.803). When comparing observed richness in severe ME/CFS patients to their matched household controls, patients from pairs 1, 2 and 3 had higher and patients from pairs 4 and 5 had lower scores compared to their matched household controls (**Figure 5.15C**).

5.3.1.3 Beta diversity

Beta diversity was measured using Bray-Curtis dissimilarity and distances between samples were visualised using a NMDS plot (**Figure 5.16**). For both RMP and QMP patients from pairs 3, 4 and 5 were most dissimilar from all other samples. Whereas patients from pairs 1 and 2 were clustered together with their matched household controls.

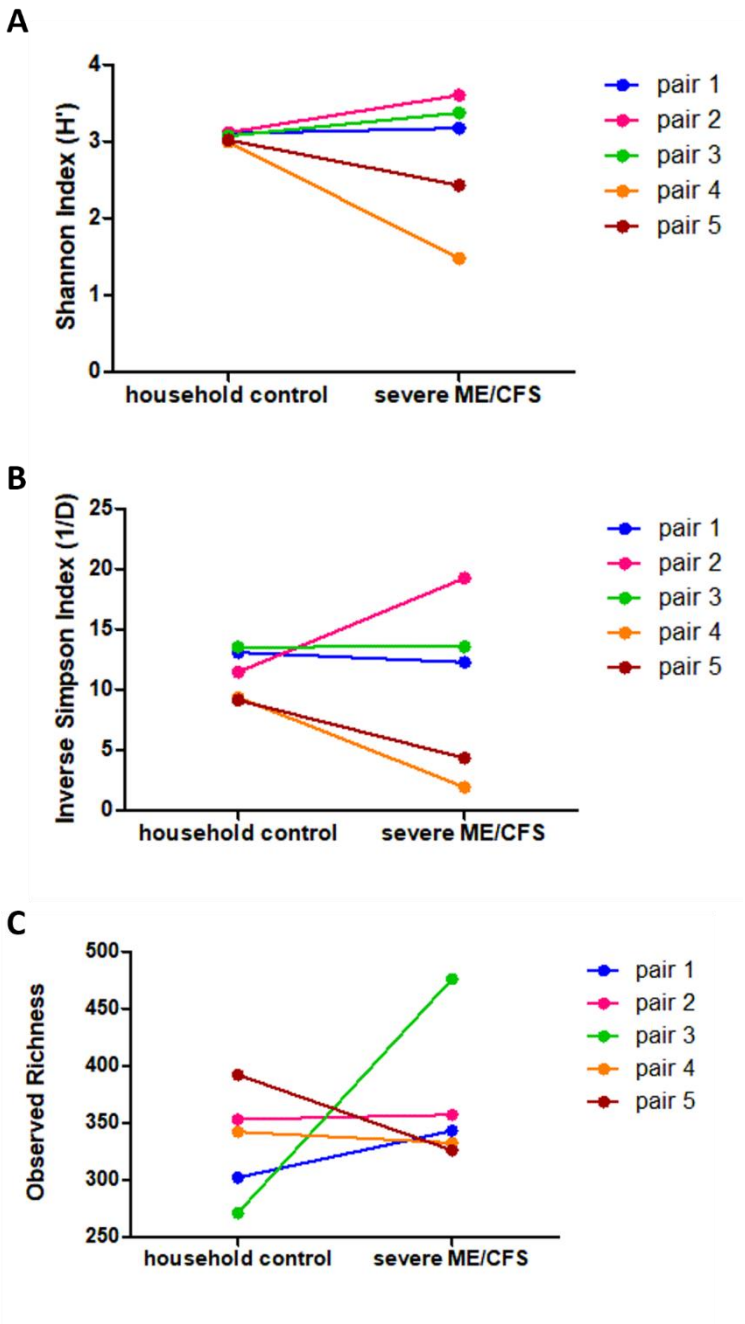

Figure 5.15: Alpha diversity measures in stool samples from severe ME/CFS patients and their matched household controls. *A) Shannon index, B) inverse Simpson index and C) observed richness of 'all' cells from stool microbes from severe ME/CFS patients (n=5) and their matched household controls (n=5).*

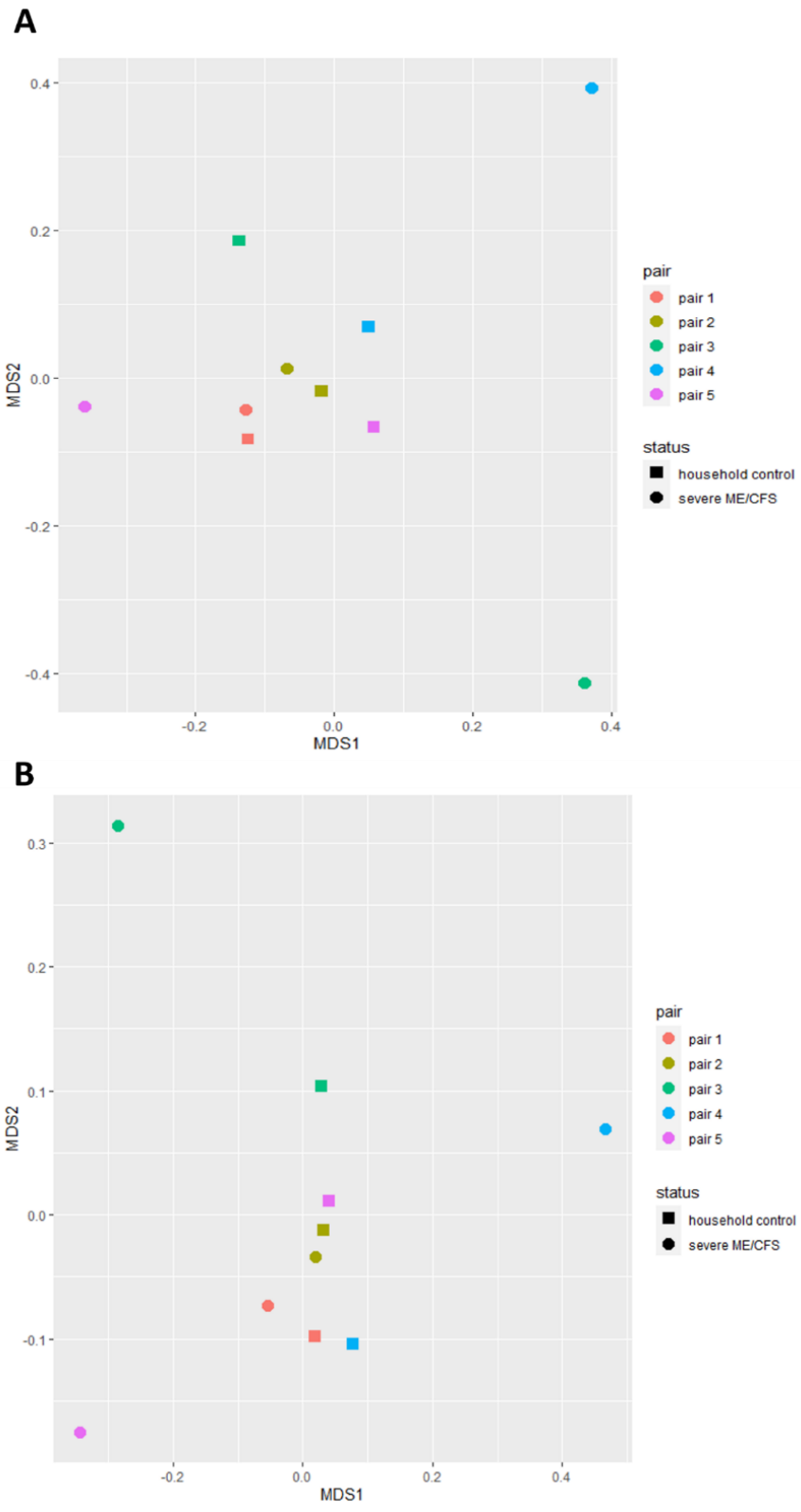

Figure 5.16: Beta diversity in stool samples from severe ME/CFS patients and their matched household controls. *Beta diversity was calculated using Bray-Curtis dissimilarity on A) species relative abundances and B) species microbial load of 'all' stool microbes from severe ME/CFS patients (n = 5) and matched household controls (n = 5). Scores were plotted on an NMDS plot.*

5.3.2 Taxonomic analysis of 'IgG positive' and 'IgG negative' stool microbes

The average number of 'IgG positive' microbes collected on the Sony SH800S cell sorter from a pool of 'all' cells from five pairs of severe ME/CFS patients and matched household controls stool samples was 1,046,734 cells (*SD* = 417575.8). The average number of 'IgG negative' microbes collected were 1,300,144 cells (*SD* = 330938.4). Taxa were removed if they were not observed in the 'all' fraction from the respective participant. Taxa present at a relative abundance less than 1 x 10^{-6} were excluded from downstream analysis.

5.3.2.1 Taxonomic composition

The taxonomic composition of 'IgG positive' and 'IgG negative' stool microbes were examined using the relative abundance of taxa in each taxonomic level. Taxonomic composition was compared between severe ME/CFS patient 'IgG positive' fraction, severe ME/CFS patient 'IgG negative' fraction, household control 'IgG positive' fraction and household control 'IgG negative' fraction using bubble plots at each taxonomic level. For taxonomic levels with more than 20 taxa present, only the top 20 most abundant taxa across all samples were shown.

5.3.2.1.1 Domain

At the domain-level only bacteria and viruses were detected in every participant's positive and negative fraction (**Figure 5.17**). The relative abundance of bacteria in every participant was comparable in the 'IgG positive' fraction and 'IgG negative' fraction, except for the severe ME/CFS patient from pair 3. This participant had a higher relative abundance of bacteria in the 'IgG negative' fraction than the 'IgG positive' fraction. Similarly, the relative abundance of viruses in every participant was comparable in the 'IgG positive' fraction and 'IgG negative' fraction, except for the severe ME/CFS patient from pair 3. This participant had a higher relative abundance of viruses in the 'IgG positive' fraction than the 'IgG negative' fraction. Archaea was detected in both the 'IgG positive' and 'IgG negative' fractions of three household controls and three patients. Archaea was not detected in the 'IgG positive' or 'IgG negative' fractions of two severe ME/CFS patients, was only detected in the 'IgG negative' fraction from the household control in pair one and was only detected in the 'IgG positive' fraction from the household control in pair five.

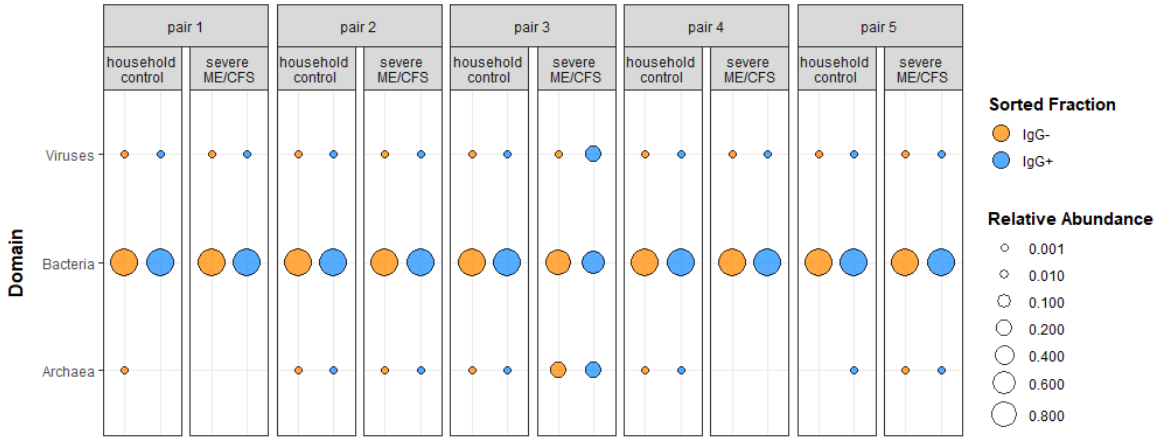

Figure 5.17: Composition of 'IgG positive' fractions and 'IgG negative' fractions in stool samples from severe ME/CFS patients and their matched household controls at the domain-level. *Stool microbes from severe ME/CFS patients (n=5) and their matched household controls (n=5) were incubated with serum IgG in vitro. 'IgG positive' fractions and 'IgG negative' fractions were subsequently collected using the Sony SH800S cell sorter and shotgun metagenomic sequencing was performed to identify the relative abundance of taxa present in the sorted fractions from each participant.*

5.3.2.1.2 Phylum

At the phylum-level 5 taxa were detected in the 'IgG positive' fraction and 'IgG negative' fraction of every participant: Firmicutes, Bacteroidetes, Proteobacteria, Verrucomicrobia, Actinobacteria and Uroviricota (**Figure 5.18**). When looking at the taxa that were only detected in the 'IgG positive' fraction or only detected in the 'IgG negative' fraction there were no patterns emerging in participant pairs or participant cohorts. The differences found instead were on an individual level; the patient from pair 1 had Basidiomycota only detected in the 'IgG negative' fraction, the household control from pair 1 had Euryarchaeota only detected in the 'IgG negative' fraction, the patient from pair 2 had Basidiomycota only detected in the 'IgG negative' fraction and Ascomycota only detected in the 'IgG positive' fraction, the household control from pair 2 had Crenarchaeota only detected in the 'IgG positive' fraction and Spirochaetes and Ascomycota only detected in the 'IgG negative' fraction, the patient from pair 3 had Cyanobacteria only detected in the 'IgG negative' fraction, the patient from pair 4 had Spirochaetes, Basidiomycota and Apicomplexa only detected in the 'IgG negative' fraction, the control from pair 4 had Ascomycota only detected in the 'IgG positive' fraction and Candidatus Saccharibacteria only detected in the 'IgG negative' fraction, the patient from pair 5 had Cressdnaviricota and Elusimicrobia only detected in the 'IgG positive' fraction, the control from pair 5 had Fusobacteria only detected in the 'IgG negative' fraction and Euryarchaeota only detected in the 'IgG positive' fraction. Another interesting finding was that the relative abundance of Uroviricota was 4000-fold higher in the 'IgG positive' fraction than the 'IgG negative' fraction in the severe ME/CFS patient from pair 3.

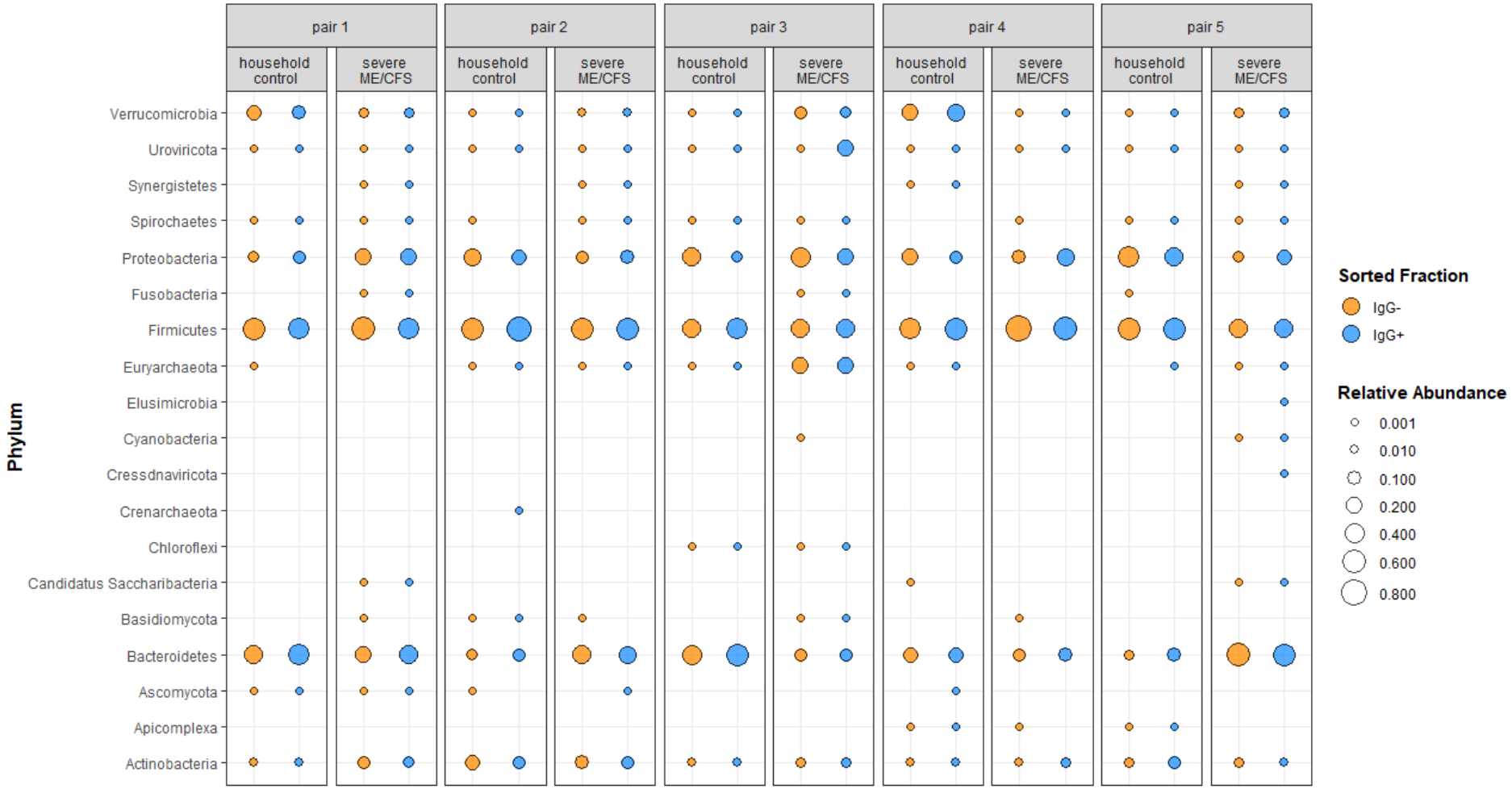
pair 1
pair 2
pair 3
pair 4
pair 5
household control
severe ME/CFS
Phylum
Verrucomicrobia
Uroviricota
Synergistetes
Spirochaetes
Proteobacteria
Fusobacteria
Firmicutes
Euryarchaeota
Elusimicrobia
Cyanobacteria
Cressdnaviricota
Crenarchaeota
Chloroflexi
Candidatus Saccharibacteria
Basidiomycota
Bacteroidetes
Ascomycota
Apicomplexa
Actinobacteria
Sorted Fraction
IgG-
IgG+
Relative Abundance
0.001
0.010
0.100
0.200
0.400
0.600
0.800

← Figure 5.18: Composition of 'IgG positive' fractions and 'IgG negative' fractions in stool samples from severe ME/CFS patients and their matched household controls at the phylum-level. *Stool microbes from severe ME/CFS patients (n=5) and their matched household controls (n=5) were incubated with serum IgG in vitro. 'IgG positive' fractions and 'IgG negative' fractions were subsequently collected using the Sony SH800S cell sorter and shotgun metagenomic sequencing was performed to identify the relative abundance of taxa present in the sorted fractions from each participant*

5.3.2.1.3 Class

At the class-level 13 taxa were detected in the 'IgG positive' fraction and 'IgG negative' fraction of every participant. Like the phylum-level, differences at the class-level were found between individuals (**Figure 5.19**). The severe ME/CFS patient from pair 1 had Malasseziomycetes only detected in the 'IgG negative' fraction, the household control from pair 1 had Methanobacteria only detected in the 'IgG negative' fraction, the patient from pair 2 had Saccharomycetes only detected in the 'IgG positive' fraction and Malasseziomycetes only detected in the 'IgG negative' fraction, the control from pair 2 had Thermoprotei only detected in the 'IgG positive' fraction and Spirochaetia, Saccharomycetes and Flavobacteriia only detected in the 'IgG negative' fraction. The patient from pair 3 had Sphingobacteria and Deltaproteobacteria only present in the 'IgG negative' fraction, the patient from pair 4 had Sphingobacteria, Malasseziomycetes and Spirochaetia only detected in the 'IgG negative' fraction, the control from pair 4 had Candidatus Saccharimonia, Flavobacteriia and Deltaproteobacteria detected only in the 'IgG negative' fraction and Sacchromycetes only detected in the 'IgG positive' fraction, the patient from pair 5 had Elusimicrobia and Arfiviricetes detected only in the 'IgG positive' fraction and the control from pair 5 had Fusobacteriia detected only in the 'IgG negative' fraction and Methanobacteria detected only in the 'IgG positive' fraction. When comparing relative abundances of taxa in 'IgG positive' and 'IgG negative' fractions Caudoviricetes was found to be 4000-fold higher in the 'IgG positive' fraction than the 'IgG negative' fraction in the severe ME/CFS patient from pair 3.

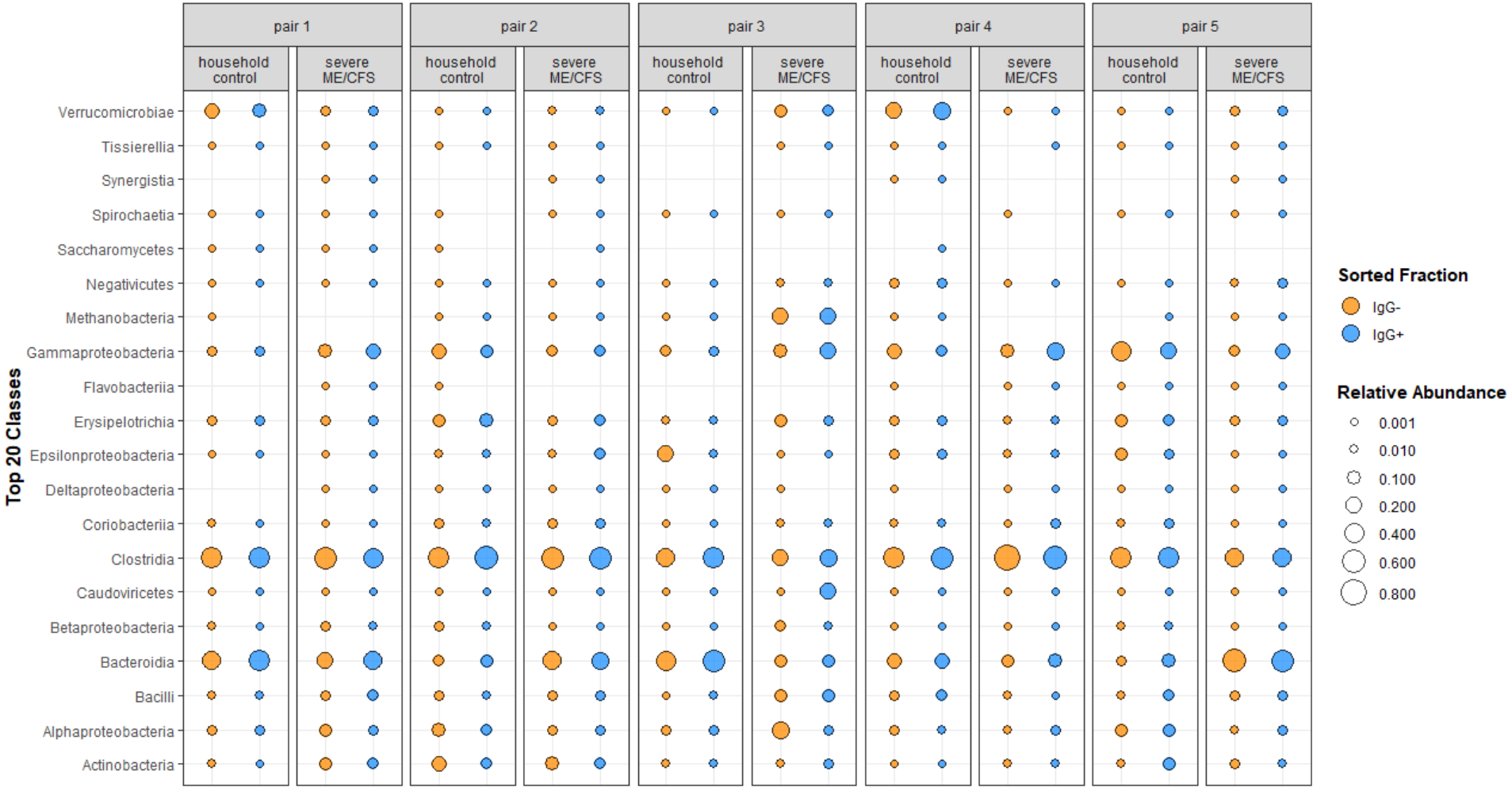
pair 1
pair 2
pair 3
pair 4
pair 5
household control
severe ME/CFS
Top 20 Classes
Verrucomicrobiae
Tissierellia
Synergistia
Spirochaetia
Saccharomycetes
Negativicutes
Methanobacteria
Gammaproteobacteria
Flavobacteriia
Erysipelotrichia
Epsilonproteobacteria
Deltaproteobacteria
Coriobacteriia
Clostridia
Caudoviricetes
Betaproteobacteria
Bacteroidia
Bacilli
Alphaproteobacteria
Actinobacteria
Sorted Fraction
IgG-
IgG+
Relative Abundance
0.001
0.010
0.100
0.200
0.400
0.600
0.800

← ***Figure 5.19: Top 20 classes in 'IgG positive' fractions and 'IgG negative' fractions in stool samples from severe ME/CFS patients and their matched household controls.*** *Stool microbes from severe ME/CFS patients (n=5) and their matched household controls (n=5) were incubated with serum IgG in vitro. 'IgG positive' fractions and 'IgG negative' fractions were subsequently collected using the Sony SH800S cell sorter and shotgun metagenomic sequencing was performed to identify the relative abundance of taxa present in the sorted fractions from each participant.*

5.3.2.1.4 Order

At the order-level 21 taxa were detected in the 'IgG positive' and 'IgG negative' fraction of every participant (**Figure 5.20**). The number of taxa detected in the 'IgG positive' fraction but not in the 'IgG negative' fraction varied between individuals; in pair 1 the severe ME/CFS patient had 0 and the matched household control had 1 taxa that was only detected in the 'IgG positive' fraction, in pair 2 the patient had 2 and the control had 2 taxa that were only detected in the 'IgG positive' fraction, in pair 3 both the patient and control had no taxa that were only detected in the 'IgG positive' fraction, in pair 4 the patient had 3 and the control had 1 taxa that were only detected in the 'IgG positive' fraction and in pair 5 the patient had 2 and the control had 2 taxa that were only detected in the 'IgG positive' fraction. Interestingly, the relative abundance of Propionibacteriales was more than 10-fold higher in the 'IgG positive' fraction than the 'IgG negative' fraction in 2 patients and 3 household controls. Caudovirales was 4000-fold higher in the 'IgG positive' fraction than the 'IgG negative' fraction in the severe ME/CFS patient in pair 3. The number of taxa detected in the 'IgG negative' fraction but not in the 'IgG positive' fraction also varied between individuals; in pair 1 the patient had 1 and the control had 2 taxa that were only detected in the 'IgG negative' fraction, in pair 2 the patient had 1 and the control had 3 taxa that were only detected in the 'IgG negative' fraction, in pair 3 the patient had 7 and the control had 3 taxa that were only detected in the 'IgG negative' fraction, in pair 4 the patient had 4 and the control had 4 taxa that were only detected in the 'IgG negative' fraction and in pair 5 the patient had 1 and the control had 1 taxa that were only detected in the 'IgG negative' fraction. When comparing the taxa only detected in the 'IgG negative' fraction there were some similarities in severe ME/CFS patients; two patients only had Springobacteriales in the 'IgG negative' fraction and three patients only had Malasseziales in the 'IgG negative' fraction. When making comparisons within pairs, the only taxa that had similarities within a pair was Rhodocyclales which was only detected in the 'IgG negative' fraction in the patient and matched household control from pair 3.

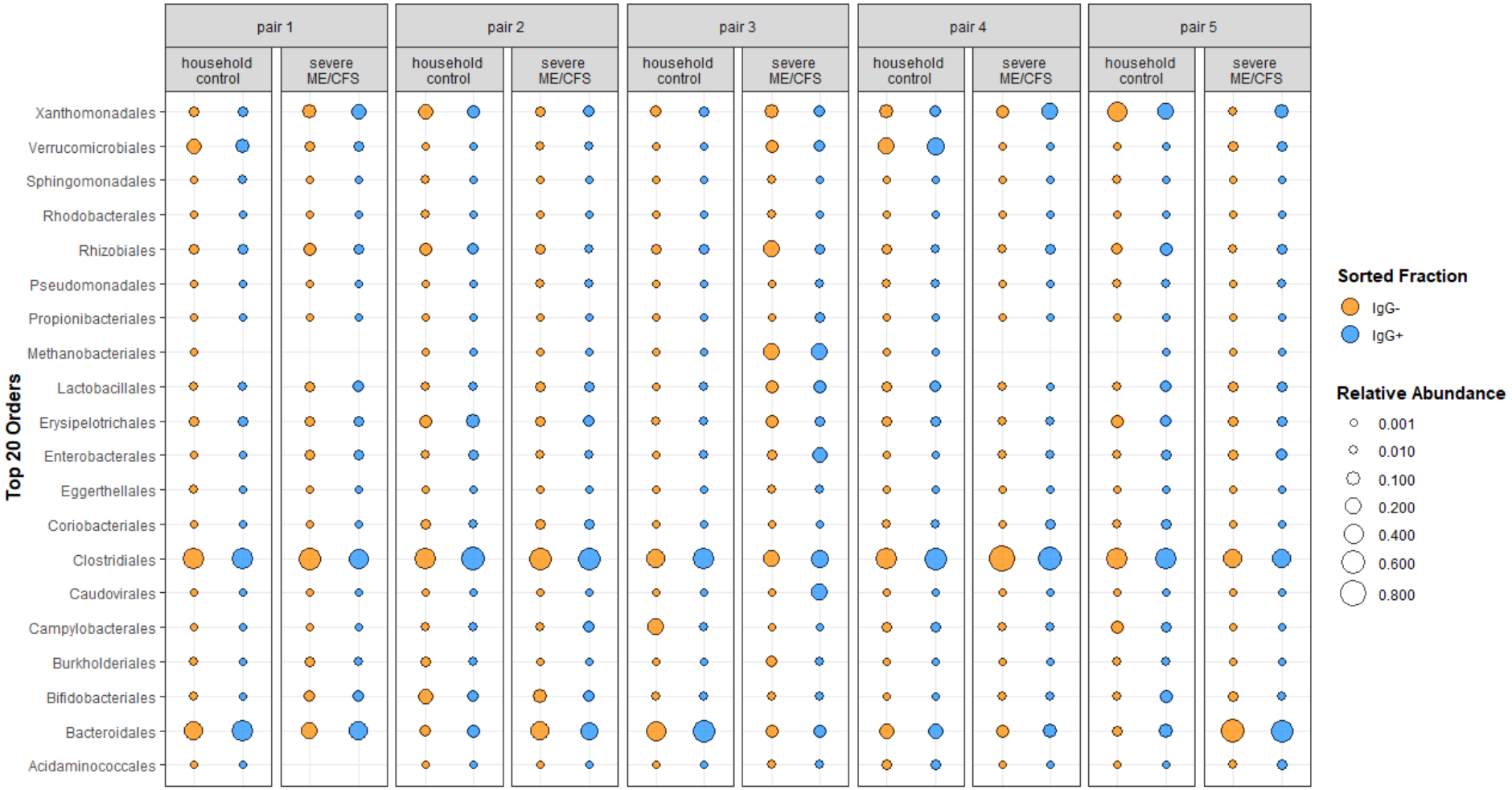
pair 1
pair 2
pair 3
pair 4
pair 5
household control
severe ME/CFS
Top 20 Orders
Xanthomonadales
Verrucomicrobiales
Sphingomonadales
Rhodobacterales
Rhizobiales
Pseudomonadales
Propionibacteriales
Methanobacteriales
Lactobacillales
Erysipelotrichales
Enterobacterales
Eggerthellales
Coriobacteriales
Clostridiales
Caudovirales
Campylobacterales
Burkholderiales
Bifidobacteriales
Bacteroidales
Acidaminococcales
Sorted Fraction
IgG-
IgG+
Relative Abundance
0.001
0.010
0.100
0.200
0.400
0.600
0.800

← ***Figure 5.20: Top 20 orders in 'IgG positive' fractions and 'IgG negative' fractions in stool samples from severe ME/CFS patients and their matched household controls.*** *Stool microbes from severe ME/CFS patients (n=5) and their matched household controls (n=5) were incubated with serum IgG in vitro. 'IgG positive' fractions and 'IgG negative' fractions were subsequently collected using the Sony SH800S cell sorter and shotgun metagenomic sequencing was performed to identify the relative abundance of taxa present in the sorted fractions from each participant.*

5.3.2.1.5 Family

At the family-level 41 taxa were detected in both the 'IgG positive' fraction and the 'IgG negative' fraction of every participant (**Figure 5.21**). The number of taxa detected in the 'IgG positive' fraction but not in the 'IgG negative' fraction also varied between individuals at the family-level; in pair 1 the patient had 1 and the control had 5 taxa that were only detected in the 'IgG positive' fraction, in pair 2 the patient had 3 and the control had 2 taxa that were only detected in the 'IgG positive' fraction, in pair 3 the patient had 2 and the control had 1 taxa that were only detected in the 'IgG positive' fraction, in pair 4 the patient had 9 and the control had 1 taxa that were only detected in the 'IgG positive' fraction and in pair 5 the patient had 3 and the control had 3 taxa that were only detected in the 'IgG positive' fraction. The number of taxa detected in the 'IgG negative' fraction but not in the 'IgG positive' fraction also varied between individuals; in pair 1 the patient had 3 and the control had 2 taxa that were only detected in the 'IgG negative' fraction, in pair 2 the patient had 2 and the control had 5 taxa that were only detected in the 'IgG negative' fraction, in pair 3 the patient had 16 and the control had 3 taxa that were only detected in the 'IgG negative' fraction, in pair 4 the patient had 6 and the control had 10 taxa that were only detected in the 'IgG negative' fraction and in pair 5 the patient had 1 and the control had 4 taxa that were only detected in the 'IgG negative' fraction. When trying to establish patterns among groups there were no taxa associated with either severe ME/CFS patients or controls. However, 3 ME/CFS patients only had Hyphomicrobiaceae detected in the 'IgG negative' fraction, 3 patients had Malasseziaceae only detected in the 'IgG negative' fraction, 2 patients had Sphingobacteriaceae only detected in the 'IgG negative' fraction and 2 patients had Porphyromonadaceae only detected in the 'IgG positive' fraction. Interestingly, Moraxellaceae was detected in the 'IgG negative', but not 'IgG positive' fraction in 4 household controls, was not detected in the microbiome from 2 patients and the relative abundance of Moraxellaceae was 10-fold higher in the 'IgG positive' fraction than the 'IgG negative' fraction in the severe ME/CFS patient from pair 3. In addition, the patient from pair 3 also had more than 100-fold higher relative abundance of Propionibacteriaceae in the 'IgG positive' fraction compared to the 'IgG negative' fraction and more than 100-fold higher relative abundance of Xanthobacteriaceae in the 'IgG negative' fraction than the 'IgG positive' fraction.

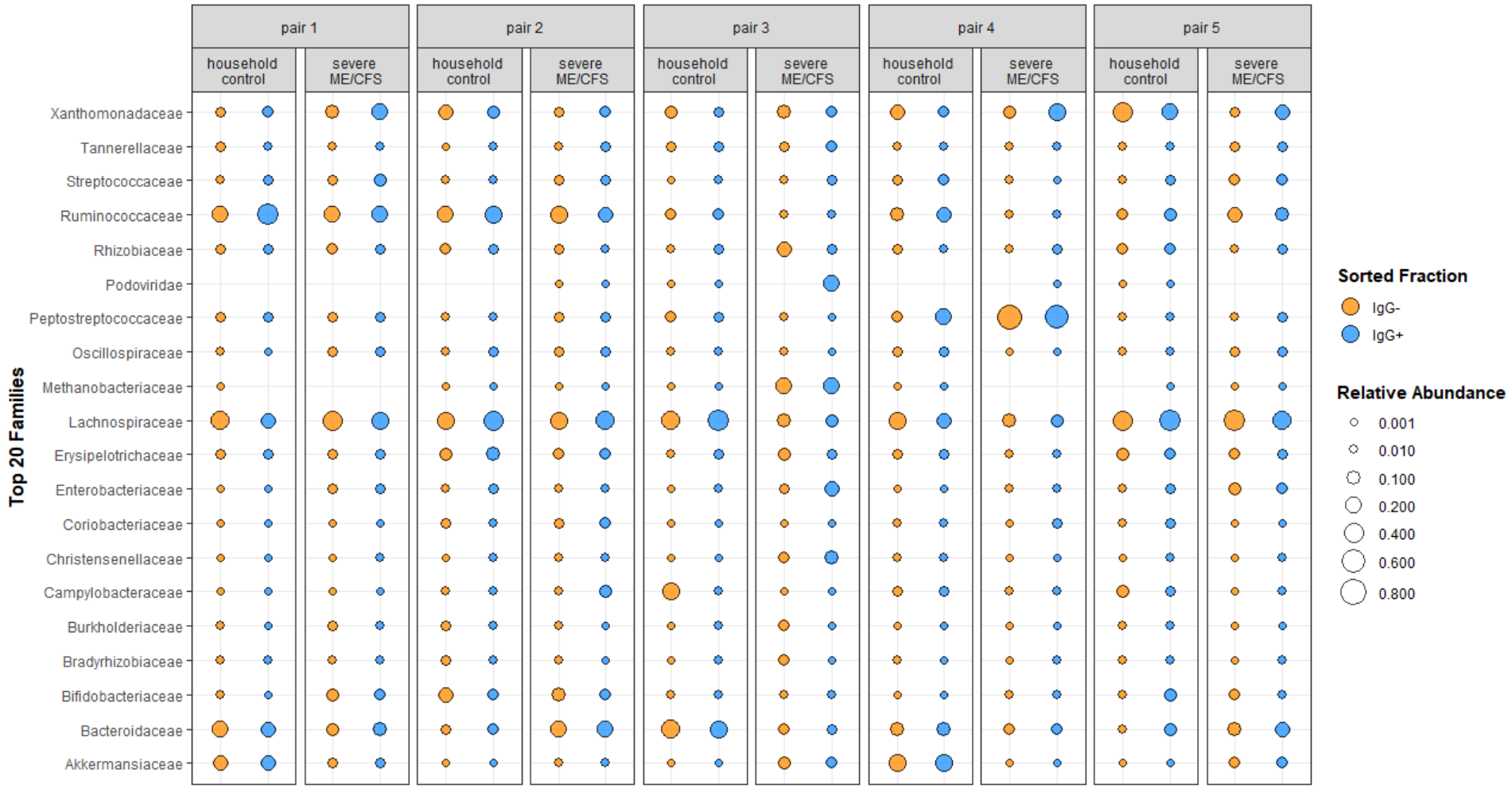
pair 1
pair 2
pair 3
pair 4
pair 5
household control
severe ME/CFS
Top 20 Families
Xanthomonadaceae
Tannerellaceae
Streptococcaceae
Ruminococcaceae
Rhizobiaceae
Podoviridae
Peptostreptococcaceae
Oscillospiraceae
Methanobacteriaceae
Lachnospiraceae
Erysipelotrichaceae
Enterobacteriaceae
Coriobacteriaceae
Christensenellaceae
Campylobacteraceae
Burkholderiaceae
Bradyrhizobiaceae
Bifidobacteriaceae
Bacteroidaceae
Akkermansiaceae
Sorted Fraction
IgG-
IgG+
Relative Abundance
0.001
0.010
0.100
0.200
0.400
0.600
0.800

← ***Figure 5.21: Top 20 families in 'IgG positive' fractions and 'IgG negative' fractions in stool samples from severe ME/CFS patients and their matched household controls.*** *Stool microbes from severe ME/CFS patients (n=5) and their matched household controls (n=5) were incubated with serum IgG in vitro. 'IgG positive' fractions and 'IgG negative' fractions were subsequently collected using the Sony SH800S cell sorter and shotgun metagenomic sequencing was performed to identify the relative abundance of taxa present in the sorted fractions from each participant.*

5.3.2.1.6 Genus

At the genus-level 72 taxa were detected in both the 'IgG positive' fraction and 'IgG negative' fraction of every participant (**Figure 5.22**). At this level the number of taxa detected in the 'IgG positive' fraction but not in the 'IgG negative' fraction also varied between individuals with no clear patterns; in pair 1 the patient had 3 and the control had 6 taxa, in pair 2 the patient had 9 and the control had 7 taxa, in pair 3 the patient had 2 and the control had 3 taxa, in pair 4 the patient had 23 and the control had 2 taxa and in pair 5 the patient had 14 and the control had 17 taxa. Again, the number of taxa detected in the 'IgG negative' fraction but not in the 'IgG positive' fraction also varied between individuals; in pair 1 the patient had 5 and the control had 10 taxa, in pair 2 the patient had 8 and the control had 9 taxa, in pair 3 the patient had 56 and the control had 4 taxa, in pair 4 the patient had 9 and the control had 30 taxa and in pair 5 the patient had 6 and the control had 6 taxa. In addition to having 56 taxa detected in the 'IgG negative' fraction but not in the 'IgG positive' fraction, the patient from pair 3 also had 5 taxa with relative abundances in the 'IgG negative' fraction that were more than 80-fold higher than in the 'IgG positive' fraction. Interestingly, the relative abundance of *Starkeya* was more than 1000-fold higher in the 'IgG negative' fraction than the 'IgG positive' fraction. *Azospira* was detected in all participants' stool samples, but pair 3 were the only pair with *Azospira* not detected in the 'IgG positive' fraction. *Malassezia* was detected in the 'IgG negative' but not the 'IgG positive' fraction of 3 patients. Another interesting observation was that in 3 patients *Devosia* was detected in the 'IgG negative' but not the 'IgG positive' fraction, and *Devosia* was only detected in one other participant, a household control who had *Devosia* present in both the 'IgG positive' and the 'IgG negative' fraction. Finally, *Methylobacterium* was only detected in the stool samples of pair 3. Interestingly the patient only had *Methylobacterium* detected in the 'IgG negative' fraction whereas the control only had *Methylobacterium* detected in the 'IgG positive' fraction.

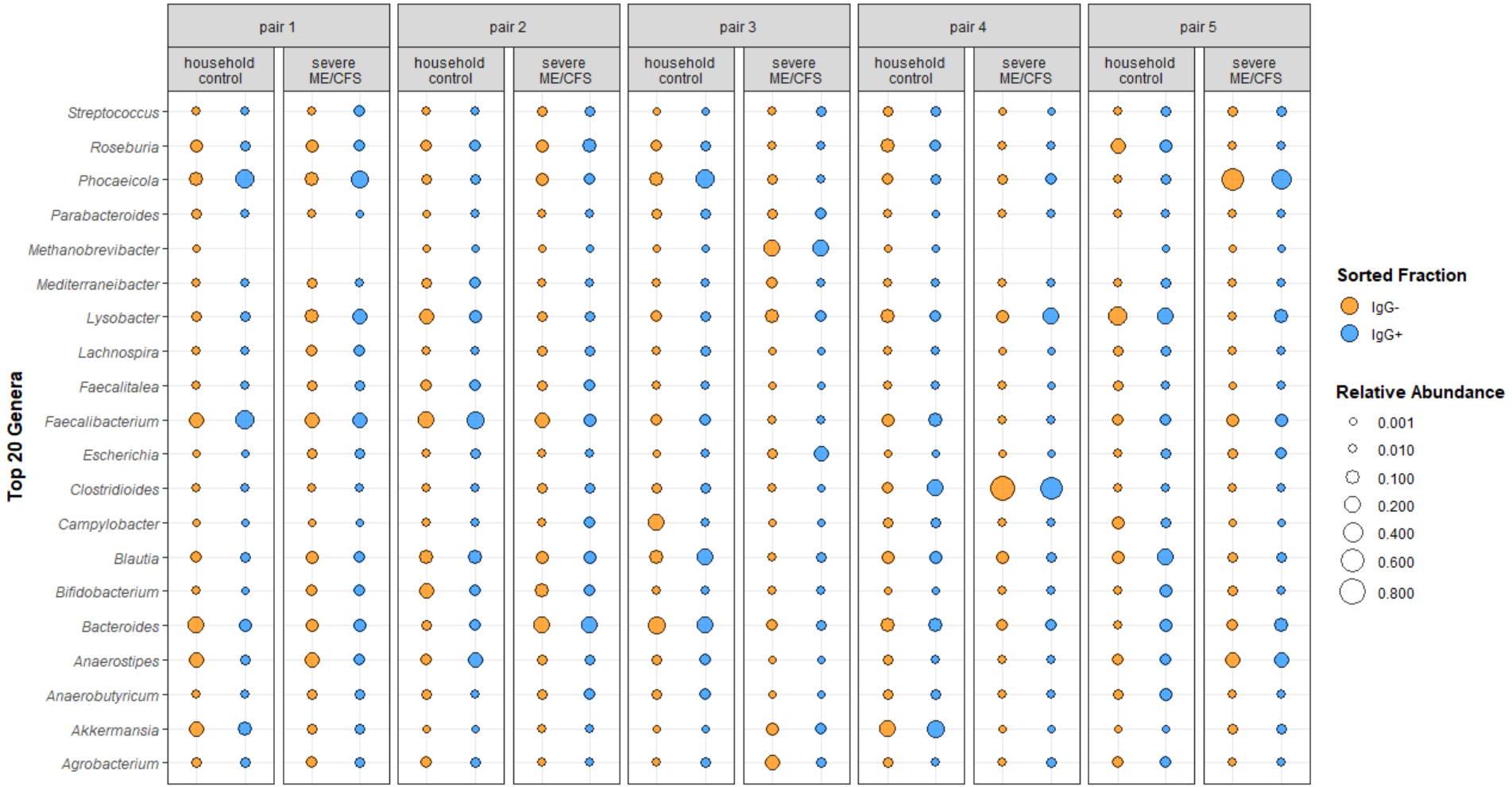
pair 1
pair 2
pair 3
pair 4
pair 5
household control
severe ME/CFS
Top 20 Genera
Streptococcus
Roseburia
Phocaeicola
Parabacteroides
Methanobrevibacter
Mediterraneibacter
Lysobacter
Lachnospira
Faecalitalea
Faecalibacterium
Escherichia
Clostridioides
Campylobacter
Blautia
Bifidobacterium
Bacteroides
Anaerostipes
Anaerobutyricum
Akkermansia
Agrobacterium
Sorted Fraction
IgG-
IgG+
Relative Abundance
0.001
0.010
0.100
0.200
0.400
0.600
0.800

← ***Figure 5.22: Top 20 genera in 'IgG positive' fractions and 'IgG negative' fractions in stool samples from severe ME/CFS patients and their matched household controls.*** *Stool microbes from severe ME/CFS patients (n=5) and their matched household controls (n=5) were incubated with serum IgG in vitro. 'IgG positive' fractions and 'IgG negative' fractions were subsequently collected using the Sony SH800S cell sorter and shotgun metagenomic sequencing was performed to identify the relative abundance of taxa present in the sorted fractions from each participant*

5.3.2.1.7 Species

At the species-level 122 taxa were detected in both the 'IgG positive' fraction and the 'IgG negative' fraction of every participant (**Figure 5.23**). At this level the number of taxa detected in the 'IgG positive' fraction but not in the 'IgG negative' fraction also varied between individuals with no clear patterns; in pair 1 the patient had 15 and the control had 11 taxa, in pair 2 the patient had 18 and the control had 15 taxa, in pair 3 the patient had 6 and the control had 9 taxa, in pair 4 the patient had 47 and the control had 3 taxa, in pair 5 the patient had 31 and the control had 39 taxa. Again, the number of taxa detected in the 'IgG negative' fraction but not in the 'IgG positive' fraction also varied between individuals; in pair 1 the patient had 15 and the control had 17 taxa, in pair 2 the patient had 25 and the control had 25 taxa, in pair 3 the patient had 176 and the control had 20 taxa, in pair 4 the patient had 12 and the control had 81 taxa and in pair 5 the patient had 18 and the control had 26 taxa. Another interesting observation in the patient from pair 3 was that they had 5 taxa whose relative abundance was more than 100-fold greater in the 'IgG negative' fraction than 'IgG positive' fraction, and 1 taxon whose relative abundance was more than 1000-fold greater in the 'IgG negative' fraction than the 'IgG positive' fraction. Species which may be of interest were *Romboutsia hominis*, *Devosia sp. I507* and *M. restricta* because they were all detected in the 'IgG negative' but not the 'IgG positive' fraction in 3 patients. Another interesting finding was that *Acidovorax carolinensis* was only detected in two patients, in both of which this taxon was only detected in the 'IgG negative' fraction. *Pseudomonas putida* was detected in stool samples from 2 patients and 1 household control, and in the patients this taxon was only detected in the 'IgG positive' fraction whereas the household control only had this taxon detected in the 'IgG negative' fraction. Finally, *Rhodococcus erthropolis* was only detected in stool samples from 2 patients and 1 household control and in those 2 patients it was only detected in the 'IgG negative' fraction whereas it was detected in the positive and negative fraction of the household control.

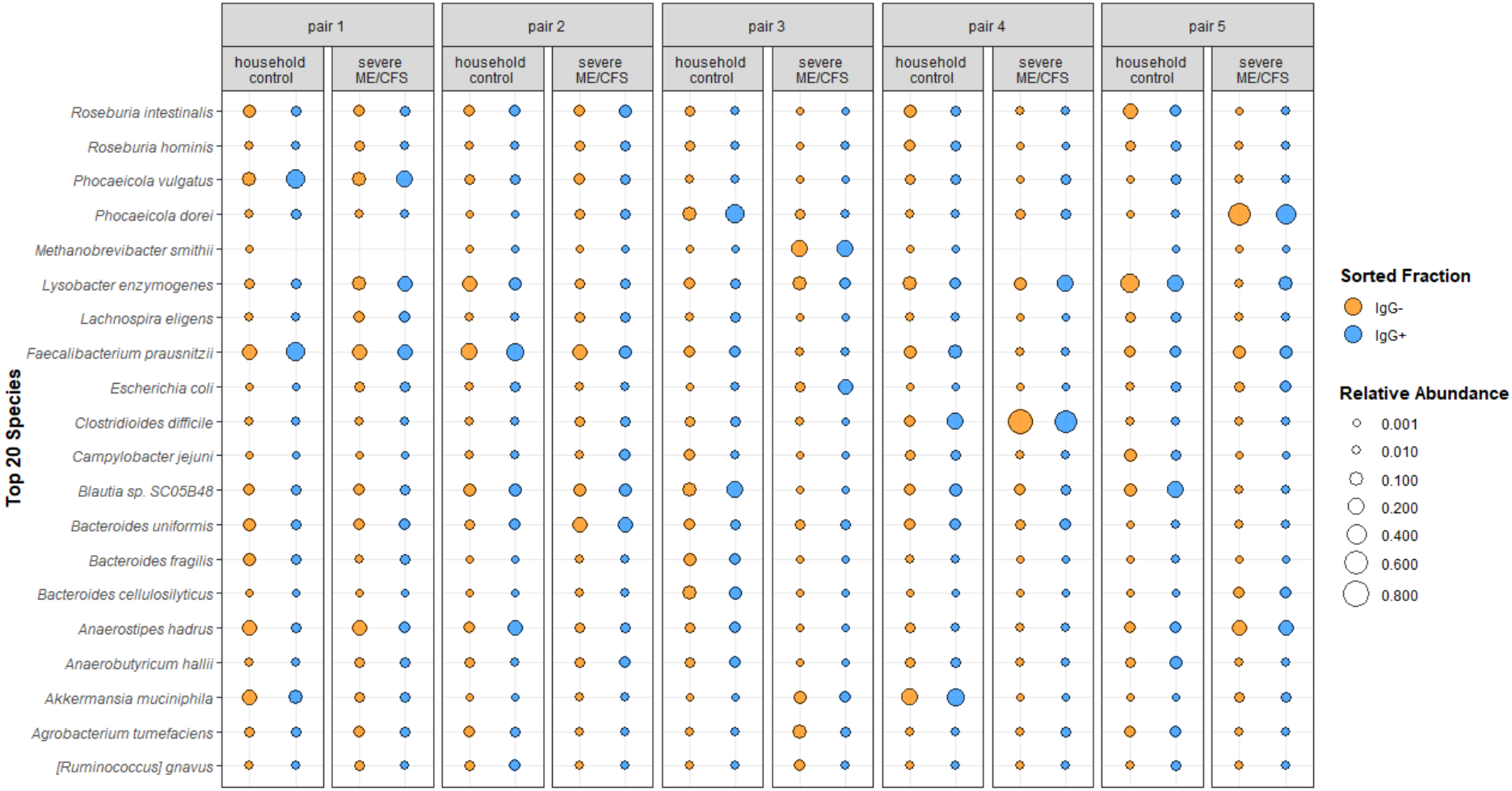
pair 1
pair 2
pair 3
pair 4
pair 5
household control
severe ME/CFS
Top 20 Species
Roseburia intestinalis
Roseburia hominis
Phocaeicola vulgatus
Phocaeicola dorei
Methanobrevibacter smithii
Lysobacter enzymogenes
Lachnospira eligens
Faecalibacterium prausnitzii
Escherichia coli
Clostridioides difficile
Campylobacter jejuni
Blautia sp. SC05B48
Bacteroides uniformis
Bacteroides fragilis
Bacteroides cellulosilyticus
Anaerostipes hadrus
Anaerobutyricum hallii
Akkermansia muciniphila
Agrobacterium tumefaciens
[Ruminococcus] gnavus
Sorted Fraction
IgG-
IgG+
Relative Abundance
0.001
0.010
0.100
0.200
0.400
0.600
0.800

← *Figure 5.23: Top 20 species in 'IgG positive' fractions and 'IgG negative' fractions in stool samples from severe ME/CFS patients and their matched household controls.* *Stool microbes from severe ME/CFS patients (n=5) and their matched household controls (n=5) were incubated with serum IgG in vitro. 'IgG positive' fractions and 'IgG negative' fractions were subsequently collected using the Sony SH800S cell sorter and shotgun metagenomic sequencing was performed to identify the relative abundance of taxa present in the sorted fractions from each participant.*

5.3.2.1.8 Summary

In conclusion, when comparing the taxonomic composition of 'IgG positive' microbes and 'IgG negative' microbes between severe ME/CFS patients and their matched household controls no global differences were identified. For most taxa, if they were detected in the 'IgG positive' fraction they were also detected in that participants 'IgG negative' fraction. There were a few taxa which were exceptions as they were only detected in one fraction. For each participant these exceptions were different taxa. When comparing taxa in a participant's 'IgG positive' fraction to that participant's 'IgG negative' fraction the relative abundances were similar. The severe ME/CFS patient from pair 3 was an exception as they had taxa detected at a relative abundance 100-fold or more higher in the 'IgG positive' fraction compared to the 'IgG negative' fraction and vice versa.

5.3.2.2 Alpha diversity

Numbers of species found in 'IgG positive' fractions and 'IgG negative' fractions from stool were measured using observed richness on rarefied reads (**Figure 5.24**). When comparing the 'IgG positive' fraction (*M* = 321.540, *SD* = 48.148) to the 'IgG negative' fraction (*M* = 357.981, *SD* = 34.030) from household controls the average observed richness score was higher in the 'IgG negative' fraction. Interestingly in 4 of the household controls the observed richness scores were similar in the 'IgG positive' and 'IgG negative' fraction, and the household control from pair 4 had nearly half of the observed richness score in the 'IgG positive' fraction compared to their 'IgG negative' fraction. The average observed richness score was also lower in the 'IgG positive' fraction (*M* = 338.662, *SD* = 45.592) than the 'IgG negative' fraction (*M* = 365.129, *SD* = 91.075) in severe ME/CFS patients. Unlike the household control, the severe ME/CFS patient from pair 4 had a higher observed richness score in the 'IgG positive' fraction than the 'IgG negative' fraction. In addition, the observed richness score of the 'IgG positive' fraction in the patient from pair 3 was nearly half the score measured in their 'IgG negative' fraction. When comparing 'IgG positive' fractions of severe ME/CFS patients (*M* = 338.662, *SD* = 45.592) to their matched household controls (*M* = 321.540, *SD* = 48.148) three patients had lower and two patients had higher observed richness scores than their matched household control.

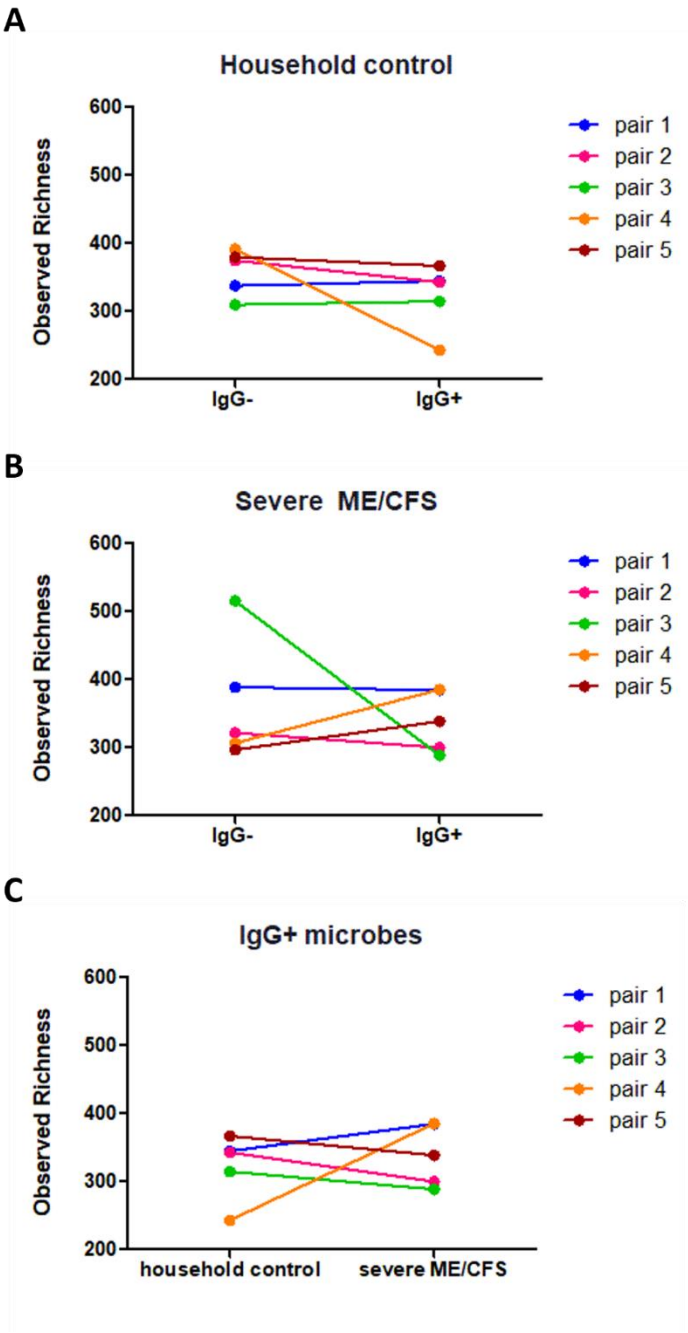

Figure 5.24: Observed richness of species from stool samples that were 'IgG positive' and 'IgG negative'. *A) comparing the observed richness of the 'IgG positive' (n = 5) and 'IgG negative' fractions (n = 5) in household controls B) comparing the observed richness of the 'IgG positive' (n = 5) and 'IgG negative' fractions (n = 5) in severe ME/CFS patients C) comparing the observed richness of the 'IgG positive' fractions between severe ME/CFS patients (n = 5) and their matched household controls (n=5).*

5.3.2.3 Beta diversity

Dissimilarity between the 'IgG positive' and 'IgG negative' fractions in severe ME/CFS patients and their matched household controls was measured using the Jaccard index. Distances between samples were visualised using a NMDS plot (**Figure 5.25**). The distance between the 'IgG positive' and 'IgG negative' fraction in every participant was shorter than the distance to another participant's sample. The 'IgG positive' and 'IgG negative' fractions in patients from pairs 3 and 4 had the greatest distance from the rest of the samples, with both patients' 'IgG positive' fraction having the greatest distance. Interestingly, the 'IgG negative' fraction from the patient in pair 5 had a greater distance than the 'IgG positive' fraction from the cluster of samples.

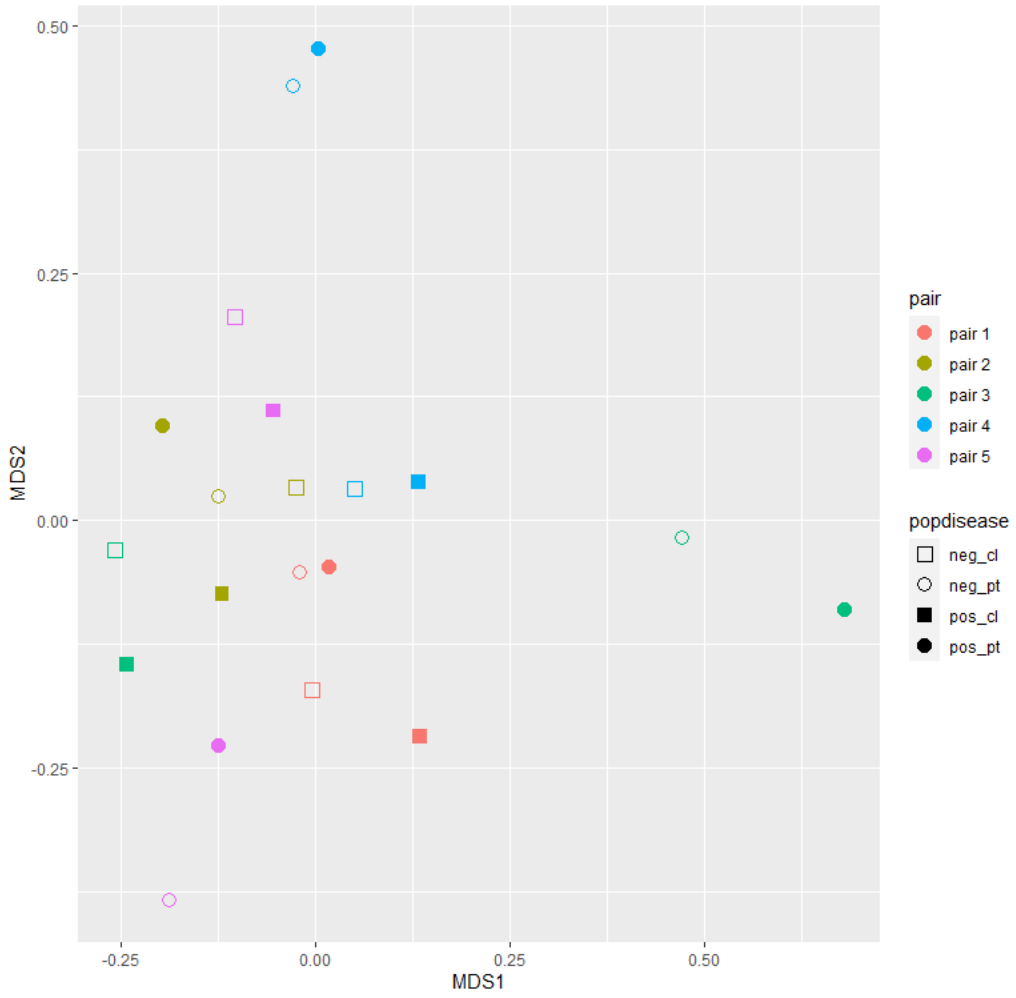

Figure 5.25: Beta diversity of species from stool samples that were 'IgG positive' and 'IgG negative'. *Beta diversity was calculated using the Jaccard index to measure the dissimilarity between severe ME/CFS patients' 'IgG positive' fraction (n = 5), severe ME/CFS patients' 'IgG negative' fraction (n = 5), household controls' 'IgG positive' fraction (n = 5) and household controls' 'IgG negative' fraction. Neg_cl = 'IgG negative' sample from the household control, neg_pt = 'IgG negative' sample from the severe ME/CFS patient, pos_cl = 'IgG positive' sample from the household control, pos_pt = 'IgG positive' sample from the severe ME/CFS patient.*

5.3.2.4 IgG probability ratio

The probability of a microbe within a given taxa being bound by IgG was calculated using the IgG probability ratio. Positive IgG probability ratios indicate that a taxon is more likely to be coated than uncoated by IgG whereas negative IgG probability ratios indicate a taxon is more likely to be uncoated. IgG probability ratios were absent when a taxa was not detected in the 'IgG positive' or 'IgG negative' fraction of a participant. IgG probability ratios were calculated for microbes and compared between severe ME/CFS patients and their matched household controls at the following taxonomic levels: phylum, class, order, family, genus and species.

5.3.2.4.1 Phylum

At the phylum-level only 7 out of a possible 19 taxa had IgG probability ratios in 4 or more complete participant pairs (**Figure 5.26**). When analysing these 7 taxa for differential IgG binding none of the taxa were significantly different between severe ME/CFS patients and their matched household controls.

Interestingly, when analysing IgG probability ratios of all taxa some patterns began to emerge (**Supplementary figure 5.4**). For example, 4 patients and 1 household control had IgG probability ratio scores for Basidiomycota. All four of these severe ME/CFS patients had negative IgG probability ratio scores whereas the household control had a positive IgG probability ratio score.

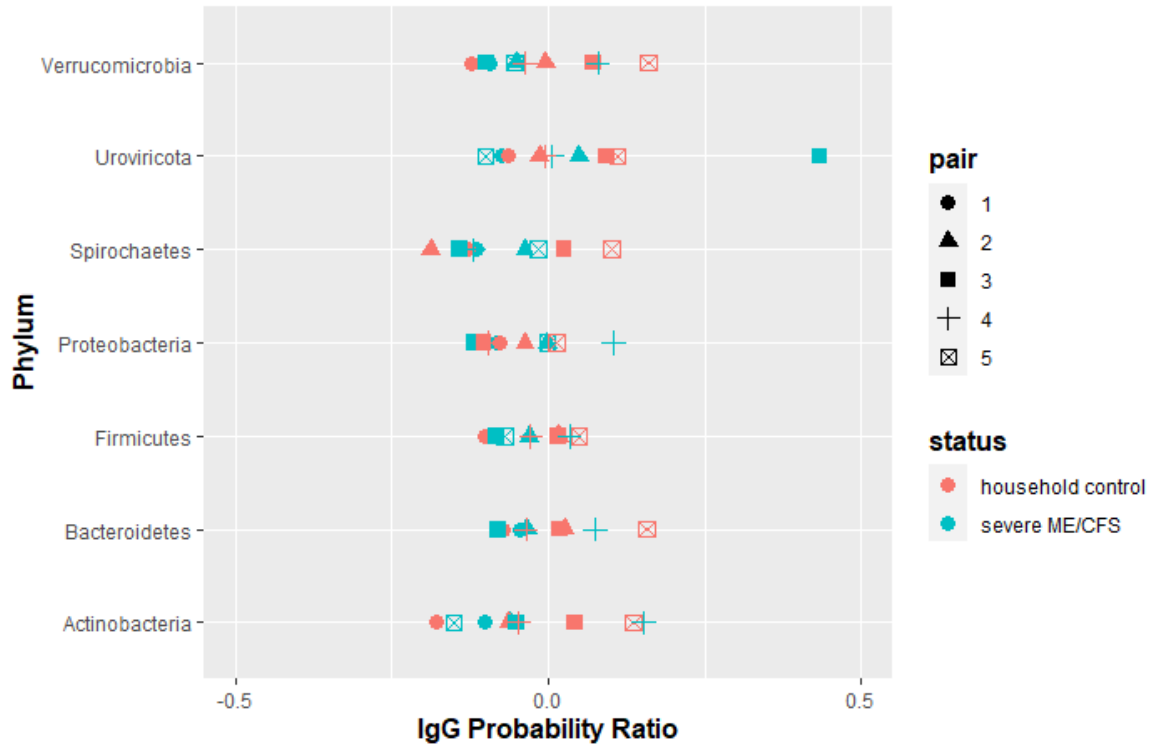

Figure 5.26: Summary plot of IgG probability ratios on taxa at the phylum-level. *Stool microbes from severe ME/CFS patients (n=5) and their matched household controls (n=5) were incubated with serum IgG in vitro. 'IgG positive' fractions and 'IgG negative' fractions were subsequently collected using the Sony SH800S cell sorter and shotgun metagenomic sequencing was performed to identify the relative abundance of taxa present in the sorted fractions from each participant. The IgG probability ratio was used to calculate the likelihood of a taxon being coated by IgG. Taxa with IgG probability ratios present for 4 or more complete participant pairs are shown on the graph.*

5.3.2.4.2 Class

At the class-level only 16 out of a possible 29 taxa had IgG probability ratios in 4 or more complete participant pairs (**Figure 5.27**). When comparing IgG probability ratios for these taxa, Epsilonproteobacteria IgG probability ratios were higher in all 5 severe ME/CFS patients compared to their matched household controls. In addition, in 4 pairs of participants the Alphaproteobacteria IgG probability ratios were lower in severe ME/CFS patients compared to their matched household control. However, none of the taxa were significantly different between severe ME/CFS patients and their matched household controls.

Analysis was then expanded to taxa including those with IgG probability ratios in less than 4 complete participant pairs (**Supplementary figure 5.5**). Malasseziomycetes, a class within the Basidiomycota phylum, was found to have negative IgG probability ratios and positive IgG probability ratios in patients and controls respectively. When comparing patients' IgG probability ratios to their matched household controls' other interesting findings were made. In pair 3 only 2 of 17 taxa that had IgG probability ratio scores in both the patient and the household control were higher in the patient compared to the control. Similarly, in pair 5 only 2 of 18 taxa with IgG probability ratio scores in both the patient and the household control were higher in the patient compared to the control. In contrast, the patient in pair 4 had IgG probability ratios higher than the matched household control in 16 taxa and only 1 taxon was lower than the matched household control.

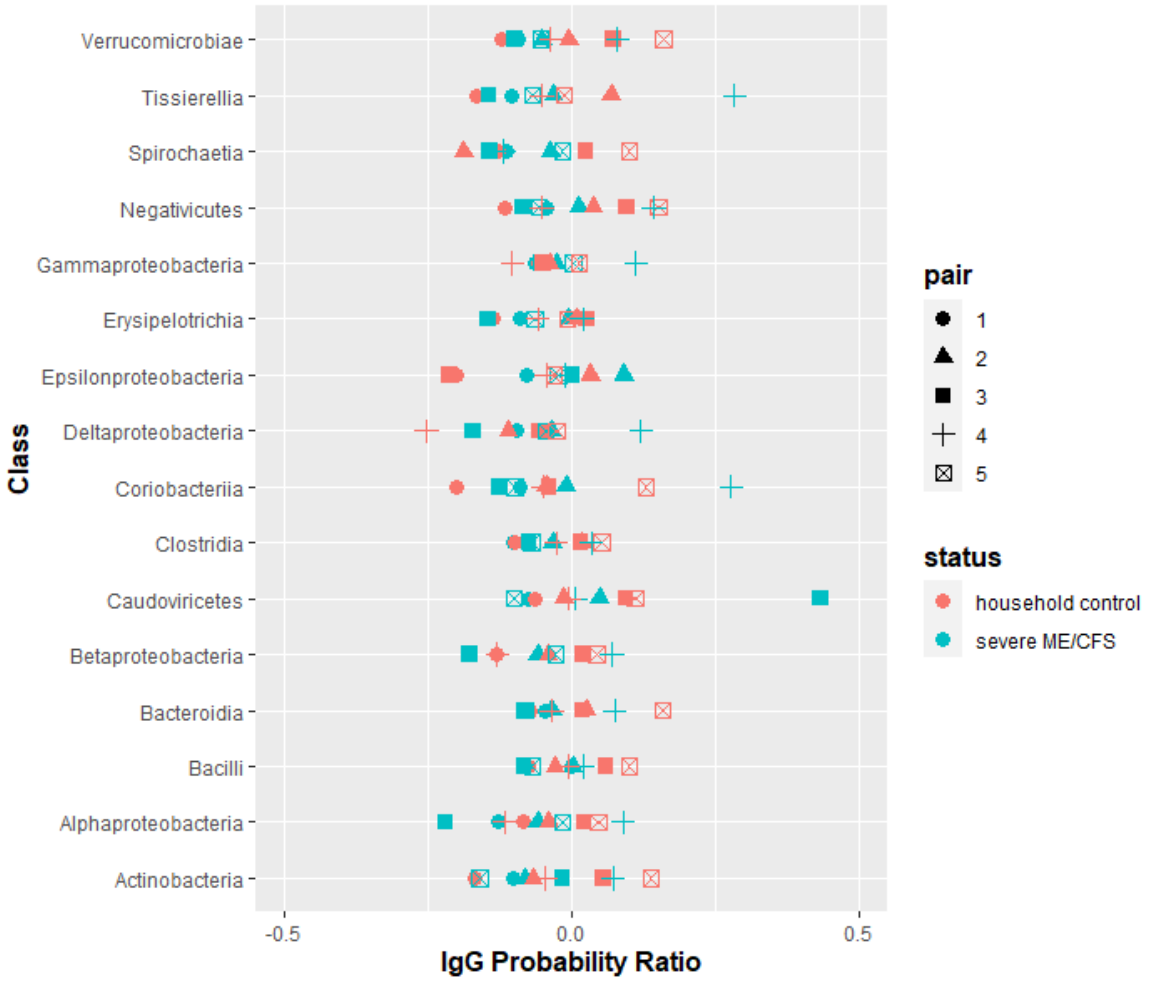

Figure 5.27: Summary plot of IgG probability ratios on taxa at the class-level. *Stool microbes from severe ME/CFS patients (n=5) and their matched household controls (n=5) were incubated with serum IgG in vitro. 'IgG positive' fractions and 'IgG negative' fractions were subsequently collected using the Sony SH800S cell sorter and shotgun metagenomic sequencing was performed to identify the relative abundance of taxa present in the sorted fractions from each participant. The IgG probability ratio was used to calculate the likelihood of a taxon being coated by IgG. Taxa with IgG probability ratios present for 4 or more complete participant pairs are shown on the graph.*

5.3.2.4.3 Order

At the order-level only 28 out of a possible 52 taxa had IgG probability ratios in 4 or more complete participant pairs (**Figure 5.28**). IgG probability ratios for Pseudomonas and Campylobacterales were higher in all severe ME/CFS patients compared to their matched household controls. In addition, the IgG probability ratio scores of Rhizobiales, Micrococcales and Caulobacterales were lower in severe ME/CFS patients compared to controls in pairs 1, 2, 3 and 5. Paired *t*-tests were performed to determine whether there were any taxa that were significantly different between severe ME/CFS patients and controls. No taxa were significantly different between severe ME/CFS patients and matched household controls before or after FDR correction.

When analysis was expanded to include taxa present in less than 4 complete pairs more interesting findings emerged (**Supplementary figure 5.6**). Malasseziales was detected in 4 patients and 1 household control, and in all 4 patients the IgG probability ratios were negative whereas the household control had a positive IgG probability ratio. Similarly, Brachyspirales was detected in 3 patients and 1 household control and in all 3 patients the IgG probability ratios were negative whereas the household control had a positive IgG probability ratio. When comparing patients' IgG probability ratios to that of their matched household controls' it was again found that the patient from pair 4 had IgG probability ratios higher than their matched household control in all but one taxon. This is in contrast to the other patients, 3 of which had IgG probability scores lower when compared to their matched household controls in more than half the taxa.

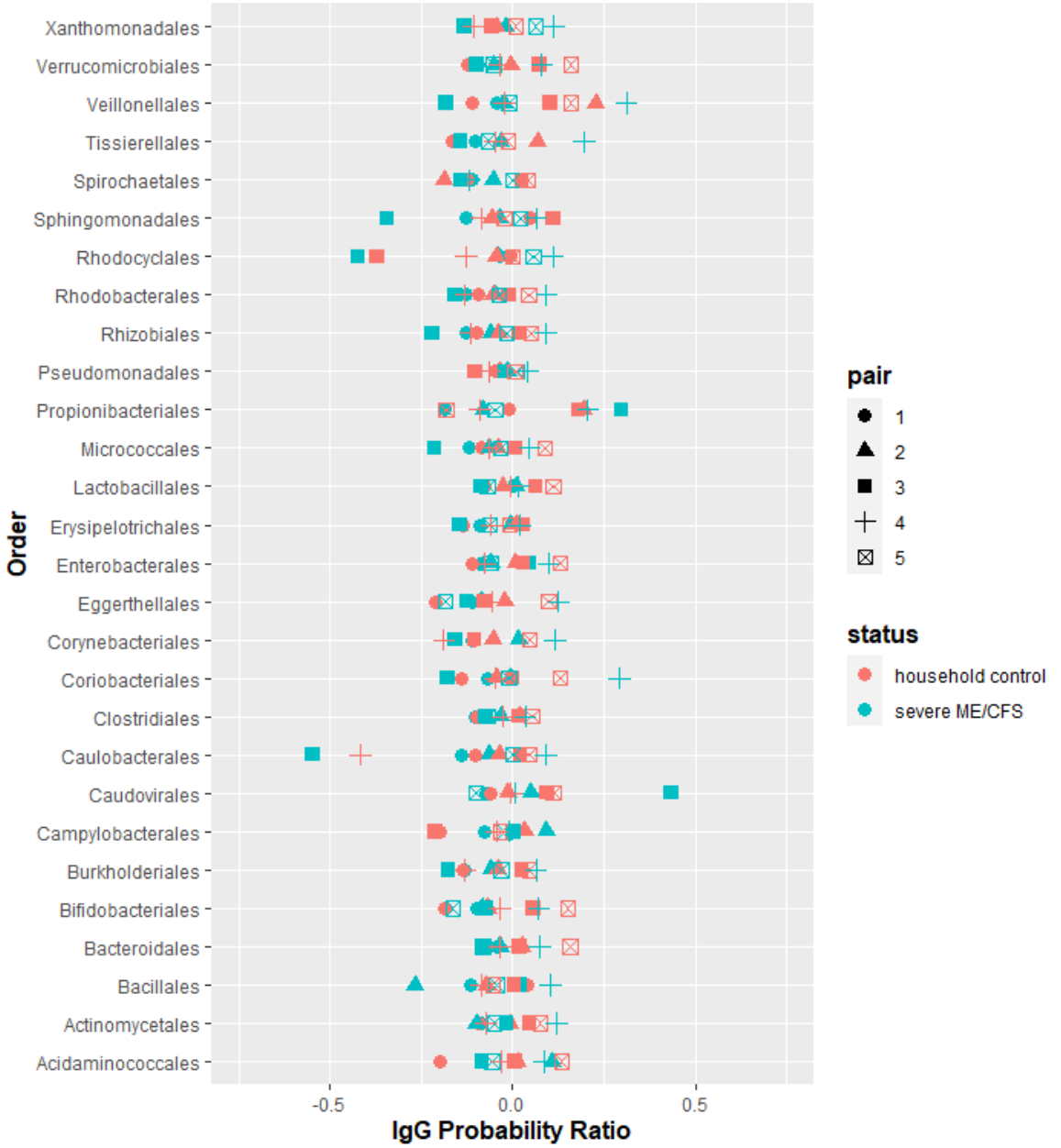

Figure 5.28: Summary plot of IgG probability ratios on taxa at the order-level. *Stool microbes from severe ME/CFS patients (n=5) and their matched household controls (n=5) were incubated with serum IgG in vitro. 'IgG positive' fractions and 'IgG negative' fractions were subsequently collected using the Sony SH800S cell sorter and shotgun metagenomic sequencing was performed to identify the relative abundance of taxa present in the sorted fractions from each participant. The IgG probability ratio was used to calculate the likelihood of a taxon being coated by IgG. Taxa with IgG probability ratios present for 4 or more complete participant pairs are shown on the graph.*

5.3.2.4.4 Family

At the family-level only 51 out of a possible 101 taxa had IgG probability ratios in 4 or more complete participant pairs (**Figure 5.29**). Interestingly the IgG probability ratio scores of Actinomycetaceae, Alcaligenaceae, Bradyrhizobiaceae, Caulobacteraceae, Microbacteriaceae, Phyllobacteriaceae, Prevotellaceae, Rhizobiaceae, Ruminococcaceae and Xanthobacteraceae were lower in severe ME/CFS patients compared to their matched household controls in all pairs except pair 4, where the patient had higher IgG probability ratios compared to the control for the aforementioned taxa. In addition, the IgG probability ratio for Siphoviridae was lower in severe ME/CFS patients compared to controls in pairs 1, 2, 3 and 5. Comparisons could not be made in pair 4 as Siphoviridae was not detected in the patient sample. Campylobacteraceae and Pseudomonadaceae had higher IgG probability ratio scores in severe ME/CFS patients compared to their matched household controls in pairs 1, 2, 4 and 5. Whereas the severe ME/CFS patient from pair 3 had lower IgG probability ratios for Campylobacteraceae and Pseudomonadaceae than the matched household control. In addition, this patient had the lowest IgG probability ratio scores for 31 taxa when compared to all other participants. The patient from pair 3 also had the highest IgG probability ratio recorded, which was for Podoviridae. However, no taxa were significantly different between severe ME/CFS patients and matched household controls before or after FDR correction.

Analysis was then expanded to include taxa present in less than 4 complete pairs (**Supplementary figure 5.7**). Malasseziaceae, part of the Malasseziales order, was detected in 4 patients and 1 household control, and in all 4 patients the IgG probability ratios were negative whereas the household control had a positive IgG probability ratio. Similarly, Brachyspiraceae, part of the Brachyspirales order, was detected in 3 patients and 1 household control and in all 3 patients the IgG probability ratios were negative whereas the household control had a positive IgG probability ratio.

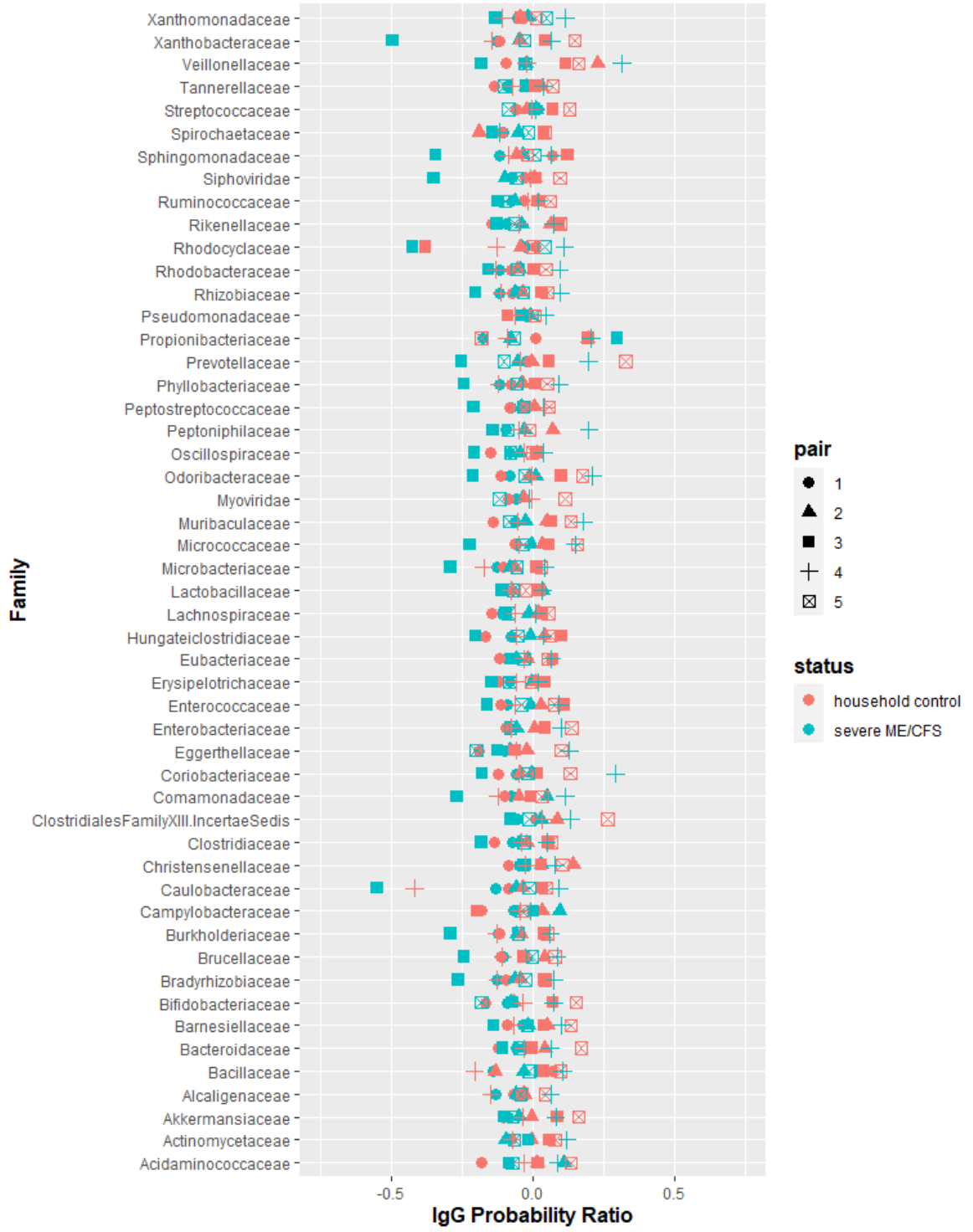

Figure 5.29: Summary plot of IgG probability ratios on taxa at the family-level. *Stool microbes from severe ME/CFS patients (n=5) and their matched household controls (n=5) were incubated with serum IgG in vitro. 'IgG positive' fractions and 'IgG negative' fractions were subsequently collected using the Sony SH800S cell sorter and shotgun metagenomic sequencing was performed to identify the relative abundance of taxa present in the sorted fractions from each participant. The IgG probability ratio was used to calculate the likelihood of a taxon being coated by IgG. Taxa with IgG probability ratios present for 4 or more complete participant pairs are shown on the graph.*

5.3.2.4.5 Genus

At the genus-level only 105 out of a possible 251 taxa had IgG probability ratios for 4 or more complete participant pairs (**Figure 5.30**). *Campylobacter* and *Pseudomonas* were detected in all participants and the IgG probability ratios were higher in all severe ME/CFS patients compared to their matched household controls. *Peribacillus* was detected in four complete pairs with severe ME/CFS patients having higher IgG probability ratios than their matched household controls. In addition, *Faecalibaculum* and *Taranisvirus* were detected in four complete participant pairs and the IgG probability ratios were lower in severe ME/CFS patients compared to their matched household controls. *Agrobacterium*, *Aminobacter*, *Bradyrhizobium*, *Brevundimonas*, *Faecalibacterium*, *Intestinibaculum, Labrys, Mesorhizobium, Microbacterium, Paraprevotella, Phocaeicola, Rhizobium, Rhodopseudomonas, Romboutsia, Shinella* and *Sphingopyxis* had IgG probability ratio scores in all participants, with lower scores in severe ME/CFS patients compared to their matched household controls in all pairs apart from pair 4, whose patient had higher IgG probability ratios compared to their matched household control. Other taxa of interest were *Clostridioides* and *Lachnoclostridium* because in four pairs of participants the IgG probability ratio was lower in severe ME/CFS patients compared to their matched household controls but the patient from pair 1 had higher IgG probability ratios compared to their matched household control. In addition, IgG probability ratios for *Phoenicibacter* were higher in severe ME/CFS patients compared to their matched household controls in all pairs except for pair 1, where the patient had a lower IgG probability ratio compared to their matched household control. When severe ME/CFS patients were compared to their matched household controls and analysed for significance, no taxa had significantly different IgG probability ratio scores between severe ME/CFS patients and matched household controls before or after FDR correction.

When analysis was expanded to include taxa present in less than 4 complete pairs more patterns emerged (**Supplementary figure 5.8**). *Malassezia*, part of the Malasseziaceae family, was detected in 4 patients and 1 household control, and all 4 patients had negative IgG probability ratios whereas the control had a positive IgG probability ratio. Similarly, *Brachyspira* was detected in 3 patients and 1 household control and all 3 patients had negative IgG probability ratios whereas the household control had a positive IgG probability ratio. Finally, the highest IgG probability ratio recorded was 0.784 which was measured for the patient from pair 3 for the *Salasvirus* genus. This genus was not detected in any other participant.

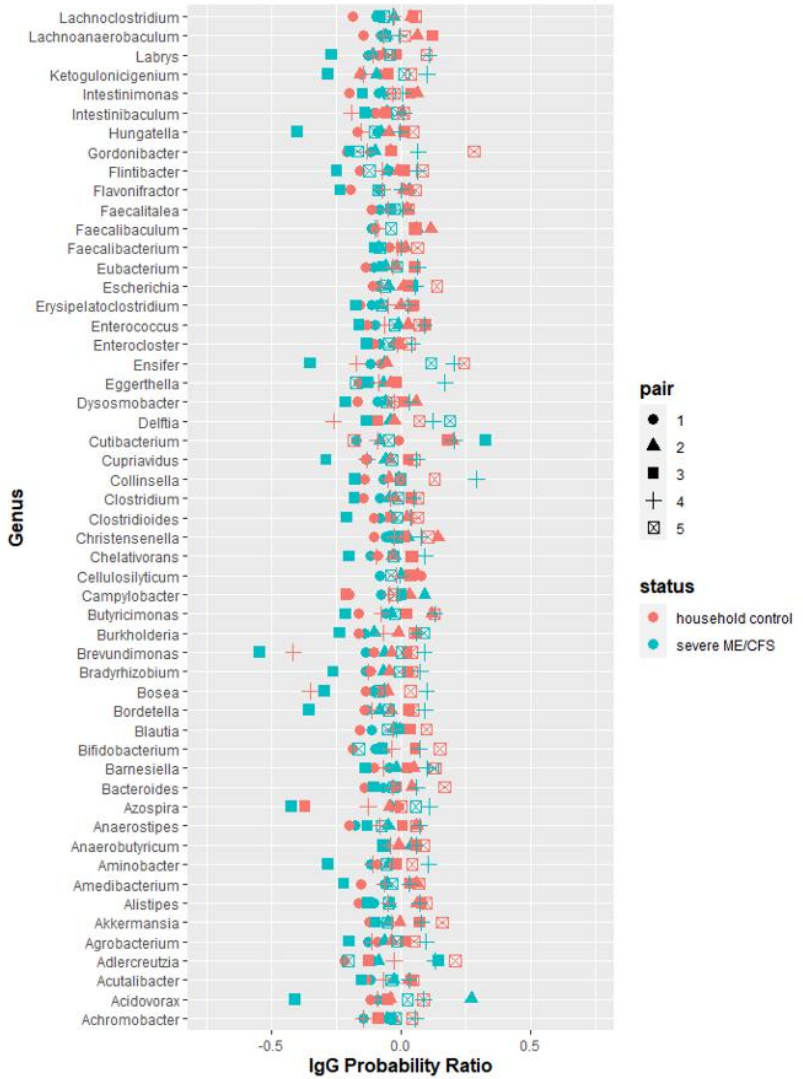
Lachnoclostridium
Lachnoanaerobaculum
Labrys
Ketogulonicigenium
Intestinimonas
Intestinibaculum
Hungatella
Gordonibacter
Flintibacter
Flavonifractor
Faecalitalea
Faecalibaculum
Faecalibacterium
Eubacterium
Escherichia
Erysipelatoclostridium
Enterococcus
Enterocloster
Ensifer
Eggerthella
Dysosmobacter
Delftia
Cutibacterium
Cupriavidus
Collinsella
Clostridium
Clostridioides
Christensenella
Chelativorans
Cellulosilyticum
Campylobacter
Butyricimonas
Burkholderia
Brevundimonas
Bradyrhizobium
Bosea
Bordetella
Blautia
Bifidobacterium
Barnesiella
Bacteroides
Azospira
Anaerostipes
Anaerobutyricum
Aminobacter
Amedibacterium
Alistipes
Akkermansia
Agrobacterium
Adlercreutzia
Acutalibacter
Acidovorax
Achromobacter
Genus
-0.5
0.0
0.5
IgG Probability Ratio
pair
1
2
3
4
5
status
household control
severe ME/CFS

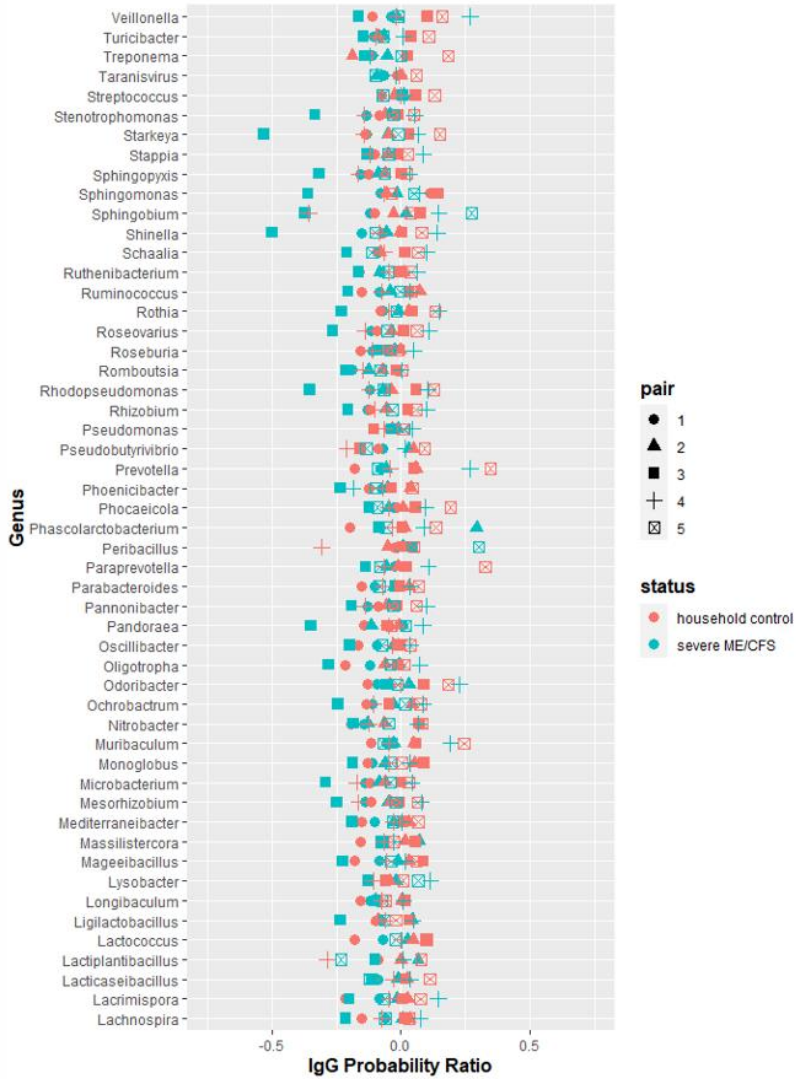
Veillonella
Turicibacter
Treponema
Taranisvirus
Streptococcus
Stenotrophomonas
Starkeya
Stappia
Sphingopyxis
Sphingomonas
Sphingobium
Shinella
Schaalia
Ruthenibacterium
Ruminococcus
Rothia
Roseovarius
Roseburia
Romboutsia
Rhodopseudomonas
Rhizobium
Pseudomonas
Pseudobutyrivibrio
Prevotella
Phoenicibacter
Phocaeicola
Phascolarctobacterium
Peribacillus
Paraprevotella
Parabacteroides
Pannonibacter
Pandoraea
Oscillibacter
Oligotropha
Odoribacter
Ochrobactrum
Nitrobacter
Muribaculum
Monoglobus
Microbacterium
Mesorhizobium
Mediterraneibacter
Massilistercora
Mageeibacillus
Lysobacter
Longibaculum
Ligilactobacillus
Lactococcus
Lactiplantibacillus
Lacticaseibacillus
Lacrimispora
Lachnospira
Genus
-0.5
0.0
0.5
IgG Probability Ratio
pair
1
2
3
4
5
status
household control
severe ME/CFS

← ***Figure 5.30: Summary plot of IgG probability ratios on taxa at the genus-level.*** *Stool microbes from severe ME/CFS patients (n=5) and their matched household controls (n=5) were incubated with serum IgG in vitro. 'IgG positive' fractions and 'IgG negative' fractions were subsequently collected using the Sony SH800S cell sorter and shotgun metagenomic sequencing was performed to identify the relative abundance of taxa present in the sorted fractions from each participant. The IgG probability ratio was used to calculate the likelihood of a taxon being coated by IgG. Taxa with IgG probability ratios present for 4 or more complete participant pairs are shown on the graph.*

5.3.2.4.6 Species

At the species-level only 204 out of a possible 619 taxa had IgG probability ratios for 4 or more complete participant pairs (**Figure 5.31**). *C. jejuni* was detected in all participants and the IgG probability ratios were higher in all severe ME/CFS patients compared to their matched household controls. *Peribacillus simplex* and *Pseudomonas viridiflava* were detected in four complete participant pairs and the IgG probability ratios were higher in the severe ME/CFS patients compared to their matched household controls. In addition, *Cupriavidus basilensis, Faecalibacterium virus Taranis, Faecalibaculum rodentium, Microbacterium sp. CBA3102* and *Rothia dentocariosa* were detected in four complete participant pairs and the IgG probability ratios were lower in the severe ME/CFS patients compared to their matched household controls. However, when performing paired *t*-tests to assess significance of these differences only *C. jejuni* and *P. viridiflava* had $p < 0.05$ prior to FDR correction, and no taxa remained significant following FDR correction (**Figure 5.32, Table 2**).

When analysis was expanded to all taxa more patterns emerged (**Supplementary figure 5.9**). Another interesting finding was that the patient from pair 3 had IgG probability ratios less than -0.5 in *Brevundimonas vancanneytii*, *Mesorhizobium cicero*, *Sphingopyxis sp. MG* and *Starkeya novella*. The only other participants with IgG probability ratios less than -0.5 were household controls from pairs 3 and 5 for *Bacteroides sp. PHL2737.* The only taxa that had an IgG probability ratio greater than 0.5 was *Bacillus virus phi29* in the patient from pair 3. *M. restricta* was detected in 4 patients and 1 household control, with all 4 patients having negative IgG probability ratios where the household control had a positive IgG probability ratio close to zero. In addition, *Brachyspira pilosicoli* was detected in 3 patients and 1 control with all patients having negative IgG probability ratios whereas the control had a positive IgG probability ratio.


Species
Bifidobacterium bifidum
Bifidobacterium animalis
Bifidobacterium adolescentis
Barnesiella viscericola
Bacteroides xylanisolvens
Bacteroides uniformis
Bacteroides thetaiotaomicron
Bacteroides sp. M10
Bacteroides sp. HF-5287
Bacteroides sp. HF-5141
Bacteroides sp. HF-162
Bacteroides sp. CBA7301
Bacteroides sp. CACC 737
Bacteroides sp. A1C1
Bacteroides ovatus
Bacteroides intestinalis
Bacteroides helcogenes
Bacteroides fragilis
Bacteroides cellulosilyticus
Bacteroides caecimuris
Bacteroides caccae
Azospira sp. I09
Anaerostipes rhamnosivorans
Anaerostipes hadrus
Anaerostipes caccae
Anaerobutyricum hallii
Aminobacter sp. SR38
Aminobacter sp. MSH1
Amedibacterium intestinale
Alistipes shahii
Alistipes onderdonkii
Alistipes megaguti
Alistipes indistinctus
Alistipes finegoldii
Alistipes dispar
Alistipes communis
Akkermansia muciniphila
Agrobacterium tumefaciens
Agrobacterium sp. CGMCC 11546
Agrobacterium genomosp. 3
Agrobacterium fabrum
Adlercreutzia sp. 8CFCBH1
Adlercreutzia equolifaciens
Acutalibacter muris
Acidovorax sp. KKS102
Achromobacter xylosoxidans
[Ruminococcus] gnavus
[Eubacterium] cellulosolvens
[Clostridium] scindens
[Clostridium] innocuum
[Clostridium] hylemonae
-0.5
0.0
0.5
IgG Probability Ratio
Species
Eubacterium callanderi
Escherichia coli
Erysipelatoclostridium ramosum
Enterococcus saigonensis
Enterococcus faecium
Enterococcus faecalis
Enterococcus cecorum
Enterocloster clostridioformis
Enterocloster bolteae
Ensifer sojae
Eggerthella lenta
Dysosmobacter welbionis
Delftia tsuruhatensis
Dechlorosoma suillum
Cutibacterium acnes
Cupriavidus pauculus
Cupriavidus necator
Cupriavidus metallidurans
Cupriavidus campinensis
Cupriavidus basilensis
Collinsella aerofaciens
Clostridium sp. SY8519
Clostridium perfringens
Clostridioides difficile
Clostridiales bacterium Choco116
Christensenella sp. Marseille-P3954
Christensenella minuta
Chelativorans sp. BNC1
Cellulosilyticum sp. WCF-2
Campylobacter jejuni
Campylobacter coli
Butyricimonas faecalis
Burkholderia contaminans
Brevundimonas sp. LM2
Brevundimonas mediterranea
Bradyrhizobium sp. SK17
Bradyrhizobium sp. BTAi1
Bradyrhizobium sp.
Bradyrhizobium betae
Bosea sp. Tri-49
Bosea sp. AS-1
Bordetella petrii
Blautia sp. SC05B48
Blautia sp. LZLJ-3
Blautia producta
Blautia hansenii
Blautia argi
Bifidobacterium pseudocatenulatum
Bifidobacterium longum
Bifidobacterium catenulatum
Bifidobacterium breve
-0.5
0.0
0.5
IgG Probability Ratio
pair
1
2
3
4
5
status
household control
severe ME/CFS

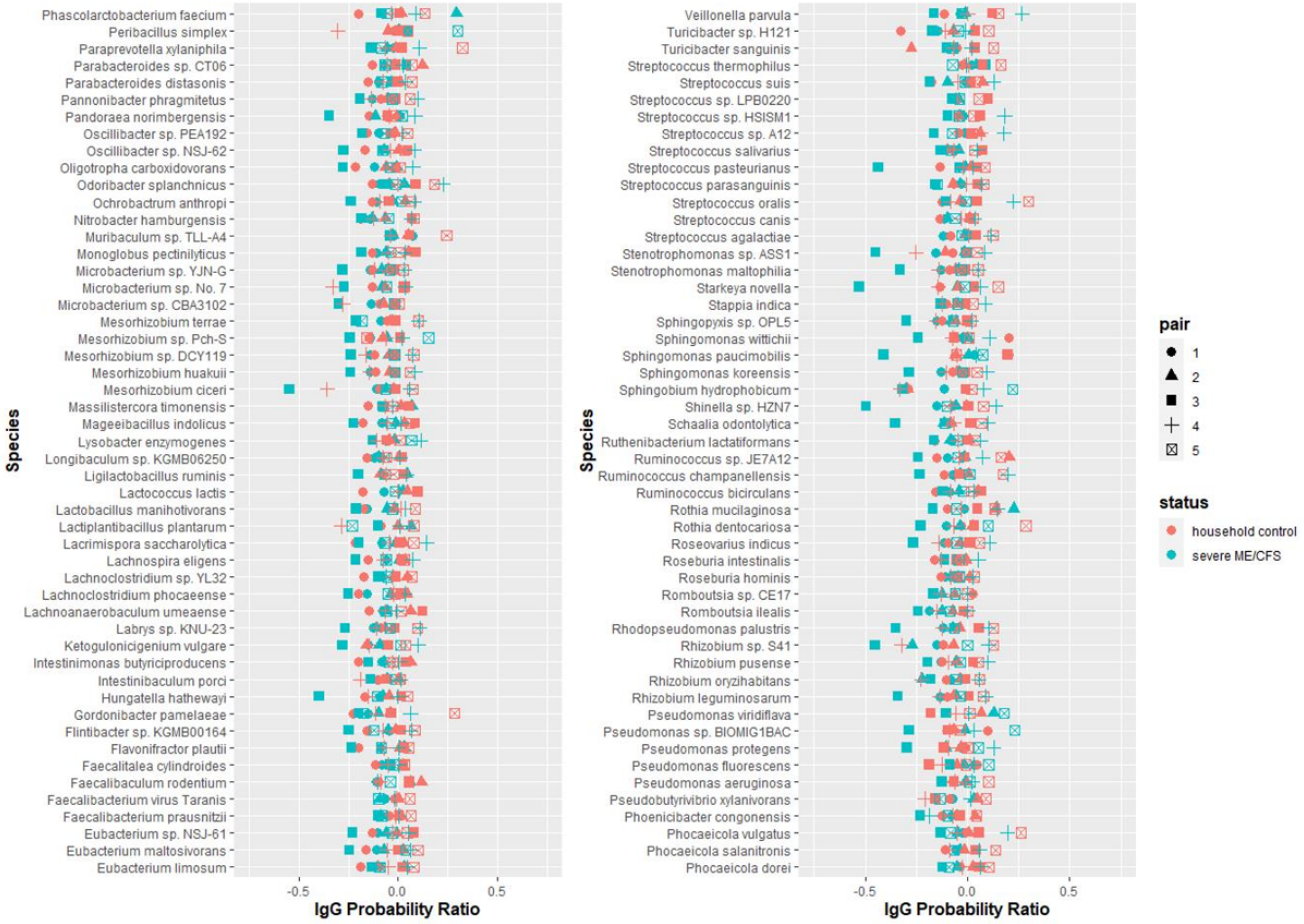
Species
Phascolarctobacterium faecium
Peribacillus simplex
Paraprevotella xylaniphila
Parabacteroides sp. CT06
Parabacteroides distasonis
Pannonibacter phragmitetus
Pandoraea norimbergensis
Oscillibacter sp. PEA192
Oscillibacter sp. NSJ-62
Oligotropha carboxidovorans
Odoribacter splanchnicus
Ochrobactrum anthropi
Nitrobacter hamburgensis
Muribaculum sp. TLL-A4
Monoglobus pectinilyticus
Microbacterium sp. YJN-G
Microbacterium sp. No. 7
Microbacterium sp. CBA3102
Mesorhizobium terrae
Mesorhizobium sp. Pch-S
Mesorhizobium sp. DCY119
Mesorhizobium huakuii
Mesorhizobium ciceri
Massilistercora timonensis
Mageeibacillus indolicus
Lysobacter enzymogenes
Longibaculum sp. KGMB06250
Ligilactobacillus ruminis
Lactococcus lactis
Lactobacillus manihotivorans
Lactiplantibacillus plantarum
Lacrimispora saccharolytica
Lachnospira eligens
Lachnoclostridium sp. YL32
Lachnoclostridium phocaeense
Lachnoanaerobaculum umeaense
Labrys sp. KNU-23
Ketogulonicigenium vulgare
Intestinimonas butyriciproducens
Intestinibaculum porci
Hungatella hathewayi
Gordonibacter pamelaeae
Flintibacter sp. KGMB00164
Flavonifractor plautii
Faecalitalea cylindroides
Faecalibaculum rodentium
Faecalibacterium virus Taranis
Faecalibacterium prausnitzii
Eubacterium sp. NSJ-61
Eubacterium maltosivorans
Eubacterium limosum
-0.5
0.0
0.5
IgG Probability Ratio
Species
Veillonella parvula
Turicibacter sp. H121
Turicibacter sanguinis
Streptococcus thermophilus
Streptococcus suis
Streptococcus sp. LPB0220
Streptococcus sp. HSISM1
Streptococcus sp. A12
Streptococcus salivarius
Streptococcus pasteurianus
Streptococcus parasanguinis
Streptococcus oralis
Streptococcus canis
Streptococcus agalactiae
Stenotrophomonas sp. ASS1
Stenotrophomonas maltophilia
Starkeya novella
Stappia indica
Sphingopyxis sp. OPL5
Sphingomonas wittichii
Sphingomonas paucimobilis
Sphingomonas koreensis
Sphingobium hydrophobicum
Shinella sp. HZN7
Schaalia odontolytica
Ruthenibacterium lactatiformans
Ruminococcus sp. JE7A12
Ruminococcus champanellensis
Ruminococcus bicirculans
Rothia mucilaginosa
Rothia dentocariosa
Roseovarius indicus
Roseburia intestinalis
Roseburia hominis
Romboutsia sp. CE17
Romboutsia ilealis
Rhodopseudomonas palustris
Rhizobium sp. S41
Rhizobium pusense
Rhizobium oryzihabitans
Rhizobium leguminosarum
Pseudomonas viridiflava
Pseudomonas sp. BIOMIG1BAC
Pseudomonas protegens
Pseudomonas fluorescens
Pseudomonas aeruginosa
Pseudobutyrivibrio xylanivorans
Phoenicibacter congonensis
Phocaeicola vulgatus
Phocaeicola salanitronis
Phocaeicola dorei
-0.5
0.0
0.5
IgG Probability Ratio
pair
1
2
3
4
5
status
household control
severe ME/CFS

←Figure 5.31: Summary plot of IgG probability ratios on taxa at the species-level. *Stool microbes from severe ME/CFS patients (n=5) and their matched household controls (n=5) were incubated with serum IgG in vitro. 'IgG positive' fractions and 'IgG negative' fractions were subsequently collected using the Sony SH800S cell sorter and shotgun metagenomic sequencing was performed to identify the relative abundance of taxa present in the sorted fractions from each participant. The IgG probability ratio was used to calculate the likelihood of a taxa being coated by IgG. Taxa with IgG probability ratios present for 4 or more complete participant pairs were shown on the graph.*

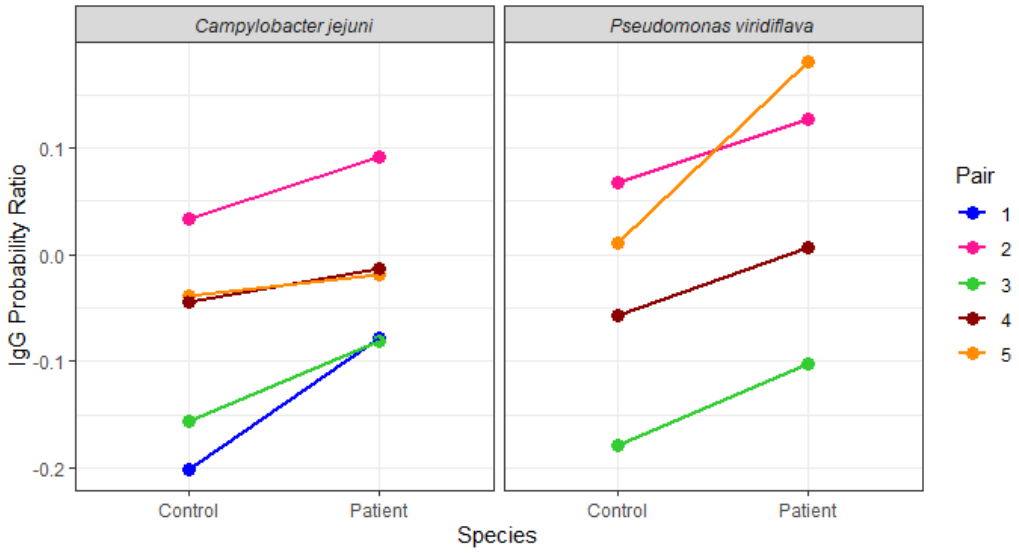

Figure 5.32: Pairwise comparisons of species-level IgG probability ratios in severe ME/CFS patients and their matched household controls. *Paired* t*-tests were performed on taxa present in at least four complete participant pairs to determine whether IgG probability ratios were significantly different between severe ME/CFS patients (n=5) and their matched household controls (n = 5). Taxa with a p-value < 0.05 (prior to FDR correction) are shown on the graph.*

Table 5.2:* P *values pre and post FDR correction from differential abundance analysis on IgG probability ratios. *Paired* t*-tests were performed on taxa present in at least four complete participant pairs to determine whether IgG probability ratios were significantly different between severe ME/CFS patients (n=5) and their matched household controls (n = 5). Taxa with a* p*-value < 0.05 (prior to FDR correction) are shown.*

Taxa	*p*-value prior to FDR correction	*p*-value with FDR correction
Campylobacter jejuni	0.028	0.995
Pseudomonas viridiflava	0.037	0.995

5.3.2.4.7 Summary

Comparing taxa with IgG probability ratios in four or more complete participant pairs found a non-significant increase in IgG binding to *C. jejuni* and *P. viridiflava* in severe ME/CFS patients compared to their matched household controls. Comparing the IgG probability ratios in all taxa showed heterogenous IgG binding profiles in both severe ME/CFS patients and household controls. In all of the 4 severe ME/CFS patients that *M. restricta* was detected the IgG probability ratios were negative, whereas in the 1 household control *M. restricta* was detected in the IgG probability ratio was positive. This pattern was seen from the phylum-level to the species-level for this taxon. Similarly, in all of the 3 severe ME/CFS patients that *B. pilosicoli* was detected in the IgG probability ratios were negative, whereas in the 1 household control *B. pilosicoli* was detected in the IgG probability ratio was positive. This pattern was seen from the order-level to the species-level for this taxon. Comparing all IgG probability ratios within pairs found that the patient from pair 4 had IgG probability ratios higher than their matched household control for most taxa. In contrast, in 3 pairs of participants the severe ME/CFS patients had lower IgG probability ratios than their matched household control in over half the taxa.

5.3.3 The functional potential of the gut microbiome

The abundance of gene families in the 'all' sorted fractions from severe ME/CFS patients and their matched household controls were analysed to determine whether there were functional differences of the microbiome between patients and controls. A total of 1,337,702 gene families were detected, 464,263 of which remained after applying the threshold. The final filtering step removed gene families that were below the threshold in more than 7 samples, which left 84,888 gene families. With such a large number of variables, univariate analysis was not appropriate to determine if there were differences in the gene families between severe ME/CFS patients and matched household controls. Therefore, multivariate analysis was used. PCA was used to reduce the number of variables by defining principal components (PC) that highlight the largest sources of variation in the data. 94 % of variance across samples was explained by eight PCs which indicated a

large variation amongst participants (**Figure 5.33**). PC4 highlighted variation attributable to differences between severe ME/CFS patients and household controls; patients had higher sample scores than controls. However, only 11 % of variance was explained by PC4. From analysing the gene families with the 20 highest and 20 lowest loadings on PC4 an overlap of relative abundances between patients and controls can be seen in all the gene families, with a greater variation of gene families' relative abundances in the controls (**Figure 5.34**). When comparing the relative abundances of the 20 gene families with the highest loadings between severe ME/CFS patients and their matched household controls, 3 of the gene families had a higher relative abundance in all 5 patients when compared to their matched household controls (**Supplementary figure 5.10**). In addition, comparing the relative abundances of the 20 gene families with the lowest loading scores revealed 50 % had lower relative abundances in all 5 patients when compared to their matched household controls (**Supplementary figure 5.11**).

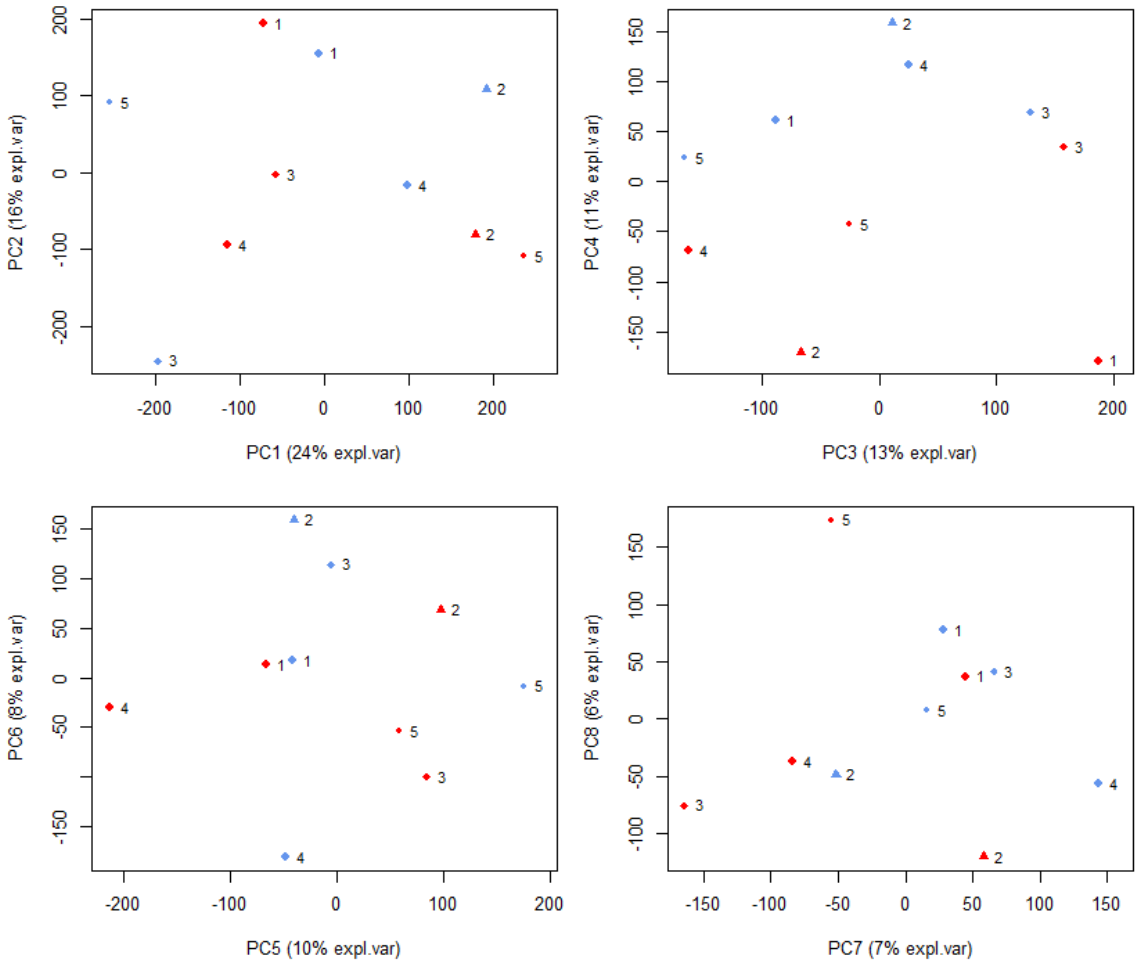

Figure 5.33: Principal component analysis of gene families from stool microbial communities in severe ME/CFS patients (blue) and household controls (red). *Stool microbes from severe ME/CFS patients (n=5) and their matched household controls (n=5) were stained with SYBR™ green I nucleic acid gel stain and 'all' cells were collected using the Sony SH800S cell sorter. Shotgun metagenomic sequencing was performed to identify gene families present in each sample. PCA was performed on gene families with 4 or more values over the threshold. Pair numbers are denoted on the graphs but were not used in the analysis.*

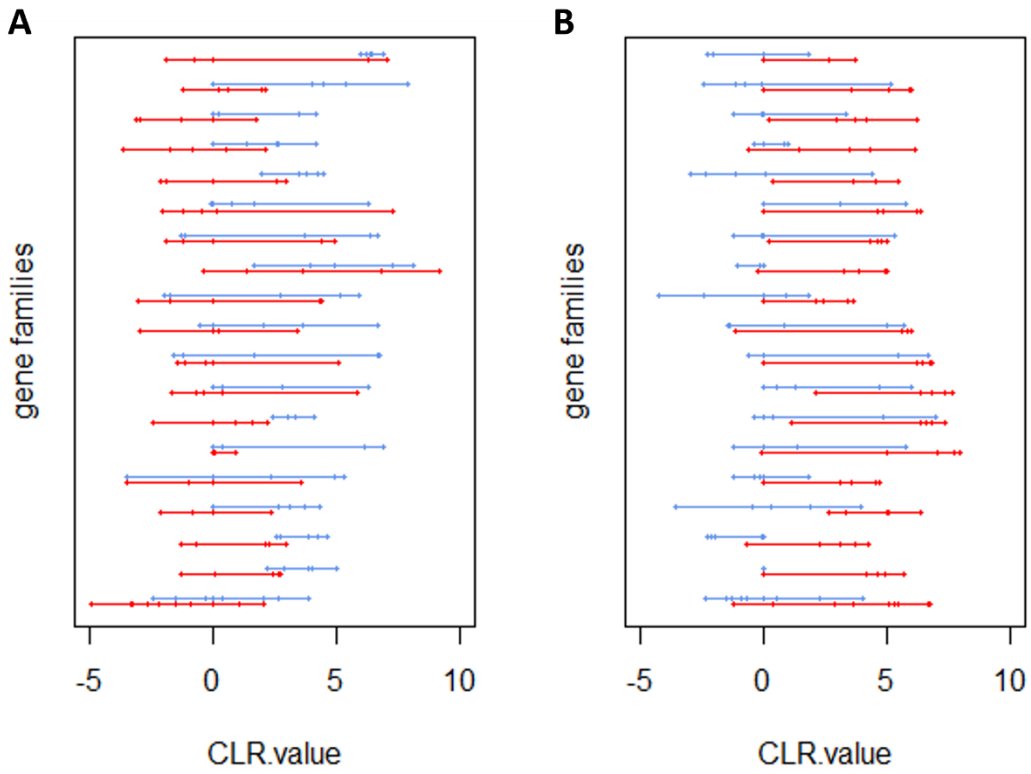

Figure 5.34: A summary of CLR transformed relative abundances of gene families contributing to variation separating severe ME/CFS patients (blue) from household controls (red). *Stool microbes from severe ME/CFS patients (n=5) and their matched household controls (n=5) were stained with SYBR™ green I nucleic acid gel stain and 'all' cells were collected using the Sony SH800S cell sorter. Shotgun metagenomic sequencing was performed to identify gene families present in each sample. PCA was performed on gene families with 4 or more values over the threshold. CLR transformed relative abundances of gene families with A) the 20 highest and B) the 20 lowest loadings on PC4 are shown.*

5.3.4 Functional analysis of 'IgG positive' and 'IgG negative' stool microbes

The relationship between IgG binding of stool microbes and the microbial community function was assessed by analysing the abundance of gene families present in 'IgG positive' and 'IgG negative' stool microbes. The likelihood of a gene family being more or less abundant in the 'IgG positive' fraction was determined on the 464,263 gene families detected above the threshold using the IgG probability ratio. 1,724 gene families had IgG probability ratio scores in all participants and therefore were used in the PCA. 13 % of the variance separated severe ME/CFS patients from four household controls, demonstrated on PC2 (**Figure 5.35**). The 20 highest and lowest loadings on PC2 were visualised to confirm that the IgG probability ratios scores of these gene families were contributing to the separation of severe ME/CFS patients from controls (**Figure 5.36**). For both the positive and negative loadings IgG probability ratios recorded in patients overlapped with the IgG probability ratios recorded in household controls. A greater variation of IgG probability ratio scores was seen in the control group for the 20 highest loading scores (**Figure 5.36A**). Conversely, the patient group had a greater variation of IgG probability ratio scores for the 20 lowest loading scores (**Figure 5.36B**).

The largest variance seen amongst samples was on PC1, which explained 67 % of variance. PC1 highlighted a difference between the patient from pair three and the rest of the participants (**Figure 5.35**). The majority of loadings for gene families on PC1 were positive (**Figure 5.37A**). Analysing the gene families with the 20 highest positive loadings found that these gene families had lower IgG probability ratios in the patient from pair 3 compared to other participants (**Figure 5.37B**). Conversely, gene families with the 20 lowest loadings had higher probability ratios in the patient from pair 3 compared to the other participants (**Figure 5.37C**).

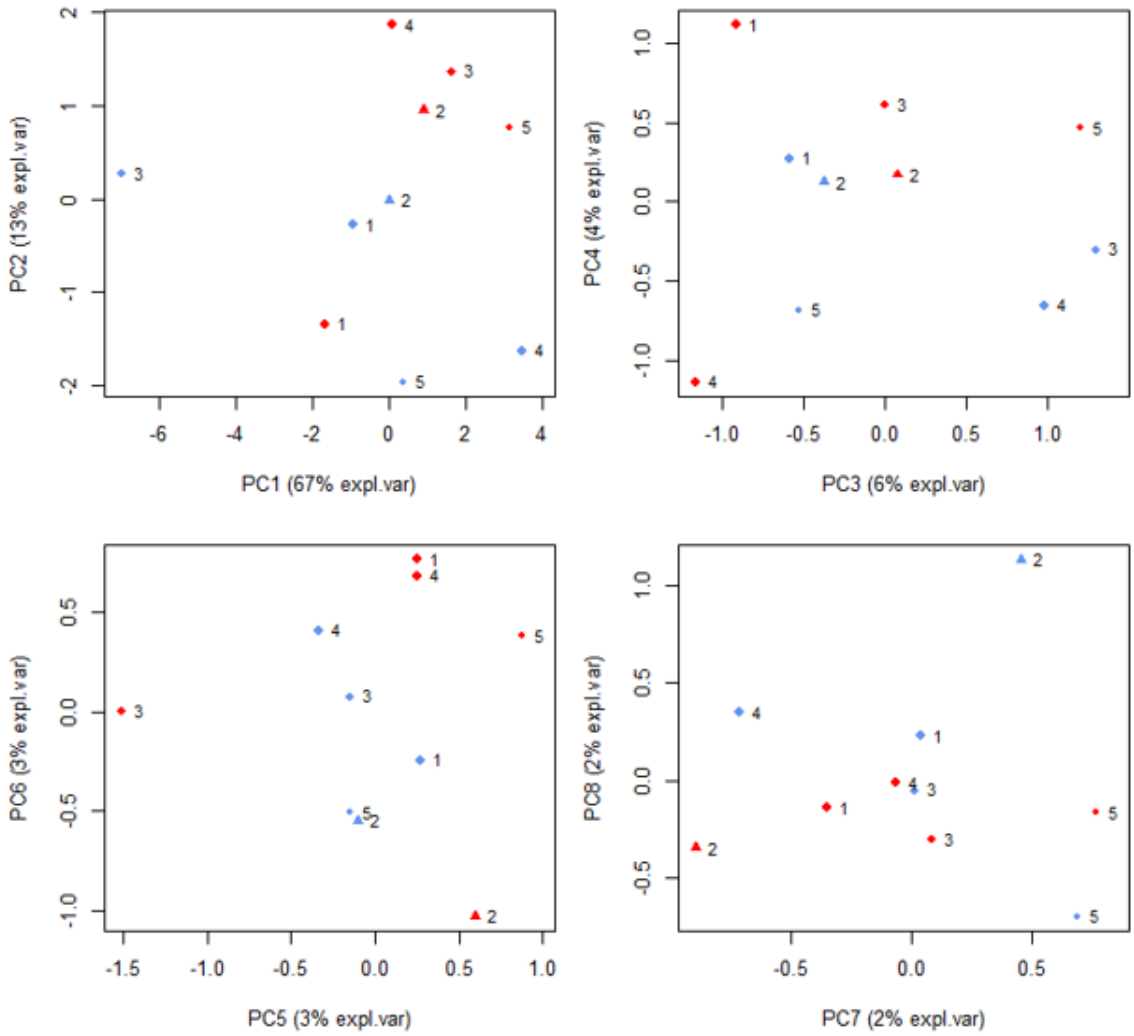

Figure 5.35: Principal component analysis of IgG probability ratios of gene families from stool microbial communities in severe ME/CFS patients (blue) and household controls (red). *Stool microbes from severe ME/CFS patients (n=5) and their matched household controls (n=5) were incubated with serum IgG in vitro. 'IgG positive' and 'IgG negative' microbes were subsequently collected using the Sony SH800S cell sorter and shotgun metagenomic sequencing was performed to identify the relative abundance of gene families present in the sorted fractions from each participant. The IgG probability ratio was used to calculate the likelihood of a gene family being more or less abundant in the 'IgG positive' fraction. PCA was performed on gene families with IgG probability ratios in all participants. Pair numbers are denoted on the graphs but were not used in the analysis.*

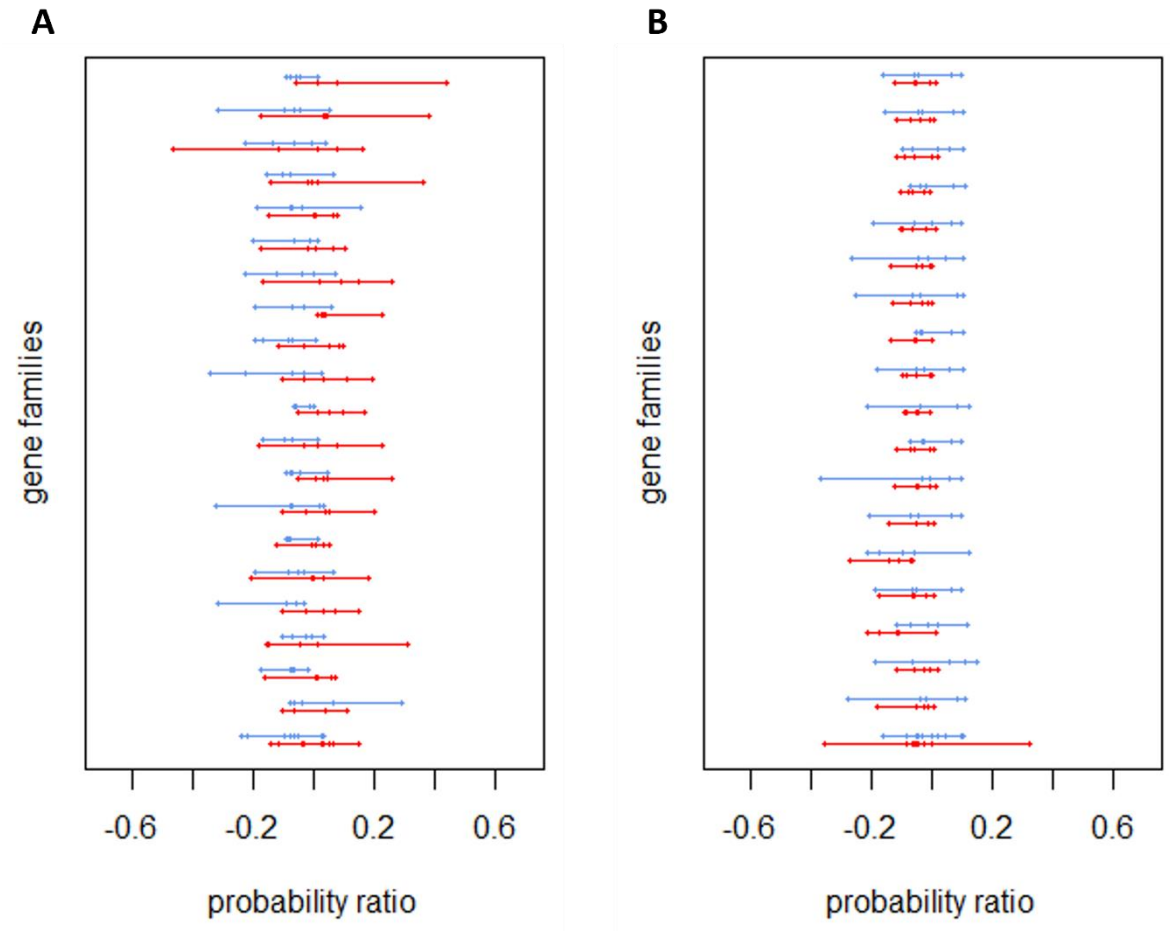

Figure 5.36: A summary of gene families with IgG probability ratios contributing to variation separating severe ME/CFS patient samples (blue) from household control samples (red). *Stool microbes from severe ME/CFS patients (n=5) and their matched household controls (n=5) were incubated with serum IgG in vitro. 'IgG positive' and 'IgG negative' microbes were subsequently collected using the Sony SH800S cell sorter and shotgun metagenomic sequencing was performed to identify the relative abundance of gene families present in the sorted fractions from each participant. The IgG probability ratio was used to calculate the likelihood of a gene family being more or less abundant in the 'IgG positive' fraction. PCA was performed on gene families with IgG probability ratios in all participants. IgG probability ratios of gene families with A) the 20 highest and B) the 20 lowest loadings on PC2 are shown.*

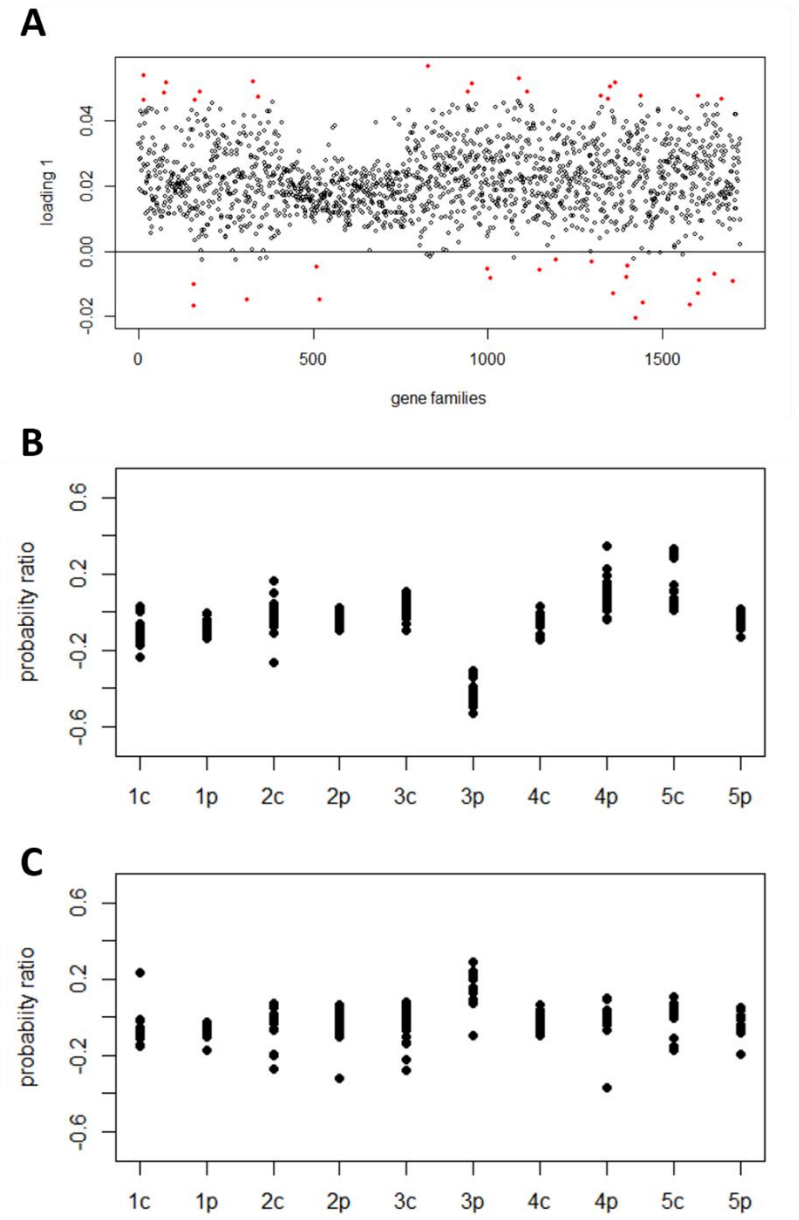

Figure 5.37: Loadings and probability ratios of gene families of interest from PC1. *Stool microbes from severe ME/CFS patients (n=5) and their matched household controls (n=5) were incubated with serum IgG in vitro. 'IgG positive' and 'IgG negative' microbes were subsequently collected using the Sony SH800S cell sorter and shotgun metagenomic sequencing was performed to identify the relative abundance of gene families present in the sorted fractions from each participant. The IgG probability ratio was used to calculate the likelihood of a gene family being more or less abundant in the 'IgG positive' fraction. PCA was performed on gene families with IgG probability ratios in all participants. A) loading scores of gene families on PC1, B) probability ratios of gene families with the 20 highest values on PC1, C) probability ratios of gene families with the 20 lowest values on PC1. In B) and C) participant pairs are shown by numbers 1-5 and severe ME/CFS patients are referred to as "p" and matched household controls are referred to as "c".*

5.4 DISCUSSION

5.4.1 Summary of key findings

This chapter describes the first attempt to analyse serum IgG antibody binding to intestinal microbes in severe ME/CFS patients.

Both non-significant increases and decreases in the relative abundance and microbial load of taxa at the phylum-, class-, order-, family-, genus- and species-level are seen in severe ME/CFS patients compared to their matched household controls. RMP and QMP analysis found different taxa with abundance alterations. When analysing the community structure of stool samples in severe ME/CFS patients and matched household controls no significant differences in alpha diversity measures are found. When analysing the inter-individual differences only clustering amongst household controls is observed.

Separation of 'IgG positive' stool microbes from 'IgG negative' stool microbes was done to compare the preferential binding of IgG to stool microbes in severe ME/CFS patients and their matched household controls. The number of species binding serum IgG is similar to the number of species not bound by serum IgG in severe ME/CFS patients. The same pattern was seen in household controls. In addition, an individual severe ME/CFS patient's 'IgG positive' microbial community is more similar to their own 'IgG negative' microbial community than 'IgG positive' microbes of other patients. Comparisons of the number of species binding serum IgG in severe ME/CFS patients to the number of species binding serum IgG in matched household controls did not find any significant differences. When analysing the probability of a microbe within a given taxa being bound by IgG, *C. jejuni* and *P. viridiflava* have a non-significant increase in likelihood of being coated by IgG in severe ME/CFS patients compared to matched household controls.

Finally, predictive functional profiling of the stool microbiome revealed 11 % of the explained variance in the abundance of gene families separates severe ME/CFS patients from household controls. In addition, 13 % of the explained variance in the likelihood of gene families being more or less abundant in 'IgG positive' stool microbes compared to 'IgG negative' stool microbes separate 5 severe ME/CFS patients from 4 household controls.

5.4.2 Taxonomic composition of both severe ME/CFS patients' stool microbes and their matched household controls' stool microbes

This study does not provide any evidence against the null hypothesis that there are no differences in the RMP and QMP of severe ME/CFS patients compared to their matched household controls. This is due to the small study size of 5 pairs of severe ME/CFS patients and matched household controls having insufficient power to detect differences between groups following correction for multiple comparisons. However, from investigating individual taxa, there were differences in both

the RMP and QMP of severe ME/CFS patients compared to their matched household controls prior to FDR correction, that may have been significant if there was the power to detect them. This highlights the need for caution when interpreting findings from *p* values prior to FDR correction as false positive results (type I errors) are not removed.

At the phylum-level both the relative abundance and microbial load of Basidiomycota, a Eukaryote, are higher in severe ME/CFS patients compared to their matched household controls, with $p < 0.05$ prior to FDR correction. Furthermore, the phyla Apicomplexa and Ascomycota from the Eukaryote domain have lower relative abundances in severe ME/CFS patients compared to their matched household controls, with $p < 0.05$ prior to FDR correction. Interestingly, a previous study has also found an increase in the relative abundance of Basidiomycota and a decrease in the relative abundance of Ascomycota in ME/CFS patients (Mandarano et al., 2018). In addition, the fungi *M. restricta* has higher relative abundances and microbial loads in severe ME/CFS patients compared to their matched household controls at both the genus- and species-level, with $p < 0.05$ prior to FDR correction. Fungi cannot be detected using 16S rRNA sequencing which leaves a limited number of ME/CFS microbiome studies for comparison. None of the studies using WGS sequencing found altered levels of *Malassezia* or *M. restricta* in ME/CFS patients (Guo et al., 2021, Nagy-Szakal et al., 2017, Raijmakers et al., 2020).

Both the relative abundances and microbial loads of 6 genera are lower in severe ME/CFS patients compared to their matched household controls, with $p < 0.05$ prior to FDR correction; *Citrobacter, Ligilactobacillus, Longibaculum, Microvirgula, Pluribacter* and *Roseburia*. Furthermore, the relative abundances and microbial loads of 6 species are lower in severe ME/CFS patients compared to their matched household controls, with $p < 0.05$ prior to FDR correction; *A. megaguti, L. ruminis, L. sp. KGMB06250, M. aerodenitrificans, P. gergoviae* and *R. intestinalis*. However, only a decrease in the relative abundance of *Roseburia* and *R. intestinalis* in ME/CFS patients is also found by others (Frémont et al., 2013, Guo et al., 2021, Nagy-Szakal et al., 2017). It is important to note that two of these studies further stratified ME/CFS patients into those with and those without IBS, with one study finding a decrease in *Roseburia* only in patients with comorbid IBS (Guo et al., 2021, Nagy-Szakal et al., 2017). However, Guo et al. (2021) found a decrease in the microbial load of *Roseburia* in ME/CFS patients with IBS and ME/CFS patients without IBS, suggesting ME/CFS associated shifts in *Roseburia* levels. Depletion of *R. intestinalis* in ME/CFS patients with IBS but not ME/CFS patients without IBS has been noted previously (Nagy-Szakal et al., 2017). Our study only compares severe ME/CFS patients with IBS to matched household controls without ME/CFS or IBS, so associations with ME/CFS patient status independent of IBS status cannot be made.

The community structure of the intestinal microbiome was assessed using alpha and beta diversity measures, which assess the intra- and inter- sample diversity respectively. The sample size in the

current study had the statistical power to reject the null hypothesis that there was no significant difference in alpha diversity measures between severe ME/CFS patients and matched household controls. However, all measures of alpha diversity are not significantly different between severe ME/CFS patients and their matched household controls, supporting the null hypothesis. This is in contrast to a previous study conducted by Giloteaux et al. (2016) who found a significant reduction in species richness, Shannon H and Chao1 diversity scores in ME/CFS patients. These differences could be due to the sequencing method used. Giloteaux et al. (2016) used 16S rRNA sequencing which identifies bacteria and archaea whereas the present study used WGS sequencing which, in addition to bacteria and archaea, identifies viruses, protozoa and fungi. Also, 16S rRNA sequencing does not identify rare taxa whereas WGS does. Only one other study has measured alpha diversity on WGS sequencing data and found significantly lower evenness and Shannon diversity scores in ME/CFS patients but no significant differences in observed species scores (Guo et al., 2021).

The sample size was too small to apply statistical methods to determine whether beta diversity was significantly different between severe ME/CFS patients and their matched household controls. Instead, the Bray-Curtis dissimilarities had to be interpreted visually. Samples from household controls had the smallest distances clustering together whereas samples from the severe ME/CFS patients did not form clusters and instead had large distances from the household control cluster and from other patient samples. This visual interpretation indicates the household control cohort are more homogeneous than the severe ME/CFS patient cohort.

Overall, this research was unable to confirm that severe ME/CFS patients have microbial dysbiosis or enriched or depleted taxa. Comparing the taxa that were different between severe ME/CFS patients and matched household controls prior to FDR correction to previous studies highlights which taxa may be significant had this study had the power to detect them. The taxa found in this study to be different between severe ME/CFS patients and matched household controls, which were not found in previous studies, may be examples of false positive results. Alternatively, these taxa may not have been found to be enriched or depleted in ME/CFS patients in previous studies because of the geographic location used in this study. Fremont et al. (2013) demonstrated microbiome studies in different geographic locations find different taxa that are enriched or depleted in ME/CFS patients. To date no microbiome studies in ME/CFS patients conducted in the UK have been published. Therefore, further studies with larger sample sizes are needed to determine microbiome alterations in UK ME/CFS patients.

5.4.3 Functional potential of the intestinal microbiome in severe ME/CFS patients compared to household controls

This chapter investigates the functional potential of the microbiome using the abundance of gene families found in severe ME/CFS patients and household controls. However, as this study was

underpowered with regards to carrying out univariate analyses, the null hypothesis that there was no significant difference between the abundance of gene families in severe ME/CFS patients compared to their matched household controls could not be tested. Therefore, multivariate analysis of gene families' abundance in severe ME/CFS patients compared to household controls was undertaken and only 11 % of the variance of gene families' relative abundances can be explained by disease status. This suggests that there are other variables causing larger variation amongst the participants. For example diet, lifestyle and genetics are all known factors to affect the microbiome and therefore could also affect the functional potential of the microbiome (Conlon and Bird, 2014, Goodrich et al., 2014, Redondo-Useros et al., 2020). The impact of environmental factors on microbiome variation can be overcome using paired samples, which were used within the current study. However, one limitation of the multivariate analysis was that the patients and controls were treated as individual groups, instead of paired samples.

It is also important to note that the patient cohort had ME/CFS with IBS and the control cohort did not have ME/CFS or IBS. This means that it is not known if the explained variance of gene families separating patients from controls is due to the presence of ME/CFS, IBS or both. Nagy-Szakal et al. (2017) demonstrated the importance of subgrouping ME/CFS patients into those with IBS and those without IBS when analysing the functional capacity of the microbiome. Therefore, future studies should ensure IBS comorbidity is accounted for in study design.

5.4.4 Taxa from the intestinal microbiome binding to serum IgG in severe ME/CFS patients compared to matched household controls

Based on the hypothesis that ME/CFS patients have a leaky gut which allows the dissemination of intestinal microbes into the systemic circulation and to then stimulate B cell production of microbiome reactive IgG antibodies, either a higher number of taxa bound by serum IgG or a stronger serum IgG response to taxa in severe ME/CFS patients compared to their matched household controls was expected. Surprisingly, there is a high number of taxa bound by serum IgG in both severe ME/CFS patients and their matched household controls. A possible explanation as to why healthy household controls also have a high number of taxa reactive with serum IgG is the persistence of microbiome reactive IgG antibodies in the circulation in health following events such as excessive exercise, excessive alcohol consumption and the use of PPIs and NSAIDs (Haas et al., 2011, Mannon, 2019).

However, chapter 4 demonstrated that there is a large variation in the proportion of stool microbes bound by IgG in both the severe ME/CFS patients and matched household controls. Comparing the relative abundance of a taxon in the 'IgG positive' fraction to the 'IgG negative' fraction is limited in its interpretation because it does not account for the size of the 'IgG positive' and 'IgG negative' fractions. To overcome this limitation Jackson et al. (2021) proposed the use of probability ratios.

Therefore, the IgG probability ratio to quantify serum IgG binding to individual taxon was used. This study is unable to provide any evidence against the null hypothesis that there are no differences in the IgG probability ratios of severe ME/CFS patients compared to their matched household controls because the study was underpowered and therefore not able to detect significant differences between groups following correction for multiple comparisons. However, species *C. jejuni* and *P. viridiflava* have higher IgG probability ratios in severe ME/CFS patients compared to that of their matched household controls, with $p < 0.05$ prior to FDR correction. It is important to note that the IgG probability ratio does not consider the abundance of taxa within a stool sample. Therefore, follow-up studies to quantify the levels of IgG binding to cellular isolates at a constant concentration should be done to complement this analysis. Undertaking this would confirm if severe ME/CFS patients have higher levels of IgG binding to *C. jejuni* and *P. viridiflava* than their matched household controls.

IgG probability ratio scores for each taxa are heterogenous amongst severe ME/CFS patients and household controls. Despite *C. jejuni* and *P. viridiflava* having higher IgG probability ratios in all severe ME/CFS patients compared to their matched household controls, the IgG probability ratio scores for *C. jejuni* and *P. viridiflava* are not the taxa with the highest IgG probability ratios for each severe ME/CFS patient. For example, the maximum IgG probability ratio scores recorded in severe ME/CFS patients for *C. jejuni* and *P. viridiflava* is 0.09 and 0.18 respectively. The maximum IgG probability ratio score in the patient from pair 1 is 0.43 for *Streptococcus sp. 'group B'*, patient from pair 2 is 0.32 for *Sphingobium cloaecae*, patient from pair 3 is 0.78 for *Bacillus virus phi 29,* patient from pair 4 is 0.33 for *Brevundimonas diminuta* and patient from pair 5 is 0.31 for *Decholorosama suillum*. This demonstrates that the immune reactivity to intestinal microbes is individualised in each severe ME/CFS patient. This finding is in line with the aetiology of ME/CFS as the infectious onset seen in patients may not be caused by a single pathogen (Chu et al., 2019).

Finally, analysing the functional potential of intestinal microbes preferentially binding IgG complements the analysis of taxa preferentially bound by IgG as it enables the identification of gene families involved in the immunogenic function of those taxa. The IgG probability ratio was used to investigate gene families present in taxa that are preferentially bound by serum IgG. As this study was underpowered univariate analysis could not be undertaken and therefore gene families more or less prevalent in the 'IgG positive' fraction could not be determined. Instead, multivariate analysis was undertaken and only 13 % of the variance in gene families' IgG probability ratio scores can be explained by disease status. This analysis demonstrates the need to consider other control groups. The largest explained variance amongst the samples separates the patient in pair 3 from the rest of the participants which shows there is a factor other than disease status driving the preferential binding of serum IgG to microbes. In addition, matching controls to patients based on

households was not effective as paired participants did not cluster together. Other factors known to affect immune status include age, gender and BMI. Therefore, future studies should be undertaken comparing ME/CFS patients to age, gender and BMI matched controls.

6 CHAPTER SIX: GENERAL DISCUSSION

6.1 SUMMARY OF THESIS OUTCOMES

The main finding of this thesis was that severe ME/CFS patients have significantly lower levels of serum IgG reactive with heterologous stool bacteria compared to their matched household controls and no significant difference in levels of serum IgG reactive with autologous stool bacteria. These findings do not support the study hypothesis that ME/CFS patients have increased immune reactivity to the microbiome as a consequence of a leaky gut. Instead they suggest ME/CFS patients have an impaired IgG reactivity to intestinal microbes. This chapter discusses the impact of these findings on ME/CFS research and the strengths and weaknesses of the study. Finally, suggestions on the direction of future research are provided.

6.2 IMPACT OF THESIS FINDINGS

The primary aim of this thesis, addressed in chapter 4, was to determine whether severe ME/CFS patients have elevated levels of serum IgG antibodies to the microbiome. Instead, the results presented within this thesis showed that severe ME/CFS patients have significantly lower levels of serum IgG reactive with heterologous stool bacteria compared to their matched household controls. One explanation for the reduced levels of serum IgG to heterologous stool bacteria is that ME/CFS patients have a weakened immune response against 'foreign' antigens. Indeed, there is published evidence of impaired pathogen clearance in ME/CFS patients (reviewed in **section 1.2.1**). In addition, despite hypothesising that ME/CFS patients have a leaky gut and bacterial translocation, the severe ME/CFS patients did not have elevated serum IgG to autologous stool bacteria. These findings were unexpected because in patients with active IBD, a disease involving intestinal inflammation and a leaky gut, autologous immune reactivity was greater in patients than in healthy controls (Duchmann et al., 1995). This thesis findings together with what is already known about a leaky gut supports a weakened IgG immune response in ME/CFS. However, as a leaky gut and bacteria translocation is only present in a proportion of ME/CFS patients (Maes et al., 2007), there is the possibility that the severe ME/CFS patients recruited onto the AI-ME/CFS study did not have a leaky gut, which would also explain why the severe ME/CFS patients do not have higher IgG reactivity to autologous stool bacteria than their matched household controls. Confirmation that ME/CFS patients have reduced serum IgG to autologous stool microbes because of a weakened immune response in the presence of a leaky gut will require further studies.

Healthy household controls have higher serum IgG reactivity to heterologous stool bacteria than serum IgG reactivity to autologous stool bacteria. This was in line with a previous study which found immune tolerance exists towards autologous stool bacteria, presumably due to an intact gut

barrier, but an adaptive immune response is mounted against heterologous stool bacteria in health (Duchmann et al., 1995). In contrast, in severe ME/CFS patients serum IgG reactivity to autologous stool bacteria was comparable to serum IgG reactivity to heterologous stool bacteria. This supports the other findings presented in this thesis that ME/CFS patients have an impaired IgG immune response with hypo reactivity to both autologous and heterologous intestinal microbes. IgG deficiency is one mechanism which causes impaired IgG immune responses. However, the results in this thesis found no significant difference in the concentration of serum IgG between severe ME/CFS patients and matched household controls. Another mechanism which involves an impaired IgG immune response is immunosenescence (Aiello et al., 2019). Immunosenescence leads to a reduction in the function of the adaptive immune system, including reduced ability to produce high affinity antibodies to new antigens. Therefore, ME/CFS patients could have immunosenescence which impairs IgG immune response to recently translocated autologous stool bacteria and heterologous stool bacteria.

The secondary aim of this thesis, addressed in chapter 5, was to identify which autologous stool microbes had a serum IgG immune response. Based on the hypothesis, severe ME/CFS patients were expected to have a higher number of species evoking a serum IgG immune response, due to intestinal microbe translocation into the systemic circulation. However, the findings discussed in chapter 4 of an impaired serum IgG immune response suggest that patients would not have an IgG response to all translocated microbes. Indeed, severe ME/CFS patients and their matched household controls have a comparable number of species evoking a serum IgG immune response. However, when investigating the level of IgG binding to each species there was a non-significant increase in IgG binding to *C. jejuni* and *P. viridiflava* in severe ME/CFS patients compared to their matched household controls. *C. jejuni* is a foodborne pathogen which causes gastroenteritis and can predispose the onset of the autoimmune disease Guillain-Barré syndrome (Rodríguez et al., 2018). *P. viridiflava* is not a gut commensal but a plant pathogen which could be ingested when eating vegetables (Lipps et al., 2022). The increased IgG binding to *C. jejuni* and *P. viridiflava* could not be explained by the increased exposure of the systemic immune system to these species, as there were no significant differences in the abundance of these species within the stool sample. However, as anti-microbiota IgG antibodies are robust and circulate the periphery for many years, it could be that at an earlier date these species could have been elevated in severe ME/CFS patients. Longitudinal studies analysing the microbiome composition and immune reactivity would be able to identify the influence of dynamic changes of the microbiome on the level and diversity of anti-stool microbe IgG antibodies circulating in the blood.

This is the first study to analyse mucosal IgA reactivity to the intestinal microbiome in ME/CFS patients. Based upon the hypothesis that ME/CFS patients have microbial dysbiosis and intestinal

inflammation, it was anticipated that the severe ME/CFS patients would have higher secretory IgA which binds intestinal microbes, as this is what occurs in IBD (Palm et al., 2014). However, no significant differences in bound and non-bound secretory IgA concentrations were found between severe ME/CFS patients and their matched household controls. Stratifying the severe ME/CFS patients based on disease duration, as suggested by Hornig et al. (2015), the two patients with a disease duration greater than 5 years had higher microbe bound IgA concentrations compared to their matched household controls. This suggests that microbial dysbiosis and intestinal inflammation occur later in the course of disease progression. As previous studies have not compared microbial dysbiosis or intestinal inflammation in long versus short duration of illness these findings cannot be corroborated.

6.3 LIMITATIONS

6.3.1 Recruitment and sample collection

The biggest limitation of this thesis was participant recruitment. Five pairs of severe ME/CFS patients and matched household controls were recruited onto the AI-ME/CFS study, which was half of the target sample size. Analysing microbial composition of 5 pairs of severe ME/CFS patients and matched household controls was insufficient to detect significant changes following correction for multiplicity. Other microbiome studies in ME/CFS patients with significant findings recruited more than 30 cases and controls (Frémont et al., 2013, Giloteaux et al., 2016a, Guo et al., 2021, Nagy-Szakal et al., 2017, Raijmakers et al., 2020).

The choice to analyse severe ME/CFS patients in order to define a homogeneous group of ME/CFS patients hindered participant recruitment. This was because only 25 % of ME/CFS patients are categorised as severe (Pendergrast et al., 2016), resulting in a small pool of eligible patients. Furthermore, some severe ME/CFS patients lacked the capacity to provide informed consent, due to the severity of cognitive symptoms, which excluded them from the study. As a result, only 36 of 3812 ME/CFS patients registered with the ESTH CFS Service and the ECCHC ME/CFS Service were invited to participate in the study. Recruitment of matched household controls also hindered recruitment as severe ME/CFS patients were often unable to identify matched household controls who were healthy and fulfilled eligibility criteria.

Sample collection from severe ME/CFS patients introduced logistical challenges to the study as home visits had to be scheduled. This meant that both the chief investigator and phlebotomist had to travel to participants' homes to undertake the consenting procedure and sample collection. Collecting samples from ECCHC patients involved up to a two hour round trip and collecting samples from ESTH patients involved up to a 7 hour round trip. The study team attempted to schedule ESTH home visits for the same day and ECCHC home visits for the same day to minimise the length of

time travelling. However, this was further complicated because of the severity of symptoms these patients experienced, as patients only had a short window within a day during which they felt well enough to receive visitors.

6.3.2 The missing components of the intestinal microbiome

Chapter 3 describes how the 'bug FACS' method first developed by Palm et al. (2014) to detect mucosal IgA binding to stool bacteria was modified and optimised to enable the detection of serum IgG binding to both bacteria and fungi found within the stool. However, the method was not optimised for the detection of the virome and archaeome which are other components of the stool microbiome. Despite the 'bug FACS' method not being optimised to detect these additional components, archaea and viruses were detected in the stool samples of severe ME/CFS patients and matched household controls.

The detection of viruses using 'bug FACS' was not optimised due to the small size of viruses (ranging from 17 nm to 350 nm) being below the limit of detection of conventional flow cytometers (300-500 nm) (Lippé, 2018). Eukaryotic viruses are suspected to play a part in the onset of ME/CFS, as many researchers propose ME/CFS is triggered by an infectious disease (Blomberg et al., 2018). In addition, infections with specific viruses such as EBV and RRV have been recorded to predate ME/CFS onset (Hickie et al., 2006, Katz et al., 2009). In addition, viruses are a crucial component of the gut microbiome, termed the virome. The virome consists of bacteriophages (97.7 %), eukaryotic viruses (2.1 %) and archaeal viruses (0.1 %) (Gregory et al., 2020), which outnumber bacterial cells by as much as 10:1 (Mukhopadhya et al., 2019). Bacteriophages are thought to be able to shape the microbiome composition through the proposed mechanisms; kill the winner, biological weapon, community shuffling and emerging new bacterial strain (review in Mukhopadhya et al., 2019). They can indirectly modulate the immune system by lysing bacterial cells, releasing PAMPs which stimulate proinflammatory responses (Sinha and Maurice, 2019). In contrast, eukaryotic viruses directly modulate the immune system during both homeostasis and viral infection (Li et al., 2021). By excluding viruses from 'bug FACS' analysis the impact of the virome on the immune system in ME/CFS patients cannot be assessed.

6.3.3 Confounding variables

Microbiome studies are often limited by confounding variables, which reduce the capacity to identify disease specific microbiome alterations. One confounding variable demonstrated to affect the identification of ME/CFS disease associated microbiome changes is lifestyle and geographical location (Lupo et al., 2021). The results presented within this thesis also accounted for the effect of lifestyle and geographical location by recruiting matched household controls. However, there are additional confounding variables of microbiome studies which include gender, age, BMI, medications, stool consistency and frequency (Falony et al., 2019, Vujkovic-Cvijin et al., 2020).

Gender (Klein and Flanagan, 2016), age (Milan-Mattos et al., 2019) and BMI (Ilavská et al., 2012) are also confounding variables when studying the immune system. These confounding variables were not accounted for when matching patients and controls in this study. An alternative way to account for microbiome covariates is to adjust for these factors during multivariate differential abundance analysis. However, it was not possible to adjust for any further covariates in this study due to the small sample size. Another confounding variable of ME/CFS microbiome studies not accounted for in the AI-ME/CFS study patient cohort was IBS comorbidity (Nagy-Szakal et al., 2017). All severe ME/CFS patients in this study had comorbid IBS, whereas none of the controls had comorbid IBS. IBS patients have previously been shown to have changes in their microbiome composition (Wang et al., 2020). Therefore, it cannot be ruled out that microbiome changes found within this thesis were due to IBS comorbidity.

6.4 RECOMMENDATIONS FOR FUTURE WORK

6.4.1 Confirmation of thesis findings in a larger ME/CFS patient cohort

To confirm the findings presented in this thesis a second human study should be set up recruiting a larger cohort of ME/CFS patients. Power calculations using the results from this thesis would enable the determination of an appropriate sample size which would enable significant associations to be found.

To overcome the restrictions encountered recruiting severe ME/CFS patients, patient selection should instead focus on recruiting moderate ME/CFS patients who are able to attend appointments at recruitment centres. By recruiting moderate ME/CFS patients, who make up 50 % of the ME/CFS population, the target sample size is more likely to be met. However, the distinction between mild and moderate ME/CFS is not clearly defined by current case definitions. Therefore, the heterogeneity amongst the ME/CFS patient cohort will increase. One way to reduce this heterogeneity is to only recruit moderate ME/CFS patients who have evidence of a leaky gut. A leaky gut can be confirmed either by assessing sugar absorption in the gut by measuring sugars in urine (Khoshbin et al., 2021) or by measuring the intestinal permeability biomarkers in the blood such as LPS, LBP, intestinal fatty acid-binding protein (I-FABP), zonulin and sCD14 (Ohlsson et al., 2019).

The identification of a matched household control by the ME/CFS patients also restricted participant recruitment. This was because many ME/CFS patients were unable to identify somebody who lived with or cared for them who was free of health conditions and willing to participate in human trials. Therefore, age, gender and BMI matched healthy controls should instead be recruited. However, microbiome associated confounding variables such as diet, lifestyle and behaviour will need to be accounted for. One way to account for environmental influences is

to collect information on lifestyle and hygiene using 'the microbiome health questionnaire' used at the QIB. Previous microbiome studies have assessed study participants' diet using food frequency questionnaires or a 24-hour dietary recall (Johnson et al., 2020). However, these methods have disadvantages such as recall bias and not including information on food brands, which contain different nutrient contents. Phone apps, like Nutritics, is an alternative way to record diet and enables brands of food to be easily recorded.

To account for the contribution of IBS comorbidity to microbiome composition alterations found in ME/CFS patients three study cohorts should be recruited. These three study cohorts should either be: a) healthy controls, IBS controls and ME/CFS patients with comorbid IBS, or b) healthy controls, ME/CFS patients with IBS and ME/CFS patients without IBS.

6.4.2 'Bug FACS' modification for the detection of viruses

Conventional flow cytometers are unable to detect small particles sizes such as viruses. However, flow virometry can be performed by using either laboratory-built nano-flow cytometers, which have previously been optimised to detect light scattering of viruses as small as 27 nm (Ma et al., 2016), or by fluorescently labelling nucleic acids or lipids or by conjugating fluorescent antibodies to nanoparticles to enable detection of light scattering (Lippé, 2018). A number of flow cytometers have previously been modified to enable detection of viruses. These include the Guava® eacyCyte™ 8HT and BD® LSRFortessa II (Zamora and Aguilar, 2018). Therefore, flow virometry is a promising technique which could be included into 'bug FACS' protocols. The modification of the 'bug FACS' protocol to determine antibody binding to the virome using flow virometry should be considered.

6.5 CONCLUSION

This is the first study to investigate serum IgG immune reactivity to the intestinal microbiome in ME/CFS patients and it provides novel findings which suggest ME/CFS patients have an impaired serum IgG immune response to intestinal microbes. It also provides the basis for further investigation into the leaky gut hypothesis in ME/CFS patients.

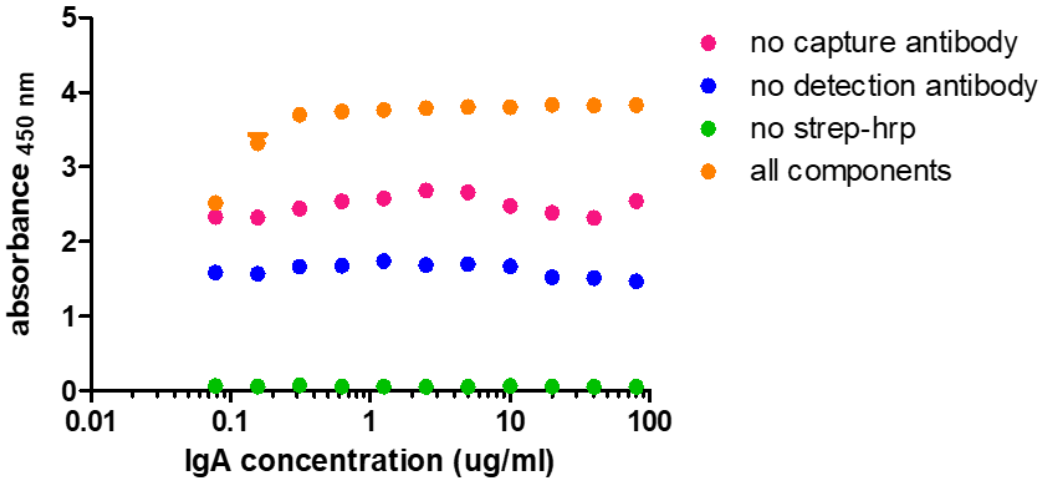

Supplementary figure 4.1: Trialling a previously published protocol for the detection of IgA1/2 in stool samples. *Stool IgA1/2 was measured in duplicate following Scholtens et al. (2008). The assay was performed with all components (orange), without capture antibody (pink), without detection antibody (blue) and without Streptavidin-HRP (green). Measurements were taken in duplicate. Mean ± SEM is represented on the graph.*

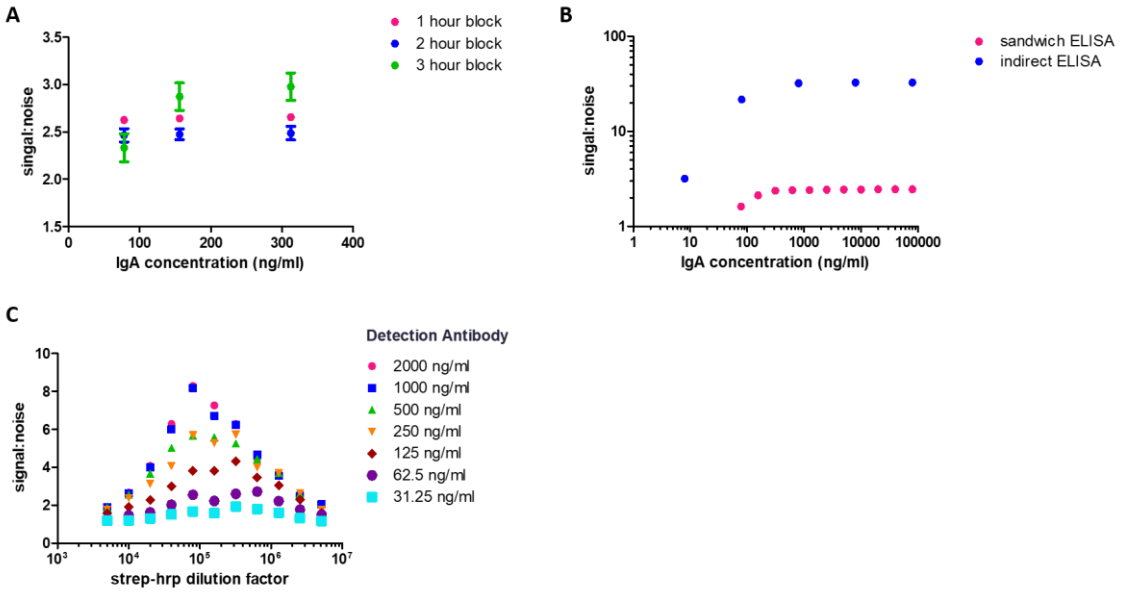

Supplementary figure 4.2: Optimising the ELISA method for detection of muscoal IgA in stool samples. *IgA from a human colostrum sample was used to optimise this method. A) comparing signal to noise ratio from different lengths of time plates were blocked. B) comparing signal to noise ratio of the published protocol (sandwich ELISA) to a modified version where ELISA plates were coated with stool samples instead of a capture antibody (indirect ELISA). C) Titrating streptavidin-HRP and detection antibodies to compare how the signal to noise ratio alters. All graphs display mean and the range of duplicate readings.*

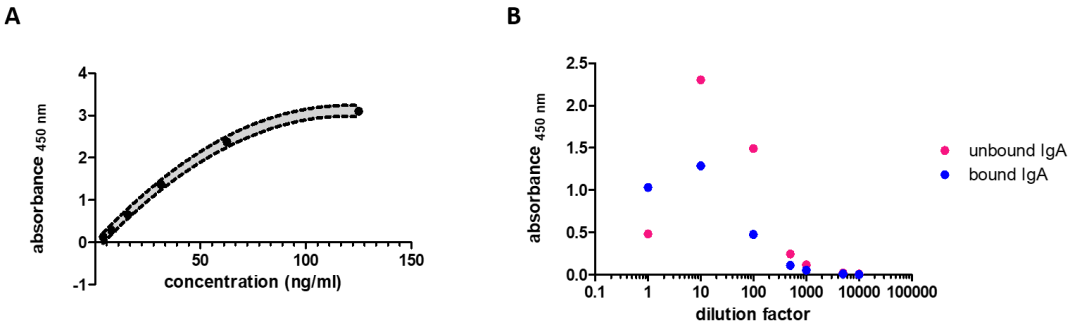

Supplementary figure 4.3: Standard curve for stool IgA measurement. *Representative sample of A) a standard curve and B) absorbance readings of stool IgA1/2. The standard curve was generated using quadratic logistic regression curve fit. The 95 % prediction band is displayed in grey. Mean± SEM is displayed on the graphs.*

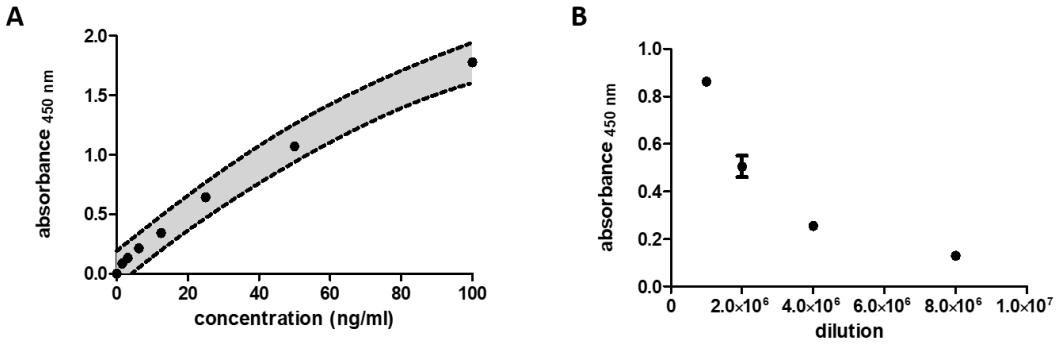

Supplementary figure 4.4: Standard curve for serum IgG measurement. *Representative sample of A) a standard curve and B) absorbance readings of serum IgG. The standard curve was generated using quadratic logistic regression curve fit. The 95 % prediction band is displayed in grey. Mean± SEM is displayed on the graphs.*

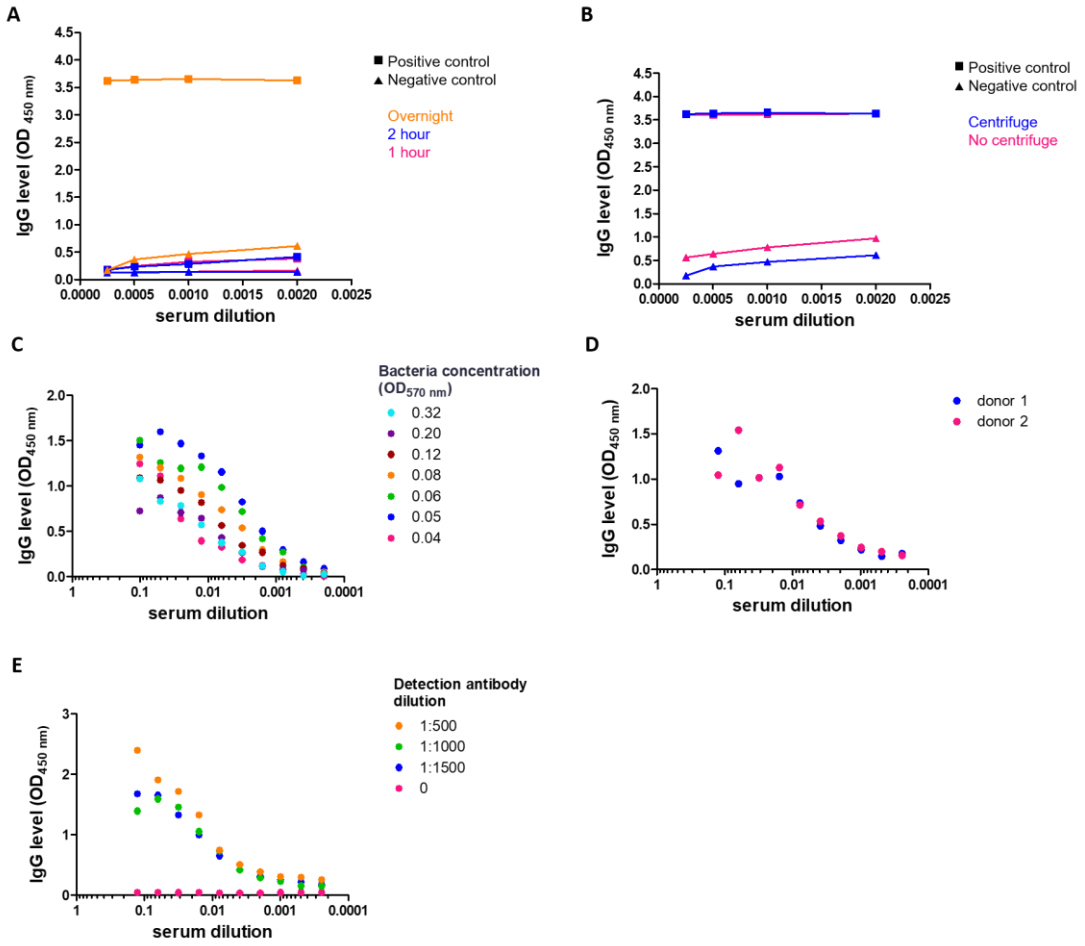

Supplementary figure 4.5: Optimising an ELISA based method for detecting autologous and heterologous stool microbe reactivity to serum IgG. *Stool microbes were incubated in Nunc ELISA MaxiSorp™ plates. Plates were washed and blocked, incubated with serum, then the detection antibody goat anti-human IgG-HRP, the TMB for colour development and sulphuric acid to quench the reaction. A) optimising the length of time stool microbes were incubated in the ELISA plate during the coating step, B) optimising the washing step by comparing plates undergoing centrifugation and plates not undergoing centrifugation, C) optimising the bacterial concentration used to coat the plates, D) optimising the serum dilution used, E) optiminising the concentration of detection antibody used. Serum from rabbits innoculated with stool microbes collected on day 0 (negative control) and day 57 (positive control) was used for optimisation in graphs A and B. Healthy donors' stool and serum samples were used for optimisation in graphs C, D and E. All points represent single values.*

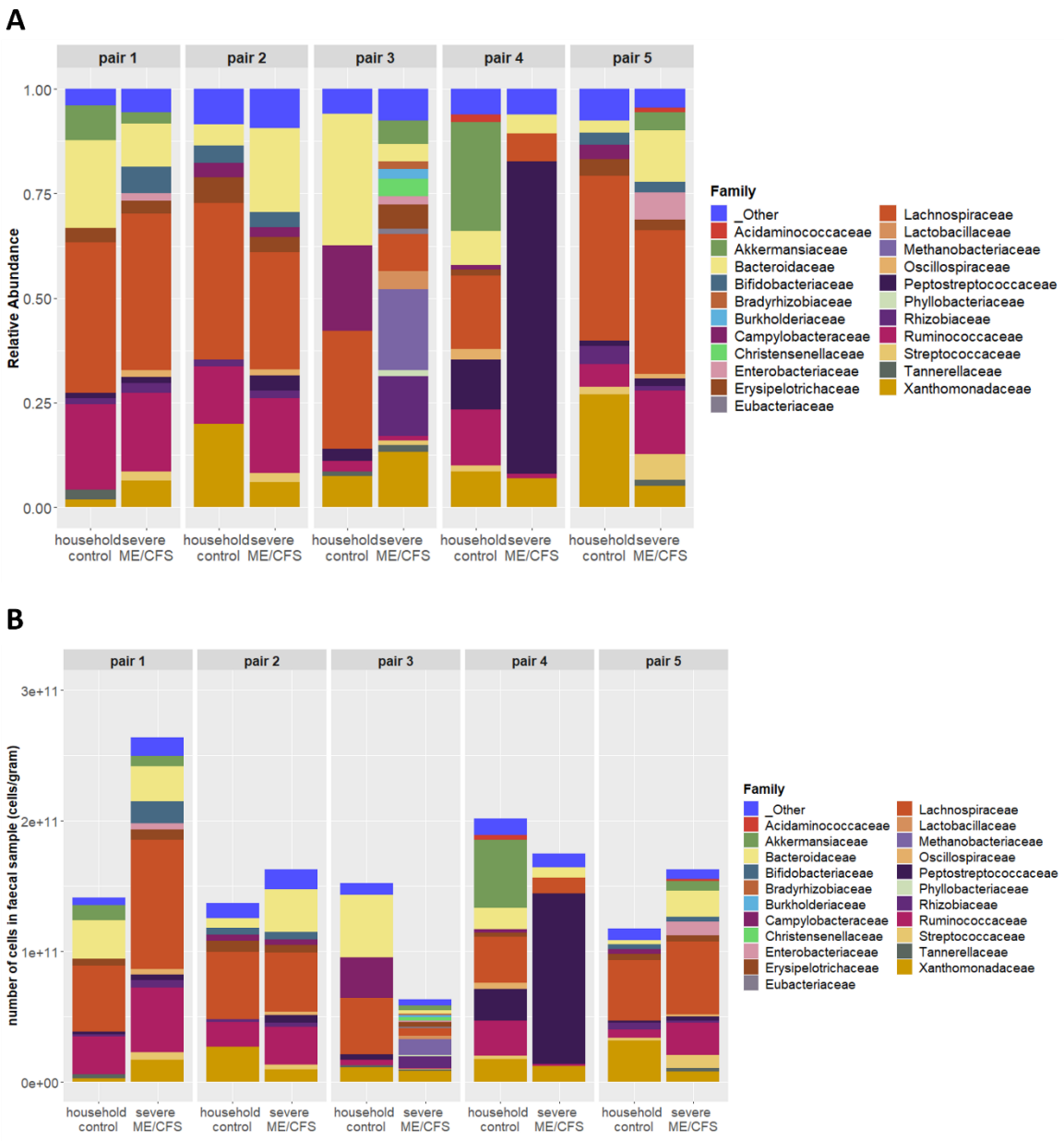

Supplementary figure 5.1: Composition of stool samples from severe ME/CFS patients and their matched household controls at the family-level. *A) Relative microbiome profiling and B) quantitative microbiome profiling of taxa present at a relative abundance greater than 0.01. Stool microbes from severe ME/CFS patients (n=5) and their matched household controls (n=5) were stained with SYBR™ green I nucleic acid gel stain and 'sybr green high' cells were collected using the Sony SH800S cell sorter and shotgun metagenomic sequencing was performed to identify the taxa present in each sample.*

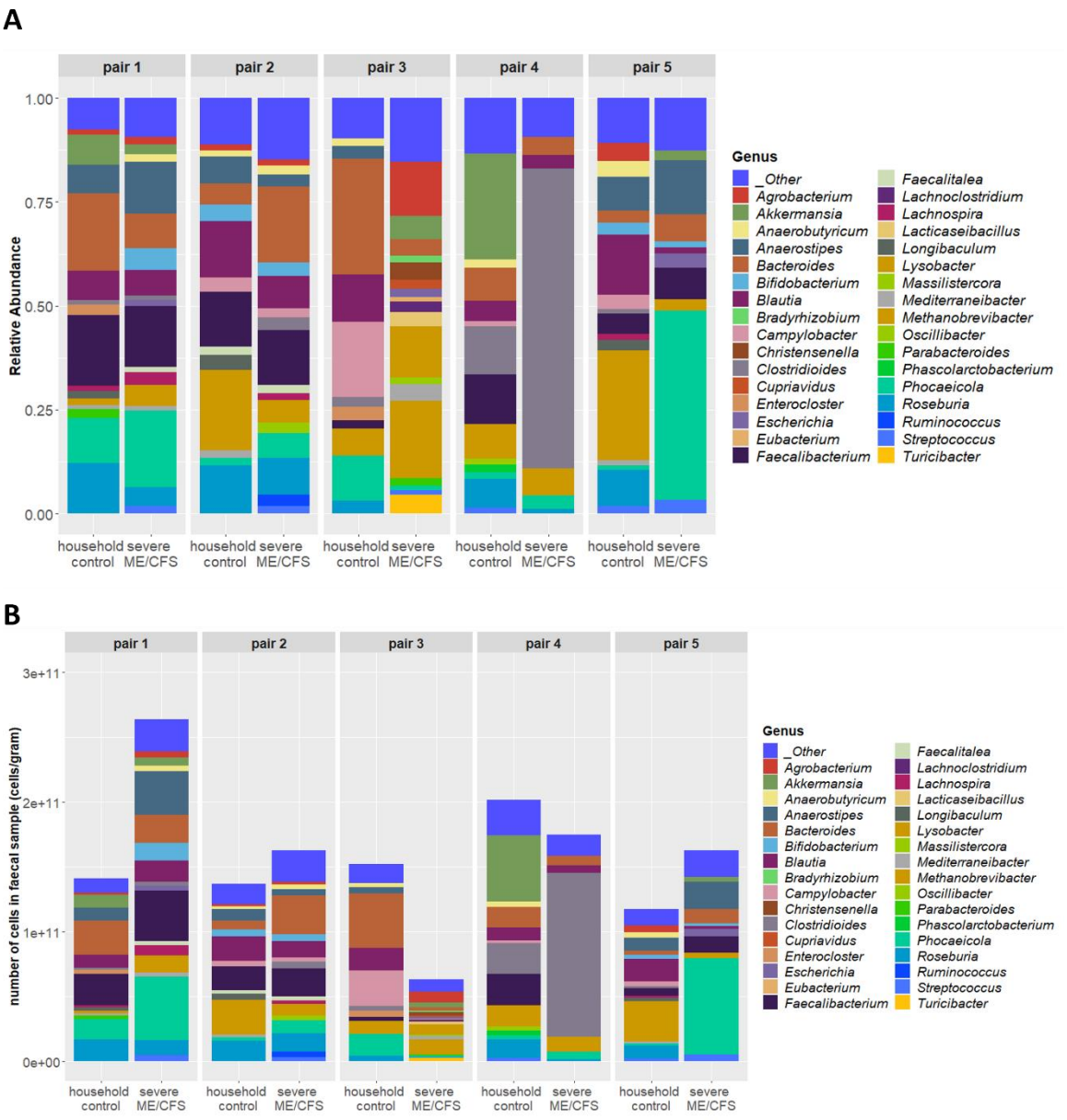

Supplementary figure 5.2: Composition of stool samples from severe ME/CFS patients and their matched household controls at the genus-level. *A) Relative microbiome profiling and B) quantitative microbiome profiling of taxa present at a relative abundance greater than 0.01. Stool microbes from severe ME/CFS patients (n=5) and their matched household controls (n=5) were stained with SYBR™ green I nucleic acid gel stain and 'sybr green high' cells were collected using the Sony SH800S cell sorter and shotgun metagenomic sequencing was performed to identify the taxa present in each sample.*

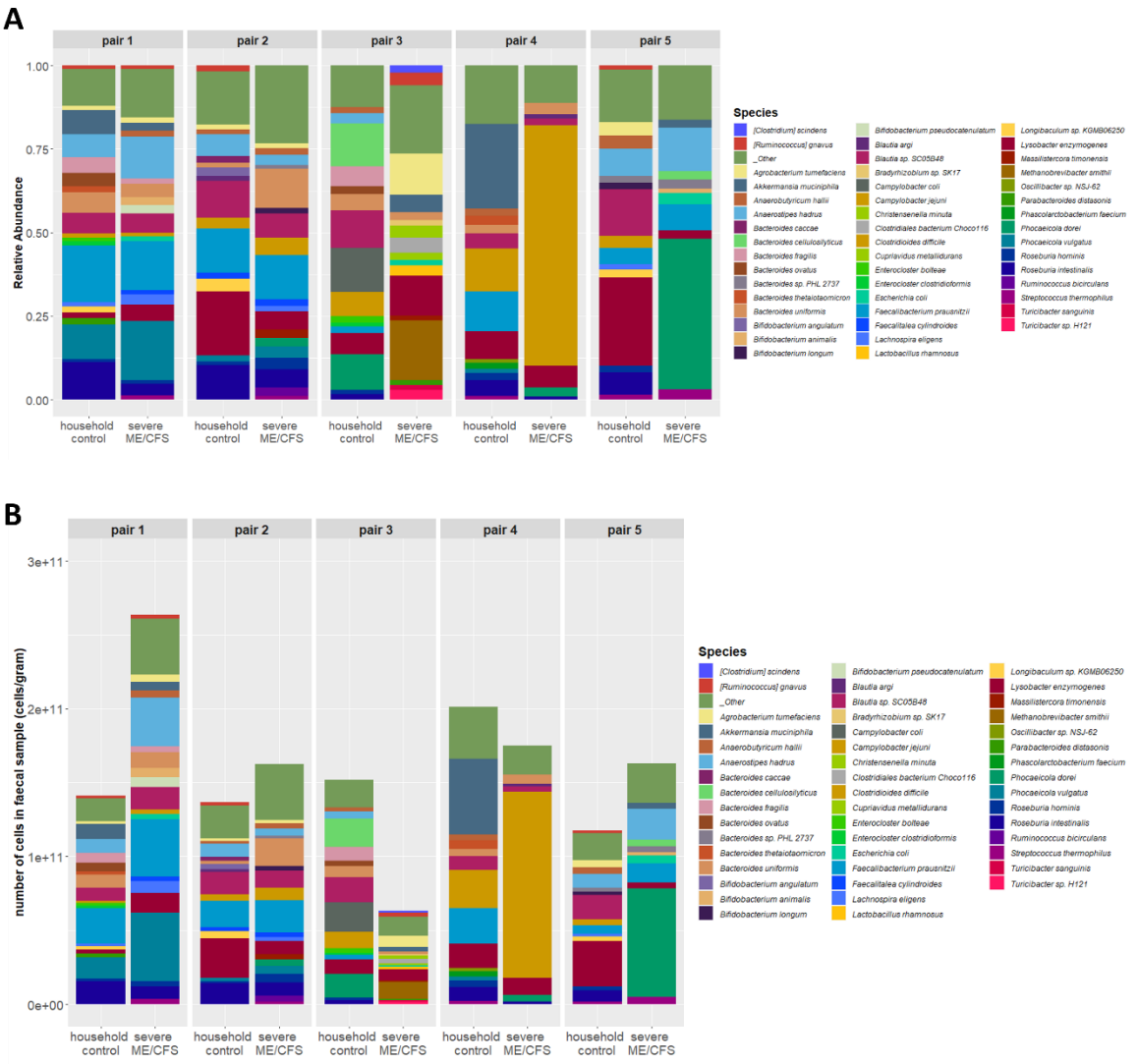

Supplementary figure 5.3: Composition of stool samples from severe ME/CFS patients and their matched household controls at the species-level. *A) Relative microbiome profiling and B) quantitative microbiome profiling of taxa present at a relative abundance greater than 0.01. Stool microbes from severe ME/CFS patients (n=5) and their matched household controls (n=5) were stained with SYBR™ green I nucleic acid gel stain and 'sybr green high' cells were collected using the Sony SH800S cell sorter and shotgun metagenomic sequencing was performed to identify the taxa present in each sample.*

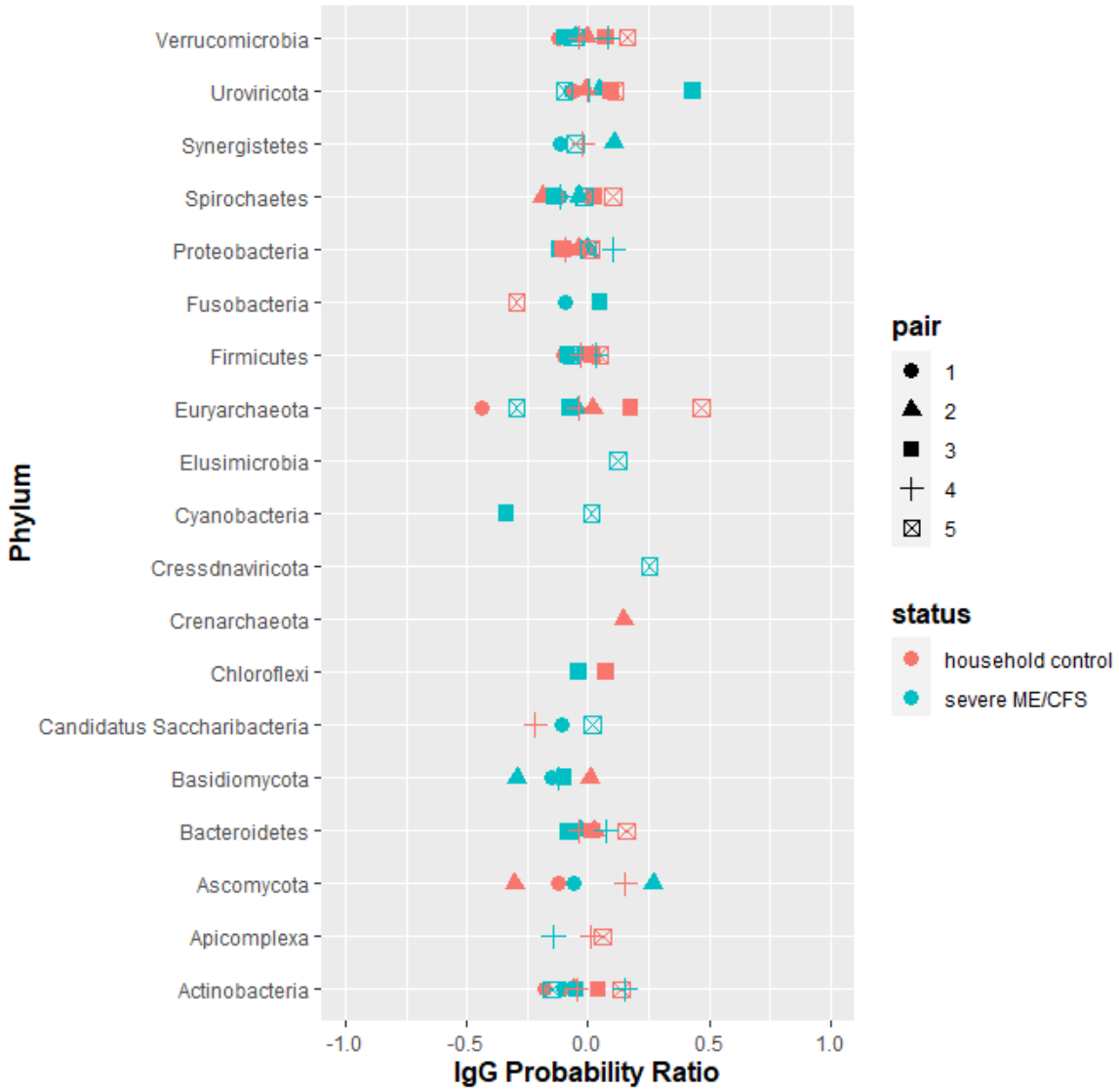

Supplementary figure 5.4: IgG probability ratios on taxa at the phylum-level. *Stool microbes from severe ME/CFS patients (n=5) and their matched household controls (n=5) were incubated with serum IgG in vitro. 'IgG positive' fractions and 'IgG negative' fractions were subsequently collected using the Sony SH800S cell sorter and shotgun metagenomic sequencing was performed to identify the relative abundance of taxa present in the sorted fractions from each participant. The IgG probability ratio was used to calculate the likelihood of a taxon being coated by IgG.*

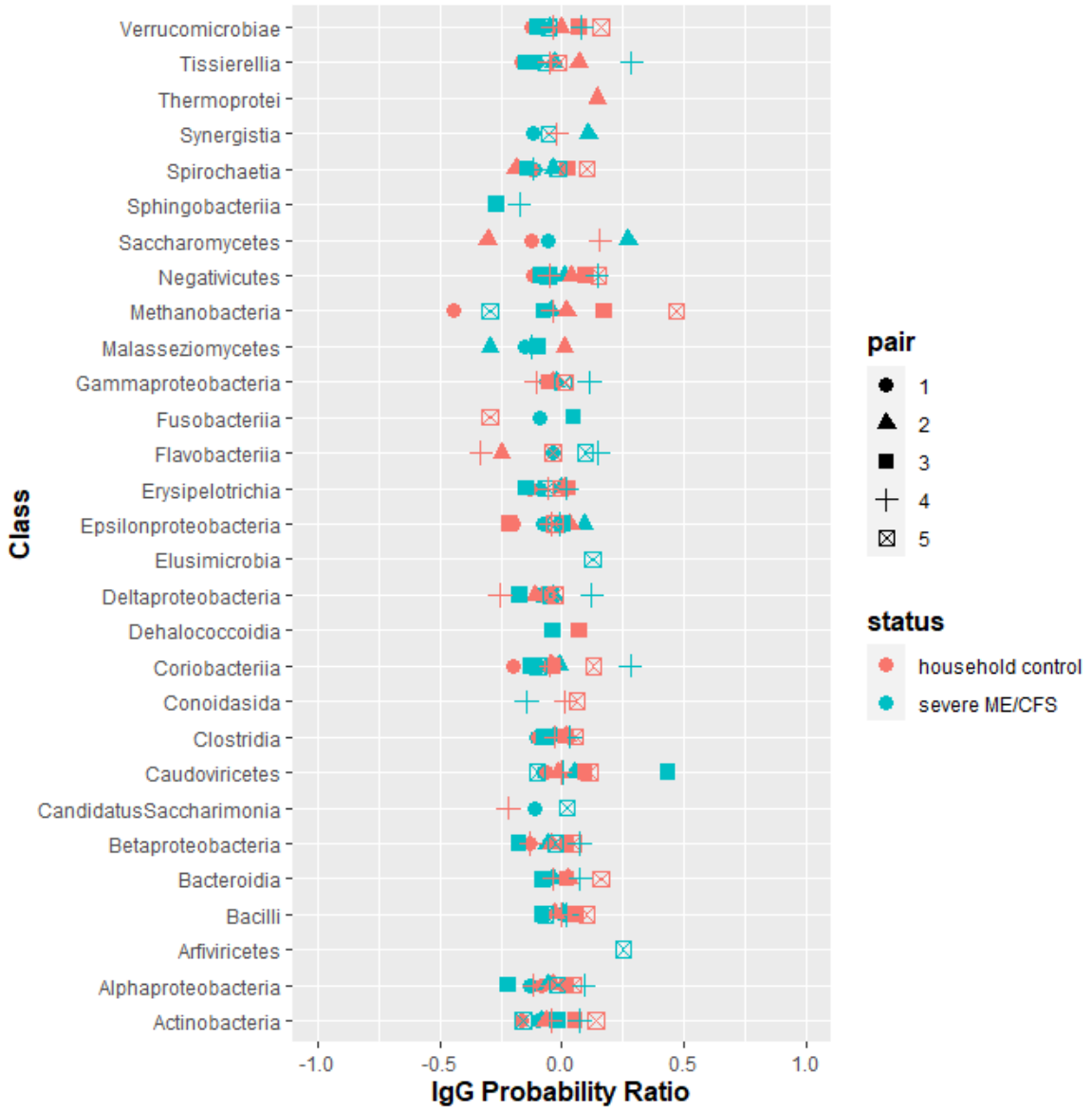

Supplementary figure 5.5: IgG probability ratios on taxa at the class-level. *Stool microbes from severe ME/CFS patients (n=5) and their matched household controls (n=5) were incubated with serum IgG in vitro. 'IgG positive' fractions and 'IgG negative' fractions were subsequently collected using the Sony SH800S cell sorter and shotgun metagenomic sequencing was performed to identify the relative abundance of taxa present in the sorted fractions from each participant. The IgG probability ratio was used to calculate the likelihood of a taxon being coated by IgG.*

Supplementary figure 5.6: IgG probability ratios on taxa at the order-level. *Stool microbes from severe ME/CFS patients (n=5) and their matched household controls (n=5) were incubated with serum IgG in vitro. 'IgG positive' fractions and 'IgG negative' fractions were subsequently collected using the Sony SH800S cell sorter and shotgun metagenomic sequencing was performed to identify the relative abundance of taxa present in the sorted fractions from each participant. The IgG probability ratio was used to calculate the likelihood of a taxon being coated by IgG.*

pair
1
2
3
4
5
status
household control
severe ME/CFS
Family
IgG Probability Ratio
1.0
0.5
0.0
-0.5
-1.0
Xanthomonadaceae
Xanthobacteraceae
Weeksellaceae
Veillonellaceae
Tissierellaceae
Tannerellaceae
Synergistaceae
Sutterellaceae
Sulfuricellaceae
Sulfolobaceae
Streptococcaceae
Staphylococcaceae
Spirochaetaceae
Sphingomonadaceae
Sphingobacteriaceae
Siphoviridae
Shewanellaceae
Selenomonadaceae
Sarcocystidae
Saccharomycetaceae
Ruminococcaceae
Rikenellaceae
Rhodocyclaceae
Rhodobacteraceae
Rhizobiaceae
Pseudomonadaceae
Propionibacteriaceae
Prevotellaceae
Porphyromonadaceae
Podoviridae
Phyllobacteriaceae
Peptostreptococcaceae
Peptoniphilaceae
Pasteurellaceae
Paenibacillaceae
Oxalobacteraceae
Oscillospiraceae
Oscillatoriaceae
Odoribacteraceae
Nostocaceae
Nocardiaceae
Myoviridae
Mycobacteriaceae
Muribaculaceae
Morganellaceae
Moraxellaceae
Micrococcaceae
Microbacteriaceae
Methylobacteriaceae
Methanobacteriaceae
Malasseziaceae
Family
IgG Probability Ratio
1.0
0.5
0.0
-0.5
-1.0
Leuconostocaceae
Leptotrichiaceae
Lactobacillaceae
Lachnospiraceae
Hyphomicrobiaceae
Hungateiclostridiaceae
Fusobacteriaceae
Flavobacteriaceae
Eubacteriaceae
Erythrobacteraceae
Erysipelotrichaceae
Enterococcaceae
Enterobacteriaceae
Elusimicrobiaceae
Eggerthellaceae
Dysgonomonadaceae
Desulfovibrionaceae
Desulfomicrobiaceae
Dermabacteraceae
Dehalococcoidaceae
Debaryomycetaceae
Corynebacteriaceae
Coriobacteriaceae
Comamonadaceae
ClostridialesFamilyXIII.IncertaeSedis
Clostridiaceae
Circoviridae
Chromobacteriaceae
Christensenellaceae
Caulobacteraceae
Carnobacteriaceae
CandidatusNanosynbacteraceae
Campylobacteraceae
Burkholderiaceae
Brucellaceae
Brevibacteriaceae
Bradyrhizobiaceae
Brachyspiraceae
Bifidobacteriaceae
Barnesiellaceae
Bacteroidaceae
Bacillaceae
Atopobiaceae
Alcaligenaceae
Akkermansiaceae
Aeromonadaceae
Aerococcaceae
Actinomycetaceae
Acidaminococcaceae
Acetobacteraceae

← ***Supplementary figure 5.7: IgG probability ratios on taxa at the family-level.*** *Stool microbes from severe ME/CFS patients (n=5) and their matched household controls (n=5) were incubated with serum IgG in vitro. 'IgG positive' fractions and 'IgG negative' fractions were subsequently collected using the Sony SH800S cell sorter and shotgun metagenomic sequencing was performed to identify the relative abundance of taxa present in the sorted fractions from each participant. The IgG probability ratio was used to calculate the likelihood of a taxon being coated by IgG.*

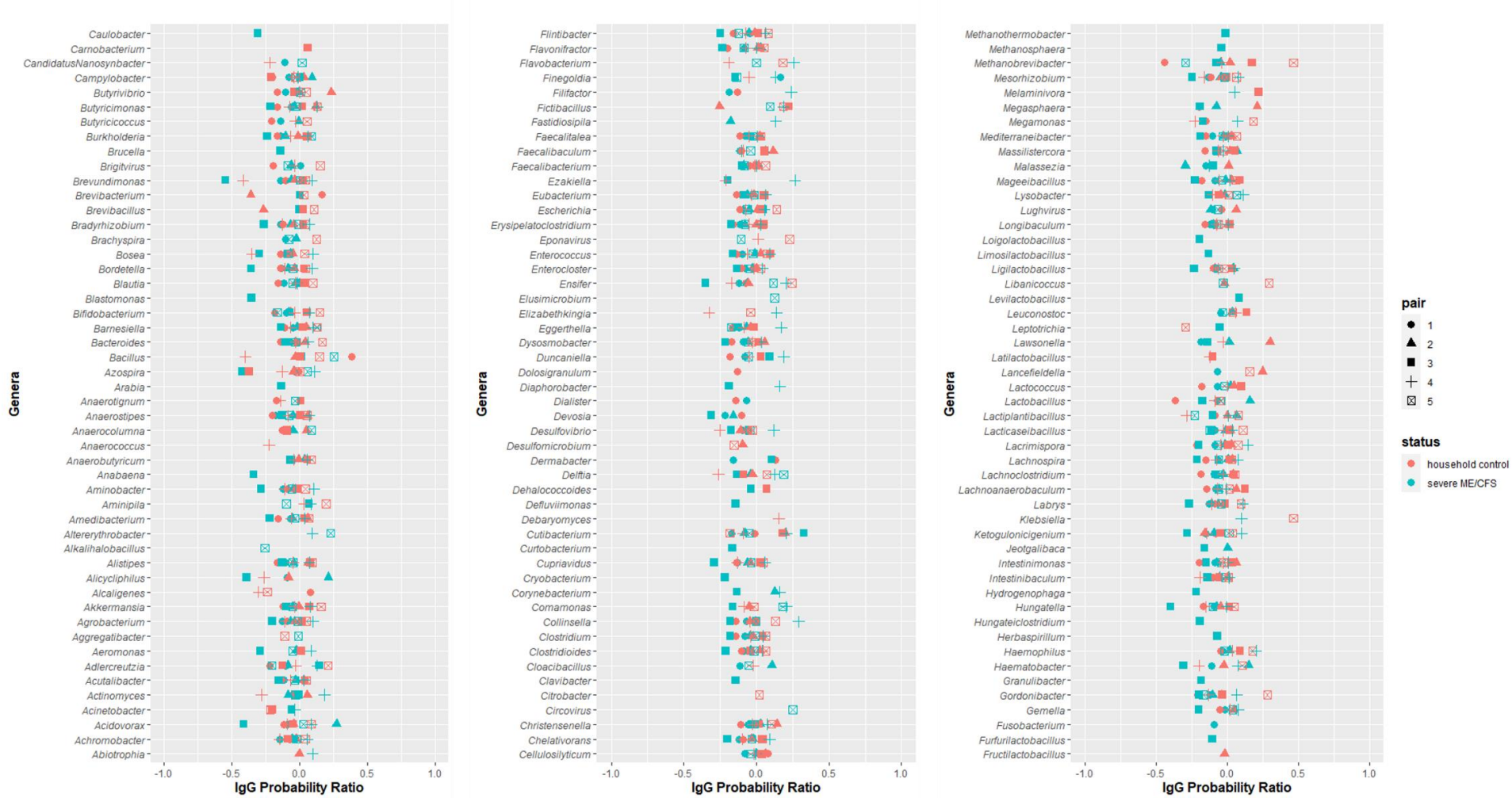
Genera
Caulobacter
Carnobacterium
CandidatusNanosynbacter
Campylobacter
Butyrivibrio
Butyricimonas
Butyricicoccus
Burkholderia
Brucella
Brigitvirus
Brevundimonas
Brevibacterium
Brevibacillus
Bradyrhizobium
Brachyspira
Bosea
Bordetella
Blautia
Blastomonas
Bifidobacterium
Barnesiella
Bacteroides
Bacillus
Azospira
Arabia
Anaerotignum
Anaerostipes
Anaerocolumna
Anaerococcus
Anaerobutyricum
Anabaena
Aminobacter
Aminipila
Amedibacterium
Altererythrobacter
Alkalihalobacillus
Alistipes
Alicycliphilus
Alcaligenes
Akkermansia
Agrobacterium
Aggregatibacter
Aeromonas
Adlercreutzia
Acutalibacter
Actinomyces
Acinetobacter
Acidovorax
Achromobacter
Abiotrophia
-1.0
-0.5
0.0
0.5
1.0
IgG Probability Ratio
Genera
Flintibacter
Flavonifractor
Flavobacterium
Finegoldia
Filifactor
Fictibacillus
Fastidiosipila
Faecalitalea
Faecalibaculum
Faecalibacterium
Ezakiella
Eubacterium
Escherichia
Erysipelatoclostridium
Eponavirus
Enterococcus
Enterocloster
Ensifer
Elusimicrobium
Elizabethkingia
Eggerthella
Dysosmobacter
Duncaniella
Dolosigranulum
Diaphorobacter
Dialister
Devosia
Desulfovibrio
Desulfomicrobium
Dermabacter
Delftia
Dehalococcoides
Defluviimonas
Debaryomyces
Cutibacterium
Curtobacterium
Cupriavidus
Cryobacterium
Corynebacterium
Comamonas
Collinsella
Clostridium
Clostridioides
Cloacibacillus
Clavibacter
Citrobacter
Circovirus
Christensenella
Chelativorans
Cellulosilyticum
-1.0
-0.5
0.0
0.5
1.0
IgG Probability Ratio
Genera
Methanothermobacter
Methanosphaera
Methanobrevibacter
Mesorhizobium
Melaminivora
Megasphaera
Megamonas
Mediterraneibacter
Massilistercora
Malassezia
Mageeibacillus
Lysobacter
Lughvirus
Longibaculum
Loigolactobacillus
Limosilactobacillus
Ligilactobacillus
Libanicoccus
Levilactobacillus
Leuconostoc
Leptotrichia
Lawsonella
Latilactobacillus
Lancefieldella
Lactococcus
Lactobacillus
Lactiplantibacillus
Lacticaseibacillus
Lacrimispora
Lachnospira
Lachnoclostridium
Lachnoanaerobaculum
Labrys
Klebsiella
Ketogulonicigenium
Jeotgalibaca
Intestinimonas
Intestinibaculum
Hydrogenophaga
Hungatella
Hungateiclostridium
Herbaspirillum
Haemophilus
Haematobacter
Granulibacter
Gordonibacter
Gemella
Fusobacterium
Furfurilactobacillus
Fructilactobacillus
-1.0
-0.5
0.0
0.5
1.0
IgG Probability Ratio
pair
1
2
3
4
5
status
household control
severe ME/CFS

pair
1
2
3
4
5
status
household control
severe ME/CFS
IgG Probability Ratio
1.0
0.5
0.0
-0.5
-1.0
Genera
Xanthobacter
Weissella
Veillonella
Turicibacter
Trueperella
Treponema
Toxoplasma
Toutatisvirus
Tissierella
Thermoclostridium
Tetragenococcus
Tardiphaga
Tardibacter
Taranisvirus
Tannerella
Sutterella
Sulfuriferula
Streptococcus
Stenotrophomonas
Starkeya
Stappia
Staphylococcus
Sphingopyxis
Sphingomonas
Sphingobium
Sphingobacterium
Sinorhizobium
Shinella
Shewanella
Schleiferilactobacillus
Schaalia
Scardovia
Salmonella
Salasvirus
Saccharomyces
Saccharolobus
Ruthenibacterium
Ruminococcus
Rothia
Roseovarius
Roseburia
Romboutsia
Rhodopseudomonas
Rhodococcus
Rhizobium
Ralstonia
Pseudoxanthomonas
Pseudomonas
Pseudobutyrivibrio
Propionimicrobium
Prevotella
Porphyromonas
Porphyrobacter
Polymorphum
Pluralibacter
Pigmentiphaga
Phoenicibacter
Phocaeicola
Phascolarctobacterium
Petrimonas
Peribacillus
Peptoniphilus
Peptacetobacter
Pediococcus
Pauljensenia
Paucibacter
Parvimonas
Parolsenella
Parascardovia
Paraprevotella
Paracoccus
Parabacteroides
Pannonibacter
Pandoraea
Paeniclostridium
Paenibacillus
Oxalobacter
Oscillibacter
Oscillatoria
Olsenella
Oligotropha
Oengusvirus
Odoribacter
Ochrobactrum
Novosphingobium
Nitrobacter
Nitratireductor
Ndongobacter
Myroides
Mycolicibacterium
Muribaculum
Murdochiella
Morganella
Moraxella
Monoglobus
Mogibacterium
Mobiluncus
Microvirgula
Microbacterium
Methylorubrum
Methylobacterium

← *Supplementary figure 5.8: IgG probability ratios on taxa at the genus-level.* *Stool microbes from severe ME/CFS patients (n=5) and their matched household controls (n=5) were incubated with serum IgG in vitro. 'IgG positive' fractions and 'IgG negative' fractions were subsequently collected using the Sony SH800S cell sorter and shotgun metagenomic sequencing was performed to identify the relative abundance of taxa present in the sorted fractions from each participant. The IgG probability ratio was used to calculate the likelihood of a taxon being coated by IgG.*

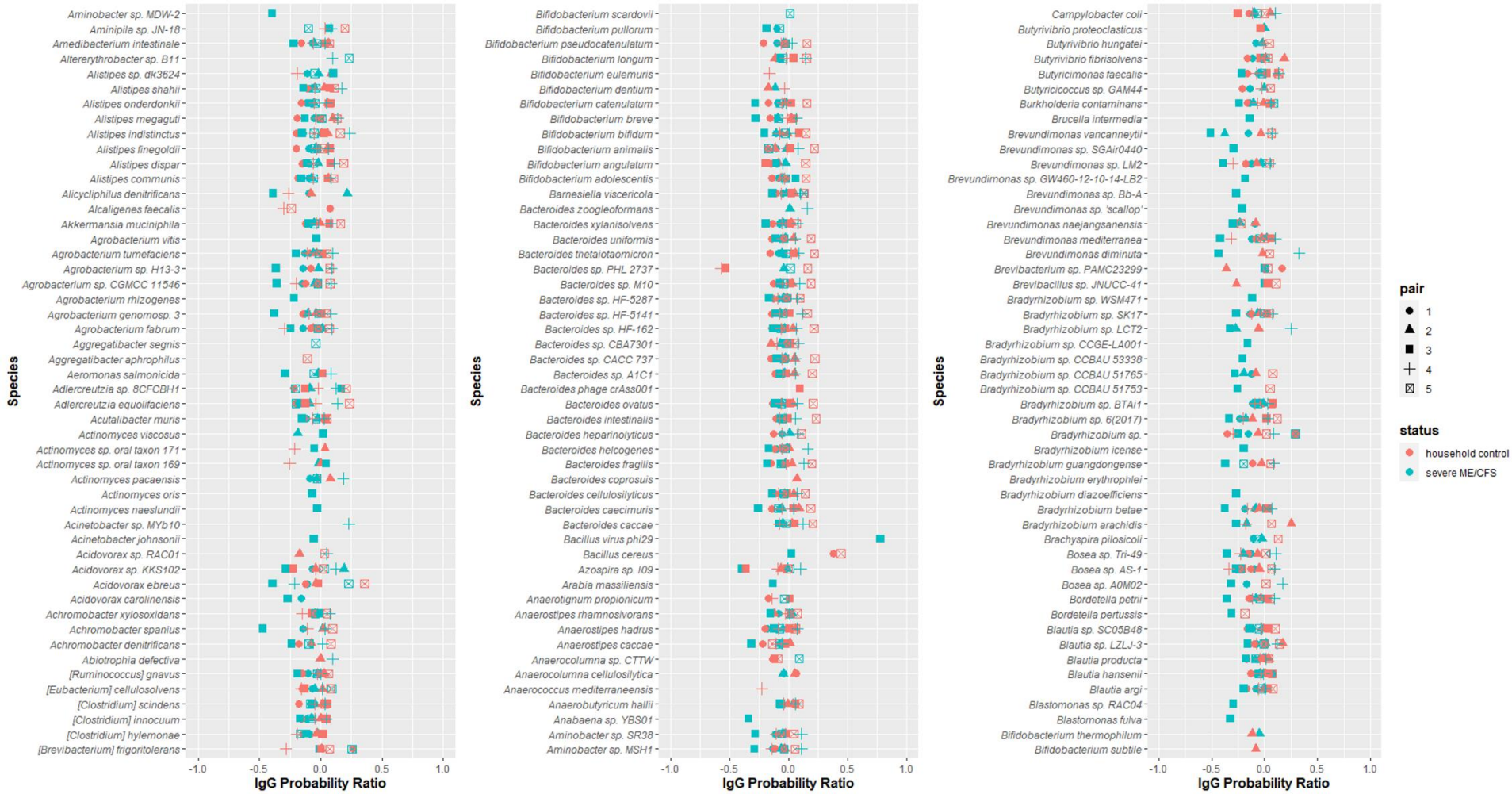
Species
Aminobacter sp. MDW-2
Aminipila sp. JN-18
Amedibacterium intestinale
Altererythrobacter sp. B11
Alistipes sp. dk3624
Alistipes shahii
Alistipes onderdonkii
Alistipes megaguti
Alistipes indistinctus
Alistipes finegoldii
Alistipes dispar
Alistipes communis
Alicycliphilus denitrificans
Alcaligenes faecalis
Akkermansia muciniphila
Agrobacterium vitis
Agrobacterium tumefaciens
Agrobacterium sp. H13-3
Agrobacterium sp. CGMCC 11546
Agrobacterium rhizogenes
Agrobacterium genomosp. 3
Agrobacterium fabrum
Aggregatibacter segnis
Aggregatibacter aphrophilus
Aeromonas salmonicida
Adlercreutzia sp. 8CFCBH1
Adlercreutzia equolifaciens
Acutalibacter muris
Actinomyces viscosus
Actinomyces sp. oral taxon 171
Actinomyces sp. oral taxon 169
Actinomyces pacaensis
Actinomyces oris
Actinomyces naeslundii
Acinetobacter sp. MYb10
Acinetobacter johnsonii
Acidovorax sp. RAC01
Acidovorax sp. KKS102
Acidovorax ebreus
Acidovorax carolinensis
Achromobacter xylosoxidans
Achromobacter spanius
Achromobacter denitrificans
Abiotrophia defectiva
[Ruminococcus] gnavus
[Eubacterium] cellulosolvens
[Clostridium] scindens
[Clostridium] innocuum
[Clostridium] hylemonae
[Brevibacterium] frigoritolerans
-1.0
-0.5
0.0
0.5
1.0
IgG Probability Ratio
Species
Bifidobacterium scardovii
Bifidobacterium pullorum
Bifidobacterium pseudocatenulatum
Bifidobacterium longum
Bifidobacterium eulemuris
Bifidobacterium dentium
Bifidobacterium catenulatum
Bifidobacterium breve
Bifidobacterium bifidum
Bifidobacterium animalis
Bifidobacterium angulatum
Bifidobacterium adolescentis
Barnesiella viscericola
Bacteroides zoogleoformans
Bacteroides xylanisolvens
Bacteroides uniformis
Bacteroides thetaiotaomicron
Bacteroides sp. PHL 2737
Bacteroides sp. M10
Bacteroides sp. HF-5287
Bacteroides sp. HF-5141
Bacteroides sp. HF-162
Bacteroides sp. CBA7301
Bacteroides sp. CACC 737
Bacteroides sp. A1C1
Bacteroides phage crAss001
Bacteroides ovatus
Bacteroides intestinalis
Bacteroides heparinolyticus
Bacteroides helcogenes
Bacteroides fragilis
Bacteroides coprosuis
Bacteroides cellulosilyticus
Bacteroides caecimuris
Bacteroides caccae
Bacillus virus phi29
Bacillus cereus
Azospira sp. I09
Arabia massiliensis
Anaerotignum propionicum
Anaerostipes rhamnosivorans
Anaerostipes hadrus
Anaerostipes caccae
Anaerocolumna sp. CTTW
Anaerocolumna cellulosilytica
Anaerococcus mediterraneensis
Anaerobutyricum hallii
Anabaena sp. YBS01
Aminobacter sp. SR38
Aminobacter sp. MSH1
-1.0
-0.5
0.0
0.5
1.0
IgG Probability Ratio
Species
Campylobacter coli
Butyrivibrio proteoclasticus
Butyrivibrio hungatei
Butyrivibrio fibrisolvens
Butyricimonas faecalis
Butyricicoccus sp. GAM44
Burkholderia contaminans
Brucella intermedia
Brevundimonas vancanneytii
Brevundimonas sp. SGAir0440
Brevundimonas sp. LM2
Brevundimonas sp. GW460-12-10-14-LB2
Brevundimonas sp. Bb-A
Brevundimonas sp. 'scallop'
Brevundimonas naejangsanensis
Brevundimonas mediterranea
Brevundimonas diminuta
Brevibacterium sp. PAMC23299
Brevibacillus sp. JNUCC-41
Bradyrhizobium sp. WSM471
Bradyrhizobium sp. SK17
Bradyrhizobium sp. LCT2
Bradyrhizobium sp. CCGE-LA001
Bradyrhizobium sp. CCBAU 53338
Bradyrhizobium sp. CCBAU 51765
Bradyrhizobium sp. CCBAU 51753
Bradyrhizobium sp. BTAi1
Bradyrhizobium sp. 6(2017)
Bradyrhizobium sp.
Bradyrhizobium icense
Bradyrhizobium guangdongense
Bradyrhizobium erythrophlei
Bradyrhizobium diazoefficiens
Bradyrhizobium betae
Bradyrhizobium arachidis
Brachyspira pilosicoli
Bosea sp. Tri-49
Bosea sp. AS-1
Bosea sp. A0M02
Bordetella petrii
Bordetella pertussis
Blautia sp. SC05B48
Blautia sp. LZLJ-3
Blautia producta
Blautia hansenii
Blautia argi
Blastomonas sp. RAC04
Blastomonas fulva
Bifidobacterium thermophilum
Bifidobacterium subtile
-1.0
-0.5
0.0
0.5
1.0
IgG Probability Ratio
pair
1
2
3
4
5
status
household control
severe ME/CFS

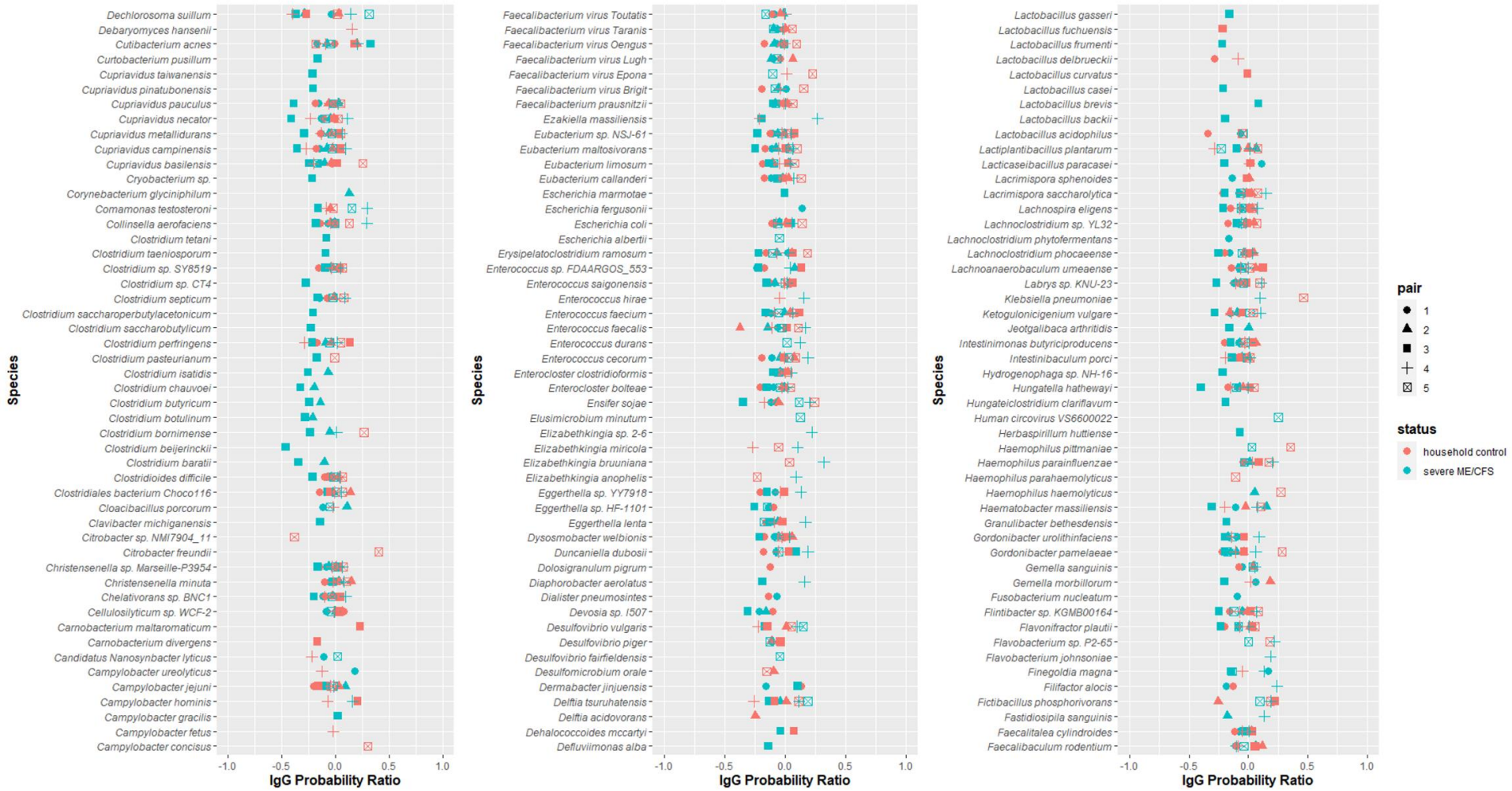
Species
Dechlorosoma suillum
Debaryomyces hansenii
Cutibacterium acnes
Curtobacterium pusillum
Cupriavidus taiwanensis
Cupriavidus pinatubonensis
Cupriavidus pauculus
Cupriavidus necator
Cupriavidus metallidurans
Cupriavidus campinensis
Cupriavidus basilensis
Cryobacterium sp.
Corynebacterium glyciniphilum
Comamonas testosteroni
Collinsella aerofaciens
Clostridium tetani
Clostridium taeniosporum
Clostridium sp. SY8519
Clostridium sp. CT4
Clostridium septicum
Clostridium saccharoperbutylacetonicum
Clostridium saccharobutylicum
Clostridium perfringens
Clostridium pasteurianum
Clostridium isatidis
Clostridium chauvoei
Clostridium butyricum
Clostridium botulinum
Clostridium bornimense
Clostridium beijerinckii
Clostridium baratii
Clostridioides difficile
Clostridiales bacterium Choco116
Cloacibacillus porcorum
Clavibacter michiganensis
Citrobacter sp. NMI7904_11
Citrobacter freundii
Christensenella sp. Marseille-P3954
Christensenella minuta
Chelativorans sp. BNC1
Cellulosilyticum sp. WCF-2
Carnobacterium maltaromaticum
Carnobacterium divergens
Candidatus Nanosynbacter lyticus
Campylobacter ureolyticus
Campylobacter jejuni
Campylobacter hominis
Campylobacter gracilis
Campylobacter fetus
Campylobacter concisus
-1.0
-0.5
0.0
0.5
1.0
IgG Probability Ratio
Species
Faecalibacterium virus Toutatis
Faecalibacterium virus Taranis
Faecalibacterium virus Oengus
Faecalibacterium virus Lugh
Faecalibacterium virus Epona
Faecalibacterium virus Brigit
Faecalibacterium prausnitzii
Ezakiella massiliensis
Eubacterium sp. NSJ-61
Eubacterium maltosivorans
Eubacterium limosum
Eubacterium callanderi
Escherichia marmotae
Escherichia fergusonii
Escherichia coli
Escherichia albertii
Erysipelatoclostridium ramosum
Enterococcus sp. FDAARGOS_553
Enterococcus saigonensis
Enterococcus hirae
Enterococcus faecium
Enterococcus faecalis
Enterococcus durans
Enterococcus cecorum
Enterocloster clostridioformis
Enterocloster bolteae
Ensifer sojae
Elusimicrobium minutum
Elizabethkingia sp. 2-6
Elizabethkingia miricola
Elizabethkingia bruuniana
Elizabethkingia anophelis
Eggerthella sp. YY7918
Eggerthella sp. HF-1101
Eggerthella lenta
Dysosmobacter welbionis
Duncaniella dubosii
Dolosigranulum pigrum
Diaphorobacter aerolatus
Dialister pneumosintes
Devosia sp. I507
Desulfovibrio vulgaris
Desulfovibrio piger
Desulfovibrio fairfieldensis
Desulfomicrobium orale
Dermabacter jinjuensis
Delftia tsuruhatensis
Delftia acidovorans
Dehalococcoides mccartyi
Defluviimonas alba
-1.0
-0.5
0.0
0.5
1.0
IgG Probability Ratio
Species
Lactobacillus gasseri
Lactobacillus fuchuensis
Lactobacillus frumenti
Lactobacillus delbrueckii
Lactobacillus curvatus
Lactobacillus casei
Lactobacillus brevis
Lactobacillus backii
Lactobacillus acidophilus
Lactiplantibacillus plantarum
Lacticaseibacillus paracasei
Lacrimispora sphenoides
Lacrimispora saccharolytica
Lachnospira eligens
Lachnoclostridium sp. YL32
Lachnoclostridium phytofermentans
Lachnoclostridium phocaeense
Lachnoanaerobaculum umeaense
Labrys sp. KNU-23
Klebsiella pneumoniae
Ketogulonicigenium vulgare
Jeotgalibaca arthritidis
Intestinimonas butyriciproducens
Intestinibaculum porci
Hydrogenophaga sp. NH-16
Hungatella hathewayi
Hungateiclostridium clariflavum
Human circovirus VS6600022
Herbaspirillum huttiense
Haemophilus pittmaniae
Haemophilus parainfluenzae
Haemophilus parahaemolyticus
Haemophilus haemolyticus
Haematobacter massiliensis
Granulibacter bethesdensis
Gordonibacter urolithinfaciens
Gordonibacter pamelaeae
Gemella sanguinis
Gemella morbillorum
Fusobacterium nucleatum
Flintibacter sp. KGMB00164
Flavonifractor plautii
Flavobacterium sp. P2-65
Flavobacterium johnsoniae
Finegoldia magna
Filifactor alocis
Fictibacillus phosphorivorans
Fastidiosipila sanguinis
Faecalitalea cylindroides
Faecalibaculum rodentium
-1.0
-0.5
0.0
0.5
1.0
IgG Probability Ratio
pair
1
2
3
4
5
status
household control
severe ME/CFS

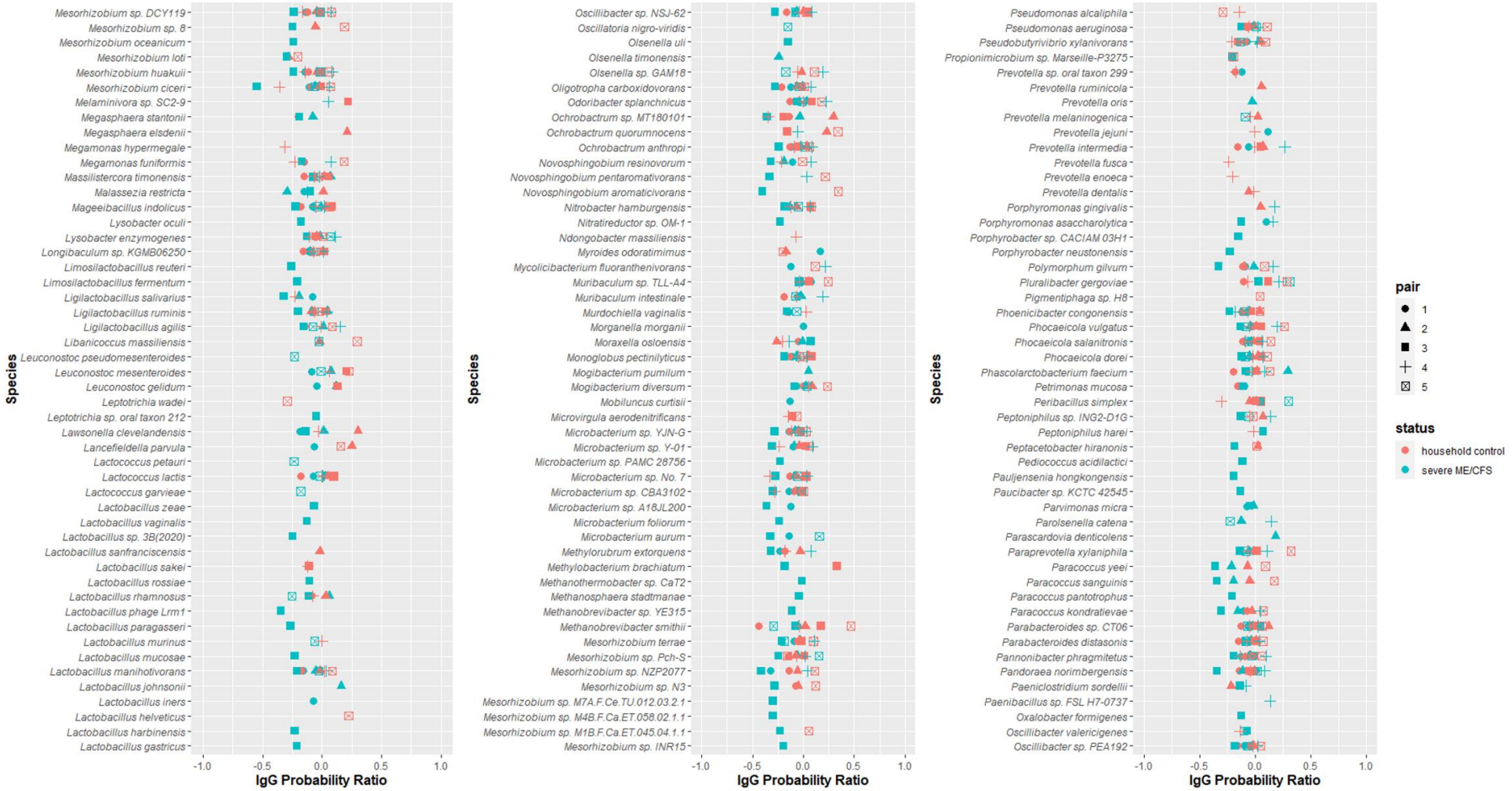
Species
Mesorhizobium sp. DCY119
Mesorhizobium sp. 8
Mesorhizobium oceanicum
Mesorhizobium loti
Mesorhizobium huakuii
Mesorhizobium ciceri
Melaminivora sp. SC2-9
Megasphaera stantonii
Megasphaera elsdenii
Megamonas hypermegale
Megamonas funiformis
Massilistercora timonensis
Malassezia restricta
Mageeibacillus indolicus
Lysobacter oculi
Lysobacter enzymogenes
Longibaculum sp. KGMB06250
Limosilactobacillus reuteri
Limosilactobacillus fermentum
Ligilactobacillus salivarius
Ligilactobacillus ruminis
Ligilactobacillus agilis
Libanicoccus massiliensis
Leuconostoc pseudomesenteroides
Leuconostoc mesenteroides
Leuconostoc gelidum
Leptotrichia wadei
Leptotrichia sp. oral taxon 212
Lawsonella clevelandensis
Lancefieldella parvula
Lactococcus petauri
Lactococcus lactis
Lactococcus garvieae
Lactobacillus zeae
Lactobacillus vaginalis
Lactobacillus sp. 3B(2020)
Lactobacillus sanfranciscensis
Lactobacillus sakei
Lactobacillus rossiae
Lactobacillus rhamnosus
Lactobacillus phage Lrm1
Lactobacillus paragasseri
Lactobacillus murinus
Lactobacillus mucosae
Lactobacillus manihotivorans
Lactobacillus johnsonii
Lactobacillus iners
Lactobacillus helveticus
Lactobacillus harbinensis
Lactobacillus gastricus
-1.0
-0.5
0.0
0.5
1.0
IgG Probability Ratio
Species
Oscillibacter sp. NSJ-62
Oscillatoria nigro-viridis
Olsenella uli
Olsenella timonensis
Olsenella sp. GAM18
Oligotropha carboxidovorans
Odoribacter splanchnicus
Ochrobactrum sp. MT180101
Ochrobactrum quorumnocens
Ochrobactrum anthropi
Novosphingobium resinovorum
Novosphingobium pentaromativorans
Novosphingobium aromaticivorans
Nitrobacter hamburgensis
Nitratireductor sp. OM-1
Ndongobacter massiliensis
Myroides odoratimimus
Mycolicibacterium fluoranthenivorans
Muribaculum sp. TLL-A4
Muribaculum intestinale
Murdochiella vaginalis
Morganella morganii
Moraxella osloensis
Monoglobus pectinilyticus
Mogibacterium pumilum
Mogibacterium diversum
Mobiluncus curtisii
Microvirgula aerodenitrificans
Microbacterium sp. YJN-G
Microbacterium sp. Y-01
Microbacterium sp. PAMC 28756
Microbacterium sp. No. 7
Microbacterium sp. CBA3102
Microbacterium sp. A18JL200
Microbacterium foliorum
Microbacterium aurum
Methylorubrum extorquens
Methylobacterium brachiatum
Methanothermobacter sp. CaT2
Methanosphaera stadtmanae
Methanobrevibacter sp. YE315
Methanobrevibacter smithii
Mesorhizobium terrae
Mesorhizobium sp. Pch-S
Mesorhizobium sp. NZP2077
Mesorhizobium sp. N3
Mesorhizobium sp. M7A.F.Ce.TU.012.03.2.1
Mesorhizobium sp. M4B.F.Ca.ET.058.02.1.1
Mesorhizobium sp. M1B.F.Ca.ET.045.04.1.1
Mesorhizobium sp. INR15
-1.0
-0.5
0.0
0.5
1.0
IgG Probability Ratio
Species
Pseudomonas alcaliphila
Pseudomonas aeruginosa
Pseudobutyrivibrio xylanivorans
Propionimicrobium sp. Marseille-P3275
Prevotella sp. oral taxon 299
Prevotella ruminicola
Prevotella oris
Prevotella melaninogenica
Prevotella jejuni
Prevotella intermedia
Prevotella fusca
Prevotella enoeca
Prevotella dentalis
Porphyromonas gingivalis
Porphyromonas asaccharolytica
Porphyrobacter sp. CACIAM 03H1
Porphyrobacter neustonensis
Polymorphum gilvum
Pluralibacter gergoviae
Pigmentiphaga sp. H8
Phoenicibacter congonensis
Phocaeicola vulgatus
Phocaeicola salanitronis
Phocaeicola dorei
Phascolarctobacterium faecium
Petrimonas mucosa
Peribacillus simplex
Peptoniphilus sp. ING2-D1G
Peptoniphilus harei
Peptacetobacter hiranonis
Pediococcus acidilactici
Pauljensenia hongkongensis
Paucibacter sp. KCTC 42545
Parvimonas micra
Parolsenella catena
Parascardovia denticolens
Paraprevotella xylaniphila
Paracoccus yeei
Paracoccus sanguinis
Paracoccus pantotrophus
Paracoccus kondratievae
Parabacteroides sp. CT06
Parabacteroides distasonis
Pannonibacter phragmitetus
Pandoraea norimbergensis
Paeniclostridium sordellii
Paenibacillus sp. FSL H7-0737
Oxalobacter formigenes
Oscillibacter valericigenes
Oscillibacter sp. PEA192
-1.0
-0.5
0.0
0.5
1.0
IgG Probability Ratio
pair
1
2
3
4
5
status
household control
severe ME/CFS

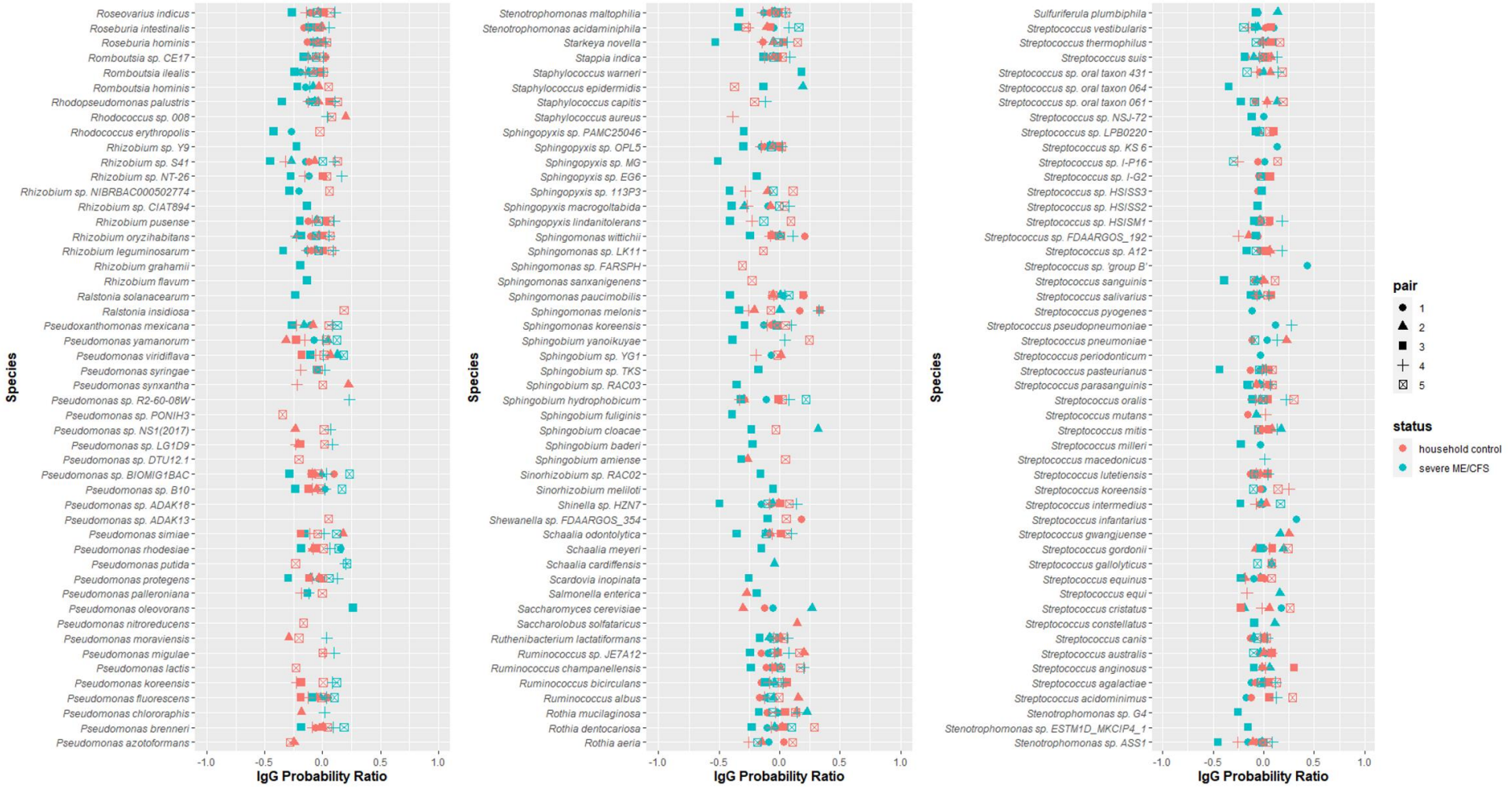
Species
Roseovarius indicus
Roseburia intestinalis
Roseburia hominis
Romboutsia sp. CE17
Romboutsia ilealis
Romboutsia hominis
Rhodopseudomonas palustris
Rhodococcus sp. 008
Rhodococcus erythropolis
Rhizobium sp. Y9
Rhizobium sp. S41
Rhizobium sp. NT-26
Rhizobium sp. NIBRBAC000502774
Rhizobium sp. CIAT894
Rhizobium pusense
Rhizobium oryzihabitans
Rhizobium leguminosarum
Rhizobium grahamii
Rhizobium flavum
Ralstonia solanacearum
Ralstonia insidiosa
Pseudoxanthomonas mexicana
Pseudomonas yamanorum
Pseudomonas viridiflava
Pseudomonas syringae
Pseudomonas synxantha
Pseudomonas sp. R2-60-08W
Pseudomonas sp. PONIH3
Pseudomonas sp. NS1(2017)
Pseudomonas sp. LG1D9
Pseudomonas sp. DTU12.1
Pseudomonas sp. BIOMIG1BAC
Pseudomonas sp. B10
Pseudomonas sp. ADAK18
Pseudomonas sp. ADAK13
Pseudomonas simiae
Pseudomonas rhodesiae
Pseudomonas putida
Pseudomonas protegens
Pseudomonas palleroniana
Pseudomonas oleovorans
Pseudomonas nitroreducens
Pseudomonas moraviensis
Pseudomonas migulae
Pseudomonas lactis
Pseudomonas koreensis
Pseudomonas fluorescens
Pseudomonas chlororaphis
Pseudomonas brenneri
Pseudomonas azotoformans
-1.0
-0.5
0.0
0.5
1.0
IgG Probability Ratio
Species
Stenotrophomonas maltophilia
Stenotrophomonas acidaminiphila
Starkeya novella
Stappia indica
Staphylococcus warneri
Staphylococcus epidermidis
Staphylococcus capitis
Staphylococcus aureus
Sphingopyxis sp. PAMC25046
Sphingopyxis sp. OPL5
Sphingopyxis sp. MG
Sphingopyxis sp. EG6
Sphingopyxis sp. 113P3
Sphingopyxis macrogoltabida
Sphingopyxis lindanitolerans
Sphingomonas wittichii
Sphingomonas sp. LK11
Sphingomonas sp. FARSPH
Sphingomonas sanxanigenens
Sphingomonas paucimobilis
Sphingomonas melonis
Sphingomonas koreensis
Sphingobium yanoikuyae
Sphingobium sp. YG1
Sphingobium sp. TKS
Sphingobium sp. RAC03
Sphingobium hydrophobicum
Sphingobium fuliginis
Sphingobium cloacae
Sphingobium baderi
Sphingobium amiense
Sinorhizobium sp. RAC02
Sinorhizobium meliloti
Shinella sp. HZN7
Shewanella sp. FDAARGOS_354
Schaalia odontolytica
Schaalia meyeri
Schaalia cardiffensis
Scardovia inopinata
Salmonella enterica
Saccharomyces cerevisiae
Saccharolobus solfataricus
Ruthenibacterium lactatiformans
Ruminococcus sp. JE7A12
Ruminococcus champanellensis
Ruminococcus bicirculans
Ruminococcus albus
Rothia mucilaginosa
Rothia dentocariosa
Rothia aeria
-1.0
-0.5
0.0
0.5
1.0
IgG Probability Ratio
Species
Sulfuriferula plumbiphila
Streptococcus vestibularis
Streptococcus thermophilus
Streptococcus suis
Streptococcus sp. oral taxon 431
Streptococcus sp. oral taxon 064
Streptococcus sp. oral taxon 061
Streptococcus sp. NSJ-72
Streptococcus sp. LPB0220
Streptococcus sp. KS 6
Streptococcus sp. I-P16
Streptococcus sp. I-G2
Streptococcus sp. HSISS3
Streptococcus sp. HSISS2
Streptococcus sp. HSISM1
Streptococcus sp. FDAARGOS_192
Streptococcus sp. A12
Streptococcus sp. 'group B'
Streptococcus sanguinis
Streptococcus salivarius
Streptococcus pyogenes
Streptococcus pseudopneumoniae
Streptococcus pneumoniae
Streptococcus periodonticum
Streptococcus pasteurianus
Streptococcus parasanguinis
Streptococcus oralis
Streptococcus mutans
Streptococcus mitis
Streptococcus milleri
Streptococcus macedonicus
Streptococcus lutetiensis
Streptococcus koreensis
Streptococcus intermedius
Streptococcus infantarius
Streptococcus gwangjuense
Streptococcus gordonii
Streptococcus gallolyticus
Streptococcus equinus
Streptococcus equi
Streptococcus cristatus
Streptococcus constellatus
Streptococcus canis
Streptococcus australis
Streptococcus anginosus
Streptococcus agalactiae
Streptococcus acidominimus
Stenotrophomonas sp. G4
Stenotrophomonas sp. ESTM1D_MKCIP4_1
Stenotrophomonas sp. ASS1
-1.0
-0.5
0.0
0.5
1.0
IgG Probability Ratio
pair
1
2
3
4
5
status
household control
severe ME/CFS

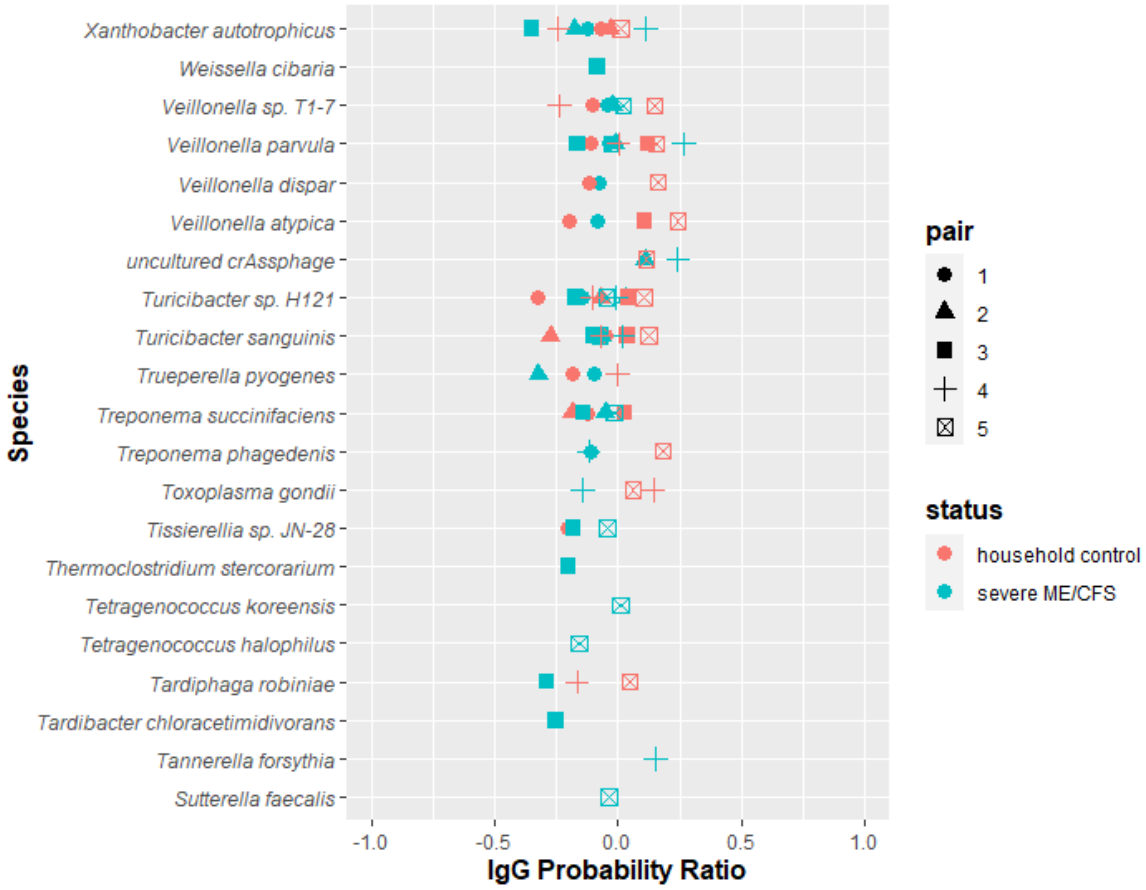
Xanthobacter autotrophicus
Weissella cibaria
Veillonella sp. T1-7
Veillonella parvula
Veillonella dispar
Veillonella atypica
uncultured crAssphage
Turicibacter sp. H121
Turicibacter sanguinis
Trueperella pyogenes
Treponema succinifaciens
Treponema phagedenis
Toxoplasma gondii
Tissierellia sp. JN-28
Thermoclostridium stercorarium
Tetragenococcus koreensis
Tetragenococcus halophilus
Tardiphaga robiniae
Tardibacter chloracetimidivorans
Tannerella forsythia
Sutterella faecalis
Species
-1.0
-0.5
0.0
0.5
1.0
IgG Probability Ratio
pair
1
2
3
4
5
status
household control
severe ME/CFS

← ***Supplementary figure 5.9: IgG probability ratios on taxa at the species-level.*** *Stool microbes from severe ME/CFS patients (n=5) and their matched household controls (n=5) were incubated with serum IgG in vitro. 'IgG positive' fractions and 'IgG negative' fractions were subsequently collected using the Sony SH800S cell sorter and shotgun metagenomic sequencing was performed to identify the relative abundance of taxa present in the sorted fractions from each participant. The IgG probability ratio was used to calculate the likelihood of a taxon being coated by IgG.*

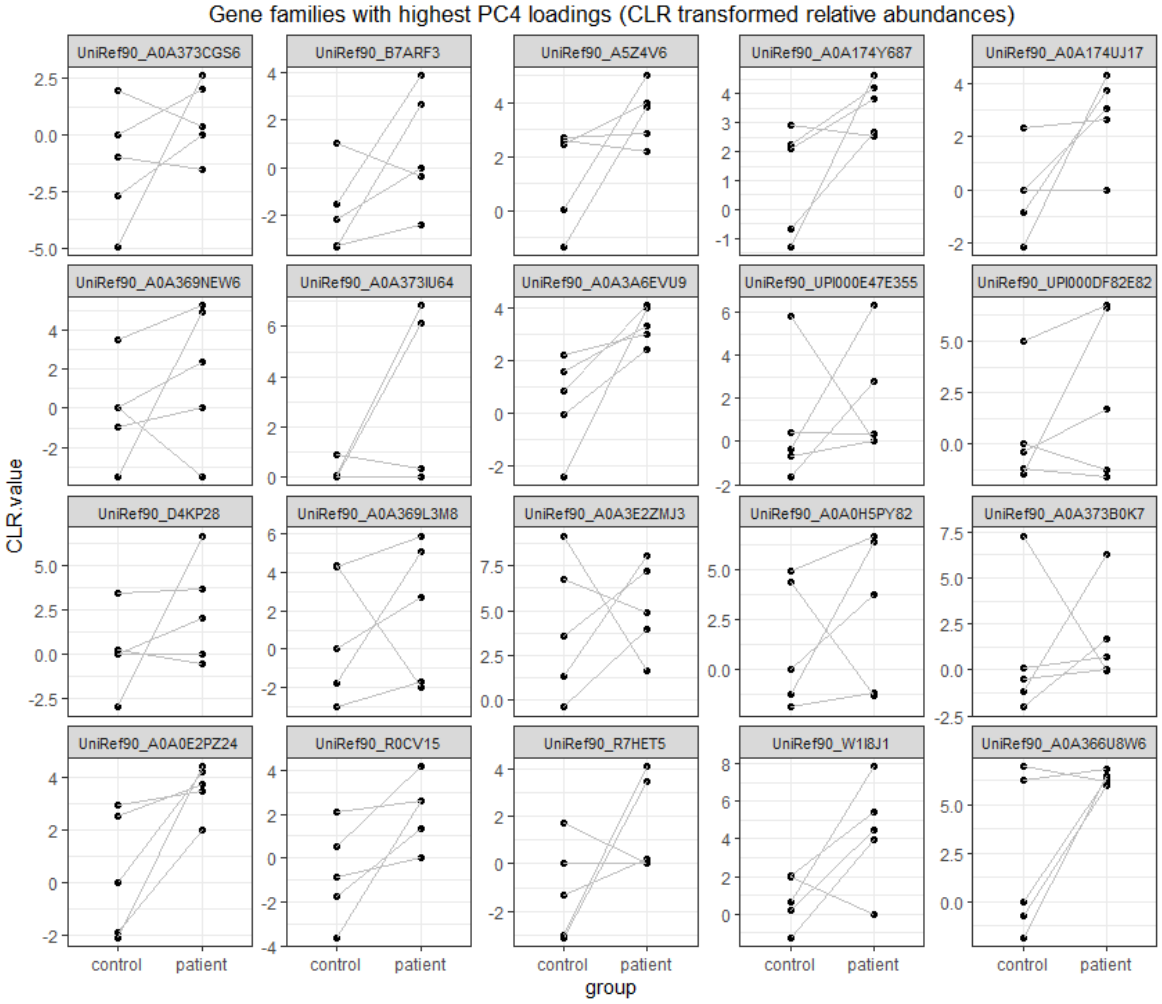

Supplementary figure 5.10: Pairwise comparisons of the 20 gene families with the highest loadings on PC4. *Stool microbes from severe ME/CFS patients (n=5) and their matched household controls (n=5) were stained with SYBR™ green I nucleic acid gel stain and 'sybr green high' cells were collected using the Sony SH800S cell sorter. Shotgun metagenomic sequencing was performed to identify gene families present in each sample. PCA was performed on gene families with 4 or more values over the threshold. CLR transformed relative abundances of gene families with the 20 highest loadings on PC4 are shown.*

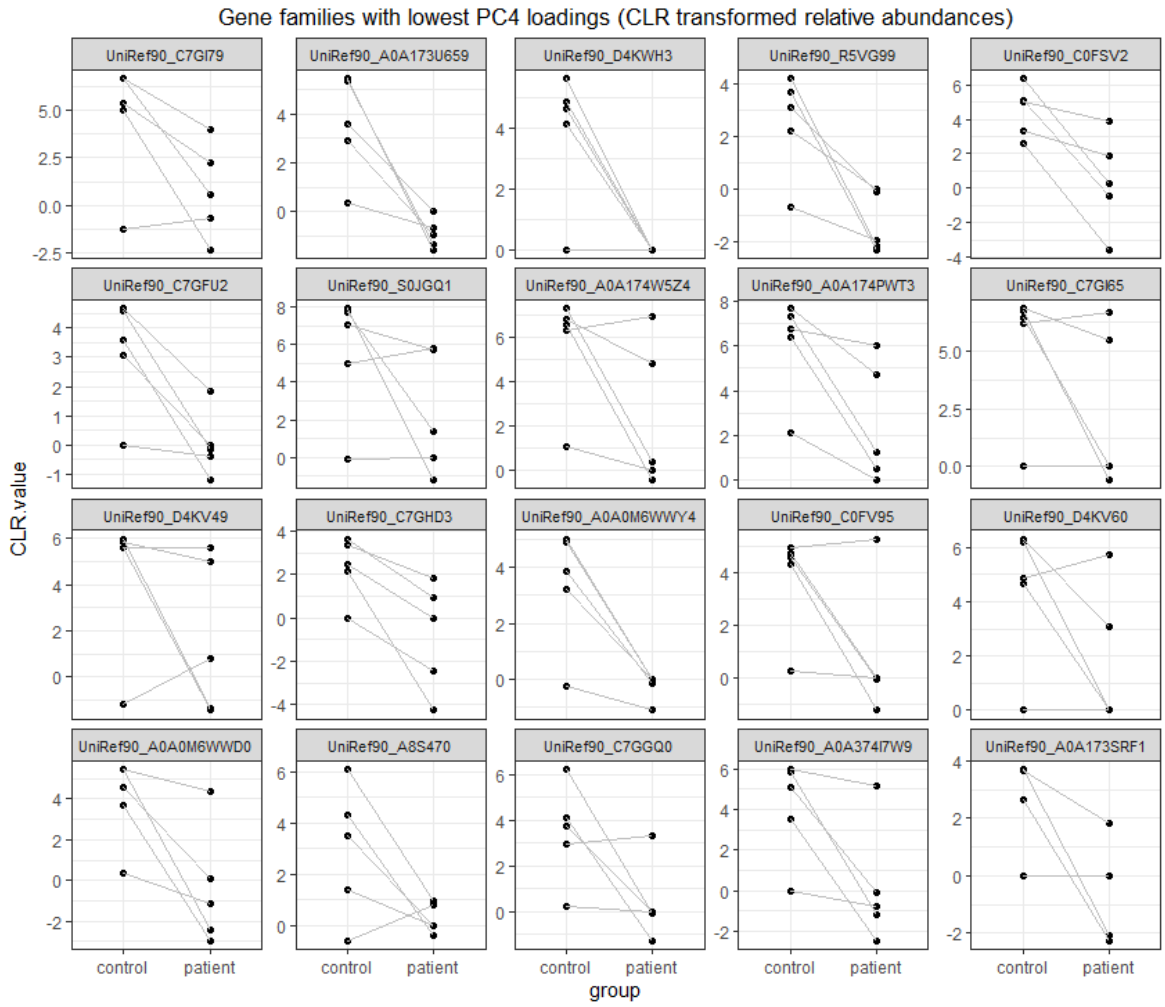

Supplementary figure 5.11: Pairwise comparisons of the 20 gene families with the lowest loadings on PC4. *Stool microbes from severe ME/CFS patients (n=5) and their matched household controls (n=5) were stained with SYBR™ green I nucleic acid gel stain and 'sybr green high' cells were collected using the Sony SH800S cell sorter. Shotgun metagenomic sequencing was performed to identify gene families present in each sample. PCA was performed on gene families with 4 or more values over the threshold. CLR transformed relative abundances of gene families with the 20 lowest loadings on PC4 are shown.*

APPENDICES

Appendix I: AI-ME/CFS HRA ethical approval

NHS
Health Research Authority

Miss Katharine Seton
Quadram Institute Bioscience
Norwich Research Park
Colney Lane
NR4 7UA

Email: hra.approval@nhs.net

19 July 2017

Dear Miss Seton,

Letter of HRA Approval

Study title:	**Defining autoimmune aspects of Myalgic Encephalomyelitis/Chronic Fatigue Syndrome (ME/CFS)**
IRAS project ID:	**218545**
REC reference:	**17/LO/1102**
Sponsor	**University of East Anglia**

I am pleased to confirm that HRA Approval has been given for the above referenced study, on the basis described in the application form, protocol, supporting documentation and any clarifications noted in this letter.

Appendix II: Example of AI-ME/CFS study letter of invitation

Epsom and St Helier University Hospitals NHS
NHS Trust

Dear Date:

Human Study: "Defining autoimmune aspects of Myalgic Encephalomyelitis/Chronic Fatigue Syndrome (ME/CFS)"

On behalf of the CFS clinic at Epsom and St Helier University Hospitals, we would like to inform you of a new research study, based at the Quadram Institute in Norwich, that aims to assess possible links between aspects of the digestive system and Myalgic Encephalomyelitis/ Chronic Fatigue Syndrome (ME/CFS). This study will be testing whether there is the presence of an immune response directed against gut microbes or food in patients diagnosed with severe ME/CFS.

For this study a single blood and stool samples will be asked to be donated. As you are suffering from severe ME/CFS, home visits are scheduled for collection of your donations.

In addition, this study also requires healthy household controls. A household control is defined as someone who is a relative, friend or carer and who regularly visits you. For every patient recruited onto this study one household control needs to be recruited. Household controls are crucial in this study because gut microbes vary between people living in different environments. Therefore, the use of household controls will enable the identification of disease-specific alterations in your gut microbes.

Before you decide whether to take part, it is important for you to understand why the research is being done and what it will involve. We have produced the summary information sheet which will give you a brief introduction to the study. Please ensure you all read the full information sheet enclosed as this describes the study in much more detail. Please read this carefully and discuss it with relatives and friends or your GP if you wish. However, it is entirely your decision whether to participate in this study. Please take your time to carefully consider whether to take part.

I have also enclosed a Household Control Information Sheet. This details who is eligible and what is required from household control volunteers. If you identify someone who potentially fills the "household control" criteria, we would really appreciate it if you could give them this Household Control Information Sheet to read.

If you and your household control are both interested in participating in this study, or if either of you have any queries please contact the study chief investigator, Katharine Seton, by either telephoning 01603 255148 or by emailing katharine.seton@quadram.ac.uk.

Yours sincerely,

Dr Amolak Bansal

CFS Clinic, Epsom and St Helier University Hospitals

10/06/2019 Annex 18: cover letter for ESTH patients version 2

Appendix III: Example of AI-ME/CFS study summary participant information sheet

IRAS ID: 218545

Defining autoimmune aspects of Myalgic Encephalomyelitis/Chronic Fatigue Syndrome (ME/CFS):

EPSOM AND ST HELIER CFS SERVICE PATIENT SUMMARY INFORMATION SHEET

Study background

We would like to invite you to take part in a new research study undertaken by the University of East Anglia in collaboration with the Quadram Institute Bioscience looking at possible links between aspects of the digestive system and autoimmunity in Myalgic Encephalomyelitis/Chronic Fatigue Syndrome (ME/CFS). This study aims to find out if there is an abnormal immune response against gut microbes in severe ME/CFS patients.

We aim to recruit 10 pairs of severe ME/CFS patients and healthy household controls. Although defined as a household control, it is not required that the household control lives with you. A household control can be anyone who comes into regular contact with you. This person could be a relative, friend or carer.

What's involved

- Donation of a 50 ml of **blood** and **stool** sample during a scheduled **home visit**
- Completion of 48 hour **food diaries** prior to stool sample collection

Study schedule

1. **Identification of household control:** if you are interested in this study, please identify and provide a household control with the "household control information sheet".
2. **Study telephone call:** If you and your household control are interested in this study please contact the study team to arrange a telephone call (where the study will be explained in more detail).
3. **Consideration period:** after the study telephone call, take 3 days to consider whether to take part.
4. **Consenting process:** If you and your household control decide you would like to take part, contact the study team to arrange the first study visit for signed and written consent to be taken.
5. **First study visit:** The study team will take you through the consenting process. You will receive stool sample collection kits with instructions and the 48 hour food diary with instructions.
6. **Second study visit:** The study team will collect your stool sample and blood sample donations and collect your 48 hour food diary.

Contacting the study team

Katharine Seton is the Chief Investigator of this study. To contact her either call 01603 255148 or email katharine.seton@quadram.ac.uk

If you are interested in participating in this study, please read the full patient information sheet.

All personal data you provide will comply with the EU General Data Protection Regulations and the UK Data Protection Act 2018

Thank you

10/09/2019 Annex 15: Epsom and St Helier CFS Service summary patient information sheet version 2

Appendix IV: Example of AI-ME/CFS study full participant information sheet for severe ME/CFS patients

IRAS ID: 218545

Defining autoimmune aspects of Myalgic Encephalomyelitis/ Chronic Fatigue Syndrome (ME/CFS): PATIENT INFORMATION SHEET

Thank you for reading the summary patient information sheet and subsequently being interested in this study.

Summary

We would like to invite you to take part in a new research study looking at possible links between aspects of the digestive system and Myalgic Encephalomyelitis/Chronic Fatigue Syndrome (ME/CFS). The study aims to find out if there is the presence of an immune response directed against gut microbes or food in patients diagnosed with severe ME/CFS. We would also like to determine whether there is an immune response directed against other parts of the body (e.g. proteins in the brain) within severe ME/CFS patients.

This study is undertaken by the University of East Anglia (UEA) in collaboration with the Quadram Institute Bioscience (QIB), Norwich. It has been made possible by funds raised across the UK and globally, by the patient charity Invest in ME Research UK. We aim to recruit 10 patients with confirmed severe ME/CFS. We also aim to recruit 10 volunteers who fulfil the "household control" criteria. Household control volunteers will be used to compare your data to in order to find disease specific alterations in the immune response to gut microbes.

If you are willing to take part in this study, we ask for a blood and stool sample to be donated to this research. You will be provided with a stool sample collection kit together with instructions for use. In addition, we ask that you complete a 48 hour food diary to record your food, fluid and supplement intake for the 48 hour period prior to collecting your stool sample. We will provide you with instructions for completing the food diary.

Please take your time to fully read and understand what this study involves and what will be required from you. Any questions you have can be answered by a member of our research team (see contact details below). Please take as much time as you need to consider carefully whether you would like to participate. Whether or not you decide to take part in this study will **not** alter your current clinical care or ongoing treatment.

What is the purpose of this study?

Very little is currently known about the onset of ME/CFS or the cause of symptoms that patients suffer from.

The wall of your gut acts as a barrier to keep food and bacteria living within the gut separate from internal organs and the bloodstream. If this wall becomes 'leaky' it will no longer act as a barrier and bacteria living within the gut and food could pass into the bloodstream. If bacteria get into the bloodstream they could react with cells of the immune system to trigger systemic (whole body) inflammation. This immune reaction could target components of the body, such as parts of the brain, and lead to some of the symptoms that patients experience.

Usually, the immune system fights infection from bacteria and viruses to keep us healthy. Sometimes the immune system reacts to bacteria, food or even parts of cells in our own body, which can make us feel ill. In this case, we are testing to see if there is an inappropriate immune response triggered by bacteria that has leaked across the gut wall.

We already known that there is evidence of both an inappropriate immune response in ME/CFS patients and gut involvement as some patients experience abdominal pain and bloating (gastro-intestinal disturbances). We would like to see whether there is an inappropriate immune response that originates in the gut.

If sufficient evidence is found to confirm an inappropriate immune response resulting from a leaky gut, investigations into the use of future treatments may be initiated. These may include drugs to suppress the inappropriate immune response, or the use of healthy probiotic bacteria to restore a balanced community of gut microbes and aim to reduce gut wall leakiness.

Why have I been chosen?

Your clinician at the Epsom and St Helier CFS Service will have identified you as a suitable candidate for this study based on a confirmed **clinical diagnosis** for severe ME/CFS in the absence of significant anxiety and depression.

Do I have to take part?

No, you do not have to take part. Once you have read this information sheet you will be given as much time as you need to decide if you would like to donate blood and stool samples to our study. It is your decision alone to participate and you can choose to withdraw at any time. **Please note any results relating to samples you have provided up until the moment you decide to withdraw will still be kept and included in the study.** However, your confidentiality will remain protected and it will not be possible to identify you in person, as all samples will be anonymised and given a unique identification number.

What would I have to do?

If you are interested in participating in this study please contact the research team (contact details are provided at the end of this sheet). We will arrange a telephone call with you to explain the study in more detail. You will then have 72 hours to decide whether you would be willing to take part. After this time, if you decide you would like to participate you can arrange the first study visit. If we do not hear from you after 72 hours we will assume you do not wish to participate and we will not contact you again.

Study visits

Study visits are carried out at your home as we are aware that ME/CFS symptoms make it difficult for you to leave your home. They will be mutually agreed in advance on dates and times that suit you and your household control volunteer.

During the first study visit, a member of the research team will discuss the sampling process in more detail and answer any questions you may have. If you are still happy to take part, a member of the research team will take you through the consenting process. You will also be asked to sign a consent form for the Norwich Biorepository, as once the study has ended any remaining sample material will be banked for future research. Once you have consented onto the study the study team will give you a food diary with instructions and a stool sampling kit with instructions.

The second study visit is scheduled for sample collection to take place. You will be asked to collect your stool sample within 24 hours of your arranged home visit and you will be asked to record your food, fluid, medication and supplement intake within the food diary for the 48 hours prior to when you collect your stool sample. At the home visit a trained phlebotomist or nurse will collect 50ml (approximately 10 teaspoons) of blood from a suitable vein in your arm.

Important information:

- You must not have received antibiotic or probiotic treatment (such as probiotic tablets) **six weeks prior** to when samples are scheduled to be collected.
- You cannot have an active infection at the time the blood tests are taken, as an infection, such as a cold, will affect the immune system and results collected.
- Your general practitioner will be informed about your participation in this study.
- You must be able to understand the requirements of the study and be **able to provide signed and dated informed consent.**

What will I have to do?

1. Volunteer recruitment:
   - severe ME/CFS patients informed about the study through post

2. Study explained:
   - Phone call with a member of the research team to discuss the study
   - Opportunity to ask questions
   - Then 72 hours to consider participation
   - Volunteers interested in participating arrange appointment for 1st study visit

3. 1st study visit:
   - Consent taken
   - Given stool sample kit and instructions
   - Given 48 hour food diary and instructions

4. 2nd study visit:
   - Blood sample taken
   - Stool sample taken less than 24 hours prior to house visit
   - 48 hour food diary taken

What will happen to the samples I give?

When you give your samples to the courier, the courier will transport the samples to the Quadram Institute Bioscience (QIB), Norwich. Here we will process the blood and stool samples that you provided. At the QIB and collaborating institutes we will examine the immune cells within the blood to see whether they react with microbes in your stool sample. We will then see whether these immune cells are capable of moving from the gut to the brain and react with proteins on brain cells.

We will also be looking at the presence of antibodies (proteins produced by immune cells) within your blood to see whether they are specific to microbes from stool samples, or specific to certain types of food. The results we collect will be compared to results from household controls.

The levels and diversity of microbes within your stool samples will also be analysed and compared to the household control samples.

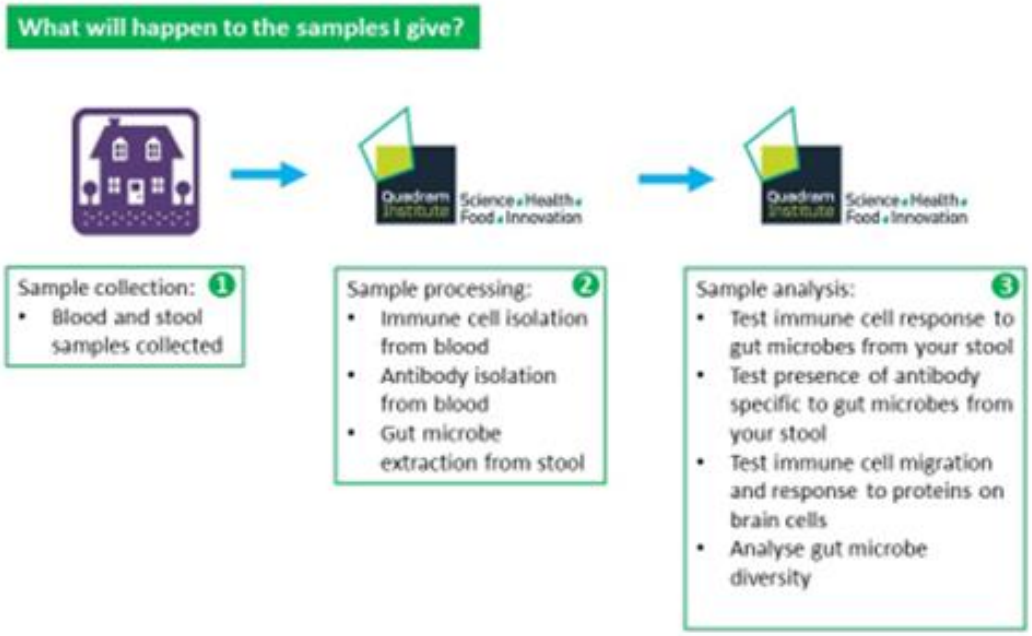

Sample analysis at collaborating research centres

Part of the research aims require samples to be sent to external research centres for analysis. Examples of this includes DNA from the gut microbes for sequencing.

You will be given the option to donate your samples to ethically approved animal research undertaken at King's College London by Dr David Andersson, with whom we are collaborating. The animal research involves serum IgG being used to identify biomarkers for ME/CFS and research symptom manifestation. Fatigue and pain symptoms will be examined in mice following the administration of serum IgG. Samples sent to collaborating research groups will be anonymised. **You are still able to participate in this human study if you do not wish for your samples to be used in animal research.**

What will happen to the samples I give after this research project has been completed?

We will transfer any unused blood and stool samples to the Norwich Biorepository for long term storage and for use in subsequent research projects that wish to address similar research questions. These samples will be kept anonymised to maintain confidentiality.

Do I have to donate both types of sample, or can I just donate blood or stool samples?

The priority for this study is to assess whether there is the presence of an immune response directed against gut microbes. Stool samples will be used to acquire gut microbes and the blood will be used to isolate immune cells and immune cell products. Analysing whether immune cells from blood can target and react with gut microbes from stools will determine whether patients have an immune response generated against gut microbes. Therefore, for this study we will need volunteers to donate both blood and stool samples.

Can I still take part if I do not have a household control?

In research studies, controls act as comparison groups in order to confirm the significance of results. Control groups are crucial to determine whether what is found within the patient group is the same or different to a group of healthy people.

In this study a control group is crucial to determine whether the presence of an immune response directed against gut microbes or food is only seen in ME/CFS patients, or in both patients and healthy controls. Knowing whether the presence of an immune response directed against gut microbes is specific to ME/CFS will help to determine further possible causes of disease initiation, progression and symptoms.

Gut microbes vary between people living in different environments. Therefore, household controls will enable the identification of disease-specific alterations in gut microbes.

This study requires that each patient has one household control to compare results with, otherwise the results found in patients cannot be confirmed.

What are the possible risks of taking part?

Possible risks of taking part are associated with blood donation. Like any blood test you have, there is a risk of experiencing discomfort, pain, bleeding, bruising or infection during or after blood collection.

The precise procedure for getting your blood sample is simple. Prior to having your blood sample taken you will be seated comfortably and the area on your arm that will be used to donate blood will be cleaned with a swab. A tourniquet will be applied to your upper arm and tightened. Blood will be taken from a suitable vein in your arm by a trained phlebotomist or nurse. After the needle is removed you should firmly press on this area for a minute to prevent bruising which can be uncomfortable and sometimes painful. Microtape will be used to adhere cotton wool to the site of venous access.

What are the possible benefits of taking part in this study?

It is unlikely that you will directly benefit from the study. However, if we discover more about the cause or illness progression of ME/CFS there is the possibility we may be able to develop better diagnostic tests and more effective treatments which will be made available to patients like you.

Will my details be kept confidential?

All data will be handled in compliance with EU GDPR and UK Data Protection Act 2018. All samples you donate will be anonymised and assigned a unique identification number. As the research team will be collecting samples from your homes identifiable data such as personal addresses, telephone number and email address will be stored on a password protected computer accessed by the chief investigator and academic supervisors only.

This means that you will not be identifiable to researchers as any samples or information leaving the hospital will be referred to only by the unique number that is allocated to you. All information collected about you during the research project will be kept strictly confidential.

Please note we require access to information related to your gender, age and diagnosis of ME/CFS. Researchers will not have direct access to your medical records. Dr Bansal will provide us with details of the severity, duration and symptoms of your ME/CFS. This information will be stored on a password protected computer accessed by the chief investigator and academic supervisors only.

No one other than the chief investigator or academic supervisors will have access to identifiable data. Identifiable data, such as information on your gender, age and diagnosis of ME/CFS will be retained for 12 months to 3 years following the end of the study. This information will be stored on a password protected computer or in a lockable filing cabinet.

What will happen to the results of this research study?

Results from this study will be published in international scientific journals and presented at conferences. At the end of the study results will be made available on the Invest in ME Research UK website (www.investinme.org). It will also form the basis of an educational project and PhD thesis to be submitted to the University of East Anglia. At no point will you be identifiable, in person, from any publications of work presented at scientific conferences.

Please note we will **not** be able to give you your individual results at any point during or after this study.

How can I make an appointment to give my consent?

You can make an appointment by contacting either Katharine Seton, chief investigator and PhD student, by calling 01603 255148 or emailing katharine.seton@quadram.ac.uk.

Thank you for taking the time to consider your involvement in this study

Appendix V: Example of AI-ME/CFS study participant information sheet for matched household controls

IRAS ID: 218545

Defining autoimmune aspects of Myalgic Encephalomyelitis/ Chronic Fatigue Syndrome (ME/CFS): HOUSEHOLD CONTROL INFORMATION SHEET

Summary

We would like to invite you to take part in a new research study looking at possible links between aspects of the digestive system and Myalgic Encephalomyelitis/Chronic Fatigue Syndrome (ME/CFS). The study aims to find out if there is the presence of an immune response directed against gut microbes or food in patients diagnosed with severe ME/CFS. We would also like to determine whether there is an immune response directed against other parts of the body (e.g. proteins in the brain) within severe ME/CFS patients.

This study is undertaken by the University of East Anglia (UEA) in collaboration with the Quadram Institute Bioscience (QIB), Norwich. It has been made possible by funds raised across the UK and globally, by the patient charity Invest in ME Research UK. We aim to recruit 10 healthy household controls, one household control for every severe ME/CFS patient recruited onto our study. A household control is someone who is healthy to compare with the patient's results.

If you decide to take part in this study we ask for a blood and stool sample to be donated to this research.. You will be provided with a stool sample collection kit together with instructions for use. In addition, we ask that you complete a 48 hour food diary to record your food, fluid and supplement intake for the 48 hour period prior to collecting your stool sample. The **home visit will be scheduled to coincide with home visits for the patient you are matched with.**

Please take your time to fully read and understand what this study involves and what will be required from you. Any questions you have can be answered by a member of our research team (see contact details below). Please take as much time as you need to consider carefully whether you would like to participate.

What is the purpose of this study?

Very little is currently known about the onset of ME/CFS or the cause of symptoms that patients suffer from.

The wall of your gut acts as a barrier to keep food and bacteria living within the gut separate from internal organs and the bloodstream. If this wall becomes 'leaky' it will no longer act as a barrier and bacteria living within the gut and food could pass into the bloodstream. If bacteria get into the bloodstream they could react with cells of the immune system to trigger systemic (whole body) inflammation. This immune reaction could target components of the body, such as parts of the brain, and lead to some of the symptoms that ME/CFS patients experience.

Usually, the immune system fights infection from bacteria and viruses to keep us healthy. Sometimes the immune system reacts to bacteria, food or even parts of cells in our own body, which can make us feel ill. In ME/CFS patients there could be an inappropriate immune response triggered by bacteria that has leaked across the gut wall.

We already know that there is evidence of both an inappropriate immune response in ME/CFS patients and gut involvement as some patients experience abdominal pain and bloating (gastro-intestinal disturbances). We would like to see whether there is an inappropriate immune response that originates from the gut.

If sufficient evidence is found to confirm an inappropriate immune response resulting from a leaky gut, investigations into the use of future treatments may be initiated. These may include drugs to suppress the inappropriate immune response, or the use of healthy probiotic bacteria to restore a balanced community of gut microbes and aim to reduce gut wall leakiness.

Why have I been chosen?

If you have been given this information sheet to read, a severe ME/CFS patient interested in participating in this study has identified you as a potential household control.

How are household controls defined and why are we needed?

A household control is someone who is a relative, friend or carer of the patient and who regularly visits the patient. It is crucial that you are healthy and free from any medical conditions affecting your gut, autoimmune diseases or anxiety. In addition, you will not qualify as a household control if you are in recipient of immunomodulatory drugs, statins, beta blockers or steroids. You cannot have taken any antibiotics or probiotic capsules up to six weeks prior to enrolment in this study. If you are interested in participating in this study, we will help you complete an eligibility questionnaire to determine whether you qualify.

Household controls are needed to act as a comparison group. Gut microbes differ between people living in different environments. The composition of gut microbes is strongly influenced by the environment we live in. Comparing differences in gut microbes between patients and people living in different environments would limit the ability to identify ME/CFS specific alterations associated with gut microbes. Therefore, the use of household controls will allow us to identify ME/CFS specific alterations, as the effect of local environmental factors influencing gut microbe composition will be accounted for.

Do I have to take part?

No, you do not have to take part. Once you have read this information sheet you will be given as much time as you need to decide if you would like to donate a blood and stool sample to our study. It is your decision alone to participate and you can choose to withdraw at any time. **Please note any results relating to samples you have provided up until the moment you decide to withdraw will still be kept and included in the study.** However, your confidentiality will remain protected and it will not be possible to identify you in person, as all samples will be anonymised and given a unique identification number.

What would I have to do?

If you are interested in participating in this study please contact the research team (contact details are at the end of this sheet). We will arrange a telephone call with you to explain the study in more detail. You will then have 72 hours to decide whether you would be willing to take part. After this time, if you decide you would like to participate you can arrange the first study visit. If we do not hear from you after 72 hours we will assume you do not wish to participate and we will not contact you again.

Study visits

The first study visit is to confirm eligibility and to take you through the consenting process. All study visits will take place at the home of the severe ME/CFS patient you are matched with, as we are aware that patients may be unable to leave the house without a detrimental effect on their health, due to the severity of their symptoms. A member of the research team will take you through an eligibility questionnaire. Once eligibility is confirmed you will be taken through the consenting process by a member of the research team. You will also be asked to sign a consent form for the Norwich Biorepository, as once the study has ended, any remaining sample material will be banked for future research. Once you have consented onto the study, the study team will give you aa food diary with instructions and a stool sampling kit and instructions on how to use the stool sampling kit.

The second study visit is scheduled for sample collection to take place. You will be asked to collect your stool sample within 24 hours of your arranged home visit and you will be asked to record your food, fluid, medication and supplement intake within the food diary, for 48 hours prior to when you collect your stool sample. At the home visit

a trained phlebotomist or nurse will collect 50ml (approximately 10 teaspoons) of blood from a suitable vein in your arm. The research team will take the stool sample, blood sample and 48 hour food diary back to the Quadram Institute Bioscience for processing.

Important information:

- You must not have received antibiotic or probiotic treatment (such as probiotic tablets) **six weeks prior** to when samples are scheduled to be collected.
- You cannot have an active infection at the time the blood tests are taken, as a current infection, such as a cold, will affect the immune system and results collected.
- You will not be eligible for this study if you have any long term medical conditions, in particular, ones affecting your stomach and bowel.
- You should also ensure that you do not have any significant anxiety or depression and that you are not on any regular medication with the exception of oral contraceptives.
- Your general practitioner will be informed about your participation in this study.
- You must be able to understand the requirements of the study and be able to provide signed and dated informed consent.

What will I have to do?

1. Volunteer recruitment:
   - severe ME/CFS patients informed about the study through post
   - Patients provide healthy household controls with information sheet
2. Study explained:
   - Phone call with a member of the research team to discuss the study
   - Opportunity to ask questions
   - Then 72 hours to consider participation
   - Volunteers interested in participating arrange appointment for 1st study visit
3. 1st study visit:
   - Eligibility questionnaire completed
   - Consent taken
   - Given stool sample kit and instructions
   - Given 48 hour food diary and instructions
4. 2nd study visit:
   - Blood sample taken
   - Stool sample taken less than 24 hours prior to house visit

What will happen to the samples I give?

When you give your samples to the courier, the courier will transport the samples to the Quadram Institute Bioscience (QIB), Norwich. Here we will process the blood and stool samples that you provided. At the QIB and collaborating institutes we will examine the immune cells within the blood to see whether they react with microbes in your stool sample. We will then see whether these immune cells are capable of moving from the gut to the brain and react with proteins on brain cells.

We will also be looking at the presence of antibodies (proteins produced by immune cells) within your blood to see whether they are specific to microbes from stool samples, or specific to certain types of food.

The levels and diversity of microbes within your stool samples will also be analysed.

The data collected from the samples you donate will be used as a control and will be compared to results collected from the patient you are matched with to determine whether the presence of an immune response directed against gut bacteria is specific to ME/CFS patients.

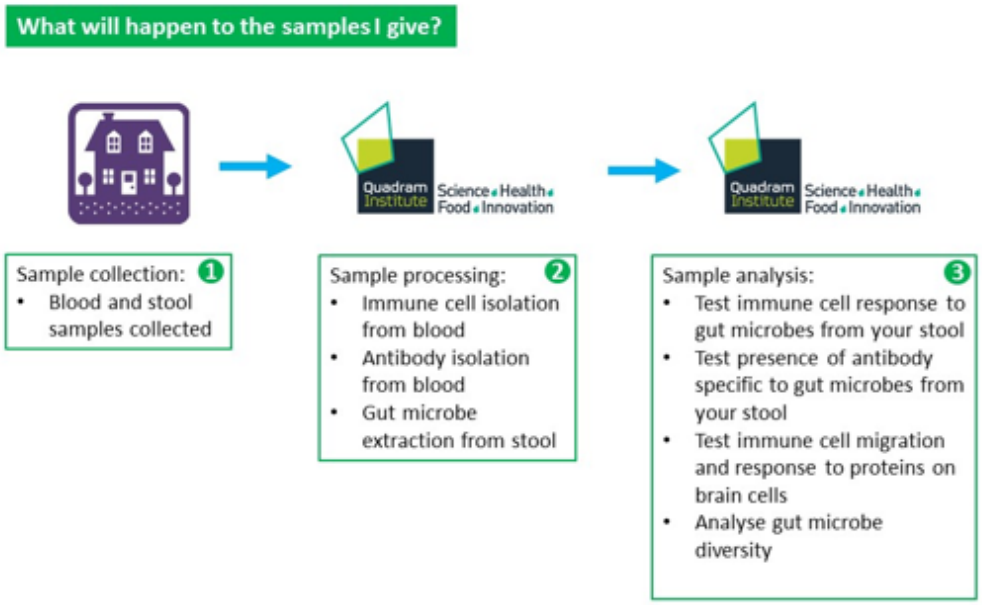

Sample analysis at collaborating research centres

Part of the research aims require samples to be sent to external research centres for analysis. Examples of this includes DNA from the gut microbes for sequencing.

You will be given the option to donate your samples to ethically approved animal research undertaken at King's College London by Dr David Andersson, with whom we are collaborating. The animal research involves serum IgG being used to identify biomarkers for ME/CFS and research symptom manifestation. Fatigue and pain symptoms will be examined in mice following the administration of serum IgG. Samples sent to collaborating research groups will be anonymised. **You are still able to participate in this human study if you do not wish for your samples to be used in animal research.**

What will happen to the samples I give after this research project has been completed?

We will transfer any unused blood and stool samples to the Norwich Biorepository for long term storage and subsequent use in research projects that wish to address similar research questions. These samples will be kept anonymised to maintain confidentiality.

Do I have to donate both types of sample, or can I just donate blood or stool samples?

The priority for this study is to assess whether there is the presence of an immune response directed against gut microbes. Stool samples will be used to acquire gut microbes and the blood will be used to isolate immune cells and immune cell products. Analysing whether immune cells from the blood can target and react with gut microbes from stool will determine whether patients have an immune response generated against gut microbes. Therefore, for this study we will need both blood and stool samples to be donated.

What are the possible risks of taking part?

Possible risks of taking part are associated with blood donation. Like any blood test you have, there is a risk of experiencing discomfort, pain, bleeding, bruising or infection during or after blood collection.

The precise procedure for getting your blood sample is simple. Prior to having your blood sample taken you will be seated comfortably and the area on your arm that will be used to donate blood will be cleaned with a swab. A tourniquet will be applied to your upper arm and tightened. Blood will be taken from a suitable vein in your arm by a trained phlebotomist or nurse. After the needle is removed you should firmly press on this area for a minute to prevent bruising which can be uncomfortable and sometimes painful. Microtape will be used to adhere cotton wool to the site of venous access.

What are the possible benefits of taking part in this study?

By taking part in this study you could help to progress ME/CFS research, discovering more about the causes or illness progression of ME/CFS. The results from this study could lead to better diagnostic tests and more effective treatments being made available to ME/CFS patients in future.

Will my details be kept confidential?

All data will be handled in compliance with EU GDPR and UK Data Protection Act 2018. All samples you donate will be anonymised and assigned a unique identification number. As the research team will be collecting samples from your homes identifiable data such as personal addresses, telephone number and email address will be stored on a password protected computer accessed by the chief investigator and academic supervisors only.

This means that you will not be identifiable to researchers, as any samples or information leaving the hospital will be referred to only by the unique number that is allocated to you. All information collected about you during the research project will be kept strictly confidential.

What will happen to the results of this research study?

Results from this study will be published in international scientific journals and presented at conferences. At the end of the study results will be made available on the Invest in ME Research UK website (www.investinme.org). It will also form the basis of an educational project and PhD thesis to be submitted to the University of East Anglia. At no point will you be identifiable, in person, from any publications of work presented at scientific conferences

Please note we will **not** be able to give you your individual results at any point during or after this study.

How can I make an appointment to give my consent?

You can make an appointment by contacting either Katharine Seton, chief investigator and PhD student, by calling 01603 255148 or emailing katharine.seton@quadram.ac.uk.

Thank you for taking the time to consider your involvement in this study

Appendix VI: AI-ME/CFS study eligibility questionnaire

IRAS ID: 218545

Defining autoimmune aspects of Myalgic Encephalomyelitis/ Chronic Fatigue Syndrome (ME/CFS): ELIGIBILITY QUESTIONNAIRE

Complete the following details:
Donor's name ……
Date of Birth ……

Thank you for expressing an interest to participate as a household control in this study. Please ensure you have read the information sheet and understand what this study involves.

In order to check that you are eligible to take part in this study, please answer the following questions (circle yes or no):

1. How old are you? ……
2. Are you male or female? ……
3. Do you have any long term medical conditions affecting the gut (e.g. IBD, IBS, bowel cancer)?

   YES/NO

   If yes, please give details:

   ……

   ……
4. Have you been previously diagnosed with an autoimmune condition (e.g. systemic lupus erythematous or rheumatoid arthritis)? **YES/NO**

   If yes, please give details:

   ……

   ……

5. Do you suffer from significant anxiety of depression? **YES/NO**
6. Do you take statins on a regular basis? **YES/NO**
7. Do you take beta blockers on a regular basis? **YES/NO**
8. Do you take steroids on a regular basis? (e.g. prednisolone, cortisone, hydrocortisone) **YES/NO**
9. Do you take immunomodulatory drugs on a regular basis? **YES/NO**
10. Do you take any other drugs (not stated above) on a regular basis? **YES/NO**

    If yes, please give details:

    .....

    .....

11. Have you taken any antibiotics or probiotics in the past 6 weeks? **YES/NO**
12. What is your relationship to the ME/CFS patient you are willing to be matched with in this study?

    .....

Appendix VII: Example of AI-ME/CFS study patient consent form

Defining autoimmune aspects of Myalgic Encephalomyelitis/ Chronic Fatigue Syndrome (ME/CFS): Patient consent form

IRAS ID: 218545

Participant Identification Number for this trial:

Participant please initial each box

I confirm that I have read and understand the information sheet **dated** _____ version **no.**__for the above study, and I have had the opportunity to consider the information, discuss the study and ask questions. ☐

I confirm that I have received satisfactory answers to my questions. ☐

I understand that my participation is voluntary, and I am free to withdraw from the study (1) at any time without giving a reason and (2) without my legal rights being affected (3) and without my medical care being affected ☐

With whom have you discussed the information for this research study?

Name: _____ **Role: Chief Investigator/Study Scientist**

I understand that any of my personal information and data collected during the study may be looked at by individuals at **QIB**, where it is relevant to participation in this study and used anonymously to support other Research at QIB in the future and may be shared with other researchers, including those in other countries. ☐

I give permission for these individuals to have access to my information and data, including information on disease severity, disease duration and symptoms experienced (provided by your clinician). ☐

I understand that relevant sections of my medical notes and data collected during the study may be looked at by individuals from regulatory authorities from the NHS trust where it is relevant to my taking part in this research. I give permission for these individuals to have access to my records. ☐

I understand that my personal information and data will be held confidentially at **QIB** and that it will be destroyed after 15 years. ☐

I agree to my GP being informed of my participation in the study. ☐

Name and address of your General Practitioner:

.....

.....

.....

I understand that all research is subject to inspection and audit. ☐
NB: although your records may be accessed for this purpose your personal information remains confidential

I am happy to provide blood and stool sample donations, and for them to be collected from my home. ☐

1 copy of the signed consent form must be given to the participant to keep.
1 copy of the signed consent form must be kept in the study records at QIB.

OPTIONAL

I have been informed that as part of the study, the procedures outlined below are entirely optional.
I understand that I am not obliged to agree to these points and that declining any of these will not affect my participation in the study.

1. I give permission for my samples to be used in ethically approved animal research

yes	no

2. If yes, I understand that my samples, without my name and contact details, may be transferred to a research group in Kings College London for analysis.

3. I give permission for researchers to store my donated samples for an indefinite amount of time at the Norwich Research Park Biorepository (NNUH Tissue Bank). I understand that my donated samples may be used in ethically approved research in the future.

yes	no

4. I agree to be contacted by the investigators to be invited to participate in future research for which I may be eligible. I give permission for my contact details to be stored for this purpose.

yes	no

I agree to take part in the above study. ☐

Signed: …… (Name of participant in BLOCK letters)……

Date: …… **Date of Birth:** ……

I confirm that the participant above has been given a full verbal and written explanation of the study.

Name of person taking consent

Signed: …… (Name in BLOCK letters)……

Role: **Chief Investigator / Study Scientist** **Date:** ……

1 copy of the signed consent form must be given to the participant to keep.
1 copy of the signed consent form must be kept in the study records at QIB.

Appendix VIII: Example of AI-ME/CFS study control consent form

Defining autoimmune aspects of Myalgic Encephalomyelitis/Chronic Fatigue Syndrome (ME/CFS): Household control consent form

IRAS ID: 218545
Participant Identification Number for this trial:

Participant please initial each box

I confirm that I have read and understand the information sheet **dated** _____ version **no.**__for the above study, and I have had the opportunity to consider the information, discuss the study and ask questions. ☐

I confirm that I have received satisfactory answers to my questions. ☐

I understand that my participation is voluntary, and I am free to withdraw from the study (1) at any time without giving a reason and (2) without my legal rights being affected ☐

With whom have you discussed the information for this research study?

Name: _____ **Role: Chief Investigator/Study Scientist**

I understand that any of my personal information and data collected during the study may be looked at by individuals at **QIB**, where it is relevant to participation in this study and used anonymously to support other Research at QIB in the future and may be shared with other researchers, including those in other countries. ☐

I give permission for these individuals to have access to my information and data. ☐

I understand that my personal information and data will be held confidentially at **QIB** and that it will be destroyed after 15 years. ☐

I agree to my GP being informed of my participation in the study. ☐

Name and address of your General Practitioner:

.....

.....

.....

I understand that all research is subject to inspection and audit. ☐
NB: although your records may be accessed for this purpose your personal information remains confidential

I am happy to provide blood and stool sample donations, and for them to be collected from my home. ☐

OPTIONAL
I have been informed that as part of the study, the procedures outlined below are entirely optional.
I understand that I am not obliged to agree to these points and that declining any of these will not affect my participation in the study.

yes	no

1 copy of the signed consent form must be given to the participant to keep.
1 copy of the signed consent form must be kept in the study records at QIB.

1. I give permission for my samples to be used in ethically approved animal research

2. If yes, I understand that my samples, without my name and contact details, will be transferred to a research group in Kings College London for analysis. ☐

3. I give permission for researchers to store my donated samples for an indefinite amount of time at the Norwich Research Park Biorepository (NNUH Tissue Bank). I understand that my donated samples may be used in ethically approved research in the future.

yes	no

4. I agree to be contacted by the investigators to be invited to participate in future research for which I may be eligible. I give permission for my contact details to be stored for this purpose.

yes	no

I agree to take part in the above study.

Signed: …… (Name of participant in BLOCK letters)……

Date: …… **Date of Birth:** ……

I confirm that the participant above has been given a full verbal and written explanation of the study.

Name of person taking consent

Signed: …… (Name in BLOCK letters)……

Role: Chief Investigator / Study Scientist **Date:** ……

1 copy of the signed consent form must be given to the participant to keep.
1 copy of the signed consent form must be kept in the study records at QIB.

IRAS ID: 218545

Defining autoimmune aspects of Myalgic Encephalomyelitis/ Chronic Fatigue Syndrome (ME/CFS): INSTRUCTIONS FOR STOOL SAMPLE COLLECTION

As you have expressed interest in participating in this study, you have been provided with a "Faecescollector Fecocontainer" to facilitate stool sample collection. Please collect your stool sample **within 24 hours of your scheduled home visit**, where you will be taken through the consenting process and have your first blood sample donated. Stool samples will be handed over to a member of the research team, along with the food diary, once consent has been taken. Instructions on how to use the kit are given below:

1. Remove the faecescollector out of the box and check if the product is not damaged. If damaged asked a member of the research team for another item. Wash your hands and unscrew the cover (anti-clockwise; Figure 1).
2. Push the white receptacle downwards until it is fully extended (Figure 2).
3. Fold down the brackets (Figure 3).
4. Prior to the collection of stool: make sure you have urinated. Put the toilet seat up and place the faecescollector carefully under the toilet seat (Figure 4). Then put the toilet seat down.
5. Collect your stool in the white receptacle (Figure 5). Make sure you only collect stool, so **no urine or toilet paper** in the receptacle. Be aware that the outside of the stool collector stays clean.
6. Next take the AnaeroGen Compact, tear open, **do not use scissors**, take out the satchet and place into the collection bowl.
7. After the stool, you can cover the faecescollector (clockwise). Make sure the blue lid closes well (Figure 6) and double-check this. Write down your unique identification number, sample number, date and time you collected the stool and your date of birth with a ballpoint pen on the sticker. Stick the sticker on the lid.
8. Fold the brackets inwards and place the faecescollector in the supplied plastic bag (Figure 7).
9. Pull the string of the plastic bag securely (Figure 8).
10. Place the sample into the fridge and await collection.


1
2
3
4
5
6
7
8
Please read first the Instructions for Use.

Appendix X: Shortened medical outcomes study 36-item short form health survey (SF-36)

Study title: Defining autoimmune aspects of Myalgic Encephalomyelitis/ Chronic Fatigue Syndrome (ME/CFS)

Participant unique ID:

ID Code: MDS

Flag F

1 - Pre 5 - 24 mth
2 - 6 wk 6 - Misc
3 - 6 mth 7 - D/C
4 - 12 mth

CFS/NHS/DEPT - *Specialist help for ME* NHS

MOS (SF-36)

The following questions are about ACTIVITIES you might do during a typical day.
Does your health now limit you in these activities? If so, how much?

Please cross only one box in each line ☒

		Yes, limited a lot	Yes, limited a little	No, not limited at all
1.1	Vigorous activities, such as running, lifting heavy objects, participating in strenuous sports	1 ☐	2 ☐	3 ☐
1.2	Moderate activities, such as moving a table, pushing a vacuum cleaner, bowling, or playing golf	1 ☐	2 ☐	3 ☐
1.3	Lifting or carrying groceries	1 ☐	2 ☐	3 ☐
1.4	Climbing several flights of stairs	1 ☐	2 ☐	3 ☐
1.5	Climbing one flight of stairs	1 ☐	2 ☐	3 ☐
1.6	Bending, kneeling, or stooping	1 ☐	2 ☐	3 ☐
1.7	Walking more than a mile	1 ☐	2 ☐	3 ☐
1.8	Walking half a mile	1 ☐	2 ☐	3 ☐
1.9	Walking one hundred yards	1 ☐	2 ☐	3 ☐
1.10	Bathing or dressing yourself	1 ☐	2 ☐	3 ☐

Appendix XI: Chalder fatigue questionnaire

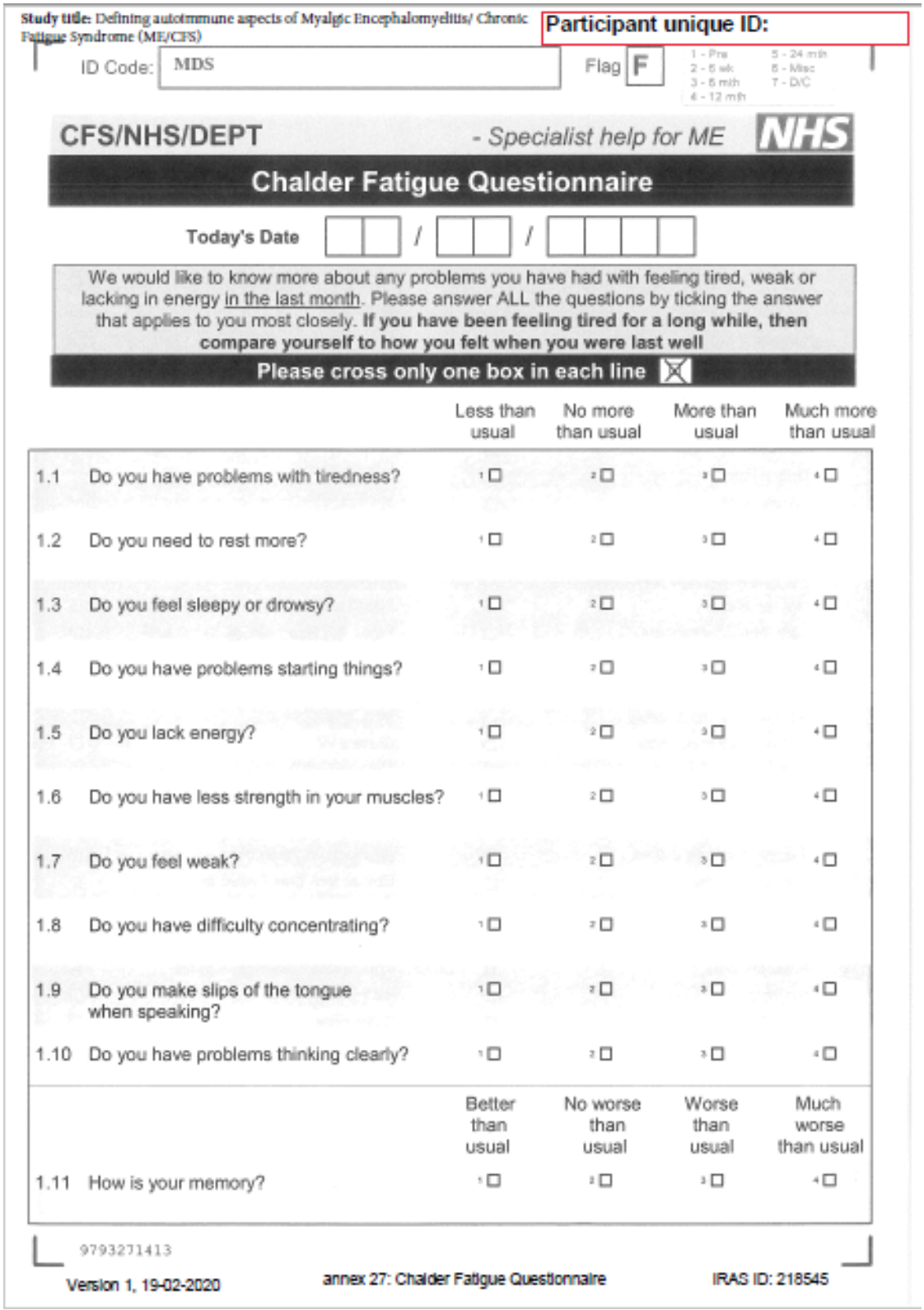

Study title: Defining autoimmune aspects of Myalgic Encephalomyelitis/ Chronic Fatigue Syndrome (ME/CFS)

Participant unique ID:

ID Code: MDS

Flag F

1 - Pre 2 - 5 wk 3 - 5 mth 4 - 12 mth 5 - 24 mth 6 - Misc 7 - D/C

CFS/NHS/DEPT - *Specialist help for ME* NHS

Chalder Fatigue Questionnaire

Today's Date ☐☐ / ☐☐ / ☐☐☐☐

We would like to know more about any problems you have had with feeling tired, weak or lacking in energy in the last month. Please answer ALL the questions by ticking the answer that applies to you most closely. **If you have been feeling tired for a long while, then compare yourself to how you felt when you were last well**

Please cross only one box in each line ☒

		Less than usual	No more than usual	More than usual	Much more than usual
1.1	Do you have problems with tiredness?	1 ☐	2 ☐	3 ☐	4 ☐
1.2	Do you need to rest more?	1 ☐	2 ☐	3 ☐	4 ☐
1.3	Do you feel sleepy or drowsy?	1 ☐	2 ☐	3 ☐	4 ☐
1.4	Do you have problems starting things?	1 ☐	2 ☐	3 ☐	4 ☐
1.5	Do you lack energy?	1 ☐	2 ☐	3 ☐	4 ☐
1.6	Do you have less strength in your muscles?	1 ☐	2 ☐	3 ☐	4 ☐
1.7	Do you feel weak?	1 ☐	2 ☐	3 ☐	4 ☐
1.8	Do you have difficulty concentrating?	1 ☐	2 ☐	3 ☐	4 ☐
1.9	Do you make slips of the tongue when speaking?	1 ☐	2 ☐	3 ☐	4 ☐
1.10	Do you have problems thinking clearly?	1 ☐	2 ☐	3 ☐	4 ☐

		Better than usual	No worse than usual	Worse than usual	Much worse than usual
1.11	How is your memory?	1 ☐	2 ☐	3 ☐	4 ☐

9793271413

Version 1, 19-02-2020 annex 27: Chalder Fatigue Questionnaire IRAS ID: 218545

Appendix XII: Hospital anxiety and depression scale (HADS)

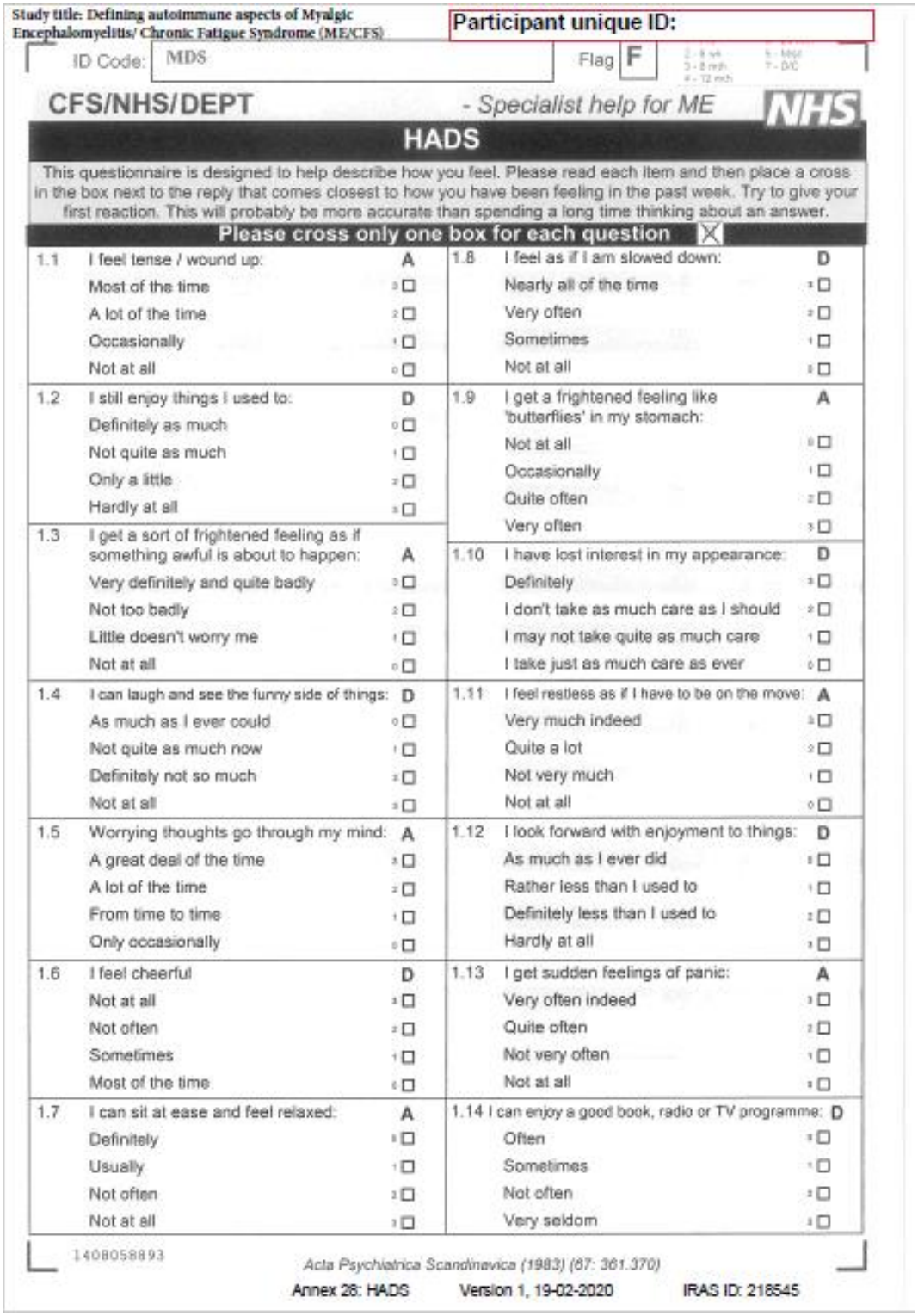

Study title: Defining autoimmune aspects of Myalgic Encephalomyelitis/ Chronic Fatigue Syndrome (ME/CFS)

Participant unique ID:

ID Code: MDS Flag F

CFS/NHS/DEPT - Specialist help for ME NHS

HADS

This questionnaire is designed to help describe how you feel. Please read each item and then place a cross in the box next to the reply that comes closest to how you have been feeling in the past week. Try to give your first reaction. This will probably be more accurate than spending a long time thinking about an answer.

Please cross only one box for each question

1.1	I feel tense / wound up:	A	1.8	I feel as if I am slowed down:	D
	Most of the time	3 ☐		Nearly all of the time	3 ☐
	A lot of the time	2 ☐		Very often	2 ☐
	Occasionally	1 ☐		Sometimes	1 ☐
	Not at all	0 ☐		Not at all	0 ☐
1.2	I still enjoy things I used to:	D	1.9	I get a frightened feeling like 'butterflies' in my stomach:	A
	Definitely as much	0 ☐		Not at all	0 ☐
	Not quite as much	1 ☐		Occasionally	1 ☐
	Only a little	2 ☐		Quite often	2 ☐
	Hardly at all	3 ☐		Very often	3 ☐
1.3	I get a sort of frightened feeling as if something awful is about to happen:	A	1.10	I have lost interest in my appearance:	D
	Very definitely and quite badly	3 ☐		Definitely	3 ☐
	Not too badly	2 ☐		I don't take as much care as I should	2 ☐
	Little doesn't worry me	1 ☐		I may not take quite as much care	1 ☐
	Not at all	0 ☐		I take just as much care as ever	0 ☐
1.4	I can laugh and see the funny side of things:	D	1.11	I feel restless as if I have to be on the move:	A
	As much as I ever could	0 ☐		Very much indeed	3 ☐
	Not quite as much now	1 ☐		Quite a lot	2 ☐
	Definitely not so much	2 ☐		Not very much	1 ☐
	Not at all	3 ☐		Not at all	0 ☐
1.5	Worrying thoughts go through my mind:	A	1.12	I look forward with enjoyment to things:	D
	A great deal of the time	3 ☐		As much as I ever did	0 ☐
	A lot of the time	2 ☐		Rather less than I used to	1 ☐
	From time to time	1 ☐		Definitely less than I used to	2 ☐
	Only occasionally	0 ☐		Hardly at all	3 ☐
1.6	I feel cheerful	D	1.13	I get sudden feelings of panic:	A
	Not at all	3 ☐		Very often indeed	3 ☐
	Not often	2 ☐		Quite often	2 ☐
	Sometimes	1 ☐		Not very often	1 ☐
	Most of the time	0 ☐		Not at all	0 ☐
1.7	I can sit at ease and feel relaxed:	A	1.14	I can enjoy a good book, radio or TV programme:	D
	Definitely	0 ☐		Often	0 ☐
	Usually	1 ☐		Sometimes	1 ☐
	Not often	2 ☐		Not often	2 ☐
	Not at all	3 ☐		Very seldom	3 ☐

1408058893

Acta Psychiatrica Scandinavica (1983) (67: 361-370)

Annex 28: HADS Version 1, 19-02-2020 IRAS ID: 216545

Appendix XIII: Self-efficacy questionnaire

Study title: Defining autoimmune aspects of Myalgic Encephalomyelitis/ Chronic Fatigue Syndrome (ME/CFS)
MDS

F

NHS

Participant unique ID:

CHRONIC FATIGUE SERVICE
Self-efficacy Questionnaire

Please rate how confident you are that you *can do* the following things, *despite the symptoms*. To answer, circle *one* of the numbers on the scale under each item, where 0 = 'not at all confident' and 6 = 'completely confident'

This questionnaire is not asking about whether or not you have been doing these things, but rather *how confident you are that you can do them*, despite the symptoms.

1. I can still enjoy things despite the symptoms

0 1 2 3 4 5 6
Not at all Confident **completely confident**

2. I can still do most of the household chores (e.g. tidying up, washing dishes etc) despite the symptoms

0 1 2 3 4 5 6
Not at all Confident **completely confident**

3. I can socialise with my friends or family members as often as I used to, despite the symptoms

0 1 2 3 4 5 6
Not at all Confident **completely confident**

4. I can cope with my symptoms in most situations

0 1 2 3 4 5 6
Not at all Confident **completely confident**

5. I can do some sort of work despite the symptoms ('work' includes housework, paid or unpaid work)

0 1 2 3 4 5 6
Not at all Confident **completely confident**

6. I can still do many of the things I enjoy doing, such as hobbies or leisure activities, despite the symptoms

0 1 2 3 4 5 6
Not at all Confident **completely confident**

7. I can cope with my symptoms without medication

0 1 2 3 4 5 6
Not at all Confident **completely confident**

Appendix XIV: Visual analogue pain rating scale

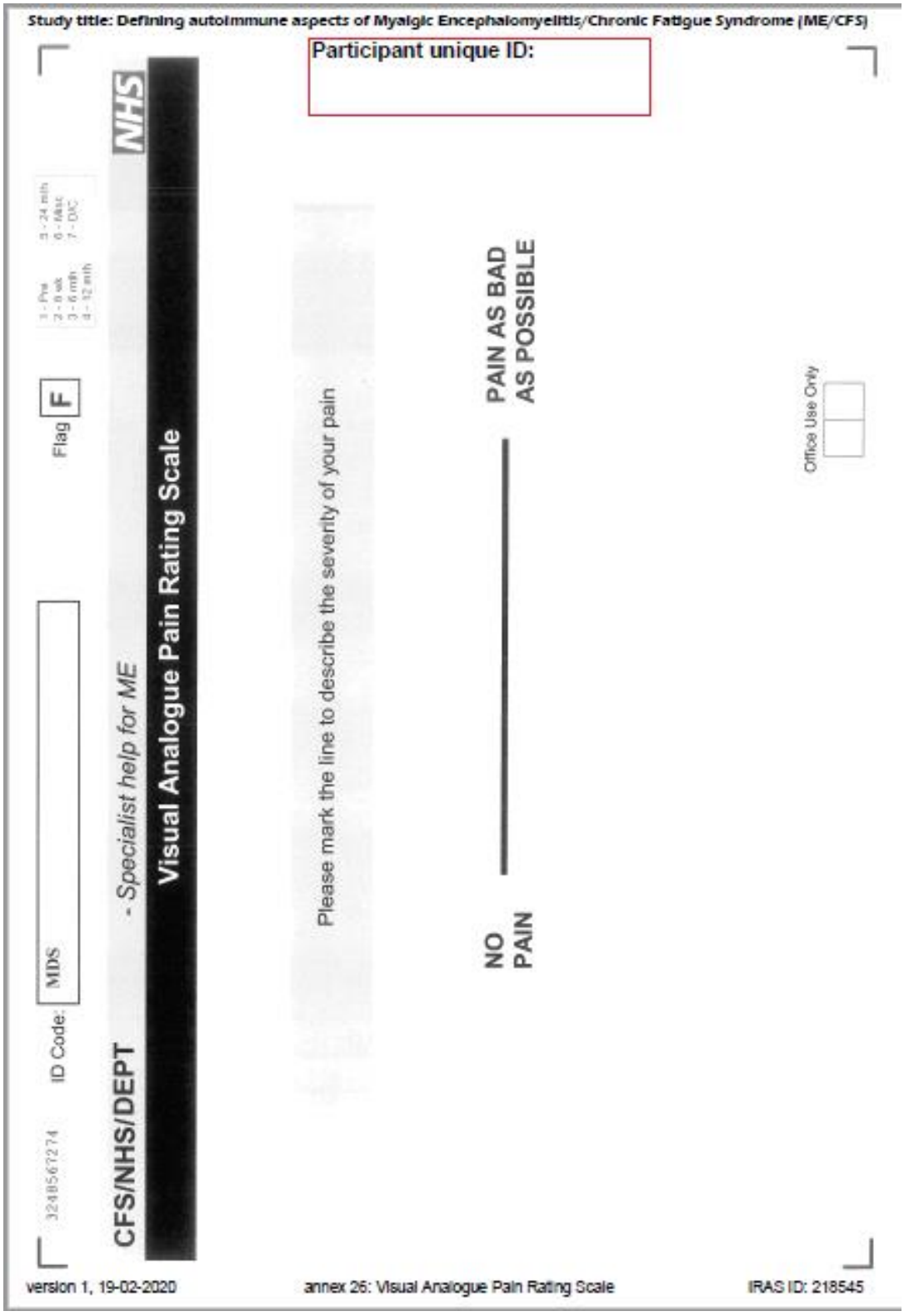

Appendix XV: Epworth sleepiness scale

IRAS ID: 218545 Annex 24: Epworth Sleepiness Scale Version 1, 19-02-2020

Study title: Defining autoimmune aspects of Myalgic Encephalomyelitis/ Chronic Fatigue Syndrome (ME/CFS)

Participant unique identification number:

ID Code: MDS MDS

Flag: 1

1 - Pre 5 - 24 mth
2 - 6 wk 6 - Exit
3 - 6 mth 7 - D/C
4 - 12 mth

1

CFS/NHS/ADULT - *Specialist help for ME* NHS

Epworth Sleepiness Scale

How likely are you to doze off or fall asleep in the following situations, in contrast to feeling just tired?

This refers to your usual way of life in recent times.

Please cross only one box in each line ☒

It is important that you answer each question as best you can

		would never doze	slight chance of dozing	moderate chance of dozing	high chance of dozing
1.1	Sitting and reading	0 ☐	1 ☐	2 ☐	3 ☐
1.2	Watching TV	0 ☐	1 ☐	2 ☐	3 ☐
1.3	Sitting, inactive in a public place like a theatre or meeting	0 ☐	1 ☐	2 ☐	3 ☐
1.4	As a passenger in a car for an hour without a break	0 ☐	1 ☐	2 ☐	3 ☐
1.5	Lying down to rest in the afternoon when circumstances permit	0 ☐	1 ☐	2 ☐	3 ☐
1.6	Sitting and talking to someone	0 ☐	1 ☐	2 ☐	3 ☐
1.7	Sitting quietly after lunch without alcohol	0 ☐	1 ☐	2 ☐	3 ☐
1.8	In a car, while stopped for a few minutes in traffic	0 ☐	1 ☐	2 ☐	3 ☐

Appendix XVI: AI-ME/CFS study ME/CFS symptom questionnaire

IRAS ID: 218545

Participant Unique identification number:

CFS/ME symptom questionnaire

Please answer the questionnaire below to give the researchers an idea of which symptoms you experience. Answer each question by circling either yes or no.

The study team is happy to help you completing this questionnaire.

Symptoms	please circle the one that applies to you	Comments
Do you experience post-exertional malaise? (fatigue made worse by any significant physical or mental activity)	yes/no	
Do you experience non-restorative sleep? (do you find your sleep is non-refreshing and that you wake up feeling as though you haven't slept at all)	yes/no	
Do you experience headaches that are new, more frequent or different in character?	yes/no	
Do you experience recurrent sore throat with enlarged glands in the neck?	yes/no	

Participant Unique identification number:

Symptoms	please circle the one that applies to you	Comments
Do you have trouble concentrating?	yes/no	
Do you have a reduced short-term memory (e.g. being able to recall what you ate the day before)	yes/no	
Do you experience joint pain or stiffness lasting several hours?	yes/no	
Do you experience aches affecting several muscle groups?	yes/no	
Are you intolerant to bright lights?	yes/no	
Are you intolerant to noise?	yes/no	
Do you often feel faint on standing?	yes/no	

Participant Unique identification number:

Symptoms	please circle the one that applies to you	Comments
Do you experience frequent nausea or vomiting?	yes/no	
Have you ever been diagnosed with fibromyalgia?	yes/no	
Do you experience irritable bowel syndrome like problems, or have ever been diagnosed with IBS?	yes/no	
Do you have cold extremities (cold hands and feet)?	yes/no	
Do you find it difficult to regulate your temperature (do you get unusually warm or cold for seasonal climates)?	yes/no	
Do you experience giddiness/dizziness/imbalance?	yes/no	
Do you experience clumsiness or poor coordination?	yes/no	
Do you experience bladder problems?	yes/no	

Participant Unique identification number:

Onset of fatigue:

Date of onset: .....

Was the onset gradual or sudden (circle answer):

- Gradual / sudden

Did you experience any of the following during or prior to onset of fatigue (circle the options that apply to you):

- Stress / viral infection / bacterial infection / surgery / toxin exposure

REFERENCES

ACHESON, E. D. 1959. The clinical syndrome variously called benign myalgic encephalomyelitis, Iceland disease and epidemic neuromyasthenia. *The American Journal of Medicine,* 26**,** 569-95.

ADAMS, R. J., HEAZLEWOOD, S. P., GILSHENAN, K. S., O'BRIEN, M., MCGUCKIN, M. A. & FLORIN, T. H. 2008. IgG antibodies against common gut bacteria are more diagnostic for Crohn's disease than IgG against mannan or flagellin. *The American Journal of Gastroenterology,* 103**,** 386-96.

AIELLO, A., FARZANEH, F., CANDORE, G., CARUSO, C., DAVINELLI, S., GAMBINO, C. M., LIGOTTI, M. E., ZAREIAN, N. & ACCARDI, G. 2019. Immunosenescence and Its Hallmarks: How to Oppose Aging Strategically? A Review of Potential Options for Therapeutic Intervention. *Frontiers in Immunology,* 10.

ALBERT-BAYO, M., PARACUELLOS, I., GONZÁLEZ-CASTRO, A. M., RODRÍGUEZ-URRUTIA, A., RODRÍGUEZ-LAGUNAS, M. J., ALONSO-COTONER, C., SANTOS, J. & VICARIO, M. 2019. Intestinal Mucosal Mast Cells: Key Modulators of Barrier Function and Homeostasis. *Cells*, 8(2), 135.

ARIMATSU, K., YAMADA, H., MIYAZAWA, H., MINAGAWA, T., NAKAJIMA, M., RYDER, M. I., GOTOH, K., MOTOOKA, D., NAKAMURA, S., IIDA, T. & YAMAZAKI, K. 2014. Oral pathobiont induces systemic inflammation and metabolic changes associated with alteration of gut microbiota. *Scientific Reports,* 4**,** 4828.

ARMSTRONG, C. W., MCGREGOR, N. R., LEWIS, D. P., BUTT, H. L. & GOOLEY, P. R. 2015. Metabolic profiling reveals anomalous energy metabolism and oxidative stress pathways in chronic fatigue syndrome patients. *Metabolomics,* 11**,** 1626-1639.

ARMSTRONG, C. W., MCGREGOR, N. R., SHEEDY, J. R., BUTTFIELD, I., BUTT, H. L. & GOOLEY, P. R. 2012. NMR metabolic profiling of serum identifies amino acid disturbances in chronic fatigue syndrome. *Clinica Chimica Acta,* 413**,** 1525-31.

ARMSTRONG, C., MCGREGOR, N., LEWIS, D., BUTT, H. & GOOLEY, P. 2016. The association of fecal microbiota and fecal, blood serum and urine metabolites in myalgic encephalomyelitis/chronic fatigue syndrome. *Metabolomics,* 13.

ATARASHI, K., TANOUE, T., ANDO, M., KAMADA, N., NAGANO, Y., NARUSHIMA, S., SUDA, W., IMAOKA, A., SETOYAMA, H., NAGAMORI, T., ISHIKAWA, E., SHIMA, T., HARA, T., KADO, S., JINNOHARA, T., OHNO, H., KONDO, T., TOYOOKA, K., WATANABE, E., YOKOYAMA, S., TOKORO, S., MORI, H., NOGUCHI, Y., MORITA, H., IVANOV, II, SUGIYAMA, T., NUÑEZ, G., CAMP, J. G., HATTORI, M., UMESAKI, Y. & HONDA, K. 2015. Th17 Cell Induction by Adhesion of Microbes to Intestinal Epithelial Cells. *Cell,* 163**,** 367-80.

AZZOUZ, D., OMARBEKOVA, A., HEGUY, A., SCHWUDKE, D., GISCH, N., ROVIN, B. H., CARICCHIO, R., BUYON, J. P., ALEKSEYENKO, A. V. & SILVERMAN, G. J. 2019. Lupus nephritis is linked to disease-activity associated expansions and immunity to a gut commensal. *Annals of the Rheumatic Diseases,* 78**,** 947.

BAKER, R. & SHAW, E. J. 2007. Diagnosis and management of chronic fatigue syndrome or myalgic encephalomyelitis (or encephalopathy): summary of NICE guidance. *Bmj,* 335**,** 446-8.

BAKKEN, I. J., TVEITO, K., GUNNES, N., GHADERI, S., STOLTENBERG, C., TROGSTAD, L., H ÅBERG, S. E. & MAGNUS, P. 2014. Two age peaks in the incidence of chronic fatigue syndrome/myalgic encephalomyelitis: a population-based registry study from Norway 2008-2012. *BMC Medicine,* 12**,** 167.

BALA, S., MARCOS, M., GATTU, A., CATALANO, D. & SZABO, G. 2014. Acute Binge Drinking Increases Serum Endotoxin and Bacterial DNA Levels in Healthy Individuals. *PLOS ONE,* 9**,** e96864.

BALINAS, C., CABANAS, H., STAINES, D. & MARSHALL-GRADISNIK, S. 2019. Transient receptor potential melastatin 2 channels are overexpressed in myalgic encephalomyelitis/chronic fatigue syndrome patients. *Journal of Translational Medicine,* 17**,** 401.

BALMER, M. L., SLACK, E., DE GOTTARDI, A., LAWSON, M. A., HAPFELMEIER, S., MIELE, L., GRIECO, A., VAN VLIERBERGHE, H., FAHRNER, R., PATUTO, N., BERNSMEIER, C., RONCHI, F., WYSS, M., STROKA, D., DICKGREBER, N., HEIM, M. H., MCCOY, K. D. & MACPHERSON, A. J. 2014. The liver may act as a firewall mediating mutualism between the host and its gut commensal microbiota. *Science Translational Medicine,* 6**,** 237ra66.

BANSAL, A. S. 2016. Investigating unexplained fatigue in general practice with a particular focus on CFS/ME. *BMC Family Practice,* 17**,** 81.

BARLOW, J. T., BOGATYREV, S. R. & ISMAGILOV, R. F. 2020. A quantitative sequencing framework for absolute abundance measurements of mucosal and lumenal microbial communities. *Nature Communications,* 11**,** 2590.

BARNDEN, L. R., CROUCH, B., KWIATEK, R., BURNET, R. & DEL FANTE, P. 2015. Evidence in chronic fatigue syndrome for severity-dependent upregulation of prefrontal myelination that is independent of anxiety and depression. *NMR in Biomedicine,* 28**,** 404-13.

BARNDEN, L. R., CROUCH, B., KWIATEK, R., BURNET, R., MERNONE, A., CHRYSSIDIS, S., SCROOP, G. & DEL FANTE, P. 2011. A brain MRI study of chronic fatigue syndrome: evidence of brainstem dysfunction and altered homeostasis. *NMR in Biomedicine,* 24**,** 1302-12.

BAVINTON, J., DARBISHIRE, L. & WHITE, P. 2004. PACE Manual for Therapists: Graded Exercise Therapy for CFS/ME. ME-PediaOrg.

BEGHINI, F., MCIVER, L. J., BLANCO-MÍGUEZ, A., DUBOIS, L., ASNICAR, F., MAHARJAN, S., MAILYAN, A., MANGHI, P., SCHOLZ, M., THOMAS, A. M., VALLES-COLOMER, M., WEINGART, G., ZHANG, Y., ZOLFO, M., HUTTENHOWER, C., FRANZOSA, E. A. & SEGATA, N. 2021. Integrating

taxonomic, functional, and strain-level profiling of diverse microbial communities with bioBakery 3. *Elife,* 10.

BELKAID, Y. & HAND, T. W. 2014. Role of the microbiota in immunity and inflammation. *Cell,* 157**,** 121-41.

BENJAMINI, Y. & HOCHBERG, Y. 1995. Controlling The False Discovery Rate - A Practical And Powerful Approach To Multiple Testing. *Journal of Royal Statistical Society: Series B,* 57**,** 289-300.

BJÖRKQVIST, O., REPSILBER, D., SEIFERT, M., BRISLAWN, C., JANSSON, J., ENGSTRAND, L., RANGEL, I. & HALFVARSON, J. 2019. Alterations in the relative abundance of *Faecalibacterium prausnitzii* correlate with changes in fecal calprotectin in patients with ileal Crohn's disease: a longitudinal study. *Scandinavian Journal of Gastroenterology,* 54**,** 577-585.

BLAKE, M. R., RAKER, J. M. & WHELAN, K. 2016. Validity and reliability of the Bristol Stool Form Scale in healthy adults and patients with diarrhoea-predominant irritable bowel syndrome. *Alimentary Pharmacology & Therapeutics,* 44**,** 693-703.

BLEASE, C. & GERAGHTY, K. J. 2018. Are ME/CFS Patient Organizations "Militant"? *Journal of Bioethical Inquiry,* 15**,** 393-401.

BLOMBERG, J., GOTTFRIES, C. G., ELFAITOURI, A., RIZWAN, M. & ROSÉN, A. 2018. Infection Elicited Autoimmunity and Myalgic Encephalomyelitis/Chronic Fatigue Syndrome: An Explanatory Model. *Frontiers in Immunology,* 9**,** 229.

BLUNDELL, S., RAY, K. K., BUCKLAND, M. & WHITE, P. D. 2015. Chronic fatigue syndrome and circulating cytokines: A systematic review. *Brain, Behavior, and Immunity,* 50**,** 186-195.

BOISSONEAULT, J., LETZEN, J., LAI, S., O'SHEA, A., CRAGGS, J., ROBINSON, M. E. & STAUD, R. 2016. Abnormal resting state functional connectivity in patients with chronic fatigue syndrome: an arterial spin-labeling fMRI study. *Journal of Magnetic Resonance Imaging,* 34**,** 603-8.

BOISSONEAULT, J., LETZEN, J., LAI, S., ROBINSON, M. E. & STAUD, R. 2018. Static and dynamic functional connectivity in patients with chronic fatigue syndrome: use of arterial spin labelling fMRI. *Clinical Physiology and Functional Imaging,* 38**,** 128-137.

BORODY, T. J., NOWAK, A. & FINLAYSON, S. 2012. The GI microbiome and its role in Chronic Fatigue Syndrome: A summary of bacteriotherapy. *Journal of the Australasian College of Nutritional and Environmental Medicine,* 31**,** 3.

BRAGÉE, B., MICHOS, A., DRUM, B., FAHLGREN, M., SZULKIN, R. & BERTILSON, B. C. 2020. Signs of Intracranial Hypertension, Hypermobility, and Craniocervical Obstructions in Patients With Myalgic Encephalomyelitis/Chronic Fatigue Syndrome. *Frontiers in Neurology,* 11.

BRENU, E. W., HUTH, T. K., HARDCASTLE, S. L., FULLER, K., KAUR, M., JOHNSTON, S., RAMOS, S. B., STAINES, D. R. & MARSHALL-GRADISNIK, S. M. 2014. Role of adaptive and innate immune

cells in chronic fatigue syndrome/myalgic encephalomyelitis. *International Immunology,* 26**,** 233-42.

BRENU, E. W., STAINES, D. R., BASKURT, O. K., ASHTON, K. J., RAMOS, S. B., CHRISTY, R. M. & MARSHALL-GRADISNIK, S. M. 2010. Immune and hemorheological changes in chronic fatigue syndrome. *Journal of Translational Medicine,* 8**,** 1.

BRENU, E. W., VAN DRIEL, M. L., STAINES, D. R., ASHTON, K. J., RAMOS, S. B., KEANE, J., KLIMAS, N. G. & MARSHALL-GRADISNIK, S. M. 2011. Immunological abnormalities as potential biomarkers in Chronic Fatigue Syndrome/Myalgic Encephalomyelitis. *Journal of Translational Medicine,* 9**,** 81.

BROWN, A. A., JASON, L. A., EVANS, M. A. & FLORES, S. 2013. Contrasting Case Definitions: The ME International Consensus Criteria vs. the Fukuda et al. CFS Criteria. *Northern American Journal of Psychology,* 15**,** 103-120.

BROWN, M. M., BELL, D. S., JASON, L. A., CHRISTOS, C. & BELL, D. E. 2012. Understanding long-term outcomes of chronic fatigue syndrome. *Journal of Clinical Psychology,* 68**,** 1028-35.

BRURBERG, K. G., FØNHUS, M. S., LARUN, L., FLOTTORP, S. & MALTERUD, K. 2014. Case definitions for chronic fatigue syndrome/myalgic encephalomyelitis (CFS/ME): a systematic review. *British Medical Journal Open,* 4**,** e003973.

BUNKER, J. J., ERICKSON, S. A., FLYNN, T. M., HENRY, C., KOVAL, J. C., MEISEL, M., JABRI, B., ANTONOPOULOS, D. A., WILSON, P. C. & BENDELAC, A. 2017. Natural polyreactive IgA antibodies coat the intestinal microbiota. *Science,* 358.

BUNKER, J. J., FLYNN, T. M., KOVAL, J. C., SHAW, D. G., MEISEL, M., MCDONALD, B. D., ISHIZUKA, I. E., DENT, A. L., WILSON, P. C., JABRI, B., ANTONOPOULOS, D. A. & BENDELAC, A. 2015. Innate and Adaptive Humoral Responses Coat Distinct Commensal Bacteria with Immunoglobulin A. *Immunity,* 43**,** 541-53.

BURGER-VAN PAASSEN, N., VINCENT, A., PUIMAN, P. J., VAN DER SLUIS, M., BOUMA, J., BOEHM, G., VAN GOUDOEVER, J. B., VAN SEUNINGEN, I. & RENES, I. B. 2009. The regulation of intestinal mucin MUC2 expression by short-chain fatty acids: implications for epithelial protection. *The Biochemical journal*, 420(2), 211–219.

BUSCARINU, M. C., ROMANO, S., MECHELLI, R., PIZZOLATO UMETON, R., FERRALDESCHI, M., FORNASIERO, A., RENIÈ, R., CERASOLI, B., MORENA, E., ROMANO, C., LOIZZO, N. D., UMETON, R., SALVETTI, M. & RISTORI, G. 2018. Intestinal Permeability in Relapsing-Remitting Multiple Sclerosis. *Neurotherapeutics,* 15**,** 68-74.

BYNKE, A., JULIN, P., GOTTFRIES, C.-G., HEIDECKE, H., SCHEIBENBOGEN, C. & BERGQUIST, J. 2020. Autoantibodies to beta-adrenergic and muscarinic cholinergic receptors in Myalgic Encephalomyelitis (ME) patients – A validation study in plasma and cerebrospinal fluid from two Swedish cohorts. *Brain, Behavior, & Immunity - Health,* 7**,** 100107.

CABANAS, H., MURAKI, K., BALINAS, C., EATON-FITCH, N., STAINES, D. & MARSHALL-GRADISNIK, S. 2019. Validation of impaired Transient Receptor Potential Melastatin 3 ion channel activity in natural killer cells from Chronic Fatigue Syndrome/ Myalgic Encephalomyelitis patients. *Molecular Medicine,* 25**,** 14.

CABANAS, H., MURAKI, K., EATON, N., BALINAS, C., STAINES, D. & MARSHALL-GRADISNIK, S. 2018. Loss of Transient Receptor Potential Melastatin 3 ion channel function in natural killer cells from Chronic Fatigue Syndrome/Myalgic Encephalomyelitis patients. *Molecular Medicine,* 24**,** 44.

VAN CAMPEN, C. M., ROWE, P. C. & VISSER, F. C. 2020. Reductions in Cerebral Blood Flow Can Be Provoked by Sitting in Severe Myalgic Encephalomyelitis/Chronic Fatigue Syndrome Patients. *Healthcare,* 8**,** 394.

CAPALDO, C. T. & NUSRAT, A. 2009. Cytokine regulation of tight junctions. *Biochimica et biophysica acta*, 1788(4), 864–871.

CARRUTHERS, B. M., JAIN, A. K., DE MEIRLEIR, K. L., PETERSON, D. L., KLIMAS, N. G., LERNER, A. M., BESTED, A. C., FLOR-HENRY, P., JOSHI, P., POWLES, A. C. P., SHERKEY, J. A. & VAN DE SANDE, M. I. 2003. Myalgic Encephalomyelitis/Chronic Fatigue Syndrome. *Journal of Chronic Fatigue Syndrome,* 11**,** 7-115.

CARRUTHERS, B. M., VAN DE SANDE, M. I., DE MEIRLEIR, K. L., KLIMAS, N. G., BRODERICK, G., MITCHELL, T., STAINES, D., POWLES, A. C. P., SPEIGHT, N., VALLINGS, R., BATEMAN, L., BAUMGARTEN-AUSTRHEIM, B., BELL, D. S., CARLO-STELLA, N., CHIA, J., DARRAGH, A., JO, D., LEWIS, D., LIGHT, A. R., MARSHALL-GRADISBIK, S., MENA, I., MIKOVITS, J. A., MIWA, K., MUROVSKA, M., PALL, M. L. & STEVENS, S. 2011. Myalgic encephalomyelitis: International Consensus Criteria. *Journal of Internal Medicine,* 270**,** 327-338.

CASTRO-MARRERO, J., CORDERO, M. D., SÁEZ-FRANCAS, N., JIMENEZ-GUTIERREZ, C., AGUILAR-MONTILLA, F. J., ALISTE, L. & ALEGRE-MARTIN, J. 2013. Could mitochondrial dysfunction be a differentiating marker between chronic fatigue syndrome and fibromyalgia? *Antioxidants & Redox Signalling,* 19**,** 1855-60.

CASTRO-MARRERO, J., FARO, M., ALISTE, L., SÁEZ-FRANCÀS, N., CALVO, N., MARTÍNEZ-MARTÍNEZ, A., DE SEVILLA, T. F. & ALEGRE, J. 2017. Comorbidity in Chronic Fatigue Syndrome/Myalgic Encephalomyelitis: A Nationwide Population-Based Cohort Study. *Psychosomatics,* 58**,** 533-543.

CHELAKKOT, C., GHIM, J. & RYU, S. H. 2018. Mechanisms regulating intestinal barrier integrity and its pathological implications. *Experimental & Molecular Medicine*, 50, 1–9.

CHEN, J., BITTINGER, K., CHARLSON, E. S., HOFFMANN, C., LEWIS, J., WU, G. D., COLLMAN, R. G., BUSHMAN, F. D. & LI, H. 2012. Associating microbiome composition with environmental covariates using generalized UniFrac distances. *Bioinformatics,* 28**,** 2106-2113.

CHEN, S., ZHOU, Y., CHEN, Y. & GU, J. 2018. fastp: an ultra-fast all-in-one FASTQ preprocessor. *Bioinformatics,* 34**,** i884-i890.

CHEN, Y., LU, D., CHUROV, A. & FU, R. 2020. Research Progress on NK Cell Receptors and Their Signaling Pathways. *Mediators of Inflammation,* 2020**,** 6437057.

CHRISTMANN, B. S., ABRAHAMSSON, T. R., BERNSTEIN, C. N., DUCK, L. W., MANNON, P. J., BERG, G., BJÖRKSTÉN, B., JENMALM, M. C. & ELSON, C. O. 2015. Human seroreactivity to gut microbiota antigens. *Journal of Allergy and Clinical Immunology,* 136**,** 1378-86.e1-5.

CHU, L., VALENCIA, I. J., GARVERT, D. W. & MONTOYA, J. G. 2019. Onset Patterns and Course of Myalgic Encephalomyelitis/Chronic Fatigue Syndrome. *Frontiers in Pediatrics,* 7**,** 12.

CICCIA, F., GUGGINO, G., RIZZO, A., ALESSANDRO, R., LUCHETTI, M. M., MILLING, S., SAIEVA, L., CYPERS, H., STAMPONE, T., DI BENEDETTO, P., GABRIELLI, A., FASANO, A., ELEWAUT, D. & TRIOLO, G. 2017. Dysbiosis and zonulin upregulation alter gut epithelial and vascular barriers in patients with ankylosing spondylitis. *Annals of Rheumatic Disease,* 76**,** 1123-1132.

CLEARE, A. J., MESSA, C., RABINER, E. A. & GRASBY, P. M. 2005. Brain 5-HT1A receptor binding in chronic fatigue syndrome measured using positron emission tomography and [11C]WAY-100635. *Biological Psychiatry,* 57**,** 239-246.

COLE, J. R., CHAI, B., FARRIS, R. J., WANG, Q., KULAM, S. A., MCGARRELL, D. M., GARRITY, G. M. & TIEDJE, J. M. 2005. The Ribosomal Database Project (RDP-II): sequences and tools for high-throughput rRNA analysis. *Nucleic Acids Research,* 33**,** D294-6.

COLLIN, S. M., NIKOLAUS, S., HERON, J., KNOOP, H., WHITE, P. D. & CRAWLEY, E. 2016. Chronic fatigue syndrome (CFS) symptom-based phenotypes in two clinical cohorts of adult patients in the UK and The Netherlands. *Journal of Psychosomatic Research,* 81**,** 14-23.

CONLON, M. A. & BIRD, A. R. 2014. The impact of diet and lifestyle on gut microbiota and human health. *Nutrients,* 7**,** 17-44.

CORBITT, M., CAMPAGNOLO, N., STAINES, D. & MARSHALL-GRADISNIK, S. 2018. A Systematic Review of Probiotic Interventions for Gastrointestinal Symptoms and Irritable Bowel Syndrome in Chronic Fatigue Syndrome/Myalgic Encephalomyelitis (CFS/ME). *Probiotics and Antimicrobial Proteins,* 10**,** 466-477.

CRYAN, J. F., O'RIORDAN, K. J., COWAN, C. S. M., SANDHU, K. V., BASTIAANSSEN, T. F. S., BOEHME, M., CODAGNONE, M. G., CUSSOTTO, S., FULLING, C., GOLUBEVA, A. V., GUZZETTA, K. E., JAGGAR, M., LONG-SMITH, C. M., LYTE, J. M., MARTIN, J. A., MOLINERO-PEREZ, A., MOLONEY, G., MORELLI, E., MORILLAS, E., O'CONNOR, R., CRUZ-PEREIRA, J. S., PETERSON, V. L., REA, K., RITZ, N. L., SHERWIN, E., SPICHAK, S., TEICHMAN, E. M., VAN DE WOUW, M., VENTURA-SILVA, A. P., WALLACE-FITZSIMONS, S. E., HYLAND, N., CLARKE, G. & DINAN, T. G. 2019. The Microbiota-Gut-Brain Axis. *Physiological Reviews,* 99**,** 1877-2013.

CURRIU, M., CARRILLO, J., MASSANELLA, M., RIGAU, J., ALEGRE, J., PUIG, J., GARCIA-QUINTANA, A. M., CASTRO-MARRERO, J., NEGREDO, E., CLOTET, B., CABRERA, C. & BLANCO, J. 2013. Screening NK-, B- and T-cell phenotype and function in patients suffering from Chronic Fatigue Syndrome. *Journal of translational medicine,* 11**,** 68-68.

DE BELLIS, A., BELLASTELLA, G., PERNICE, V., CIRILLO, P., LONGO, M., MAIO, A., SCAPPATICCIO, L., MAIORINO, M. I., BELLASTELLA, A., ESPOSITO, K. & MONTOYA, J. G. 2021. Hypothalamic-Pituitary Autoimmunity and Related Impairment of Hormone Secretions in Chronic Fatigue Syndrome. *The Journal of Clinical Endocrinology & Metabolism,* 106**,** e5147-e5155.

DE LANGE, F. P., KALKMAN, J. S., BLEIJENBERG, G., HAGOORT, P., VAN DER WERF, S. P., VAN DER MEER, J. W. & TONI, I. 2004. Neural correlates of the chronic fatigue syndrome--an fMRI study. *Brain,* 127**,** 1948-57.

DE SOUSA-PEREIRA, P. & WOOF, J. M. 2019. IgA: Structure, Function, and Developability. *Antibodies (Basal, Switzerland)*, 8(4), 57.

DECKER, M. J., TABASSUM, H., LIN, J. M. & REEVES, W. C. 2009. Electroencephalographic correlates of Chronic Fatigue Syndrome. *Behavioral and Brain Functions,* 5**,** 43.

DEGRUTTOLA, A. K., LOW, D., MIZOGUCHI, A. & MIZOGUCHI, E. 2016. Current Understanding of Dysbiosis in Disease in Human and Animal Models. *Inflammatory Bowel Diseases,* 22**,** 1137-50.

DEMITRACK, M. A., DALE, J. K., STRAUS, S. E., LAUE, L., LISTWAK, S. J., KRUESI, M. J., CHROUSOS, G. P. & GOLD, P. W. 1991. Evidence for impaired activation of the hypothalamic-pituitary-adrenal axis in patients with chronic fatigue syndrome. *The Journal of Clinical Endocrinology & Metabolism,* 73**,** 1224-34.

DI TOMMASO, N., GASBARRINI, A. & PONZIANI, F. R. 2021. Intestinal Barrier in Human Health and Disease. *International Journal of Environmental Research and Public Health,* 18.

DINAN, T. G., MAJEED, T., LAVELLE, E., SCOTT, L. V., BERTI, C. & BEHAN, P. 1997. Blunted serotonin-mediated activation of the hypothalamic-pituitary-adrenal axis in chronic fatigue syndrome. *Psychoneuroendocrinology,* 22**,** 261-7.

DORON, I., LEONARDI, I., LI, X. V., FIERS, W. D., SEMON, A., BIALT-DECELIE, M., MIGAUD, M., GAO, I. H., LIN, W. Y., KUSAKABE, T., PUEL, A. & ILIEV, I. D. 2021. Human gut mycobiota tune immunity via CARD9-dependent induction of anti-fungal IgG antibodies. *Cell,* 184**,** 1017-1031.e14.

DOWSETT, E. G., GOUDSMIT, E., MACINTYRE, A. & SHEPHERD, C. B. 1994. *Report from The National Task Force on Chronic Fatigue Syndrome (CFS), Post Viral Fatigue Syndrome (PVFS), Myalgic Encephalomyelitis (ME).* Westcare.

DOWSETT, E. G., RAMSAY, A. M., MCCARTNEY, R. A. & BELL, E. J. 1990. Myalgic encephalomyelitis--a persistent enteroviral infection? *Postgraduate medical journal,* 66**,** 526-530.

DU CLOS, T. W. 2000. Function of C-reactive protein. *Annals of Medicine,* 32**,** 274-278.

DUCHMANN, R., KAISER, I., HERMANN, E., MAYET, W., EWE, K. & MEYER ZUM BÜSCHENFELDE, K. H. 1995. Tolerance exists towards resident intestinal flora but is broken in active inflammatory bowel disease (IBD). *Clinical & Experimental Immunology,* 102**,** 448-55.

DUNKELBERGER, J. R. & SONG, W.-C. 2010. Complement and its role in innate and adaptive immune responses. *Cell Research,* 20**,** 34-50.

EATON-FITCH, N., DU PREEZ, S., CABANAS, H., STAINES, D. & MARSHALL-GRADISNIK, S. 2019. A systematic review of natural killer cells profile and cytotoxic function in myalgic encephalomyelitis/chronic fatigue syndrome. *Systematic Reviews,* 8**,** 279.

EDGAR, R. C. 2013. UPARSE: highly accurate OTU sequences from microbial amplicon reads. *Nature Methods,* 10**,** 996-998.

ESCORIHUELA, R. M., CAPDEVILA, L., CASTRO, J. R., ZARAGOZÀ, M. C., MAUREL, S., ALEGRE, J. & CASTRO-MARRERO, J. 2020. Reduced heart rate variability predicts fatigue severity in individuals with chronic fatigue syndrome/myalgic encephalomyelitis. *Journal of Translational Medicine,* 18**,** 4.

EVENGÅRD, B., GRÄNS, H., WAHLUND, E. & NORD, C. E. 2007. Increased number of *Candida albicans* in the faecal microflora of chronic fatigue syndrome patients during the acute phase of illness. *Scandinavian Journal of Gastroenterology,* 42**,** 1514-5.

FADLALLAH, J., STERLIN, D., FIESCHI, C., PARIZOT, C., DORGHAM, K., EL KAFSI, H., AUTAA, G., GHILLANI-DALBIN, P., JUSTE, C., LEPAGE, P., MALPHETTES, M., GALICIER, L., BOUTBOUL, D., CLÉMENT, K., ANDRÉ, S., MARQUET, F., TRESALLET, C., MATHIAN, A., MIYARA, M., OKSENHENDLER, E., AMOURA, Z., YSSEL, H., LARSEN, M. & GOROCHOV, G. 2019. Synergistic convergence of microbiota-specific systemic IgG and secretory IgA. *Journal of Allergy and Clinical Immunology,* 143**,** 1575-1585.e4.

FALONY, G., VANDEPUTTE, D., CAENEPEEL, C., VIEIRA-SILVA, S., DARYOUSH, T., VERMEIRE, S. & RAES, J. 2019. The human microbiome in health and disease: hype or hope. *Acta Clinica Belgica,* 74**,** 53-64.

FERREIRA-HALDER, C. V., FARIA, A. V. S. & ANDRADE, S. S. 2017. Action and function of *Faecalibacterium prausnitzii* in health and disease. *Best Practice and Research in Clinical Gastroenterology,* 31**,** 643-648.

FIEDOROVÁ, K., RADVANSKÝ, M., NĚMCOVÁ, E., GROMBIŘÍKOVÁ, H., BOSÁK, J., ČERNOCHOVÁ, M., LEXA, M., ŠMAJS, D. & FREIBERGER, T. 2019. The Impact of DNA Extraction Methods on Stool Bacterial and Fungal Microbiota Community Recovery. *Frontiers in Microbiology,* 10.

FINKELMEYER, A., HE, J., MACLACHLAN, L., WATSON, S., GALLAGHER, P., NEWTON, J. L. & BLAMIRE, A. M. 2018. Grey and white matter differences in Chronic Fatigue Syndrome - A voxel-based morphometry study. *NeuroImage: Clinical,* 17**,** 24-30.

FLETCHER, M. A., ZENG, X. R., BARNES, Z., LEVIS, S. & KLIMAS, N. G. 2009. Plasma cytokines in women with chronic fatigue syndrome. *Journal of Translational Medicine,* 7**,** 96.

FLOR-HENRY, P., LIND, J. C. & KOLES, Z. J. 2010. EEG source analysis of chronic fatigue syndrome. *Psychiatry Research,* 181**,** 155-64.

FLUGE, Ø. & MELLA, O. 2009. Clinical impact of B-cell depletion with the anti-CD20 antibody rituximab in chronic fatigue syndrome: a preliminary case series. *BMC Neurology,* 9**,** 28.

FLUGE, Ø., BRULAND, O., RISA, K., STORSTEIN, A., KRISTOFFERSEN, E. K., SAPKOTA, D., NÆSS, H., DAHL, O., NYLAND, H. & MELLA, O. 2011. Benefit from B-lymphocyte depletion using the anti-CD20 antibody rituximab in chronic fatigue syndrome. A double-blind and placebo-controlled study. *PLOS One,* 6**,** e26358.

FLUGE, Ø., MELLA, O., BRULAND, O., RISA, K., DYRSTAD, S. E., ALME, K., REKELAND, I. G., SAPKOTA, D., RØSLAND, G. V., FOSSÅ, A., KTORIDOU-VALEN, I., LUNDE, S., SØRLAND, K., LIEN, K., HERDER, I., THÜRMER, H., GOTAAS, M. E., BARANOWSKA, K. A., BOHNEN, L. M., SCHÄFER, C., MCCANN, A., SOMMERFELT, K., HELGELAND, L., UELAND, P. M., DAHL, O. & TRONSTAD, K. J. 2016. Metabolic profiling indicates impaired pyruvate dehydrogenase function in myalgic encephalopathy/chronic fatigue syndrome. *JCI Insight,* 1**,** e89376.

FLUGE, Ø., REKELAND, I. G., LIEN, K., THÜRMER, H., BORCHGREVINK, P. C., SCHÄFER, C., SØRLAND, K., AßMUS, J., KTORIDOU-VALEN, I., HERDER, I. & ET AL. 2019. B-Lymphocyte Depletion in Patients With Myalgic Encephalomyelitis/Chronic Fatigue Syndrome: A Randomized, Double-Blind, Placebo-Controlled Trial. *Annals of Internal Medicine,* 170**,** 585-593.

FLUGE, Ø., RISA, K., LUNDE, S., ALME, K., REKELAND, I. G., SAPKOTA, D., KRISTOFFERSEN, E. K., SØRLAND, K., BRULAND, O., DAHL, O. & MELLA, O. 2015. B-Lymphocyte Depletion in Myalgic Encephalopathy/ Chronic Fatigue Syndrome. An Open-Label Phase II Study with Rituximab Maintenance Treatment. *PLOS One,* 10**,** e0129898.

FRANZOSA, E. A., HSU, T., SIROTA-MADI, A., SHAFQUAT, A., ABU-ALI, G., MORGAN, X. C. & HUTTENHOWER, C. 2015. Sequencing and beyond: integrating molecular 'omics' for microbial community profiling. *Nature Reviews Microbiology,* 13**,** 360-372.

FREITAG, H., SZKLARSKI, M., LORENZ, S., SOTZNY, F., BAUER, S., PHILIPPE, A., KEDOR, C., GRABOWSKI, P., LANGE, T., RIEMEKASTEN, G., HEIDECKE, H. & SCHEIBENBOGEN, C. 2021. Autoantibodies to Vasoregulative G-Protein-Coupled Receptors Correlate with Symptom Severity, Autonomic Dysfunction and Disability in Myalgic Encephalomyelitis/Chronic Fatigue Syndrome. *Journal of Clinical Medicine,* 10.

FRÉMONT, M., COOMANS, D., MASSART, S. & DE MEIRLEIR, K. 2013. High-throughput 16S rRNA gene sequencing reveals alterations of intestinal microbiota in myalgic encephalomyelitis/chronic fatigue syndrome patients. *Anaerobe,* 22**,** 50-6.

FRÉMONT, M., METZGER, K., RADY, H., HULSTAERT, J. & DE MEIRLEIR, K. 2009. Detection of herpesviruses and parvovirus B19 in gastric and intestinal mucosa of chronic fatigue syndrome patients. *In Vivo,* 23**,** 209-13.

FUJII, H., SATO, W., KIMURA, Y., MATSUDA, H., OTA, M., MAIKUSA, N., SUZUKI, F., AMANO, K., SHIN, I., YAMAMURA, T., MORI, H. & SATO, N. 2020. Altered Structural Brain Networks Related to Adrenergic/Muscarinic Receptor Autoantibodies in Chronic Fatigue Syndrome. *J Neuroimaging,* 30**,** 822-827.

FUKUDA, K., STRAUS, S. E., HICKIE, I., SHARPE, M. C., DOBBINS, J. G. & KOMAROFF, A. 1994. The chronic fatigue syndrome: a comprehensive approach to its definition and study. International Chronic Fatigue Syndrome Study Group. *Annals of Internal Medicine,* 121**,** 953-9.

GALAZZO, G., VAN BEST, N., BENEDIKTER, B. J., JANSSEN, K., BERVOETS, L., DRIESSEN, C., OOMEN, M., LUCCHESI, M., VAN EIJCK, P. H., BECKER, H. E. F., HORNEF, M. W., SAVELKOUL, P. H., STASSEN, F. R. M., WOLFFS, P. F. & PENDERS, J. 2020. How to Count Our Microbes? The Effect of Different Quantitative Microbiome Profiling Approaches. *Frontiers in Cellular and Infection Microbiology,* 10.

GARCIA-RUBIO, R., DE OLIVEIRA, H. C., RIVERA, J. & TREVIJANO-CONTADOR, N. 2020. The Fungal Cell Wall: *Candida*, *Cryptococcus*, and *Aspergillus* Species. *Frontiers in Microbiology,* 10.

GENSOLLEN, T., IYER, S. S., KASPER, D. L. & BLUMBERG, R. S. 2016. How colonization by microbiota in early life shapes the immune system. *Science (New York, N.Y.),* 352**,** 539-544.

GERMAIN, A., BARUPAL, D. K., LEVINE, S. M. & HANSON, M. R. 2020. Comprehensive Circulatory Metabolomics in ME/CFS Reveals Disrupted Metabolism of Acyl Lipids and Steroids. *Metabolites,* 10.

GERMAIN, A., RUPPERT, D., LEVINE, S. M. & HANSON, M. R. 2017. Metabolic profiling of a myalgic encephalomyelitis/chronic fatigue syndrome discovery cohort reveals disturbances in fatty acid and lipid metabolism. *Molecular BioSystems,* 13**,** 371-379.

GERMAIN, A., RUPPERT, D., LEVINE, S. M. & HANSON, M. R. 2018. Prospective Biomarkers from Plasma Metabolomics of Myalgic Encephalomyelitis/Chronic Fatigue Syndrome Implicate Redox Imbalance in Disease Symptomatology. *Metabolites,* 8.

GHALI, A., RICHA, P., LACOUT, C., GURY, A., BEUCHER, A.-B., HOMEDAN, C., LAVIGNE, C. & URBANSKI, G. 2020. Epidemiological and clinical factors associated with post-exertional malaise severity in patients with myalgic encephalomyelitis/chronic fatigue syndrome. *Journal of translational medicine,* 18**,** 246-246.

GILOTEAUX, L., GOODRICH, J. K., WALTERS, W. A., LEVINE, S. M., LEY, R. E. & HANSON, M. R. 2016a. Reduced diversity and altered composition of the gut microbiome in individuals with myalgic encephalomyelitis/chronic fatigue syndrome. *Microbiome,* 4**,** 30.

GILOTEAUX, L., HANSON, M. R. & KELLER, B. A. 2016b. A Pair of Identical Twins Discordant for Myalgic Encephalomyelitis/Chronic Fatigue Syndrome Differ in Physiological Parameters and Gut Microbiome Composition. *American Journal of Case Reports,* 17**,** 720-729.

GOODRICH, J. K., WATERS, J. L., POOLE, A. C., SUTTER, J. L., KOREN, O., BLEKHMAN, R., BEAUMONT, M., VAN TREUREN, W., KNIGHT, R., BELL, J. T., SPECTOR, T. D., CLARK, A. G. & LEY, R. E. 2014. Human genetics shape the gut microbiome. *Cell,* 159**,** 789-799.

GREGORY, A. C., ZABLOCKI, O., ZAYED, A. A., HOWELL, A., BOLDUC, B. & SULLIVAN, M. B. 2020. The Gut Virome Database Reveals Age-Dependent Patterns of Virome Diversity in the Human Gut. *Cell Host Microbe,* 28**,** 724-740.e8.

GREILING, T. M., DEHNER, C., CHEN, X., HUGHES, K., IÑIGUEZ, A. J., BOCCITTO, M., RUIZ, D. Z., RENFROE, S. C., VIEIRA, S. M., RUFF, W. E., SIM, S., KRIEGEL, C., GLANTERNIK, J., CHEN, X., GIRARDI, M., DEGNAN, P., COSTENBADER, K. H., GOODMAN, A. L., WOLIN, S. L. & KRIEGEL, M. A. 2018. Commensal orthologs of the human autoantigen Ro60 as triggers of autoimmunity in lupus. *Science Translational Medicine,* 10.

GROEGER, D., O'MAHONY, L., MURPHY, E. F., BOURKE, J. F., DINAN, T. G., KIELY, B., SHANAHAN, F. & QUIGLEY, E. M. 2013. *Bifidobacterium infantis* 35624 modulates host inflammatory processes beyond the gut. *Gut Microbes,* 4**,** 325-39.

GROVEN, N., FORS, E. A. & REITAN, S. K. 2019. Patients with Fibromyalgia and Chronic Fatigue Syndrome show increased hsCRP compared to healthy controls. *Brain, Behavior, and Immunity,* 81**,** 172-177.

GRÜNING, B., DALE, R., SJÖDIN, A., CHAPMAN, B. A., ROWE, J., TOMKINS-TINCH, C. H., VALIERIS, R., KÖSTER, J. & THE BIOCONDA, T. 2018. Bioconda: sustainable and comprehensive software distribution for the life sciences. *Nature Methods,* 15**,** 475-476.

GUDNASON, H., DUFVA, M., BANG, D. D., & WOLFF, A. 2007. Comparison of multiple DNA dyes for real-time PCR: effects of dye concentration and sequence composition on DNA amplification and melting temperature. *Nucleic acids research*, 35(19), e127.

GUENTHER, S., LOEBEL, M., MOOSLECHNER, A. A., KNOPS, M., HANITSCH, L. G., GRABOWSKI, P., WITTKE, K., MEISEL, C., UNTERWALDER, N., VOLK, H. D. & SCHEIBENBOGEN, C. 2015. Frequent IgG subclass and mannose binding lectin deficiency in patients with chronic fatigue syndrome. *Human Immunology,* 76**,** 729-35.

GÜNTHER, S., HÜBSCHMANN, T., RUDOLF, M., ESCHENHAGEN, M., RÖSKE, I., HARMS, H. & MÜLLER, S. 2008. Fixation procedures for flow cytometric analysis of environmental bacteria. *Journal of Microbiological Methods,* 75**,** 127-134.

GUO, C., CHE, X., BRIESE, T., ALLICOCK, O., YATES, R. A., CHENG, A., RANJAN, A., MARCH, D., HORNIG, M., KOMAROFF, A. L., LEVINE, S., BATEMAN, L., VERNON, S. D., KLIMAS, N. G., MONTOYA, J. G., PETERSON, D. L., LIPKIN, W. I. & WILLIAMS, B. L. 2021. Deficient butyrate-

producing capacity in the gut microbiome of Myalgic Encephalomyelitis/Chronic Fatigue Syndrome patients is associated with fatigue symptoms. *medRxiv***,** 2021.10.27.21265575.

GUO, S., AL-SADI, R., SAID, H. M. & MA, T. Y. 2013. Lipopolysaccharide causes an increase in intestinal tight junction permeability in vitro and in vivo by inducing enterocyte membrane expression and localization of TLR-4 and CD14. *The American Journal of Pathology*, 182(2), 375–387.

GUR, A., CEVIK, R., NAS, K., COLPAN, L. & SARAC, S. 2004. Cortisol and hypothalamic-pituitary-gonadal axis hormones in follicular-phase women with fibromyalgia and chronic fatigue syndrome and effect of depressive symptoms on these hormones. *Arthritis Research & Therapy,* 6**,** R232-8.

HAAS, A., ZIMMERMANN, K., GRAW, F., SLACK, E., RUSERT, P., LEDERGERBER, B., BOSSART, W., WEBER, R., THURNHEER, M. C., BATTEGAY, M., HIRSCHEL, B., VERNAZZA, P., PATUTO, N., MACPHERSON, A. J., GÜNTHARD, H. F. & OXENIUS, A. 2011. Systemic antibody responses to gut commensal bacteria during chronic HIV-1 infection. *Gut,* 60**,** 1506-19.

HARBISON, J. E., ROTH-SCHULZE, A. J., GILES, L. C., TRAN, C. D., NGUI, K. M., PENNO, M. A., THOMSON, R. L., WENTWORTH, J. M., COLMAN, P. G., CRAIG, M. E., MORAHAN, G., PAPENFUSS, A. T., BARRY, S. C., HARRISON, L. C. & COUPER, J. J. 2019. Gut microbiome dysbiosis and increased intestinal permeability in children with islet autoimmunity and type 1 diabetes: A prospective cohort study. *Pediatric Diabetes,* 20**,** 574-583.

HARDCASTLE, S. L., BRENU, E. W., JOHNSTON, S., NGUYEN, T., HUTH, T., RAMOS, S., STAINES, D. & MARSHALL-GRADISNIK, S. 2015b. Serum Immune Proteins in Moderate and Severe Chronic Fatigue Syndrome/Myalgic Encephalomyelitis Patients. *International Journal of Medical Sciences,* 12**,** 764-72.

HARDCASTLE, S. L., BRENU, E. W., JOHNSTON, S., NGUYEN, T., HUTH, T., WONG, N., RAMOS, S., STAINES, D. & MARSHALL-GRADISNIK, S. 2015c. Characterisation of cell functions and receptors in Chronic Fatigue Syndrome/Myalgic Encephalomyelitis (CFS/ME). *BMC Immunology,* 16**,** 35.

HARDCASTLE, S., BRENU, E., JOHNSTON, S., NGUYEN, T., HUTH, T., RAMOS, S., STAINES, D. & MARSHALL-GRADISNIK, S. 2015a. Longitudinal analysis of immune abnormalities in varying severities of Chronic Fatigue Syndrome/Myalgic Encephalomyelitis patients. *Journal of translational medicine,* 13**,** 299.

HARMSEN, H. J., POUWELS, S. D., FUNKE, A., BOS, N. A. & DIJKSTRA, G. 2012. Crohn's disease patients have more IgG-binding fecal bacteria than controls. *Clinical and Vaccine Immunology,* 19**,** 515-21.

HARTZ, A. J., KUHN, E. M. & LEVINE, P. H. 1998. Characteristics of Fatigued Persons Associated with Features of Chronic Fatigue Syndrome. *Journal of Chronic Fatigue Syndrome,* 4**,** 71-97.

HAYWOOD, K. L., STANISZEWSKA, S. & CHAPMAN, S. 2012. Quality and acceptability of patient-reported outcome measures used in chronic fatigue syndrome/myalgic encephalomyelitis (CFS/ME): a systematic review. *Quality of Life Research,* 21**,** 35-52.

HAZAN, R., QUE, Y.-A., MAURA, D. & RAHME, L. G. 2012. A method for high throughput determination of viable bacteria cell counts in 96-well plates. *BMC Microbiology,* 12**,** 259.

HE, B., XU, W., SANTINI, P. A., POLYDORIDES, A. D., CHIU, A., ESTRELLA, J., SHAN, M., CHADBURN, A., VILLANACCI, V., PLEBANI, A., KNOWLES, D. M., RESCIGNO, M. & CERUTTI, A. 2007. Intestinal bacteria trigger T cell-independent immunoglobulin A(2) class switching by inducing epithelial-cell secretion of the cytokine APRIL. *Immunity,* 26**,** 812-26.

HICKIE, I., DAVENPORT, T., WAKEFIELD, D., VOLLMER-CONNA, U., CAMERON, B., VERNON, S. D., REEVES, W. C. & LLOYD, A. 2006. Post-infective and chronic fatigue syndromes precipitated by viral and non-viral pathogens: prospective cohort study. *British Medical Journal,* 333**,** 575.

HILDEBRAND, F., TADEO, R., VOIGT, A. Y., BORK, P. & RAES, J. 2014. LotuS: an efficient and user-friendly OTU processing pipeline. *Microbiome,* 2**,** 30.

HILL, C., GUARNER, F., REID, G., GIBSON, G. R., MERENSTEIN, D. J., POT, B., MORELLI, L., CANANI, R. B., FLINT, H. J., SALMINEN, S., CALDER, P. C. & SANDERS, M. E. 2014. The International Scientific Association for Probiotics and Prebiotics consensus statement on the scope and appropriate use of the term probiotic. *Nature Reviews Gastroenterology & Hepatology,* 11**,** 506-514.

HOEFLICH, C., UNTERWALDER, N., SCHUETT, S., SCHMOLKE, K., BOENISCH, O., HAMMER, M., SCHEUFELE, R., MICHAEL, D., VOLK, H. D., SCHEIBENBOGEN, C., VON BAEHR, V. & MEISEL, C. 2009. Clinical manifestation of mannose-binding lectin deficiency in adults independent of concomitant immunodeficiency. *Human Immunology,* 70**,** 809-12.

HOLMES, G. P., KAPLAN, J. E., GANTZ, N. M., KOMAROFF, A. L., SCHONBERGER, L. B., STRAUS, S. E., JONES, J. F., DUBOIS, R. E., CUNNINGHAM-RUNDLES, C., PAHWA, S. & ET AL. 1988. Chronic fatigue syndrome: a working case definition. *Annals of Internal Medicine,* 108**,** 387-9.

HORNIG, M., GOTTSCHALK, C. G., EDDY, M. L., CHE, X., UKAIGWE, J. E., PETERSON, D. L. & LIPKIN, W. I. 2017. Immune network analysis of cerebrospinal fluid in myalgic encephalomyelitis/chronic fatigue syndrome with atypical and classical presentations. *Translational Psychiatry,* 7**,** e1080.

HORNIG, M., GOTTSCHALK, G., PETERSON, D. L., KNOX, K. K., SCHULTZ, A. F., EDDY, M. L., CHE, X. & LIPKIN, W. I. 2016. Cytokine network analysis of cerebrospinal fluid in myalgic encephalomyelitis/chronic fatigue syndrome. *Molecular Psychiatry,* 21**,** 261-9.

HORNIG, M., MONTOYA, J. G., KLIMAS, N. G., LEVINE, S., FELSENSTEIN, D., BATEMAN, L., PETERSON, D. L., GOTTSCHALK, C. G., SCHULTZ, A. F., CHE, X., EDDY, M. L., KOMAROFF, A. L. & LIPKIN,

W. I. 2015. Distinct plasma immune signatures in ME/CFS are present early in the course of illness. *Science Advances,* 1.

HOUSER, M. C. & TANSEY, M. G. 2017. The gut-brain axis: is intestinal inflammation a silent driver of Parkinson's disease pathogenesis? *npj Parkinson's Disease,* 3**,** 3.

HO-YEN, D. O. 1990. Patient management of post-viral fatigue syndrome. *The British journal of general practice : the journal of the Royal College of General Practitioners,* 40**,** 37-39.

HUANG, K. C., MUKHOPADHYAY, R., WEN, B., GITAI, Z. & WINGREEN, N. S. 2008. Cell shape and cell-wall organization in Gram-negative bacteria. *Proceedings of the National Academy of Sciences,* 105**,** 19282-19287.

HUSEYIN, C. E., RUBIO, R. C., O'SULLIVAN, O., COTTER, P. D. & SCANLAN, P. D. 2017. The Fungal Frontier: A Comparative Analysis of Methods Used in the Study of the Human Gut Mycobiome. *Frontiers in Microbiology,* 8.

HUTH, T. K., BRENU, E. W., RAMOS, S., NGUYEN, T., BROADLEY, S., STAINES, D. & MARSHALL-GRADISNIK, S. 2016a. Pilot Study of Natural Killer Cells in Chronic Fatigue Syndrome/Myalgic Encephalomyelitis and Multiple Sclerosis. *Scandinavian Journal of Immunology,* 83**,** 44-51.

HUTH, T. K., STAINES, D. & MARSHALL-GRADISNIK, S. 2016b. ERK1/2, MEK1/2 and p38 downstream signalling molecules impaired in CD56 dim CD16+ and CD56 bright CD16 dim/- natural killer cells in Chronic Fatigue Syndrome/Myalgic Encephalomyelitis patients. *Journal of Translational Medicine,* 14**,** 97.

HUTH, T., BRENU, E. W., NGUYEN, T., HARDCASTLE, S., JOHNSTON, S. & RAMOS, S. 2014. Characterization of Natural Killer Cell Phenotypes in Chronic Fatigue Syndrome/Myalgic Encephalomyelitis. *Journal of Clinical & Cellular Immunology,* 5.

HUUS, K. E., FRANKOWSKI, M., PUČIĆ-BAKOVIĆ, M., VUČKOVIĆ, F., LAUC, G., MULLISH, B. H., MARCHESI, J. R., MONAGHAN, T. M., KAO, D. & FINLAY, B. B. 2021. Changes in IgA-targeted microbiota following fecal transplantation for recurrent *Clostridioides difficile* infection. *Gut Microbes,* 13**,** 1-12.

HYDE, B. M. 2007. *The Nightingale, Myalgic Encephalomyelitis (M.E.) Definition.,* The Nightingale Research Foundation.

ICD-11. 2022. *International classification of disease (ICD)-11 for mortality and morbidity statistics: Postviral fatigue syndrome [8E49]* [Online]. World Health Organization (WHO). Available: https://icd.who.int/browse11/l-m/en#/http://id.who.int/icd/entity/569175314 [Accessed 16 March 2022].

ILAVSKÁ, S., HORVÁTHOVÁ, M., SZABOVÁ, M., NEMESSÁNYI, T., JAHNOVÁ, E., TULINSKÁ, J., LÍŠKOVÁ, A., WSOLOVÁ, L., STARUCHOVÁ, M. & VOLKOVOVÁ, K. 2012. Association between the human immune response and body mass index. *Human Immunology,* 73**,** 480-5.

IOM 2015. The National Academies Collection: Reports funded by National Institutes of Health. *Beyond Myalgic Encephalomyelitis/Chronic Fatigue Syndrome: Redefining an Illness.* Washington (DC): National Academies Press (US) Copyright 2015 by the National Academy of Sciences. All rights reserved.

IRWIN, M. R., WANG, M., CAMPOMAYOR, C. O., COLLADO-HIDALGO, A. & COLE, S. 2006. Sleep deprivation and activation of morning levels of cellular and genomic markers of inflammation. *Archives of Internal Medicine,* 166**,** 1756-62.

JACKSON, M. A., PEARSON, C., ILOTT, N. E., HUUS, K. E., HEGAZY, A. N., WEBBER, J., FINLAY, B. B., MACPHERSON, A. J., POWRIE, F. & LAM, L. H. 2021. Accurate identification and quantification of commensal microbiota bound by host immunoglobulins. *Microbiome,* 9**,** 33.

JAMES, E. A., PIETROPAOLO, M. & MAMULA, M. J. 2018. Immune Recognition of β-Cells: Neoepitopes as Key Players in the Loss of Tolerance. *Diabetes,* 67**,** 1035-1042.

JANZON, A., GOODRICH, J. K., KOREN, O., WATERS, J. L. & LEY, R. E. 2019. Interactions between the Gut Microbiome and Mucosal Immunoglobulins A, M, and G in the Developing Infant Gut. *mSystems,* 4.

JASON, L. A., BROWN, A., CLYNE, E., BARTGIS, L., EVANS, M. & BROWN, M. 2012. Contrasting case definitions for chronic fatigue syndrome, Myalgic Encephalomyelitis/chronic fatigue syndrome and myalgic encephalomyelitis. *Evaluation & the Health Professions,* 35**,** 280-304.

JASON, L. A., CORRADI, K. & TORRESHARDING, S. 2007. Toward an Empirical Case Definition of CFS. *Journal of Social Service Research,* 34**,** 43-54.

JASON, L. A., CORRADI, K., TORRES-HARDING, S., TAYLOR, R. R. & KING, C. 2005. Chronic fatigue syndrome: the need for subtypes. *Neuropsychology Review,* 15**,** 29-58.

JASON, L. A., EVANS, M. A., PORTER, N. S., BROWN, M. M., BROWN, A. A., HUNNELL, J., ANDERSON, V. R., LERCH, A. & FRIEDBERG, F. 2010. The Development of a Revised Canadian Myalgic Encephalomyelitis Chronic Fatigue Syndrome Case Definition. *American Journal of Biochemistry and Biotechnology,* 6**,** 120-135.

JASON, L. A., EVANS, M., BROWN, M., PORTER, N., BROWN, A., HUNNELL, J., ANDERSON, V. & LERCH, A. 2011. Fatigue Scales and Chronic Fatigue Syndrome: Issues of Sensitivity and Specificity. *Disability Studies Quarterly,* 31.

JASON, L. A., KOT, B., SUNNQUIST, M., BROWN, A., EVANS, M., JANTKE, R., WILLIAMS, Y., FURST, J. & VERNON, S. D. 2015. Chronic Fatigue Syndrome and Myalgic Encephalomyelitis: Toward An Empirical Case Definition. *Health Psychology and Behavioral Medicine,* 3**,** 82-93.

JERJES, W. K., CLEARE, A. J., WESSELY, S., WOOD, P. J. & TAYLOR, N. F. 2005. Diurnal patterns of salivary cortisol and cortisone output in chronic fatigue syndrome. *Journal of Affective Disorders,* 87**,** 299-304.

JERJES, W. K., TAYLOR, N. F., WOOD, P. J. & CLEARE, A. J. 2007. Enhanced feedback sensitivity to prednisolone in chronic fatigue syndrome. *Psychoneuroendocrinology,* 32**,** 192-198.

JIANG, S. & DONG, C. 2013. A complex issue on CD4+ T-cell subsets. *Immunological Reviews,* 252**,** 5-11.

JOHNSON, A. J., ZHENG, J. J., KANG, J. W., SABOE, A., KNIGHTS, D. & ZIVKOVIC, A. M. 2020. A Guide to Diet-Microbiome Study Design. *Frontiers in Nutrition,* 7.

JONES, J. F., KOHL, K. S., AHMADIPOUR, N., BLEIJENBERG, G., BUCHWALD, D., EVENGARD, B., JASON, L. A., KLIMAS, N. G., LLOYD, A., MCCLEARY, K., OLESKE, J. M. & WHITE, P. D. 2007. Fatigue: case definition and guidelines for collection, analysis, and presentation of immunization safety data. *Vaccine,* 25**,** 5685-96.

JONES, M. G., COOPER, E., AMJAD, S., GOODWIN, C. S., BARRON, J. L. & CHALMERS, R. A. 2005. Urinary and plasma organic acids and amino acids in chronic fatigue syndrome. *Clinica Chimica Acta,* 361**,** 150-8.

JONSJÖ, M. A., OLSSON, G. L., WICKSELL, R. K., ALVING, K., HOLMSTRÖM, L. & ANDREASSON, A. 2020. The role of low-grade inflammation in ME/CFS (Myalgic Encephalomyelitis/Chronic Fatigue Syndrome) - associations with symptoms. *Psychoneuroendocrinology,* 113**,** 104578.

JOST, L. 2006. Entropy and diversity. *Oikos,* 113**,** 363-375.

KARHU, E., FORSGÅRD, R. A., ALANKO, L., ALFTHAN, H., PUSSINEN, P., HÄMÄLÄINEN, E. & KORPELA, R. 2017. Exercise and gastrointestinal symptoms: running-induced changes in intestinal permeability and markers of gastrointestinal function in asymptomatic and symptomatic runners. *European Journal of Applied Physiology,* 117**,** 2519-2526.

KATZ, B. Z., SHIRAISHI, Y., MEARS, C. J., BINNS, H. J. & TAYLOR, R. 2009. Chronic fatigue syndrome after infectious mononucleosis in adolescents. *Pediatrics,* 124**,** 189-193.

KELLY, CALEB J., ZHENG, L., CAMPBELL, ERIC L., SAEEDI, B., SCHOLZ, CARSTEN C., BAYLESS, AMANDA J., WILSON, KELLY E., GLOVER, LOUISE E., KOMINSKY, DOUGLAS J., MAGNUSON, A., WEIR, TIFFANY L., EHRENTRAUT, STEFAN F., PICKEL, C., KUHN, KRISTINE A., LANIS, JORDI M., NGUYEN, V., TAYLOR, CORMAC T. & COLGAN, SEAN P. 2015. Crosstalk between Microbiota-Derived Short-Chain Fatty Acids and Intestinal Epithelial HIF Augments Tissue Barrier Function. *Cell Host & Microbe,* 17**,** 662-671.

KENYON, J. N., COE, S. & IZADI, H. 2019. A retrospective outcome study of 42 patients with Chronic Fatigue Syndrome, 30 of whom had Irritable Bowel Syndrome. Half were treated with oral approaches, and half were treated with Faecal Microbiome Transplantation. *Human Microbiome Journal,* 13**,** 100061.

KEYT, B. A., BALIGA, R., SINCLAIR, A. M, CARROLL, S. F. & PETERSON, M. S. 2020. Structure, Function and Therapeutic Use of IgM Antibodies. *Antibodies (Basel, Switzerland)*, 9(4), 53.

KHAN MIRZAEI, M., XUE, J., COSTA, R., RU, J., SCHULZ, S., TARANU, Z. E. & DENG, L. 2021. Challenges of Studying the Human Virome – Relevant Emerging Technologies. *Trends in Microbiology,* 29**,** 171-181.

KHAN, A. A., YURKOVETSKIY, L., O'GRADY, K., PICKARD, J. M., DE POOTER, R., ANTONOPOULOS, D. A., GOLOVKINA, T. & CHERVONSKY, A. 2019. Polymorphic Immune Mechanisms Regulate Commensal Repertoire. *Cell Reports,* 29**,** 541-550.e4.

KHOSHBIN, K., KHANNA, L., MASELLI, D., ATIEH, J., BREEN-LYLES, M., ARNDT, K., RHOTEN, D., DYER, R. B., SINGH, R. J., NAYAR, S., BJERKNESS, S., HARMSEN, W. S., BUSCIGLIO, I., & CAMILLERI, M. (2021). Development and Validation of Test for "Leaky Gut" Small Intestinal and Colonic Permeability Using Sugars in Healthy Adults. *Gastroenterology*, 161(2), 463–475.e13.

KIECOLT-GLASER, J. K., WILSON, S. J., BAILEY, M. L., ANDRIDGE, R., PENG, J., JAREMKA, L. M., FAGUNDES, C. P., MALARKEY, W. B., LASKOWSKI, B. & BELURY, M. A. 2018. Marital distress, depression, and a leaky gut: Translocation of bacterial endotoxin as a pathway to inflammation. *Psychoneuroendocrinology,* 98**,** 52-60.

KIM, B. H., NAMKOONG, K., KIM, J. J., LEE, S., YOON, K. J., CHOI, M. & JUNG, Y. C. 2015. Altered resting-state functional connectivity in women with chronic fatigue syndrome. *Psychiatry Research,* 234**,** 292-7.

KIM, D. Y., LEE, J. S. & SON, C. G. 2020. Systematic Review of Primary Outcome Measurements for Chronic Fatigue Syndrome/Myalgic Encephalomyelitis (CFS/ME) in Randomized Controlled Trials. *Journal of Clinical Medicine,* 9.

KINASHI, Y. & HASE, K. 2021. Partners in Leaky Gut Syndrome: Intestinal Dysbiosis and Autoimmunity. *Frontiers in Immunology,* 12**,** 673708.

KITAMI, T., FUKUDA, S., KATO, T., YAMAGUTI, K., NAKATOMI, Y., YAMANO, E., KATAOKA, Y., MIZUNO, K., TSUBOI, Y., KOGO, Y., SUZUKI, H., ITOH, M., MORIOKA, M. S., KAWAJI, H., KOSEKI, H., KIKUCHI, J., HAYASHIZAKI, Y., OHNO, H., KURATSUNE, H. & WATANABE, Y. 2020. Deep phenotyping of myalgic encephalomyelitis/chronic fatigue syndrome in Japanese population. *Scientific Reports,* 10**,** 19933.

KLANN, E. M., DISSANAYAKE, U., GURRALA, A., FARRER, M., SHUKLA, A. W., RAMIREZ-ZAMORA, A., MAI, V. & VEDAM-MAI, V. 2022. The Gut–Brain Axis and Its Relation to Parkinson's Disease: A Review. *Frontiers in Aging Neuroscience,* 13.

KLEIN, S. L. & FLANAGAN, K. L. 2016. Sex differences in immune responses. *Nature Reviews Immunology,* 16**,** 626-638.

KNIGHT, R., VRBANAC, A., TAYLOR, B. C., AKSENOV, A., CALLEWAERT, C., DEBELIUS, J., GONZALEZ, A., KOSCIOLEK, T., MCCALL, L.-I., MCDONALD, D., MELNIK, A. V., MORTON, J. T., NAVAS, J.,

QUINN, R. A., SANDERS, J. G., SWAFFORD, A. D., THOMPSON, L. R., TRIPATHI, A., XU, Z. Z., ZANEVELD, J. R., ZHU, Q., CAPORASO, J. G. & DORRESTEIN, P. C. 2018. Best practices for analysing microbiomes. *Nature Reviews Microbiology,* 16**,** 410-422.

KOMAROFF, A. L., FAGIOLI, L. R., GEIGER, A. M., DOOLITTLE, T. H., LEE, J., KORNISH, R. J., GLEIT, M. A. & GUERRIERO, R. T. 1996. An examination of the working case definition of chronic fatigue syndrome. *The American Journal of Medicine,* 100**,** 56-64.

KÖNIG, R. S., ALBRICH, W. C., KAHLERT, C. R., BAHR, L. S., LÖBER, U., VERNAZZA, P., SCHEIBENBOGEN, C. & FORSLUND, S. K. 2021. The Gut Microbiome in Myalgic Encephalomyelitis (ME)/Chronic Fatigue Syndrome (CFS). *Frontiers in Immunology,* 12**,** 628741.

KONTUREK, P. C., HARSCH, I. A., KONTUREK, K., SCHINK, M., KONTUREK, T., NEURATH, M. F. & ZOPF, Y. 2018. Gut¯Liver Axis: How Do Gut Bacteria Influence the Liver? *Medical Sciences (Basel),* 6.

KRZEWSKI, K. & COLIGAN, J. E. 2012. Human NK cell lytic granules and regulation of their exocytosis. *Frontiers in Immunology,* 3**,** 335.

LACY, B. E. & PATEL, N. K. 2017. Rome Criteria and a Diagnostic Approach to Irritable Bowel Syndrome. *Journal of clinical medicine,* 6**,** 99.

LAGKOUVARDOS, I., FISCHER, S., KUMAR, N. & CLAVEL, T. 2017. Rhea: a transparent and modular R pipeline for microbial profiling based on 16S rRNA gene amplicons. *PeerJ,* 5**,** e2836.

LANDERS, C. J., COHAVY, O., MISRA, R., YANG, H., LIN, Y. C., BRAUN, J. & TARGAN, S. R. 2002. Selected loss of tolerance evidenced by Crohn's disease-associated immune responses to auto- and microbial antigens. *Gastroenterology,* 123**,** 689-99.

LAX, S., SMITH, D. P., HAMPTON-MARCELL, J., OWENS, S. M., HANDLEY, K. M., SCOTT, N. M., GIBBONS, S. M., LARSEN, P., SHOGAN, B. D., WEISS, S., METCALF, J. L., URSELL, L. K., VÁZQUEZ-BAEZA, Y., VAN TREUREN, W., HANSAN, N. A., GIBSON, M. K., COLWELL, R., DANTAS, G., KNIGHT, R., & GILBERT, J. A. 2014. Longitudinal analysis of microbial interaction between humans and the indoor environment. *Science (New York, N.Y.),* 345(6200), 1048–1052.

LE BON, O., NEU, D., BERQUIN, Y., LANQUART, J. P., HOFFMANN, R., MAIRESSE, O. & ARMITAGE, R. 2012. Ultra-slow delta power in chronic fatigue syndrome. *Psychiatry Research,* 200**,** 742-7.

LEBARON, P., SERVAIS, P., BAUDOUX, A. C., BOURRAIN, M., COURTIES, C. & PARTHUISOT, N. 2002. Variations of bacterial-specific activity with cell size and nucleic acid content assessed by flow cytometry. *Aquatic Mircobial Ecology,* 28**,** 131-140.

LEE, J. S., JEON, Y. J., PARK, S. Y. & SON, C. G. 2020. An Adrenalectomy Mouse Model Reflecting Clinical Features for Chronic Fatigue Syndrome. *Biomolecules,* 10.

LEE, J.-S., LACERDA, E. M., NACUL, L., KINGDON, C. C., NORRIS, J., O'BOYLE, S., ROBERTS, C. H., PALLA, L., RILEY, E. M. & CLIFF, J. M. 2021. Salivary DNA loads for human herpes viruses 6 and 7 are correlated with disease phenotype in Myalgic Encephalomyelitis/ Chronic Fatigue Syndrome. *medRxiv***,** 2021.01.06.20248486.

LEWIS, S. J., & HEATON, K. W. 1997. Stool form scale as a useful guide to intestinal transit time. *Scandinavian journal of gastroenterology*, *32*(9), 920–924.

LI, Q., WANG, C., TANG, C., HE, Q., LI, N. & LI, J. 2014. Dysbiosis of gut fungal microbiota is associated with mucosal inflammation in Crohn's disease. *Journal of Clinical Gastroenterology,* 48**,** 513-23.

LI, Y., HANDLEY, S. A. & BALDRIDGE, M. T. 2021. The dark side of the gut: Virome-host interactions in intestinal homeostasis and disease. *Journal of Experimental Medicine,* 218.

LIANG, S., WU, X., HU, X., WANG, T. & JIN, F. 2018. Recognizing Depression from the Microbiota¯Gut¯Brain Axis. *International Journal of Molecular Sciences,* 19.

LIM, E. J. & SON, C. G. 2020. Review of case definitions for myalgic encephalomyelitis/chronic fatigue syndrome (ME/CFS). *Journal of Translational Medicine,* 18**,** 289.

LIM, E. J., AHN, Y. C., JANG, E. S., LEE, S. W., LEE, S. H. & SON, C. G. 2020. Systematic review and meta-analysis of the prevalence of chronic fatigue syndrome/myalgic encephalomyelitis (CFS/ME). *Journal of Translational Medicine,* 18**,** 100.

LIN, R., CHEN, H., SHU, W., SUN, M., FANG, L., SHI, Y., PANG, Z., WU, W. & LIU, Z. 2018. Clinical significance of soluble immunoglobulins A and G and their coated bacteria in feces of patients with inflammatory bowel disease. *Journal of Translational Medicine,* 16**,** 359.

LINDAN, R. 1956. Benign Myalgic Encephalomyelitis. *Canadian Medical Association Journal,* 75**,** 596-7.

LIPPÉ, R. 2018. Flow Virometry: a Powerful Tool To Functionally Characterize Viruses. *J Virol,* 92.

LIPPS, S. M., & SAMAC, D. A. (2022). Pseudomonas viridiflava: An internal outsider of the Pseudomonas syringae species complex. *Molecular plant pathology*, 23(1), 3–15.

LIU, Y., YUAN, X., LI, L., LIN, L., ZUO, X., CONG, Y. & LI, Y. 2020. Increased Ileal Immunoglobulin A Production and Immunoglobulin A-Coated Bacteria in Diarrhea-Predominant Irritable Bowel Syndrome. *Clinical and translational gastroenterology,* 11**,** e00146-e00146.

LLOYD, A. R., HICKIE, I., BOUGHTON, C. R., SPENCER, O. & WAKEFIELD, D. 1990. Prevalence of chronic fatigue syndrome in an Australian population. *The Medical Journal of Australia,* 153**,** 522-8.

LOEBEL, M., GRABOWSKI, P., HEIDECKE, H., BAUER, S., HANITSCH, L. G., WITTKE, K., MEISEL, C., REINKE, P., VOLK, H.-D., FLUGE, Ø., MELLA, O. & SCHEIBENBOGEN, C. 2016. Antibodies to β adrenergic and muscarinic cholinergic receptors in patients with Chronic Fatigue Syndrome. *Brain, Behavior, and Immunity,* 52**,** 32-39.

LOZUPONE, C. A., HAMADY, M., KELLEY, S. T. & KNIGHT, R. 2007. Quantitative and qualitative beta diversity measures lead to different insights into factors that structure microbial communities. *Applied and Environmental Microbiology,* 73**,** 1576-85.

LU J, B. F., THIELEN P, SALZBERG SL. 2017. Bracken: estimating species abundance in metagenomics data. *PeerJ Computer Science,* 3**,** e104.

LUDWIG, R. J., VANHOORELBEKE, K., LEYPOLDT, F., KAYA, Z., BIEBER, K., MCLACHLAN, S. M., KOMOROWSKI, L., LUO, J., CABRAL-MARQUES, O., HAMMERS, C. M., LINDSTROM, J. M., LAMPRECHT, P., FISCHER, A., RIEMEKASTEN, G., TERSTEEG, C., SONDERMANN, P., RAPOPORT, B., WANDINGER, K. P., PROBST, C., EL BEIDAQ, A., SCHMIDT, E., VERKMAN, A., MANZ, R. A. & NIMMERJAHN, F. 2017. Mechanisms of Autoantibody-Induced Pathology. *Frontiers in Immunology,* 8**,** 603.

LUNDBERG, K., KINLOCH, A., FISHER, B. A., WEGNER, N., WAIT, R., CHARLES, P., MIKULS, T. R. & VENABLES, P. J. 2008. Antibodies to citrullinated alpha-enolase peptide 1 are specific for rheumatoid arthritis and cross-react with bacterial enolase. *Arthritis & Rheumatology,* 58**,** 3009-19.

LUPO, G. F. D., ROCCHETTI, G., LUCINI, L., LORUSSO, L., MANARA, E., BERTELLI, M., PUGLISI, E. & CAPELLI, E. 2021. Potential role of microbiome in Chronic Fatigue Syndrome/Myalgic Encephalomyelits (CFS/ME). *Scientific Reports,* 11**,** 7043.

LUTZ, L., ROHRHOFER, J., ZEHETMAYER, S., STINGL, M. & UNTERSMAYR, E. 2021. Evaluation of Immune Dysregulation in an Austrian Patient Cohort Suffering from Myalgic Encephalomyelitis/Chronic Fatigue Syndrome. *Biomolecules,* 11.

MA, J., PRINCE, A. & AAGAARD, K. M. 2014. Use of whole genome shotgun metagenomics: a practical guide for the microbiome-minded physician scientist. *Seminars in Reproductive Medicine,* 32**,** 5-13.

MA, L., ZHU, S., TIAN, Y., ZHANG, W., WANG, S., CHEN, C., WU, L. & YAN, X. 2016. Label-Free Analysis of Single Viruses with a Resolution Comparable to That of Electron Microscopy and the Throughput of Flow Cytometry. *Angewandte Chemie International Edition in English,* 55**,** 10239-43.

MACPHERSON, A., KHOO, U. Y., FORGACS, I., PHILPOTT-HOWARD, J. & BJARNASON, I. 1996. Mucosal antibodies in inflammatory bowel disease are directed against intestinal bacteria. *Gut,* 38**,** 365-75.

MAES, M. & LEUNIS, J. C. 2008. Normalization of leaky gut in chronic fatigue syndrome (CFS) is accompanied by a clinical improvement: effects of age, duration of illness and the translocation of LPS from gram-negative bacteria. *Neuroendocrinology Letters,* 29**,** 902-10.

MAES, M. 2015. A new case definition of Neuro-Inflammatory and Oxidative Fatigue (NIOF), a neuroprogressive disorder, formerly known as chronic fatigue syndrome or Myalgic

Encephalomyelitis: results of multivariate pattern recognition methods and external validation by neuro-immune biomarkers. *Neuroendocrinology Letters,* 36**,** 320-9.

MAES, M., LEUNIS, J. C., GEFFARD, M. & BERK, M. 2014. Evidence for the existence of Myalgic Encephalomyelitis/Chronic Fatigue Syndrome (ME/CFS) with and without abdominal discomfort (irritable bowel) syndrome. *Neuroendocrinology Letters,* 35**,** 445-53.

MAES, M., MIHAYLOVA, I. & LEUNIS, J. C. 2007. Increased serum IgA and IgM against LPS of enterobacteria in chronic fatigue syndrome (CFS): indication for the involvement of gram-negative enterobacteria in the etiology of CFS and for the presence of an increased gut-intestinal permeability. *Journal of Affective Disorders,* 99**,** 237-40.

MAES, M., MIHAYLOVA, I., KUBERA, M., LEUNIS, J. C., TWISK, F. N. & GEFFARD, M. 2012a. IgM-mediated autoimmune responses directed against anchorage epitopes are greater in Myalgic Encephalomyelitis/Chronic Fatigue Syndrome (ME/CFS) than in major depression. *Metabolic Brain Disease,* 27**,** 415-23.

MAES, M., MIHAYLOVA, I., KUBERA, M., UYTTERHOEVEN, M., VRYDAGS, N. & BOSMANS, E. 2009. Coenzyme Q10 deficiency in myalgic encephalomyelitis / chronic fatigue syndrome (ME/CFS) is related to fatigue, autonomic and neurocognitive symptoms and is another risk factor explaining the early mortality in ME/CFS due to cardiovascular disorder. *Neuro endocrinology letters,* 30**,** 470-6.

MAES, M., RINGEL, K., KUBERA, M., ANDERSON, G., MORRIS, G., GALECKI, P. & GEFFARD, M. 2013. In myalgic encephalomyelitis/chronic fatigue syndrome, increased autoimmune activity against 5-HT is associated with immuno-inflammatory pathways and bacterial translocation. *Journal of Affective Disorders,* 150**,** 223-30.

MAES, M., TWISK, F. N. & JOHNSON, C. 2012b. Myalgic Encephalomyelitis (ME), Chronic Fatigue Syndrome (CFS), and Chronic Fatigue (CF) are distinguished accurately: results of supervised learning techniques applied on clinical and inflammatory data. *Psychiatry Research,* 200**,** 754-60.

MAES, M., TWISK, F. N., KUBERA, M. & RINGEL, K. 2012c. Evidence for inflammation and activation of cell-mediated immunity in Myalgic Encephalomyelitis/Chronic Fatigue Syndrome (ME/CFS): increased interleukin-1, tumor necrosis factor-α, PMN-elastase, lysozyme and neopterin. *Journal of Affective Disorders,* 136**,** 933-9.

MAES, M., TWISK, F. N., KUBERA, M., RINGEL, K., LEUNIS, J. C. & GEFFARD, M. 2012d. Increased IgA responses to the LPS of commensal bacteria is associated with inflammation and activation of cell-mediated immunity in chronic fatigue syndrome. *Journal of Affective Disorders,* 136**,** 909-17.

MAHER, K. J., KLIMAS, N. G. & FLETCHER, M. A. 2005. Chronic fatigue syndrome is associated with diminished intracellular perforin. *Clinical & Experimental Immunology,* 142**,** 505-11.

MANDARANO, A. H., GILOTEAUX, L., KELLER, B. A., LEVINE, S. M. & HANSON, M. R. 2018. Eukaryotes in the gut microbiota in myalgic encephalomyelitis/chronic fatigue syndrome. *PeerJ,* 6**,** e4282.

MANDARANO, A. H., MAYA, J., GILOTEAUX, L., PETERSON, D. L., MAYNARD, M., GOTTSCHALK, C. G. & HANSON, M. R. 2020. Myalgic encephalomyelitis/chronic fatigue syndrome patients exhibit altered T cell metabolism and cytokine associations. *The Journal of Clinical Investigation,* 130**,** 1491-1505.

MANNON, P. J. 2019. Systemic antibody responses to gut commensal bacteria: How and why do I know you? *Journal of Allergy and Clinical Immunology,* 143**,** 1353-1354.

MATSUDA, K., AKIYAMA, T., TSUJIBE, S., OKI, K., GAWAD, A. & FUJIMOTO, J. 2021. Direct measurement of stool consistency by texture analyzer and calculation of reference value in Belgian general population. *Scientific reports,* 11**,** 2400-2400.

MCEVEDY, C. P. & BEARD, A. W. 1970. Royal Free epidemic of 1955: a reconsideration. *British Medical Journal,* 1**,** 7-11.

MCIVER, L. J., ABU-ALI, G., FRANZOSA, E. A., SCHWAGER, R., MORGAN, X. C., WALDRON, L., SEGATA, N. & HUTTENHOWER, C. 2018. bioBakery: a meta'omic analysis environment. *Bioinformatics,* 34**,** 1235-1237.

MCPHEE, G., BALDWIN, A., KINDLON, T. & HUGHES, B. M. 2021. Monitoring treatment harm in myalgic encephalomyelitis/chronic fatigue syndrome: A freedom-of-information study of National Health Service specialist centres in England. *Journal of Health Psychology,* 26**,** 975-984.

MCPHERSON, A. C., PANDEY, S. P., BENDER, M. J. & MEISEL, M. 2021. Systemic Immunoregulatory Consequences of Gut Commensal Translocation. *Trends in Immunology,* 42**,** 137-150.

MEGUR, A., BALTRIUKIENĖ, D., BUKELSKIENĖ, V. & BUROKAS, A. 2020. The Microbiota-Gut-Brain Axis and Alzheimer's Disease: Neuroinflammation Is to Blame? *Nutrients,* 13.

MILAN-MATTOS, J. C., ANIBAL, F. F., PERSEGUINI, N. M., MINATEL, V., REHDER-SANTOS, P., CASTRO, C. A., VASILCEAC, F. A., MATTIELLO, S. M., FACCIOLI, L. H. & CATAI, A. M. 2019. Effects of natural aging and gender on pro-inflammatory markers. *Brazilian Journal of Medical and Biological Research,* 52**,** e8392.

MILRAD, S. F., HALL, D. L., JUTAGIR, D. R., LATTIE, E. G., IRONSON, G. H., WOHLGEMUTH, W., NUNEZ, M. V., GARCIA, L., CZAJA, S. J., PERDOMO, D. M., FLETCHER, M. A., KLIMAS, N. & ANTONI, M. H. 2017. Poor sleep quality is associated with greater circulating pro-inflammatory cytokines and severity and frequency of chronic fatigue syndrome/myalgic encephalomyelitis (CFS/ME) symptoms in women. *Journal of Neuroimmunology,* 303**,** 43-50.

MISSAILIDIS, D., ANNESLEY, S. J. & FISHER, P. R. 2019. Pathological Mechanisms Underlying Myalgic Encephalomyelitis/Chronic Fatigue Syndrome. *Diagnostics (Basel),* 9.

MISSAILIDIS, D., ANNESLEY, S. J., ALLAN, C. Y., SANISLAV, O., LIDBURY, B. A., LEWIS, D. P. & FISHER, P. R. 2020. An Isolated Complex V Inefficiency and Dysregulated Mitochondrial Function in Immortalized Lymphocytes from ME/CFS Patients. *International Journal of Molecular Sciences,* 21.

MIWA, K. 2017. Down-regulation of renin-aldosterone and antidiuretic hormone systems in patients with myalgic encephalomyelitis/chronic fatigue syndrome. *Journal of Cardiology,* 69**,** 684-688.

MONTOYA, J. G., HOLMES, T. H., ANDERSON, J. N., MAECKER, H. T., ROSENBERG-HASSON, Y., VALENCIA, I. J., CHU, L., YOUNGER, J. W., TATO, C. M. & DAVIS, M. M. 2017. Cytokine signature associated with disease severity in chronic fatigue syndrome patients. *Proceedings of the National Academy of Sciences of the United States of America,* 114**,** E7150-e7158.

MOON, C., BALDRIDGE, M. T., WALLACE, M. A., D, C. A., BURNHAM, VIRGIN, H. W. & STAPPENBECK, T. S. 2015. Vertically transmitted faecal IgA levels determine extra-chromosomal phenotypic variation. *Nature,* 521**,** 90-93.

MØRCH, K., HANEVIK, K., RIVENES, A. C., BØDTKER, J. E., NÆSS, H., STUBHAUG, B., WENSAAS, K. A., RORTVEIT, G., EIDE, G. E., HAUSKEN, T. & LANGELAND, N. 2013. Chronic fatigue syndrome 5 years after giardiasis: differential diagnoses, characteristics and natural course. *BMC Gastroenterology,* 13**,** 28.

MORENO-SABATER, A., AUTAA, G., STERLIN, D., JERBI, A., VILLETTE, R., HOLM, J. B., PARIZOT, C., SELIM, S., SENGHOR, Y., GHILLANI-DALBIN, P., BACHMEYER, C., HENNEQUIN, C., GOROCHOV, G. & LARSEN, M. 2020. Systemic anti-commensal response to fungi analyzed by flow cytometry is related to gut mycobiome ecology. *Microbiome,* 8**,** 159.

MORRIS, G. & MAES, M. 2014. Oxidative and Nitrosative Stress and Immune-Inflammatory Pathways in Patients with Myalgic Encephalomyelitis (ME)/Chronic Fatigue Syndrome (CFS). *Current Neuropharmacology,* 12**,** 168-85.

MORRIS, G., BERK, M., CARVALHO, A. F., CASO, J. R., SANZ, Y. & MAES, M. 2016. The Role of Microbiota and Intestinal Permeability in the Pathophysiology of Autoimmune and Neuroimmune Processes with an Emphasis on Inflammatory Bowel Disease Type 1 Diabetes and Chronic Fatigue Syndrome. *Current Pharmaceutical Design,* 22**,** 6058-6075.

MOWAT, A. M. 2018. To respond or not to respond - a personal perspective of intestinal tolerance. *Nature Reviews Immunology,* 18**,** 405-415.

MUKHOPADHYA, I., SEGAL, J. P., CARDING, S. R., HART, A. L. & HOLD, G. L. 2019. The gut virome: the 'missing link' between gut bacteria and host immunity? *Therapeutic Advances in Gastroenterology,* 12**,** 1756284819836620.

MÜLLER, S., ULLRICH, S., LÖSCHE, A., LOFFHAGEN, N. & BABEL, W. 2000. Flow cytometric techniques to characterise physiological states of Acinetobacter calcoaceticus. *Journal of Microbiological Methods,* 40**,** 67-77.

MURDOCK, K. W., WANG, X. S., SHI, Q., CLEELAND, C. S., FAGUNDES, C. P. & VERNON, S. D. 2017. The utility of patient-reported outcome measures among patients with myalgic encephalomyelitis/chronic fatigue syndrome. *Quality of Life Research,* 26**,** 913-921.

MURTAGH, F. & LEGENDRE, P. 2014. Ward's Hierarchical Agglomerative Clustering Method: Which Algorithms Implement Ward's Criterion? *Journal of Classification,* 31**,** 274-295.

NACUL, L. C., LACERDA, E. M., PHEBY, D., CAMPION, P., MOLOKHIA, M., FAYYAZ, S., LEITE, J. C., POLAND, F., HOWE, A. & DRACHLER, M. L. 2011. Prevalence of myalgic encephalomyelitis/chronic fatigue syndrome (ME/CFS) in three regions of England: a repeated cross-sectional study in primary care. *BMC Medicine,* 9**,** 91.

NACUL, L., O'BOYLE, S., PALLA, L., NACUL, F. E., MUDIE, K., KINGDON, C. C., CLIFF, J. M., CLARK, T. G., DOCKRELL, H. M. & LACERDA, E. M. 2020. How Myalgic Encephalomyelitis/Chronic Fatigue Syndrome (ME/CFS) Progresses: The Natural History of ME/CFS. *Frontiers in Neurology,* 11.

NAGAFUSA, H. & SAYAMA, K. 2020. Age-related chemokine alterations affect IgA secretion and gut immunity in female mice. *Biogerontology,* 21**,** 609-618.

NAGPAL, R. & YADAV, H. 2017. Bacterial Translocation from the Gut to the Distant Organs: An Overview. *Annals of Nutrition & Metabolism,* 71 Suppl 1**,** 11-16.

NAGY-SZAKAL, D., BARUPAL, D. K., LEE, B., CHE, X., WILLIAMS, B. L., KAHN, E. J. R., UKAIGWE, J. E., BATEMAN, L., KLIMAS, N. G., KOMAROFF, A. L., LEVINE, S., MONTOYA, J. G., PETERSON, D. L., LEVIN, B., HORNIG, M., FIEHN, O. & LIPKIN, W. I. 2018. Insights into myalgic encephalomyelitis/chronic fatigue syndrome phenotypes through comprehensive metabolomics. *Scientific Reports,* 8**,** 10056.

NAGY-SZAKAL, D., WILLIAMS, B. L., MISHRA, N., CHE, X., LEE, B., BATEMAN, L., KLIMAS, N. G., KOMAROFF, A. L., LEVINE, S., MONTOYA, J. G., PETERSON, D. L., RAMANAN, D., JAIN, K., EDDY, M. L., HORNIG, M. & LIPKIN, W. I. 2017. Fecal metagenomic profiles in subgroups of patients with myalgic encephalomyelitis/chronic fatigue syndrome. *Microbiome,* 5**,** 44.

NAKATOMI, Y., MIZUNO, K., ISHII, A., WADA, Y., TANAKA, M., TAZAWA, S., ONOE, K., FUKUDA, S., KAWABE, J., TAKAHASHI, K., KATAOKA, Y., SHIOMI, S., YAMAGUTI, K., INABA, M., KURATSUNE, H. & WATANABE, Y. 2014. Neuroinflammation in Patients with Chronic

Fatigue Syndrome/Myalgic Encephalomyelitis: An ^{11}C-(R)-PK$_{11195}$ PET Study. *Journal of Nuclear Medicine,* 55**,** 945-950.

NAYFACH, S. & POLLARD, K. S. 2015. Average genome size estimation improves comparative metagenomics and sheds light on the functional ecology of the human microbiome. *Genome Biology,* 16**,** 51.

NEWBERRY, F., HSIEH, S.-Y., WILEMAN, T. & CARDING, S. 2018. Does the microbiome and virome contribute to myalgic encephalomyelitis/chronic fatigue syndrome? *Clinical Science,* 132**,** 523-542.

NGUYEN, T., JOHNSTON, S., CLARKE, L., SMITH, P., STAINES, D. & MARSHALL-GRADISNIK, S. 2016a. Impaired calcium mobilization in natural killer cells from chronic fatigue syndrome/myalgic encephalomyelitis patients is associated with transient receptor potential melastatin 3 ion channels. *Clinical and Experimental Immunology,* 187**,** 284-293.

NGUYEN, T., STAINES, D., NILIUS, B., SMITH, P. & MARSHALL-GRADISNIK, S. 2016b. Novel identification and characterisation of Transient receptor potential melastatin 3 ion channels on Natural Killer cells and B lymphocytes: effects on cell signalling in Chronic fatigue syndrome/Myalgic encephalomyelitis patients. *Biological Research,* 49**,** 27.

NICE. 2021. *Myalgic encephalomyelitis (or encephalopathy)/chronic fatigue syndrome: diagnosis and management: NICE guidelines [NG206]* [Online]. Available: https://www.nice.org.uk/guidance/ng206 [Accessed 16 March 2022].

NIJHOF, S. L., RUTTEN, J. M., UITERWAAL, C. S., BLEIJENBERG, G., KIMPEN, J. L. & PUTTE, E. M. 2014. The role of hypocortisolism in chronic fatigue syndrome. *Psychoneuroendocrinology,* 42**,** 199-206.

NILSSON, R. H., LARSSON, K. H., TAYLOR, A. F. S., BENGTSSON-PALME, J., JEPPESEN, T. S., SCHIGEL, D., KENNEDY, P., PICARD, K., GLÖCKNER, F. O., TEDERSOO, L., SAAR, I., KÕLJALG, U. & ABARENKOV, K. 2019. The UNITE database for molecular identification of fungi: handling dark taxa and parallel taxonomic classifications. *Nucleic Acids Research,* 47**,** D259-d264.

NORMAN, J. M., HANDLEY, S. A., BALDRIDGE, M. T., DROIT, L., LIU, C. Y., KELLER, B. C., KAMBAL, A., MONACO, C. L., ZHAO, G., FLESHNER, P., STAPPENBECK, T. S., MCGOVERN, D. P., KESHAVARZIAN, A., MUTLU, E. A., SAUK, J., GEVERS, D., XAVIER, R. J., WANG, D., PARKES, M. & VIRGIN, H. W. 2015. Disease-specific alterations in the enteric virome in inflammatory bowel disease. *Cell,* 160**,** 447-60.

NOTO, D. & MIYAKE, S. 2022. Gut dysbiosis and multiple sclerosis. *Clinical Immunology,* 235**,** 108380.

OHLSSON, L., GUSTAFSSON, A., LAVANT, E., SUNESON, K., BRUNDIN, L., WESTRIN, Å., LJUNGGREN, L. & LINDQVIST, D. 2019. Leaky gut biomarkers in depression and suicidal behavior. *Acta Psychiatrica Scandinavica,* 139**,** 185-193.

OKADA, T., TANAKA, M., KURATSUNE, H., WATANABE, Y. & SADATO, N. 2004. Mechanisms underlying fatigue: a voxel-based morphometric study of chronic fatigue syndrome. *BMC Neurology,* 4**,** 14.

OLIPHANT, K. & ALLEN-VERCOE, E. 2019. Macronutrient metabolism by the human gut microbiome: major fermentation by-products and their impact on host health. *Microbiome,* 7**,** 91.

O'NEAL, A. J. & HANSON, M. R. 2021. The Enterovirus Theory of Disease Etiology in Myalgic Encephalomyelitis/Chronic Fatigue Syndrome: A Critical Review. *Frontiers in Medicine,* 8.

OSOBA, T., PHEBY, D., GRAY, S. & NACUL, L. 2007. The Development of an Epidemiological Definition for Myalgic Encephalomyelitis/Chronic Fatigue Syndrome. *Journal of Chronic Fatigue Syndrome,* 14**,** 61-84.

PACHECO, Y., ACOSTA-AMPUDIA, Y., MONSALVE, D. M., CHANG, C., GERSHWIN, M. E. & ANAYA, J.-M. 2019. Bystander activation and autoimmunity. *Journal of Autoimmunity,* 103**,** 102301.

PALM, N. W., DE ZOETE, M. R., CULLEN, T. W., BARRY, N. A., STEFANOWSKI, J., HAO, L., DEGNAN, P. H., HU, J., PETER, I., ZHANG, W., RUGGIERO, E., CHO, J. H., GOODMAN, A. L. & FLAVELL, R. A. 2014. Immunoglobulin A coating identifies colitogenic bacteria in inflammatory bowel disease. *Cell,* 158**,** 1000-1010.

PALSSON, O. S., BAGGISH, J. S., TURNER, M. J. & WHITEHEAD, W. E. 2012. IBS patients show frequent fluctuations between loose/watery and hard/lumpy stools: implications for treatment. *The American journal of gastroenterology,* 107**,** 286-295.

PAONE, P. & CANI P. D. 2020. Mucus barrier, mucins and gut microbiota: the expected slimy partners? *Gut*, 2020;69:2232-2243.

PARODI, B. & KERLERO DE ROSBO, N. 2021. The Gut-Brain Axis in Multiple Sclerosis. Is Its Dysfunction a Pathological Trigger or a Consequence of the Disease? *Frontiers in Immunology,* 12.

PASCAL, V., POZUELO, M., BORRUEL, N., CASELLAS, F., CAMPOS, D., SANTIAGO, A., MARTINEZ, X., VARELA, E., SARRABAYROUSE, G., MACHIELS, K., VERMEIRE, S., SOKOL, H., GUARNER, F. & MANICHANH, C. 2017. A microbial signature for Crohn's disease. *Gut,* 66**,** 813-822.

PENDERGRAST, T., BROWN, A., SUNNQUIST, M., JANTKE, R., NEWTON, J. L., STRAND, E. B. & JASON, L. A. 2016. Housebound versus nonhousebound patients with myalgic encephalomyelitis and chronic fatigue syndrome. *Chronic Illness,* 12**,** 292-307.

PENNY, H. A., DOMINGUES, R. G., KRAUSS, M. Z., MELO-GONZALEZ, F., DICKSON, S., PARKINSON, J., HURRY, M., PURSE, C., JEGHAM, E., GODINHO-SILVA, C., RENDAS, M., VEIGA-FERNANDES, H., BECHTOLD, D., GRENCIS, R. K., TOELLNER, K.-M., WAISMAN, A., SWANN, J. R., GIBBS, J. E. & HEPWORTH, M. R. 2021. Rhythmicity of Intestinal IgA Responses Confers Oscillatory Commensal Microbiota Mutualism. *bioRxiv***,** 2021.10.11.463908.

PERFETTO, S. P., CHATTOPADHYAY, P. K., LAMOREAUX, L., NGUYEN, R., AMBROZAK, D., KOUP, R. A., & ROEDERER, M. 2010. Amine-reactive dyes for dead cell discrimination in fixed samples. *Current protocols in cytometry*, Chapter 9, Unit–9.34.

PETERSON, D., BRENU, E. W., GOTTSCHALK, G., RAMOS, S., NGUYEN, T., STAINES, D. & MARSHALL-GRADISNIK, S. 2015. Cytokines in the cerebrospinal fluids of patients with chronic fatigue syndrome/myalgic encephalomyelitis. *Mediators of Inflammation,* 2015**,** 929720.

PETERSON, P. K., SHEPARD, J., MACRES, M., SCHENCK, C., CROSSON, J., RECHTMAN, D. & LURIE, N. 1990. A controlled trial of intravenous immunoglobulin G in chronic fatigue syndrome. *The American Journal of Medicine,* 89**,** 554-60.

PIANTA, A., ARVIKAR, S., STRLE, K., DROUIN, E. E., WANG, Q., COSTELLO, C. E. & STEERE, A. C. 2017. Evidence of the Immune Relevance of *Prevotella copri*, a Gut Microbe, in Patients With Rheumatoid Arthritis. *Arthritis & Rheumatology,* 69**,** 964-975.

PICKARD, J. M., ZENG, M. Y., CARUSO, R. & NÚÑEZ, G. 2017. Gut microbiota: Role in pathogen colonization, immune responses, and inflammatory disease. *Immunological reviews,* 279**,** 70-89.

PIMENTEL, M. & LEMBO, A. 2020. Microbiome and Its Role in Irritable Bowel Syndrome. *Digestive Diseases and Sciences,* 65**,** 829-839.

PLANAS, R., SANTOS, R., TOMAS-OJER, P., CRUCIANI, C., LUTTEROTTI, A., FAIGLE, W., SCHAEREN-WIEMERS, N., ESPEJO, C., EIXARCH, H., PINILLA, C., MARTIN, R. & SOSPEDRA, M. 2018. GDP-l-fucose synthase is a CD4(+) T cell-specific autoantigen in DRB3*02:02 patients with multiple sclerosis. *Science Translational Medicine,* 10.

POWELL, D. J. H., LIOSSI, C., MOSS-MORRIS, R. & SCHLOTZ, W. 2013. Unstimulated cortisol secretory activity in everyday life and its relationship with fatigue and chronic fatigue syndrome: A systematic review and subset meta-analysis. *Psychoneuroendocrinology,* 38**,** 2405-2422.

PRAGER, I. & WATZL, C. 2019. Mechanisms of natural killer cell-mediated cellular cytotoxicity. *Journal of Leukocyte Biology,* 105**,** 1319-1329.

PREST, E. I., HAMMES, F., KÖTZSCH, S., VAN LOOSDRECHT, M. C. M. & VROUWENVELDER, J. S. 2013. Monitoring microbiological changes in drinking water systems using a fast and reproducible flow cytometric method. *Water Research,* 47**,** 7131-7142.

PURI, B. K., JAKEMAN, P. M., AGOUR, M., GUNATILAKE, K. D., FERNANDO, K. A., GURUSINGHE, A. I., TREASADEN, I. H., WALDMAN, A. D. & GISHEN, P. 2012. Regional grey and white matter volumetric changes in myalgic encephalomyelitis (chronic fatigue syndrome): a voxel-based morphometry 3 T MRI study. *The British Journal of Radiology,* 85**,** e270-3.

QIN, J., LI, R., RAES, J., ARUMUGAM, M., BURGDORF, K. S., MANICHANH, C., NIELSEN, T., PONS, N., LEVENEZ, F., YAMADA, T., MENDE, D. R., LI, J., XU, J., LI, S., LI, D., CAO, J., WANG, B., LIANG, H., ZHENG, H., XIE, Y., TAP, J., LEPAGE, P., BERTALAN, M., BATTO, J.-M., HANSEN, T., LE

PASLIER, D., LINNEBERG, A., NIELSEN, H. B., PELLETIER, E., RENAULT, P., SICHERITZ-PONTEN, T., TURNER, K., ZHU, H., YU, C., LI, S., JIAN, M., ZHOU, Y., LI, Y., ZHANG, X., LI, S., QIN, N., YANG, H., WANG, J., BRUNAK, S., DORÉ, J., GUARNER, F., KRISTIANSEN, K., PEDERSEN, O., PARKHILL, J., WEISSENBACH, J., ANTOLIN, M., ARTIGUENAVE, F., BLOTTIERE, H., BORRUEL, N., BRULS, T., CASELLAS, F., CHERVAUX, C., CULTRONE, A., DELORME, C., DENARIAZ, G., DERVYN, R., FORTE, M., FRISS, C., VAN DE GUCHTE, M., GUEDON, E., HAIMET, F., JAMET, A., JUSTE, C., KACI, G., KLEEREBEZEM, M., KNOL, J., KRISTENSEN, M., LAYEC, S., LE ROUX, K., LECLERC, M., MAGUIN, E., MELO MINARDI, R., OOZEER, R., RESCIGNO, M., SANCHEZ, N., TIMS, S., TORREJON, T., VARELA, E., DE VOS, W., WINOGRADSKY, Y., ZOETENDAL, E., BORK, P., EHRLICH, S. D., WANG, J. & META, H. I. T. C. 2010. A human gut microbial gene catalogue established by metagenomic sequencing. *Nature,* 464**,** 59-65.

QIU, X., ZHAO, X., CUI, X., MAO, X., TANG, N., JIAO, C., WANG, D., ZHANG, Y., YE, Z. & ZHANG, H. 2020. Characterization of fungal and bacterial dysbiosis in young adult Chinese patients with Crohn's disease. *Therapeutic Advances in Gastroenterology,* 13**,** 1756284820971202.

QUAST, C., PRUESSE, E., YILMAZ, P., GERKEN, J., SCHWEER, T., YARZA, P., PEPLIES, J. & GLÖCKNER, F. O. 2013. The SILVA ribosomal RNA gene database project: improved data processing and web-based tools. *Nucleic Acids Research,* 41**,** D590-6.

QUINCE, C., WALKER, A. W., SIMPSON, J. T., LOMAN, N. J. & SEGATA, N. 2017. Shotgun metagenomics, from sampling to analysis. *Nature Biotechnology,* 35**,** 833-844.

RAIJMAKERS, R. P. H., ROERINK, M. E., JANSEN, A. F. M., KEIJMEL, S. P., GACESA, R., LI, Y., JOOSTEN, L. A. B., VAN DER MEER, J. W. M., NETEA, M. G., BLEEKER-ROVERS, C. P. & XU, C.-J. 2020. Multi-omics examination of Q fever fatigue syndrome identifies similarities with chronic fatigue syndrome. *Journal of Translational Medicine,* 18**,** 448.

RAISON, C. L., LIN, J. M. & REEVES, W. C. 2009. Association of peripheral inflammatory markers with chronic fatigue in a population-based sample. *Brain, Behavior, and Immunity,* 23**,** 327-37.

RAMSAY, A. M. 1978. 'Epidemic neuromyasthenia' 1955-1978. *Postgraduate Medical Journal,* 54**,** 718-21.

RAMSAY, M. 1986. *Postviral Fatigue Syndrome: The Saga of Royal Free Disease,* London, Gower Medical Publishing.

RAO, A. V., BESTED, A. C., BEAULNE, T. M., KATZMAN, M. A., IORIO, C., BERARDI, J. M. & LOGAN, A. C. 2009. A randomized, double-blind, placebo-controlled pilot study of a probiotic in emotional symptoms of chronic fatigue syndrome. *Gut Pathogens,* 1**,** 6.

REDONDO-USEROS, N., NOVA, E., GONZÁLEZ-ZANCADA, N., DÍAZ, L. E., GÓMEZ-MARTÍNEZ, S. & MARCOS, A. 2020. Microbiota and Lifestyle: A Special Focus on Diet. *Nutrients,* 12**,** 1776.

REEVES, W. C., WAGNER, D., NISENBAUM, R., JONES, J. F., GURBAXANI, B., SOLOMON, L., PAPANICOLAOU, D. A., UNGER, E. R., VERNON, S. D. & HEIM, C. 2005. Chronic fatigue syndrome--a clinically empirical approach to its definition and study. *BMC Medicine,* 3**,** 19.

REVERBERI, R., & REVERBERI L. (2007). Factors affecting the antigen-antibody reaction. *Blood Transfusion*, 5(4), 227–240.

RIMES, K. A., GOODMAN, R., HOTOPF, M., WESSELY, S., MELTZER, H. & CHALDER, T. 2007. Incidence, Prognosis, and Risk Factors for Fatigue and Chronic Fatigue Syndrome in Adolescents: A Prospective Community Study. *Pediatrics,* 119**,** e603-e609.

RINNINELLA, E., RAOUL, P., CINTONI, M., FRANCESCHI, F., MIGGIANO, G. A. D., GASBARRINI, A. & MELE, M. C. 2019. What is the Healthy Gut Microbiota Composition? A Changing Ecosystem across Age, Environment, Diet, and Diseases. *Microorganisms,* 7**,** 14.

RIVAS, J. L., PALENCIA, T., FERNÁNDEZ, G. & GARCÍA, M. 2018. Association of T and NK Cell Phenotype With the Diagnosis of Myalgic Encephalomyelitis/Chronic Fatigue Syndrome (ME/CFS). *Frontiers in Immunology,* 9**,** 1028.

ROBERTS, A. D., WESSELY, S., CHALDER, T., PAPADOPOULOS, A. & CLEARE, A. J. 2004. Salivary cortisol response to awakening in chronic fatigue syndrome. *The British Journal of Psychiatry,* 184**,** 136-41.

RODRÍGUEZ, Y., ROJAS, M., PACHECO, Y., ACOSTA-AMPUDIA, Y., RAMÍREZ-SANTANA, C., MONSALVE, D. M., GERSHWIN, M. E., & ANAYA, J. M. 2018. Guillain-Barré syndrome, transverse myelitis and infectious diseases. *Cellular & molecular immunology*, 15(6), 547–562.

ROHR, M. W., NARASIMHULU, C. A., RUDESKI-ROHR, T. A. & PARTHASARATHY, S. 2019. Negative Effects of a High-Fat Diet on Intestinal Permeability: A Review. *Advances in Nutrition,* 11**,** 77-91.

ROLLENSKE, T., SZIJARTO, V., LUKASIEWICZ, J., GUACHALLA, L. M., STOJKOVIC, K., HARTL, K., STULIK, L., KOCHER, S., LASITSCHKA, F., AL-SAEEDI, M., SCHRÖDER-BRAUNSTEIN, J., VON FRANKENBERG, M., GAEBELEIN, G., HOFFMANN, P., KLEIN, S., HEEG, K., NAGY, E., NAGY, G. & WARDEMANN, H. 2018. Cross-specificity of protective human antibodies against *Klebsiella pneumoniae* LPS O-antigen. *Nature Immunology,* 19**,** 617-624.

ROSEN, C. E. & PALM, N. W. 2017. Functional Classification of the Gut Microbiota: The Key to Cracking the Microbiota Composition Code: Functional classifications of the gut microbiota reveal previously hidden contributions of indigenous gut bacteria to human health and disease. *Bioessays,* 39.

ROWE, P. C., UNDERHILL, R. A., FRIEDMAN, K. J., GURWITT, A., MEDOW, M. S., SCHWARTZ, M. S., SPEIGHT, N., STEWART, J. M., VALLINGS, R. & ROWE, K. S. 2017. Myalgic

Encephalomyelitis/Chronic Fatigue Syndrome Diagnosis and Management in Young People: A Primer. *Frontiers in Pediatrics,* 5.

RUFF, W. E., DEHNER, C., KIM, W. J., PAGOVICH, O., AGUIAR, C. L., YU, A. T., ROTH, A. S., VIEIRA, S. M., KRIEGEL, C., ADENIYI, O., MULLA, M. J., ABRAHAMS, V. M., KWOK, W. W., NUSSINOV, R., ERKAN, D., GOODMAN, A. L. & KRIEGEL, M. A. 2019. Pathogenic Autoreactive T and B Cells Cross-React with Mimotopes Expressed by a Common Human Gut Commensal to Trigger Autoimmunity. *Cell Host & Microbe,* 26**,** 100-113.e8.

RUFF, W. E., GREILING, T. M. & KRIEGEL, M. A. 2020. Host-microbiota interactions in immune-mediated diseases. *Nat Reviews Microbiology,* 18**,** 521-538.

RUIZ-NÚÑEZ, B., TARASSE, R., VOGELAAR, E. F., JANNEKE DIJCK-BROUWER, D. A. & MUSKIET, F. A. J. 2018. Higher Prevalence of "Low T3 Syndrome" in Patients With Chronic Fatigue Syndrome: A Case-Control Study. *Frontiers in Endocrinology (Lausanne),* 9**,** 97.

SANADA, K., NAKAJIMA, S., KUROKAWA, S., BARCELÓ-SOLER, A., IKUSE, D., HIRATA, A., YOSHIZAWA, A., TOMIZAWA, Y., SALAS-VALERO, M., NODA, Y., MIMURA, M., IWANAMI, A. & KISHIMOTO, T. 2020. Gut microbiota and major depressive disorder: A systematic review and meta-analysis. *Journal of Affective Disorders,* 266**,** 1-13.

SCHEIBENBOGEN, C., LOEBEL, M., FREITAG, H., KRUEGER, A., BAUER, S., ANTELMANN, M., DOEHNER, W., SCHERBAKOV, N., HEIDECKE, H., REINKE, P., VOLK, H. D. & GRABOWSKI, P. 2018. Immunoadsorption to remove ß2 adrenergic receptor antibodies in Chronic Fatigue Syndrome CFS/ME. *PLOS One,* 13**,** e0193672.

SCHEIBENBOGEN, C., SOTZNY, F., HARTWIG, J., BAUER, S., FREITAG, H., WITTKE, K., DOEHNER, W., SCHERBAKOV, N., LOEBEL, M. & GRABOWSKI, P. 2021. Tolerability and Efficacy of s.c. IgG Self-Treatment in ME/CFS Patients with IgG/IgG Subclass Deficiency: A Proof-of-Concept Study. *Journal of Clinical Medicine,* 10.

SCHLUEDERBERG, A., STRAUS, S. E., PETERSON, P., BLUMENTHAL, S., KOMAROFF, A. L., SPRING, S. B., LANDAY, A. & BUCHWALD, D. 1992. Chronic Fatigue Syndrome Research. *Annals of Internal Medicine,* 117**,** 325-331.

SCHOLTENS, P. A., ALLIET, P., RAES, M., ALLES, M. S., KROES, H., BOEHM, G., KNIPPELS, L. M., KNOL, J. & VANDENPLAS, Y. 2008. Fecal secretory immunoglobulin A is increased in healthy infants who receive a formula with short-chain galacto-oligosaccharides and long-chain fructo-oligosaccharides. *The Journal of Nutrition,* 138**,** 1141-7.

SCHROEDER, H. W., JR, & CAVACINI, L. 2010. Structure and function of immunoglobulins. *The Journal of allergy and clinical immunology*, 125(2 Suppl 2), S41-S52.

SCHULTHESS, J., PANDEY, S., CAPITANI, M., RUE-ALBRECHT, K. C., ARNOLD, I., FRANCHINI, F., CHOMKA, A., ILOTT, N. E., JOHNSTON, D. G. W., PIRES, E., MCCULLAGH, J., SANSOM, S. N.,

ARANCIBIA-CÁRCAMO, C. V., UHLIG, H. H. & POWRIE, F. 2019. The Short Chain Fatty Acid Butyrate Imprints an Antimicrobial Program in Macrophages. *Immunity,* 50**,** 432-445.e7.

SCHWARZ, E. C., QU, B. & HOTH, M. 2013. Calcium, cancer and killing: the role of calcium in killing cancer cells by cytotoxic T lymphocytes and natural killer cells. *Biochimica et Biophysica Acta,* 1833**,** 1603-11.

SCOTT, L. V., MEDBAK, S. & DINAN, T. G. 1998. Blunted adrenocorticotropin and cortisol responses to corticotropin-releasing hormone stimulation in chronic fatigue syndrome. *Acta Psychiatrica Scandinavica,* 97**,** 450-7.

SCOTT, L. V., SALAHUDDIN, F., COONEY, J., SVEC, F. & DINAN, T. G. 1999. Differences in adrenal steroid profile in chronic fatigue syndrome, in depression and in health. *Journal of Affective Disorders,* 54**,** 129-137.

SHAN, Z. Y., KWIATEK, R., BURNET, R., DEL FANTE, P., STAINES, D. R., MARSHALL-GRADISNIK, S. M. & BARNDEN, L. R. 2016. Progressive brain changes in patients with chronic fatigue syndrome: A longitudinal MRI study. *Journal of Magnetic Resonance Imaging,* 44**,** 1301-1311.

SHAN, Z. Y., KWIATEK, R., BURNET, R., DEL FANTE, P., STAINES, D. R., MARSHALL-GRADISNIK, S. M. & BARNDEN, L. R. 2017. Medial prefrontal cortex deficits correlate with unrefreshing sleep in patients with chronic fatigue syndrome. *NMR in Biomedical Research,* 30.

SHAPIRO, J. M., DE ZOETE, M. R., PALM, N. W., LAENEN, Y., BRIGHT, R., MALLETTE, M., BU, K., BIELECKA, A. A., XU, F., HURTADO-LORENZO, A., SHAH, S. A., CHO, J. H., LELEIKO, N. S., SANDS, B. E., FLAVELL, R. A. & CLEMENTE, J. C. 2021. Immunoglobulin A Targets a Unique Subset of the Microbiota in Inflammatory Bowel Disease. *Cell Host Microbe,* 29**,** 83-93.e3.

SHARPE, M. 1991. A report–chronic fatigue syndrome: guidelines for research. *Journal of the Royal Society of Medicine,* 84**,** 118-121.

SHARPE, M. C., ARCHARD, L. C., BANATVALA, J. E., BORYSIEWICZ, L. K., CLARE, A. W., DAVID, A., EDWARDS, R. H., HAWTON, K. E., LAMBERT, H. P., LANE, R. J. & ET AL. 1991. A report--chronic fatigue syndrome: guidelines for research. *Journal of the Royal Society of Medicine,* 84**,** 118-21.

SHERLIN, L., BUDZYNSKI, T., KOGAN BUDZYNSKI, H., CONGEDO, M., FISCHER, M. E. & BUCHWALD, D. 2007. Low-resolution electromagnetic brain tomography (LORETA) of monozygotic twins discordant for chronic fatigue syndrome. *Neuroimage,* 34**,** 1438-42.

SHUKLA, S. K., COOK, D., MEYER, J., VERNON, S. D., LE, T., CLEVIDENCE, D., ROBERTSON, C. E., SCHRODI, S. J., YALE, S. & FRANK, D. N. 2015. Changes in Gut and Plasma Microbiome following Exercise Challenge in Myalgic Encephalomyelitis/Chronic Fatigue Syndrome (ME/CFS). *PLOS One,* 10**,** e0145453.

SIEGEL, Z. A., BROWN, A., DEVENDORF, A., COLLIER, J. & JASON, L. A. 2018. A content analysis of chronic fatigue syndrome and myalgic encephalomyelitis in the news from 1987 to 2013. *Chronic Illness,* 14**,** 3-12.

SINGH, P., SILVESTER, J., CHEN, X., XU, H., SAWHNEY, V., RANGAN, V., ITURRINO, J., NEE, J., DUERKSEN, D. R. & LEMBO, A. 2019. Serum zonulin is elevated in IBS and correlates with stool frequency in IBS-D. *United European Gastroenterology Journal,* 7**,** 709-715.

SINHA, A. & MAURICE, C. F. 2019. Bacteriophages: Uncharacterized and Dynamic Regulators of the Immune System. *Mediators of Inflammation,* 2019**,** 3730519.

SKOWERA, A., CLEARE, A., BLAIR, D., BEVIS, L., WESSELY, S. C. & PEAKMAN, M. 2004. High levels of type 2 cytokine-producing cells in chronic fatigue syndrome. *Clinical & Experimental Immunology,* 135**,** 294-302.

SPENCE, V. A., KENNEDY, G., BELCH, J. J., HILL, A. & KHAN, F. 2008. Low-grade inflammation and arterial wave reflection in patients with chronic fatigue syndrome. *Clinical Science (London),* 114**,** 561-6.

SPERBER, A. D. & DEKEL, R. 2010. Irritable Bowel Syndrome and Co-morbid Gastrointestinal and Extra-gastrointestinal Functional Syndromes. *Journal of Neurogastroenterology and Motility,* 16**,** 113-9.

ST. PAUL, M. & OHASHI, P. S. 2020. The Roles of $CD8^+$ T Cell Subsets in Antitumor Immunity. *Trends in Cell Biology,* 30**,** 695-704.

STAGG, A. J. 2018. Intestinal Dendritic Cells in Health and Gut Inflammation. *Frontiers in Immunology,* 9.

STERLIN, D., FADLALLAH, J., ADAMS, O., FIESCHI, C., PARIZOT, C., DORGHAM, K., RAJKUMAR, A., AUTAA, G., EL-KAFSI, H., CHARUEL, J. L., JUSTE, C., JÖNSSON, F., CANDELA, T., WARDEMANN, H., AUBRY, A., CAPITO, C., BRISSON, H., TRESALLET, C., CUMMINGS, R. D., LARSEN, M., YSSEL, H., VON GUNTEN, S. & GOROCHOV, G. 2020. Human IgA binds a diverse array of commensal bacteria. *Journal of Experimental Medicine,* 217.

STERLIN, D., FADLALLAH, J., SLACK, E. & GOROCHOV, G. 2020. The antibody/microbiota interface in health and disease. *Mucosal Immunology,* 13**,** 3-11.

STRAWBRIDGE, R., SARTOR, M. L., SCOTT, F. & CLEARE, A. J. 2019. Inflammatory proteins are altered in chronic fatigue syndrome-A systematic review and meta-analysis. *Neuroscience & Biobehavioral Reviews,* 107**,** 69-83.

SUGAHARA, H., OKAI, S., ODAMAKI, T., WONG, C. B., KATO, K., MITSUYAMA, E., XIAO, J. Z. & SHINKURA, R. 2017. Decreased Taxon-Specific IgA Response in Relation to the Changes of Gut Microbiota Composition in the Elderly. *Frontiers in Microbiology,* 8**,** 1757.

SULHEIM, D., FAGERMOEN, E., WINGER, A., ANDERSEN, A. M., GODANG, K., MÜLLER, F., ROWE, P. C., SAUL, J. P., SKOVLUND, E., ØIE, M. G. & WYLLER, V. B. 2014. Disease mechanisms and

clonidine treatment in adolescent chronic fatigue syndrome: a combined cross-sectional and randomized clinical trial. *JAMA Pediatrics,* 168**,** 351-60.

SULLIVAN, A., NORD, C. E. & EVENGÅRD, B. 2009. Effect of supplement with lactic-acid producing bacteria on fatigue and physical activity in patients with chronic fatigue syndrome. *Nutrition Journal,* 8**,** 4.

SZYMULA, A., ROSENTHAL, J., SZCZERBA, B. M., BAGAVANT, H., FU, S. M. & DESHMUKH, U. S. 2014. T cell epitope mimicry between Sjögren's syndrome Antigen A (SSA)/Ro60 and oral, gut, skin and vaginal bacteria. *Clinical Immunology,* 152**,** 1-9.

TAIT, C. & SAYUK, G. S. 2021. The Brain-Gut-Microbiotal Axis: A framework for understanding functional GI illness and their therapeutic interventions. *European Journal of Internal Medicine,* 84**,** 1-9.

TAJIK, N., FRECH, M., SCHULZ, O., SCHÄLTER, F., LUCAS, S., AZIZOV, V., DÜRHOLZ, K., STEFFEN, F., OMATA, Y., RINGS, A., BERTOG, M., RIZZO, A., ILJAZOVIC, A., BASIC, M., KLEYER, A., CULEMANN, S., KRÖNKE, G., LUO, Y., ÜBERLA, K., GAIPL, U. S., FREY, B., STROWIG, T., SARTER, K., BISCHOFF, S. C., WIRTZ, S., CAÑETE, J. D., CICCIA, F., SCHETT, G. & ZAISS, M. M. 2020. Targeting zonulin and intestinal epithelial barrier function to prevent onset of arthritis. *Nature Communications,* 11**,** 1995.

TAK, L. M., CLEARE, A. J., ORMEL, J., MANOHARAN, A., KOK, I. C., WESSELY, S. & ROSMALEN, J. G. 2011. Meta-analysis and meta-regression of hypothalamic-pituitary-adrenal axis activity in functional somatic disorders. *Biological Psychology,* 87**,** 183-94.

TAKAKURA, W. & PIMENTEL, M. 2020. Small Intestinal Bacterial Overgrowth and Irritable Bowel Syndrome - An Update. *Frontiers in psychiatry,* 11**,** 664-664.

TARGAN, S. R., LANDERS, C. J., YANG, H., LODES, M. J., CONG, Y., PAPADAKIS, K. A., VASILIAUSKAS, E., ELSON, C. O. & HERSHBERG, R. M. 2005. Antibodies to CBir1 flagellin define a unique response that is associated independently with complicated Crohn's disease. *Gastroenterology,* 128**,** 2020-8.

TELATIN, A., FARISELLI, P. & BIROLO, G. 2021. SeqFu: A Suite of Utilities for the Robust and Reproducible Manipulation of Sequence Files. *Bioengineering (Basel, Switzerland),* 8**,** 59.

TERZO, S., MULÈ, F., CALDARA, G. F., BALDASSANO, S., PULEIO, R., VITALE, M., CASSATA, G., FERRANTELLI, V. & AMATO, A. 2020. Pistachio Consumption Alleviates Inflammation and Improves Gut Microbiota Composition in Mice Fed a High-Fat Diet. *International Journal of Molecular Sciences,* 21.

TEZUKA, H. & OHTEKI, T. 2019. Regulation of IgA Production by Intestinal Dendritic Cells and Related Cells. *Frontiers in Immunology,* 10.

THE MEDICAL STAFF OF THE ROYAL FREE HOSPITAL 1957. AN OUTBREAK of encephalomyelitis in the Royal Free Hospital Group, London, in 1955. *British medical journal,* 2**,** 895-904.

THOMAS, N., GURVICH, C., HUANG, K., GOOLEY, P. R. & ARMSTRONG, C. W. 2022. The underlying sex differences in neuroendocrine adaptations relevant to Myalgic Encephalomyelitis Chronic Fatigue Syndrome. *Frontiers in Neuroendocrinology***,** 100995.

TIEW, P. Y., MAC AOGAIN, M., ALI, N., THNG, K. X., GOH, K., LAU, K. J. X. & CHOTIRMALL, S. H. 2020. The Mycobiome in Health and Disease: Emerging Concepts, Methodologies and Challenges. *Mycopathologia,* 185**,** 207-231.

TOKUMASU, K., HONDA, H., SUNADA, N., SAKURADA, Y., MATSUDA, Y., YAMAMOTO, K., NAKANO, Y., HASEGAWA, T., YAMAMOTO, Y., OTSUKA, Y., HAGIYA, H., KATAOKA, H., UEDA, K., & OTSUKA, F. (2022). Clinical Characteristics of Myalgic Encephalomyelitis/Chronic Fatigue Syndrome (ME/CFS) Diagnosed in Patients with Long COVID. *Medicina (Kaunas, Lithuania)*, 58(7), 850.

TOMAS, C., BROWN, A., STRASSHEIM, V., ELSON, J. L., NEWTON, J. & MANNING, P. 2017. Cellular bioenergetics is impaired in patients with chronic fatigue syndrome. *PLOS One,* 12**,** e0186802.

TORDESILLAS, L. & BERIN, M. C. 2018. Mechanisms of Oral Tolerance. *Clinical Reviews in Allergy & Immunology,* 55**,** 107-117.

UNDERHILL, R. A. 2015. Myalgic encephalomyelitis, chronic fatigue syndrome: An infectious disease. *Medical Hypotheses,* 85**,** 765-73.

VAN CAMPEN, C. M. C., ROWE, P. C. & VISSER, F. C. 2020a. Cerebral Blood Flow Is Reduced in Severe Myalgic Encephalomyelitis/Chronic Fatigue Syndrome Patients During Mild Orthostatic Stress Testing: An Exploratory Study at 20 Degrees of Head-Up Tilt Testing. *Healthcare,* 8**,** 169.

VAN CAMPEN, C. M. C., ROWE, P. C. & VISSER, F. C. 2020b. Validation of the Severity of Myalgic Encephalomyelitis/Chronic Fatigue Syndrome by Other Measures than History: Activity Bracelet, Cardiopulmonary Exercise Testing and a Validated Activity Questionnaire: SF-36. *Healthcare,* 8**,** 273.

VAN CAMPEN, C. M. C., ROWE, P. C. & VISSER, F. C. 2021. Cerebral blood flow remains reduced after tilt testing in myalgic encephalomyelitis/chronic fatigue syndrome patients. *Clinical Neurophysiology Practice,* 6**,** 245-255.

VAN CAMPEN, C. M. C., VERHEUGT, F. W. A., ROWE, P. C. & VISSER, F. C. 2020c. Cerebral blood flow is reduced in ME/CFS during head-up tilt testing even in the absence of hypotension or tachycardia: A quantitative, controlled study using Doppler echography. *Clinical Neurophysiology Practice,* 5**,** 50-58.

VANDEPUTTE, D., KATHAGEN, G., D'HOE, K., VIEIRA-SILVA, S., VALLES-COLOMER, M., SABINO, J., WANG, J., TITO, R. Y., DE COMMER, L., DARZI, Y., VERMEIRE, S., FALONY, G. & RAES, J. 2017.

Quantitative microbiome profiling links gut community variation to microbial load. *Nature,* 551**,** 507-511.

VASILIAUSKAS, E. A., KAM, L. Y., KARP, L. C., GAIENNIE, J., YANG, H. & TARGAN, S. R. 2000. Marker antibody expression stratifies Crohn's disease into immunologically homogeneous subgroups with distinct clinical characteristics. *Gut,* 47**,** 487.

VENTURINI, L., BACCHI, S., CAPELLI, E., LORUSSO, L., RICEVUTI, G. & CUSA, C. 2019. Modification of Immunological Parameters, Oxidative Stress Markers, Mood Symptoms, and Well-Being Status in CFS Patients after Probiotic Intake: Observations from a Pilot Study. *Oxidative Medicine and Cellular Longevity,* 2019**,** 1684198.

VISSER, J. T., DE KLOET, E. R. & NAGELKERKEN, L. 2000. Altered glucocorticoid regulation of the immune response in the chronic fatigue syndrome. *Annals of the New York Academy of Sciences,* 917**,** 868-75.

VISSER, J., LENTJES, E., HASPELS, I., GRAFFELMAN, W., BLAUW, B., DE KLOET, R. & NAGELKERKEN, L. 2001. Increased Sensitivity to Glucocorticoids in Peripheral Blood Mononuclear Cells of Chronic Fatigue Syndrome Patients, Without Evidence for Altered Density or Affinity of Glucocorticoid Receptors. *Journal of Investigative Medicine,* 49**,** 195-204.

VIVIER, E., TOMASELLO, E., BARATIN, M., WALZER, T. & UGOLINI, S. 2008. Functions of natural killer cells. *Nature Immunology,* 9**,** 503-510.

VOGL, T., KLOMPUS, S., LEVIATAN, S., KALKA, I. N., WEINBERGER, A., WIJMENGA, C., FU, J., ZHERNAKOVA, A., WEERSMA, R. K. & SEGAL, E. 2021. Population-wide diversity and stability of serum antibody epitope repertoires against human microbiota. *Nature Medicine,* 27**,** 1442-1450.

VUJKOVIC-CVIJIN, I., SKLAR, J., JIANG, L., NATARAJAN, L., KNIGHT, R. & BELKAID, Y. 2020. Host variables confound gut microbiota studies of human disease. *Nature,* 587**,** 448-454.

WANG, L., ALAMMAR, N., SINGH, R., NANAVATI, J., SONG, Y., CHAUDHARY, R. & MULLIN, G. E. 2020. Gut Microbial Dysbiosis in the Irritable Bowel Syndrome: A Systematic Review and Meta-Analysis of Case-Control Studies. *Journal of the Academy of Nutrition and Dietetics,* 120**,** 565-586.

WANG, Y., FEI, Y., LIU, L., XIAO, Y., PANG, Y., KANG, J. & WANG, Z. 2018. *Polygonatum odoratum* Polysaccharides Modulate Gut Microbiota and Mitigate Experimentally Induced Obesity in Rats. *International Journal of Molecular Sciences,* 19.

WESSELY, S. 1996. Chronic fatigue syndrome: summary of a report of a joint committee of the Royal Colleges of Physicians, Psychiatrists and General Practitioners. *Journal of the Royal College of Physicians of London,* 30**,** 497.

WIRTH, K. & SCHEIBENBOGEN, C. 2020. A Unifying Hypothesis of the Pathophysiology of Myalgic Encephalomyelitis/Chronic Fatigue Syndrome (ME/CFS): Recognitions from the finding of autoantibodies against ß2-adrenergic receptors. *Autoimmunity Reviews,* 19**,** 102527.

WOOD, D. E., LU, J. & LANGMEAD, B. 2019. Improved metagenomic analysis with Kraken 2. *Genome Biology,* 20**,** 257.

WRIGHT, M. H., ADELSKOV, J. & GREENE, A. C. 2017. Bacterial DNA Extraction Using Individual Enzymes and Phenol/Chloroform Separation. *Journal of Microbiology & Biology Education,* 18.

WU, K. Q., SUN, W. J., LI, N., CHEN, Y. Q., WEI, Y. L. & CHEN, D. F. 2019. Small intestinal bacterial overgrowth is associated with Diarrhea-predominant irritable bowel syndrome by increasing mainly Prevotella abundance. *Scandinavian Journal of Gastroenterology,* 54**,** 1419-1425.

WU, T., QI, X., SU, Y., TENG, J. & XU, X. 2016. Electroencephalogram characteristics in patients with chronic fatigue syndrome. *Neuropsychiatric Disease and Treatment,* 12**,** 241-9.

XIONG, N. & HU, S. 2015. Regulation of intestinal IgA responses. *Cellular and molecular life sciences : CMLS,* 72**,** 2645-2655.

YAMANO, E., SUGIMOTO, M., HIRAYAMA, A., KUME, S., YAMATO, M., JIN, G., TAJIMA, S., GODA, N., IWAI, K., FUKUDA, S., YAMAGUTI, K., KURATSUNE, H., SOGA, T., WATANABE, Y. & KATAOKA, Y. 2016. Index markers of chronic fatigue syndrome with dysfunction of TCA and urea cycles. *Scientific Reports,* 6**,** 34990.

YOSHIUCHI, K., FARKAS, J. & NATELSON, B. H. 2006. Patients with chronic fatigue syndrome have reduced absolute cortical blood flow. *Clinical Physiology and Functional Imaging,* 26**,** 83-86.

YU, Y. & ZHAO, F. 2021. Microbiota-gut-brain axis in autism spectrum disorder. *Journal of Genetics and Genomics,* 48**,** 755-762.

ZAMORA, J. L. R. & AGUILAR, H. C. 2018. Flow virometry as a tool to study viruses. *Methods,* 134-135**,** 87-97.

ZENG, M. Y., CISALPINO, D., VARADARAJAN, S., HELLMAN, J., WARREN, H. S., CASCALHO, M., INOHARA, N. & NÚÑEZ, G. 2016. Gut Microbiota-Induced Immunoglobulin G Controls Systemic Infection by Symbiotic Bacteria and Pathogens. *Immunity,* 44**,** 647-658.

ZHANG, H., LI, P., WU, D., XU, D., HOU, Y., WANG, Q., LI, M., LI, Y., ZENG, X., ZHANG, F. & SHI, Q. 2015. Serum IgG subclasses in autoimmune diseases. *Medicine,* 94**,** e387-e387.

ZHANG, N. & BEVAN, M. J. 2011. CD8(+) T cells: foot soldiers of the immune system. *Immunity,* 35**,** 161-8.

ZHENG, D., LIWINSKI, T. & ELINAV, E. 2020. Interaction between microbiota and immunity in health and disease. *Cell Research,* 30**,** 492-506.

ZIMMERMANN, K., HAAS, A. & OXENIUS, A. 2012. Systemic antibody responses to gut microbes in health and disease. *Gut Microbes,* 3**,** 42-7.

ZINN, M. A., ZINN, M. L., VALENCIA, I., JASON, L. A. & MONTOYA, J. G. 2018. Cortical hypoactivation during resting EEG suggests central nervous system pathology in patients with chronic fatigue syndrome. *Biological Psychology,* 136**,** 87-99.

ZINN, M. L., ZINN, M. A. & JASON, L. A. 2016. Intrinsic Functional Hypoconnectivity in Core Neurocognitive Networks Suggests Central Nervous System Pathology in Patients with Myalgic Encephalomyelitis: A Pilot Study. *Applied Psychophysiology and Biofeedback,* 41**,** 283-300.

ZIPPER, H., BRUNNER, H., BERNHAGEN, J. & VITZTHUM, F. 2004. Investigations on DNA intercalation and surface binding by SYBR Green I, its structure determination and methodological implications. *Nucleic acids research,* 32**,** e103-e103.